

Federal/Provincial Research and
Monitoring Coordinating Committee (RMCC)



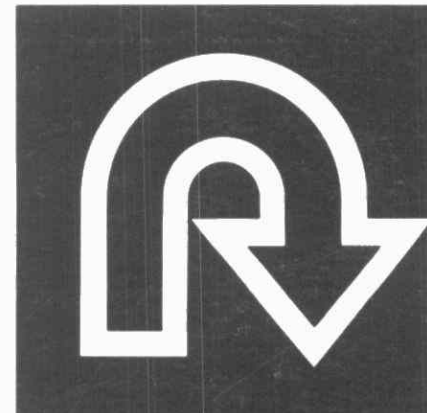
THE 1990 CANADIAN
LONG-RANGE TRANSPORT OF
AIR POLLUTANTS AND
ACID DEPOSITION
ASSESSMENT REPORT

Part 3

ATMOSPHERIC SCIENCES

TD
195.54
.C36
1990
part 3
MOE

1990



ACID RAIN

PLUIES
ACIDES

BC
Environment

Gouvernement
du Québec
Ministère de
l'Environnement

Alberta
ENVIRONMENT

New Brunswick
Nouveau Brunswick

Saskatchewan
Environment and
Public Safety

Prince Edward Island
Department of the
Environment

Manitoba
Environment



Nova Scotia
Department of the
Environment

Environment
Ontario



Province of Newfoundland
Department of Environment & Lands

Canada

TD
195.54
.C36
1990
part 3

The 1990 Canadian long-range
transport of air pollutants and
acid deposition assessment
report.

77963

Copyright Provisions and Restrictions on Copying:

This Ontario Ministry of the Environment work is protected by Crown copyright (unless otherwise indicated), which is held by the Queen's Printer for Ontario. It may be reproduced for non-commercial purposes if credit is given and Crown copyright is acknowledged.

It may not be reproduced, in all or in part, part, for any commercial purpose except under a licence from the Queen's Printer for Ontario.

For information on reproducing Government of Ontario works, please contact Service Ontario Publications at copyright@ontario.ca

JAN 26 1995

FEDERAL/PROVINCIAL
RESEARCH AND MONITORING
COORDINATING COMMITTEE (RMCC)

MOEE
SCI & TECH BRANCH
LIBRARY

**THE 1990 CANADIAN LONG-RANGE TRANSPORT
OF AIR POLLUTANTS AND ACID DEPOSITION
ASSESSMENT REPORT**

**PART 3
ATMOSPHERIC SCIENCES
1990**

EDITORS

M.A. Lusiš	Air Resources Branch, Ontario Ministry of Environment
M.L. Phillips	Atmospheric Environment Service, Environment Canada

AUTHORS/CONTRIBUTORS

L.A. Barrie	Atmospheric Environment Service, Environment Canada
B.L. Beattie	Atmospheric Environment Service, Environment Canada
R. Bloxam	Air Resources Branch, Ontario Ministry of Environment
J. Bottenheim	Atmospheric Environment Service, Environment Canada
D. Davies	Atmospheric Environment Service, Environment Canada
M. Ferland	Direction de la Météorologie, Environnement Québec
C. Fung	Air Resources Branch, Ontario Ministry of Environment
P.K. Misra	Air Resources Branch, Ontario Ministry of Environment
J. Ogden	Department of Biology, Dalhousie University
M.P. Olson	Atmospheric Environment Service, Environment Canada
N.W. Reid	Air Resources Branch, Ontario Ministry of Environment
C.U. Ro	Atmospheric Environment Service, Environment Canada
A. Sirois	Atmospheric Environment Service, Environment Canada
W.B. Sukloff	Atmospheric Environment Service, Environment Canada
P.W. Summers	Atmospheric Environment Service, Environment Canada
A.J.S. Tang	Air Resources Branch, Ontario Ministry of Environment
J. Underwood	Environmental Assessment Division, Nova Scotia Department of the Environment
F. Vena	Conservation and Protection, Environment Canada
R.J. Vet	Atmospheric Environment Service, Environment Canada

D.H. Waller	Technical University of Nova Scotia
D. Yap	Air Resources Branch, Ontario Ministry of Environment
J.W.S. Young	Atmospheric Environment Service, Environment Canada

EXTERNAL REVIEWERS

R.G. Derwent	Environmental and Medical Sciences Division, Harwell Laboratory
H. Dovland	Norwegian Institute for Air Research

TABLE OF CONTENTS

SECTION	PAGE#
LIST OF TABLES	3-iv
LIST OF FIGURES	3-vi
SUMMARY	3-1
3.1 INTRODUCTION	3-7
3.2 INSIGHT INTO SOURCE-RECEPTOR RELATIONSHIPS GAINED FROM PATTERN ASSOCIATIONS, TRENDS AND RELATED STUDIES	3-9
3.2.1 INTRODUCTION	3-9
3.2.2 EMISSIONS AND ATMOSPHERIC OBSERVATIONS	3-9
3.2.2.a EMISSIONS	3-9
3.2.2.b PATTERNS OF PRECIPITATION COMPOSITION AND DEPOSITION OF ACIDS IN CANADA	3-27
3.2.2.c THE SPATIAL AND TEMPORAL PATTERNS OF SULPHUR DIOXIDE, SULPHATE AND NITRATE CONCENTRATIONS IN AIR IN ONTARIO	3-44
3.2.3 TRENDS IN OBSERVED ACIDIC CONSTITUENTS IN EASTERN CANADA	3-60
3.2.3.a TEMPORAL VARIATIONS OF SULPHATE AND NITRATE IN AIR AND PRECIPITATION AT FIVE FEDERAL SITES IN EASTERN CANADA	3-60
3.2.3.b TEMPORAL VARIATIONS OF INTEGRATED WET DEPOSIT OF SULPHATE AND NITRATE IN EASTERN NORTH AMERICA	3-70
3.2.3.c TEMPORAL VARIATIONS OF SULPHATE AND NITRATE IN AIR AND PRECIPITATION AT DORSET ONTARIO	3-76
3.2.3.d SOURCE-RECEPTOR RELATIONSHIPS FROM EMISSION DEPOSITION PATTERN ASSOCIATIONS IN QUEBEC	3-79
3.2.3.e TRENDS IN SURFACE OZONE CONCENTRATIONS IN ONTARIO	3-81
3.2.4 SOURCE-RECEPTOR RELATIONSHIPS FROM ATMOSPHERIC TRACERS	3-86
3.2.4.a INTRODUCTION	3-86

TABLE OF CONTENTS (continued)

SECTION	PAGE#
3.2.4.b WIND SECTOR STRATIFICATION AT MONITORING SITES	3-88
3.2.4.c AIRMASS TRAJECTORY ANALYSES	3-89
3.2.4.d RECEPTOR MODELLING	3-94
3.2.4.e IMPACT OF MAJOR POINT SOURCE SHUT-DOWN	3-99
3.2.4.f THE CROSS APPALACHIAN TRACER EXPERIMENT (CAPTEX)	3-100
3.2.4.g THE ACROSS NORTH AMERICA TRACER EXPERIMENT (ANATEX)	3-100
3.2.4.h AN UPDATED ATMOSPHERIC SULPHUR BUDGET FOR EASTERN CANADA	3-100
3.2.4.i ARCTIC HAZE	3-103
3.2.5 SUMMARY AND CONCLUSIONS	3-104
3.3 SOURCE-RECEPTOR RELATIONSHIPS FROM NUMERICAL MODELS	3-111
3.3.1 INTRODUCTION	3-111
3.3.2 MAJOR CONSIDERATIONS IN MODELLING SOURCE-RECEPTOR RELATIONSHIPS	3-114
3.3.2.a MODEL FORMULATION	3-115
3.3.2.b INPUT DATA	3-117
3.3.2.c PRACTICAL COMPUTATION CONSTRAINTS	3-119
3.3.3 NONLINEARITY QUESTIONS	3-119
3.3.4 LINEAR MODELS	3-122
3.3.4.a INTRODUCTION	3-122
3.3.4.b MODELLING APPROACHES	3-122
3.3.4.c EVALUATIONS OF LINEAR LONG-RANGE TRANSPORT MODELS	3-124
3.3.4.d THE INTERNATIONAL SULPHUR DEPOSITION MODEL EVALUATION (ISDME)	3-139
3.3.4.e CURRENT OR FUTURE USE OF "LINEAR MODELS"	3-149

TABLE OF CONTENTS (continued)

SECTION	PAGE#
3.3.5 NONLINEAR EULERIAN MODELS	3-149
3.3.5.a BRIEF DESCRIPTION OF THE ADOM MODEL	3-150
3.3.5.b OSCAR MODEL RUNS	3-152
3.3.5.c ANATEX MODEL RUNS	3-159
3.3.5.d SUMMER OZONE EPISODE	3-163
3.3.5.e WINTER STUDY	3-163
3.3.5.f EULERIAN MODEL EVALUATION FIELD STUDY	3-165
3.3.5.g PRELIMINARY COMPARISON OF LINEAR AND COMPREHENSIVE MODELS	3-187
3.3.6 DISCUSSION AND CONCLUSIONS	3-193
APPENDICES	3-196
APPENDIX 3A The best estimate of total deposition that is dry deposition in eastern Canada.	3-197
APPENDIX 3B Concentration and deposition patterns.	3-203
APPENDIX 3C The spatial and temporal patterns of sulphate and nitrate concentrations in air in Ontario.	3-257
APPENDIX 3D Temporal variation of sulphate and nitrate concentrations in air and precipitation at five sites in eastern Canada.	3-262
APPENDIX 3E Trends in precipitation chemistry in Nova Scotia: 1978-1987.	3-306
APPENDIX 3F Temporal variation of sulphate and nitrate concentrations in air and precipitation at Dorset, Ontario.	3-311
APPENDIX 3G Lagrangian model scenario runs.	3-344
REFERENCES	3-350

LIST OF TABLES

Table#		Page#
3.2.1	1980-1985 SO _x Emissions in Canada (by source regions - 1,000 tonnes/year).	3-18
3.2.2	1980-1985 SO _x Emissions in the United States (by source regions - 1,000 tonnes/year).	3-19
3.2.3	1980-1985 NO _x Emissions in Canada (by source regions - 1,000 tonnes/year).	3-20
3.2.4	1980-1985 NO _x Emissions in the United States (by source regions - 1,000 tonnes/year).	3-21
3.2.5	Annual Eastern North American SO ₂ and NO _x Emissions for the Period 1980-1987.	3-22
3.2.6	Wet Deposition Monitoring Networks.	3-28
3.2.7	Summary of results of time series analysis of SO ₄ ⁼ and NO ₃ ⁻ concentration in precipitation at 5 rural locations in eastern Canada.	3-63
3.2.8	Summary of results of time series analysis of SO ₄ ⁼ , SO ₂ and Total NO ₃ ⁻ concentration in air at 5 rural locations in eastern Canada.	3-64
3.2.9	Total annual deposition integrated over the area shown in Figure 3.2.31 for eastern North America over the period 1980-1987. Units MT yr ⁻¹ .	3-71
3.2.10	Standard Error of the integrated wet deposition of SO ₄ ⁼ and NO ₃ ⁻ and the deposition values $\pm 3\sigma$ at the beginning and end of period.	3-72
3.2.11	Source-receptor matrix for wet deposition of SO ₄ ⁼ and NO ₃ ⁻ at 2 sites in southern Ontario, showing % contribution from US and Canadian sources.	3-91
3.2.12	The concentration-weighted apportionment of atmospheric Pb using the Pb-206/207 ratio observed in hi-vol air samples at 3 sites in eastern Canada in the Autumn of 1984. Absolute uncertainties of one standard deviation are shown.	3-97
3.2.13	Estimates of contribution of sources to Pb in air at Dorset in two seasons. Absolute uncertainties of one standard deviation are given.	3-98
3.2.14	The main flux terms in regional atmospheric budgets for eastern Canada and the eastern US 1985-1987.	3-102
3.3.1	Targetted sensitive receptor sites.	3-129

LIST OF TABLES (continued)

Table#		Page#
3.3.2	Spearman's Rank Correlation Coefficient Summary for ground level $\text{SO}_4^{=}$ concentration from MOI (1982b) at Muskoka.	3-132
3.3.3	Spearman's Rank Correlation Coefficient Summary for dry deposition from MOI (1982b) at Muskoka.	3-133
3.3.4	Spearman's Rank Correlation Coefficient Summary for wet deposition from MOI (1982b) at Muskoka.	3-133
3.3.5	Model ranking for Muskoka, Ontario - annual (1978) wet sulphur deposition.	3-136
3.3.6	AES-LRT Model annual (1978) $\text{SO}_4^{=}$ unit matrix in micrograms per cubic metre per Tg emitted.	3-137
3.3.7	AES-LRT Model annual (1978) wet deposition unit matrix in kilograms S per hectare per Tg emitted.	3-138
3.3.8	The models and participants in ISDME.	3-140
3.3.9	Summary of model performance measures for Winter 1980.	3-145
3.3.10	Summary of model performance measures for Autumn 1980.	3-146
3.3.11	Summary of model performance measures for Spring 1980.	3-147
3.3.12	Summary of model performance measures for Summer 1980.	3-148
3.3.13	Ratios of $\text{NO}_3^-/\text{SO}_4^{=}$ found in precipitation during OSCAR II and IV (springtime) and a winter period.	3-169

LIST OF FIGURES

Figure#		Page#
	Summary	
3.S.1	Trends in SO ₂ emissions and precipitation excess sulphate concentrations in eastern North America. The different shaded areas on the map show the percent difference between 1980-82 and 1985-87 average concentration fields. The box directly underneath the map shows the eastern North American SO ₂ emission changes normalized to 1980. The outer boxes show the year to year observations at a number of specific sites normalized to 1980.	3-5
3.S.2	Trends in NO _x emissions and precipitation excess sulphate concentrations in eastern North America. The different shaded areas on the map show the percent difference between 1980-82 and 1985-87 average concentration fields. The box directly underneath the map shows the eastern North American NO _x emission changes normalized to 1980. The outer boxes show the year to year observations at a number of specific sites normalized to 1980.	3-6
	Section 3.2	
3.2.1	Schematic map showing regions that currently have acidification problems, and regions where, based on soil sensitivity, expected future emissions and population density, acidification might become severe in the future (from Rhode and Herrera, 1988).	3-11
3.2.2	Eastern North American pattern of non-marine SO ₄ ⁼ precipitation-weighted-mean concentration (1982-1987).	3-12
3.2.3	The global nature of acid rain in the early 1980s.	3-13
3.2.4	NATCHEM 1980-87 Precipitation chemistry stations in the NATCHEM DATA BASE.	3-14
3.2.5	North America SO _x Emissions by Source Regions: Year - 1980	3-15
3.2.6	North America SO _x Emissions by Source Regions: Year - 1985.	3-16
3.2.7	North America SO _x Emissions 85-80 Variation by Source Region.	3-17
3.2.8	North America NO _x Emissions by Source Regions: Year -1980.	3-24
3.2.9	North America NO _x Emissions by Source Regions: Year -1985.	3-25

LIST OF FIGURES (continued)

Figure#		Page#
3.2.10	North America NO _x Emissions 85-80 Variation by Source Region.	3-26
3.2.11a	Canadian and US wet deposition monitoring sites used to generate spatial patterns of concentration and deposition from 1980 to 1983.	3-29
3.2.11b	Canadian and US wet deposition monitoring sites used to generate spatial patterns of concentration and deposition from 1984 to 1987.	3-30
3.2.12a	Patterns of annual precipitation-weighted-mean concentrations of excess SO ₄ ⁼ (mg/l):1980-1983.	3-35
3.2.12b	Patterns of annual precipitation-weighted-mean concentrations of excess SO ₄ ⁼ (mg/l):1984-1987.	3-36
3.2.13a	Patterns of annual wet deposition of excess of SO ₄ ⁼ (kg/ha/yr):1980-1983.	3-37
3.2.13b	Patterns of annual wet deposition of excess of SO ₄ ⁼ (kg/ha/yr):1984-1987.	3-38
3.2.14a	Envelope of annual 20 kg/ha/y excess sulphate deposition isopleths for all years from 1980 to 1987.	3-39
3.2.14b	Superposition of the 20 kg/ha/y excess sulphate deposition isopleths for the periods of 1980-82 and 1985-87.	3-39
3.2.15a	Envelope of annual 15 kg/ha/y nitrate deposition isopleths for the periods 1980 to 1987.	3-40
3.2.15b	Superposition of the 15 kg/ha/y nitrate deposition isopleths for the periods 1980-82 and 1985-87.	3-40
3.2.16	Six-year-average (1982-1987) concentration and deposition patterns of excess sulphate.	3-46
3.2.17	Superposition of the 1982-87 six-year-average excess sulphate concentration isopleths (2 and 3 mg/l) on the 1985 SO ₂ emission pattern.	3-47
3.2.18	Six-year-average (1982-87) concentration and deposition patterns of nitrate.	3-48

LIST OF FIGURES (continued)

Figure#		Page#
3.2.19	Superposition of the 1982-87 six-year-average nitrate concentration isopleths (1.5 and 2 mg/l) on the 1985 NO _x emission pattern.	3-49
3.2.20	Trajectory roses (2-day back trajectories at the 925 mb level) for precipitation sulphate (top) and nitrate (bottom) concentrations measured at several Canadian sites (MOI, 1982).	3-50
3.2.21	Six-year-average (1982-87) concentration and deposition patterns of H ⁺ .	3-51
3.2.22	Changes in the precipitation-weighted mean concentrations of SO ₄ ⁼ between the two periods 1980-1982 and 1985-1987 expressed as a spatial pattern of a) absolute changes in mg/l and b) % changes against the first period as the base.	3-52
3.2.23	Changes in the precipitation-weighted mean concentrations of NO ₃ ⁻ between the two periods 1980-1982 and 1985-1987 expressed as a spatial pattern of a) absolute changes in mg/l and b) % changes against the first period as the base.	3-53
3.2.24a	Annual average 28-day air concentrations of SO ₂ (μg m ⁻³) in Ontario: 1982-1986.	3-54
3.2.24b	Annual average 28-day air concentrations of SO ₄ ⁼ (μg m ⁻³) in Ontario: 1982-1986.	3-55
3.2.24c	Annual average 28-day air concentrations of t-NO ₃ ⁻ (μg N m ⁻³) in Ontario: 1982-1986.	3-56
3.2.25	Variation of Sulphur Dioxide concentration in air (μg m ⁻³) in Ontario: 1982/1983 compared to 1985/1986.	3-57
3.2.26	Variation of Sulphate concentration in air (μg m ⁻³) in Ontario: 1982/1983 to 1985/1986.	3-58
3.2.27	Variation in Total Nitrate concentration in air (μg N m ⁻³) in Ontario: 1982/1983 compared to 1985/1986.	3-59
3.2.28	Map showing long term air and precipitation monitoring sites.	3-62
3.2.29a	Significant normalized precipitation SO ₄ ⁼ concentration trends (corrected for influence of precipitation amount and seasonal cycles removed).	3-65

LIST OF FIGURES (continued)

Figure#		Page#
3.2.29b	Significant normalized precipitation NO_3^- concentration trends (corrected for influence of precipitation amount and seasonal cycles removed).	3-66
3.2.30a	Significant normalized air SO_2 concentration variations (seasonal cycles removed).	3-67
3.2.30b	Significant normalized air $\text{SO}_4^{=}$ concentration variations (seasonal cycles removed).	3-68
3.2.30c	Significant normalized air NO_3^- concentration variations (seasonal cycles removed).	3-69
3.2.31	Area used to obtain the integrated wet deposition of $\text{SO}_4^{=}$ and NO_3^- over eastern North America.	3-73
3.2.32	Time series showing the annual emissions and annual integrated wet deposition over eastern North America from 1980 to 1987. (a) SO_2 and excess $\text{SO}_4^{=}$ (b) NO_x and NO_3^- . All values are normalized to 1980 as unity.	3-74
3.2.33	Correlation between the annual emissions and integrated annual wet deposition over eastern North America from 1980 to 1987. (a) excess $\text{SO}_4^{=}$ (b) NO_3^- . All values are normalized to 1980 as unity. The best fit regression lines and Pearson correlation coefficient (R) are included.	3-75
3.2.34	Temporal variation of sulphate and nitrate concentrations in air and precipitation at Dorset, Ontario.	3-78
3.2.35	Precipitation amount corrected seasonal sulphate and nitrate concentrations at Dorset, Ontario.	3-80
3.2.36	Ten year trends for O_3 concentrations and 80 ppb exceedences across Ontario.	3-83
3.2.37	"Episode days" - days on which widespread elevated O_3 levels greater than 80 ppb occurred at more than 8 monitoring sites in southern Ontario from 1979 to 1985.	3-84
3.2.38	Average hourly O_3 maxima for 144 episode days in southern Ontario.	3-85
3.2.39	Schematic diagram illustrating the main pathways for reactive and non-reactive pollutants/tracers through the atmosphere.	3-87

LIST OF FIGURES (continued)

Figure#		Page#
3.2.40	Apportionment of a) sulphate, and b) nitrate wet deposition between Canadian and USA sources at Longwoods and Railton using 1981-1983 monitoring data classified by air trajectory origin.	3-92
3.2.41	The percentage contributions of the emissions in each region to the ambient air episodes observed at Montmorency, Quebec during the period 1980-1984 for a) SO_4^{2-} and b) NO_3^- . Episodes are defined as days in the top 5% of observed concentrations.	3-96
3.2.42	Trends in SO_2 emissions and precipitation excess sulphate concentrations in eastern North America. The different shaded areas on the map show the percent difference between 1980-82 and 1985-87 average concentration fields. The box directly underneath the map shows the eastern North American SO_2 emission changes normalized to 1980. The outer boxes show the year to year observations at a number of sites normalized to 1980.	3-109
3.2.43	Trends in NO_x emissions and precipitation excess sulphate concentrations in eastern North America. The different shaded areas on the map show the percent difference between 1980-82 and 1985-87 average concentration fields. The box directly underneath the map shows the eastern North American NO_x emission changes normalized to 1980. The outer boxes show the year to year observations at a number of sites normalized to 1980.	3-110
Section 3.3		
3.3.1	Model trajectories starting from Sudbury, Ontario in January 1978.	3-127
3.3.2	Model trajectories starting from Sudbury, Ontario in July 1978.	3-128
3.3.3	North American emissions source regions.	3-130
3.3.4	Aggregated emissions source regions in North America.	3-131
3.3.5	The mean percentage of annual 1980 sulphur wet deposition observed and predicted for each season at 30 ISDME sites.	3-144

LIST OF FIGURES (continued)

Figure#		Page#
3.3.6	Total SO ₂ emission rate (metric tonnes per day) during springtime within each ADOM (127 x 127 km ²) grid.	3-151
3.3.7	The total precipitation amount (mm) during OSCAR II, III and IV (10-29 April 1981) plotted on the ADOM domain.	3-153
3.3.8	(a) OSCAR II SO ₄ ⁼ concentrations in precipitation (new scavenging module).	3-154
	(b) OSCAR IV SO ₄ ⁼ concentrations in precipitation (new scavenging module).	3-154
3.3.9	(a) OSCAR II nitrate concentrations in precipitation (new scavenging module).	3-155
	(b) OSCAR IV nitrate concentrations in precipitation (new scavenging module).	3-155
3.3.10	16-day averaged (April 10-25, 1981) wet flux (μg m ⁻² h ⁻¹) of SO ₄ ⁼ predicted by the Lagrangian model. This is given on the ADOM grid domain. A background deposition of 67 μg m ⁻² h ⁻¹ is added to the model output to account for non-anthropogenic and out-of-domain contributions.	3-156
3.3.11	16-day averaged (April 10-25, 1981) wet flux (μg m ⁻² h ⁻¹) of SO ₄ ⁼ predicted by ADOM.	3-157
3.3.12	20-day averaged (April 10-29, 1981) ADOM predicted percentage reduction in SO ₄ ⁼ precipitation concentration as a result of a 50% across-the-domain reduction of SO ₂ and SO ₄ ⁼ emissions.	3-158
3.3.13	Primary ground-level ANATEX sampling network. Exact station locations is at the centre of each site number.	3-160
3.3.14	The observed and predicted PDCH pattern for the first 44 days of the ANATEX run. The contours are 0.5, 1, 2, 5, 10, 20, 50, 100, fl/l with the outermost contour being 0.5.	3-161
3.3.15	The observed and predicted PDCH pattern for the first three days of the first release of the ANATEX run. The observed contours start at a fl/l on the outside and increase in steps of 4 fl/l. The predicted contours start at 1 fl/l on the outside and increase in steps of 10 fl/l.	3-162

LIST OF FIGURES (continued)

Figure#		Page#
3.3.16	Ozone concentrations, June 9-17, 1983, southern Ontario and northern Ohio.	3-164
3.3.17	Event averaged $\text{SO}_4^{=}$ concentrations in precipitation.	3-166
3.3.18	Reduction (%) in wet sulphur deposition in response to 50% reduction in grid SO_x emissions.	3-167
3.3.19	Eulerian Model Evaluation Field Study (EMEFS) monitoring sites and regions.	3-168
3.3.20	Model predictions vs. observed ground level concentrations of SO_2 ($\mu\text{g}/\text{m}^3$) during July 28 - August 8 and August 25 - September 5, 1988.	3-171
3.3.21	Time series plot of averaged concentrations of observed and predicted SO_2 ($\mu\text{g}/\text{m}^3$) for Regions 3 and 5 during Periods 1 and 2.	3-172
3.3.22	Model predictions vs. observed ground level concentrations of $\text{SO}_4^{=}$ ($\mu\text{g}/\text{m}^3$) during July 28 - August 8, and August 25 - September 5, 1988.	3-173
3.3.23	Time series plots of averaged concentrations of observed and predicted $\text{SO}_4^{=}$ ($\mu\text{g}/\text{m}^3$) for Regions 3 and 6 during Periods 1 and 2.	3-175
3.3.24	Model predictions vs. observed ground level concentrations of total sulphur ($\mu\text{g}/\text{m}^3$) during July 28 - August 8 and August 25 - September 5, 1988.	3-176
3.3.25	Model predictions vs. observed concentrations in precipitation $\text{SO}_4^{=}$ (mg/l) during July 28 - August 8 and August 25 - September 5, 1988.	3-177
3.3.26	Model predictions vs. observed concentrations NO_2 ($\mu\text{g}/\text{m}^3$) during July 28 - August 8 and August 25 - September 5, 1988.	3-179
3.3.27	Time series plots of averaged concentrations of observed and predicted NO_2 ($\mu\text{g}/\text{m}^3$) for Regions 3 and 6 during Periods 1 and 2.	3-180
3.3.28	Model predictions vs. observed ground level concentrations of total nitrate ($\mu\text{g}/\text{m}^3$) during July 28 - August 8 and August 25 - September 5, 1988.	3-181

LIST OF FIGURES (continued)

Figure#		Page#
3.3.29	Time series plots of averaged concentrations of observed and predicted nitrate concentration ($\mu\text{g}/\text{m}^3$) for Regions 3 and 5 during Periods 1 and 2.	3-182
3.3.30	Model predictions vs. observed concentrations in precipitation of total nitrate (mg/l) during July 28 - August 8 and August 25 - September 5, 1988.	3-184
3.3.31	Model predictions (dashes) vs. observed ozone concentrations (x's) at selected sites and model grid points in Ontario (16,18), Michigan (13,13) and Maine (23,19) for Period 1 (July 28 - August 8) and Period 2 (August 25 - September 6).	3-185
3.3.32	Ontario Ministry of the Environment Lagrangian Model Predictions for the EMEFS period - SO_2 ($\mu\text{g}/\text{m}^3$).	3-190
3.3.33	Ontario Ministry of the Environment Lagrangian Model predictions for the EMEFS period - $\text{SO}_4^{=}$ ($\mu\text{g}/\text{m}^3$).	3-191
3.3.34	Ontario Ministry of the Environment Lagrangian Model predictions for the EMEFS period - $\text{SO}_4^{=}$ in precipitation (mg/l).	3-192

SUMMARY

Various approaches to evaluating source-receptor relationships (i.e. the quantitative relationships between current and future emissions, and receptor exposure) have been examined in this report, in the context of the North American acid precipitation problem. Particular emphasis has been placed on Canadian studies. Air and precipitation monitoring programs have been in place in Canada since the early 1980's, and have by now yielded a substantial, high-quality data set. The development and evaluation of various acid rain mathematical models, including Lagrangian and the more advanced Eulerian Acid Deposition and Oxidants Model (ADOM), has also spanned this time period.

The variation in acid gas emissions in eastern North America has been examined, and some significant changes that have occurred since 1980 in Canada and the adjoining States have been identified. The response of deposition spatial patterns, as well as air and precipitation concentrations in eastern Canada to these changes has been examined.

In spite of the noise introduced by meteorological variability, data analysis has shown the temporal and spatial variations in air and precipitation concentrations of sulphate to be consistent with the changes in emissions in eastern North America. Other types of data analyses - using tracers, and trajectory analyses of various types - clearly show the impact of acid gas emission regions on downwind receptor areas. However, with such analyses it is usually not possible to quantify the contribution of a specific source area to the acid deposition at a particular receptor area.

The present status of our understanding about the capability of the available models to predict source-receptor relationships has been examined in this report. Unfortunately, the full results of a major field study to evaluate a number of Eulerian models for acid gas transport, transformation and deposition - the Eulerian Model Evaluation Field Study (EMEFS) - are not yet available, although the findings of a preliminary Eulerian model evaluation have been included. Nevertheless it is possible to come to some conclusions about the severity of the much-disputed non-linearity problem when various emission scenarios are being evaluated, and the applicability of the relatively simple linear models which were used in the mid-1980's to formulate Canada's acid gas emission control policy.

We address below two questions regarding source-receptor relationships:

1. How well does present knowledge enable us to establish current and future source-receptor relationships?

There are various approaches currently available for evaluating source-receptor relationships, based both on the analysis of atmospheric measurements and the predictions of long-range transport mathematical models.

Qualitatively, on a continental scale, acidic gas emission spatial patterns are clearly related to measured air concentration and wet deposition patterns. While it is not possible to determine specific source-receptor relationships from this association, one can at least reasonably deduce that, on the large spatial scale, changes in eastern North American sulphur emissions have resulted in changes in air and precipitation chemistry as well as deposition over the area. The shrinkage in the total area in eastern Canada receiving sulphate wet deposition loadings greater than 20 kg per hectare per year between 1980 and 1987, and the concurrent decrease of airborne sulphur dioxide, is no doubt partly due to general decreases of SO₂ emissions in Canada and adjoining states. There are also a number of other contributing factors, most notably meteorological influence. In the same area, there is no clear trend in NO_x emissions over the same period, and no large scale change in precipitation nitrate patterns is evident in the data.

Temporal trend analyses using air and precipitation chemistry data from specific sites also yield interesting information when interpreted in the light of regional emission changes. The interpretation is complicated by noise introduced by meteorological variability although some of this can be removed by applying various statistical techniques. The temporal variations in observations are consistent with the broad-scale changes in spatial emission patterns. Thus, at a number of locations in eastern Canada, where aerometric measurements have been made since the late 1970's or early 1980's, statistically significant decreases in atmospheric SO₂, the predominant atmospheric sulphur compound in air, were observed. These locations are in, or downwind of, regions in which SO₂ emissions have decreased by more than 10%. While the statistical interpretation of the changes of sulphate and nitrate in precipitation is more difficult due to the added uncertainty caused by pollutant scavenging processes, results are still consistent with the variations in upwind SO₂ and NO_x emissions (See, for example, Figures 3.S.1 and 3.S.2).

Various types of air mass trajectory analysis have been successfully applied to a number of case studies, including analysis of episodes of sulphate and nitrate wet deposition and of ozone in Canada. They clearly implicate emission areas to the south as sources of the episodic acid or ozone levels. However, stratification of the measured concentrations by trajectory can only point to all the sources within a given sector, and does not enable discrimination to be made between local and distant sources within the sector. If empirical decay factors for pollutant concentration along the trajectory path are included, then discrimination between the impact of various source regions is possible. In this way quantitative semi-empirical source-receptor relationships have been estimated, showing the contribution of various emission areas to acidic deposition at Montmorency Park in Quebec, for example. The results are in reasonable agreement with the predictions of a number of linear long-range transport models.

Receptor modelling, using the fact that atmospheric aerosols contain many trace elements that have known sources from combustion, smelting or natural processes, has been used to distinguish between broad source regions contributing to observed atmospheric acidity

at a monitoring site. Using this approach, the impact of midwestern sources on receptors at Rhode Island and Vermont has been demonstrated to be in reasonable agreement with the predictions of simple long-range transport models. Furthermore, aerosol chemistry studies have shown that indium, arsenic and the isotopic composition of lead are useful tracers of pollution associated with acidic gas emissions particularly from northern smelters, coal combustion products and automobile exhaust from Canada or the US.

Mathematical long-range transport models currently provide our best means of establishing source-receptor relationships quantitatively. Although there is no practical direct way of determining the uncertainty in source-receptor relationships predicted by such models, one can gain confidence in them through their ability to predict observed temporal and spatial patterns of deposition and air concentration. In this regard, the simple linear models which have been used to estimate source-receptor relationships for the Canadian control program perform reasonably well. It should be emphasized that in situations of reduced emissions such as are likely to occur in the future under current control programs, there are no observations with which to check the models. Therefore, the best that can be done for future scenarios is to rely on the predictions of chemical transport models that embody the most realistic simulations of processes affecting pollution enroute from source to sink.

2. From the viewpoint of atmospheric science, what, if any, adjustments are required for the Canadian acid gas emission control program for 1994?

Recognizing that the Canadian emission control program is based on the assumption of a linear relationship between source emission and downwind deposition (as simulated in simple long-range transport models), and that it assumes that a 50% reduction in both Canada and the U.S. will reduce sulphur wet deposition below a target annual loading of 20 kg/ha, the following conclusions are drawn.

Simple linear long-range transport models, such as those used in the mid-1980's to formulate Canada's acid gas emission control policy, are probably overpredicting the extent of deposition reductions after controls are imposed. However, the results obtained to date with Eulerian models indicate that in spring a reduction of sulphur dioxide emissions by 50% from the 1980 levels will reduce the wet deposition of sulphur in eastern North America by 30-40%. This is a degree of non-linearity that, at this time, cannot be deemed significant considering model and observational uncertainty. In winter, the few available modelling simulations suggest somewhat more pronounced non-linear effects. On the other hand, the summer period, for which no modelling assessments have so far been carried out, would be expected to be more linear, because the level of oxidants, which brings about SO₂ oxidation, is greatest during this season. Moreover, it should be noted that the above statements apply only to wet deposition. The total (wet plus dry) deposition of sulphur responds to emission changes in an even more linear fashion than the wet deposition alone.

The full results of a major field study now underway to evaluate a number of more sophisticated Eulerian models, which attempt to incorporate our best current understanding of atmospheric processes leading to acid deposition, are not yet available. Only a preliminary and partial evaluation of the Eulerian models ADOM (Acid Deposition and Oxidants Model) and RADM (Regional Acid Deposition Model) has so far been carried out, and so conclusive statements about whether the simple or complex models better reproduce observations are not yet possible.

Given the above, it is concluded that the less scientifically advanced linear models can be used for regulatory purposes to provide source-receptor relationships for total sulphur deposition, especially on a seasonal or annual basis. In this regard, the atmospheric modelling results that provided an input to the planning of the Canadian acid gas emission control program can be considered to be still valid.

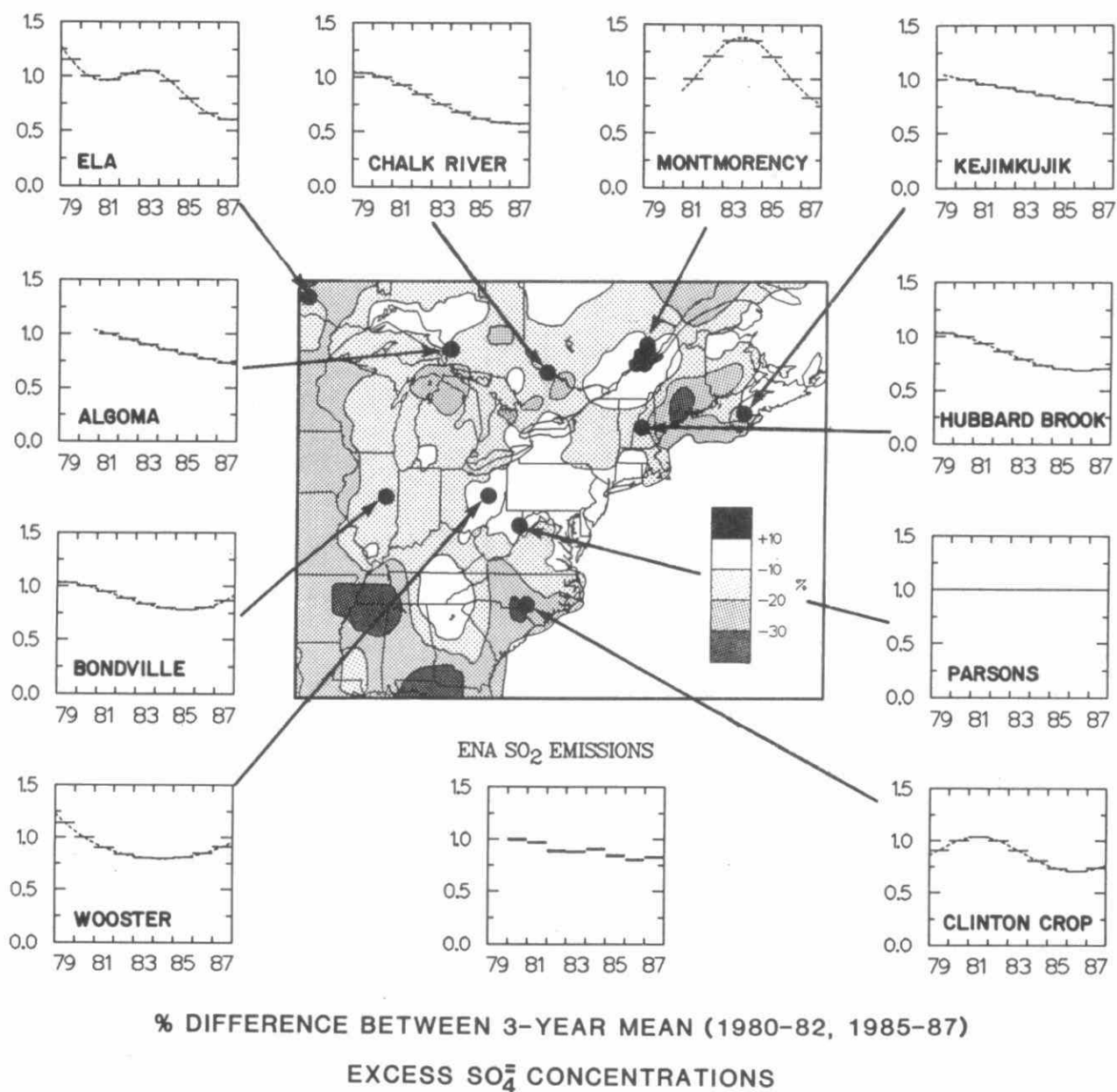
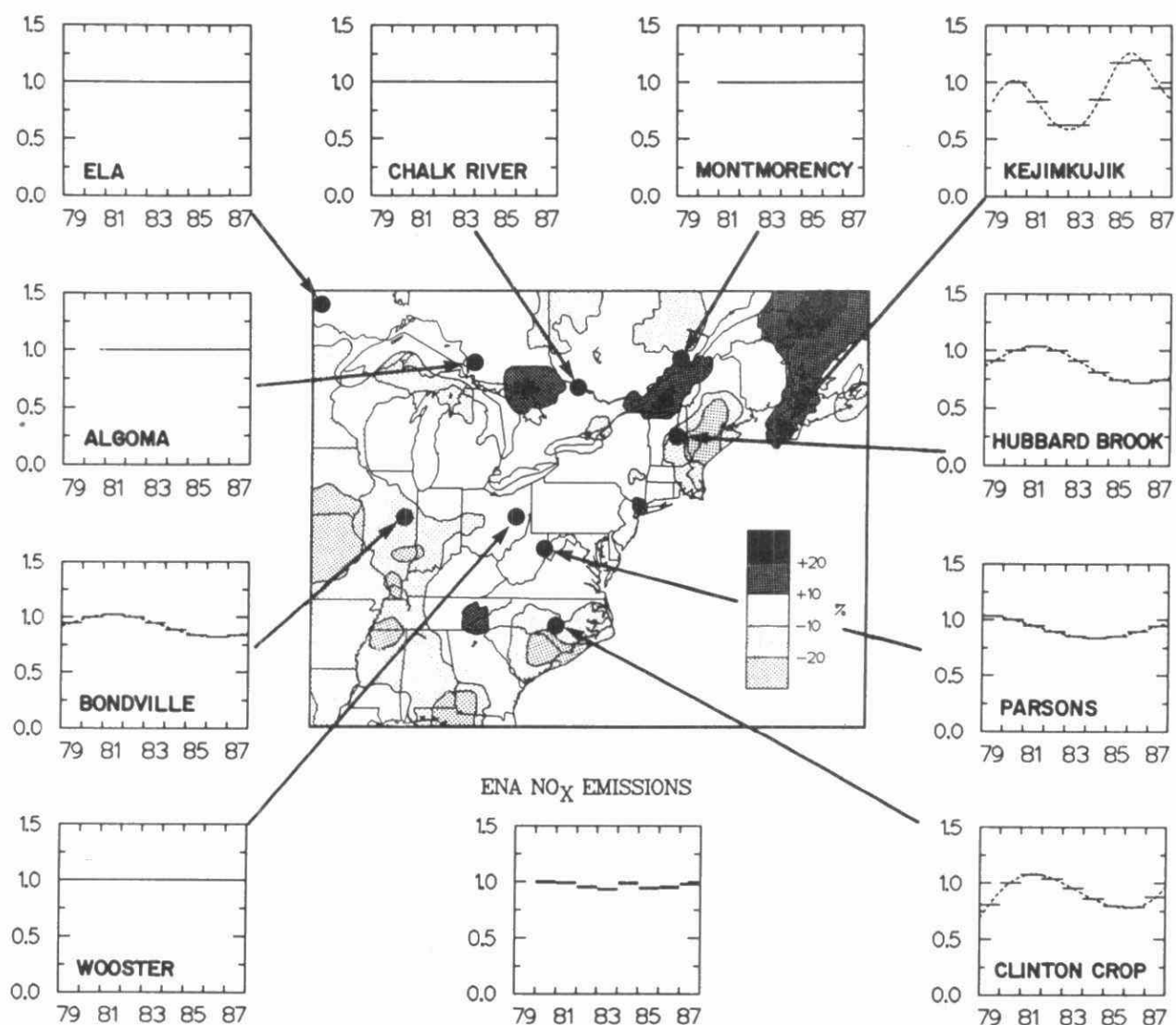


Fig. 3.S.1 Trends in SO₂ emissions and precipitation excess sulphate concentrations in eastern North America. The different shaded areas on the map show the present difference between 1980-82 and 1985-87 average concentration fields. The box directly underneath the map shows the eastern North American SO₂ emission changes normalized to 1980. The outer boxes show the year to year observations at a number of specific sites normalized to 1980.



% DIFFERENCE BETWEEN 3-YEAR MEAN (1980-82, 1985-87) NO_3 CONCENTRATIONS

Fig. 3.S.2

Trends in NO_x emissions and precipitation excess sulphate concentrations in eastern North America. The different shaded areas on the map show the percent difference between 1980-82 and 1985-87 average concentration fields. The box directly underneath the map shows the eastern North American NO_x emission changes normalized to 1980. The outer boxes show the year to year observations at a number of specific sites normalized to 1980.

3.1 INTRODUCTION

The question of source - receptor relationships - i.e., the quantitative relationship between emissions (current and future) and receptor exposure - has been one of the central issues in the acid rain control debate. It does not matter if targeted or blanket emission control strategies are under consideration: even if a blanket policy were enacted, knowing source-receptor relationships would allow one to predict how much a receptor's exposure to acidic deposition would be reduced (see, for example, Summers, 1984).

The complexity of the problem poses a dilemma for policy makers. There are strong arguments in favour of mitigative action. Damage due to acid rain is now well documented and generally accepted. The impact of anthropogenic sources has been clearly demonstrated. Control technology exists to significantly reduce acid gas emissions from those sources. On the other hand, according to many scientists our current scientific understanding of the phenomenon is incomplete and the costs of control are expected to amount to billions of dollars (e.g. see Hidy, 1984; Crocker and Regens, 1985), and there has to be an assurance that any control measures that are implemented will, in fact, result in significant environmental benefits. Our understanding of source-receptor relationships is one of the key links in the decision-making process.

In Canada in 1984, the eastern provinces and the federal government decided that enough was known to take unilateral action and reduce Canadian sulphur dioxide emissions to a ceiling of 2.3 million tonnes by 1994 (a 50% reduction from the 1980 base case year), even in the absence of control on the major emission source areas south of the border. On February 5, 1985 the provincial and federal governments agreed on a series of steps to achieve the first 1.9 million tonnes of this reduction, and committed to determining the allocations of any further reductions in sufficient time to achieve the 1994 objective.

In arriving at the emission reductions allocated to each province, currently available long-range transport models were used, as described by Young (1988) and Young and Shaw (1986). It was felt that our scientific understanding of source-receptor relationships was sufficiently sound to form the basis for control action. Subsequently, Ontario and Quebec even went beyond the commitment made at the federal/provincial meetings, with their own acid rain reduction programs, announced in 1985. According to Countdown Acid Rain, Ontario's sulphur dioxide emissions are to be reduced from the 1980 base case level of 2.19 million tonnes to 0.885 million tonnes by 1994. Quebec has committed itself to reduce sulphur dioxide emissions further, by additional reductions which will be obtained from the Noranda smelter by 1995, bringing Quebec emissions from 1.09 million tonnes in 1980 to less than 0.550 million tonnes in 1995. The emissions of nitrogen oxides are also to be controlled substantially.

By contrast, until recently there has been a reluctance on the part of the U.S. administration to act until a number of key scientific questions are resolved, hopefully by

the end of the National Acid Precipitation Assessment Program (NAPAP) in 1990. As far as source-receptor relationships are concerned, the key question is that of linearity: will there be a proportional relationship between changes in emission at a controlled source area and changes in deposition due to that source at a sensitive receptor area?

As a consequence, one of the major developments in acid rain science in recent years has been the investment of millions of dollars in Canada and the United States into the construction of advanced Eulerian models (e.g. the Canadian Acid Deposition and Oxidants Model, ADOM, and NAPAP's Regional Acid Deposition Model, RADM - see Venkatram et al., 1988; Chang et al., 1987). These attempts to incorporate (within the limitations of present day computers) our best current understanding of atmospheric processes leading to acid deposition and presumably will, after validation with field data, constitute our best tools for determining source-receptor relationships under various emission scenarios, for both acidic species and also other long-range transported pollutants, such as oxidants. In addition to mathematical modelling, there are a number of other scientific approaches available for estimating (on a variety of space and time scales) source-receptor relationships. The scientific journals and conferences in recent years have been replete with papers on this subject.

It is the purpose of the present report to review our state of knowledge on source-receptor relationships, and the implications regarding emission controls. The main emphasis is on sulphur and nitrogen oxides.

The report deals with the following subjects:

1. Insight into source-receptor relationships gained from atmospheric measurements.
2. Source-receptor relationships from long-range transport mathematical models (both simple and complex).

Seven appendices are also included. These contain maps of precipitation chemistry and wet deposition discussed in this report, and in the companion aquatic and terrestrial effects reports; trend analyses of data from various Canadian networks; and future deposition projections based on mathematical modelling.

In writing this report, the authors were asked to keep in mind two important questions:

1. How well does present knowledge enable us to establish current and future source-receptor relationships?
2. From the viewpoint of atmospheric science, what, if any, adjustments are required for the Canadian acid gas emission control program for 1994 and beyond?

3.2 INSIGHT INTO SOURCE-RECEPTOR RELATIONSHIPS OF ACIDS AND OZONE GAINED FROM PATTERN-ASSOCIATIONS, TRENDS AND RELATED STUDIES

3.2.1 INTRODUCTION

It is well recognized that acidic deposition (caused by nitrogen and sulphur oxides released to the atmosphere) when falling on acid sensitive soils is causing problems in selected regions around the globe (Fig. 3.2.1). Because the average lifetime of these acids in the atmosphere is on the order of a few days to at most a week (e.g. Summers and Fricke, 1989), the nature of acid rain is indeed a regional problem. This is best illustrated by the spatial pattern of acidic sulphur in precipitation in Eastern North America (Figure 3.2.2) and of the acidity of precipitation on this globe (Fig. 3.2.3).

In this chapter, we will focus on measurements of regional spatial distributions and temporal trends of acidic compounds in the atmosphere and in the precipitation of North America, as well as atmospheric tracers. Particular emphasis will be placed on what these tell us about the connection between pollution sources and receptors in the 1980's. At our disposal are a multitude of measurements made at over 100 regional-scale sites in Canada between 1980 and 1986 in both air and precipitation (more precipitation than air measurements available). In Figure 3.2.4, the location of the monitoring sites in Canada are shown. The combined federal/provincial data set is archived in The National Atmospheric Chemistry Data Base (NAtChem) at Environment Canada.

The Canadian measurement program is unique in North America in that it has monitored concentrations of acids in air as well as in precipitation during this period. Thus trends in regional air quality can be discussed. The United States has only recently mounted a regional air monitoring network. No trends data are available.

3.2.2 EMISSIONS AND ATMOSPHERIC OBSERVATIONS

As a qualitative assessment of the link between sources and receptors, it is useful to compare the spatial distribution of acidic emissions to the distribution of precipitation composition or deposition averaged over a year or more.

3.2.2.a. EMISSIONS

SO₂ and NO_x emissions in North America for the base years 1980 and 1985, and the emission trends between 1980 and 1985 have been compiled and developed from a number of source documents and reports. For the United States, emissions for 1980 are based on the NAPAP (National Acid Precipitation Assessment Program) Emission Inventory Versions 5.0 and 5.2 and for 1985, on the 1985 NAPAP inventory as reported by Zimmerman et al. (1988). United States trend data for the years 1981-1984 are based on the information in the Annual Report (NAPAP, 1985) and the National Air Quality and Emissions Trends Report, 1986 (EPA, 1988). For Canada, the data were compiled using

provincially and federally developed emission data to cover the period from 1980 to 1985.

Between 1980 and 1985, overall SO₂ emissions in North America declined about 16%. The estimated SO₂ emission in 1985 was 24.6 million tonnes, down from 29.1 million tonnes in 1980. In the United States, SO₂ emissions decreased about 15% (24.5 to 20.9 million tonnes) and in Canada, about 20% (4.6 to 3.7 million tonnes).

Using the North American source regions previously defined for the 1980 base year (MOI, 1982) the spatial patterns of SO₂ for 1980 and 1985 were compiled. These are depicted in Figs. 3.2.5 and 3.2.6, along with the percentage changes in emissions from 1980 to 1985 (Fig. 3.2.7). In general, SO₂ emissions declined over most areas of North America between 1980 and 1985. Significant variations occurred on the regional scale. For example, emission decreases in the range 35-40% occurred in the Pacific states, as well as in Florida and Michigan. Over the Ohio Valley region, emission decreases ranged from about 5% in the north to about 15-20% in the south. In Canada, emissions decreased about 15-20% over the high density emission areas of Ontario and 15-60% over similar areas of Quebec. The yearly emission trends between 1980 and 1985 are shown in Tables 3.2.1 and 3.2.2. For the United States, overall SO₂ emissions have declined steadily in the intervening years. In Canada, SO₂ emissions reached a minimum in 1982 and have increased slightly thereafter.

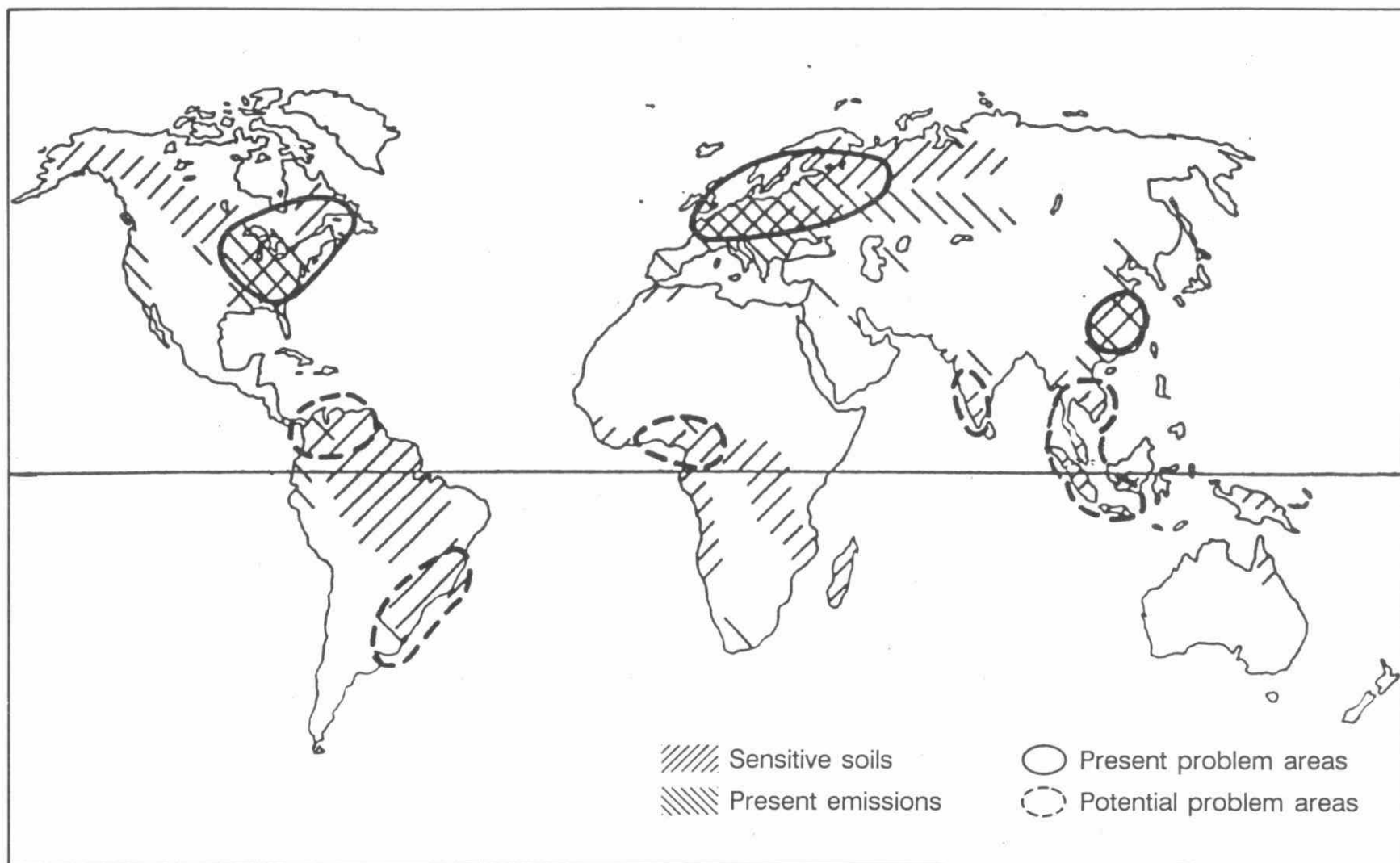


Fig. 3.2.1 Schematic map showing regions that currently have acidification problems, and regions where, based on soil sensitivity, expected future emissions and population density, acidification might become severe in the future. (from Rhode and Herrera, 1988)

6-YEAR (1982-87) MEAN XSO_4^- CONCENTRATION
IN PRECIPITATION (mg/l)

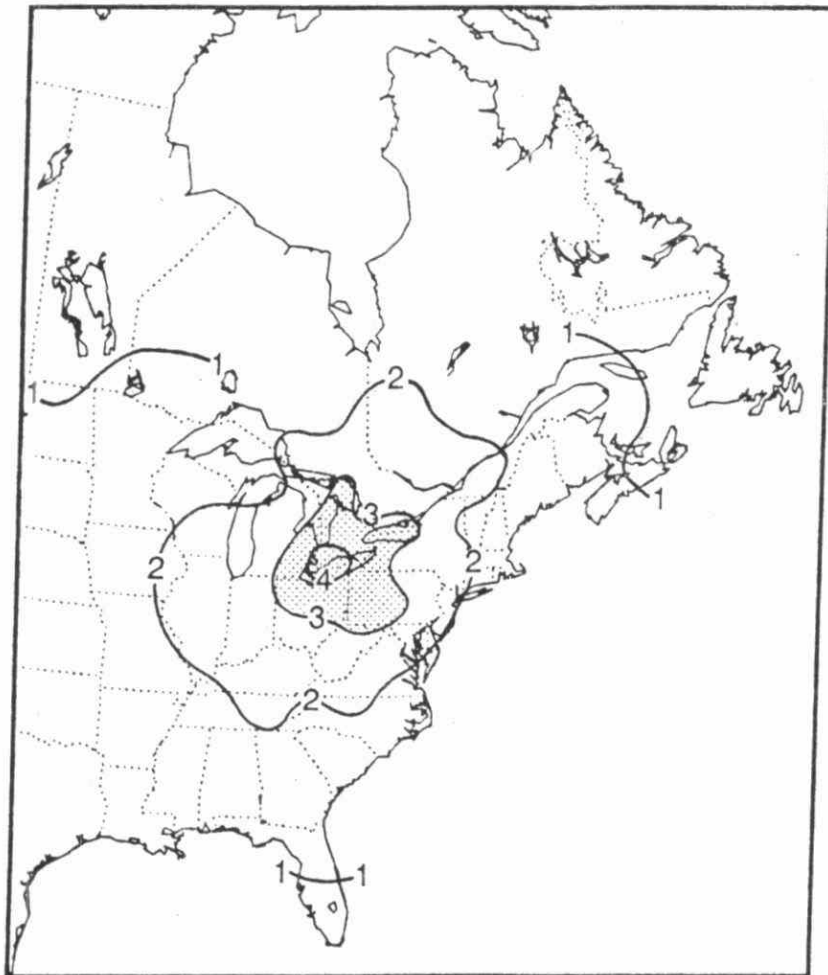


Fig. 3.2.2 Eastern North American pattern of non-marine SO_4^- precipitation-weighted-mean concentration (1982-1987).

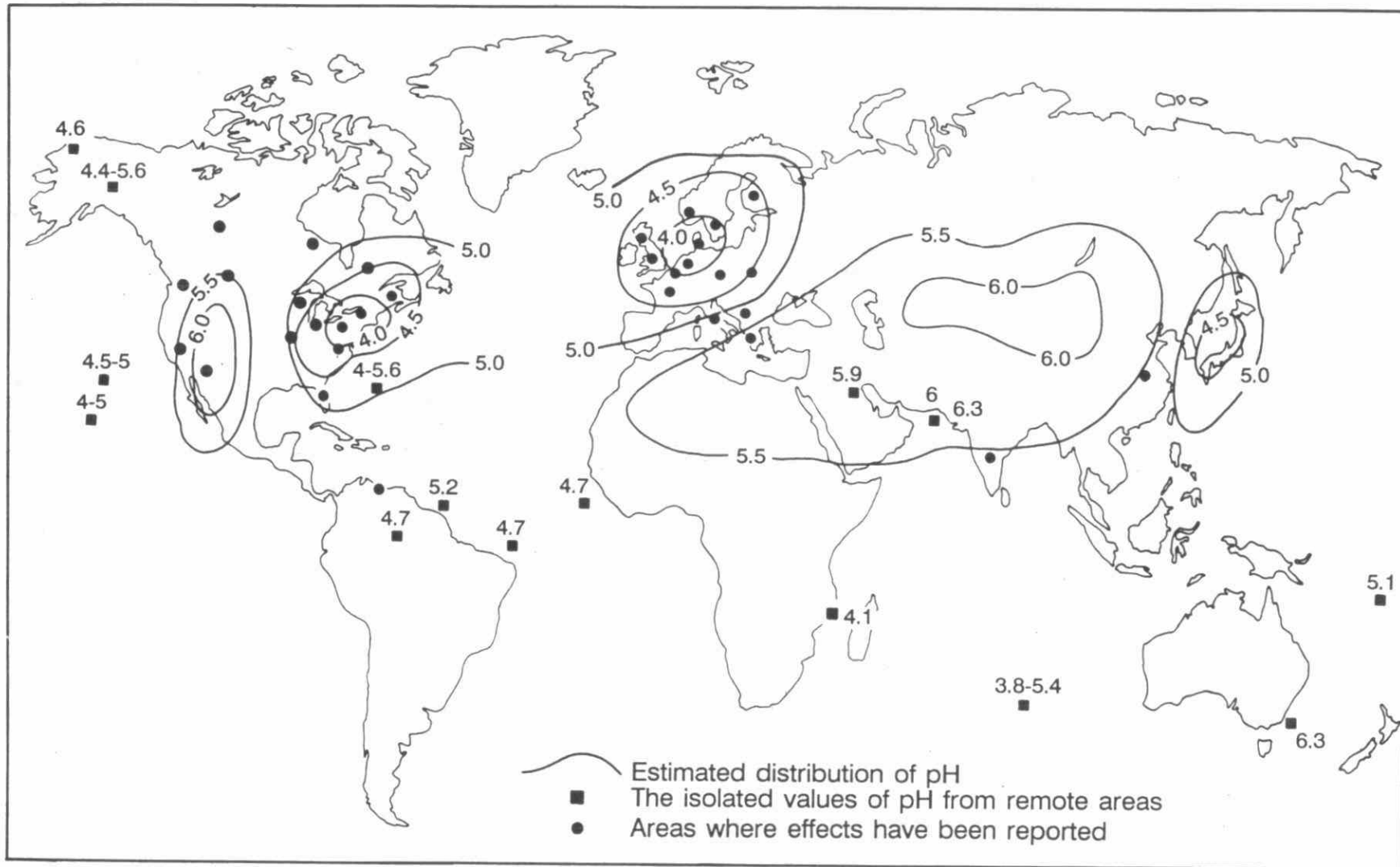


Fig. 3.2.3 The global nature of acid rain in the early 1980s.

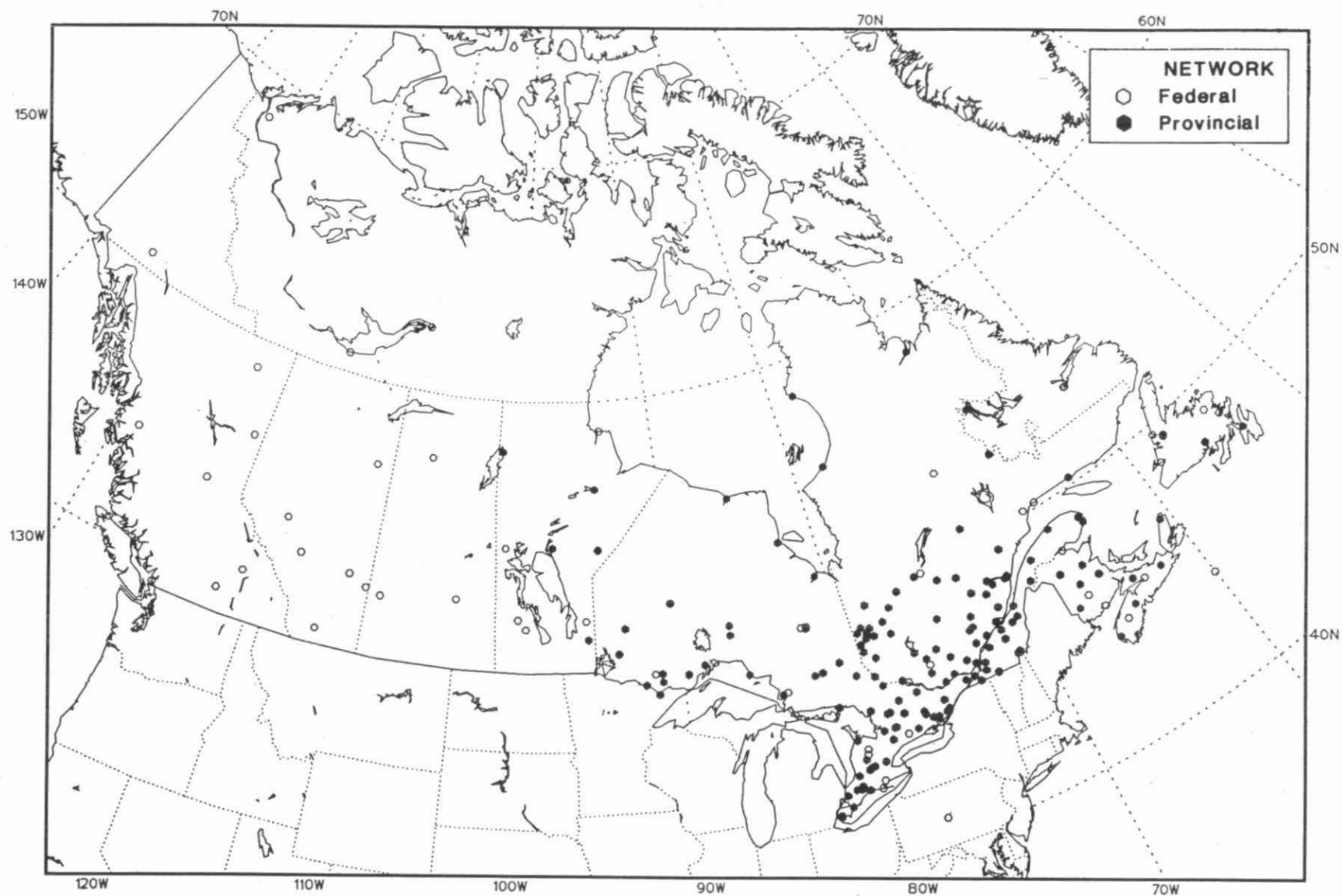


Fig. 3.2.4 NATCHEM 1980-87 Precipitation chemistry stations in the NATCHEM DATA BASE.

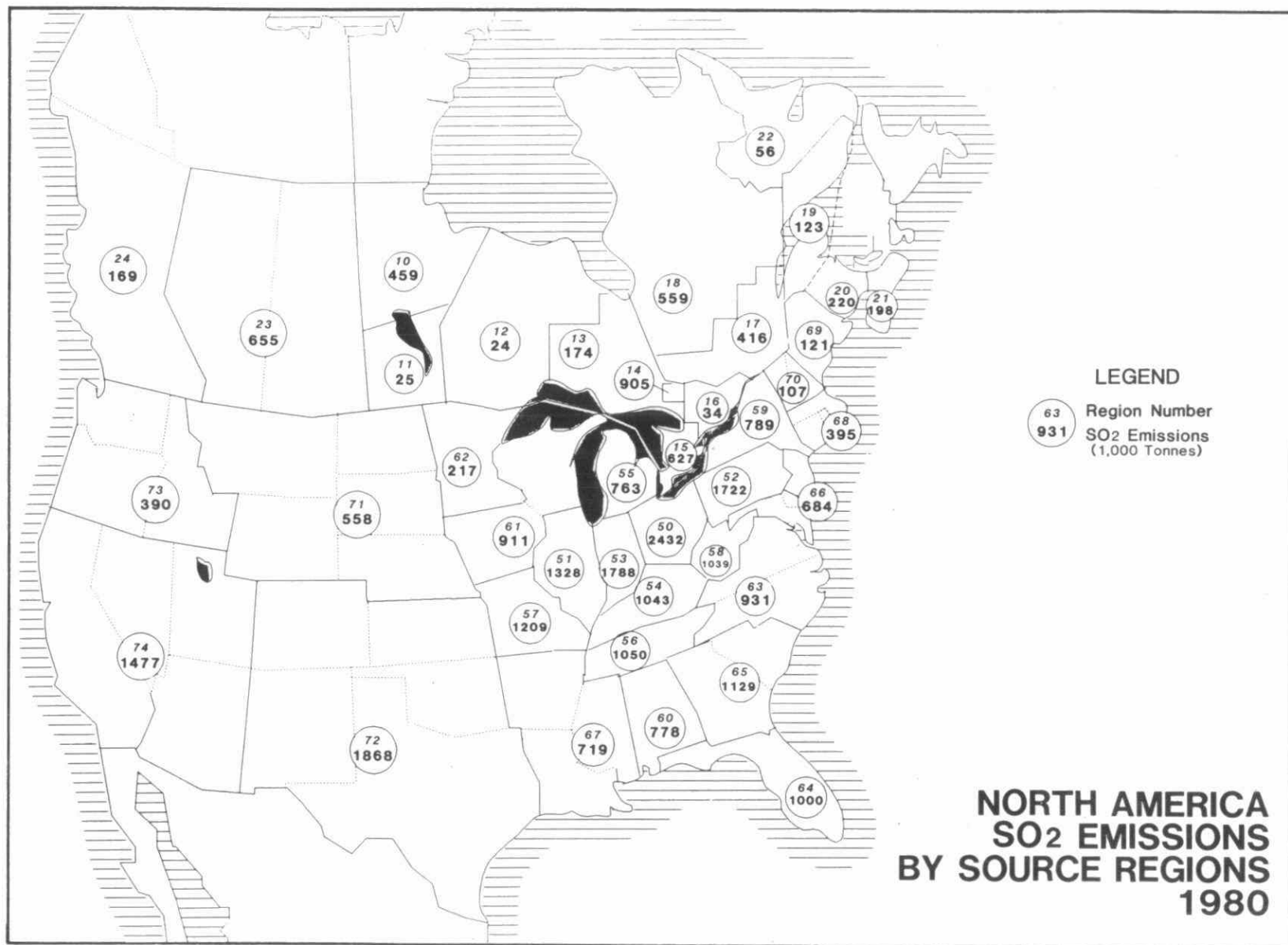


Fig. 3.2.5 North America SO_x Emissions by Source Regions: Year - 1980

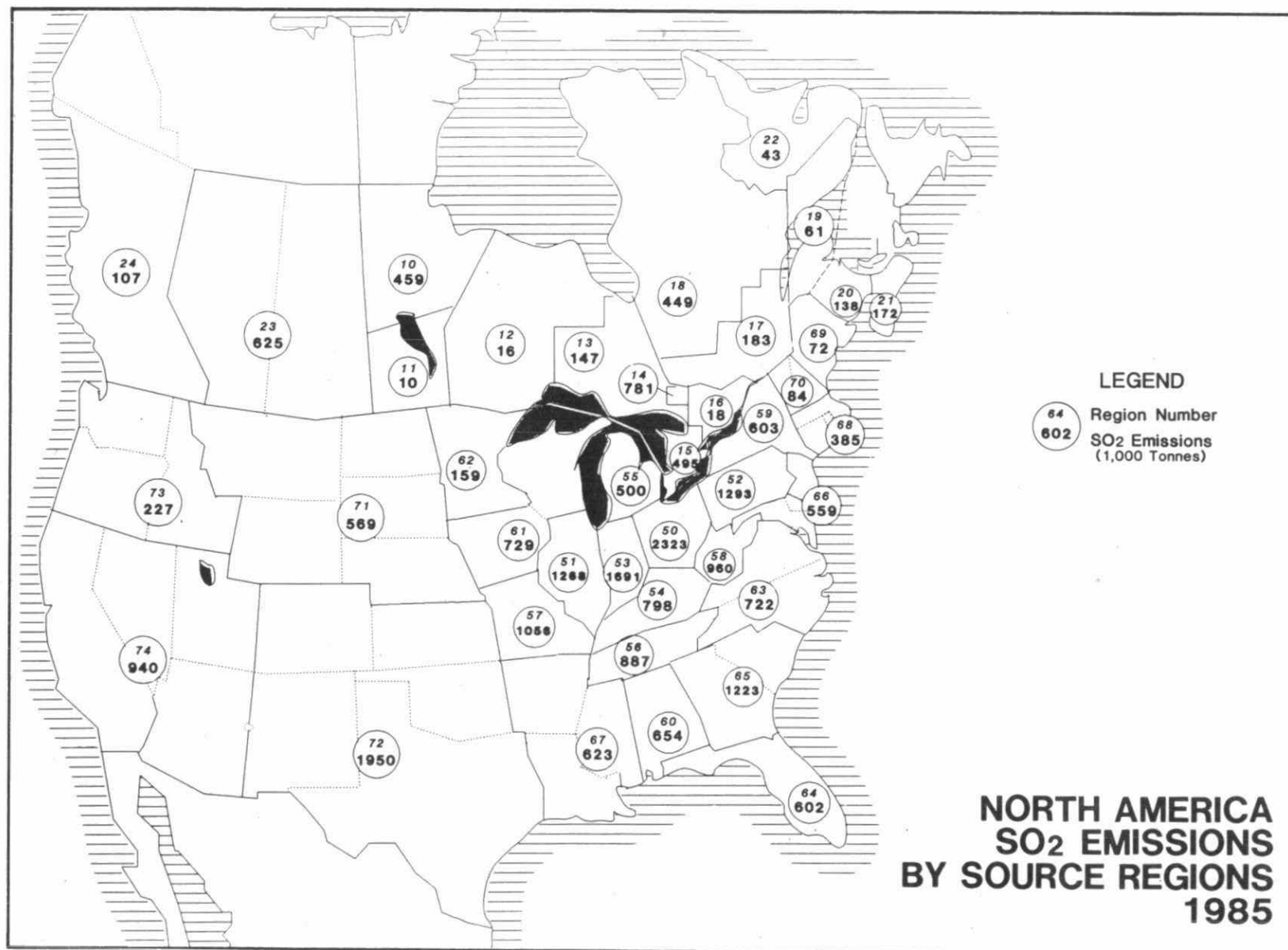


Fig. 3.2.6 North America SO_x Emissions by Source Regions: Year - 1985.

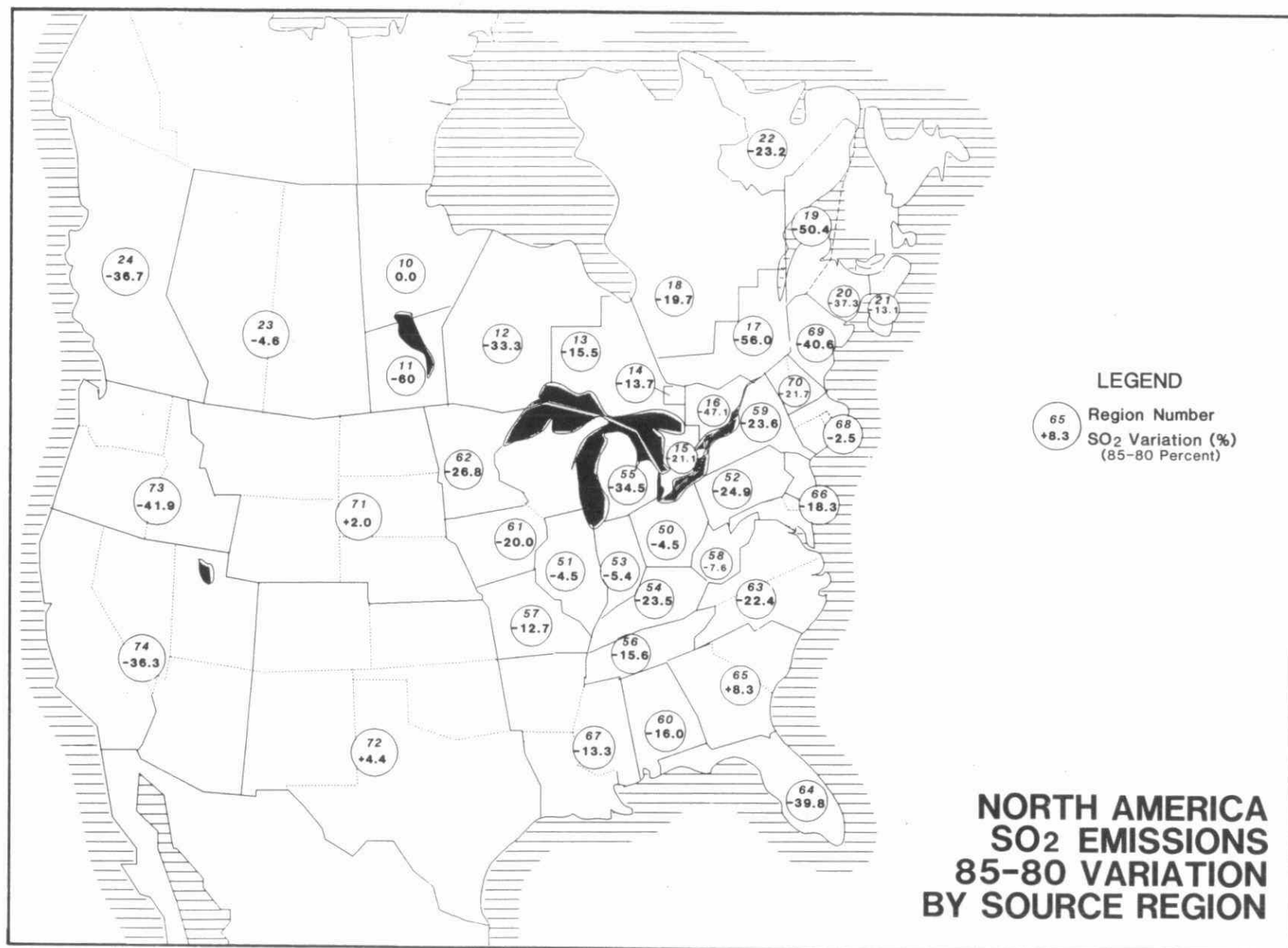


Fig. 3.2.7 North America SO_x Emissions 85-80 Variation by Source Region.

Table 3.2.1

**1980-1985 SO_x emissions in Canada
(by source regions - 1000 tonnes/year)**

REGION - PROVINCE		1980	1981	1982	1983	1984	1985	(85-80)%
10	N.MANITOBA	459	399	343	400	456	459	0.0
11	S.MANITOBA	25	22	19	9	10	10	-60.0
	sub-total	484	421	362	409	466	469	-3.1
12	N.W. ONTARIO	24	22	15	14	18	16	-33.3
13	N.E. ONTARIO & S.ALGOMA	174	162	112	128	158	147	-15.5
14	SUDBURY	905	845	586	684	842	781	-13.7
15	S.W. ONTARIO & TORONTO	627	585	407	433	533	495	-21.1
16	S.E. ONTARIO	34	31	22	16	20	18	-47.1
	sub-total	1764	1645	1142	1275	1571	1457	-17.4
17	MONTREAL,ST.LA -RENCE VALLEY	416	346	283	246	202	183	-56.0
18	NORANDA & N.C.	559	516	559	494	489	449	-19.7
19	QUEBEC GASPE BAY	123	140	90	52	46	61	-50.4
	sub-total	1098	1002	932	792	737	693	-36.9
20	NEW BRUNSWICK	220	221	206	172	162	138	-37.3
21	NOVA SCOTIA P.E.I.	193 5	193 3	179 3	175 2	201 2	170 2	-11.9 -60.0
	sub-total	198	196	182	177	203	172	-13.1
22	NEWFOUNDLAND & LABRADOR	56	41	42	36	38	43	-23.2
23	SASKATCHEWAN, ALBERTA	55 600	56 543	82 504	97 513	111 517	86 539	56.4 -10.2
	sub-total	655	599	586	610	628	625	-4.6
24	B.C.,NWT.,& YUKON	169	166	160	155	151	107	-36.7
	TOTAL:CANADA	4644	4291	3612	3625	3625	3704	-20.2

Table 3.2.2
1980-1985 SO_x emissions in the United States
(by source regions - 1000 tonnes/year)

	REGION/STATE	1980	1981	1982	1983	1984	1985	(80-85)%
50	OHIO	2432	2480	2399	2335	2425	2323	-4.5
51	ILLINOIS	1328	1261	1275	1352	1313	1268	-4.5
52	PENNSYLVANIA	1722	1586	1534	1551	1485	1293	-24.9
53	INDIANA	1788	1674	1513	1579	1764	1691	-5.4
54	KENTUCKY	1043	1085	994	818	765	798	-23.5
55	MICHIGAN	763	826	786	783	790	500	-34.5
56	TENNESSEE	1050	1000	758	859	833	887	-15.6
57	MISSOURI	1209	1175	1196	1144	1161	1056	-12.7
58	W.VIRGINIA	1039	1030	967	971	985	960	-7.6
59	NEW YORK	789	800	744	717	748	603	-23.6
60	ALABAMA	778	770	616	695	714	654	-16.0
61	WISCONSIN & IOWA	911	851	796	808	854	729	-20.0
62	MINNESOTA	217	200	178	160	171	159	-26.8
63	VIRGINIA & N. CAROLINA	931	896	842	764	779	722	-22.4
64	FLORIDA	1000	1009	915	843	818	602	-39.8
65	GEORGIA & S. CAROLINA	1129	1221	1132	1104	1198	1223	8.3
66	MARYLAND, DEL, N.J. & D.C.	684	644	622	629	561	559	-18.3
67	ARKANSAS, LOUISIANA & MISSISSIPPI	719	639	624	587	630	623	-13.3
68	MASS., CONN., & R.I.	395	377	386	358	370	385	-2.5
69	MAINE	121	103	102	81	84	72	-40.6
70	VERMONT, NEW HAMPSHIRE	107	92	84	85	101	84	-21.7
71	CENTRAL N.W. STATES*	558	548	532	502	567	569	2.0
72	CENTRAL S.W. STATES**	1868	1872	1823	1822	1938	1950	4.4
73	PACIFIC N.W. STATES***	390	400	366	355	353	227	-41.9
74	PACIFIC S.W. STATES****	1477	1626	1365	1242	1203	940	-36.3
	TOTAL: UNITED STATES	24448	24167	22552	22144	22610	20877	-14.6

* Nebraska, North Dakota, South Dakota, Montana, Wyoming
 ** Oklahoma, Kansas, Colorado, New Mexico, Texas
 *** Washington, Idaho, Oregon
 **** California, Nevada, Utah, Arizona

Table 3.2.3
1980-1985 NO_x emissions in Canada
(by source regions - 1000 tonnes/year)

	REGION/PROVINCE	1980	1981	1982	1983	1984	1985	(85-80)%
10	N.MANITOBA	6	6	5	5	4	5	-13.2
11	S.MANITOBA	74	72	70	75	72	80	8.3
12	N.W. ONTARIO	19	20	20	27	29	29	49.0
13	N.E.ONTARIO & ALGOMA	20	20	20	23	24	24	23.0
14	SUDBURY	11	11	11	10	10	10	-5.4
15	S.W. ONTARIO & TORONTO	440	441	448	421	438	442	0.5
16	S.E. ONTARIO	76	76	77	76	79	80	5.7
17	MONTREAL, ST. LAWRENCE	295	265	242	229	224	209	-29.1
18	NORANDA & N.C. QUEBEC	13	12	11	14	14	13	0.6
19	GASPE BAY	23	21	19	20	19	18	-22.5
20	NEW BRUNSWICK	58	57	52	48	49	46	-20.7
21	NOVA SCOTIA & P.E.I.	93	73	78	79	82	84	-9.6
22	NEWFOUNDLAND & LABRADOR	36	35	34	33	33	35	-1.4
23	SASKATCHEWAN & ALBERTA	555	535	547	542	565	606	9.1
24	BC, NWT & YUKON	242	230	251	255	260	279	15.5
	TOTAL: CANADA	1959	1872	1884	1856	1901	1960	0.1

CANADA SOURCE: - Environment Canada (EC) data (except Ontario from Ontario Ministry of Environment), excluding forest fire emissions.

- Breakdown to regions: 1980 MOI report ratios for 81-82 1985 EC ratios for 83-84.

US SOURCE: - 80: NAPAP versions 5.0 (area) and 5.2(points).

- 81 - 84: NAPAP national trend data (1977-1986), otherwise breakdown by 80 ratios.

- 85: 1985 NAPAP Inventory Report, EPA-600/7-88-022, Nov.88.

Table 3.2.4
1980-1985 NO_x emissions in the United States
(by source regions - 1000 tonnes/year)

	REGION/STATE	1980	1981	1982	1983	1984	1985	85-80%
50	OHIO	1104	1099	1055	1034	1015	924	-16.33
51	ILLINOIS	883	878	844	826	936	881	-0.10
52	PENNSYLVANIA	944	940	903	884	937	869	-8.00
53	INDIANA	714	710	682	668	759	799	12.00
54	KENTUCKY	500	498	478	468	516	472	-5.60
55	MICHIGAN	649	646	620	607	612	597	-7.90
56	TENNESSEE	482	480	461	451	500	464	-3.70
57	MISSOURI	499	496	477	467	517	486	-2.40
58	W.VIRGINIA	418	416	400	392	408	419	0.10
59	NEW YORK	668	665	639	626	726	568	-15.00
60	ALABAMA	442	440	422	414	485	426	-3.60
61	WISCONSIN & IOWA	647	644	618	606	638	557	-13.90
62	MINNESOTA	332	331	318	311	331	323	-2.90
63	VIRGINIA & NORTH CAROLINA	831	827	794	778	822	808	-2.70
64	FLORIDA	646	643	617	605	614	619	-4.20
65	GEORGIA & SOUTH CAROLINA	788	784	753	737	748	771	-2.10
66	MARYLAND, DEL, NJ & DC	808	804	772	756	717	671	-16.90
67	ARKANSAS, LOUISIANA & MISSISSIPPI	1101	1096	1053	1031	1101	1125	2.20
68	MASS., CONN., & R.I.	406	404	388	380	406	395	-2.70
69	MAINE	61	61	58	57	59	61	-0.30
70	VERMONT, NEW HAMPSHIRE	94	93	89	88	95	72	-22.60
71	CENTRAL NW STATES*	705	702	674	660	776	725	2.80
72	CENTRAL SW STATES**	4403	4381	4209	4122	3924	3533	-19.80
73	PACIFIC NW STATES***	556	553	532	521	477	484	-13.00
74	PACIFIC SW STATES****	1720	1712	1644	1611	1509	1609	-6.50
	TOTAL: UNITED STATES	20397	20300	19500	19100	19628	18658	-8.50

* Nebraska, North Dakota, South Dakota, Montana, Wyoming
 ** Oklahoma, Kansas, Colorado, New Mexico, Texas
 *** Washington, Idaho, Oregon
 **** California, Nevada, Utah, Arizona

Table 3.2.5

**Annual Eastern North American¹ SO₂ and NO_x Emissions
for the Period 1980 - 1987²
(Million tonnes per year)**

	1980	1981	1982	1983	1984	1985	1986	1987	change ³
SO ₂ annual total	24.0	23.3	21.3	21.1	21.7	20.2	19.2	19.9	
3-yr average	22.9						19.8		-13.5%
NO _x annual total	14.2	14.1	13.5	13.2	14.0	13.4	13.5	13.9	
3-yr average	13.9						13.6		-2.0%

¹ Defined as the region in the USA east of the Mississippi Valley and in Canada east of the Saskatchewan-Manitoba border.

² Data for 1980-1985 from Tables 3.2.1 through 3.2.4 based on NAPAP reports. Tentative data for 1986,1987 obtained from NEDS in November 1989.

³ Percentage change from the 1980-1982 average to the 1985-1987 average. Significant reductions in SO₂ emissions in Canada between 1980 and 1985 have been in the non-ferrous smelting sector. This decrease can be attributed to process improvements and regulatory initiatives. Emission decreases from fuel combustion in stationary sources, excluding utilities, have been largely due to the regulation of sulphur content, the decline in use of coal for industrial activities, and a shift to cleaner fuels.

In the United States, SO₂ emissions reductions between 1980 and 1985 reflect the use of flue gas desulphurization controls at coal-fired electric generating stations and a reduction in the average sulphur content of fuels. For other stationary sources of fuel combustion, there has been a decrease in coal combustion. Emissions from industrial processes have also declined largely as a result of controls implemented.

In North America, the overall NO_x emissions in 1980 were estimated to be 22.3 million tonnes and in 1985 to be 20.6 million tonnes. This represents a reduction of 8%. Between 1980 and 1985, the United States NO_x emissions decreased about 8.5% (20.4 to 18.7 million tonnes) whereas in Canada, the NO_x emission level was almost constant at 1.96 million tonnes. The spatial patterns of NO_x emissions in 1980 and 1985 are depicted in Figs. 3.2.8 and 3.2.9, along with the percentage changes in emissions from 1980 and 1985 (Fig. 3.2.10). In general, NO_x emission changes were less pronounced than those for SO₂. The maximum decreases in the United States over significant source regions were about 15 to 20%. Typically, NO_x decreases were about 5%. In Canada, NO_x emission levels were nearly constant between 1980 and 1985. The yearly NO_x emission trends between 1980 and 1985 are given in Tables 3.2.3 and 3.2.4. For the United States, overall NO_x emissions have steadily declined except for a slight increase in 1984. In Canada, NO_x emissions have remained relatively constant over the 6 year-period.

In Canada, NO_x emissions changes between 1980 and 1985 were negligible. For the United States, a slight decrease occurred which appears to be related to decreases in highway vehicle emissions.

In Table 3.2.5 annual emissions of SO₂ for eastern North America between 1980 and 1987 are shown. Also included are three year averages for 1980-82 and 1985-87 to be used later.

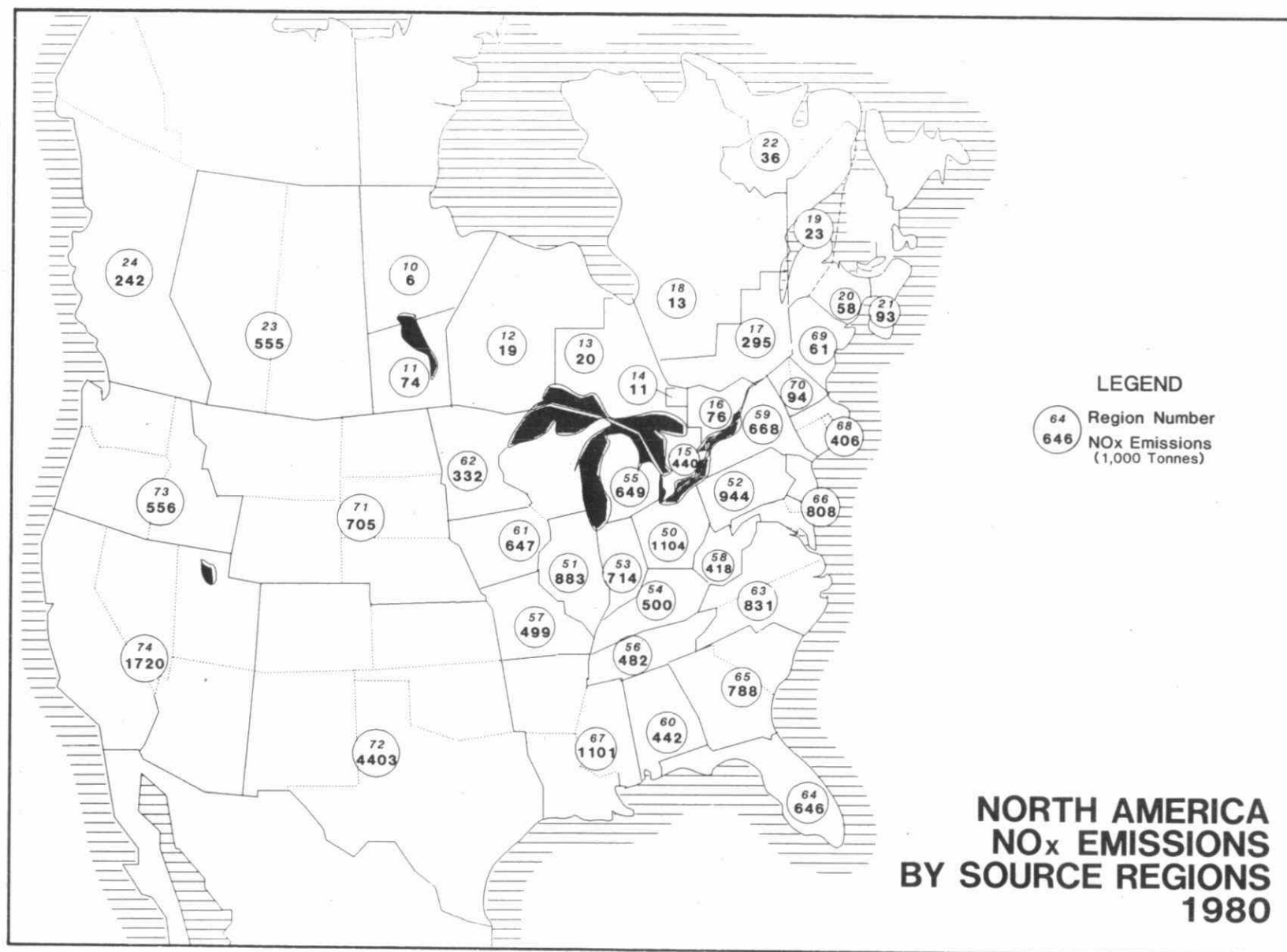


Fig. 3.2.8 North America NO_x Emissions by Source Regions: Year -1980.

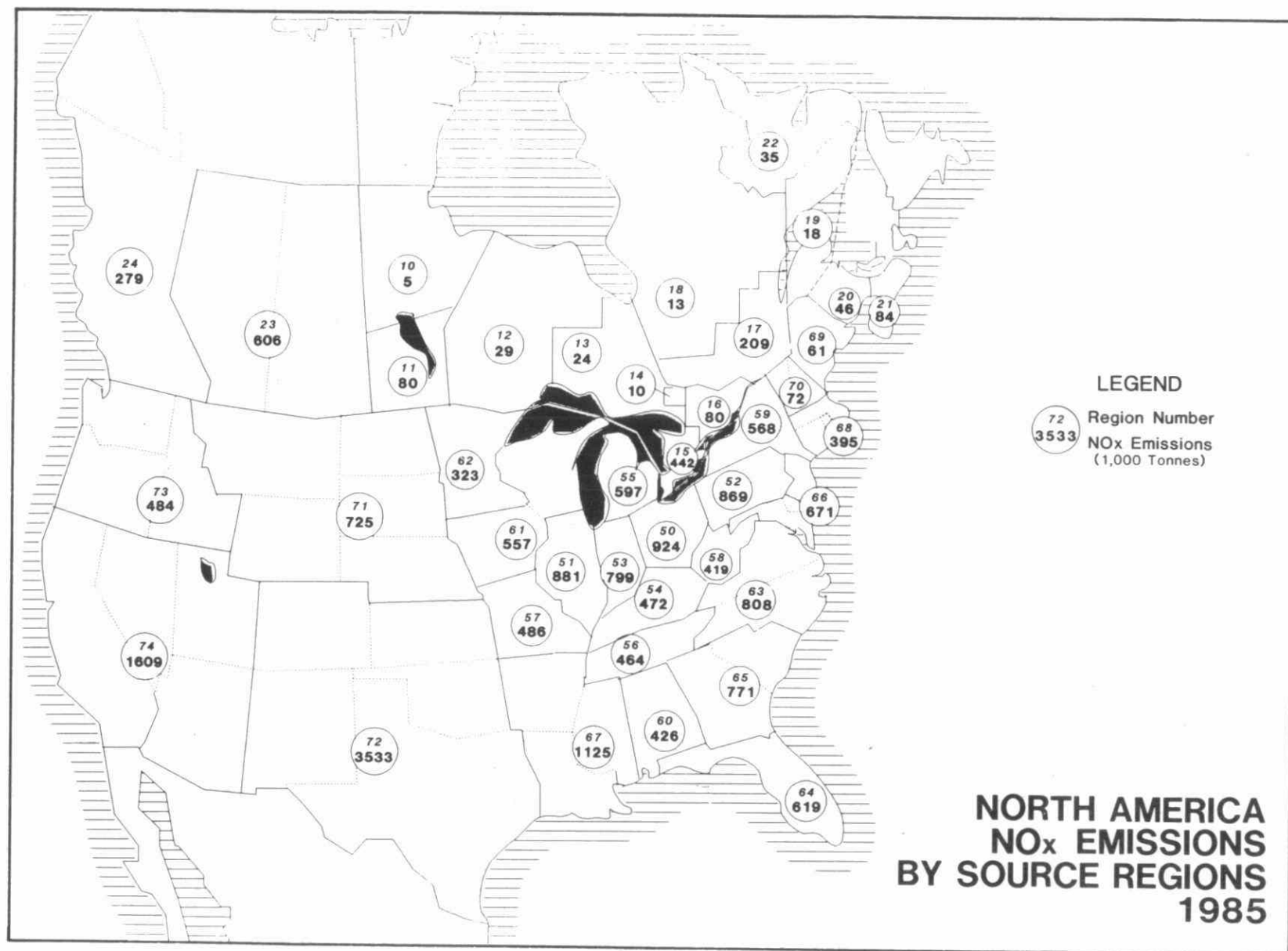


Fig. 3.2.9 North America NO_x Emissions by Source Regions: Year -1985.

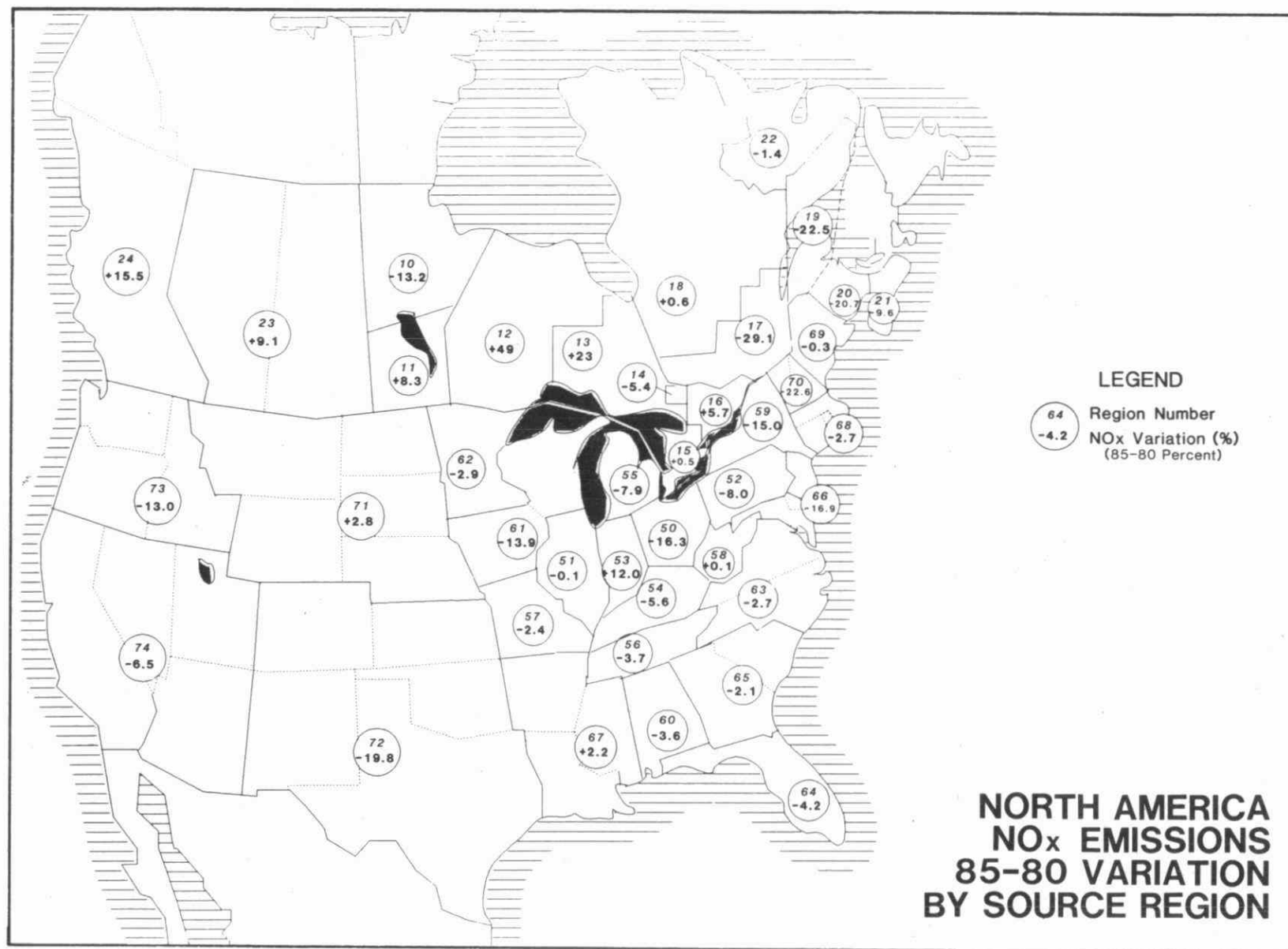


Fig. 3.2.10 North America NO_x Emissions 85-80 Variation by Source Region.

3.2.2.b PATTERNS OF PRECIPITATION COMPOSITION AND DEPOSITION OF ACIDS IN CANADA

In this section wet deposition observations are discussed. Dry deposition is not discussed, largely because of the paucity of dry deposition data in eastern Canada. A brief discussion of the relative importance of dry and wet deposition is addressed in Appendix 3A. The general conclusion is that, for sulphur, wet deposition dominates over dry deposition while for nitrogen the two are of roughly equal importance.

Maps showing the spatial patterns of precipitation-weighted mean concentration and wet deposition have been generated for all major ions for the period 1980 through 1987. The maps have several uses - they illustrate the magnitude and variability of wet deposition across eastern North America, and they provide insight into the relationship between anthropogenic emissions of sulphur and nitrogen oxides and precipitation chemistry/wet deposition. The spatial patterns and their implications for that relationship are discussed in this section. The maps do not attempt to take into account the role topography plays in increasing wet deposition at higher elevations. Deposition of acidic components can be expected to be increased in the mountainous areas of eastern North America for two reasons. First, rainfall will increase with altitude, and second, mountains are frequently immersed in fog and there is a direct input of water from the fog to the forests. The amount of the wet deposition increase has not been easily quantifiable because of the complexity of the terrain and the general lack of high elevation stations. The implications for southern Quebec, however, will be discussed in some detail below.

Data from 11 Canadian and 3 US wet deposition monitoring networks were used to generate the spatial patterns of precipitation chemistry and wet deposition. Not all networks operated during the entire period. As a result, the number of sites varied from year to year. Table 3.2.6. summarizes the names, acronyms and operating periods of the networks operative at various times in the 1980s. Note that the majority of the networks began in the early 1980s and gradually increased the number of measurement sites to a maximum in 1987. This is seen in Figure 3.2.11 which illustrates the set of sites used to generate each map from 1980 to 1987. All of the maps were generated from the National Atmospheric Chemistry Data Base (NAtChem), a federal/provincial data base resident at the Atmospheric Environment Service of Environment Canada.

Table 3.2.6
Wet Deposition Monitoring Networks

Network Acronym	Network Name	Data Period Used
CANADA		
CANSAP	Canadian Network for Sampling Precipitation	1980-1983
APN	Canadian Air and Precipitation Network	1980-1983
CAPMoN	Canadian Air and Precipitation Monitoring Network	1983-1987
MAPMN	Manitoba Acid Precipitation Monitoring Network	1984-1986
APIOS-C	Acidic Precipitation in Ontario Study - Cumulative Network	1980-1987
APIOS-D	Acidic Precipitation In Ontario Study - Daily Network	1980-1987
RE PQ	Réseau d'échantillonnage des précipitation du Québec	1981-1987
NBPN	New Brunswick Precipitation Network	1981-1987
NSPMN	Nova Scotia Precipitation Monitoring Network	1980-1987
NPMN	Newfoundland Precipitation Monitoring Network	1987
EPSN	Environmental Protection Service Network	1981-1987
UNITED STATES		
NADP/NTN	National Atmospheric Deposition Program/National Trends Network	1980-1987
MAP3S	Multi-State Atmospheric Pollution Power Production Study Network	1980-1987
UAPSP	Utility Acid Precipitation Study Program Network	1980-1987

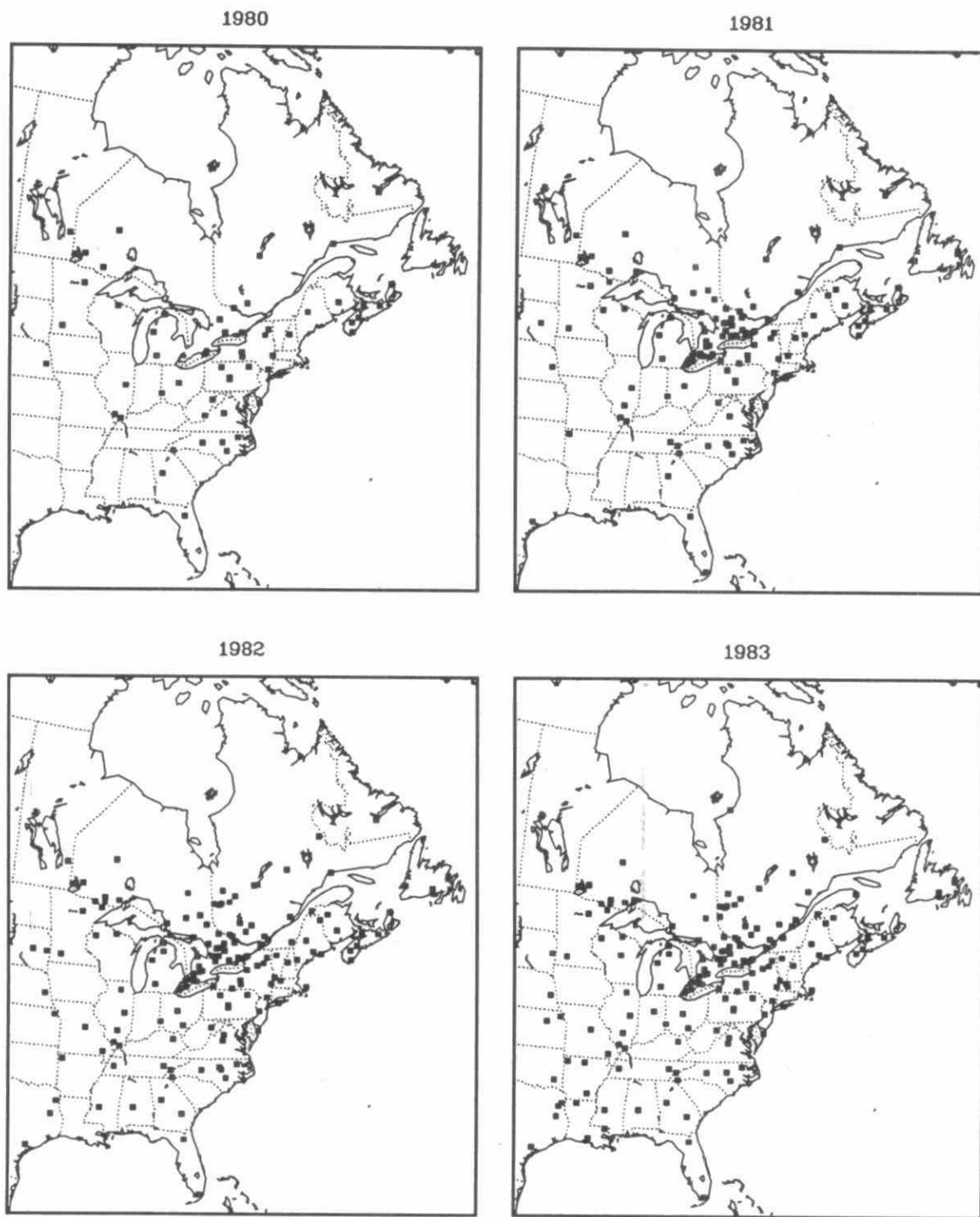


Fig. 3.2.11a Canadian and US wet deposition monitoring sites used to generate spatial patterns of concentration and deposition from 1980 to 1983.

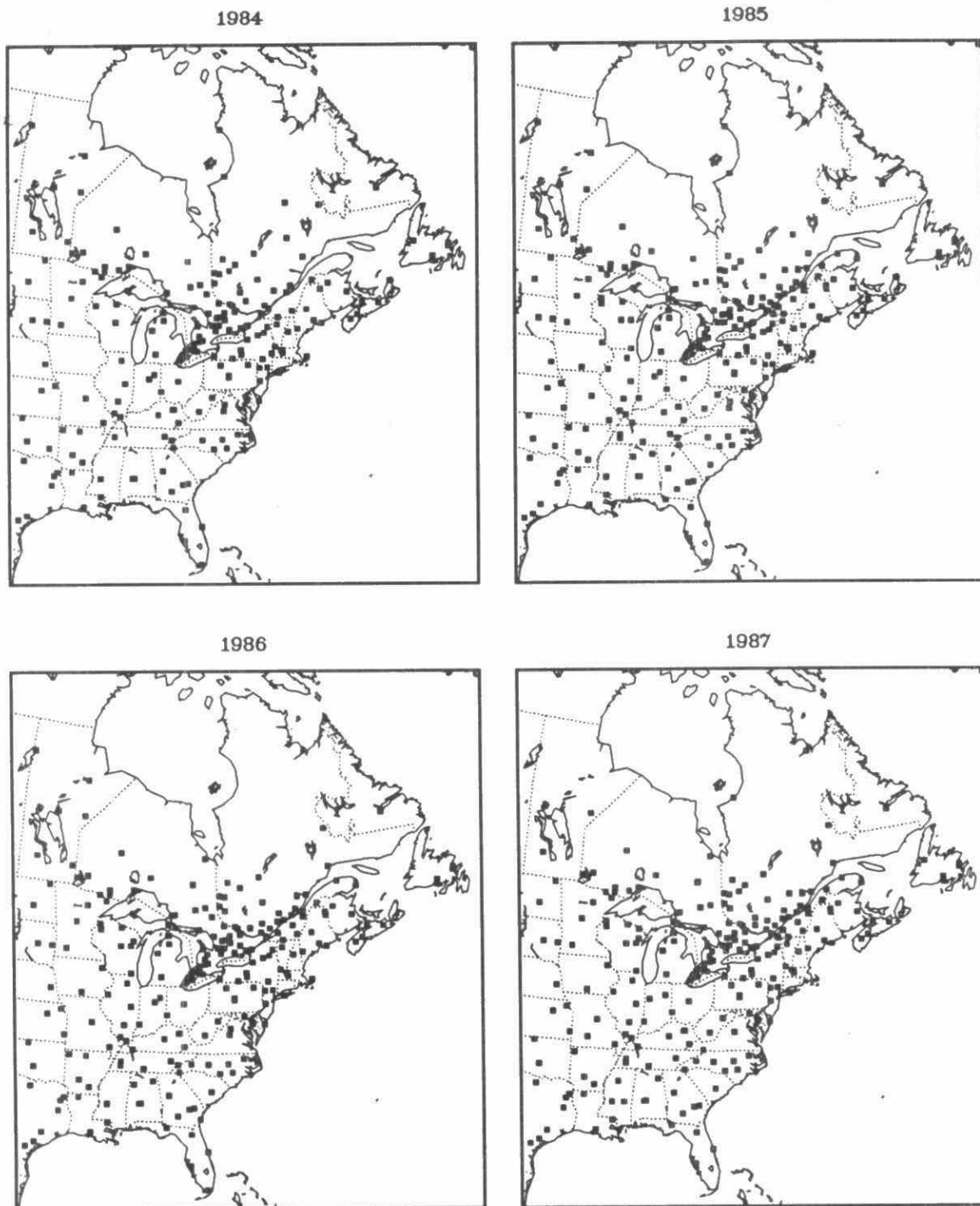


Fig. 3.2.11b Canadian and US wet deposition monitoring sites used to generate spatial patterns of concentration and deposition from 1984 to 1987.

Spatial Patterns Of Precipitation Chemistry And Wet Deposition

Two types of spatial patterns were generated from the network data:

- annual maps of precipitation-weighted mean concentration and wet deposition for each year from 1980 through 1987,
- six-year-average maps of precipitation-weighted mean concentration and wet deposition for the period 1982-1987.

Both are described below.

Annual Concentration And Deposition Patterns

The annual patterns of precipitation-weighted mean concentration and deposition are shown for $\text{SO}_4^{=}$, NO_3^- , H^+ , NH_4^+ , Ca^{++} , Mg^{++} , Na^+ , Cl^- and K^+ in Appendix 3B. The patterns for excess $\text{SO}_4^{=}$ (i.e. sea salt corrected) are shown in Figures 3.2.12 and 3.2.13). The annual precipitation-weighted mean concentration and deposition data used to generate the patterns were obtained from two sources - individual networks and the United States' Acid Deposition System (ADS) Data Base. Data from the ADS Data Base included three Canadian networks (CAPMoN, APIOS-C, and APIOS-D) and three US networks (NADP/NTN, UAPSP, MAP3S). All calculations of annual precipitation-weighted mean concentrations and wet deposition were based on the recommended equations of the Canada/US Unified Deposition Data Base Committee (UDDBC, 1985).

Data used in the production of the maps were vetted for quality. Only data meeting certain annual data completeness and site representativeness criteria were used. The criteria were:

1. Precipitation depth measurements must have been available for at least 90% of each year under consideration;
2. The depth of precipitation associated with samples having valid concentrations must have represented at least 70% of the total annual precipitation depth;
3. The site must have been regionally-representative in that it satisfied the Canada-US Unified Deposition Data Base Committee's regional representativeness rating of a Class 1, 2a or 2b site (UDDBC, 1985).

Data not meeting these criteria were used in one instance only, that is, in the case of 5 to 9 marginally non-representative CANSAP sites that were used in the years 1980, 1981, and 1982. These sites were exempted from the criteria because no other data were available in those areas for those years. Data from these sites have also been used in other mapping exercises (e.g., Clark et al, 1987; Barchet, 1987). In a few cases, data that

did satisfy the above criteria were not used because they exhibited extremely high or low values totally inconsistent with the regional concentration or deposition patterns.

The annual concentration and deposition maps shown in Figures 3.2.12 and 3.2.13 and Appendix 3B were produced using a spatial interpolation scheme known as Simple Kriging. The method used the measured data from the irregularly-spaced measurement sites (Fig.3.2.11) to estimate the concentration and deposition values at 9360 grid points over the map domain. Each grid point value represented a least squares estimate made from 25 of the nearest sampling sites, weighted by the distance from the sites to the grid point. The distance weighting scheme was based on a linear equation describing the functional dependence between measurement variance and between-site distance. From the 9360 grid point values, isopleths of constant concentration or deposition were plotted using a linear contouring routine. Complete details of the interpolation and plotting package are described in Mathews (1987). All maps were computer-generated at the Atmospheric Environment Service (Environment Canada) and were hand-drafted (with minor smoothing) for publication.

The most noticeable characteristic of the excess $\text{SO}_4^{=}$, SO_4^{-} , NO_3^{-} and H^{+} , patterns of concentration and deposition maps is their appearance as mis-shapen bullseyes. In both the concentration and deposition maps, the centre of the bullseye is typically located in the lower Great Lakes area of Canada and the United States. The bullseye exhibits a well-defined gradient toward low values along the northern, western and southern edges of the map.

The concentration and deposition patterns of all four ions show considerable year-to-year variability - in both shape and magnitude. For example, the shape and location of the isopleths shift from year to year, and the magnitude of the isopleths increases or decreases in certain years. The latter can be seen in the annual excess sulphate deposition patterns of Figures 3.2.13 where the 40 kg/ha/yr contour appears in some years but not in the other years.

Figures 3.2.14 and 3.2.15 also illustrate the year-to-year variability of the excess sulphate and nitrate deposition patterns. Shown in Figure 3.2.14 (a) is the envelope of all 20 kg/ha/yr annual deposition isopleths for the years 1980 through 1987 (the shaded area represents the region between the minimum and maximum extremes of the eight annual isopleths). The large geographical size of the envelope clearly illustrates the variability in the isopleth locations over the eight years. Typical distances between the minimum and maximum extremes are 200 to 1000 km. There is a strong suggestion that this interannual variability consists of both a systematic and a random component. The systematic is being a trend toward contraction of the area within the 20 kg/ha/yr isopleth; the random component is an annual fluctuation in the trend. Evidence for the systematic component is given in Figure 3.2.14 (b) which shows the locations of two 3-year-average isopleths, one for the period 1980-1982 and one for the period 1985-1987. The smaller

area enclosed within the 1985-1987 isopleth compared to the 1980-1982 isopleth is readily apparent.

Similarly, Figure 3.2.15 (a) shows the envelope of 15 kg/ha/yr nitrate isopleths for the years 1980 to 1987, and Figure 3.2.15 (b) shows the superposition of the 1980-82 and 1985-87 averaged isopleths. As with sulphate, the size of the 15 kg/ha/yr deposition envelope is quite large, suggesting a strong interannual variability. However, unlike sulphate, the annual nitrate variations do not appear to be systematic since the 1980-82 and 1985-87 isopleths are quite similar.

The year-to-year variability in the annual deposition patterns can be attributed to several sources including:

- changes in the annual meteorological patterns (e.g., wind direction, temperature, precipitation, etc.);
- changes in emission rates and patterns;
- changes in the number and location of measurement sites (which have a strong influence on interpolation error);
- changes in the quality of the measurement data (e.g., increasing accuracy and precision with time).

Interpretation of the patterns, and particularly their changes with time, is highly sensitive to the effects of this interannual variability. An attempt was made in Figures 3.2.14 (b) and 3.2.15 (b) to smooth out the meteorological and interpolation effects by averaging over three year periods (1980-82 and 1985-87). As mentioned above, the interesting aspect of the two diagrams is the apparent contraction of the excess sulphate deposition pattern from the early to late 1980s, and the lack of contraction in the nitrate pattern. It is particularly noteworthy that, during this same time period, SO_2 emissions decreased markedly, while NO_x emissions did not. Further discussion on the possible relationship between emissions and precipitation chemistry appears in Section 3.2.3.

As noted at the beginning of the section, all of the foregoing discussion has focussed solely on precipitation chemistry and wet deposition. Air chemistry and dry deposition were excluded because measurements were too sparse to produce large-scale spatial patterns over eastern North America. The effects of topography, particularly on enhanced precipitation and cloud/fog water deposition, have also not been included.

Topography, however, will also play a role in reshaping the patterns in certain regions in southern Quebec. If we take 500 m as an elevation above which one might expect significantly increased rainfall and frequent fog episodes, then we find there are three areas of importance in southern Quebec. One is a triangular shaped area northwest of Montreal extending 200 km north of Mont Tremblant. The second is along the eastern border of Quebec and the states of Vermont, New Hampshire and Maine. The third is

a roughly square area, 100 km on a side, to the north of Quebec City. These areas form the highest parts of the mountainous terrain that surrounds the St. Lawrence Lowlands.

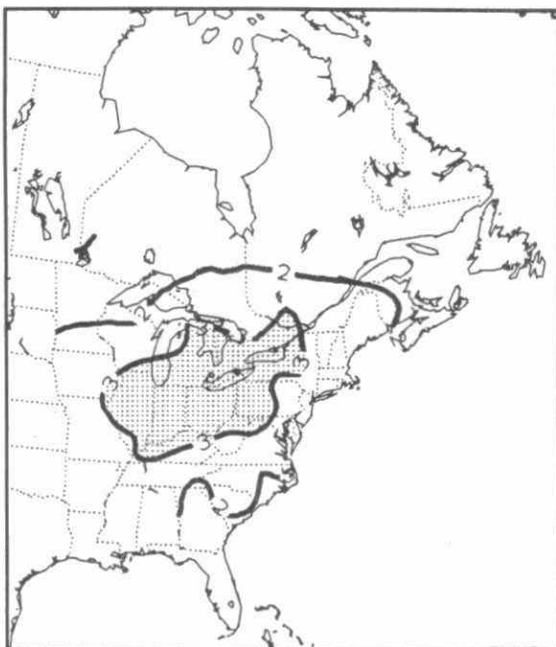
Southwesterly flows in the boundary layer will be constrained by these features to continue a motion to the northeast. In late 1985, three sites were established as part of the Chemistry of High Elevation Fog (CHEF) program (Schemenauer, 1986) to look at wet deposition, ozone concentrations and meteorological data at elevations of up to 970 m around the perimeter of the St. Lawrence Lowlands. Two of the sites, Mont Tremblant and Roundtop Mountain, remain operational in 1990.

The increase of precipitation amount with altitude in mountainous areas is well documented in the literature. In the particular geographical area of interest, Schemenauer (1986) noted an increase in precipitation amount of about 38% at Mont Tremblant and 55% at Roundtop at mountain sites about 600 m above the valley sites which were at 250 m. Vogelmann (1982), working in the Green Mountains of Vermont, recorded a 20% increase in precipitation from 550m to 850m. Presumably, below 550 m evaporation would have contributed to even lower precipitation amounts. Therefore, one might reasonably expect about 50% greater precipitation on the upper parts of mountains in southern Quebec than is normally recorded at the standard low elevation stations.

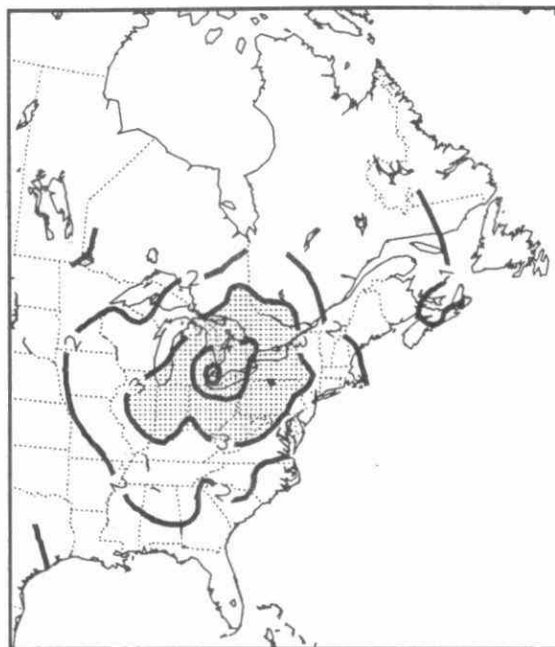
The variation of precipitation pH (Schemenauer, 1986) and precipitation chemistry (Schemenauer and Winston, 1988; Schemenauer et al., 1988) with altitude has also been reported for southern Quebec. To a good approximation, the precipitation chemistry does not vary with altitude. When coupled with the higher precipitation amounts noted above, this implies that as much as 50% more wet deposition from precipitation may be occurring in the elevated areas of southern Quebec than is currently being mapped.

The relative wet deposition components from fog and precipitation have been discussed (Barrie and Schemenauer, 1986; Barrie and Schemenauer, 1988). The chemical composition of the higher elevation fogs in southern Quebec has been reported (Schemenauer, 1986; Schemenauer and Winston, 1988; Schemenauer et al., 1988). Generally, the concentrations of all ionic species (H^+ , NH_4^+ , K^+ , Ca^{++} , Mg^{++} , $SO_4^{=}$, NO_3^- , Cl^-) are 3 to 20 times higher in fog water than in precipitation. Each site and each season show somewhat different values. The fog pH values range from 0.2 to 0.5 pH units lower than for precipitation and are typically around 3.8.

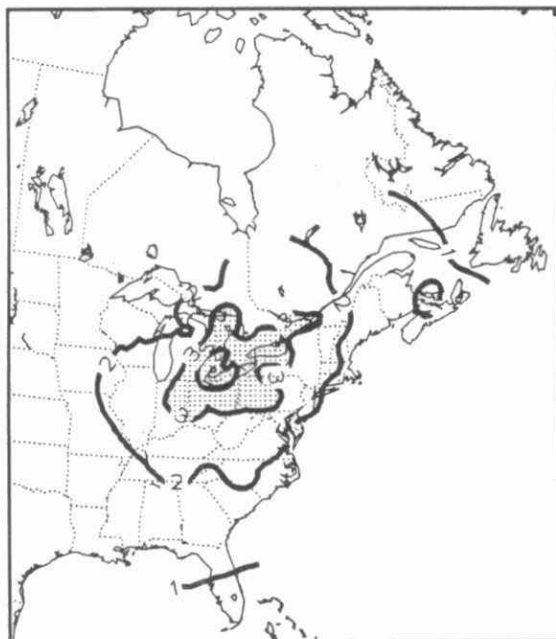
1980 ANNUAL MEAN EXCESS SO₄ CONCENTRATION IN PRECIPITATION (MG/L)



1981 ANNUAL MEAN EXCESS SO₄ CONCENTRATION IN PRECIPITATION (MG/L)



1982 ANNUAL MEAN EXCESS SO₄ CONCENTRATION IN PRECIPITATION (MG/L)



1983 ANNUAL MEAN EXCESS SO₄ CONCENTRATION IN PRECIPITATION (MG/L)

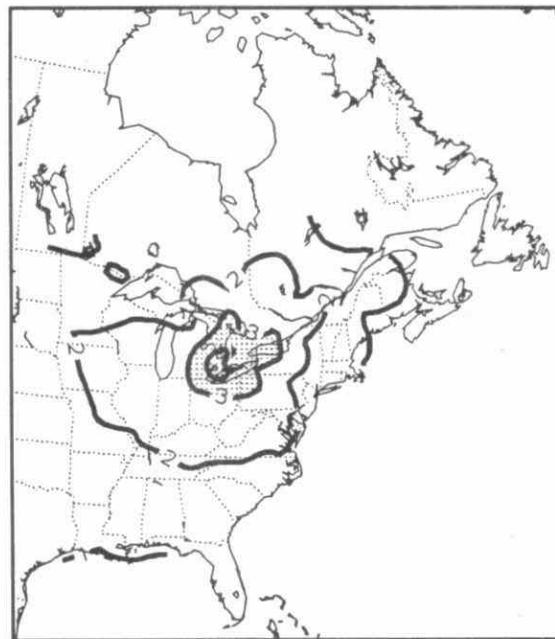
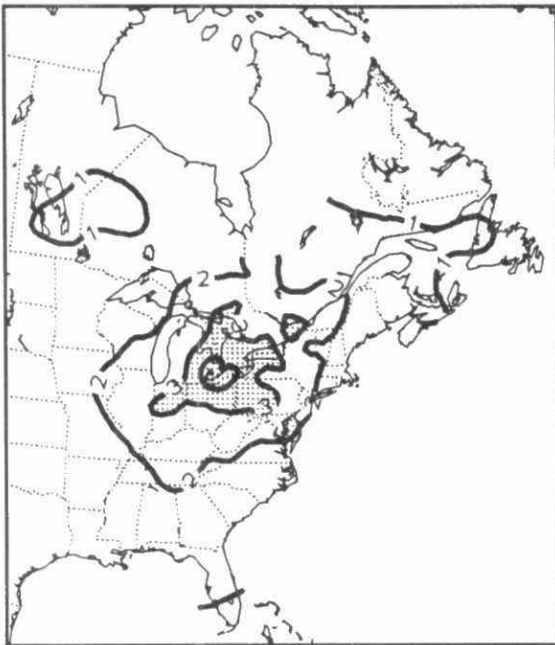
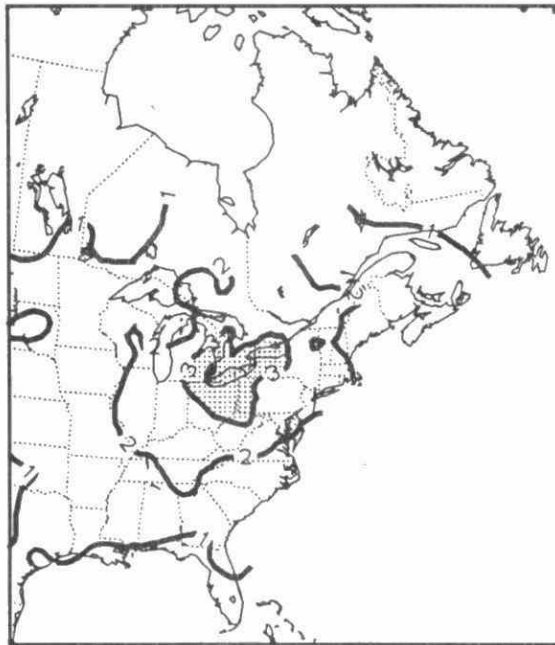


Fig. 3.2.12a Patterns of annual precipitation-weighted-mean concentrations of excess SO₄⁼ (mg/l):1980-1983.

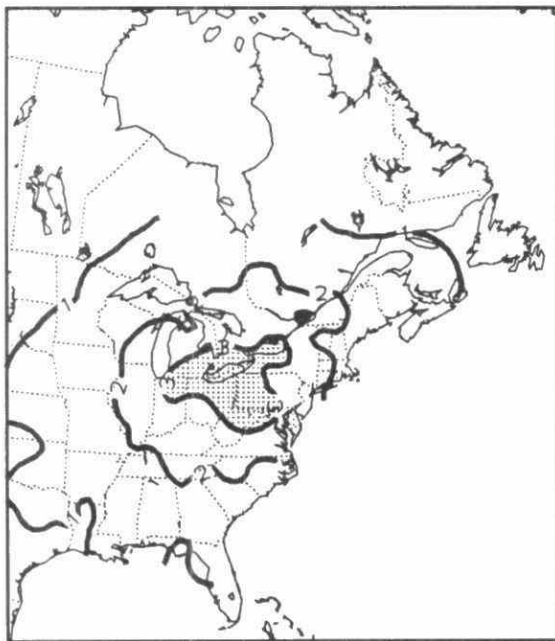
1984 ANNUAL MEAN EXCESS SO₄ CONCENTRATION IN PRECIPITATION (MG/L)



1985 ANNUAL MEAN EXCESS SO₄ CONCENTRATION IN PRECIPITATION (MG/L)



1986 ANNUAL MEAN EXCESS SO₄ CONCENTRATION IN PRECIPITATION (MG/L)



1987 ANNUAL MEAN EXCESS SO₄ CONCENTRATION IN PRECIPITATION (MG/L)

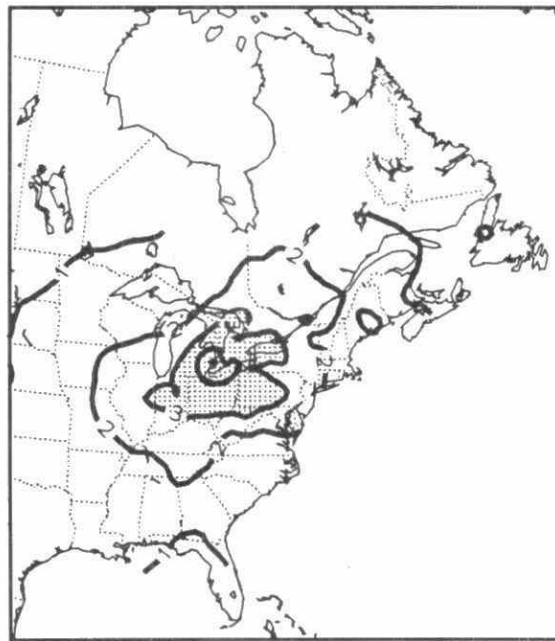
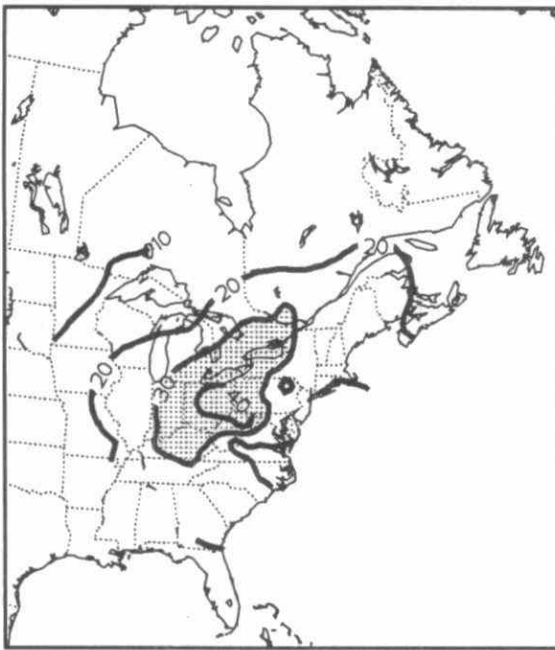
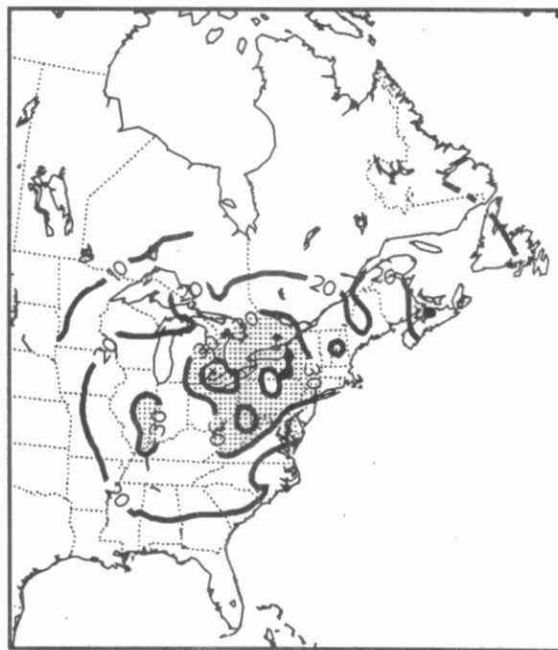


Fig. 3.2.12b Patterns of annual precipitation-weighted-mean concentrations of excess SO₄²⁻ (mg/l):1984-1987.

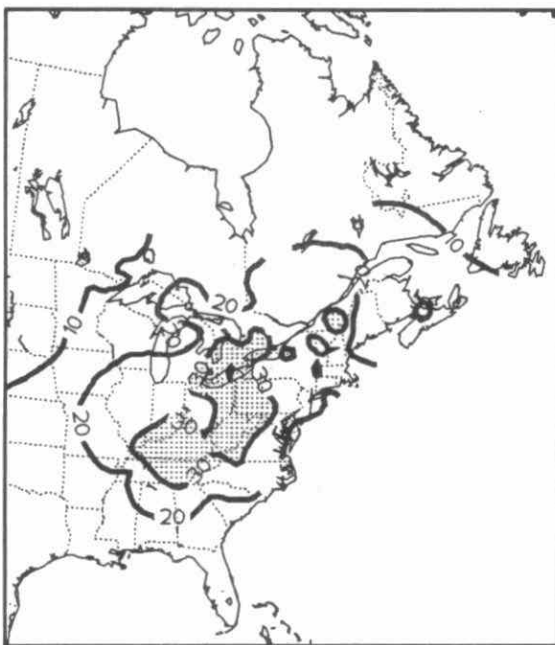
1980 WET EXCESS SO₄ DEPOSITION (KG/HA/YR)



1981 WET EXCESS SO₄ DEPOSITION (KG/HA/YR)



1982 WET EXCESS SO₄ DEPOSITION (KG/HA/YR)



1983 WET EXCESS SO₄ DEPOSITION (KG/HA/YR)

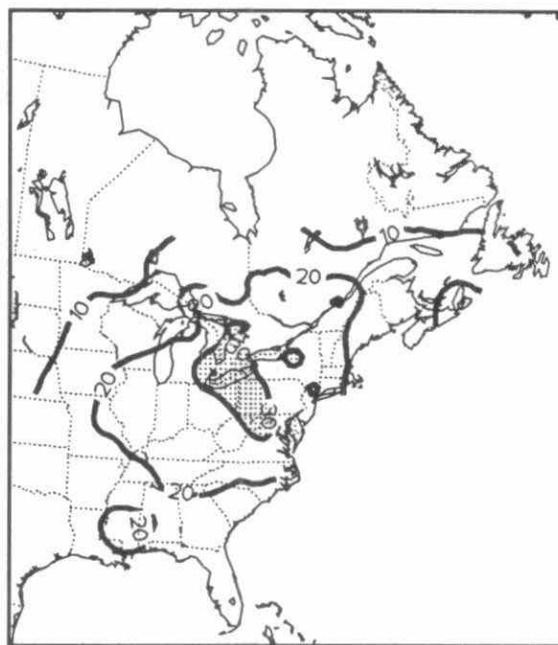
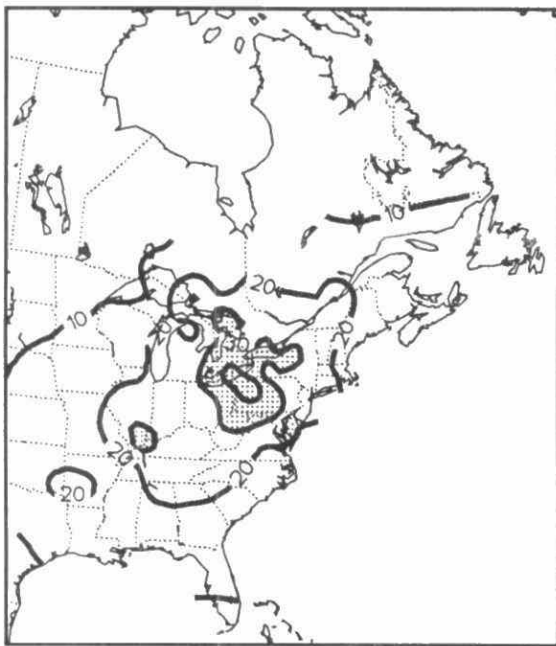
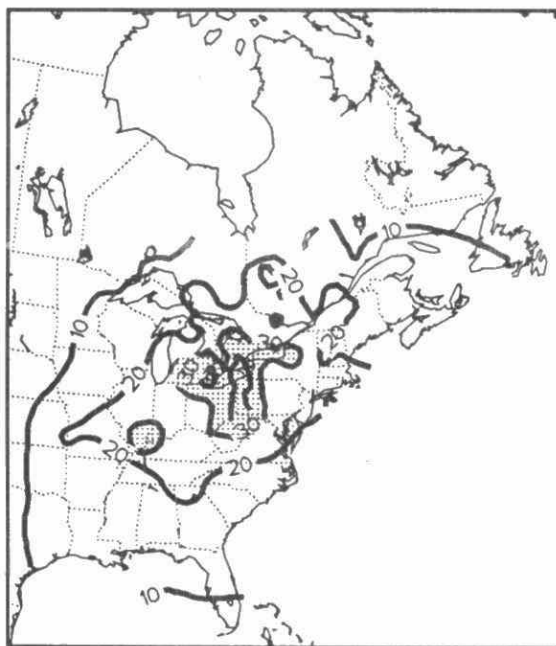


Fig. 3.2.13a Patterns of annual wet deposition of excess of SO₄⁻ (kg/ha/yr):1980-1983.

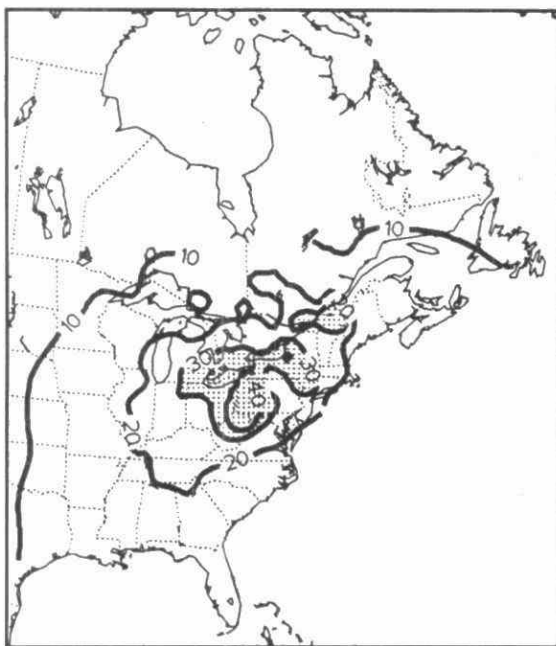
1984 WET EXCESS SO₄ DEPOSITION (KG/HA/YR)



1985 WET EXCESS SO₄ DEPOSITION (KG/HA/YR)



1986 WET EXCESS SO₄ DEPOSITION (KG/HA/YR)



1987 WET EXCESS SO₄ DEPOSITION (KG/HA/YR)

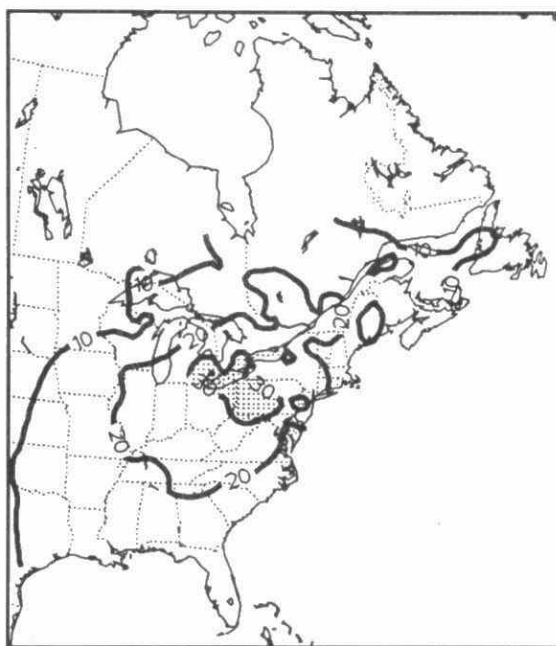


Fig. 3.2.13b Patterns of annual wet deposition of excess of SO₄²⁻ (kg/ha/yr):1984-1987.

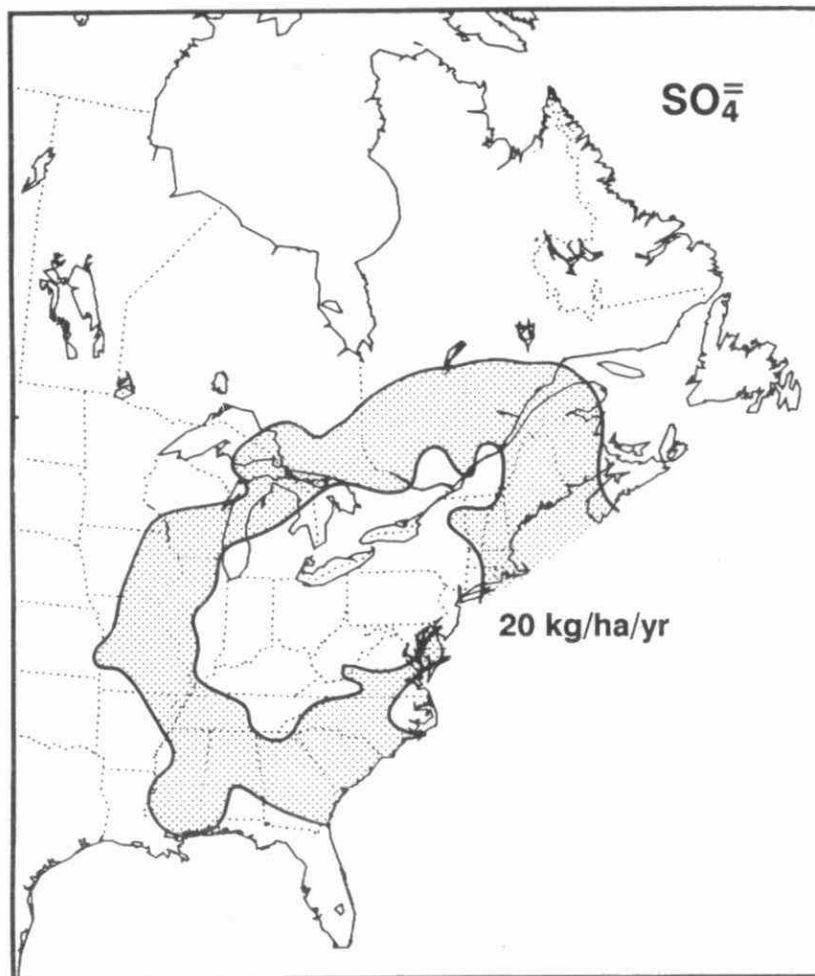


Fig. 3.2.14a Envelope of annual 20 kg/ha/y excess sulphate deposition isopleths for all years from 1980 to 1987.

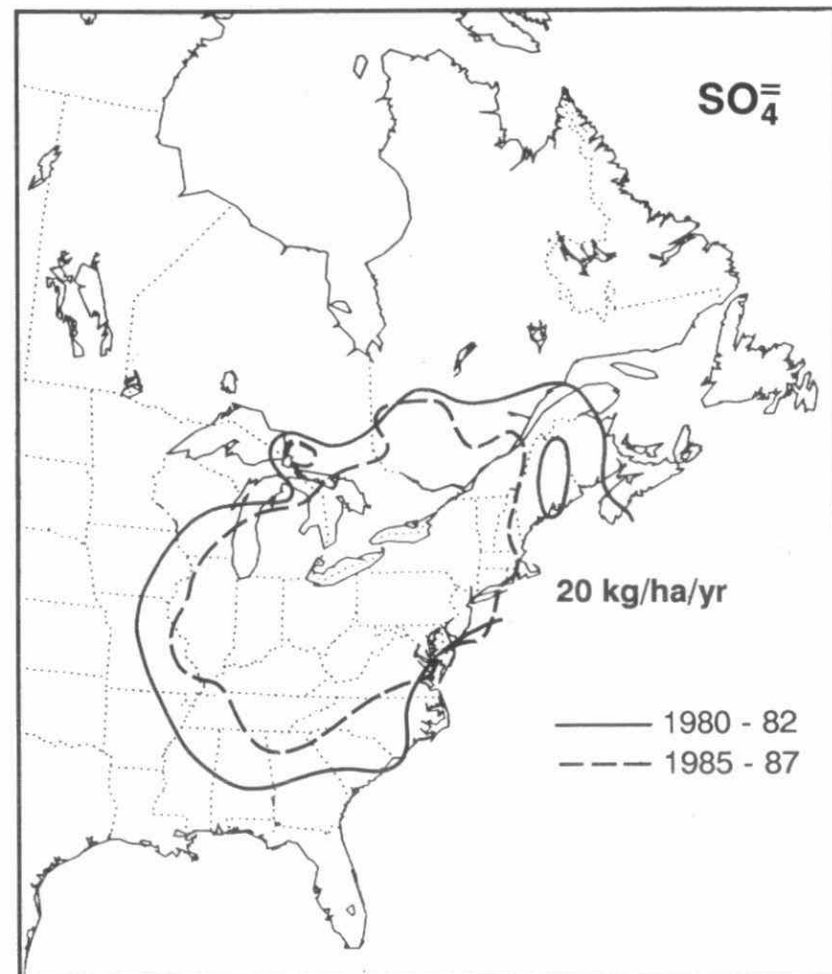


Fig. 3.2.14b Superposition of the 20 kg/ha/y excess sulphate deposition isopleths for the periods of 1980-82 and 1985-87.

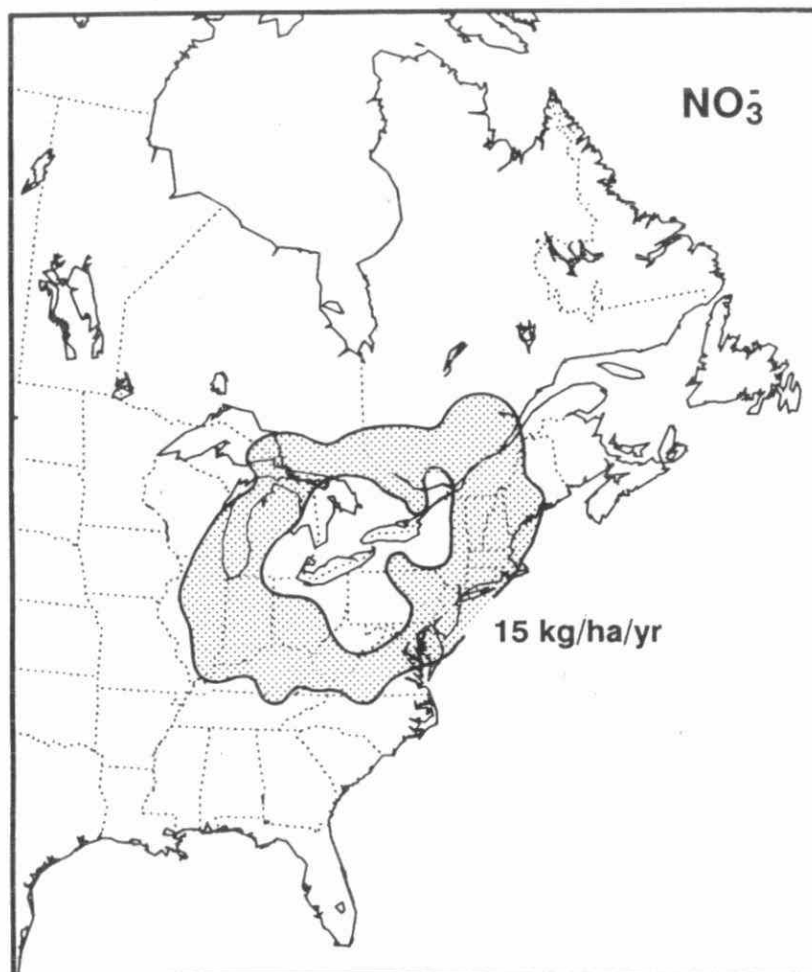


Fig. 3.2.15a Envelope of annual 15 kg/ha/y nitrate deposition isopleths for the periods 1980 to 1987.

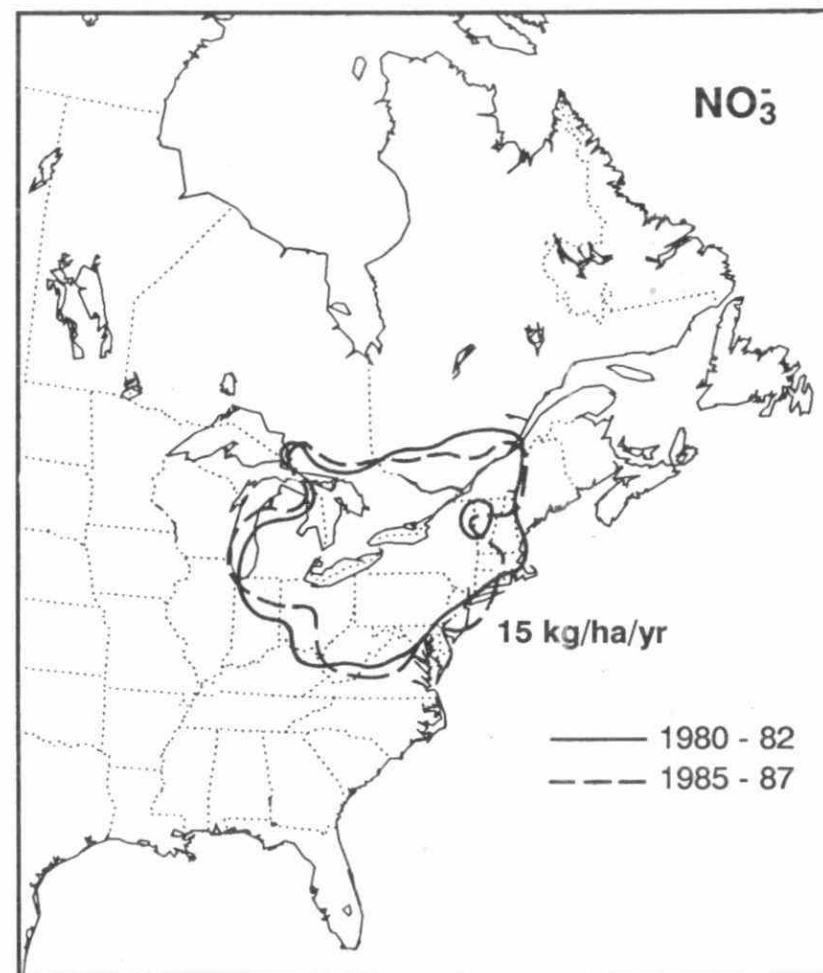


Fig. 3.2.15b Superposition of the 15 kg/ha/y nitrate deposition isopleths for the periods 1980-82 and 1985-87.

It is very difficult to quantify the deposition from fog to a forest, particularly in the complex terrain that exists in mountainous regions. Most attempts to date have utilized variations of a published deposition model (Lovett, 1984). There have also been some attempts to measure throughfall directly. Mohnen (1988), from a model study using data from high elevation sites in the eastern U.S.A., concludes that, "Cloud interception therefore has the potential to be the major and sometimes dominant process for the input of sulfur and nitrogen compounds into montane forests." Kroll and Winkler (1989) used the Lovett model to calculate wet deposition from fog to high elevation coniferous forests in Germany and found the values for sulphate and nitrate to be twice as high from the fog as from precipitation. Schemenauer et al. (1988) estimated that, conservatively, the volume of fog water impinging on higher elevation forests in southern Quebec is 10% of the volume of water from precipitation (using low elevation values). Therefore, given the order of magnitude higher ion concentrations, one might expect that the sulphate and nitrate deposition due to fog is about equivalent to that from precipitation at low elevations in the region.

The net result of the increased rainfall, and the fog water input, is that the higher elevation areas in southern Quebec may be receiving 2.5 times the sulphate and nitrate that is measured in the lowland monitoring networks. This is in the process of being quantified. The implication is that the areas of high sulphate and nitrate wet deposition mapped in this report may have to be modified to reflect anomalously high deposition figures in the three high elevation areas noted above.

Similarly, coastal areas of the Atlantic Provinces which experience extensive periods of fog, may also be receiving elevated amounts of acidic deposition from fog water (Cox et al, 1989). Again, further quantification of this phenomenon is needed.

Six-Year Mean Concentration and Deposition Patterns

Six-year mean (1982-87) patterns of concentration and deposition were produced for excess $\text{SO}_4^{=}$, NO_3^- , pH, H^+ , NH_4^+ , Ca^{++} , Mg^{++} , Na^+ , Cl^- , and K^+ . The patterns of excess $\text{SO}_4^{=}$, NO_3^- and H^+ are presented in Figures 3.2.16, 3.2.18 and 3.2.21; the others are shown in Appendix 3B. By smoothing out the year-to-year variability of the annual patterns, the six-year mean maps provide a much clearer picture of the spatial characteristics of the concentration and deposition fields over most of the decade. The six-year patterns were produced by first estimating the concentration and deposition values for each year at all 9360 grid points in the map domain (using the same simple Kriging interpolation technique used to produce the annual maps), then averaging the grid point values over the six years. In the case of the concentration maps, the six-year averages are precipitation-weighted; for the deposition maps, the averages are arithmetic. The concentration and deposition isopleths were then drawn by contouring the six-year average grid point values.

The major characteristics of the concentration and deposition patterns shown in Figures 3.2.16, 3.2.18 and 3.2.21 are summarized below. Summaries for the remaining ions are contained in Appendix 3B. Note that 5-year average deposition maps from 1982-1986 were produced in the same manner and appear in part 4 (Aquatic) and part 5 (Terrestrial) of this Assessment.

Excess $\text{SO}_4^{=}$ (Sea Salt Corrected)

In general, the 6-year mean patterns of excess $\text{SO}_4^{=}$ concentration and deposition are similar (Figure 3.2.16). Highest concentrations and deposition occurred in the area near Lake Ontario and Lake Erie in both Canada and the US, while lowest values occurred in the northern/western regions of Canada and the southern/western regions of the USA. Both the concentration and deposition patterns are both slightly elliptical and elongated along a southwest to northeast axis.

Over the 6-year averaging period, the highest mean excess $\text{SO}_4^{=}$ concentration was slightly greater than 4 mg/l (in southwestern Ontario) and the highest deposition was approximately 40 kg/ha/yr (in western Pennsylvania). Lowest concentration and deposition values were around 0.5 mg/l and 4 kg/ha/yr, respectively, in the northeastern and northwestern sections of the map.

The spatial patterns of excess $\text{SO}_4^{=}$ concentration and deposition, and the emission pattern of SO_2 strongly suggest a relationship between precipitation chemistry and emissions. This is seen in Figure 3.2.17 where the 2 and 3 mg/l excess $\text{SO}_4^{=}$ concentration isopleths are superimposed on the 1985 SO_2 emission pattern. It is clear that the area enclosed by the 2 mg/l isopleth contains most of the SO_2 emissions in eastern North America. As well, the area enclosed by the 3 mg/l isopleth corresponds very closely to the maximum emission area of eastern Ohio, western Pennsylvania, eastern Michigan and southwestern Ontario. It also corresponds to the area immediately downwind of a secondary high emission area located in Illinois and Indiana.

Of particular note in Fig. 3.2.17 is the fact that the 2 mg/l isopleth extends well into northern Ontario and northern Quebec where few emission sources existed in the period 1982-1987. This suggests that precipitation chemistry and wet deposition in these isolated areas are strongly influenced by the long-range transport of SO_2 from the high emission regions to the south and southwest. Such an assertion is supported by strong evidence that, in those areas, the predominant air flow during precipitation events is from the south and southwest. Figure 3.2.20, taken from MOI (1982) illustrates the high frequency of southerly and southwesterly air mass trajectories (from the high emission regions) at several sites in eastern Canada. Also shown is the strong association between these flow directions and high $\text{SO}_4^{=}$ concentrations in precipitation. Recent work by Summers (1987), Samson (1989) and Beattie and Whelpdale (1989) corroborates the dominant influence of southerly to westerly flow from high SO_2 emission areas to the southern areas of Ontario, Quebec, and the Maritimes.

NO_3^-

The 6-year average patterns of NO_3^- concentration and deposition shown in Fig. 3.2.18 are similar to those of excess $\text{SO}_4^{=}$. The areas of highest concentration (maximum 2.8 mg/l) and deposition (maximum 27 kg/ha/yr) are located in southern Ontario, southern Quebec and sections of Ohio, Pennsylvania and New York. Lowest concentrations (approximately 0.3 mg/l) and deposition (2.45 kg/ha/yr), occurred in northwestern Ontario and Manitoba.

A relationship between NO_x emissions and NO_3^- concentrations in precipitation and wet deposition also appears from the spatial patterns. Figure 3.2.19 shows the 1.5 and 2.0 mg/l concentration isopleths superimposed on the 1985 NO_x emission pattern. It is apparent that most large NO_x emission sources (i.e. > 200 kT/grid square) in northeastern North America are enclosed within the 1.5 mg/l NO_3^- concentration isopleth. As well, large areas of Ontario and Quebec having low NO_x emissions have very high NO_3^- concentrations wet deposition. As was the case with excess $\text{SO}_4^{=}$, this strongly suggests that long-range transport from the high emission areas of North America has a strong influence on precipitation chemistry over Ontario and Quebec. Again, this is corroborated by the air parcel trajectory analysis shown in Figure 3.2.20.

H^+ (and pH)

The concentration and deposition patterns of H^+ (Figure 3.2.21) are strikingly similar to those of excess $\text{SO}_4^{=}$ and NO_3^- , reflecting the strong influence of $\text{SO}_4^{=}$ and NO_3^- on precipitation acidity. From 1982-87, the area of maximum concentration and deposition occurred around the lower Great Lakes, and the minimum occurred in the more remote areas of northern Canada, western Canada and the western United States. The low H^+ concentrations in the west are likely related to the neutralizing influence of soil dust.

Changes In Spatial Patterns With Time

The close geographic association of the spatial patterns of the $\text{SO}_4^{=}$ and NO_3^- in precipitation with SO_2 and NO_x emissions was noted earlier on the basis of Figs. 3.2.17 and 3.2.19. This suggests that, since the emissions of SO_2 have shown a fairly steady and substantial downward trend from 1980 to 1987 (see Table 3.2.5), this should be reflected in the change in precipitation $\text{SO}_4^{=}$ concentration pattern over the same period. However, because of the large year-to-year variability in these patterns shown in Appendix 3B, the difference between any two single years may be overwhelmed by the meteorological variability. This can be partially overcome by averaging over a 3-year period near 1980 and another 3-year period near 1985 to cover roughly the same period over which emissions data are available. The results for $\text{SO}_4^{=}$ concentrations for the two periods 1980-1982 and 1985-1987 are shown in Fig. 3.2.22, both as an absolute change of concentration units and as a percentage change from the 1980-1982 base. The area shown is that for which reasonable spatial coverage of monitoring sites was available in

both periods with good quality data. The pattern for the percentage is slightly different than that for absolute changes because of the varying base against which the percentages are calculated.

If, within the limits of accuracy of the measurements, a change of less than $\pm 10\%$ is considered as no change, then Fig. 3.2.22 shows that over most of the region (except for a small area around Quebec City) the $\text{SO}_4^{=}$ concentrations have decreased with an overall average of between 10 and 20%. This is entirely consistent with the change in SO_2 emissions for eastern North America of -13.5% between the two periods (Table 3.2.5). Even on a smaller regional scale the changes correspond in most cases to the changes in upwind SO_2 emissions. For example, from Fig. 3.2.7 it can be seen that the largest percentage changes in SO_2 emissions between 1980 and 1985 occurred in a contiguous band from Wisconsin across the Great Lakes and Ontario into New York, Pennsylvania and northern New England. Apart from southern Quebec, concentration changes across the same belt were between 10 and 30%.

Immediately south of the Great Lakes, through the high emission states of Illinois, Indiana, Ohio and West Virginia, the percentage change in emissions averaged only about 5 or 6% and the precipitation concentrations changed by less than 10% in the region immediately to the east and east-northeast. In the southern United States the relationships are more confused, possibly because transport winds are more variable in direction and the year-to-year meteorological changes play a more dominant role than emissions in determining year-to-year changes in concentrations.

A similar analysis for NO_3^- concentrations in precipitation is shown in Fig. 3.2.23. Overall, the changes between the two periods are much less and, in fact, in terms of absolute changes in concentration if the same grey scale classifications had been used in Fig. 3.2.23a as in Fig. 3.2.22 the NO_3^- map would appear almost blank, i.e. except for one area >0.4 mg/l. Over most of the region the percentage change in precipitation NO_3^- concentrations is less than 10% and, as for $\text{SO}_4^{=}$, this change is entirely consistent with the change of only - 2.0% in NO_x emissions over eastern North America between the two periods (Table 3.2.5). Within the limits of accuracy of both the NO_3^- precipitation concentrations and emission estimates for NO_x the conclusion is that there has been no change in the spatial patterns.

3.2.2.c THE SPATIAL AND TEMPORAL PATTERNS OF SULPHUR DIOXIDE, SULPHATE AND NITRATE CONCENTRATIONS IN AIR IN ONTARIO

A detailed analysis of the spatial patterns of sulphur dioxide, sulphate and nitrate concentrations in air in Ontario measured by the APIOS (Acidic Precipitation in Ontario Study) network was done for the years 1982 to 1986 (Appendix 3C).

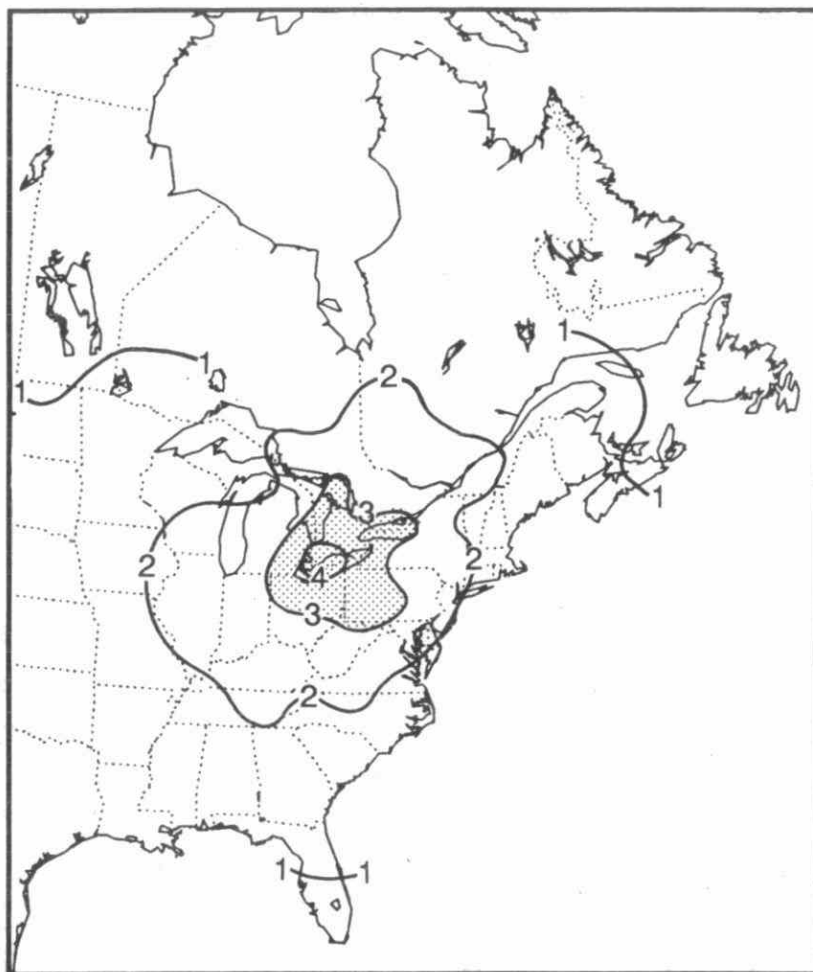
Distributions of these substances for all years 1982-1986 are shown in Figure 3.2.24. The patterns shown in this figure are consistent with those for all years showing a strong

decrease in air concentration of all constituents from south to north in Ontario. This is as one would expect from the direction of the prevailing winds and the location of emissions in eastern North America.

Isolines of SO_2 and, to a lesser extent, $\text{SO}_4^{=}$ have shown a general southward movement over the period of study corresponding to a decrease in concentrations at most locations. In contrast, those of total NO_3^- have not. This is illustrated by the comparison of average spatial distribution of each of these substances for a two year period at the beginning and end of the study (Figs. 3.2.25 to 3.2.27).

The available air concentration data are consistent with the precipitation patterns described in the previous section.

6-YEAR (1982-87) MEAN XSO_4^- CONCENTRATION
IN PRECIPITATION (mg/l)



6-YEAR (1982-87) MEAN XSO_4^- DEPOSITION (kg/ha/yr)

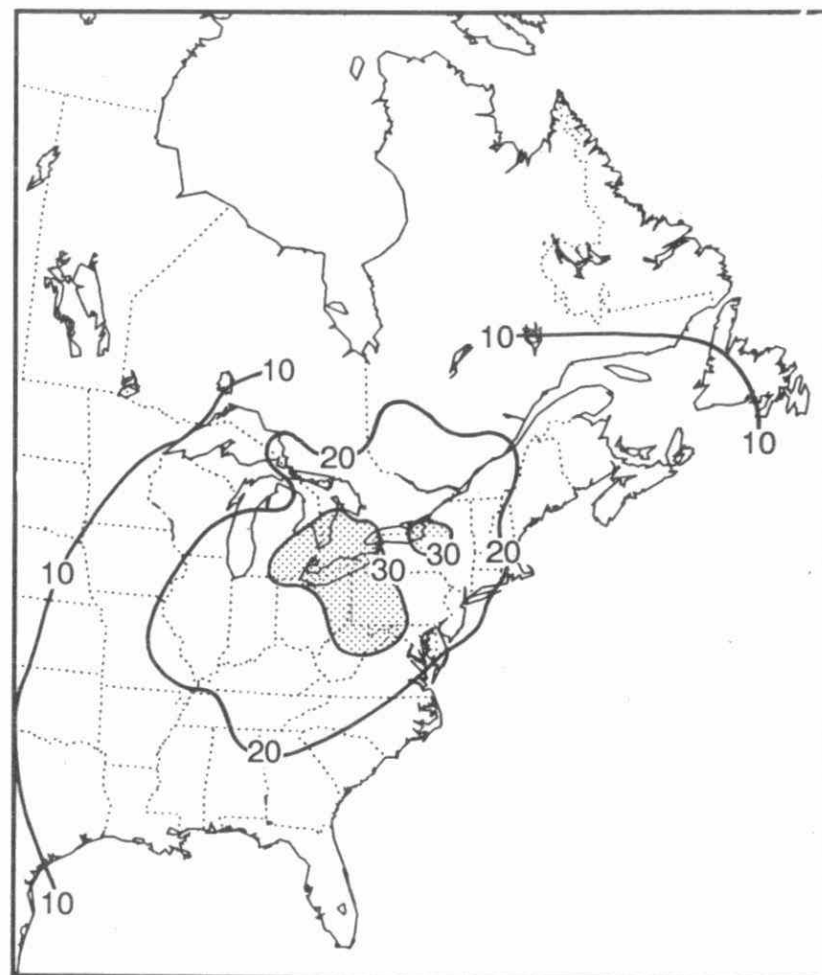


Fig. 3.2.16 Six-year-average (1982-1987) concentration and deposition patterns of excess sulphate.

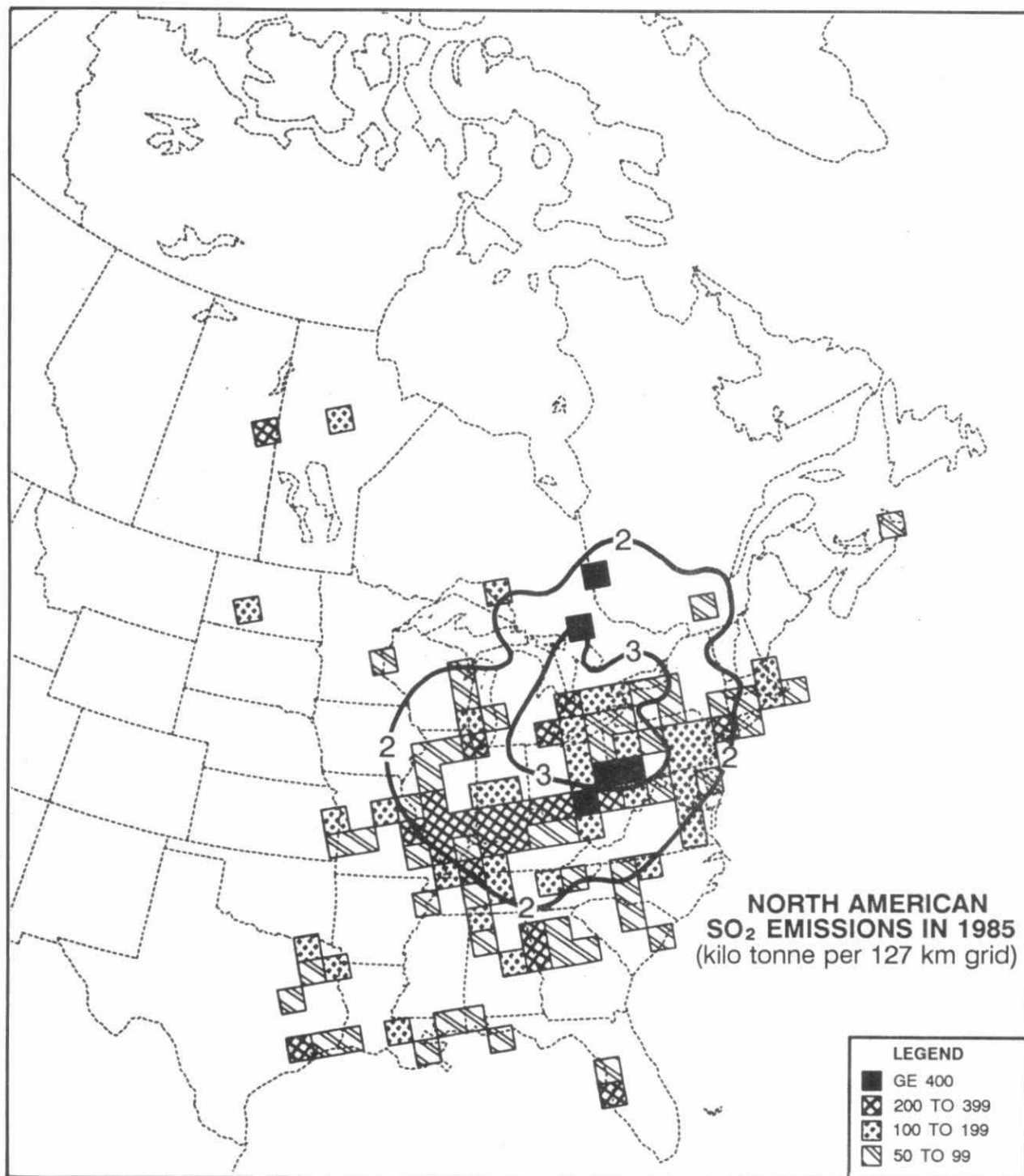
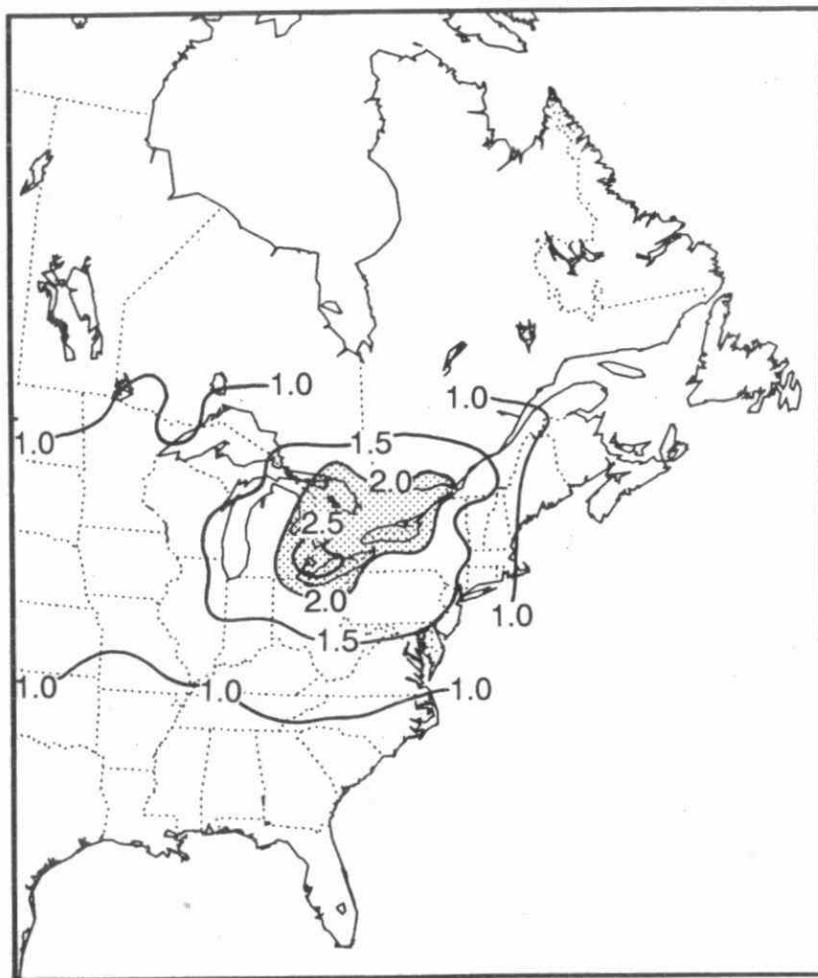


Fig. 3.2.17 Superposition of the 1982-87 six-year-average excess sulphate concentration isopleths (2 and 3 mg/l) on the 1985 SO₂ emission pattern.

6-YEAR (1982-87) MEAN NO_3^- CONCENTRATION
IN PRECIPITATION (mg/l)



6-YEAR (1982-87) MEAN NO_3^- DEPOSITION (kg/ha/yr)

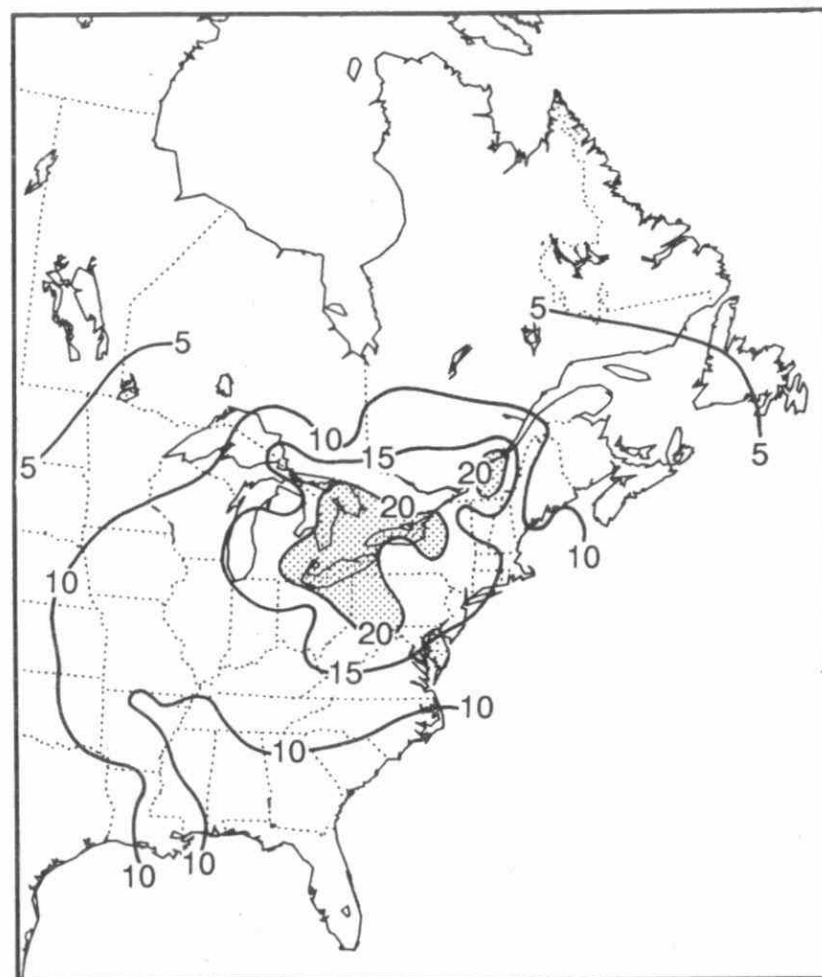


Fig. 3.2.18 Six-year-average (1982-87) concentration and deposition patterns of nitrate.

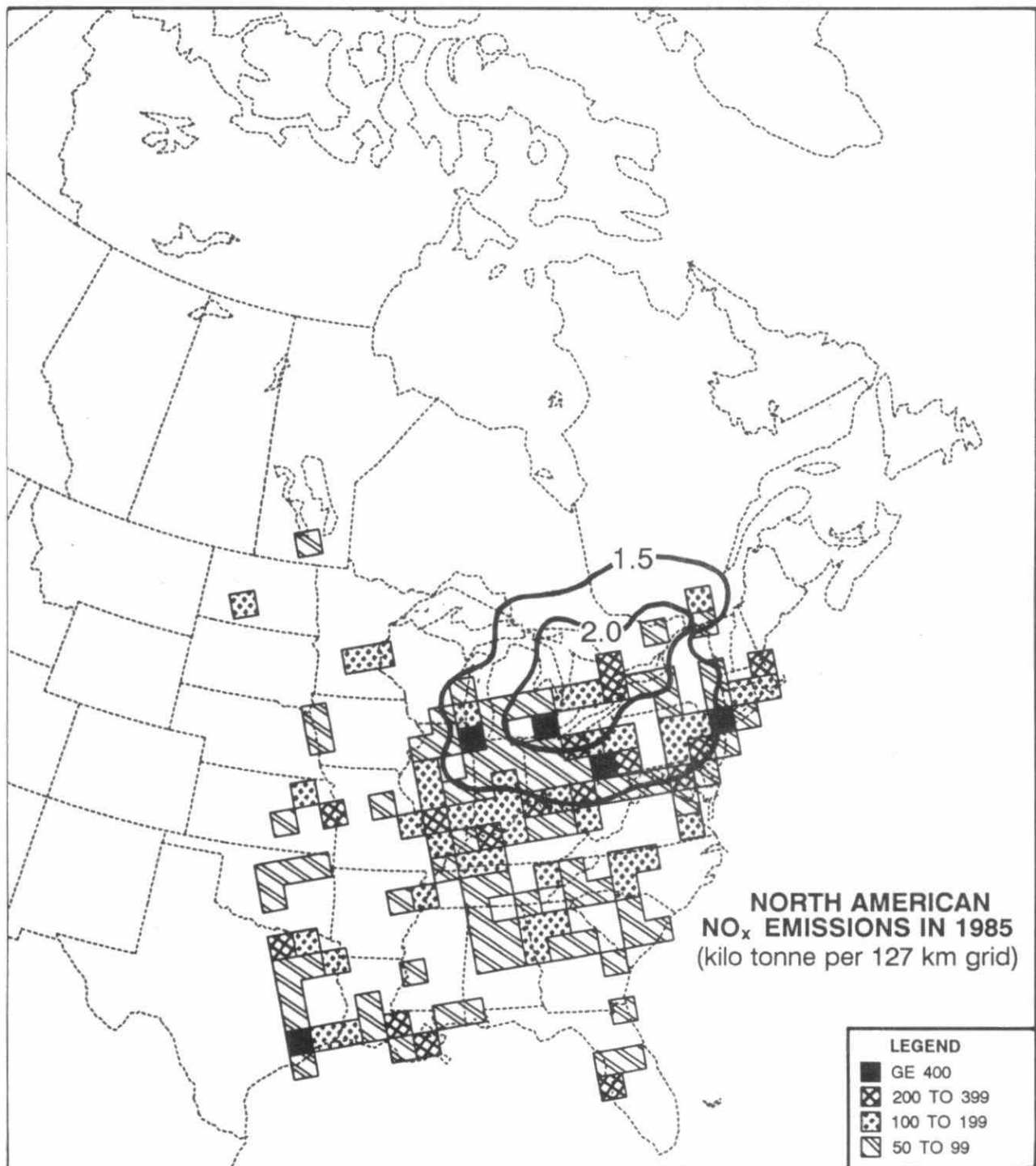


Fig. 3.2.19 Superposition of the 1982-87 six-year-average nitrate concentration isopleths (1.5 and 2 mg/l) on the 1985 NO_x emission pattern.

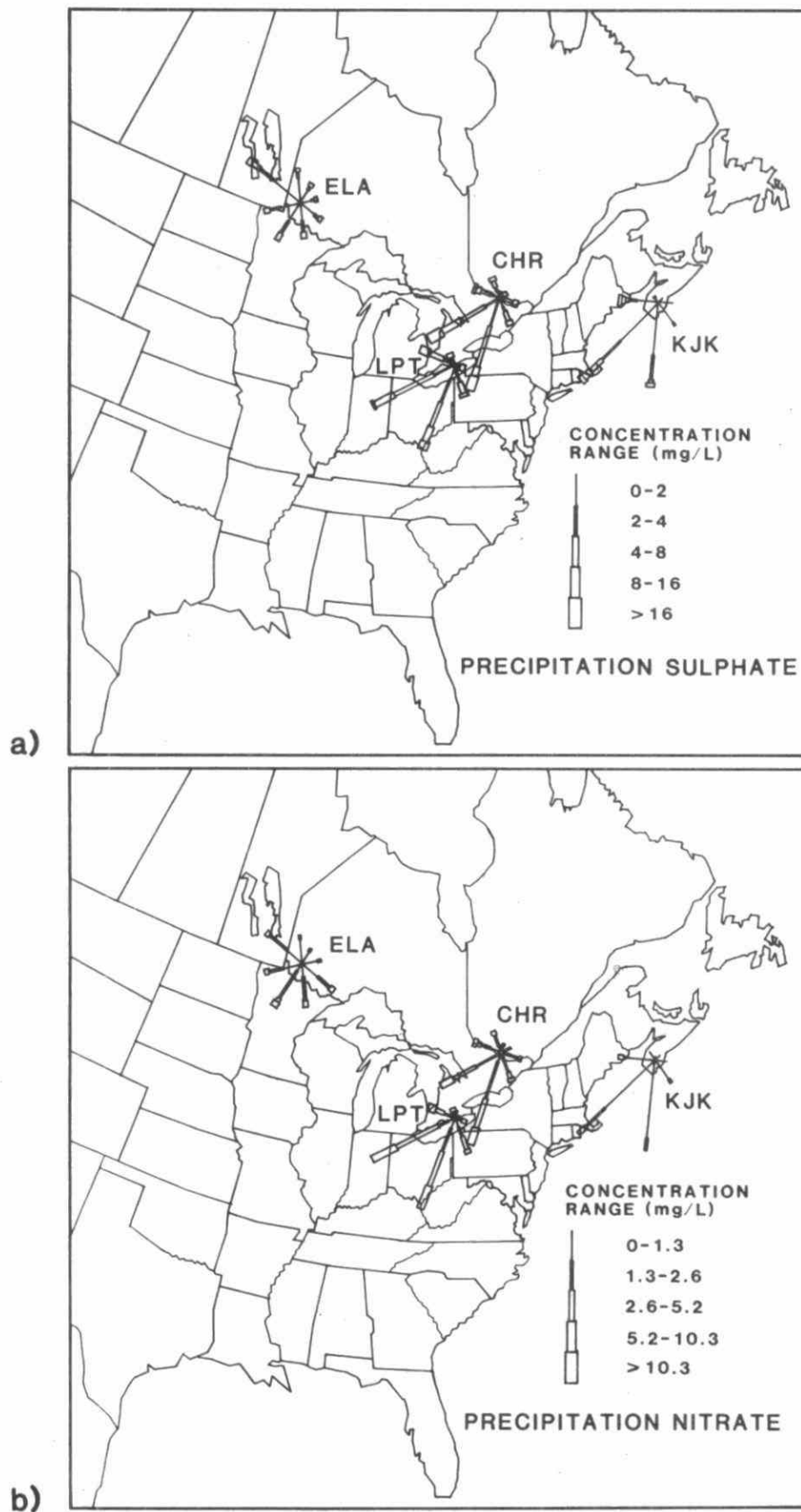
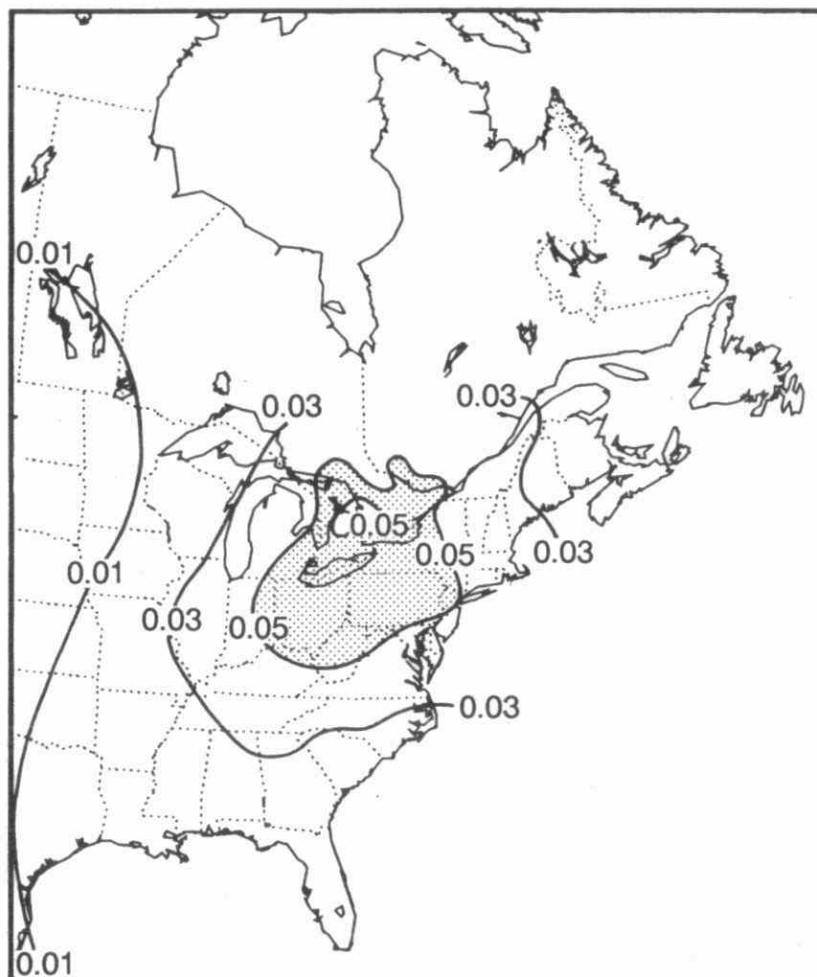


Fig. 3.2.20 Trajectory roses (2-day back trajectories at the 925 mb level) for precipitation sulphate (top) and nitrate (bottom) concentrations measured at several Canadian sites (MOI, 1982).

6-YEAR (1982-87) MEAN H^+ CONCENTRATION
IN PRECIPITATION (mg/l)



6-YEAR (1982-87) MEAN H^+ DEPOSITION (kg/ha/yr)

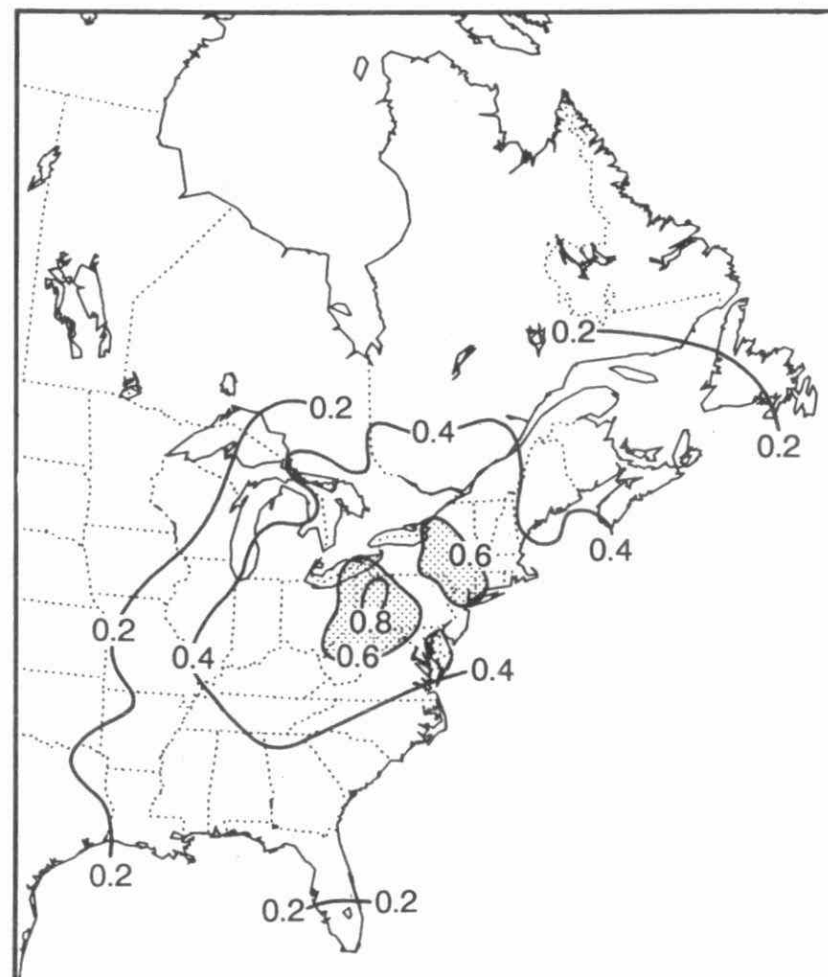
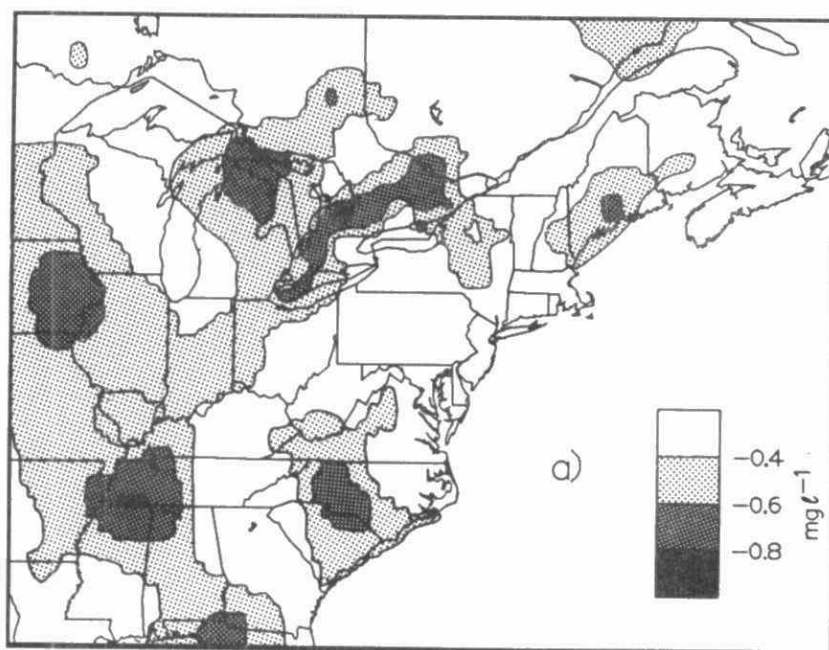


Fig. 3.2.21 Six-year-average (1982-87) concentration and deposition patterns of H^+ .

DIFFERENCE BETWEEN 3-YEAR MEAN (1980-82,1985-87) excess $\text{SO}_4^{=}$ CONCENTRATIONS



% DIFFERENCE BETWEEN 3-YEAR MEAN (1980-82,1985-87) excess $\text{SO}_4^{=}$ CONCENTRATIONS

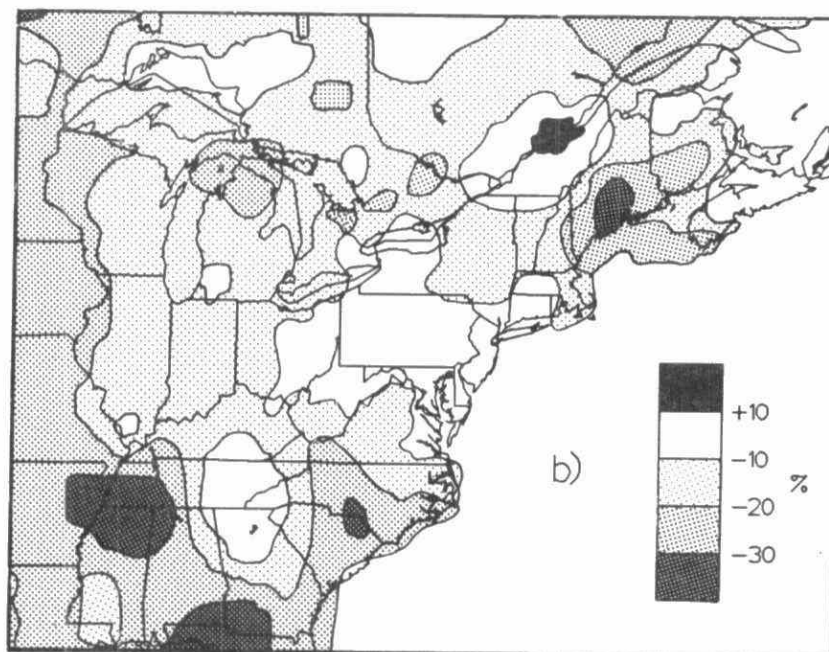
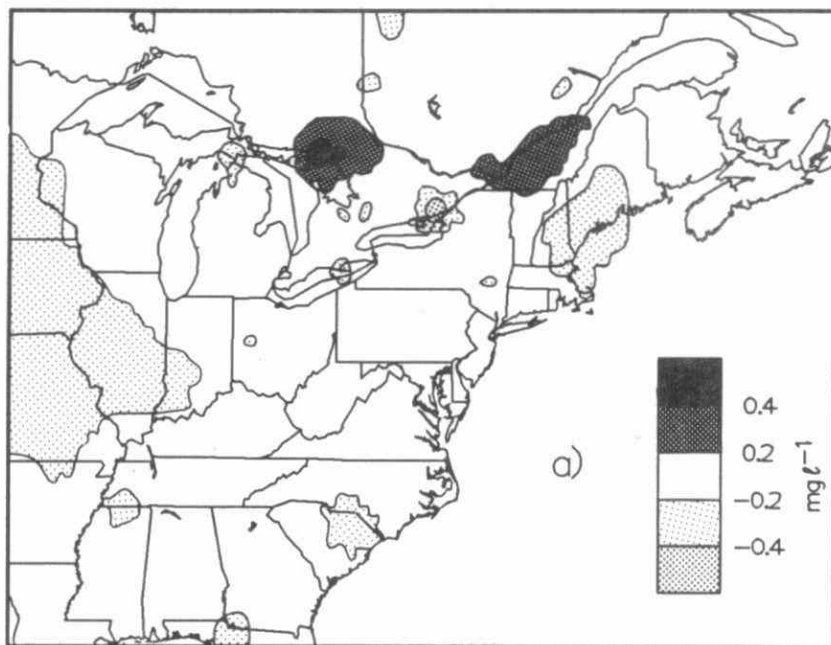


Fig. 3.2.22 Changes in the precipitation-weighted mean concentrations of $\text{SO}_4^{=}$ between the two periods 1980-1982 and 1985-1987 expressed as a spatial pattern of a) absolute changes in mg/l and b) % changes against the first period as the base.

DIFFERENCE BETWEEN 3-YEAR MEAN (1980-82, 1985-87) NO_3^- CONCENTRATIONS



% DIFFERENCE BETWEEN 3-YEAR MEAN (1980-82, 1985-87) NO_3^- CONCENTRATIONS

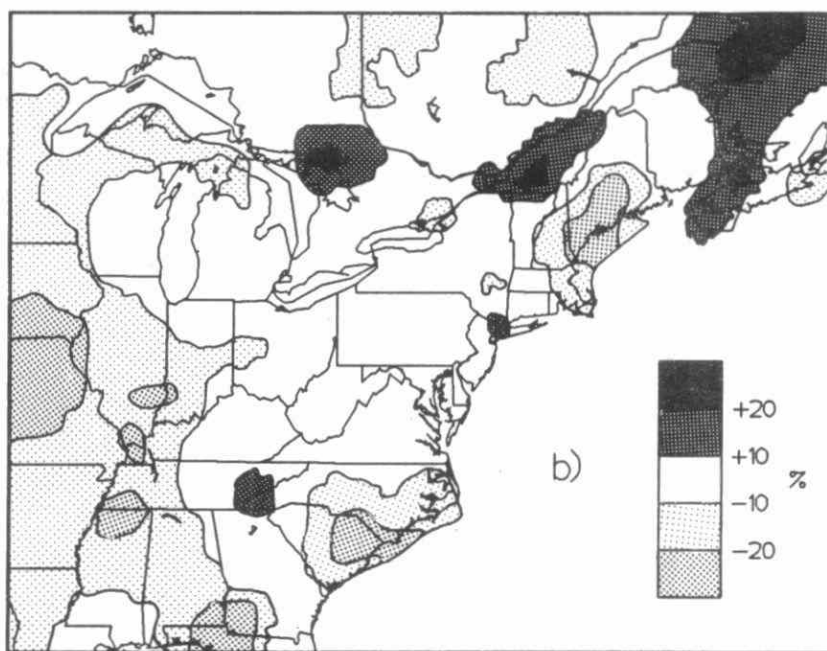


Fig. 3.2.23 Changes in the precipitation-weighted mean concentrations of NO_3^- between the two periods 1980-1982 and 1985-1987 expressed as a spatial pattern of a) absolute changes in mg/l and b) % changes against the first period as the base.

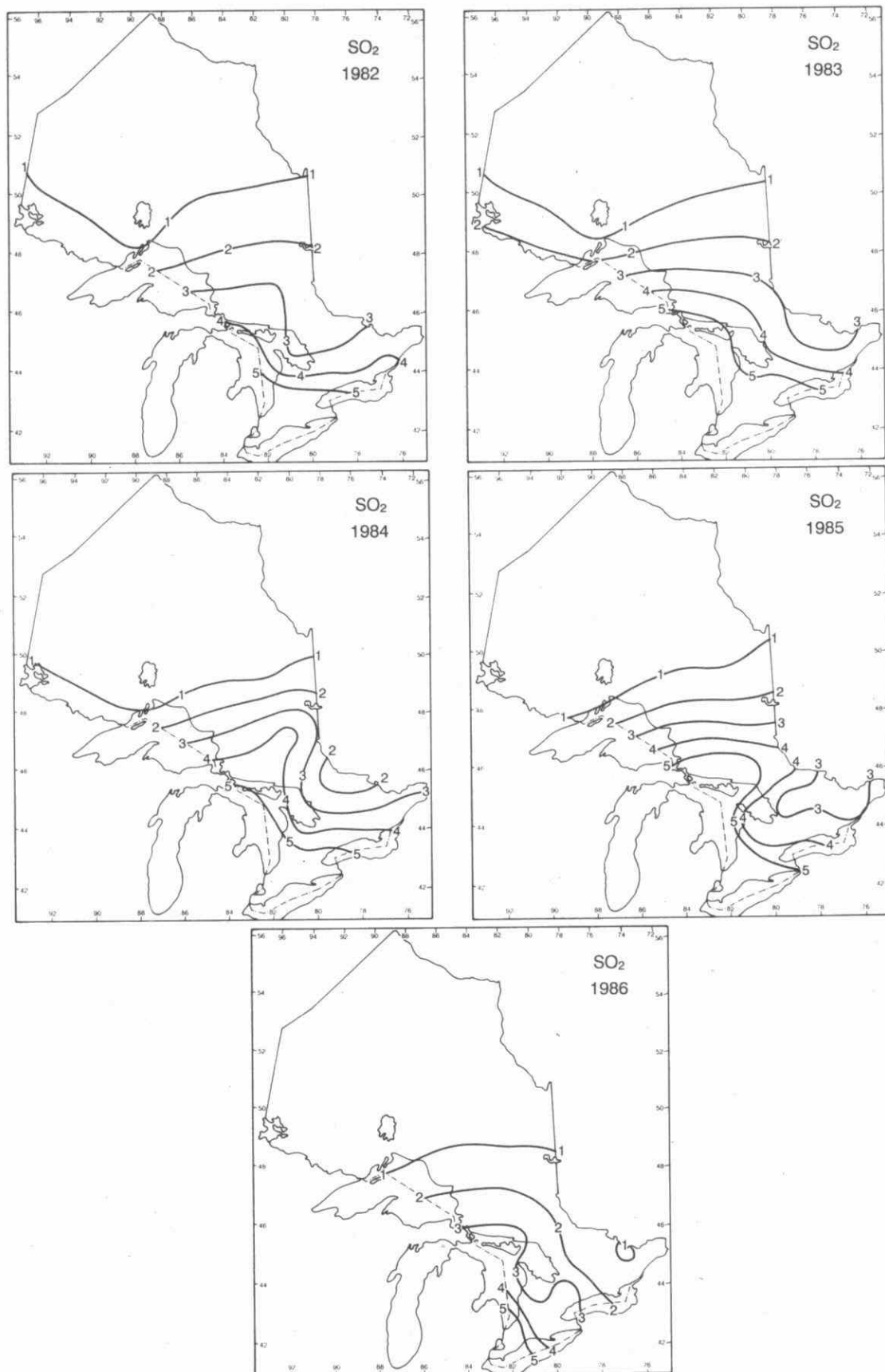


Fig. 3.2.24a Annual average 28-day air concentrations of SO_2 ($\mu\text{g m}^{-3}$) 1982-1986.

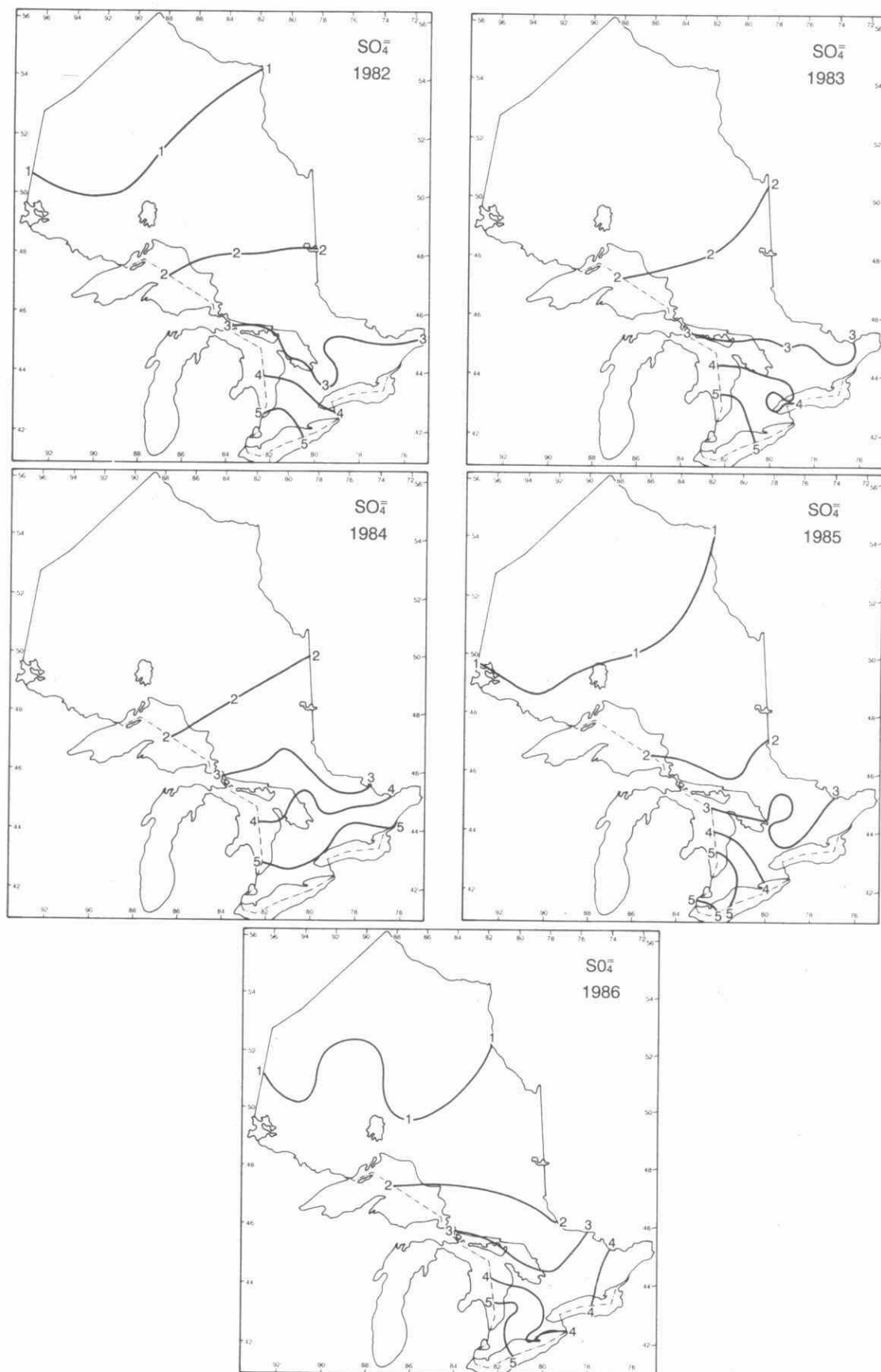


Fig. 3.2.24b Annual average 28-day air concentrations of $\text{SO}_4^{=}$ ($\mu\text{g m}^{-3}$) 1982-1986.

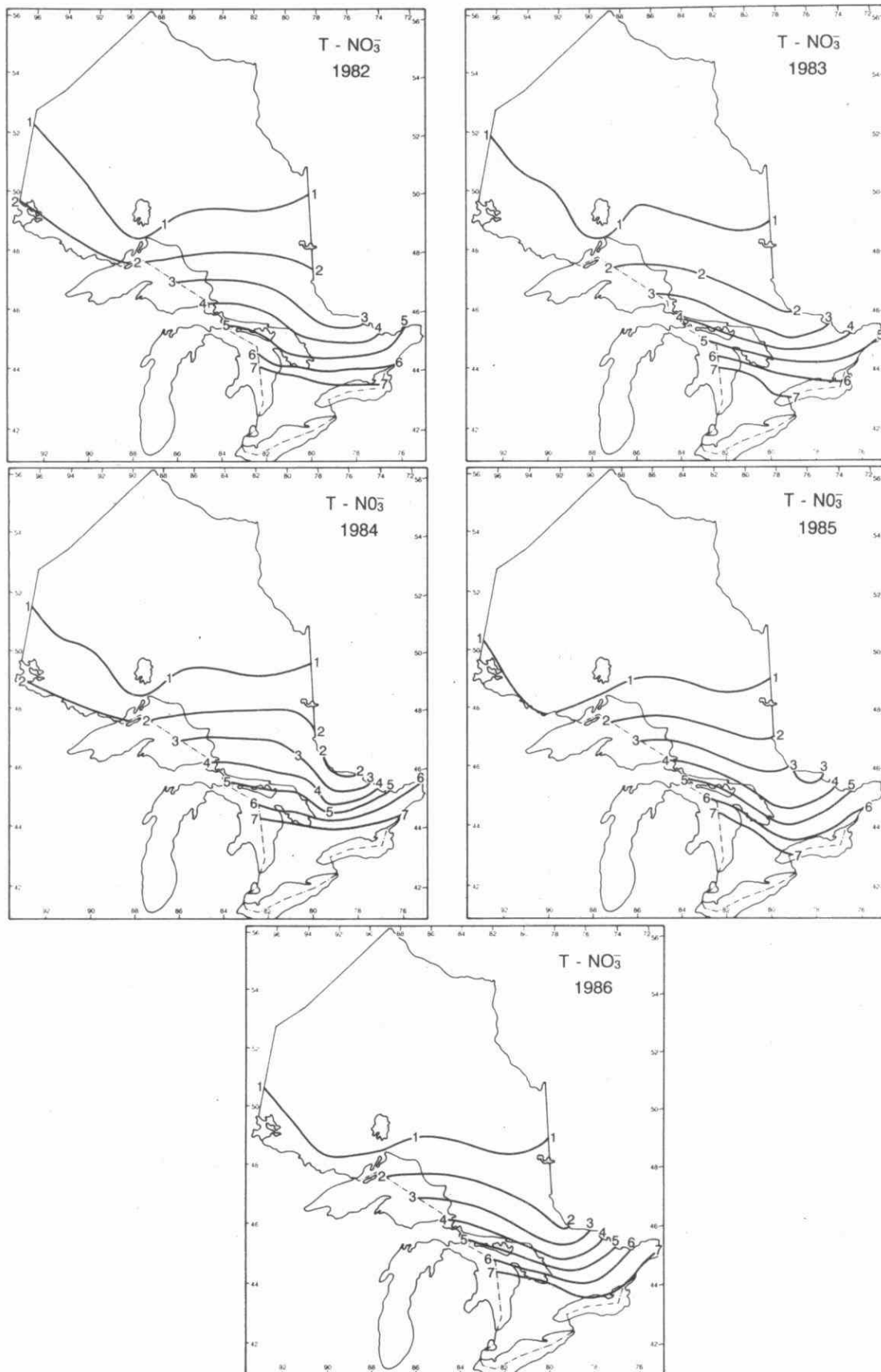


Fig. 3.2.24c Annual average 28-day air concentrations of $t\text{-NO}_3^-$ ($\mu\text{g N m}^{-3}$) 1982-1986.

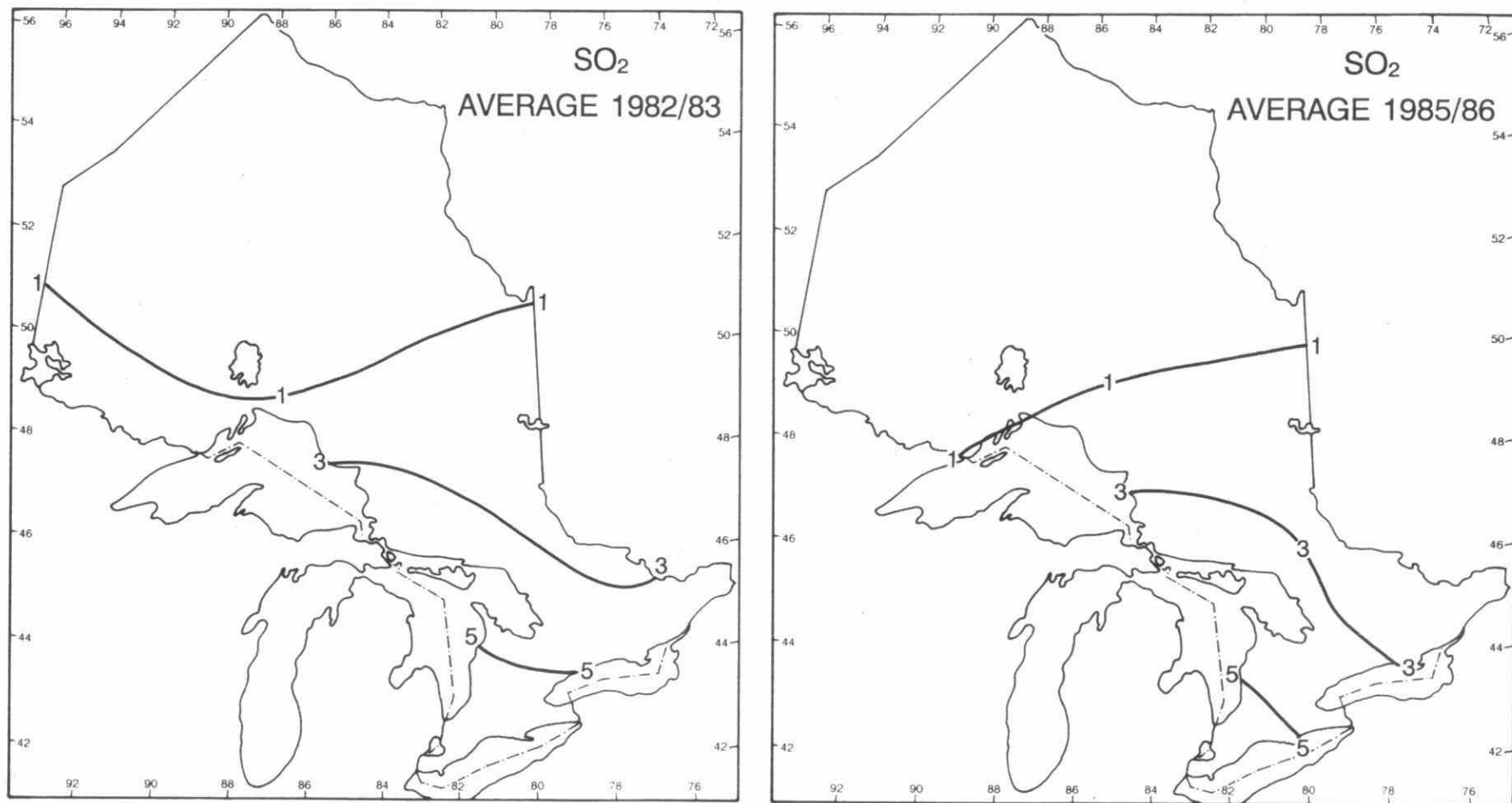


Fig. 3.2.25 Variation of Sulphur Dioxide concentration in air ($\mu\text{g}/\text{m}^3$) in Ontario:1982/1983 compared to 1985/1986.

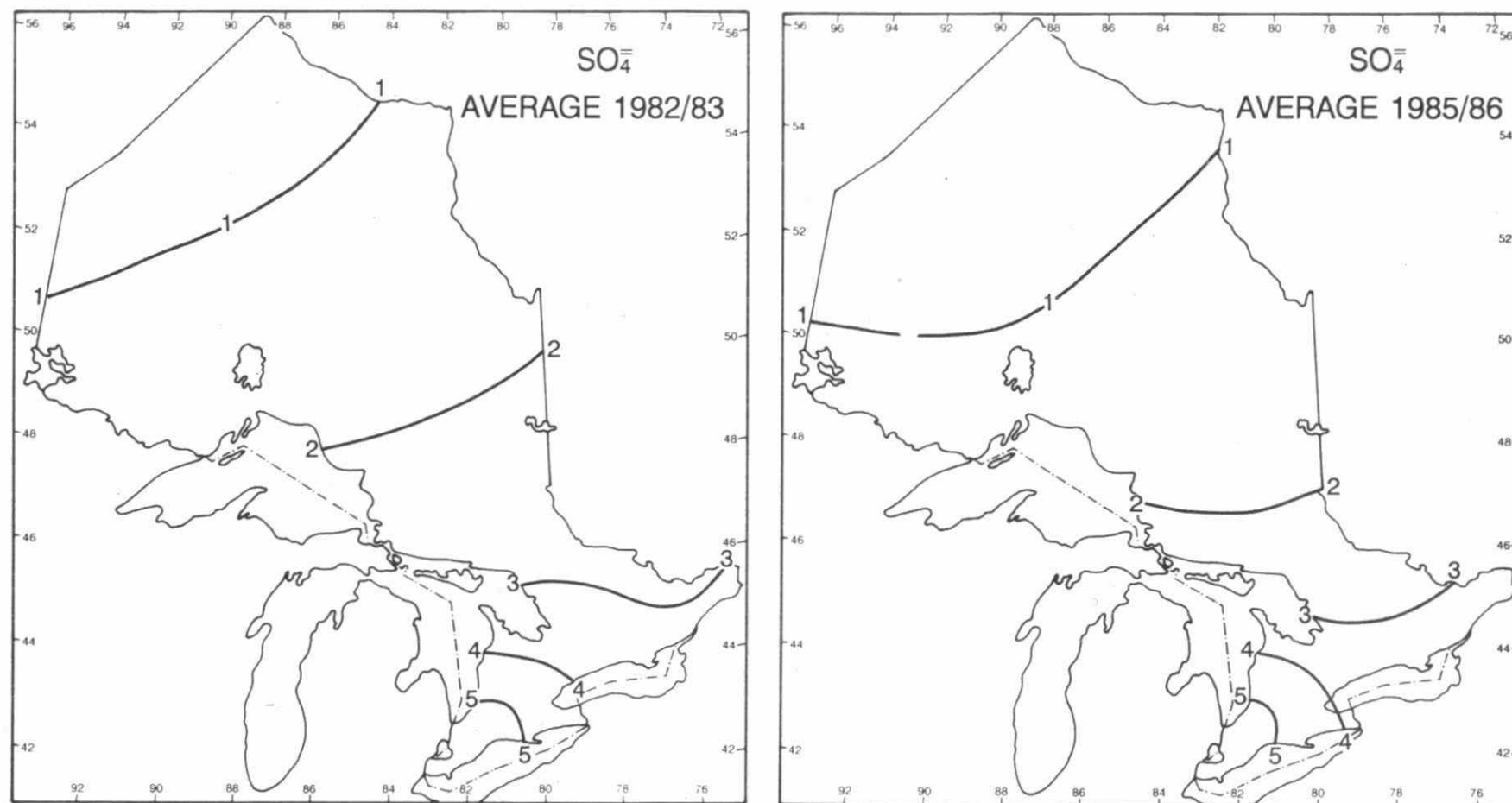


Fig. 3.2.26 Variation of Sulphate concentration in air ($\mu\text{g}/\text{m}^3$) in Ontario: 1982/1983 to 1985/1986.

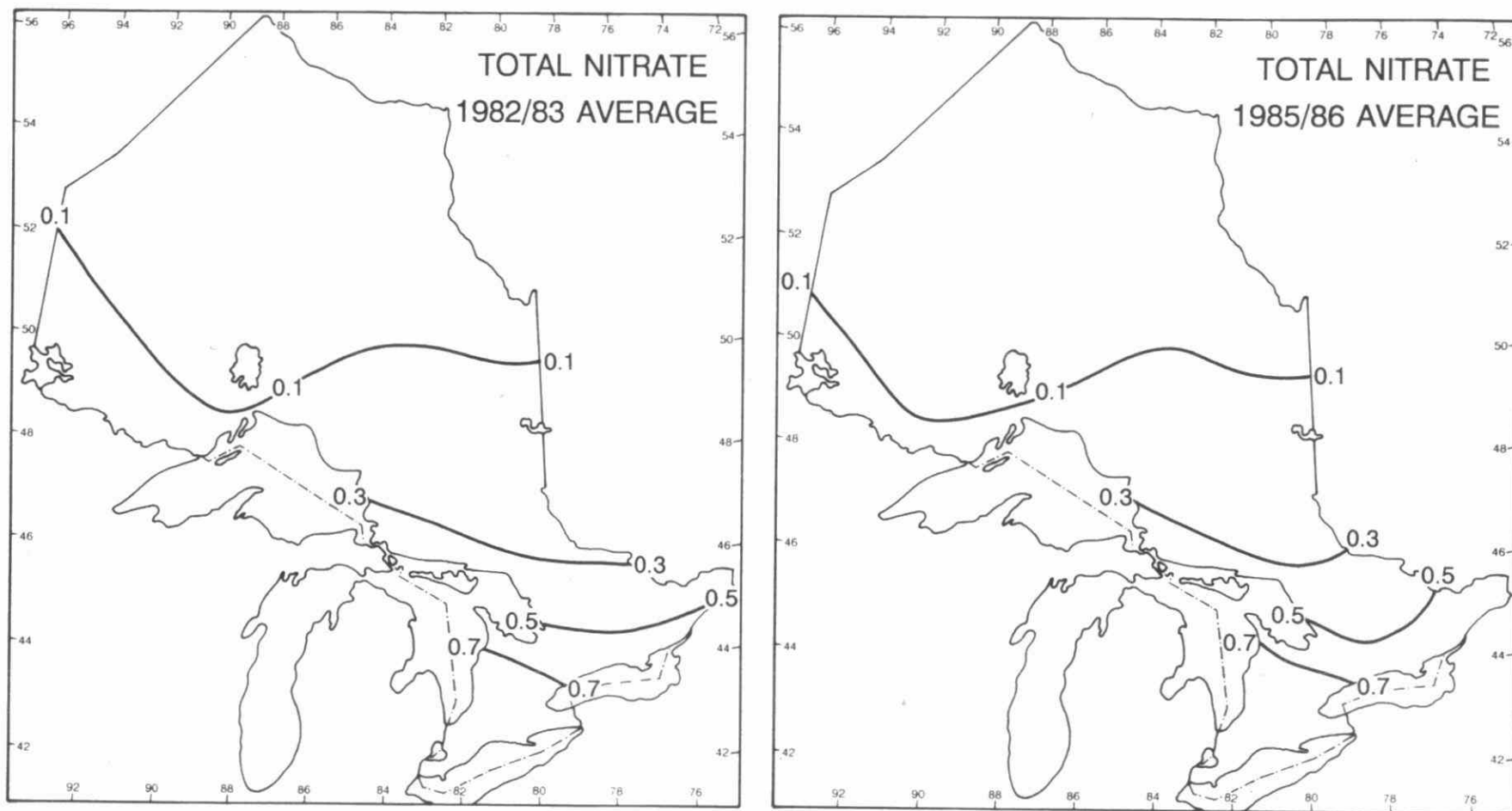


Fig. 3.2.27 Variation in Total Nitrate concentration in air ($\mu\text{g N m}^{-3}$) in Ontario: 1982/1983 compared to 1985/1986.

3.2.3 TRENDS IN OBSERVED ACIDIC CONSTITUENTS IN EASTERN CANADA

There are several studies of trends in point measurements of $\text{SO}_4^{=}$ and NO_3^- in air and precipitation in eastern Canada that, when compared with trends in emissions, may lend insight into the connection between emission sources and air and precipitation acidity at receptors.

3.2.3.a TEMPORAL VARIATIONS OF SULPHATE AND NITRATE IN AIR AND PRECIPITATION AT FIVE FEDERAL SITES IN EASTERN CANADA

Since 1979, the federal government has taken daily air and precipitation chemistry observations at selected rural locations in Canada especially in the east where the acid rain problem is most severe. Appendix 3D presents a detailed time series analysis from 1979 to 1987 of weekly precipitation-amount-weighted mean concentrations of acidic substances in precipitation, and of monthly median concentrations of acidic substances in air at five sites (Figure 3.2.28) not including Dorset. The statistical model used separated the time series into three components: i) a seasonal component ii) a long-term cyclical component having a period longer than a year and less than the length of data record and iii) a long-term trend component. For precipitation, an additional term allowing for the effect of precipitation amount was added to the model.

The results of the analysis are summarized in Tables 3.2.7 and 3.2.8. From the perspective of understanding source-receptor relationships between emissions and air quality at a downwind receptor, the trend in the sum of the long term cyclical and trend components is the salient piece of information. This is plotted for precipitation and air, respectively, in Figures 3.2.29a,b and 3.2.30a,b,c for those sites where it was significant. The plots are normalized by the average concentration in 1980 or the first subsequent complete year of record. For precipitation, the plots represent normalized variations that have been corrected for an inverse dependence of concentration on precipitation amount.

For precipitation $\text{SO}_4^{=}$ and NO_3^- , with the exception of NO_3^- at Chalk River, there was a significant non-seasonal variation at all sites. However, for NO_3^- (Fig. 3.2.29b) most of that variation was in component ii) the long-term cyclical component. No steadily changing increase or decrease was detectable except at Kejimikujik where an increase occurred between 1979 and 1987.

For precipitation $\text{SO}_4^{=}$ (Fig 3.2.29a) a significant long term trend between 1981 and 1987 was evident at all sites. It decreased at all sites except Forêt Montmorency. At this site it peaked in about 1984. The decrease at Kejimikujik is consistent with the observed decrease in Maritime Canada noted in Figure 3.2.22. Changes at Kejimikujik are typical of those occurring in the rest of Nova Scotia as indicated by good agreement with Nova Scotia provincial network observations (Appendix 3E).

In air, significant long term trends (not necessarily monotonically decreasing) were detected for $\text{SO}_4^{=}$ only at Chalk River (Fig. 3.2.30b); for total NO_3^- at Chalk River, Forêt Montmorency and Kejimikujik (Fig. 3.2.30c); and for SO_2 at all sites except Algoma (Fig. 3.2.30a).

Sector stratified trend analysis (SSTA) of air data was applied at two sites: ELA on the western edge of major North American sources and at Kejimikujik on the eastern edge. It involved the same analysis as described above but with monthly median daily data stratified according to compass sector of origin using air parcel back trajectories. At ELA, statistically significant long term trends were encountered only for SO_2 . Between January 1982 and December 1987 the long term component of SO_2 decreased by a factor of 3 to 4 for all sectors.

At Kejimikujik, a similar analysis revealed long term trends in particulate $\text{SO}_4^{=}$ for all sectors except that to the southwest where large sources on the US east coast are located. The same was true for total NO_3^- except one additional sector towards the east into the Atlantic showed no trend. For SO_2 at Kejimikujik all sectors showed significant decreases of a factor of 2 to 10 between 1981 and 1987. The largest decrease was in the sector off the Atlantic Ocean (which includes Halifax). Between 1980 and 1985 SO_2 emissions from two thermal generating stations in Halifax decreased from 25713 to 5521 tonnes per annum (J. Underwood, personal communication). The lowest decrease was in the southwest sector (the US east coast).

This analysis makes clear two important facts. Firstly, that more complicated models than a simple linear long-term trend and an annual cycle are necessary to describe the temporal variation of concentrations of acidic substances in air and precipitation. Secondly, that although long-term variations can be detected, care is required to link them with temporal variation in emissions of the order of 18 to 30%, since many factors including the meteorological variability, length of observational record and continuity of observational method are involved.



Fig. 3.2.28 Map showing long term air and precipitation monitoring sites.

Table 3.2.7

Summary of results of time series analysis
of SO_4^- and NO_3^- concentration in precipitation at 5 rural locations
in eastern Canada.

N is the number of data used and R^2 is the fraction of the total variance explained by the model.
"Y" means that model component is present and "N" that it is not present.

ION	SITE	N	R^2	PREC. DEPTH	LONG TERM TREND	LONG TERM CYCLE	ANNUAL CYCLE
SO_4^-	E.L.A.	318	.34	Y	Y	Y	Y
	ALGOMA	302	.19	Y	Y	Y	Y
	CHALK RIVER	363	.34	Y	Y	N	Y
	MONTMORENCY	257	.27	Y	Y	N	Y
	KEJIMKUJIK	364	.31	Y	Y	N	Y
NO_3^-	E.L.A.	269	.19	Y	N	Y	Y
	ALGOMA	291	.15	N	N	Y	Y
	CHALK RIVER	325	.17	Y	N	N	Y
	MONTMORENCY	248	.06	Y	N	Y	Y
	KEJIMKUJIK	347	.20	Y	Y	N	Y

Table 3.2.8

Summary of results of time series analysis
for SO_4^{2-} , SO_2 and Total NO_3^- concentration in air at 5 rural locations
in eastern Canada.

N is the number of data used and R^2 is the fraction of the total variance explained by the model.
"Y" means that model component is present and "N" that it is not present.

ION	SITE	N	R^2	LONG TERM TREND	LONG TERM CYCLE	ANNUAL CYCLE
SO_4^{2-}	E.L.A.	103	.52	N	Y	Y
	ALGOMA	84	.17	N	N	Y
	CHALK RIVER	105	.27	Y	Y	N
	MONTMORENCY	80	.35	N	Y	Y
	KEJIMKUJIK	98	.35	N	Y	Y
SO_2	E.L.A.	79	.71	Y	Y	Y
	ALGOMA	79	.71	N	Y	Y
	CHALK RIVER	104	.80	Y	N	Y
	MONTMORENCY	65	.77	Y	N	Y
	KEJIMKUJIK	83	.78	Y	Y	Y
TNO_3^-	E.L.A.	102	.37	N	Y	Y
	ALGOMA	83	.12	N	N	Y
	CHALK RIVER	103	.40	Y	Y	Y
	MONTMORENCY	76	.19	Y	N	Y
	KEJIMKUJIK	98	.24	Y	N	Y

LONG-TERM TREND AND CYCLE

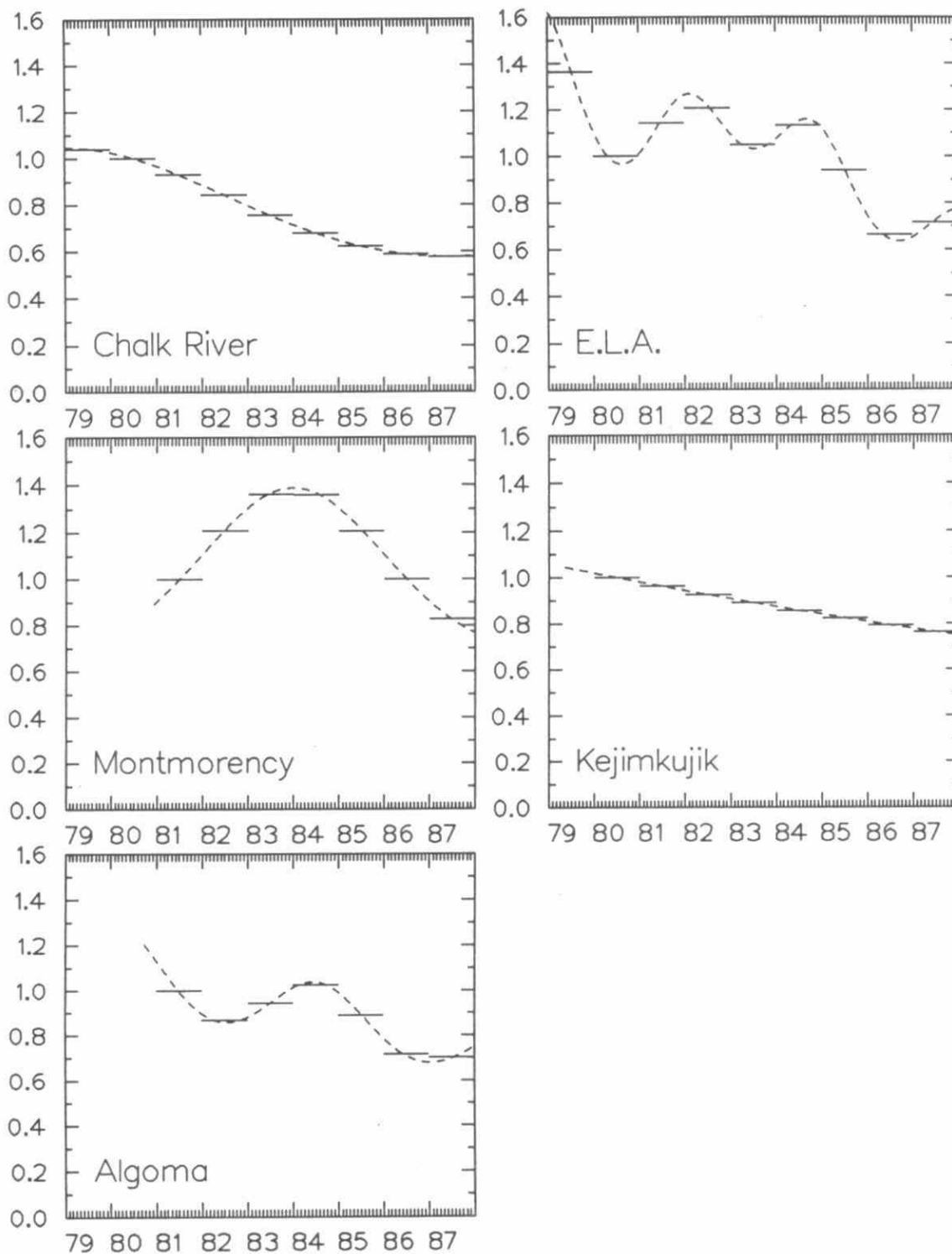


Fig. 3.2.29a Significant normalized precipitation $\text{SO}_4^{=}$ concentration trends (corrected for influence of precipitation amount and seasonal cycles removed).

LONG-TERM TREND AND CYCLE

NO_3^-

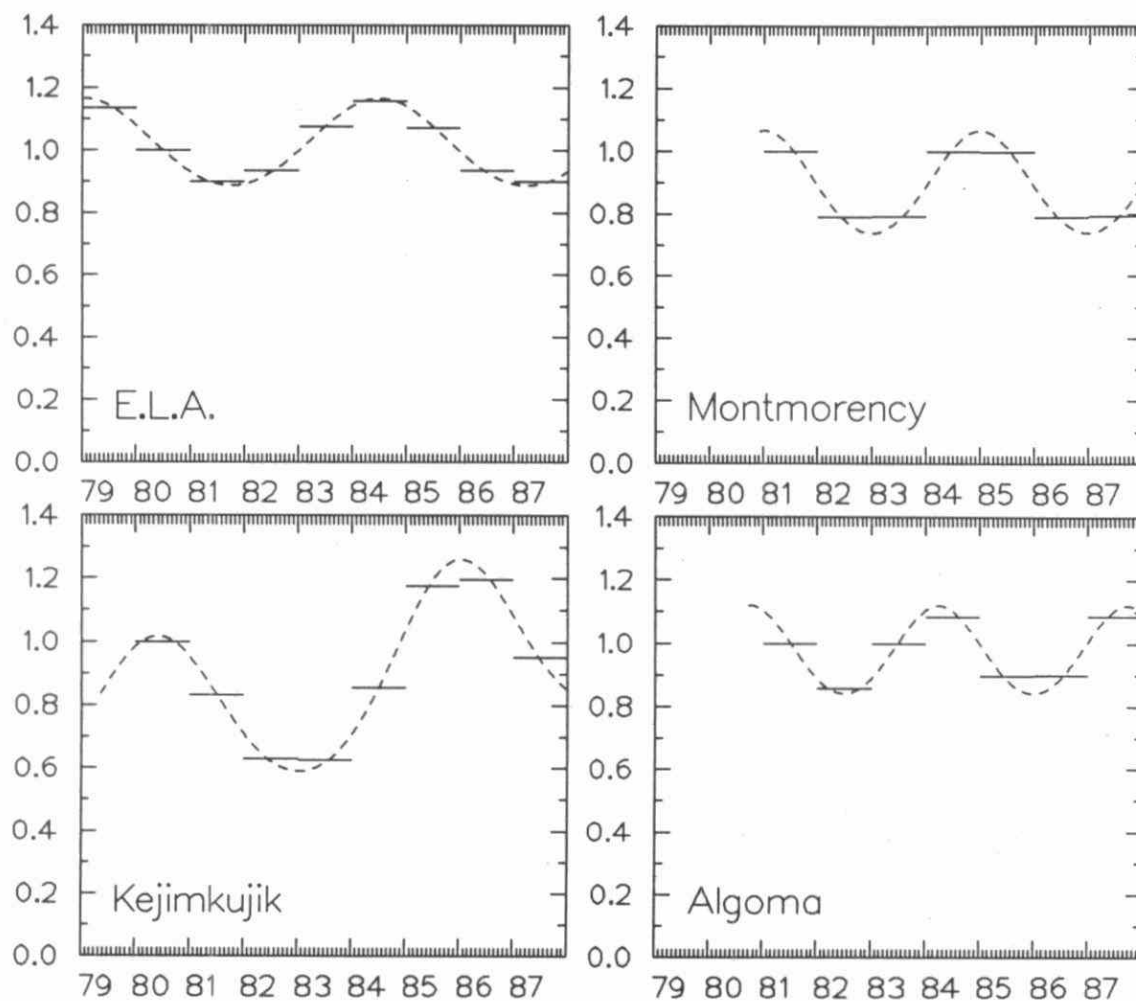


Fig. 3.2.29b Significant normalized precipitation NO_3^- concentration trends (corrected for influence of precipitation amount and seasonal cycles removed).

LONG-TERM TREND AND CYCLE

SO₂

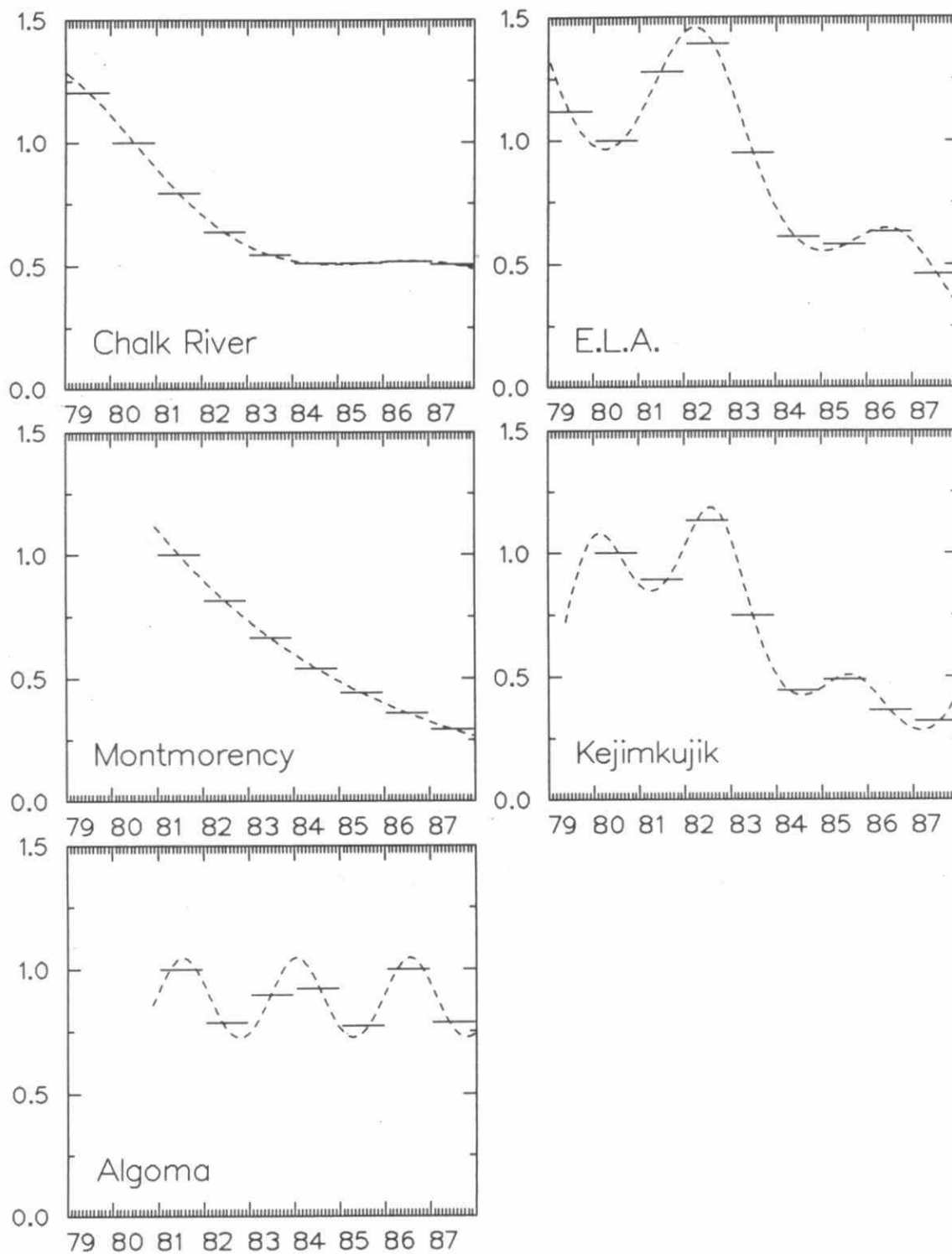


Fig. 3.2.30a Significant normalized air SO₂ concentration variations (seasonal cycles removed).

LONG-TERM TREND AND CYCLE

$\text{SO}_4^{=}$

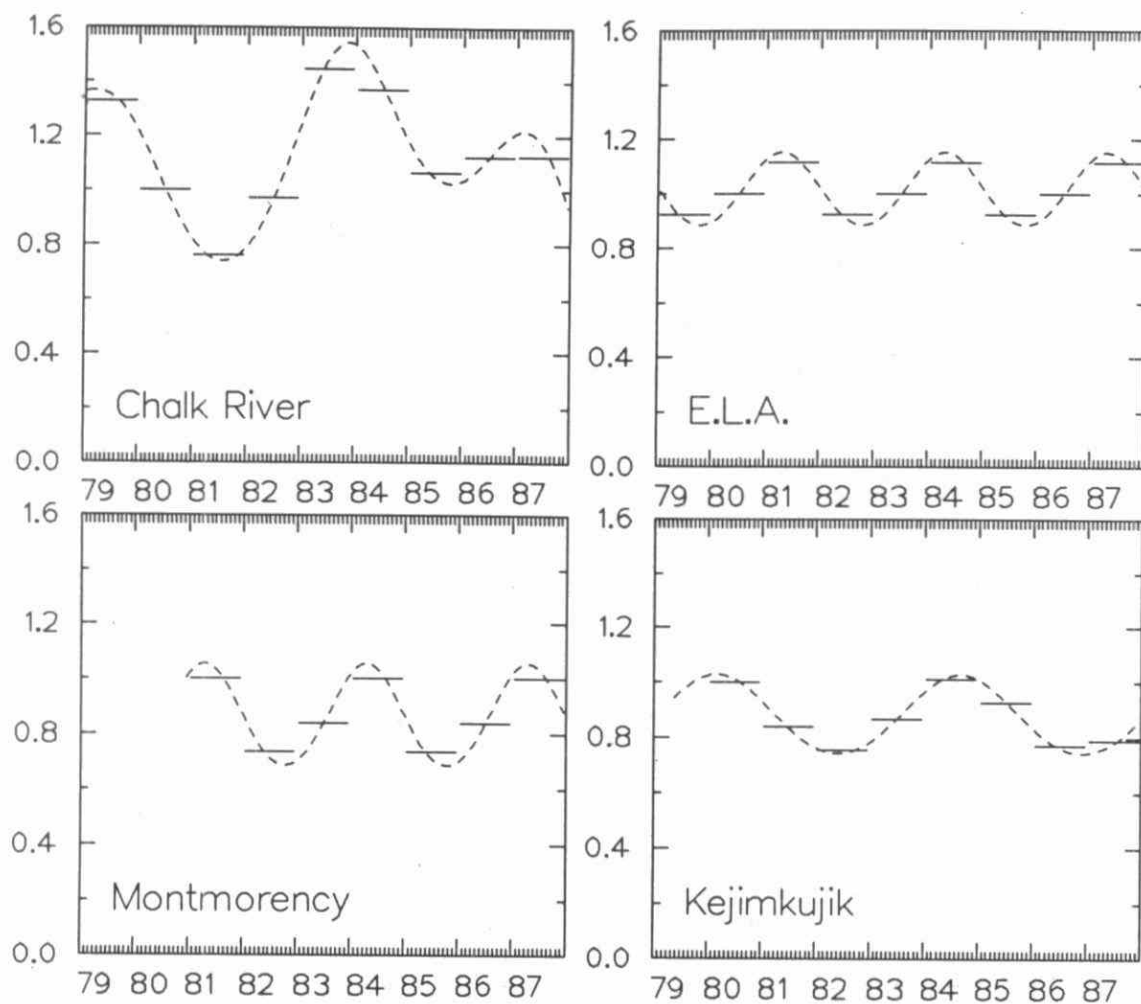


Fig. 3.2.30b Significant normalized air $\text{SO}_4^{=}$ concentration variations (seasonal cycles removed).

LONG-TERM TREND AND CYCLE

Total NO_3^-

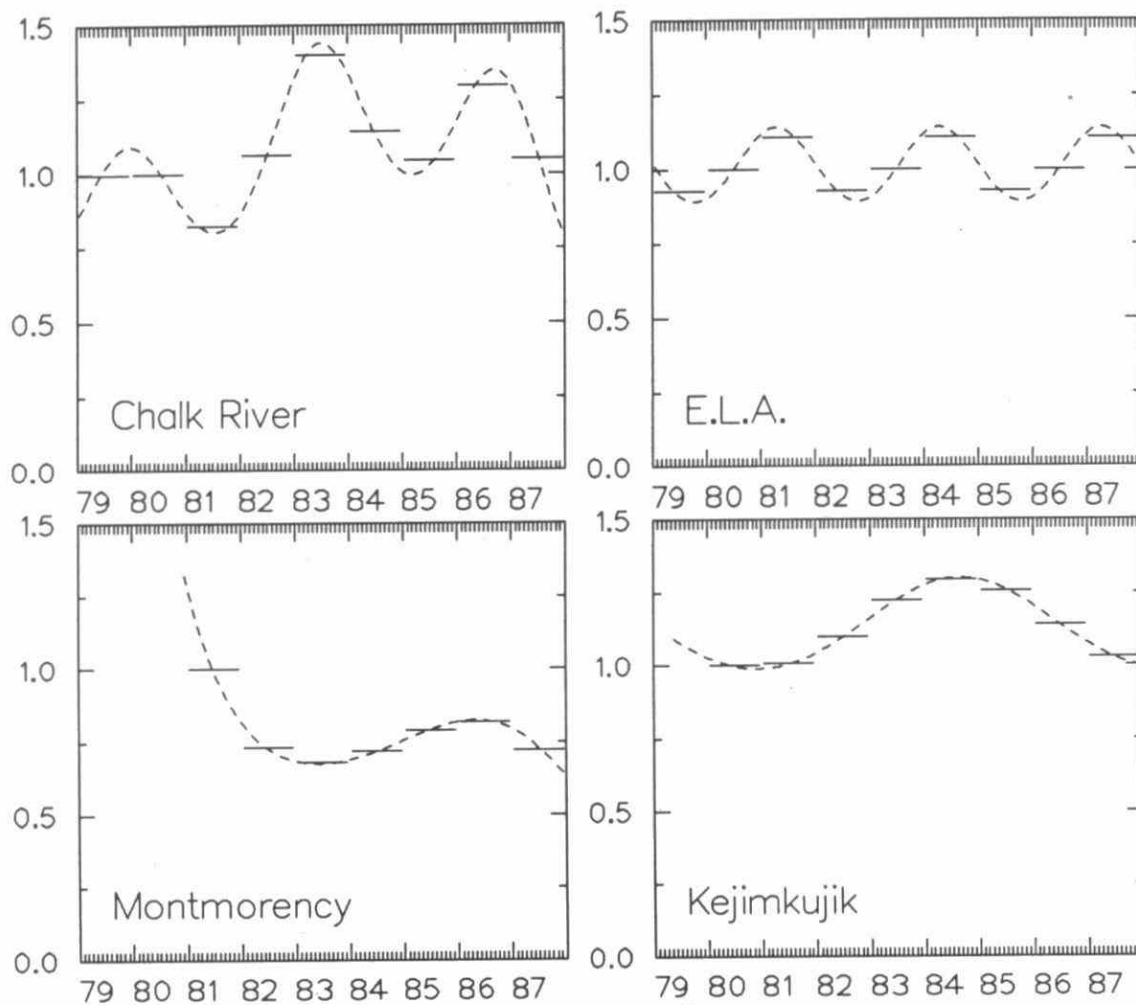


Fig. 3.2.30c Significant normalized air NO_3^- concentration variations (seasonal cycles removed).

3.2.3.b TEMPORAL VARIATIONS OF INTEGRATED WET DEPOSITION OF SULPHATE AND NITRATE IN EASTERN NORTH AMERICA

The analysis in the previous section considered the long-term variations in precipitation chemistry at a few single stations. In this section, the annual wet deposition of sulphate and nitrate integrated over the whole of eastern North America will be considered. The area selected for the integration is shown in Figure 3.2.31. The grid points shown on the figures were the ones used to produce the contour maps in Section 3.2.2.b. The values of deposition for each grid square multiplied by the area (adjusted for the map projection) are then summed over the whole area to produce the values shown in Table 3.2.9.

Plots against time of the annual wet deposition of excess $\text{SO}_4^{=}$ (corrected for sea-salt) and of NO_3^- , together with the SO_2 and NO_x emissions, are shown in Figure 3.2.32 a) and b) respectively. In both cases, the numbers are normalized to 1980 as unity. It can be seen that for sulphur, the integrated deposition is tracking closely to the change in SO_2 emissions with time. This is further illustrated in Figure 3.2.33a showing the correlation between emissions and deposition. The Pearson correlation coefficient is 0.91 and is highly significant at the 99% level.

The best-fit line, over the range of values available, shows an almost one-to-one relationship between excess $\text{SO}_4^{=}$ wet deposition and SO_2 emissions. Between the two periods 1980-1982 and 1985-1987, the SO_2 emissions in ENA decreased by 13.5% (see Table 3.2.5) and the regionally integrated wet excess $\text{SO}_4^{=}$ deposition decreased by about 17.5% (Table 3.2.9).

In contrast, between the two periods NO_x emissions showed no significant trend, just year-to-year variations of $\pm 4\%$ with the last three years 2% lower than the first three (Table 3.2.5). The wet NO_3^- deposition showed a year-to-year variation of $\pm 5\%$ with the last three years 5.1% lower than the first three. Figure 3.2.33b shows that there is not a significant correlation between NO_3^- and NO_x emissions. These variations are probably well within the uncertainties of the estimates and indicate no significant change over the period of either NO_x emissions or wet NO_3^- deposition.

Uncertainty Analysis

An analysis was done to ascertain the uncertainty introduced into the calculation of the integrated areal deposition value due to the interpolation errors in the contouring method. Using estimates of variance generated by the krigging technique for the individual grid points, the standard deviation (σ) for the integrated areal deposition was determined for each year and for the early and late period 3-yr averages. For both $\text{SO}_4^{=}$ and NO_3^- the values for σ were highest in 1980 and 1981 and showed a sharp drop in 1982. During the period 1982 through 1986 the value of σ stayed almost constant, decreasing again in 1987. The values for the beginning and end of the period are summarized in Table 3.2.10.

Table 3.2.9

**Total annual deposition integrated over the area shown in Figure 3.2.31
for eastern North America over the period 1980-1987.**

Units: MT yr⁻¹

	1980	1981	1982	1983	1984	1985	1986	1987	80-82	85-87
SO ₄ ⁻	10.68	10.51	10.18	9.20	9.38	8.97	8.57	8.32	10.45	8.62
NO ₃ ⁻	6.04	5.36	5.78	5.61	5.83	5.66	5.37	5.27	5.73	5.44

Table 3.2.10

Standard error of the integrated wet deposition of SO_4^- and NO_3^-
and the deposition values $\pm 3\sigma$ at the beginning and end of the period.

	Standard Deviation(σ) (MT yr ⁻¹)		Integrated Deposition $\pm 3\sigma$ (MT yr ⁻¹)	
	1980	1987	1980	1987
SO_4^-	0.082	0.049	10.68 \pm 0.25	8.32 \pm 0.15
NO_3^-	0.056	0.035	6.04 \pm 0.17	5.27 \pm 0.10

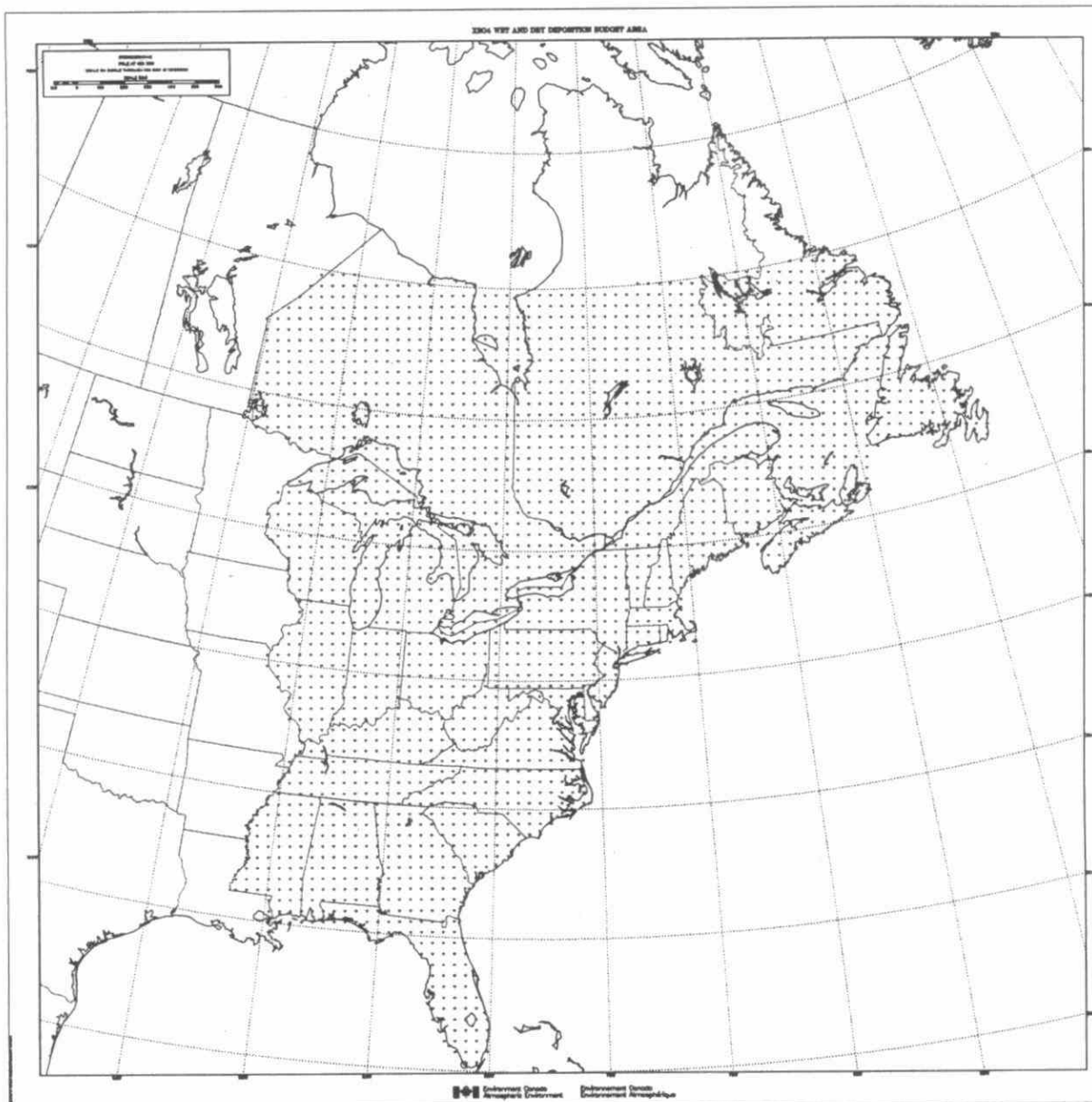


Fig. 3.2.31 Area used to obtain the integrated wet deposition of SO_4^{2-} and NO_3^- over eastern North America.

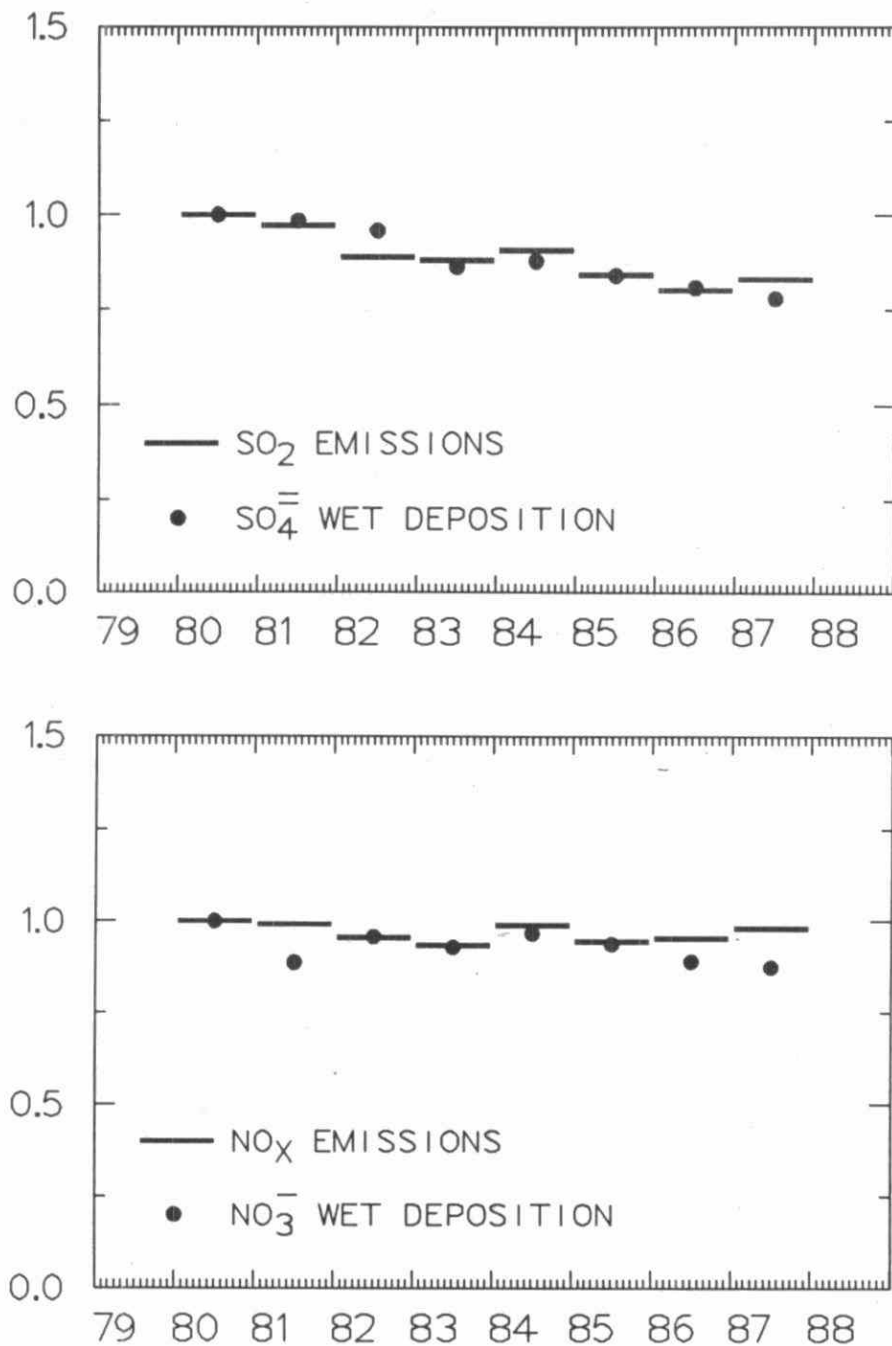


Fig. 3.2.32 Time series showing the annual emissions and annual integrated wet deposition over eastern North America from 1980 to 1987. (a) SO_2 and excess $\text{SO}_4^{=}$ (b) NO_x and NO_3^- . All values are normalized to 1980 as unity.

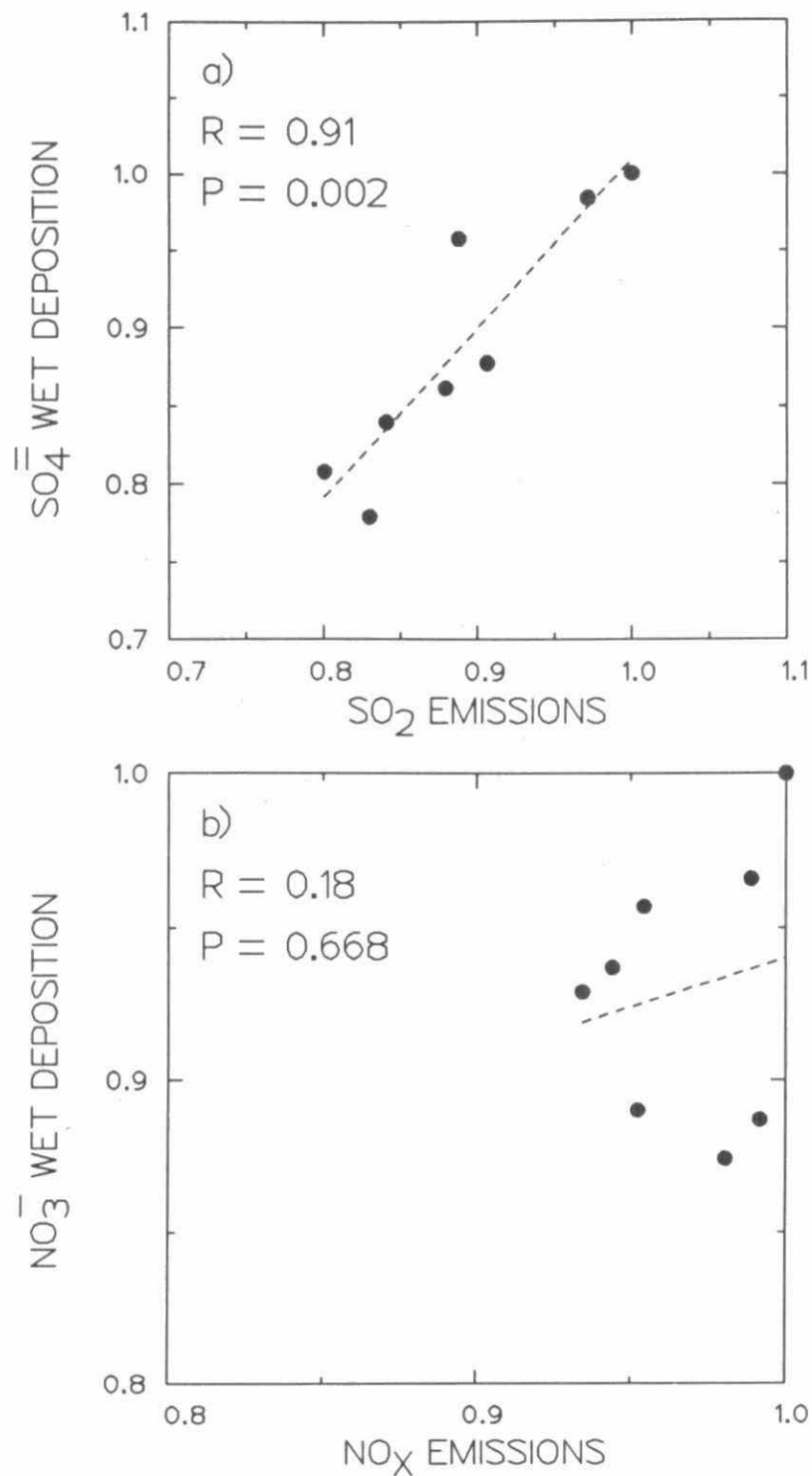


Fig. 3.2.33 Correlation between the annual emissions and integrated annual wet deposition over eastern North America from 1980 to 1987. (a) excess SO_4^{2-} (b) NO_3^- . All values are normalized to 1980 as unity. The best fit regression lines and Pearson correlation coefficient (R) are included.

The table shows that, assuming the point observations are accurate, the integrated deposition can be determined to within very narrow limits. In 1980 the $\pm 3 \sigma$ error estimate was about $\pm 2.5\%$ and by 1987 was reduced to $\pm 2.0\%$ showing that the density of existing networks is adequate to satisfactorily estimate annual integrated wet deposition values.

It is possible that the year-to-year variations in the integrated deposition estimates (Table 3.2.10) may be caused, at least partially, by year-to-year changes in the number of measurement data available in each year. In specific terms, one can reasonably question whether the small number of measurement sites available in the years 1980 through 1983 (i.e., 53, 86, and 134 respectively), compared to the later years 1985 to 1987 (195, 191, and 170 respectively) could artificially induce interpolation uncertainties.

A sensitivity test was done to investigate this effect. The results indicate that the uncertainties in the integrated deposition values caused by the smaller number of sites in the early years are relatively low. The tests were done by re-estimating the 1981 through 1987 integrated deposition values (Table 3.2.9) using only those sites (53 in total) that were operating in 1980. In some years, 1980 sites that were no longer operating were replaced by the nearest available site. The differences between the integrated deposition values based on the full suite of sites versus those calculated based on the 1980 subset of sites ranged from -0.129 to +0.402 MT (i.e., -1.4% to +4.5% of the original deposition estimates) – considerably lower than the differences seen in the integrated deposition values from the earlier to later years.

Table 3.2.10 shows that, the one standard deviation bar on the wet deposition values plotted in Figure 3.2.32 would not be much wider than the width of the dot. Thus the time changes in the integrated values are well outside the bounds of any errors caused by the integration technique itself, or by the changes in the numbers of monitoring sites over the period.

Since the wet deposition of SO_4^{2-} and NO_3^- are both controlled by the same meteorology and precipitation events, the preceding analysis shows that both are responding in a consistent way to the behaviour of the emissions.

It is concluded from the above analysis that over large space scales and long time periods the wet deposition of sulphate is clearly responding in a close to linear fashion to changes in the precursor SO_2 emissions.

3.2.3.c TEMPORAL VARIATIONS OF SULPHATE AND NITRATE CONCENTRATIONS IN AIR AND PRECIPITATION AT DORSET ONTARIO.

A classical time series analysis was carried out for data collected at Dorset, a rural site located in central Ontario (Appendix 3F). The location of the Dorset site is shown in Figure 3.2.28. The time period covered by these data is mid-1981 to 1986. The chemical species included in the analysis were sulphate and nitrate in precipitation, and

total sulphur (from the sum of sulphate and sulphur dioxide) and total nitrate (particulate nitrate plus gaseous nitric acid) in air. The analysis was applied to seasonal averages of concentration, and the statistical model took the form:

$$D = T \times S \times C \times I,$$

where D is the time series of the seasonal concentrations (the data)
 T is the trend component
 S is the seasonal component
 C is the cyclical component (a repetitive component with a period longer than one year), and
 I is the irregular component.

The time series of the data are presented in Figure 3.2.34.

Significant decreasing trends with time were observed for sulphate in precipitation, and for total sulphur in air, but nitrate concentrations in air and precipitation showed little change. The actual changes were approximately 30% for sulphate in precipitation, and close to 40% for total sulphur in air. This is consistent with observed variations in air and precipitation chemistry at Chalk River (Fig. 3.2.29 and 3.2.30) and with the changes in spatial patterns shown in Fig. 3.2.22 and 3.2.23. As can be seen from Figure 3.2.34, most of this decrease occurred in the first year or two of the data record. It is interesting to note that the largest decreases for sulphate in precipitation were seen for summer, spring and autumn, while the winter season has shown little change. This may mean that the concentrations of sulphate measured at Dorset during the winter correspond to background levels, since the amount of oxidation and scavenging of sulphur dioxide is at a minimum during the winter.

The seasonal cycle is well developed for sulphate in precipitation, but less so for the other three parameters considered.

An inverse correlation was observed between precipitation depth and the irregular component, which was interpreted as describing the dependence of concentration on precipitation amount. From this correlation an adjustment factor was derived which allows concentrations to be normalised to a standard precipitation amount. The effect of the adjustment is seen in Figure 3.2.35a,b which contains time series plots of sulphate and nitrate concentrations in precipitation after normalisation to a common precipitation depth. This process, by eliminating the major effect of meteorological variability, sharpens up the definition of the seasonal cycles and the long term trend (if any).

Fig. a Seasonal sulfate concentration
in precipitation

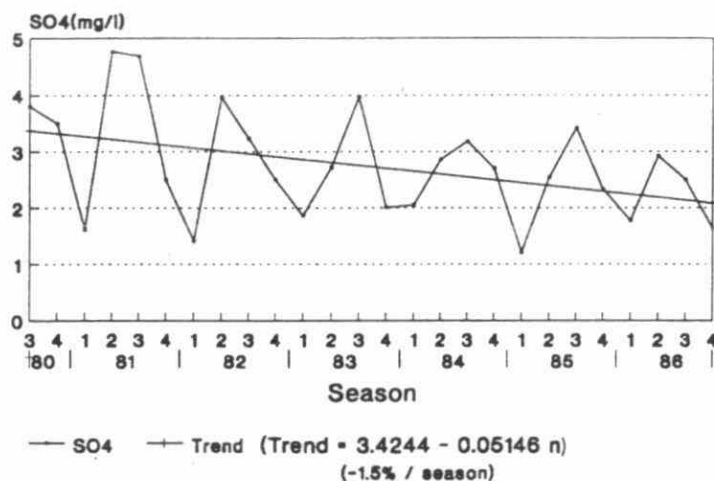


Fig. C Seasonal total sulfur
concentration in air

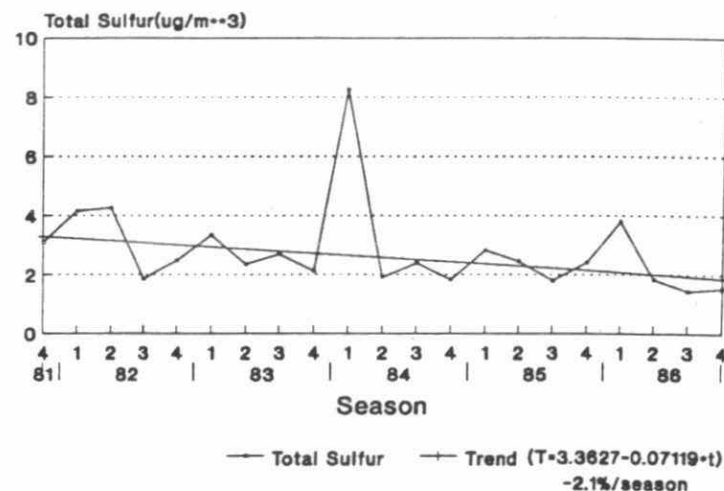


Fig. b Seasonal Nitrate concentrations
in precipitation

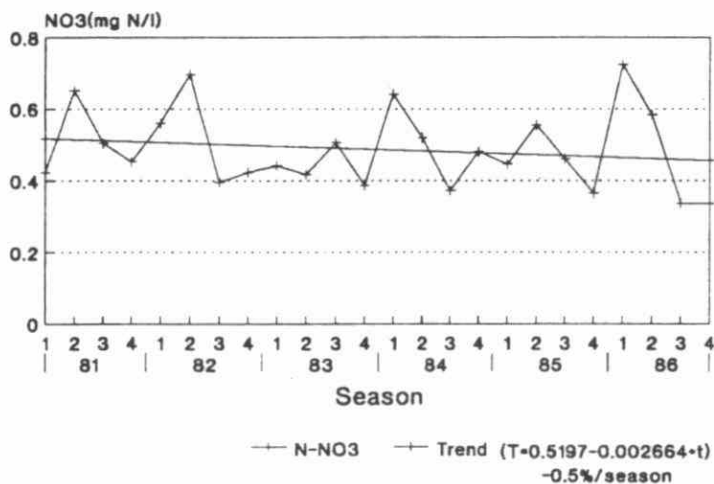


Fig. d Seasonal total nitrate
concentration in ambient air

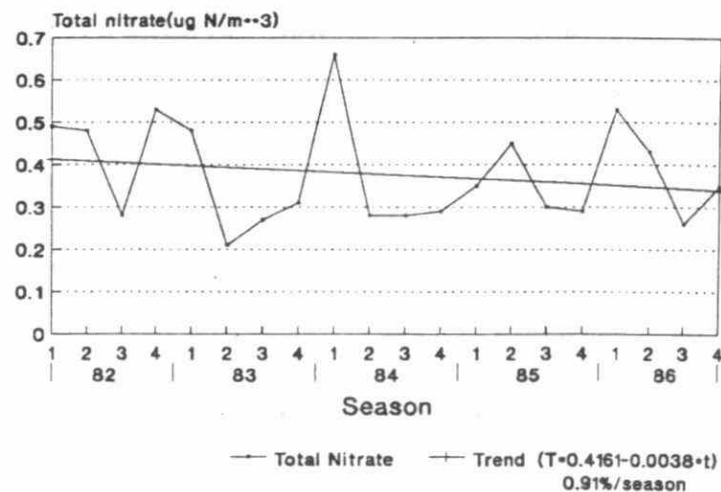


Fig. 3.2.34 Temporal variation of sulphate and nitrate concentrations in air and precipitation at Dorset, Ontario.

3.2.3.d SOURCE-RECEPTOR RELATIONSHIPS FROM EMISSION-DEPOSITION PATTERN ASSOCIATIONS IN QUEBEC

For the province of Quebec, a few studies on the statistical analysis of trends in some acid precipitation parameters have been done:

- (i) In a recent thesis, Vachon (1988) has done a statistical analysis on the temporal evolution of the concentration of three ions ($\text{SO}_4^{=}$, NH_4^{+} and NO_x), using data from four sites (including Forêt Montmorency) of the Quebec precipitation sampling network over a five year period (1982-1986). Descriptive statistics tend to indicate a seasonal component in the $\text{SO}_4^{=}$, NH_4^{+} and NO_x series, and a downward trend in the NH_4^{+} series at one site and in the NO_x at another location. Vachon has shown that this apparent seasonalities and trends are not supported by the Box and Jenkins time series models that he has used in his study.
- (ii) Pinard (1989) has examined the evolution with time of two environmental quality indicators, namely a sulphate indicator and a pH indicator, from 1981 to 1986. The pH indicator is defined as the annual total precipitation with a pH less than or equal to 4.6 for a homogeneous region. The sulphate indicator is defined as the percentage of weekly precipitation having a sulphate concentration larger than or equal to 32 $\mu\text{eq/l}$ (1.54 mg/l) on an annual basis and for a homogeneous region.

The two indicators follow approximately the same trends, characterized by a minimum value in 1983. This is not consistent with the variations in precipitation $\text{SO}_4^{=}$ observed at Montmorency (Fig. 3.2.29a) which peaked in 1983/84. For the whole of Quebec, Pinard has found a significant correlation coefficient of 0.85 between the indicators, which confirms the well-known relationship between pH and sulphates.

He has also examined the temporal evolution of the total anthropogenic SO_2 emissions from the U.S., Ontario and Quebec for the years 1982 to 1985 inclusive. The total emissions show a relative minimum in 1983, but the correlation with the above-mentioned $\text{SO}_4^{=}$ and pH indicators are not significant.

Finally, Pinard has calculated the two correlations between the annual average of the weekly precipitation and the two indicators. The correlation with the $\text{SO}_4^{=}$ indicator has a value of -0.83 and is significant at the 95 percent level.

He points out that more than five years of observations will be necessary in order to clearly demonstrate the existence of possible trends in the acidity of precipitation.

Fig. a Precipitation amount corrected
seasonal sulfate concentration

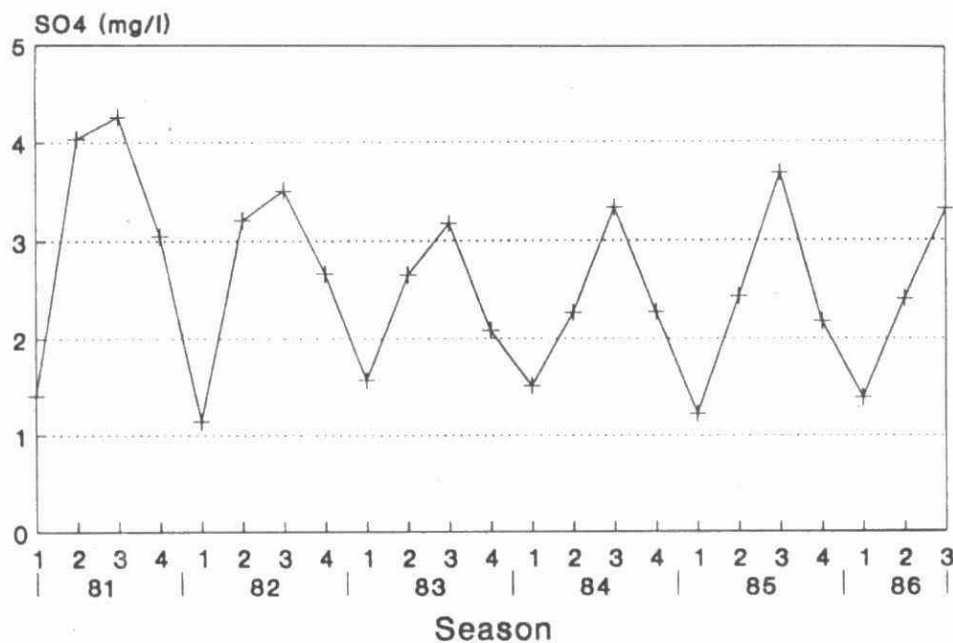
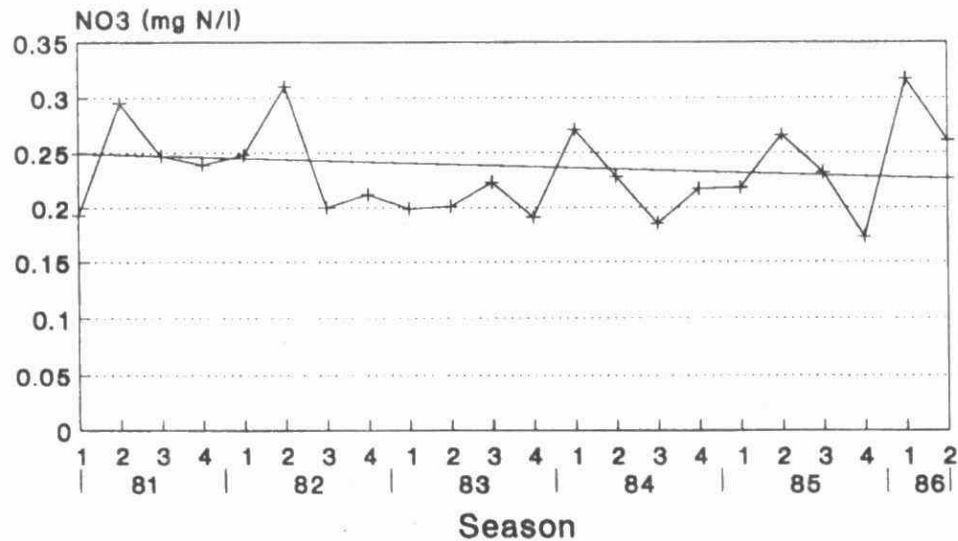


Fig. b Precipitation amount correct
seasonal nitrate concentration



—+— NO3 —+— Trend ($T=0.2505-0.001107 \cdot t$)
-0.44%/season

Fig. 3.2.35 Precipitation amount corrected seasonal sulphate and nitrate concentrations at Dorset, Ontario.

3.2.3.e TRENDS IN SURFACE OZONE CONCENTRATIONS IN ONTARIO

Ozone can be a product of photochemical smog in which nitrogen oxides and hydrocarbons react in the presence of sunlight. It is therefore linked with the acidic precipitation problem. The ozone trend and life-cycle over Ontario have been studied by numerous researchers since the mid-1970's (e.g. Chung, 1977; Yap et al., 1977, 1988; Shenfeld et al., 1978; Mukammal et al., 1982, 1985; Davis et al., 1984, 1986; Heidorn and Yap, 1986; Kurtz et al., 1989). At present, there is a network of 47 ozone stations in Ontario to investigate the potential of long-range transport of ozone into Ontario and to provide information to assess the damage of ozone to crops. Results from this network for the past decade (based on 23 stations where a 10-year record exists) show that, except for 1988, the provincial mean ozone level has remained relatively constant (Fig. 3.2.36a). There is some variability at specific sites but no apparent trend. The data also show that Ontario's air quality criterion for ozone (80 ppb 1-h average) is frequently exceeded (Fig. 3.2.36b). There is no particular trend in these ozone excursions but in 1988, summer ozone levels were unusually high, and exceedences occurred most often. The ozone exceedences are confined primarily to the summer months and are strongly influenced by meteorological conditions, particularly synoptic motion systems. Elevated ozone levels which tend to cover large regions of eastern North America (including southern Ontario) are found typically on the rear sides of anticyclones or in the warm sectors of cyclones. To analyze ozone episodes and their relationship to meteorological conditions, "episode-days" are defined as days on which widespread (hundreds of kilometres) elevated ozone levels (greater than 80 ppb maximum hourly concentration) occurred simultaneously at more than eight monitoring sites and "episodes" are defined as distinct events associated with episode days.

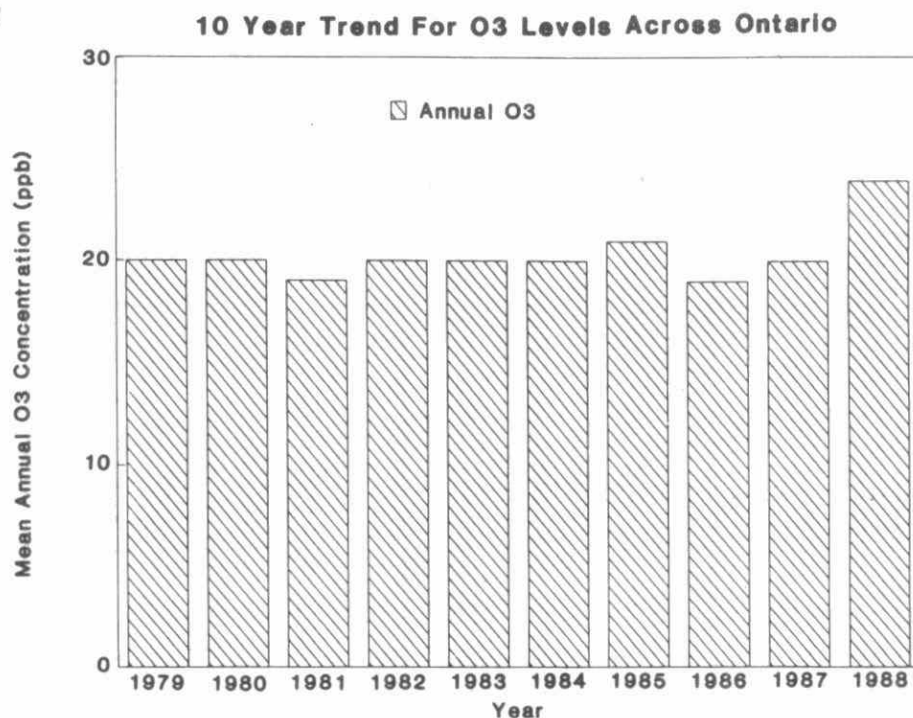
"Episode-days" in southern Ontario for the period 1979-1988 occurred on average 16 times per year with a maximum of 36 such days in 1988 and a minimum of 7 in 1982. The frequency of O_3 episode days using 2-day back trajectories of air parcels for 1979 to 1985 (Yap et al., 1988), indicates that trajectories generally reach southern Ontario from the south/southwest paths over heavily industrialized and urban areas of the U.S., which are potential source regions of O_3 and its precursors (Fig. 3.2.37). In addition, episodic conditions in southern Ontario for the period 1979-1988 invariably occurred with flows from the U.S. (about 95% of the cases during the 10 year period). The widespread occurrences of elevated O_3 levels in southern Ontario are often not unique to Ontario at any given time, but are possibly manifestations of the northern extent of the O_3 problem in eastern North America.

It has been established that high concentrations of O_3 can be generated and transported downwind of moderate to large cities. For southern Ontario, such an effect has been noted previously for areas to the east and northeast of Metropolitan Toronto and to the east of Sarnia (e.g. Lusis et al., 1976, 1985). Figure 3.2.38 depicts the spatial pattern of the average hourly O_3 maxima for the 164 episode-days during 1979-1988. In this figure there is a depression of O_3 levels in the urbanized Toronto-Hamilton area which can be

attributed to local scavenging by NO. There is some suggestion of elevated O₃ levels downwind of the Detroit-Windsor-Sarnia area, but a similar effect downwind (i.e. northeast) of the Toronto-Hamilton corridor is not evident. Climatologically, it would seem that for southern Ontario, local impacts on O₃ levels are generally small and, therefore, local control measures will be relatively ineffective in lowering exceedences of the air quality criterion for O₃.

In conclusion, an examination of ozone data in Ontario for the past decade indicates that there is no apparent long term trend in ground level ozone concentrations. This is consistent with the relatively constant NO_x emission rates in the region, although there is no solid information on the concurrent variations of hydrocarbon emissions (the other precursor of ozone). Meteorological analysis of the ozone data has clearly demonstrated the importance of emission sources in the United States to ozone air quality standard violations in southern Ontario.

a)



b)

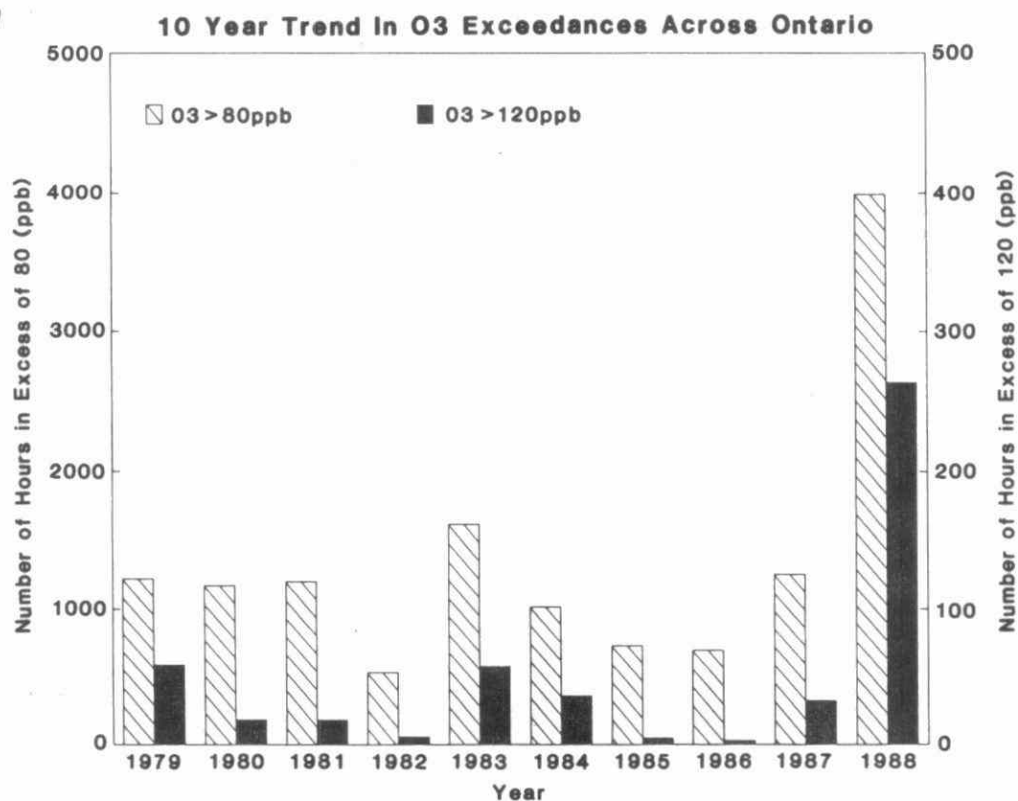


Fig. 3.2.36 Ten year trends for O₃ concentrations and 80 ppb exceedences across Ontario.

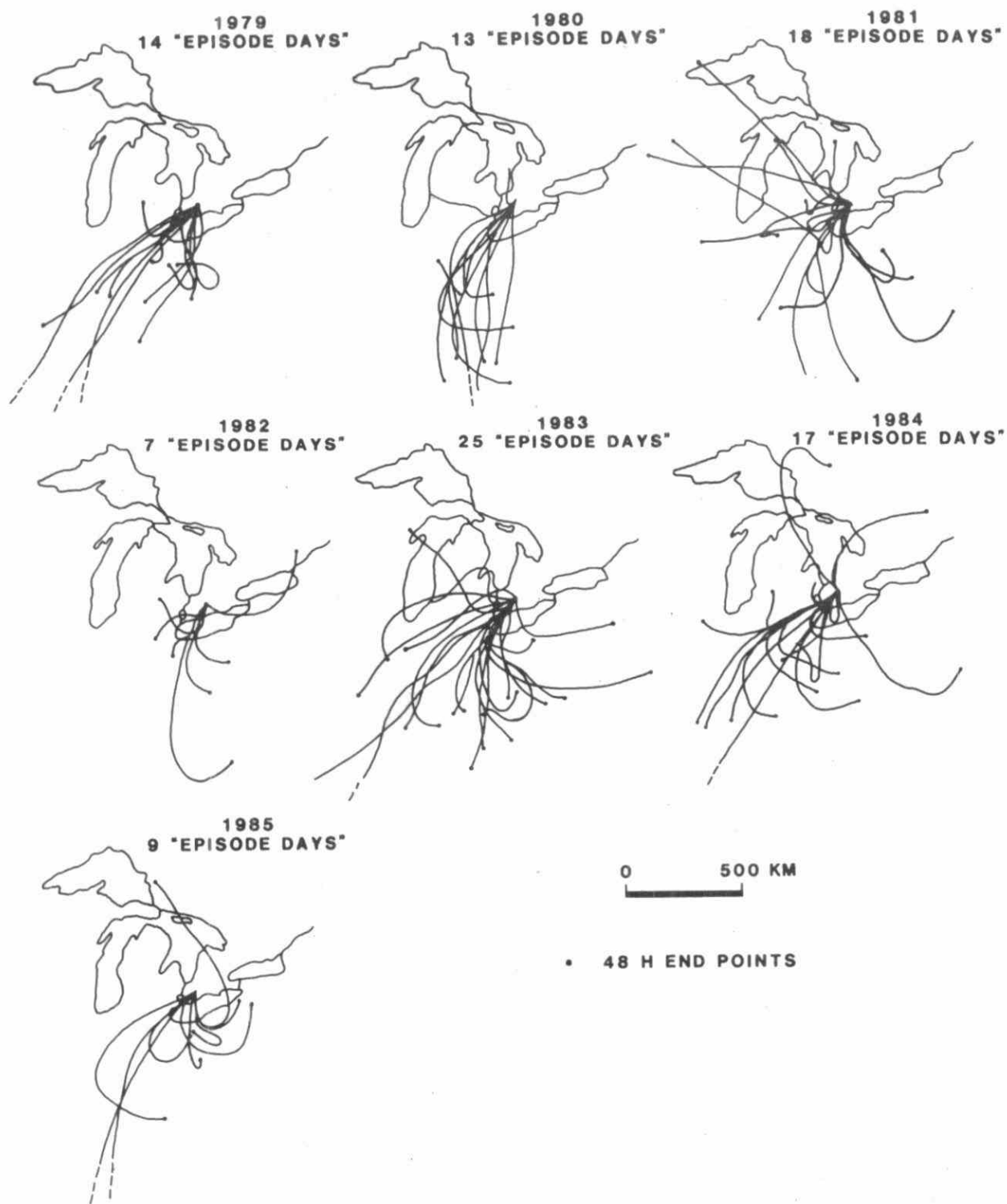


Fig. 3.2.37 "Episode days" - days on which widespread elevated O_3 levels greater than 80 ppb occurred at more than 8 monitoring sites in southern Ontario from 1979 to 1985.

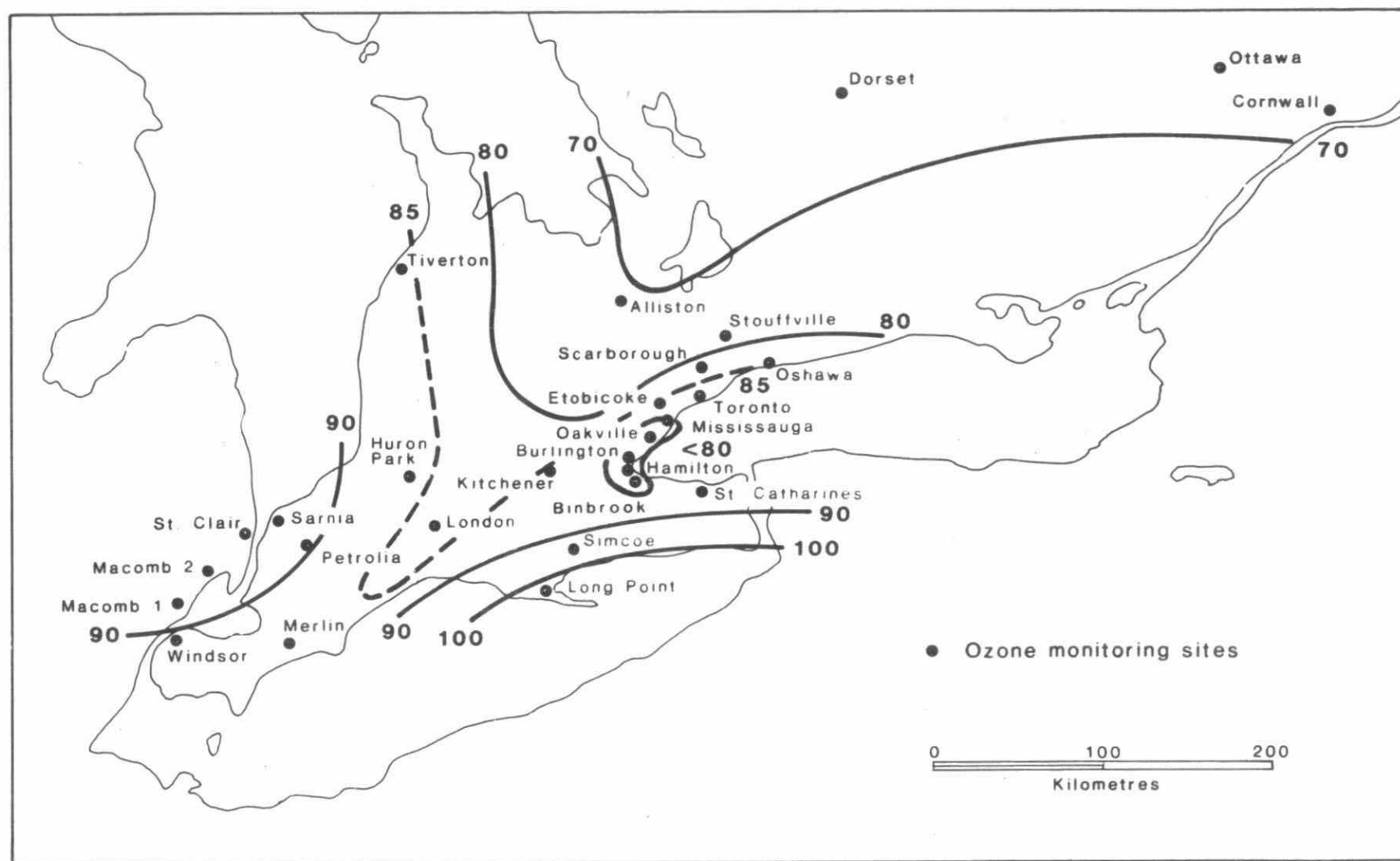


Fig. 3.2.38 Average hourly O_3 maxima for 144 episode days in southern Ontario.

3.2.4 SOURCE-RECEPTOR RELATIONSHIPS FROM ATMOSPHERIC TRACERS

3.2.4.a INTRODUCTION

In this section, atmospheric tracers will be considered in the broadest sense and thus be defined as any of the following:

- i) man made pollutants themselves;
- ii) trace elements that have a known relationship to the man-made pollutants;
- iii) natural trace substances that are released in certain known geographical regions;and
- iv) artificial tracers that are deliberately injected into the atmosphere at a known place and time - either alone or in combination with pollutants. These can be either chemically reactive or inert.

After tracers are emitted into the atmosphere they follow the general pathway, and are subjected to the processes, shown in Figure 3.2.39 (Summers, 1982). The relative importance of these processes depends on which class of tracers is being considered. For example, in the case of reactive pollutants, such as SO_2 and NO_x , or reactive artificial tracers, all processes including the chemical transformations are important. However, for non-reactive artificial tracers, such as perfluoro-monomethyl-cyclohexane (C_7F_{14}) used in the Cross Appalachian Tracer Experiment in 1983 (CAPTEX-83), and the Across North America Tracer Experiment in 1987 (ANATEX), only the transport processes are important.

On the regional and continental scale, appropriate to the long-range transport of air pollutants and the acid deposition issue, it is self-evident that the tracers cannot be transported from a source region (S) to a receptor point (R) unless the winds in fact blow from S to R. Thus, the meteorological synoptic weather pattern, which in turn determines the wind transport field, controls whether source S affects receptor R on a given day and, averaged over a given length of time, determines what fraction of the time receptor R is influenced by various sources. The quantitative estimate of the percentage contribution of a given S to a receptor is more difficult to determine for two main reasons: (i) more than one source at different distances upwind can contribute to the tracer concentration found in a given mass trajectory, and (ii) the tracers present in the air mass can be subjected to any, or all, of the transformation and depletion (wet and dry deposition) and dynamic (transport and dispersion) processes en route from the source regions to the receptor. These processes can be incorporated into mathematical simulation models and quantitative source-receptor relationships (SSRs) determined as described in Chapter 3.3.

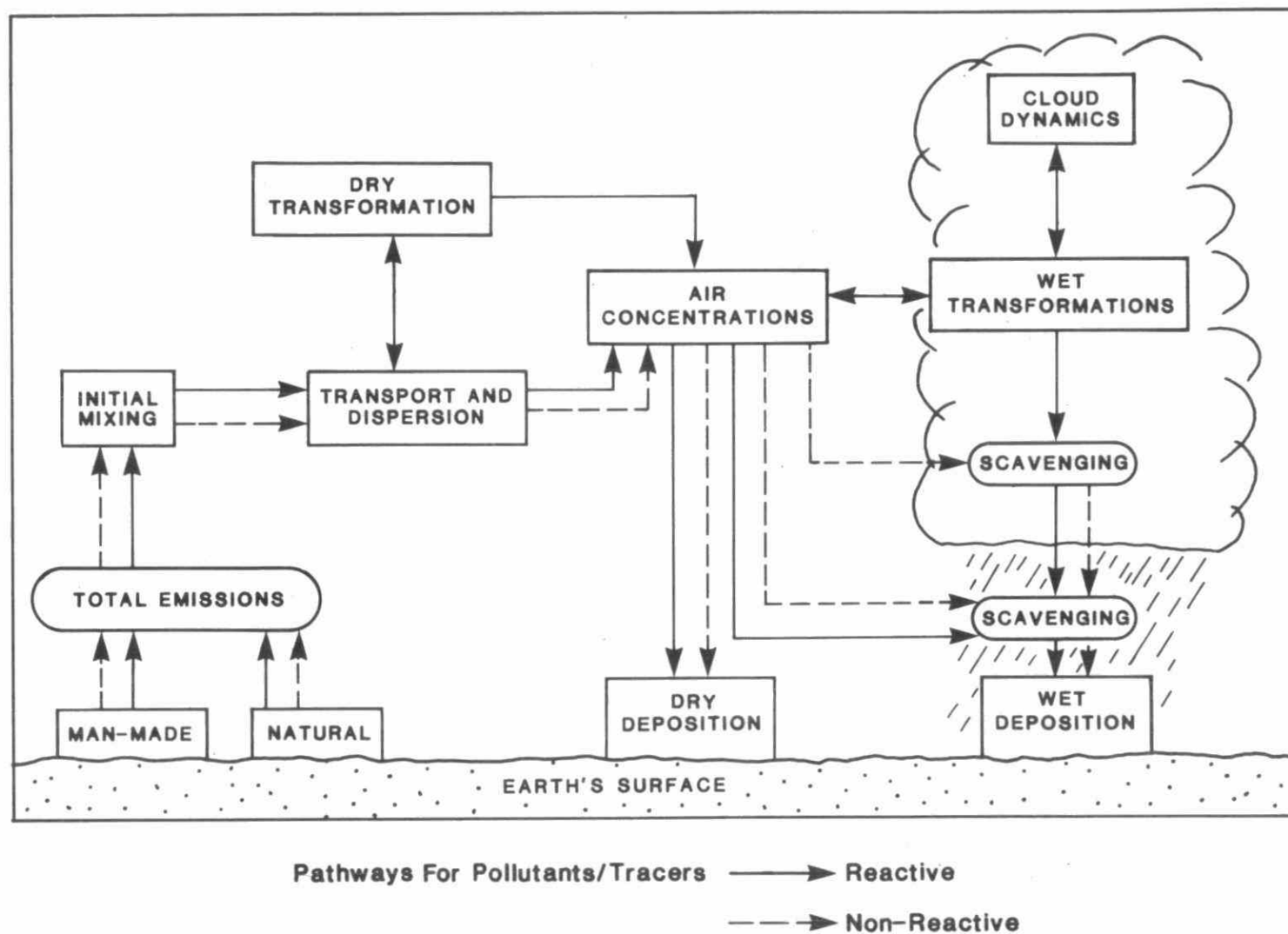


Fig. 3.2.39 Schematic diagram illustrating the main pathways for reactive and non-reactive pollutants/tracers through the atmosphere.

In this section, the use of observational data on tracers will be extended from the pattern association discussed in the previous sections by including information on atmospheric transport and some empirical or semi-quantitative knowledge of the atmospheric processes affecting the tracers. In this way SSRs can be discussed at two levels. Firstly, identification of those source regions that can affect a given receptor, and secondly, empirical estimates of the relative contribution made by various source regions to a given receptor.

Early pollution studies were concerned with two main issues. Firstly, the immediate vicinity of large industrial (smelters, power plant, etc.) point sources where the smoke emissions were an obvious tracer of the gaseous pollutants. Secondly, urban pollution problems where the smog haze, and in cold climates ice-fog, was a less well defined but still a visible tracer of the downwind drift of such pollution. Both of these issues were confined to the local (approx. 100 km) spatial scale. It was not until the early 1970's that the longer range transport of tropospheric man-made pollutants was documented in Europe, and for the first time in Canada by Munn (1973). The following sections only discuss the various techniques used to estimate SSRs on the scale of a few 100 km to several 1000 km relevant to the long-range transport of pollutants and acid deposition.

3.2.4.b WIND SECTOR STRATIFICATION AT MONITORING SITES

The geographical associations discussed in Section 3.2.2.b can be further refined by stratifying the observations at monitoring sites according to the local wind, or air-mass, arrival directions. This technique is well-suited for observing sites on the periphery of emission zones because in these cases there is a clear discrimination between air flows from the various source regions and from clean regions. Thus, Rodhe et al. (1972), Forland (1973) and Buch et al. (1976) were all able to show convincing evidence that the highest concentrations of soot and sulphates in the air, or the sulphate concentrations in precipitation, over southern Scandinavia always occurred with winds from sectors between SW and SE. These sectors contain the regions of heaviest SO_2 emissions in Europe. The first applications of sector analysis in North America were the data from Whiteface Mountain, New York State (Samson, 1978) and in Toronto, Ontario (Anlauf, et al. 1980). In both cases sulphate concentrations in air with flows in the SW sector were an order of magnitude higher than the concentrations in air arriving from Northern Canada. The SW sector contains the regions of highest SO_2 emission density along the Ohio Valley. Since these early results, wind sector analyses have now become an almost routine statistical stratification tool for interpreting observational data. Data from many sites have now been stratified by sector and confirm the earlier conclusions. The big disadvantage of the technique is that often several pollution source regions might be within a given sector and, thus, it is not possible from the observations alone to establish the relative contributions from the closer, versus the more distant, sources.

3.2.4.c AIRMASS TRAJECTORY ANALYSES

The local wind direction can be influenced by local topographical features and thus sector stratifications based on this wind may not correctly represent the sector from which the air originated several days earlier. In addition, air masses often follow curved trajectories and thus, air that arrives within one sector (eg. SW) may have originated in another sector (eg. W) further away. To overcome these problems, use of back trajectories (going back in time from 1 to 5 days), rather than the local wind, is now the preferred approach. Trajectory information can be combined with monitoring data in three different ways:

- i) case studies of particular air pollution events
- ii) generation of statistical summaries of the monitoring data at a site associated with certain trajectory classifications (eg. by sector or origin)
- iii) generation of a climatology of trajectory patterns associated with certain classifications of the monitoring data (eg. the highest 5% of the concentrations).

Methods i) and iii) depend on a particular characteristic of wet deposition at many monitoring stations, namely, that a large fraction of the annual deposition of $\text{SO}_4^{=}$ (and some other ions) is deposited on only a few days. From an examination of data in Europe, Smith and Hunt (1978) defined "episode days" at a particular place as those days with the highest wet deposition which, when summed, make up 30% of the annual wet deposition total. They further defined "episodicity" as the percentage of wet days in a year which are episode days, and considered a site to have highly episodic deposition if the episodicity was less than 5%. Over western Europe and Scandinavia the episodicity is typically in the range of 1 to 12. A similar phenomenon is observed in Canada.

Sirois and Barrie (1988) used an inverse definition of episodicity as the percentage of the total deposition in a period that occurs in the top 20% of deposition events. Air concentrations (which can be used with the deposition velocity to estimate the dry deposition flux) behave in a similar fashion (Sirois and Barrie, 1988) with a large fraction of the annual integrated exposure (concentration x time) to air pollution occurring on a small fraction of the days. On this basis, typical values for the episodicity of $\text{SO}_4^{=}$ deposition across eastern Canada are 49-61% for dry and 52-70% for wet. This range for wet is very similar to that inferred from Smith and Hunt. In Canada the episodicity for wet NO_3^- deposition is similar to that for $\text{SO}_4^{=}$.

- i) Case Studies: Detailed analysis of individual episode days can provide information on particular source regions within the gridded emissions inventory used in Europe and North America. Smith and Hunt (1978) studied the most extreme deposition event at two sites in Europe in 1974 - one in southern Norway, the other is the southern U.K. In both cases the back trajectories

could be traced back over some of the strongest emission sources in eastern Europe and western Europe, respectively.

A prolonged wet deposition episode occurred over southern Ontario from August 28 to September 4, 1981 (Kurtz et al., 1984). During this period 100 mm of rain (12% of the 1981 total) fell at Dorset with a wet deposition of $7 \text{ kg SO}_4^{=}$ ha^{-1} (28% of the 1981 total). During this period back trajectories showed a steady SSW flow from the SO_2 emissions in the lower Great Lakes region including southern Ontario and the Ohio Valley.

- ii) Stratification by Trajectory Sector: Analysis of wet deposition data at two stations operated near the Canada/U.S.A. border by the Ontario Ministry of Environment (OME) was carried out by Tang et al. (1986). Air parcel trajectories going back in time for 2 days were used to stratify each precipitation event into three categories - those passing over only U.S. sources, those passing over only Canadian sources and those of uncertain origin. Because the sites were close to the border it was relatively easy to separate the trajectories between Canadian and US origin, although, if there was any doubt, they were put in the unknown category. The percentage contribution of each of these categories to the total deposition observed over the three year period 1981-1983 was calculated for both $\text{SO}_4^{=}$ and NO_3^{-} deposition as shown in Figure 3.2.40. It is clear that US sources overwhelm the contribution of Canadian sources to wet deposition at these near-border sites. For $\text{SO}_4^{=}$, US sources contribute at least 10 times as much as Canadian sources; and for NO_3^{-} US sources contribute about 3.5 times as much as Canadian sources.

This information can be presented in another way as a simple source-receptor matrix shown in Table 3.2.11.

Table 3.2.11

Source-receptor matrix for wet deposition of SO_4^{2-} and NO_3^- at 2 sites in southern Ontario, showing % contribution from US and Canadian Sources.

Source	Receptor			
	Longwoods		Railton	
	SO_4^{2-}	NO_3^-	SO_4^{2-}	NO_3^-
USA	81	79	57	60
Canada	6	7	16	18
Uncertain	13	14	27	22

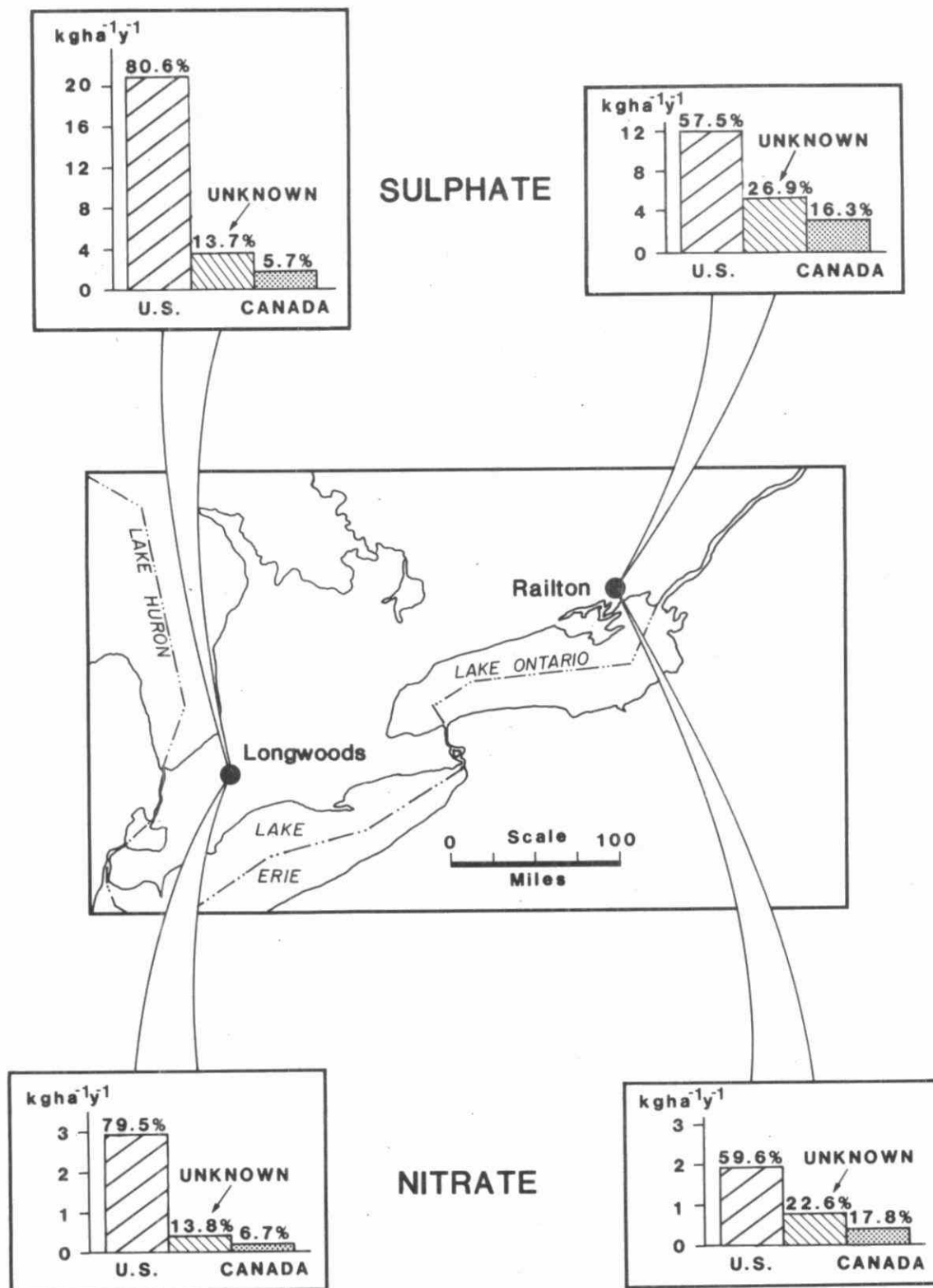


Fig. 3.2.40 Apportionment of a)sulphate, and b)nitrate wet deposition between Canadian and USA sources at Longwoods and Railton using 1981-1983 monitoring data classified by air trajectory origin.

- iii) Trajectory Climatologies: The episodic nature of deposition can be used to generate long-term statistics of the airmass trajectories associated with various data classifications. For example, by averaging the ensemble of back trajectories arriving at a monitoring site for the days contributing to an upper percentile of the deposition or concentration values, a clear climatological pattern emerges delineating the geographical region whose emissions contribute to the receptor. Several different ways of generating these statistics have been used.

As an example Ashbaugh (1983) studied trajectories arriving in the Grand Canyon area in Arizona, associated with the highest sulphate values causing reduced visibility. The trajectory positions at each six-hour time-step, prior to arriving at the Grand Canyon, were accumulated in grid squares and summed to provide a residence time in each grid cell. These times were contoured on a map and showed one predominating pathway from urban southern California and another from the regions with smelters in Utah and Nevada. This technique was expanded by Poirot and Wishinski (1986) using summer visibility observations in the northeast USA as a surrogate for sulphate concentrations. In their analysis, the number of hours the trajectories spent in each grid square was computed. Probability density maps showed a distinct pattern for high sulphate days with air arriving from the SW, and for clear days, air arriving from the northwest. A correction was applied to the probabilities to account for the geometry of the analysis (eg. the probability of a random selected trajectory crossing a given grid square depends on the distance from the observing site), and the resultant regions with high residence times are very closely associated with the regions of high SO_2 emissions in states south of the Great Lakes.

In Europe, Strauss et al. (1986) used another variant of this technique with a $1/t^2$ (t = time) correction to the back trajectories to account for the diffusion of the pollutants in passing from the source to the receptor. In this way, the contribution to the SO_2 measured at Donon in northeastern France was calculated for each grid square and then aggregated to countries. The results compared favourably with those from the EMEP numerical LRT model. Summers (1987) expanded on the technique of Poirot and Wishinski (1986) by using actual $\text{SO}_4^{=}$ and SO_2 data from the Canadian monitoring network to generate both the trajectory probability climatology and the distance decay factors (Summers and Fricke, 1989). In this way it was possible to estimate the contribution to episode-days (top 5 - 10% of the events) from each emission grid square, and thus produce quantitative, semi-empirical S-R relationships. Example results for the estimated percentage contribution from various source regions to the episodic (top 5%) values of $\text{SO}_4^{=}$ and NO_3^- air concentrations observed at Montmorency, Quebec are shown in Figure 3.2.41. Note that for $\text{SO}_4^{=}$ more distant source regions, such as Ohio and Michigan have a substantial impact, but in the case of NO_3^- the closer source regions such as Southern Quebec, New York and New England have a relatively higher contribution than for $\text{SO}_4^{=}$. This is related to both the emission strengths for SO_2 and NO_x but is also a reflection of the shorter decay distance for NO_3^- compared to $\text{SO}_4^{=}$ (Summers and Fricke, 1989). The two smelter regions of Sudbury, Ontario and Noranda, Quebec have an impact on the $\text{SO}_4^{=}$ concentrations but are undetectable as far as NO_3^- is concerned. Also, it is

interesting to note that the results shown in Figure 3.2.41 are in reasonable agreement with the predictions of a number of simple linear long-range transport models.

3.2.4.d RECEPTOR MODELLING

This method takes advantage of the fact that atmospheric aerosols contain small amounts of elemental constituents such as arsenic (As), antimony (Sb), selenium (Se), vanadium (V), manganese (Mn), zinc (Zn), copper (Cu), indium (In), lead (Pb), and others. Modern chemical analysis techniques, such as PIXE, allow these to be detected and quantified even when in extremely small amounts. If the regional variation of the emissions of these trace elements is known for various fuels such as oil and coal, or ores that are being smelted, then examination of the concentrations of the elements, or their ratios, in aerosols collected at distant sites has the potential to distinguish between the contributing source regions. Some key assumptions are made in the application of this technique. First, that sufficient elemental measurements have been made in the source regions so that representative emission functions can be established. Second, that there is no selective removal of certain elements by wet or dry deposition during transport which would cause the ratios to change with time. The first assumption is still open to question for some elements; the second appears reasonable since most elements are concentrated in fine-particle aerosols ($< 2\mu$ diameter). Applying this technique at two sites in Rhode Island and Vermont in the northeastern U.S., Rahn and Lowenthal (1984, 1985) concluded that the northeast is the most important source of aerosol elements that are broadly distributed over eastern North America or enriched in northeastern emissions (i.e. V, Sb, Zn, Mn). On the other hand, for those elements such as As and In found in Canadian smelter emissions and Se and S found in mid-west coal emissions, the contributions of distant sources may equal or exceed those from the northeast. This technique therefore provides clear evidence of long-range transport, and can begin to discriminate between source regions on the large scale.

Pacyna (1986) discusses S-R relationships for trace elements in northern Europe. The technique was applied to individual case studies with a simple transport-depletion model to estimate concentrations based on a grided emissions inventory for various trace elements. The model estimates generally agreed with observations within a factor of 2. Another approach was to use sector analysis and it was found that the ratios of Cr, Cu, As, Se, Mn and Sn relative to V were useful in differentiating western and eastern European sources.

The major limitation of this approach for acid deposition applications is that it only applies to primary particulate emissions and not for the sulphate aerosol produced by oxidation of precursor SO_2 , which is the predominating source of SO_4^{2-} in precipitation in the regions of heavy deposition. The technique is still controversial, in terms of generating S-R relationships, as evidenced by the conclusions of Dutkiewicz et al. (1987) and the discussion by Lowenthal and Rahn (1988).

Trace elemental analyses have also been made on hi-vol filter samples collected at three rural air monitoring sites in eastern Canada. In the Fall of 1984, 70 daily samples were collected at Dorset (about 200 km NNE of Toronto), and 28 weekly or daily samples were collected at Montmorency (about 70 km N of Quebec City) and at Kejimikujik National Park in the central part of southern Nova Scotia (see Fig. 3.2.28). Using the Dorset data alone, together with 925mb air mass trajectory frequency distributions, Barrie (1988) showed clearly that the highest Pb levels were observed coming from the urban areas to the south, and the highest Indium and Arsenic levels from the smelters in northern Ontario.

Carrying this technique one step further, Pb isotope ratios, which are different for Pb used in Canadian and U.S. gasoline, were used to apportion Pb observed in aerosols at 3 locations in Canada between the two countries (Hopper and Barrie, 1988). The results are shown in Table 3.2.12.

The Dorset study was repeated for another two months (April-May) in the Spring of 1986 (Sturges and Barrie, 1989). These results are compared to those obtained in the Fall of 1984 in Table 3.2.13. The differences are explained by a higher frequency of winds from the north in the Spring study providing a higher contribution from the northern smelters and a lower contribution from U.S. sources.

Another innovative use of trace elements has been developed by Samson and Keeler (1987). In this case no assumptions were made regarding the location of the trace element emissions and only the daily observations at six monitoring sites in the northeast U.S. for the month of August 1983 together with the meteorological wind and precipitation fields were used. Back trajectories were calculated from each observing site for each day and the wet and dry deposition and dispersion accounted for. In this way probability functions were developed, and for each site geographical regions producing concentrations in given ranges were determined. By overlapping the maps for all sites, clear patterns emerged showing the geographical regions associated with observations in certain ranges at all six sites. For example, the vanadium pattern showed maximum concentrations coming from the east coast consistent with its presence in fuel oil; for $\text{SO}_4^{=}$ the source region for maximum concentrations covers the Ohio Valley.

A recent analysis of event-data collected at 3 locations in southern Ontario combines principle component analysis of the chemical species in the precipitation with an air mass trajectory end-point analysis (Zeng and Hopke, 1989). The results clearly show that the Ohio Valley and east coast of the U.S.A. is the major source region for the acidic species.

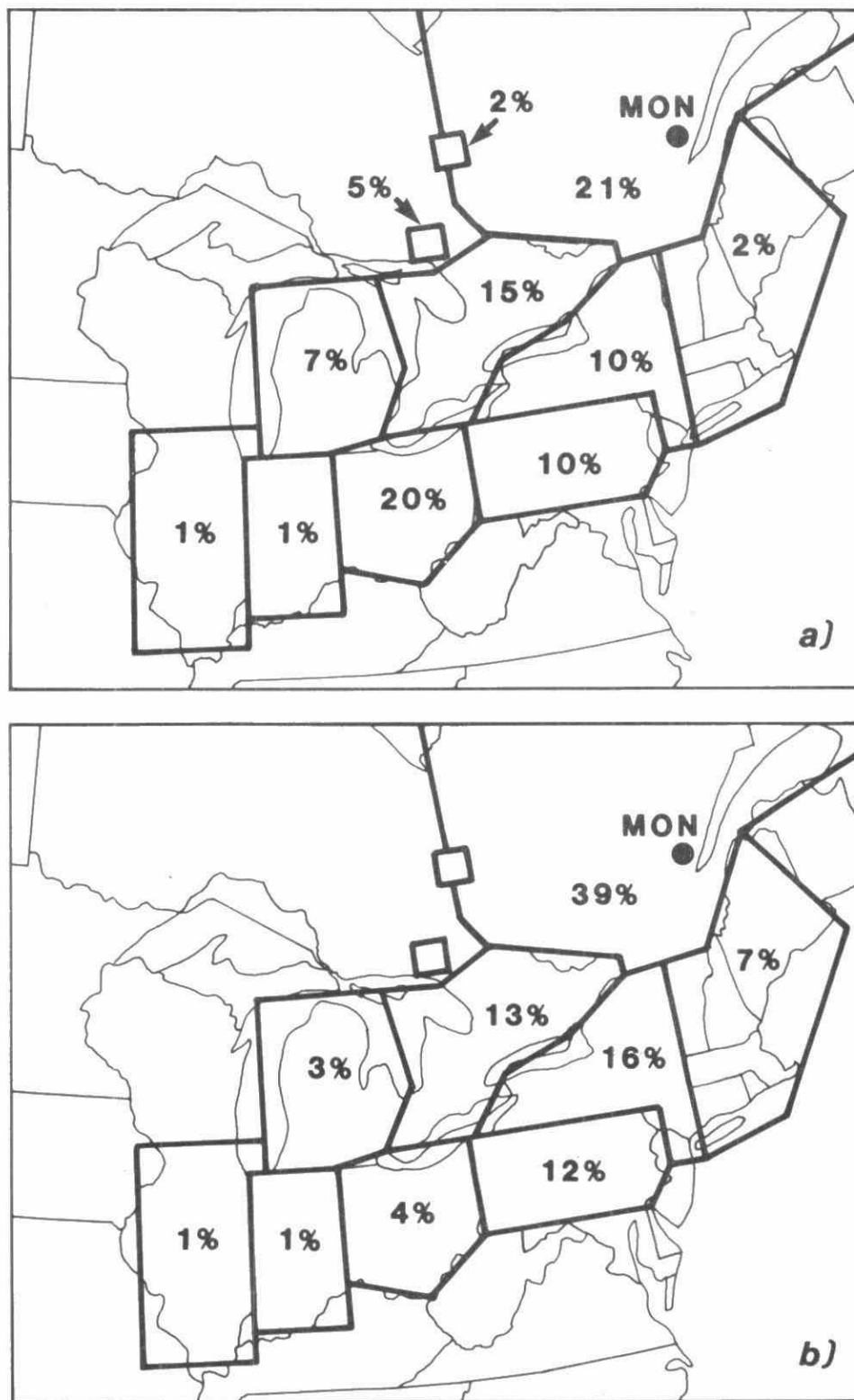


Fig. 3.2.41 The percentage contributions of the emissions in each region to the ambient air episodes observed at Montmorency, Quebec during the period 1980-1984 for a)SO₄⁼ and b)NO₃⁻. Episodes are defined as days in the top 5% of observed concentrations.

Table 3.2.12

The concentration-weighted apportionment of atmospheric Pb using the Pb-206/207 ratio observed in hi-vol air samples at 3 sites in eastern Canada in the Autumn of 1984.

Absolute uncertainties of one standard deviation are shown.

Site	No of Samples	Canadian Auto	U.S. Auto	Canadian Smelters
Contribution (%)				
Dorset	64	52 ± 3	46 ± 3	2 ± 0.3
Montmorency	23	67 ± 1.5	28 ± 2	4 ± 0.6
Kejimkujik	21	51 ± 2.5	44 ± 3	5 ± 0.4

Source: Hopper and Barrie, 1988

Table 3.2.13

**Estimates of contribution of sources to Pb in air at Dorset
in two seasons.**

Absolute uncertainties of one standard deviation are given.

Site	Fall 1984	Spring 1986
Contribution (%)		
Canada	52 ± 3	66 ± 3
U.S.	46 ± 3	25 ± 2
Northern Smelters	2 ± 3	9 ± 1

Source: Sturges and Barrie, 1989

3.2.4.e IMPACT OF MAJOR POINT SOURCE SHUT-DOWN

In the previous assessment (RMCC, 1986) the attempts to identify and quantify the impact of a prolonged shut-down of the INCO Smelter at Sudbury in the early 1980s were discussed. Although definite decreases in SO_2 air concentrations and bulk (wet plus dry) deposition of $\text{SO}_4^{=}$ could be detected within the Sudbury Basin, the impact on precipitation chemistry at distances more than 200 km downwind was hard to detect. In part, this is due to the low probability of the plume from a single point source being over the distant monitoring site at the time of a rain event. This, combined with the high regional levels of $\text{SO}_4^{=}$ deposition due to long-range transport from other sources in eastern North America, made it difficult to isolate the impact of the INCO smelter.

Since the above studies were carried out, a unique experimental opportunity presented itself on the west coast. The permanent closure in March 1985 of the large ASARCO copper smelter in Tacoma, Washington was announced well ahead of time. This enabled a precipitation monitoring network to be set up specifically to sample storm events before and after closure. Three other factors made detection of the impact of the smelter easier: i) the smelter produced a large fraction of the total SO_2 emissions in the Puget Sound area, ii) there was no significant long-range transport of $\text{SO}_4^{=}$ into the area, and iii) the topography and meteorology of the region, with the heavy rain events occurring mostly with a SW flow, enabled the rain events to be easily classified. It was concluded (Vong et al., 1988) that the $\text{SO}_4^{=}$ concentrations in rainwater in the region 25 km downwind of the source decreased significantly after the smelter closure, but that no significant changes were observed further downwind in the Seattle area. More important was the fact that an average of only 4.4% (range over all storms, 0.7% to 8.6%) of the SO_2 emitted was wet deposited as $\text{SO}_4^{=}$ within the 60 x 60 km region downwind of the source. The corollary of this last statement is that most of the sulphur is deposited by dry deposition or transported long distances downwind. The latter is corroborated by analysis of data from a precipitation chemistry monitoring network operated in B.C. just north of the U.S. border by Environment Canada since 1982. Eleven sites were operated in a chain from the west side and around the bottom of Vancouver Island, across the Strait of Georgia to Vancouver and up the Fraser Valley.

For precipitation events with a S to SW flow regime, the highest concentrations of both $\text{SO}_4^{=}$ and arsenic (As), the only significant source of which was the ASARCO smelter, occurred at those stations most exposed to a flow directly out of Puget Sound (Faulkner, 1986) at sites 150-230 km from the smelter. After the smelter closure, and with the same meteorological regime, the As concentrations dropped to background values at all sites. At most sites where As was detected before closure, the $\text{SO}_4^{=}$ concentrations dropped by an average of 0.2 mg l^{-1} , or about 25%, after closure. As a control, the averages for rain events before and after closure with winds directly off the Pacific showed no significant changes in either As or $\text{SO}_4^{=}$ concentration.

3.2.4.f THE CROSS-APPLALCHIAN TRACER EXPERIMENT (CAPTEX)

Several artificial tracers, such as SF_6 , have been used for some time to track plume diffusion and dispersion over distances up to the order of 100 m. The real breakthrough for longer range transport experiments, over distances of 1000 m or more, came in the late 1970's with the development of inert perfluorocarbon tracers. Because of the extremely low natural background concentrations of these tracers in the atmosphere and the highly sensitive laboratory analytical techniques, experiments could be carried out with the release of the order of 100 g of tracer. In the CAPTEX, carried out in eastern North America in the Fall of 1983, seven tracer releases were made about one week apart - 5 from Dayton, Ohio and 2 from Sudbury, Ontario (Ferber, 1985).

The main objective of CAPTEX was to test the ability of LRTAP models to simulate the transport and dispersion of an inert tracer gas in the atmosphere. However, plots of the ground level tracer concentration field, in six-hour time steps for the two days following each release, clearly showed the motion of the tracer across eastern North America and that ground level releases were mixed sufficiently in the lower atmosphere to be transported as a coherent gas cloud for distances of at least 1200 km.

3.2.4.g THE ACROSS NORTH AMERICA TRACER EXPERIMENT (ANATEX)

Following on from the success of CAPTEX, a larger scale experiment was conducted during the first 3 months of 1987 (Draxler and Hefter, Eds., 1989). In this experiment three different types of inert perfluorocarbon tracers were used with releases of different combinations every 2½ days (ensuring alternating daytime and night-time releases) from two sites (Glasgow, Montana and St. Cloud, Minnesota) located about 1000 km apart. Samples of 24-hour duration were collected at 77 sites covering all of the eastern U.S. and Canada east of longitude 104°W and south of latitude 54°N out to a distance of 3000 km from the release point. The two main objectives of ANATEX were to establish the ability of LRT models to separate the effects of two different sources on a receptor and to characterize the influence of synoptic scale meteorological features on continental scale transport. Again it was shown that ground level releases of material into the atmosphere could be positively tracked and identified for distances up to 3000 km. The comparisons of the tracer transport with LRT models is discussed in Section 3.3.5.c.

3.2.4.h AN UPDATED ATMOSPHERIC SULPHUR BUDGET FOR EASTERN CANADA

Additional information on source-receptor relationships on the large regional scale can be obtained by examining the atmospheric budget of sulphur. The last detailed sulphur budgets for eastern North America, based on observations, used data from the early 1980s. Since then, the input of anthropogenic SO_2 emissions has changed considerably. Some of the other terms in the budget can now be estimated more accurately based on observations from extensive monitoring networks and the results of the Western Atlantic Ocean Experiment (WATOX).

As a result of recommendations made at the International Conference sponsored by the U.S. National Acid Precipitation Assessment Program (NAPAP) in February 1990, the NAPAP is preparing a sulphur budget for the eastern United States (and perhaps eastern North America as a whole). In the meantime, some preliminary estimates of the various flux terms in the U.S.A. obtained from NAPAP (1989) will be given here pending the final results of NAPAP. The region to be discussed is that shown in Figure 3.2.31, and the estimated flux terms for Canada and the U.S. are summarized in Table 3.2.14. The sources of the estimates are briefly indicated in footnotes below the table. Note that two of the U.S. estimates (i.e. wet and dry deposition) have large uncertainties due to the large enhancement factors applied by NAPAP, although these uncertainties should be reduced in the final NAPAP report. These enhancements due to the influence of large urban areas are much less important in Canada and the rural monitoring networks give good representative measurements for the whole region.

The main emphasis in this section will, therefore, be on Canada where some of the estimates are easier to make. As far as eastern Canada is concerned there is a substantial imbalance between the estimated input and output terms and this is assumed to be the net influx across the border from the U.S.A. The "best estimate" value 1.2 Tg S yr^{-1} is within the range of values estimated recently by two Lagrangian long-range transport models (Olson and Oikawa, 1989; Shannon and Lesht, 1986), but differs substantially from the results of a statistical LRTAP model (Fay et al., 1986) as discussed by Olson (1989). This value of 1.2 Tg S yr^{-1} is slightly less than that estimated by Galloway and Whelpdale (1980) and is, therefore, consistent with the fact that the anthropogenic emission input has dropped since then. Using the best estimates of the major flux terms and omitting the smaller terms (indicated with a ? on the table), a net northward flux of about 1.4 Tg S yr^{-1} into Canada is required to balance the eastern U.S. budget. This flux is consistent with the one obtained for the Canadian budget.

This budget for eastern Canada shows that the estimated net flux of SO_2 across the border from the U.S.A. is equal in magnitude to the man-made emissions in eastern Canada. This reaffirms previous conclusions that over eastern Canada as a whole about half the sulphur deposition is due to U.S. sources and half is due to Canadian sources.

Table 3.2.14 The main flux terms in regional atmospheric budgets for eastern Canada and the eastern US 1985-1987.

Units: Tg S yr ⁻¹		Canada		USA	
Flux Term	Range	Best Estimate	Range	Best Estimate	
INPUT					
Anthropogenic Emissions	1.1 - 1.3 ⁽¹⁾	1.2	7.6 - 9.2	8.4	
Natural Emissions		<0.1 ⁽²⁾		?	
Inflow from West	0.05 - 0.01 ⁽³⁾	<0.1		?	
Total	1.2 - 1.4	1.3		8.4	
OUTPUT					
Wet Deposition ⁽⁴⁾	1.1 - 1.3	1.2	1.7 - 2.5 ⁽⁵⁾	2.1	
Dry Deposition ⁽⁶⁾	0.2 - 0.4	0.3	1.2 - 3.4 ⁽⁷⁾	2.3	
Outflow to Atlantic ⁽⁸⁾	0.7 - 1.1	0.9	2.3 - 2.9	2.6	
High elevation droplet deposition	0.0 - 0.2	0.1		?	
Total	2.0 - 3.0	2.5		7.0	
IMBALANCE - assumed to be net flux USA to Canada	0.6 - 1.8	1.2			

(1) From Tables 3.2.1, 3.2.2, 3.2.5, with an error estimate of +10%.

(2) Based on Galloway and Whelpdale (1980)- emissions in western Canada have changed little and monitoring (near border at ELA Kenora shows current mean annual air concentration as 0.5 µg S m⁻³).

(3) From Galloway and Whelpdale (1980).

(4) Integration over Canada and US regions separately by method described in Section 3.2.3b.

(5) Deposition enhanced by 25% due to urban influence as proposed by NAPAP (1989).

(6) Using a ratio of dry to total deposition based on values given in Appendix 3A and Summers (1990).

(7) Using Summers (1990), with enhancement of 100% due to bias of rural monitoring against high concentrations near point sources and in urban areas as proposed by NAPAP (1989).

(8) Based on estimates from WATOX given by Galloway and Whelpdale (1987) and apportioned between Canada and the US according to Table 9 in Galloway et al. (1984).

(9) Based on Schemenauer et al. (1988) and assuming that 5 to 10% of the total eastern Canada region is subject to high elevation droplet deposition.

? Not estimated by NAPAP - but all terms considered small, i.e. < 0.5 Tg S yr⁻¹.

3.2.4.i ARCTIC HAZE

The phenomenon of reduced visibility in the Arctic was first documented over 30 years ago, but it was not until the late 1970's that its cause was slowly recognized. Based on the strong seasonal variation of the concentration and chemical composition of suspended particulate matter in the Arctic, together with the seasonal variation of the large-scale meteorological circulation pattern, it was concluded by Rahn and Heidam (1981) that the winter time occurrence of Arctic haze was due to the long-range transport, over distances of the order of 10,000 km, of pollutants from the industrial regions in the mid-latitudes of the northern hemisphere. Further analyses of the predominant climatological air-mass pathways from the industrial source regions, together with the likelihood of precipitation being encountered while en-route to the Arctic, suggested Eurasia as being the most likely source region (Rahn, 1982). A more detailed analysis of the synoptic weather situation producing strong surges of air from mid-latitudes into the Arctic (Raatz and Shaw, 1984) showed that the link between Eurasia and the Arctic was much stronger than that between North America and the Arctic. This Eurasia link was broken down further into a predominance of surges originating from eastern Europe (west of the Urals) in the early winter (November to January); and originating from western Europe in the late winter (February to March).

Further refinements to the above analyses have been carried out in recent years using air-mass trajectory calculations. However, the accuracy of trajectory calculations over the several days it takes for the air parcel to travel from the source region to the Arctic now becomes an important issue. Several recent papers have discussed this issue and it appears that, under certain meteorological conditions, position errors of up to 500 km can occur after 72 hrs. An analysis devoted specifically to long-range transport trajectories in the Arctic (Kahl et al., 1989) shows differences in end points calculated by two different models of up to 1000 km after 5 days. Thus trajectories cannot be used to discriminate between potential emission sources for Arctic haze on a scale of less than about 1000 km. Such resolution is however, useful because a distinction can still be made between North American and Eurasian sources and even between different parts of the Eurasian continent.

3.2.5 SUMMARY AND CONCLUSIONS

Since the major acid rain research programs in North America began in the late 1970's, considerable effort has gone into determining the emissions of acids to the atmosphere and their concentrations in air and precipitation on as fine a spatial resolution as the problem warranted. In Canada the federal and provincial governments have cooperated to fill in our portion of the total North American picture. Now in the late 1980's, we possess at least 5 years of observational data with good spatial coverage and the best estimates of emissions possible. This information has been examined in this chapter to see what it reveals about source-receptor relationships. This summary first pulls information together on spatial and temporal trends of precipitation concentrations to show the large scale spatial response to eastern North American emission changes and is followed by more specific conclusions.

General Conclusion on the Overall Linkage Between Emissions and Precipitation Chemistry Changes

The strong geographical linkage between the regions of maximum emissions density and highest concentration patterns for sulphur and NO_x was established in Figs. 3.2.17 and 3.2.19. This, together with other information from several of the previous sections can now be brought together as shown in Figures 3.2.42 and 3.2.43 to summarize the time response of concentrations to emission changes. In Fig. 3.2.42 the central map is a repeat of Fig. 3.2.22b) showing the % change in the precipitation-weighted mean concentration of $\text{SO}_4^{=}$ between the periods 1980-1982 and 1985-1987. Underneath is the time change of SO_2 emissions for eastern North America (defined as that portion of Canada east of the Manitoba/ Saskatchewan border and of the U.S. east of the Mississippi Valley) showing a decline in emissions of 13.5% from the period 1980-1982 to the period 1985-1987 (see Table 3.2.5). Surrounding the central map are shown the time trends from 1979 to 1987 of the weekly-average precipitation $\text{SO}_4^{=}$ concentrations at selected monitoring stations (Appendix 3D). The methodology for calculating these trends was discussed in Section 3.2.3a and the five Canadian sites are shown. In addition, the results of a similar analysis performed on five selected U.S. sites (presented at the NADP Workshop on Trend Analysis, Provincetown, Mass., October 26-27, 1989) are shown. Note that in all cases the time trends have been corrected for the influence of precipitation amount and have had the annual and longer term (2-6 yr) cycles removed. Also the emissions and $\text{SO}_4^{=}$ concentrations have been scaled to unity for the base year 1980 (except Algoma and Montmorency which used 1981). At each monitoring site the % change of the 1985-1987 average from the 1980-1982 average matches very well with the isopleths on the map - this is not surprising since both are based on the same data. What is interesting is the different way each station responds over time to the change in emissions. One would not expect each station to respond identically because of the fact that each has different geographical pollutant source regions affecting it. This, combined with the fact that $\text{SO}_4^{=}$ has a residence time of several days and can thus travel anywhere up to a few thousand km before encountering rain, and that the meteorological flow

regimes associated with rain events differ seasonally and geographically, means that there is not a one-to-one relationship between a particular monitoring site and a given regional emissions source. Numerical modelling techniques attempt to quantify these relationships by generating source-receptor transfer matrices. None-the-less Fig. 3.2.42, based on data analysis alone, does show some important and useful linkages.

- (i) The overall downward trend in precipitation $\text{SO}_4^{=}$ concentrations shown on the map is about the same as that for the SO_2 emissions over the same area for the same period.
- (ii) The longer more detailed time trends in precipitation $\text{SO}_4^{=}$ concentrations at individual sites in most cases show significant downward trends of the same order with two exceptions.
- (iii) One exception is at Montmorency, Québec where the concentrations increased substantially from 1981 (no data are available for 1980) to 1983-84 followed by a dramatic decline which cannot easily be attributed to either local or distant emissions.
- (iv) The other exception is at Parsons, West Virginia where no significant trend was detected. However, in this case the high emissions in the three states to the west had only decreased slightly (see Fig. 3.2.7).
- (v) At several sites the downward trend in precipitation $\text{SO}_4^{=}$ concentrations was levelling off or even reversing in the last two years, again consistent with the behaviour of the emissions.

The situation for NO_3^- concentrations is quite different as shown in Fig. 3.2.43. The spatial pattern of precipitation-weighted NO_3^- concentrations only shows small changes - over most of the area less than a 10% change between the period 1980-1982 and 1985-1987. This is consistent with the overall small change in NO_x emissions of only -2.0% between the two periods (see Table 3.2.5). Of the five Canadian sites, one (Chalk River) shows neither a trend nor any long term cycle. (Table 3.2.7) Three show cycles only and one (Kejimikujik) shows a trend (in the form of a cycle greater than 5 years period). This latter response is puzzling since none of the regions to the SW showed any major fluctuations in NO_x during the period. However, the concentrations of NO_3^- are very sensitive to wind direction at this site. A band of extremely high NO_x emission density lies along the Washington-Boston urban corridor and a slight change in the frequency of wind direction along this corridor from year to year could have a significant effect, and possibly produce the cyclical trend.

The preceding analysis provides two general conclusions: (i) the overall regional response of the $\text{SO}_4^{=}$ and NO_3^- concentrations measured in precipitation over a period of only 8 years is consistent with the changes in the regional SO_2 and NO_x emissions over the

same period; and (ii) the variation in the detailed response at each monitoring station, whilst generally consistent with the above, shows that relying on too few stations for monitoring the atmospheric chemistry response to future emission changes would be difficult to interpret and could be misleading.

Specific Conclusions

1. Between 1980 and 1985, SO_x emissions in Canada have decreased by 20% (Table 3.2.1). Individual provinces have reduced emissions by amounts ranging from 3% in Manitoba to 37% in Quebec and New Brunswick. The largest producer, Ontario, reduced by 17%. There was a somewhat smaller decrease in American emissions of about 15% (Table 3.2.2). Changes in various regions or individual states ranged from +4% in the central southwest to -30 to -40% in Maine, the Pacific West, Michigan and Florida (Table 3.2.2). Changes in states adjacent to the eastern Canada/US border ranged from about -5% in Illinois, Indiana and Ohio to -20 to -40% in the other states.
2. Between 1980 and 1985, NO_x emissions change was little in Canada increasing by only 0.1% (Table 3.2.3). The range has been from -28% in Quebec to +49% in northwestern Ontario. In contrast total US NO_x emissions decreased by 8%. Changes in various regions or states ranged from +12% in Indiana to -22% in the northeast (Table 3.2.4).
3. The spatial patterns of air concentrations and wet deposition of acid substances have a strong qualitative geographical relationship to the spatial patterns of SO_2 and NO_x precursor emissions. The maxima in the atmospheric patterns tend to be over, or immediately downwind, of the maxima in the emissions density. This is not a new insight but rather a confirmation of deductions made earlier in the decade based on fewer and less dense observations.
4. Stratification of the measured concentrations using surface mixed layer air mass trajectories going back in time for up to 5 days enables the emission source regions over which the air has passed to be determined, but does not enable discrimination to be made between local and distant emission sources. However, if empirical decay factors for pollutant concentrations along the trajectory path are included, then discrimination between the impact of source regions of varying distances is possible. In this way quantitative semi-empirical source-receptor relationships can be estimated. All of these analyses reconfirm earlier estimates (from both observations and models) that a large fraction (usually $\geq 50\%$) of the air and precipitation concentrations of SO_4^{2-} observed at eastern Canadian sites close to the U.S. border is due to U.S. sources. For NO_3^- , similar results apply.
5. Receptor modelling, using the fact that atmospheric aerosols contain many trace elements that have known sources, and concentration ratios, in certain combustion

or natural processes, can be used to distinguish between the broad source regions contributing observed concentrations at a monitoring site. For example, by using the known unique isotope ratios of Pb used in Canadian and U.S. gasoline, and in the ores processed by Canadian smelters, and combining the observations at monitoring sites with air mass trajectory analysis, it is possible to apportion the sources of Pb found in the air at a few rural monitoring sites in eastern Canada. These show transport over long distances with the smelters in central Ontario and western Quebec being detected in Nova Scotia. Also Pb from U.S. auto emissions accounts for between 1/4 and 1/2 of the Pb found in the air at the Canadian sites.

6. Experiments with controlled (in space and time) releases of inert artificial tracers (such as perfluorocarbons) have clearly demonstrated long-range transport of up to 3000 km from ground releases. These experiments cannot be used to generate source-receptor relationships for reactive acidic pollutants, but are useful in establishing the uncertainties associated with the calculation of air mass trajectories from the meteorological wind fields.
7. Trends in concentrations of acidic compounds caused by changes in emissions on the order of -18 to -30% are difficult to resolve with a 5 to 9 year observational record because of meteorological variability and changes in methodology of measurement. Statistical analysis showed that not only does one need to include seasonal variations and long term trends in a model fitting the data but also variations on a time scale larger than one year and less than the data record. Despite the difficulty some interesting changes were observed.
8. In eastern Canada statistically significant decreases in atmospheric SO₂ (the predominant acidic sulphur compound in air) were observed between 1980 and 1985 at ELA-Kenora, Chalk River, Forêt Montmorency and Kejimikujik (Figure 3.2.30a). All of these sites are in or downwind of regions in which SO_x emissions have decreased by more than 10%. The exception was Algoma near Sault St. Marie where no change in SO₂ was apparent. This is understandable since a major upwind source region for this site is Illinois where emissions changed by only -4.5% (Table 3.2.2). Also consistent with these results is the deduction that total S in air at Dorset, Ontario (closest to Chalk River) decreased between 1981 and 1986.
9. An analysis of the change in SO₂ air concentration between 1982 and 1987 at ELA-Kenora and Kejimikujik, Nova Scotia as a function of air parcel trajectory sector, yielded the following result. At ELA, the decrease was a relatively uniform factor of 3 to 4 regardless of air parcel origin. At Kejimikujik, it varied from a factor of 10 in the relatively clean sector off the Atlantic over eastern Nova Scotia to a factor of 2 off the relatively polluted continental sector to the southwest. These decreases in concentration are larger than what one would expect from a simple linear relationship between emissions and downwind air concentrations. However,

meteorological variability cannot be neglected as a causative factor even though sector analysis has been conducted in an attempt to reduce it.

10. The concentration of total NO_3^- in air or in precipitation did not consistently decrease or increase at 5 rural sites in eastern Canada between 1979 and 1987 or at Dorset, Ontario between 1981 to 1986. However there were statistically significant variations observed at several locations. The cause of these variations are likely meteorological. The fact that there is little or no change in NO_3^- is not surprising considering the magnitude and complex pattern of emission changes during the early 1980's. These emissions increased in Canada but in the US a regionally variant pattern of increases and decreases occurred.
11. Between 1981 and 1987, the concentration of $\text{SO}_4^{=}$ in precipitation adjusted to account for dependence on precipitation amount varied significantly at all five sites in eastern Canada. Excluding Montmorency, all sites displayed a net decrease in this time period ranging from 18 to 40% (Figure 3.2.29a). The changes are consistent with overall pattern of change in eastern North America between the early 1980's and late 1980's (Figure 3.2.42).
12. There are no significant trends in surface level atmospheric concentrations of ozone in southern Ontario between 1979 and 1988. This is consistent with only small changes in NO_x emissions in this period in Canada and the northern U.S. states.

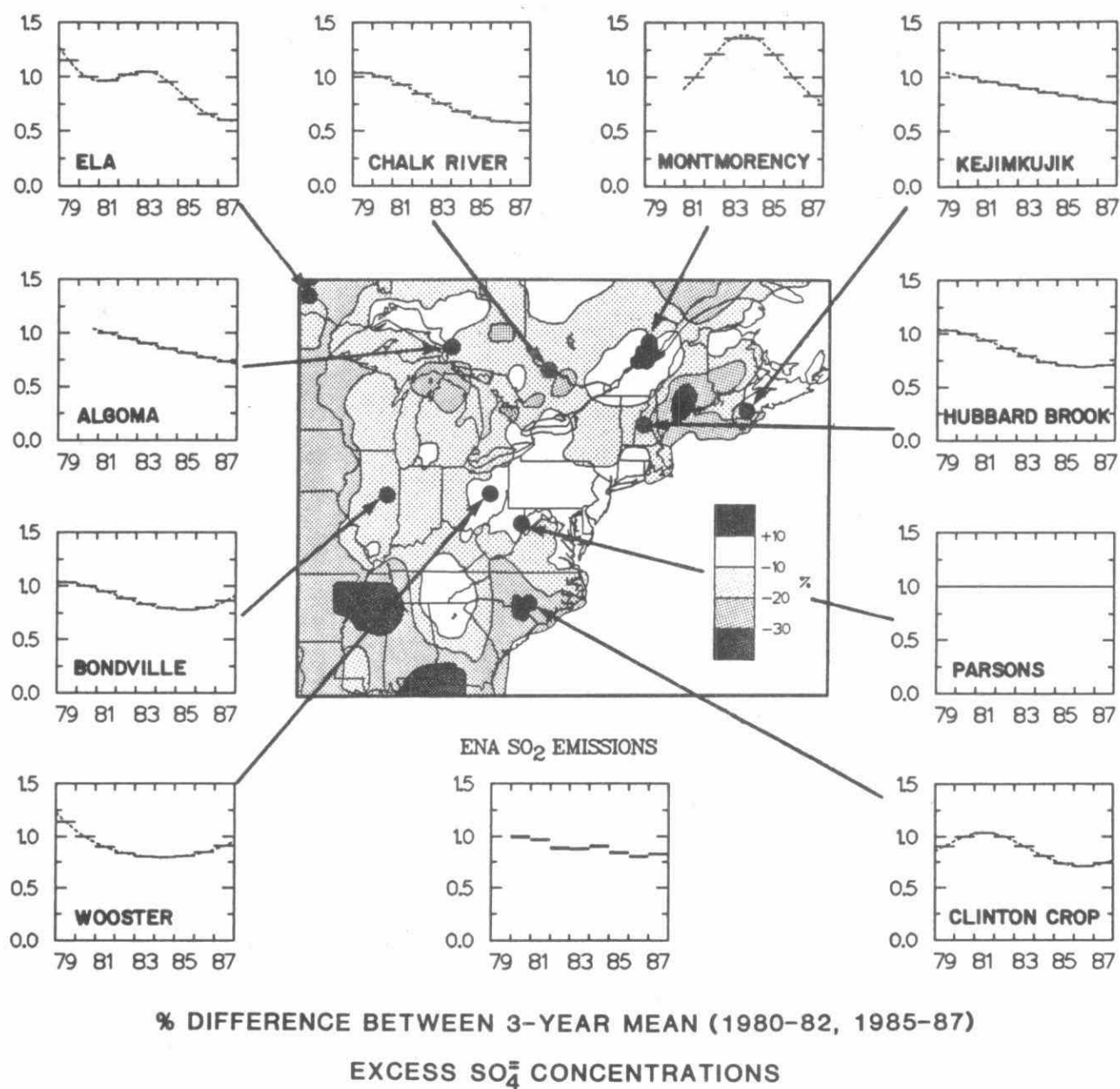
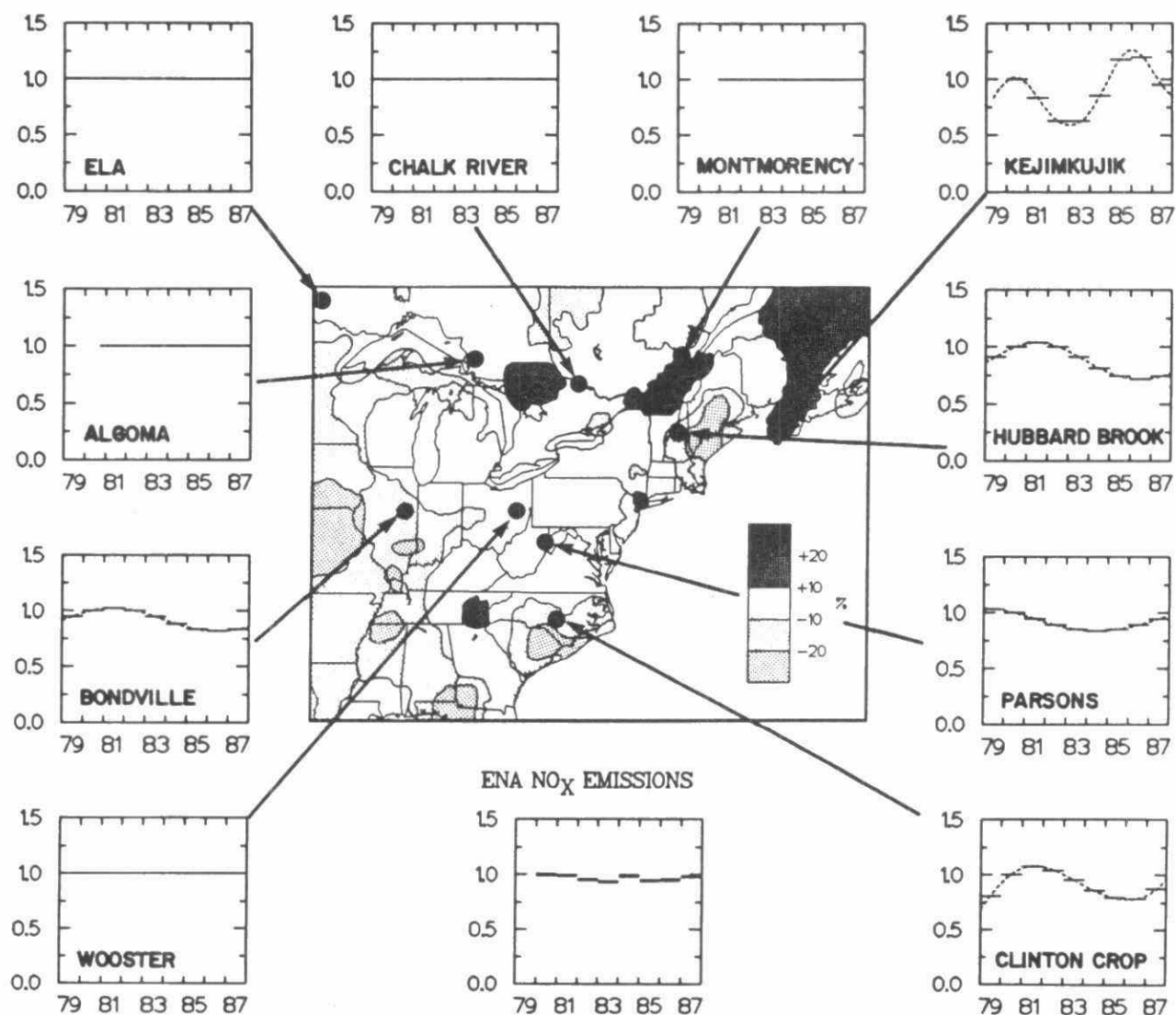


Fig. 3.2.42 Trends in SO_2 emissions and precipitation excess sulphate concentrations in eastern North America. The different shaded areas on the map show the percent difference between 1980-82 and 1985-87 average concentration fields. The box directly underneath the map shows the eastern North American SO_2 emission changes normalized to 1980. The outer boxes show the year to year observations at a number of sites normalized to 1980.



% DIFFERENCE BETWEEN 3-YEAR MEAN (1980-82, 1985-87) NO_3 CONCENTRATIONS

Fig. 3.2.43 Trends in NO_x emissions and precipitation excess sulphate concentrations in eastern North America. The different shaded areas on the map show the percent difference between 1980-82 and 1985-87 average concentration fields. The box directly underneath the map shows the eastern North American NO_x emission changes normalized to 1980. The outer boxes show the year to year observations at a number of sites normalized to 1980.

3.3 SOURCE-RECEPTOR RELATIONSHIPS FROM NUMERICAL MODELS

3.3.1 INTRODUCTION

Source-receptor relationships are defined here as the effect of a source, a group of sources, or a source area on the air quality and eco-system of any geographic location called the receptor. A source refers to a point or an area of emissions of primary atmospheric pollutants. The effect on the receptor can be due to the impact of the primary pollutants as well as secondary pollutants which form as a result of chemical reactions in the atmosphere.

The degree of impact of these pollutants on the receptor depends on the sensitivity of the receptor to the pollutants and the amount of the pollutants received. Pollutants are received by the receptor through various pathways. Here we are concerned with the atmospheric pathways; i.e. the transport of the pollutants by the wind, their chemical transformation and deposition along the way and the manner in which they are deposited at the receptor.

Mathematically the source-receptor relationship for a linear system can be given as follows:

$$D_j = \sum S_i \cdot X_{ij} + B_j \quad (1)$$

where the summation is over repeated indices, and D_j is the deposition or concentration of pollutants at the j th receptor due to the i th source, or source area (S_i). X_{ij} is the "transfer function" (sometimes also called the transfer matrix) linking the i th source to the j th receptor. For a linear system, X_{ij} is independent of S_i but X_{ij} in general is a function of S_i and in this case, a simple linear relationship is not appropriate. Since the sources are usually anthropogenic in origin, the background deposition B_j accounts for deposition from natural sources and sources outside the domain of interest. The background is relatively small in high deposition regions and dominates in remote regions. It is usually the product of a constant background concentration in precipitation times the precipitation at the site (j) (e.g. Eliassen, 1980; Barrie and Hales, 1984).

In the early stages of model development for simulations of long range transport problems, a linear relationship between D_j and S_i was assumed for the sulphur species; i.e. X_{ij} was assumed to be independent of S_i . With this assumption mathematical models were developed to determine the values of X_{ij} at various time scales. Some of the earlier models developed were due to Eliassen (1980), Shannon (1981), Venkatram et al. (1982), Fay and Rosenzweig (1980), Ellenton et al. (1985), and Voldner et al. (1981).

The various parameters used in most of these models were generally derived from a best fit to the observed deposition fields for SO_4^{2-} , and hence represented the situation of the current emissions and the associated atmospheric chemistry. Therefore, even though

these models displayed considerable skill in reproducing the seasonal, annual and often monthly and weekly deposition patterns, they suffered from the criticism that such skill was fortuitous since the parameters were derived from the observed data and the emissions have not changed significantly during the period of their evaluation. This implies that these models might not be able to be used for a situation where emissions are reduced significantly since the parameters may not be valid for these reduced emissions. It is to be noted that one of the primary reasons for developing a source-receptor relationship is to determine, along with economic models, the most cost effective manner in which control can be put in place to reduce the emissions and deposition of the primary and secondary pollutants.

Such criticism of the linear models can be better understood if one considers the mechanisms by which the primary pollutant SO_2 can affect a receptor through the chemical reactions to $\text{SO}_4^{=}$, and in the presence of precipitating clouds, as acid rain. SO_2 can be transformed to $\text{SO}_4^{=}$ aerosols in the gas phase primarily through its reaction with OH radicals. Investigations by Calvert and Stockwell (1984) have shown that such a chemical reaction is not chain terminating. In other words, OH radicals are not consumed by this reaction as more are produced in the process. Thus one can expect this chemical pathway to be approximately linear. Indeed, some more advanced modelling, such as in the Acid Deposition and Oxidants (ADOM) or Regional Acid Deposition (RADM) Models, shows this to be valid.

SO_2 can also be transformed to $\text{SO}_4^{=}$, in the aqueous phase (precipitating and non-precipitating clouds). The most dominant mechanism for this reaction is the reaction of S(iv) with H_2O_2 in the aqueous phase leading to the formation of $\text{SO}_4^{=}$ (Schwartz, 1984; Seinfeld, 1980). H_2O_2 is readily soluble in water. Thus, the degree to which atmospheric SO_2 can be transformed to $\text{SO}_4^{=}$ in the aqueous phase depends on the availability of H_2O_2 (Schwartz and Daum, 1988), which in turn depends on the photo-chemistry of other species in the atmosphere such as NO_x and reactive hydrocarbons (RHC) etc. This introduces a nonlinearity in the relationship between D_j and S_i through the limitation of H_2O_2 in certain circumstances. The reaction of S(iv) in the aqueous phase with O_3 can also be a significant process of $\text{SO}_4^{=}$ formation. This pathway, being pH dependent, is also nonlinear.

In addition to the above arguments, investigations with clouds indicate that transport of the pollutants can be significantly affected by the vertical motions inside clouds (e.g. Isaac et al., 1983; Banic et al., 1986; Ching and Alkezweeny, 1986; Dickerson et al., 1987). Thus, it was argued that only a three dimensional model with a minimum vertical domain of 10 km, which includes the details of the atmospheric photo-chemistry and the cloud processes, could reliably establish the source-receptor relationship. Being less parametric, such a detailed model could also be used to simulate scenarios with significant emissions changes.

The degree of non-linear response of the deposition fields to the source terms is expected to be a function of the space and the time scales and whether only wet deposition or total (dry plus wet) deposition is considered. For instance, over a long averaging time period and for depositions averaged over a greater geographical area (e.g. over an entire continent), the relationship between total deposition and emissions is expected to be linear (National Academy of Sciences, 1983). This can be argued mainly from the conservation of mass.

On the other hand, if one is interested in the variability of deposition on a statewide or provincial scale, then such linear relationships cannot always be expected. It has been argued that even on this scale annual deposition values may be linearly related to the emissions. However, acid wet deposition is highly episodic (Smith, 1981). In other words, a significant fraction of the total annual deposition occurs over a few precipitation episodes. If linear relationships cannot be assumed to hold on an episodic time scale, then it is doubtful that annual deposition will behave in a linear manner.

Non-linearity is a function of both the availability of H_2O_2 and O_3 in the conversion of SO_2 to SO_4^- in the aqueous phase. Consequently, one expects to find this non-linear behaviour everywhere during an episode (Fung et al., 1989).

This led to the development of several three dimensional Eulerian models (Venkatram et al., 1988; ERT, 1984, 1985; Chang et al., 1987; Lamb, 1982, 1983, 1985; Carmichael and Peters, 1984). The Acidic Deposition and Oxidants Model (ADOM) and Regional Acidic Deposition Model (RADM), given in the first four references, are more detailed in their formulations than the others.

In this section we present a review of the results of the linear models developed to date and compare them with the results of the more complex three dimensional models. It is shown that whereas the linear models predict a one-to-one correspondence between deposition (or concentration) at the receptor and the emissions at a source, the non-linear models show that the deposition (concentration) reductions would be lower at the receptor for a similar reduction in the emissions.* The trend however, is the same; i.e. one always observes a reduction in deposition for a reduction in emissions.

This implies that the degree of emissions reduction will have to be greater than the linear models would predict. Evaluations of the models are underway with an extensive data set to determine the difference from the linear model predictions with more precision. It is noted that the linear model results (e.g. Ellenton et al., 1985; Voldner et al., 1981) have been used to determine the emission reductions in Canada required by 1994. Preliminary

* This is especially true for wet deposition of sulphur. The total deposition (wet plus dry) is approximately linear.

evaluations indicate that for the sulphur species the degree of non-linearity in total deposition lies within the precision of model outputs and observed data. This suggests that the linear models, although scientifically deficient, can be used in an engineering manner to study the source-receptor relationship for total (wet plus dry) deposition of sulphur.

This chapter deals with the review of various mathematical models and their use in defining the source-receptor relationship.

3.3.2 MAJOR CONSIDERATIONS IN MODELLING SOURCE-RECEPTOR RELATIONSHIPS

Detailed information on the relationships and changes in the relationships between emission sources and specific receptors can only be obtained through the use of mathematical models. These models attempt to relate all the factors which are involved in describing source-receptor relationships. We are confining our discussion to the atmospheric components of these relationships since other RMCC Subgroups will be describing aquatic, terrestrial and other effects (health, socio-economic etc.) in their respective assessments. The atmospheric component requires information on the relevant emission sources and transport of the pollutants through the atmosphere, a description of the physical processes to move the material both in and out of clouds, the transformation of the initial pollutants by chemical processes and finally a mechanism to remove the pollutants by wet and dry deposition. In addition to these factors, the mathematical models themselves require numerical algorithms to solve conservation equations, analysis methods to prepare the meteorological, geophysical and chemical input/output data and computers of sufficient speed and storage capacity to solve the problem on a suitable time scale.

The ability of a model to simulate source-receptor relationships for various averaging times then depends on:

- (1) The detail and accuracy of the mechanisms incorporated into the transport, chemistry and scavenging aspects of the model;
- (2) The temporal and spatial resolution and accuracy of the input meteorological, emission and geophysical data.

A short discussion of these considerations follows.

3.3.2.a MODEL FORMULATION

Transport and Diffusion

There are many transport and diffusion methodologies used in atmospheric models. Statistical models use either a mean wind direction with plume standard deviations reflecting horizontal fluctuations on the synoptic scale or direction frequency classes. These models can only be used to simulate long term source-receptor relationships since they reflect only "mean" large scale meteorology.

The more complex Lagrangian models compute trajectories either from emission sources or to receptor sites (e.g. Summers and Olson, 1985; Kahl et al., 1989; Pudykiewicz, 1988; Walmsley and Mailhot, 1983 ; Haagenson et al., 1987). These trajectories are computed from analyzed or observed wind data on isobaric or isentropic surfaces or they use vertical motion to give 3-D wind fields. There are different algorithms to compute the trajectory end-points but most models use the constant acceleration method which requires iterative solutions of the trajectory equations. Tracer releases (CAPTEX, Chernobyl, etc.) and theoretical studies have been used to evaluate trajectory models and the results indicate that the trajectories in the middle of the boundary layer (950-925 mb) are reasonably representative of the pollutant transport.

Most Lagrangian models are run for a single layer and this lack of vertical resolution and wind shear effects has the potential to affect source-receptor relationships. Material mixed to higher elevations by diffusion, large scale transport or cloud mixing could travel long distances before being deposited or scavenged. Despite this problem Lagrangian models have enjoyed a high degree of success in simulating concentration and deposition patterns of sulphur species in Europe and North America.

Although Lagrangian models frequently employ plume or puff spread as a function of distance downwind, a number of trajectories must be analyzed before a statistically reliable deposition field can be produced. These models are normally used for monthly, seasonal or annual average deposition. In an Eulerian model formulation, pollutant transport is computed at many vertical levels using advection into or out of each grid cell. Thus vertical resolution and vertical wind shear concerns are handled directly. Pollutant diffusion is usually formulated in terms of 3-D eddy diffusivity (K) with values calculated as a function of space and time. In addition to real diffusion, these models are subject to artificial or numerical diffusion which is a result of approximating a continuous diffusion process by a discrete process on a grid. Eulerian models employ sophisticated advection/diffusion numerical algorithms to minimize such effects which might otherwise alter source-receptor relationships. Depending on the model resolution and the accuracy of the meteorological data this formulation allows the possibility of modelling deposition on an episodic basis.

An additional physical mechanism which can affect deposition by changing transport properties is the vertical mixing of pollutants due to clouds. If this mechanism is not included in the model, deposition patterns could be altered downwind of a source.

Chemistry Formulation

Chemical processes can have a major effect on the patterns of dry and wet deposition away from source regions. Correspondingly such processes affect source-receptor relationships.

Modelling of chemical processes has been performed by methods ranging from simple linear conversion between species (e.g. Fisher, 1978; Ellenton et al., 1985) to complex sets of equations to be solved for gaseous and aqueous phase reaction schemes (e.g. Venkatram et al., 1988; Chang et al., 1987). Sulphur chemistry is perhaps the most well known and has been modelled as a linear conversion from SO_2 to SO_4^- in many statistical and Lagrangian models. The conversion rates selected and any seasonal dependence of those rates would affect the dry deposition and scavenging rates and thus the relationships between sources and receptors. Lagrangian models can be very successful in simulating current deposition patterns because parameters such as chemical conversion rates can be calibrated for the present conditions.

More complex oxidant and sulphur chemistry mechanisms have been formulated in several Lagrangian models (e.g. Eliassen et al., 1982) although this framework has difficulty handling such processes in multisource regions. An Eulerian framework allows complex chemical mechanisms to be incorporated for both gaseous and aqueous phase processes. The non-linearity concerns in modelling source-receptor relationships are described in the next section of this chapter. Both the potential nonlinearity of the chemical mechanism and the conversion rates for different meteorological conditions and different mixes of pollutants are of concern in source-receptor relationships. More detailed treatment of such processes should result in improved model performance as long as the formulations are sufficiently complete and the reaction rates are known accurately.

Wet and Dry Deposition

Most statistical and Lagrangian models use simple wet scavenging ratio concepts (Venkatram et al., 1982; Ellenton et al., 1985; Voldner et al., 1981; Shannon, 1981) for sulphur compounds (SO_2 and SO_4^-). Scavenging is usually assumed to occur over the depth of the entire grid cell since these simple models often have only one vertical layer.

Dry deposition in statistical and Lagrangian models such as those mentioned above is derived using a dry deposition velocity which can vary with time of the year or with surface characteristics depending on the complexity of the model. For source-receptor relationships the accuracy of these parameters affects the results. These models can to

some extent be calibrated for present conditions by varying the parameters used for dry deposition and scavenging rates.

Some Eulerian models employ cloud physics modules which include more physically based scavenging assumptions (Venkatram et al., 1988; Chang et al., 1987). Also, the scavenging can be limited to the portion of the air mass encountering clouds or precipitation. Since Eulerian models can readily incorporate gridded fields of land use, roughness length as well as atmospheric stability on an hourly basis, dry deposition velocities can be formulated which include more detail and more physics than statistical or Lagrangian models. The accuracy of parameters such as the surface resistance affect the rate at which material is deposited and correspondingly the relationships between sources and receptors. There are indications that direct deposition on ground through fog and cloud droplets may be an important process in some areas (e.g. high elevation locations, see Section 3.2.2.b). This process has not been dealt with in any model so far.

3.3.2.b INPUT DATA

The resolution and accuracy of input parameters to a long range transport model can affect the absolute values of deposition and the source-receptor relationships over some averaging time.

Emission Data

Errors in either the total emissions of a species or the distribution of those emissions can affect the absolute value and/or the pattern of deposition. However, percentage changes in deposition could still be modelled fairly well if the system were linear. For source-receptor relationships or comparisons with long term deposition patterns, systematic errors in allocating the vertical level at which the material is injected can have some effect. Most statistical and Lagrangian models assign all emissions to one vertical level. In comprehensive Eulerian models where emissions for many species are used as input data (i.e. SO_2 , NO_x , RHC, NH_3 etc.) systematic errors in total emissions can bias model results and correspondingly affect source-receptor relationships. For example, omission of natural RHC's from an emission inventory would alter the oxidant concentrations in the model and thus affect the conversion of SO_2 to $\text{SO}_4^{=}$. Heisler et al. (1986) compared NAPAP and EPRI emission inventories to estimate potential errors in these inventories. The NH_3 inventory was very different in these two data sets (EPRI NH_3 emissions were about 7 times the NAPAP emissions). NH_3 acts to neutralise the acidity and hence affects the aqueous conversion of SO_2 . Further, it also determines the partitioning of particulate to gaseous NO_3^- and hence the dry deposition of NO_3^- .

Geophysical Data

There are several processes in long range transport modelling which are influenced by geophysical data. Simpler models which do not contain detailed information on surface characteristics could not resolve a factor such as reduced or enhanced dry deposition to water surfaces. More detailed geophysical data used in comprehensive Eulerian models allow the possibility of these effects being taken into account. However, the accuracy and resolution of these data can still affect deposition over episodic time scales in Eulerian models. For example, if a snow line were supplied from climatological data, dry deposition and mixing rates would depend on the location of that snow line. For an episodic evaluation a climatological average snow line might not reflect the conditions for that period of time.

Meteorological Data

The accuracy and resolution of meteorological data have a major influence on the time scale over which modelled deposition could be reliable. Statistical models which do not contain actual meteorology have the inherent limitation that they can be used to predict only long term average deposition or concentration fields. Studies with Lagrangian models have shown that meteorological variability from month to month or year to year can significantly affect deposition patterns and can account for most of the observed variations in deposition at sites (Ellenton et al., 1985, 1988; Fernau and Samson, 1986).

The factor which is of most importance for deposition models is the precipitation field. For the simplest models precipitation is modelled as a function of the duration of wet and dry periods based on climatological data. Lagrangian models usually use analyzed observed precipitation over land surfaces. When such models make use of gridded 24 hour average precipitation without taking into account nonprecipitating hours within that period, they can overestimate deposition near the source. This occurs since a washout ratio approach predicts efficient scavenging of SO_4^- even with light precipitation. Lack of precipitation data over the oceans also affects model results in coastal regions.

Comprehensive Eulerian models use either numerical model generated cloud and precipitation fields, observed fields or a combination of observed data and diagnostic fields from weather prediction models (Venkatram et al., 1988; Chang et al., 1987).

The use of dynamic models to estimate cloud and precipitation fields allows the separation of these fields into large scale and convective components. The ADOM model uses such diagnostic fields as first guess data which are then modified by observed cloud and precipitation data over land. These detailed data allow the possibility of modelling over short deposition episodes. However, experience with the models has indicated that the accuracy of the precipitation data can significantly affect model results over these short time periods. Also, when comparing model results averaged over a grid square

with station deposition, the subgrid scale precipitation variations can affect the comparisons.

Similarly, subgrid scale variations in other input fields such as wind, emissions and geophysical data can result in discrepancies between model and observed results. For example, lack of time or spatial resolution in the wind field can lead to individual large sources being advected in the wrong direction for a given episode (McCormick et al. 1989). This effect would be mitigated by averaging source-receptor relationships over longer time periods. Also, if the grid size is large, one is forced to use a grid average deposition velocity which can introduce errors in dry deposition estimates.

3.3.2.c PRACTICAL COMPUTATION CONSTRAINTS

The basic idea of a comprehensive model is to incorporate all of the relevant details known about specific processes into a common numerical framework. Lack of accurate knowledge about the processes imposes one constraint in developing such models. A second constraint is the available input data to run such a comprehensive model. The third factor which limits the accuracy and completeness of such models is the required computer resources to run the models. Compromises must be made between what is practical and what can be most rigorously justified from a theoretical viewpoint. This means that the number of variables used to formulate the model is smaller than the number required for an ideal model.

Comprehensive models such as RADM and ADOM use CRAY computers to perform the calculations. Advances in computer technology have eased the restrictions on storage and computation time but they are still a constraint when preparing model runs. Preparation of the meteorological and emission input fields also requires significant manpower and computer resources which limit the length of model simulations. The volume of output from such comprehensive models also requires a significant commitment of manpower and computer resources to analyze the results.

3.3.3 NONLINEARITY QUESTIONS

If it is possible to single out a species at the source, and control its emission without any change in the emission of other material, then this process does not introduce non-linear responses by itself. However, subsequent atmospheric processes may change in their (non) linearity, e.g. an oxidant limited process may become linear upon reduction of the species to be oxidized. Oxidant formation which depends in some respect on the ratio of RHC/NO_x may show non-linear response to NO_x reduction when this ratio is small (urban conditions).

Chemical Transformations

The process of main importance concerns the conversion of NO_x to nitrate species and SO_2 to sulphate. These processes can be summarized by the equation:

$$\text{Rate of conversion} = k [X] [Y]$$

where: k = rate coefficient of the reaction
 $[X]$ = the concentration of X (which can be NO_x or SO_2)
 $[Y]$ = the concentration of Y (which is an oxidizing species)

This process is linear as long as the change in $[X]$ has no effect on either k or $[Y]$.

A. $X = \text{NO}_2$

In this case, the predominant oxidizing species are $Y = \text{OH}$ during the day and $Y = \text{O}_3$ during the night. Since both the OH and O_3 concentrations are quite dependent on the NO_x concentration (as well as the hydrocarbon levels) (e.g. Finlayson-Pitts and Pitts, 1986), the oxidation of NO_x to nitrates is in principle always a nonlinear process. However, some smog chamber data suggest that under specific conditions the effective rate of oxidation is quite linear (Spicer, 1983; Spicer and Holdren, 1983); Lagrangian models assuming the oxidation of NO_x to nitrates to be (pseudo-) linear have been used with some success (e.g. Bottenheim et al., 1984; Olson et al., 1989a).

B. $X = \text{SO}_2$

There are two rather different ways of transforming SO_2 into sulphates: homogeneous gas phase reactions and liquid phase reactions in clouds.

- (i) Homogeneous gas phase reactions. In this process, the predominant oxidant is $Y = \text{OH}$. Since the OH concentration is determined by the NO_x -hydrocarbon chemistry and since this reaction is now known not to result in radical consumption (the OH radical is effectively transformed into HO_2 which via other reactions leads to OH being formed again, Stockwell and Calvert, 1983), this process is essentially linear.
- (ii) Liquid phase reactions in clouds. There are three distinct ways of transforming SO_2 into sulphate in clouds: oxidation by H_2O_2 , O_3 , and metal ion catalyzed reaction with O_2 . Although the details of the fundamental mechanisms are still uncertain, enough is known about these reactions that it can be stated that all are nonlinear.
 - a. $Y = \text{H}_2\text{O}_2$. Contrary to the gas phase reaction of SO_2 with OH , reaction of SO_2 with H_2O_2 has an effect on the oxidant concentration.

This is due to the fact that the rate of formation of H_2O_2 is generally much slower than the rate of reaction of H_2O_2 with SO_2 and there is no recycling of H_2O_2 from the product side. Consequently, if there is more SO_2 than H_2O_2 in the air, the supply of the H_2O_2 oxidant can be exhausted well before all SO_2 is transformed into sulphate. Such conditions occur often near the sources of SO_2 and NO_2 .

- b. $\text{Y} = \text{O}_3$. Since the Henry's Law constant for O_3 is rather low, one would normally expect that this reaction has only a marginal effect on ambient O_3 concentrations and hence oxidant limitation is not a major consideration. However, the process of oxidation of SO_2 has the effect of reducing the pH of the cloud water. Since the rate coefficient of the $\text{SO}_2 + \text{O}_3$ reaction in clouds is dependent on the pH value, and drops dramatically with decreasing pH, nonlinearity in this case does not originate from an effect on $[\text{Y}]$ but on k .
- c. $\text{Y} = \text{O}_2$, metal ion (Me^+) catalyzed. The same reasoning as used for the $\text{SO}_2 + \text{O}_3$ reaction applies here: the reaction is nonlinear due to the pH dependence of the rate coefficient.

Deposition

There are two processes of deposition: wet and dry deposition. Although at first sight they are both linear, there are some considerations which make these processes somewhat less than linear.

Dry Deposition

This process of removal from the atmosphere is essentially linear in that the species concentration does not contribute to the largely physical processes that are involved. It is only at the actual uptake of the species at the surface that chemical considerations will play a role, but it is usually these factors that cause the ultimate difference in the largely empirical "dry deposition rate" data that are used in many models. At this species-surface interaction level, it is actually possible to conceive of a saturation condition. Another case in point is the deposition of SO_2 on wet surfaces. This process can lead to substantial changes in pH and hence the apparent dry deposition velocity " V_D " becomes a function of the SO_2 concentration. The reverse is actually proposed in the Netherlands, where the often high levels of NH_3 create an alkaline environment which leads to enhanced SO_2 dry deposition.

Precipitation Deposition

As with dry deposition, this process is essentially a physical process and as such not very dependent on species concentrations. The large nonlinearity in sulphate removal is not

due to the precipitation process itself, but the way in which the cloudwater sulphate is produced. Nevertheless, there is conceivably a nonlinearity possible due to sulphate concentrations. Sulphate aerosols are generally good cloud condensation nuclei and hence it is possible that the presence of large amounts of aerosols leads to enhanced removal by precipitation of both nitrates and sulphates. This effect would be a nonlinearity in sulphate removal. Nitrate aerosols are less active cloud condensation nuclei, and generally much less abundant than sulphate aerosols; hence no nonlinearity in nitrate wet deposition is expected.

3.3.4 LINEAR MODELS

3.3.4.a INTRODUCTION

The early attempts to simulate and study the acidic deposition phenomenon by mathematical models are based on the assumption that the conversion of the primary species to secondary species can be characterized by a linear process. Nevertheless, as pointed out in earlier sections, this assumption has been increasingly found to be inadequate as more research data become available. Also, with the computer power now available, comprehensive models with detailed chemistry to specifically address the issue of non-linearity seem practical. Linear models still serve a useful purpose as engineering tools to study source-receptor relationships given their proven ability to reproduce the present deposition patterns with reasonable accuracy.

In this section, we will review the results of the linear models. The next section will give a summary of the findings of a major comprehensive model ADOM.

3.3.4.b MODELLING APPROACHES

Three types of linear models are usually referred to in the literature. The STATISTICAL models are of the simplest type of models employing statistical averages for meteorological inputs and model parameters. Consequently, the validity of the model predictions is limited by the temporal and spatial resolution of the input data and the various approximations in the model formulation. Briefly, this type of model uses the analytic solution of a simplified (approximate) form of the general transport equation on each of the source to receptor pairs. Wind frequency roses determine the direction of transport. One of the earliest attempts at this approach is that of Fisher (1975). Further development (Fisher, 1978) on this early version saw the incorporation of the stochastic approach to precipitation scavenging of Rodhe and Grandell (1972). This approach which considers the stochastic behaviour of an average precipitating (wet) and non-precipitating (dry) period over a fixed location is widely adopted in statistical models (e.g. Venkatram et al., 1982).

Next on the scale of complexity are the LAGRANGIAN models, using the parcel method employed for the advection of the effluents. Dispersion is typically idealized as puffs or

plumes moving on a horizontal surface. The model by Olson et al. (1978) uses three dimensional trajectories. This conceptually simple approach utilizes air parcel trajectories to determine the position of a puff or a plume of effluent. Changes in air concentration are a result of the balance between the source and sink terms within the puff or plume segment. Since each puff can be tracked independently, the lower limit on the temporal and spatial scales of applicability comes from the resolution of the input data and statistical nature of transport and diffusion modelled by a finite number of trajectories. The manner in which such models handle plume spread also affects the minimum time and space resolution of the output. One of the early efforts in this direction is that of Eliassen (1980) in Europe who approximated each puff as occupying the grid volume containing the end point of the trajectory. In North America, Endlich et al. (1983) simulated puffs as rigid and expanding cylinders moved by trajectories. This model ENAMAP was adopted and enhanced by the US EPA to become RELMAP (Eder et al., 1986) which was one of the models evaluated in the ISDME project to be described later. Other attempts, building on the flexibility of the Lagrangian approach, incorporated expanding Gaussian puffs for pollution dispersion away from the idealized 'centre' of the puff. Examples are Ellenton et al. (1985), Benkley and Bass (1979). The last work was cited by the US EPA as having the potential for further development and consequently was further enhanced to become MESOPUFF II (Scire et al., 1983; 1984) which has the greatest versatility among Lagrangian models.

Appendix 3G illustrates how a linear Lagrangian model can be applied to emission scenario evaluation. Four scenarios were simulated: a. the base case for 1980 emissions; b. 1980 base case emissions for the U.S. with Canadian emissions cut according to the 1994 Countdown Acid Rain Program; and c. and d. Canadian emissions cut according to the 1994 Countdown Acid Rain Program while U.S. cuts for 1995 (c) and 2000 (d) were estimated based on President Bush's proposed emission reductions of 4.5 and 9 million tonnes, respectively. It is seen that the reduction in $\text{SO}_4^{=}$ deposition due to the Canadian control program alone would not be very significant without a reduction of the U.S. emissions. In this exercise with linear models, the percentage change in deposition was deemed to be more reliable than the absolute deposition.

The Eulerian approach can also be used with linear chemistry. This framework, which is most convenient for dealing with reactive chemicals, is based on solving the transport and mass balance equations at each of the grid points of the modelling domain. Since this modelling approach requires extensive meteorological data which put a large demand on computer resources, it has not been used as frequently for modelling linear systems. The Regional Transport Model (RTM-II, Liu et al., 1981) is the only model of this type that was found suitable for detailed evaluation by the Electric Power Research Institute (EPRI, 1984).

3.3.4.c EVALUATIONS OF LINEAR LONG-RANGE TRANSPORT MODELS

In 1980, an agreement between the U.S. and Canadian governments was reached to study the issues pertaining to the acidic precipitation phenomenon with a view to recommending a course of action for the two governments. One of the subgroups (regional modelling) under this bilateral agreement (United States/ Canadian Memorandum of Intent on Transboundary Air Pollution , MOI) was charged with selecting relevant long-range transport models for intercomparison and evaluation and recommending the most appropriate model for regulation purposes (MOI, 1982b).

Eight models (AES, MEP, MOE, ASTRAP, CAPITA, ENAMAP-1, RCDM-3, UMACID) with the first three being Canadian, were selected. All eight models assumed linear chemistry. This list represents a variety of formulations and techniques employed within the modelling community and each was developed with a different end usage in mind. For example, the ASTRAP model takes the mean of an ensemble of trajectories as the advecting trajectory and is intended for simulation of long term averages. On the other hand, the AES model considers trajectories at two pressure levels (850 and 1000 mb) to capture the best short term variations. This diversity together with the uncertainty in knowledge made it impossible to select the 'best' model for regulatory or legislative purposes. Nevertheless, this study sets the direction for future modelling activities. The study's conclusions and recommendations are as follows:

"While differing opinions remain within the modelling community as to the proper method and the statistics to be used for evaluation and intercomparison of model results, the Regional Modelling Subgroup of the MOI designated common evaluation criteria for performing this task for the eight selected models.

"It is generally accepted that one should expect model predictions to deviate from measurements because a practical model cannot incorporate even current understanding of the relevant chemical and physical processes, and because our available emissions and monitoring data bases contain inaccuracies and are insufficient to estimate the ensemble average which the model is designed to predict. Due to these deficiencies, it is not possible to quantify the uncertainties in model predictions based on the differences between model predictions and observations (residuals).

"Furthermore, the assumption of linearity by the models provided for rate constants that are independent of emissions and co-pollutant concentrations. The question is raised as to whether the linear models of sulphur transport represent reasonable first approximations in the absence of operational nonlinear models. It thus becomes subject to individual scientific judgment whether or not nonlinear effects would invalidate the general seasonal and annual results of these linear models".

Based on review of the eight long-range transport models and the comparison of their predictions with observed data, some conclusions on each of the model components were derived as follows:

1. When the sample wind fields are displayed for the models as mean trajectories and standard deviations (see Figures 3.3.1 and 3.3.2) for the month of January and July for two points in the U.S. and Canada and the statistics at various travel times for these two locations, it is seen that the mean transport winds for the eight models vary widely, depending on the type of data used to generate the wind flow. Such discrepancies in the calculation of mean trajectories which are also a reflection of different raw data used are a definite factor in producing differences in model results.
2. An analogous test made for the second major meteorological input common to all models, namely precipitation, reveals that the precipitation gridding process is also quite dissimilar between models, ranging from gridding hourly observations on time and space scales compatible with the model advection time steps, e.g. ENAMAP-1 and AES to calculating the average durations of wet and dry periods over seasonal or annual time periods, e.g. MOE and CAPITA. The wide variations in input precipitation amounts are a second factor in causing differences in model results.
3. The uncertainties in the emissions data were not available at the time of model evaluation. It is not unlikely that these uncertainties are a function of source regions, which would affect the model results significantly since a constant uncertainty factor would only introduce a bias. Furthermore, since emissions were only available as annual totals, model predictions cannot be expected to accurately simulate monthly or seasonal emissions variations. To properly analyze the behaviour of model predictions, one would need to know the magnitudes and spatial variability of all the emission uncertainties.
4. Extensive screening of the observed wet sulphur deposition and sulphate concentration data was necessary to correct for errors associated with catch efficiencies, evaporation and sample contamination. Out of the three networks (EPRI SURE, MAP3S and CANSAP) operating more than sixty sites over eastern North America, not enough data were found, after screening, to perform a meaningful evaluation of the models. Instead, the 'evaluation' serves as a demonstration of the statistical methodology to be used and as a preliminary indication of model performance.
5. Comparisons of model outputs with observed data show that collectively, all models perform better for wet sulphur deposition than for sulphate air concentration predictions. SO_2 was not considered for this comparison exercise due to the unavoidable contamination of data from local sources and the errors in measurements at very low concentrations. This is somewhat surprising because

wet deposition of sulphur is very episodic (most of the depositions occurring in a few precipitation events), whereas the model results were presented as non-episodic or longer-term. Nevertheless, the right order of magnitude of the large time and space-scale features of the wet sulphur deposition fields is reproduced by the models.

6. Only a few data points were found suitable for the evaluation of the model predictions. This handicap, combined with the unknown uncertainties in the emissions inventory and precipitation data, prevents a ranking of models in terms of their absolute performance.
7. The diversity of parameterizations in these operational models reflects the fact that they were independently developed. The variations in techniques and parameterizations reflect a breadth of scientific opinions and judgment amongst modellers. It is not at all surprising that models show differences in detail when applied to a single data set. On the contrary, the extent of agreement among the model outputs and between these outputs with observed wet sulphur deposition data suggests that the models have captured the essence of long-range transport.
8. Transfer matrices for sulphur species produced by the eight long-range transport models reveal variations among the absolute magnitude of the transfer matrix elements for a single model and for the same element among different models.

Transfer matrices were produced for 40 emission regions at 9 receptors (Figure 3.3.3) and also at 11 aggregated emission regions at 9 receptors (Figure 3.3.4). These transfer matrices are based on unit emissions and do not reflect the actual impact of a region on a receptor. The 9 receptors (Table 3.3.1) represent sensitive areas over eastern North America. These transfer matrix elements were then ranked according to their magnitude at the receptors and the ranking correlated using the Spearman's rank coefficient. These coefficients for the different models for the Muskoka, Ontario (Dorset) site are given in Tables 3.3.2 to 3.3.4 for sulphate ground level concentration, dry deposition and wet deposition, respectively. Only the ranking statistics for the 11 sources and 9 receptors are shown. Nevertheless, the values for the 40 sources and 9 receptors show similar correlation for the ranking. A value of 1 indicates perfect agreement in the order of ranking of matrix elements between models.

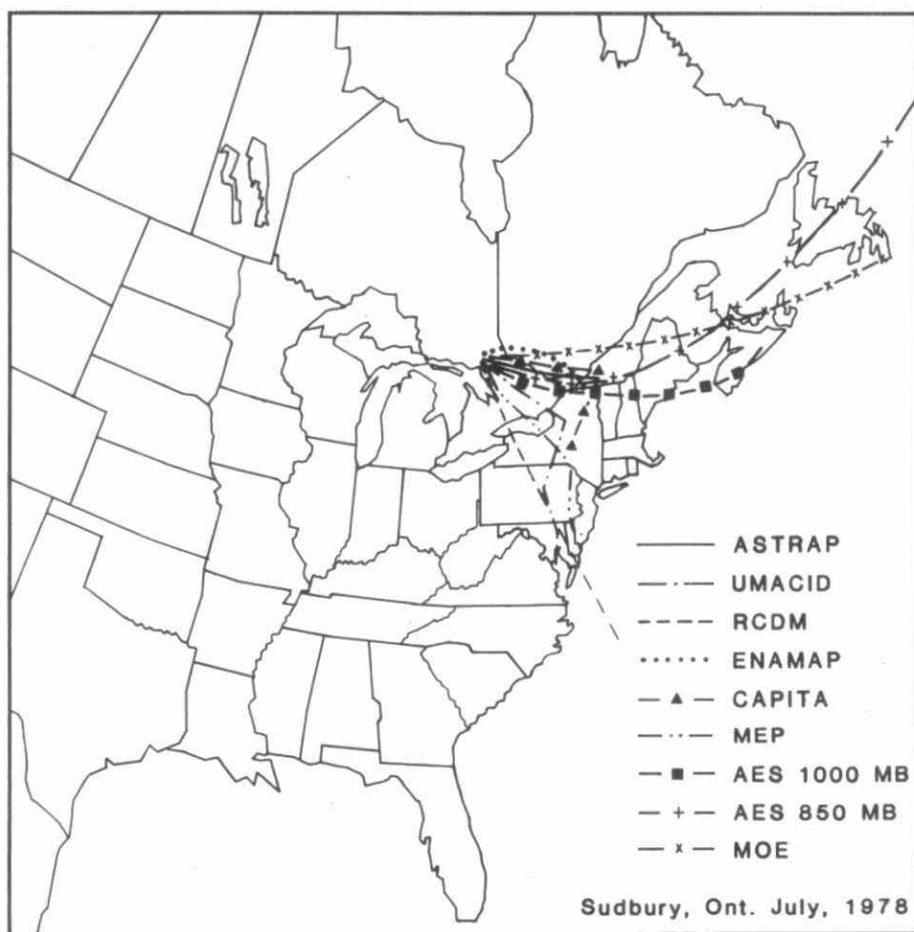


Fig. 3.3.1 Model trajectories starting from Sudbury, Ontario in January 1978.

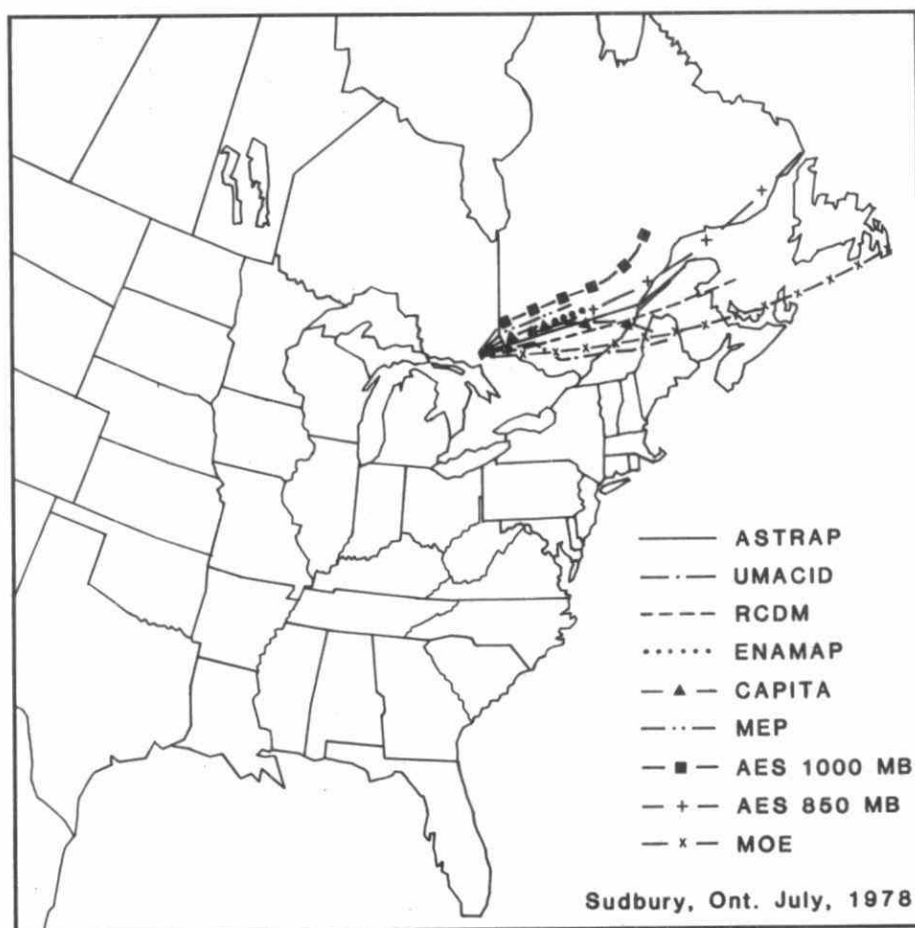


Fig. 3.3.2 Model trajectories starting from Sudbury, Ontario in July 1978.

Table 3.3.1

Targeted sensitive receptor sites

Abbreviation	Name
BW	Boundary Waters, Ontario
ALG	Algoma, Ontario
MUSK	Muskoka, Ontario (Dorset)
QUEB	Quebec City, Quebec
VT	Vermont/New Hampshire
ADIR	Adirondacks, New York
NSC	Southern Nova Scotia
PENN	Western Pennsylvania
SMOK	Southern Appalachians



Fig. 3.3.3 North American emissions source regions.

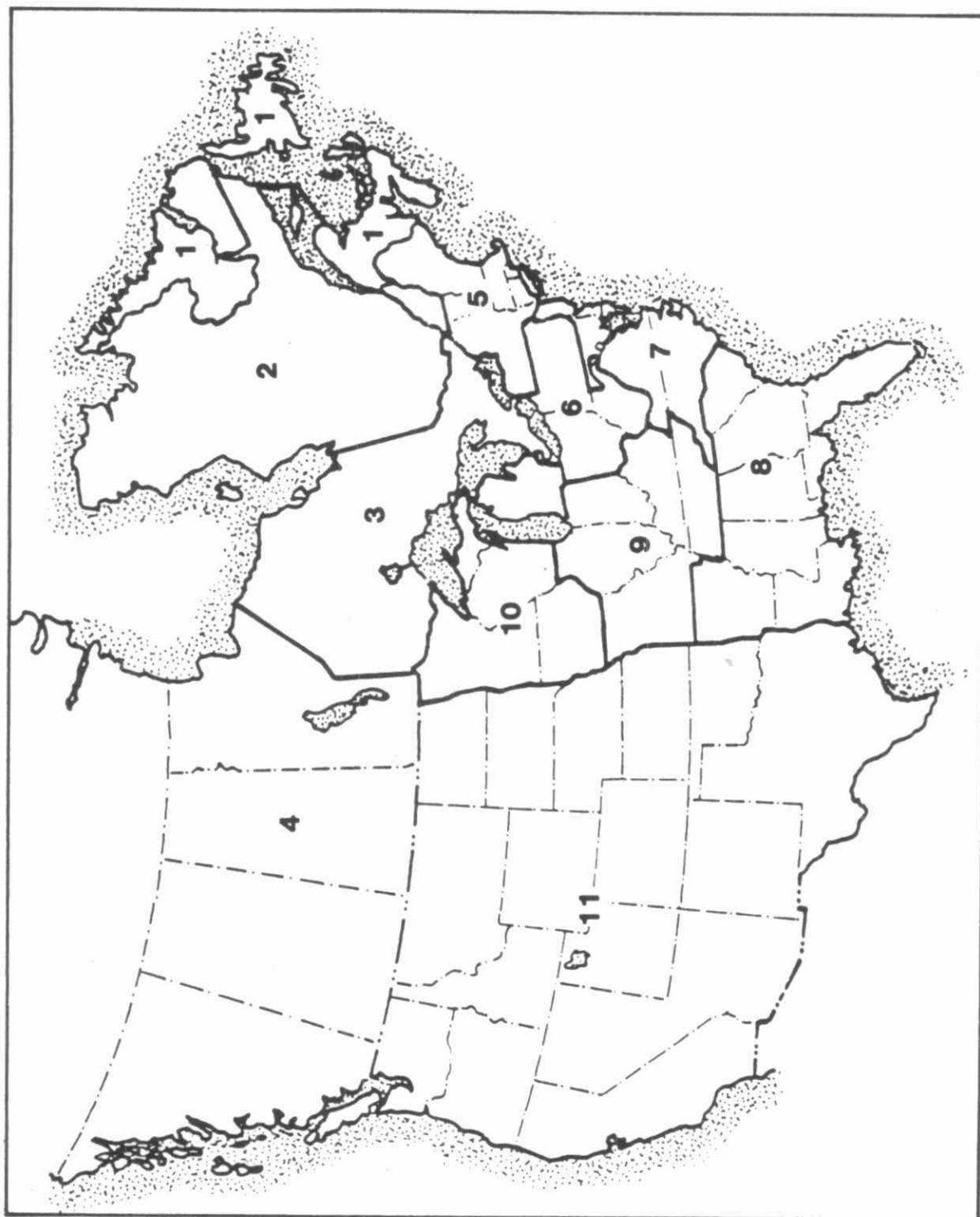


Fig. 3.3.4 Phase II aggregated emissions regions in North America.

Table 3.3.2
Spearman's Rank Correlation Coefficient Summary for ground level
SO₄²⁻ concentration from MOI (1982b) at Muskoka.

MODEL	AES	ASTRAP	CAPITA	ENAMAP	MEP	MOE	RCDM-3	UMACID
AES	-----	.82	.90	.92	.93	.98	.65	.96
ASTRAP		-----	.72	.84	.79	.81	.69	.87
CAPITA			-----	.93	.85	.89	.75	.86
ENAMAP1				-----	.89	.94	.73	.94
MEP					-----	.94	.62	.90
MOE						-----	.70	.96
RCDM-3							-----	.75
UMACID								-----

Table 3.3.3

Spearman's Rank Correlation Coefficient Summary for dry deposition from MOI (1982b) at Muskoka.

MODEL	AES	ASTRAP	CAPITA	ENAMAP	MEP	MOE	RCDM-3	UMACID
AES	----	.94	.95	.95	.93	.98	.79	.96
ASTRAP		----	.91	.95	.89	.91	.85	.95
CAPITA			----	.91	.89	.91	.84	.95
ENAMAP1				----	.94	.94	.85	.94
MEP					----	.93	.82	.92
MOE						----	.74	.95
RCDM-3							----	.85
UMACID								----

Table 3.3.4

Spearman's Rank Correlation Coefficient Summary for wet deposition from MOI (1982b) at Muskoka

MODEL	AES	ASTRAP	CAPITA	ENAMAP	MEP	MOE	RCDM-3	UMACID
AES	----	.85	.95	.91	.93	.90	.76	.94
ASTRAP		----	.78	.85	.71	.59	.88	.95
CAPITA			----	.96	.92	.89	.75	.73
ENAMAP				----	.79	.78	.80	.92
MEP					----	.93	.54	.83
MOE						----	.45	.73
RCDM-3							----	.88
UMACID								----

These results show that the models agree fairly well with each other in ranking the contributors to the receptor of Muskoka, Ontario. This is especially true for air concentration and dry deposition where most of the coefficients are between 0.8 and 1.0. The slight deterioration of the ranking coefficients for wet deposition might have been caused by the sporadic nature of precipitation coupled with the way the precipitation data were gridded.

A study by Voldner and Olson (1982) examined the rank correlation between 7 MOI models on the 40 X 9 source-receptor data. The RCDM model did not produce data for the 40 source regions. Table 3.3.5 shows the model ranking for wet sulphur deposition at Muskoka. Five models show that southwestern Ontario (SWO) ranks first for potential impact at Muskoka. The AES model shows Michigan (MCH) second and Sudbury (SUD) third, whereas the MOE model shows Sudbury first, southwestern Ontario second and Michigan third. When all ranks are correlated between models, tables similar to Table 3.3.4 are the result.

The actual unit transfer matrices or source-receptor relationships for the AES model are shown in Tables 3.3.6 and 3.3.7 (Olson et al., 1983). They are analogous to X_{ij} in equation (1) where the "i" represents the 40 source regions and the "j" represents the 9 receptor sites giving a 40 X 9 matrix. Table 3.3.6 shows the unit matrix values linking each source region with each receptor for sulphate air concentration per unit emission. The matrix shows that Sudbury (SUD) is the most important potential contributor to sulphate air concentration at Muskoka followed by Michigan (MCH) and northwestern Ontario (NWO). If all matrix values are multiplied by the proper emission for each source region (S_i), then the result is the sulphate air concentration contributed by the sources to each receptor. Summing the columns gives the model-estimated sulphate air concentration at each receptor from all sources. Similarly, Table 3.3.7 shows the unit wet deposition matrix. In this case, southwestern Ontario (SWO) is the prime potential contributor to wet deposition followed by Michigan and Sudbury as indicated in Table 3.3.5. Thus the matrices can discriminate between precipitation events (Table 3.3.7) and other meteorological events (Table 3.3.6). Once again, multiplying these matrix values by the source emissions gives the model-estimated wet sulphate deposition contributed by each source. Summing the columns gives the model estimated total wet deposition at each site from all the anthropogenic sources. When the background (B_j) is added, the total deposition (D_j) is produced as linearly expressed by equation (1).

From Table 3.3.2, the one model that shows consistently lower correlation with other models in terms of ranking is RCDM-3. If RCDM-3 is not considered, then the AES model can be said to correlate well with most other models. From the MOI report (2 F-M, 1982b), the AES model suggests that Ontario is the greatest contributor to the Muskoka site for ground level concentration, and dry and wet deposition. This is followed by aggregated Region 10 comprising Michigan, Wisconsin, Minnesota and Iowa (Figure 3.3.4). This attribution is corroborated by all the other models except CAPITA (or MCARLO) which puts Region 2 (Quebec) ahead of Region 10 in terms of contribution to

the Muskoka site for air concentration and dry deposition while ranking wet deposition in the order described. RCDM-3 ranked the contributions differently and placed either aggregated Region 6 (Pennsylvania, Ohio and West Virginia) or 9 (Indiana, Illinois, Missouri, Kentucky and Tennessee) ahead of others. This would mean Ontario is not the strongest contributor to a site within its border. There is less agreement among models on the third position in the ranking. Nevertheless, apart from RCDM-3, it is either Region 2, 6 or 9. This implies that reduction of emissions targetted to a few key states (U.S.) and provinces (Canada) would produce the maximum benefits at the receptors.

The Modelling Subgroup further made eleven recommendations in an effort to improve the performance of long-range transport models and to gain more confidence in the model results. The thrust of the recommendations was to improve the input (meteorological, precipitation and emissions) and evaluation data so as to reduce the uncertainty associated with running the model in a hope to delineate the strengths and weaknesses of the model formulations. The residuals of the uncertainties should be quantified and their impacts on model output delineated through sensitivity tests. These recommendations were later incorporated into the ISDME program to be discussed in the next section.

Two recommendations included in a list of eleven recommendations went further than suggesting improvements on the existing techniques and focussed on scientific advancements. One calls for studying the impact of nonlinearity through sensitivity analyses on oxidation and scavenging rates. Though it can now be questioned how sensitivity analyses using the techniques available to linear models can shed light on the issue of nonlinearity, it nevertheless shows the foresight of the team in facing squarely a potentially important issue. The other recommendation of note is to start evaluating regional NO_x transport and deposition models.

Table 3.3.5

Model ranking for Muskoka, Ontario -- annual (1978) wet sulphur deposition

	REGION	AES-LRT	ASTRAP	MOE	MEP	ENAMAP	CAPITA	UMACID	RCDM
10	NMN	21	2	24	33	*	*	*	*
11	SMN	16	18	10	22	35	25	31	*
12	NWO	6	16	8	18	21	16	18	*
13	NEO	14	8	5	6	4	4	4	*
14	SUD	3	6	1	3	2	2	3	*
15	SWO	1	1	2	1	3	1	1	*
16	SEO	5	3	4	5	1	6	7	*
17	SLV	22	40	16	13	34	23	26	*
18	NQU	12	17	9	14	9	7	23	*
19	GBY	40	39	34	24	33	30	34	*
20	NBK	39	38	31	23	32	33	32	*
21	NSP	38	37	35	27	31	34	33	*
22	NFL	37	36	37	32	30	35	*	*
23	ASK	31	30	23	31	*	*	*	*
24	BCA	36	35	*	*	*	*	*	*
50	OHO	4	10	11	4	6	5	5	*
51	ILL	8	4	14	12	19	9	6	*
52	PEN	7	11	15	8	8	10	9	*
53	IND	9	7	13	10	10	13	8	8
54	KEN	10	12	20	20	11	11	14	*
55	MCH	2	2	3	2	5	3	2	*
56	TEN	17	15	27	28	12	15	15	*
57	MSU	20	9	19	19	15	17	13	*
58	WVR	13	14	17	9	7	8	12	*
59	NYK	11	19	12	7	14	14	11	*
60	ALA	29	21	30	35	29	19	19	*
61	WIO	15	5	6	11	18	12	10	*
62	MIN	18	13	7	15	17	18	17	*
63	VNC	25	22	28	21	28	20	20	*
64	FLD	35	31	36	34	27	31	30	*
65	GSC	26	26	33	30	26	24	25	*
66	MDJ	19	23	22	16	13	22	16	*
67	ALM	27	20	32	29	16	21	21	*
68	MCR	24	27	25	26	25	29	22	*
69	MAN	34	34	26	25	24	32	27	*
70	VNH	23	29	21	17	23	28	24	*
71	WNE	28	24	18	*	20	27	29	*
72	WSE	30	25	29	*	22	26	28	*
73	WNW	33	33	*	*	*	*	*	*
74	WSW	32	32	*	*	*	*	*	*

* REGION ELEMENT MISSING

Table 3.3.6

AES-LRT Model

Annual (1978) SO₄⁻ unit matrix in micrograms per cubic meter per Tg emitted

REGION		BW	ALG	MUSK	QUEB	SNSC	VT	ADIR	PENN	SMOK
10	MNM	1.11	0.66	0.33	0.25	0.16	0.25	0.20	0.12	0.04
11	SMN	2.31	0.77	0.77	0.0	0.0	0.0	0.0	0.77	0.0
12	NWO	1.67	1.67	1.67	0.0	0.0	0.0	0.0	0.0	0.0
13	NEO	0.26	2.21	1.30	0.91	0.26	0.91	1.04	0.65	0.0
14	SUD	0.04	0.73	3.00	1.13	0.84	1.39	2.10	0.66	0.09
15	SWO	0.0	0.12	1.36	0.72	0.78	1.39	1.62	1.77	0.20
16	SEO	0.0	0.29	0.88	0.88	1.18	2.06	2094	0.29	0.0
17	SLV	0.0	0.05	0.14	1.02	1.58	2.33	0.93	0.19	0.05
18	NQU	0.25	0.76	1.42	1.45	0.91	1.53	1.93	0.22	0.04
19	GBY	0.0	0.0	0.0	0.18	0.73	0.18	0.0	0.0	0.0
20	NBK	0.0	0.0	0.0	0.10	1.06	0.10	0.10	0.0	0.0
21	NSP	0.0	0.0	0.0	0.17	0.34	0.0	0.0	0.0	0.0
22	NFL	0.0	0.0	0.0	0.0	0.0	0.0	0.0	0.0	0.0
23	ASK	0.38	0.10	0.07	0.0	0.0	0.03	0.03	0.07	0.07
24	BCA	0.10	0.0	0.0	0.0	0.0	0.0	0.0	0.0	0.0
50	OHO	0.0	0.04	0.57	0.17	0.31	0.41	0.64	2.19	0.60
51	ILL	0.04	0.43	0.53	0.17	0.11	0.23	0.37	0.59	1.03
52	PEN	0.0	0.03	0.30	0.19	0.35	0.49	0.86	2.31	0.10
53	IND	0.01	0.27	0.27	0.10	0.14	0.24	0.33	0.85	1.48
54	KEN	0.0	0.04	0.18	0.02	0.08	0.12	0.18	0.78	2.09
55	MCH	0.09	0.45	1.75	0.57	0.45	0.78	0.92	1.54	0.24
56	TEN	0.0	0.04	0.10	0.0	0.02	0.02	0.08	0.37	2.82
57	MSU	0.03	0.21	0.21	0.05	0.05	0.10	0.16	0.39	1.01
58	WVR	0.0	0.0	0.22	0.12	0.16	0.32	0.58	1.90	0.54
59	NYK	0.0	0.14	0.27	0.37	0.80	0.82	1.17	0.31	0.04
60	ALA	0.0	0.0	0.03	0.0	0.0	0.0	0.03	0.15	1.71
61	WIO	0.27	0.92	0.69	0.18	0.16	0.25	0.39	0.71	0.37
62	MIN	0.83	0.83	0.45	0.15	0.15	0.15	0.23	0.45	0.23
63	VNC	0.0	0.0	0.02	0.02	0.09	0.12	0.16	0.49	0.84
64	FLD	0.0	0.0	0.0	0.0	0.0	0.0	0.0	0.02	0.33
65	GSC	0.0	0.0	0.02	0.0	0.02	0.02	0.06	0.23	2.72
66	MDJ	0.0	0.03	0.13	0.16	0.51	0.32	0.45	0.27	0.0
67	ALM	0.0	0.0	0.04	0.0	0.0	0.0	0.0	0.08	0.91
68	MCR	0.03	0.0	0.20	0.27	1.20	0.30	0.37	0.10	0.0
69	MAN	0.0	0.0	0.0	0.22	2.67	0.22	0.22	0.0	0.0
70	VNH	0.0	0.0	0.0	0.36	1.25	0.36	0.36	0.0	0.0
71	WNE	0.41	0.16	0.10	0.0	0.03	0.03	0.03	0.10	0.10
72	WSE	0.07	0.03	0.03	0.01	0.01	0.01	0.02	0.04	0.11
73	WNW	0.12	0.02	0.0	0.0	0.0	0.0	0.0	0.0	0.02
74	WSW	0.0	0.0	0.0	0.0	0.0	0.0	0.0	0.0	0.0

Table 3.3.7
AES-LRT Model
Annual (1978) wet deposition unit matrix in kilograms S
per hectare per Tg emitted

REGION	BW	ALG	MUSK	QUEB	SNSC	VT	ADIR	PENN	SMOK	
10	NMN	0.45	0.45	0.25	0.12	0.04	0.20	0.29	0.04	0.0
11	SMN	1.54	0.77	0.77	0.0	0.0	0.0	0.0	0.0	0.0
12	NWO	1.67	1.67	1.67	1.67	1.67	1.67	1.67	0.0	0.0
13	NEO	0.26	2.99	0.91	1.04	0.78	1.43	1.04	0.52	0.0
14	SUD	0.06	2.25	3.10	1.86	0.47	1.56	2.21	0.71	0.0
15	SWO	0.0	1.07	4.38	1.57	0.96	1.74	2.14	2.26	0.12
16	SEO	0.0	0.59	1.76	2.06	0.88	3.53	4.12	0.29	0.0
17	SLV	0.0	0.14	0.19	4.56	1.30	5.40	1.44	0.28	0.0
18	NQU	0.04	0.51	0.95	1.42	0.76	1.35	2.11	0.15	0.0
19	GBY	0.0	0.0	0.0	0.36	0.73	0.36	0.0	0.0	0.0
20	NBK	0.0	0.0	0.0	0.29	1.73	0.29	0.29	0.0	0.0
21	NSP	0.0	0.0	0.0	0.51	1.27	0.17	0.08	0.0	0.0
22	NFL	0.0	0.0	0.0	0.0	0.0	0.0	0.0	0.0	0.0
23	ASK	0.31	0.07	0.03	0.0	0.0	0.03	0.03	0.03	0.03
24	BCA	0.10	0.0	0.0	0.0	0.0	0.0	0.0	0.0	0.0
50	OHO	0.01	0.28	1.97	0.50	0.21	1.06	1.42	4.59	0.27
51	ILL	0.19	1.38	1.18	0.50	0.10	0.26	0.37	0.99	0.73
52	PEN	0.0	0.31	1.32	0.75	0.34	1.76	2.29	7.07	0.06
53	IND	0.03	1.06	1.15	0.17	0.14	0.34	0.55	1.41	0.97
54	KEN	0.0	0.12	1.08	0.06	0.10	0.32	0.62	1.77	1.67
55	MCH	0.21	2.32	3.13	1.11	0.36	0.83	1.11	1.73	0.17
56	TEN	0.0	0.16	0.51	0.04	0.08	0.12	0.41	1.34	4.48
57	MSU	0.25	0.83	0.39	0.08	0.07	0.10	0.13	0.49	0.72
58	WVR	0.0	0.04	0.93	0.60	0.14	1.55	1.83	5.91	0.20
59	NYK	0.0	0.49	1.04	1.43	1.45	2.72	3.74	0.82	0.02
60	ALA	0.0	0.03	0.06	0.03	0.0	0.03	0.06	0.51	3.71
61	WIO	0.55	1.95	0.82	0.27	0.11	0.25	0.39	1.08	0.27
62	MIN	1.43	1.50	0.45	0.15	0.08	0.23	0.23	0.53	0.15
63	VNC	0.0	0.02	0.16	0.28	0.33	0.77	0.93	2.68	0.72
64	FLD	0.0	0.0	0.0	0.0	0.0	0.0	0.02	0.09	2.26
65	GSC	0.0	0.02	0.13	0.02	0.04	0.11	0.27	0.90	8.51
66	MDJ	0.0	0.05	0.40	0.99	0.83	1.93	2.06	1.26	0.03
67	ALM	0.0	0.12	0.08	0.0	0.0	0.0	0.08	0.25	0.95
68	MCR	0.0	0.03	0.17	1.24	2.74	2.07	1.84	0.13	0.0
69	MAN	0.0	0.0	0.0	1.11	3.78	1.11	0.67	0.0	0.0
70	VNH	0.0	0.0	0.18	1.79	2.32	2.50	1.43	0.0	0.0
71	WNE	0.41	0.19	0.06	0.03	0.0	0.03	0.0	0.10	0.10
72	WSE	0.28	0.08	0.03	0.01	0.01	0.02	0.01	0.01	0.13
73	WNW	0.07	0.05	0.0	0.0	0.0	0.0	0.0	0.0	0.0
74	WSW	0.01	0.0	0.0	0.0	0.0	0.0	0.0	0.0	0.0

3.3.4.d THE INTERNATIONAL SULPHUR DEPOSITION MODEL EVALUATION (ISDME)

The International Sulphur Deposition Model Evaluation project, initiated in 1985 and completed in 1987, was conducted jointly by the U.S. Environmental Protection Agency and the Atmospheric Environment Service of Canada. The development of linear models was essentially complete by the time the ISDME study took place. Subsequent efforts have primarily focussed on the effect non-linearity has on long range transport. The ISDME study was limited to an analysis of linear models partly because the non-linear models being developed at that time, e.g. RADM and ADOM, required far more extensive meteorological data (i.e. cloud cover, diffusivities, humidity, many vertical levels) than available in the ISDME project.

The following is taken from the ISDME report's (Clark et al., 1987) executive summary.

"ISDME evaluated eleven linear-chemistry atmospheric models of sulfur deposition for each season and the year of 1980. These models were either statistical, Lagrangian or hybrids. The selection of 1980 as the evaluation year was based, in part, on the availability of the most recent emissions inventory ". The eleven models, their nature, and affiliations are given in Table 3.3.8.

"The approach of the study was to i) compile and distribute standardized model input data sets to the modelers, ii) apply the eleven models using these data sets and iii) evaluate the models in a "blind" test mode, meaning the computer code of these models was not modified specifically to improve the results for 1980. The evaluation data consisted of sulfur wet deposition amounts calculated from screened precipitation chemistry data from the five major North American networks and daily air concentrations of sulfur dioxide and sulfate at four Canadian sites. Dry deposition data were not available during this study.

"The ISDME screening and calculation procedures were very similar to those recommended by the Unified Deposition Data Base Committee (1985) established by the Canadian Research and Monitoring Coordinating Committee and the U.S. National Acid Precipitation Assessment Program. The number of sites with data passing the ISDME criteria ranged from 32 for the annual to 46 for the spring periods.

"Unlike the evaluations of the past, the ISDME focused on the ability of the models to replicate the spatial patterns of seasonal, as well as annual amounts of sulfur wet deposition within the uncertainties of the data. Seasonal and annual evaluations, rather than only annual evaluations, were conducted to provide a more stringent test of the models. Patterns were generated by interpolating the site observations and predictions to half-degree grid cells via a technique known as kriging. This technique minimizes the interpolation errors and quantifies the uncertainties arising from both the interpolation and the errors of measurement.

TABLE 3.3.8

The models and participants in the ISDME

Atmospheric Environment Service Long-Range Transport Model (AES)	Eva Volder and Marvin Olson Environment Canada	Lagrangian
Advanced Statistical Trajectory Regional Air Pollution (ASTRAP)	Jack Shannon Argonne National Laboratory	Lagrangian/ Statistical
Ontario Ministry of the Environment (MOE) Long-Range Transport Model	Barbara Ley Ministry of Environment	Lagrangian
Regional Impacts on Visibility and Acid Deposition (RIVAD) Model	Doug Latimer Systems Applications Inc.	Lagrangian
Regional Lagrangian Model of Air Pollution (RELMAP)	Terry Clark US Environmental Protection Agency	Lagrangian
Regional Transport Model (RTM-II)	Doug Latimer Systems Applications Inc.	Eulerian/ Lagrangian
Statistical Estimates of Transport and Acidic Deposition (SERTAD) Model	Ron Portelli Concord Scientific Corp.	Statistical
Statistical Model (STATMOD)*	Akula Venkatram Environmental Research and Technology Inc.	Statistical
Tennessee Valley Authority Model-T	William Norris Tennessee Valley Authority	Statistical
University of Michigan Atmospheric Contributions to Interregional Deposition (UMACID) Model	Perry Samson University of Michigan	Lagrangian

* A second version of this model, SIMPMOD, was also applied.

"The emphasis on pattern replication is based on the fact that point measurements are not necessarily representative of the spatial resolution of the models. That is, large spatial variability of meteorological parameters and air concentrations can cause "local" effects on the measurements at a site. As a result, these measurements could be representative of only a point and not the region. Therefore, it is necessary to compare predictions and observations on commensurate spatial scales. Moreover, pattern comparisons provide at least a limited evaluation of the models in data sparse regions.

"The second unique aspect of the evaluation approach was the consideration of the uncertainties of the observed amounts of sulfur wet deposition. Rather than comparing predictions to the best estimates of the observations, this evaluation determined whether and by how much the predictions were outside the uncertainty limits of the interpolated observations. Based on these uncertainty limits, the statistical significance of the differences was determined. These uncertainties arise from sampling and analytical errors, local or nonregional effects, network protocol differences, and the interpolations of both the predictions and observations. The uncertainties of the annual pattern of sulfur wet deposition ranged from approximately $\pm 50\%$ in the region of highest sulfur wet deposition to $\pm 100\%$ across data-sparse regions of eastern North America.

"The models were evaluated using six model performance measures, which quantified the differences between the predicted and observed patterns of sulfur wet deposition. The measure receiving the most weight was the percentage of the half-degree cells where the predictions significantly differed from the measurements. The remaining five measures were assigned equal weights. Two of these measures quantified differences in pattern position, while two additional measures quantified the differences in the magnitudes and locations of the maxima. The final measure quantified differences in the seasonal distribution of the annual amounts.

"The comparison of predicted and observed patterns of seasonal sulfur wet deposition revealed that the predicted patterns tended to resemble concentric ellipses and to show less detail than the observed patterns. The predicted seasonal and annual patterns also consistently exhibited maximum amounts within the high emissions region of Ohio, western Pennsylvania and West Virginia. This behavior was not evident in the patterns of the observations, which indicated that the location of the maximum was not anchored, but migrated from northern West Virginia to southern Ontario.

"Depending on the model, distances separating the predicted and observed locations of the maxima for all seasons were less than 170 to 350 km. Most models were within the uncertainty limits of the magnitude of the seasonal and annual maxima.

"The determination of the areas of statistically significant differences between the

predictions and observations of sulfur wet deposition revealed that across 80% of the evaluation region:

- * The seasonal predictions of five of the eleven models were within the uncertainty limits of the observed seasonal patterns
- * The seasonal predictions of all but three models were within the same uncertainty limits for at least three seasons
- * The annual predictions of all but three models were within the uncertainty limits of the observed annual pattern.

"A contributing factor to this high percentage was the degree of uncertainty of the observed pattern of sulfur wet deposition, which was as high as $\pm 50\%$ across the area of greatest site density. Therefore, the models in this study were afforded a rather large statistical tolerance for differences.

"Regarding the seasonal contributions to the 1980 amount of sulfur wet deposition, nearly 40% and 30% of the annual observed amounts occurred during summer (July, August and September) and spring (April, May and June), respectively. Approximately 15% occurred during both winter (January, February and March) and autumn (October, November and December). Most of the models are within 10% of the summer and spring contributions and within 25% of the autumn and winter contributions. Three models did not mimic the observed seasonal variability as well as the other models.

"Two features of model performance were common to the statistical models but not to the other models. First, the patterns of the sulfur wet deposition, as determined by the statistical models, tended to be oriented more toward the east-west axis, as opposed to the southwest-northeast axis of the observed patterns. On the other hand, the orientation of the patterns produced by the other models tended to be closer to that of the observed patterns. This distinction could be due to the fact that the statistical models base their transport simulation on seasonal mean winds, which in North America tend to be westerly, rather than on wind measurements available twice a day. The second feature common to statistical models was the tendency to predict sulfate air concentrations higher than those of the deterministic models at both the ISDME sites and the four Canadian monitoring sites." The results of the seasonal evaluation are given in Figure 3.3.5 and Tables 3.3.9 - 3.3.12.

"Finally, the seasonal, annual and overall performances of the models were summarized by scoring and clustering procedures based on subjectively determined criteria values for each of the six performance measures. A model received points if the values of the performance measures did not exceed the criteria values. Overall performance scores were based on weighted seasonal performance scores. The weights, the sum of which equalled one, were determined by the mean relative contributions of the observed

seasonal amounts of sulfur wet deposition. Consequently, the model performance for the summer, the season of greatest sulfur wet deposition, received a weight of approximately 0.4. The distribution of overall performance scores illustrated three distinct clusters or groups of models. One model having one of the highest overall performance scores was deemed to have performed relatively well, but used an empirical "correction" (or background) term accounting for 40 to 60% of the predicted sulfur wet deposition."

The last comment in the ISDME's report executive summary points to a very important aspect of long-range-transport modelling. The fact that correlation with observed data is improved in one of the better performing models through the inclusion of a precipitation dependent background term underlines the importance of accurate precipitation data to model prediction of wet deposition. In the next section on the performance of a comprehensive (non-linear) model, it is also seen that the choice of precipitation data can markedly affect model performance results. Since precipitation is by nature episodic and local, comparison between model and observed results is difficult. If there is an accurate way to average or estimate precipitation amounts over areas the size of approximately one grid cell commonly used in these models (~ 100km x 100km) and employed as model input, then the overall wet deposition pattern will be captured. However, these results will not necessarily compare well with observations which depend on the local precipitation. To get a good comparison with observations, local precipitation amounts should be used. The conflict between these competing purposes can only be resolved by increasing coverage of wet deposition monitoring.

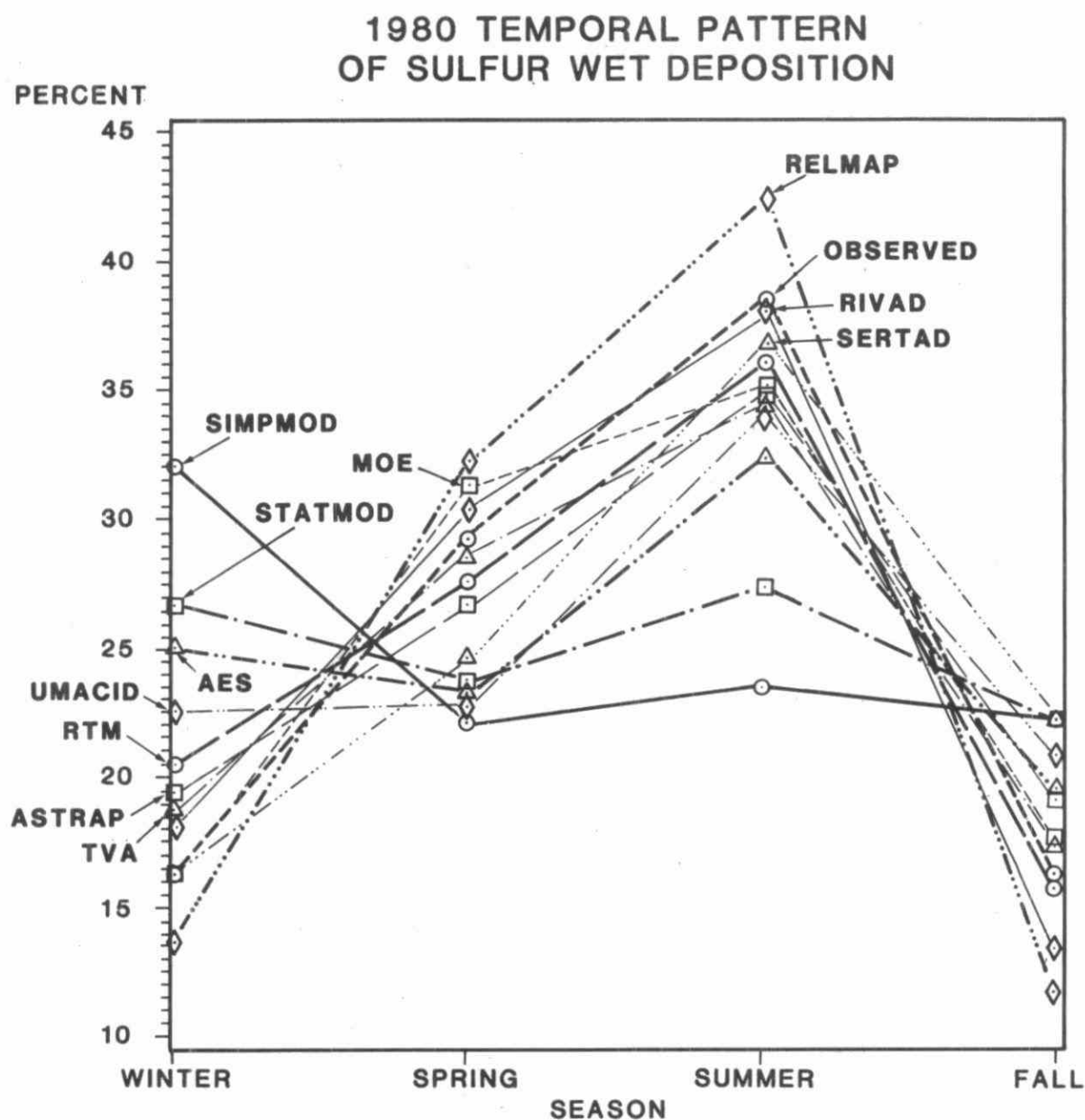


Fig. 3.3.5 The mean percentage of annual 1980 sulphur wet deposition observed and predicted for each season at 30 ISDME sites.

Table 3.3.9 Summary of model performance measures for Winter 1980

	AES	AST	MOE	REL	RIV	RTM	SER	SIM	STA	TVA	UMA	OBS
I. Spatial Patterns Replication												
A. Magnitude												
1. Area of Significant Differences (%)[*]												
a. Northeast	0.0	0.0	0.8-	0.0	0.8-	0.0	0.0	0.0	0.0	0.0	0.0	
b. North Central	0.2+	11.5+	0.0	5.4-	31.2-	27.6-	0.7+	14.7+	3.4-	0.0	0.9-	
c. Southwest	41.2+	29.4+	0.0	5.3+	4.4-	2.6-	0.0	62.3+	33.3+	4.4+	1.8+	
d. Southeast	85.5+	52.6+	5.3-	50.7+	0.0	0.0	19.7+	96.7+	32.7+	13.2+	9.2+	
e. All 4 regions	20.7+	18.2+	0.9-	10.4+	13.8-	11.8-	3.0+	32.5+	11.7+	2.8+	2.1+	
2. Median (kg S/ha) (p-value) ^{**}	2.38 0.009	2.25 0.000	1.15 0.097	1.58 0.477	0.87 0.004	0.99 0.009	1.50 0.477	2.97 0.000	2.02 0.235	1.61 0.477	1.49 0.477	1.34
3. Dispersion (kg S/ha) (p-value) ^{**}	2.12 0.000	0.75 0.064	0.29 0.113	0.78 0.052	0.13 0.000	0.17 0.003	0.50 0.359	2.01 0.000	1.05 0.007	0.59 0.203	0.58 0.212	0.44
4. Bias-High (kg S/ha) (p-value) ^{**}	-0.77 0.03	-1.06 0.00	0.18 0.18	-0.08 0.38	0.78 0.00	0.72 0.00	-0.12 0.29	-1.87 0.00	-0.22 0.25	-0.29 0.13	-0.02 0.46	
5. Bias-Low (kg S/ha) (p-value) ^{**}	-0.91 0.00	-0.48 0.00	0.44 0.00	-0.10 0.29	0.54 0.00	0.29 0.01	0.09 0.28	-1.08 0.00	-0.27 0.05	0.06 0.35	0.06 0.37	
6. Mean Squared Error (kg S/ha) ²	2.85	1.33	0.64	0.88	0.85	0.63	0.62	4.10	0.95	0.65	0.55	
B. Position												
1. Centroids (km)	146	43	82	144	66	112	42	81	151	32	87	
2. Major Axis (degrees) ^{***}	+5.3	+8.7	+13.3	+3.7	+10.2	+10.2	+9.4	+12.6	+20.1	+14.4	-0.1	37.5
3. Shift (km)	704	492	245	704	641	737	467	467	660	397	592	
C. Shape												
1. Correlation-No Shift	-0.17	0.03	0.36	-0.16	-0.06	-0.11	-0.18	-0.06	-0.02	0.11	0.08	
2. Correlation-With Shift ^{****}	0.79	0.68	0.61	0.74	0.73	0.78	0.63	0.58	0.65	0.69	0.74	
II Maxima												
A. Location-Kriged (km)	238	42	55	238	202	202	197	238	238	101	253	
B. Magnitude-Kriged (%) ^{***}	+36	0	0	0	-25	-18	0	+38	0	0	0	
Magnitude-Site (%) ^{***}	+59	+7	-19	0	-42	-37	0	+63	+1	0	0	
III Temporal Pattern Replication												
A. Seasonal Contribution (%) (Percent Difference)	25.0 +54	19.4 +20	16.2 0	13.7 -15	18.1 +12	20.5 +27	16.3 +1	32.0 +98	26.7 +65	19.3 +19	22.5 +39	16.2

Underscored measures are primary performance measures.

* "+" and "-" denote the prevalence of overpredictions and underpredictions, respectively. Significant differences detected when the prediction falls outside the uncertainty range about each interpolated observation.

** The p-value is the probability that the differences occurred by chance.

*** Values listed for each model represent the value of the prediction minus the value of the observation. Percent differences are normalized by observed values.

**** Model pattern shifted to produce the highest possible correlation with observation.

***** Kriging was used to arrive at the maximum location and magnitude.

Table 3.3.10 Summary of model performance measures for Autumn 1980

	AES	AST	MOE	REL	RIV	RTM	SER	SIM	STA	TVA	UMA	OBS
I. Spatial Patterns Replication												
A. Magnitude												
1. Area of Significant Differences (%)[*]												
a.Northeast	1.5+	1.5+	9.8-	0.0	21.4-	0.0	10.5+	0.0	0.0	13.2-	0.0	
b.North Central	9.5+	14.9+	0.0	4.1-	23.8-	18.8-	14.0+	3.2+	0.2-	0.0	0.0	
c.Southwest	0.0	11.0+	0.0	0.0	0.0	0.0	0.0	18.4+	0.0	2.6+	0.0	
d.Southeast	63.8+	53.9+	0.0	7.9+	0.0	0.0	13.8+	78.9+	14.5+	10.5+	2.6+	
e.All 4 regions	13.1+	16.3+	2.4-	2.8	14.9-	7.6-	10.2+	16.2+	2.1+	5.2	0.4+	
2. Median (kg S/ha)	1.92	2.24	1.15	1.36	0.59	0.76	2.04	2.03	1.33	1.40	1.17	1.28
(p-value)^{**}	0.006	0.000	0.254	0.649	0.000	0.000	0.000	0.000	0.649	0.649	0.362	
3. Dispersion (kg S/ha)	0.46	0.62	0.22	0.38	0.03	0.03	0.28	0.86	0.37	0.40	0.36	0.41
(p-value)^{**}	0.353	0.097	0.029	0.412	0.000	0.000	0.127	0.011	0.408	0.477	0.349	
4. Bias-High (kg S/ha)	-0.15	-1.02	0.13	0.38	1.04	1.00	-0.54	-0.76	0.09	-0.06	-0.01	
(p-value)^{**}	0.24	0.00	0.25	0.07	0.00	0.00	0.00	0.02	0.37	0.42	0.49	
5. Bias-Low (kg S/ha)	-0.46	-0.56	0.24	-0.10	0.59	0.42	-0.76	-0.50	0.03	0.09	0.21	
(p-value)^{**}	0.01	0.00	0.03	0.26	0.00	0.00	0.00	0.02	0.42	0.29	0.10	
6. Mean Squared Error (kg S/ha)²	1.03	1.39	0.51	0.76	0.98	0.80	0.81	1.76	0.79	0.82	0.46	
B. Position												
1. Centroids (km)	139	65	71	182	71	97	65	126	147	99	38	
2. Major Axis (degrees)^{***}	+7.3	+16.6	+18.2	+3.3	+12.2	+8.6	+13.3	+20.7	+23.2	+21.0	+8.7	29.0
3. Shift (km)	660	440	330	592	347	934	246	454	592	440	453	
C. Shape												
1. Correlation-No Shift	-0.39	0.37	0.59	-0.58	0.17	-0.19	0.54	-0.43	-0.50	-0.26	0.30	
2. Correlation-With Shift^{****}	0.55	0.81	0.86	0.61	0.78	0.20	0.71	0.83	0.74	0.89	0.88	
II Maxima^{*****}												
A. Location-Kriged (km)	338	183	164	338	315	135	0	338	285	338	338	
B. Magnitude-Kriged (%)^{***}	0	0	0	0	-52	-42	0	0	0	0	0	
Magnitude-Site (%)^{***}	0	+1	-24	0	-68	-61	0	+18	0	0	0	
III Temporal Pattern Replication												
A. Seasonal Contribution (%)^{***}	19.4	19.1	17.5	11.7	13.4	15.5	22.2	22.2	22.3	17.3	20.7	16.0
(Percent Difference)	+21	+19	+9	-27	-16	-3	+39	+39	+39	+8	+29	

Underscored measures are primary performance measures.

* "+" and "-" denote the prevalence of overpredictions and underpredictions, respectively. Significant differences detected when the prediction falls outside the uncertainty range about each interpolated observation.

** The p-value is the probability that the differences occurred by chance.

*** Values listed for each model represent the value of the prediction minus the value of the observation. Percent differences are normalized by observed values.

**** Model pattern shifted to produce the highest possible correlation with observation.

***** Kriging was used to arrive at the maximum location and magnitude.

Table 3.3.11 Summary of model performance measures for Spring 1980

	AES	AST	MOE	REL	RIV	RTM	SER	SIM	STA	TVA	UMA	OBS
I. Spatial Patterns Replication												
A. Magnitude												
1. Area of Significant Differences (%)[*]												
a. Northeast	0.0	0.0	0.0	0.0	0.0	0.4-	0.0	0.0	1.9-	0.0	2.3-	
b. North Central	0.5-	1.8+	0.0	1.4+	16.1-	39.1-	0.0	0.0	33.0-	0.0	12.9-	
c. Southwest	0.0	0.0	0.0	14.0+	57.5-	64.0-	0.0	0.0	1.8-	0.0	32.0-	
d. Southeast	0.0	20.4+	0.0	59.9+	25.7-	27.6-	0.0	0.0	0.0	0.0	3.3-	
e. All 4 regions	0.2-	3.6+	0.0	11.9+	22.2-	33.3-	0.0	0.0	14.2-	0.0	13.0-	
2. Median (kg S/ha) (p-value) ^{**}	2.20 0.124	3.00 0.510	2.13 0.048	3.07 0.272	1.40 0.000	1.33 0.000	2.33 0.079	2.15 0.124	1.60 0.000	2.25 0.124	1.34 0.000	2.83
3. Dispersion (kg S/ha) (p-value) ^{**}	0.80 0.316	1.53 0.055	0.90 0.456	5.5 0.000	0.15 0.000	0.10 0.000	0.53 0.038	0.90 0.461	0.76 0.268	1.11 0.285	0.67 0.154	0.92
4. Bias-High (kg S/ha) (p-value) ^{**}	0.76 0.00	-0.37 0.10	0.55 0.01	-1.39 0.02	1.77 0.00	1.93 0.00	0.64 0.00	0.72 0.00	1.33 0.00	0.42 0.03	1.44 0.00	
5. Bias-Low (kg S/ha) (p-value) ^{**}	0.49 0.00	-0.09 0.32	0.68 0.00	-0.51 0.05	1.03 0.00	1.05 0.00	0.21 0.05	0.45 0.00	0.91 0.00	0.46 0.00	1.22 0.00	
6. Mean Squared Error (kg S/ha) ²	0.93	1.23	1.00	4.32	2.34	2.52	0.65	0.89	1.64	0.77	2.13	
B. Position												
1. Centroids (km)	51	68	66	82	30	25	16	72	84	46	30	
2. Major Axis (degrees) ^{***}	-2.6	-3.1	-0.3	-0.5	-2.2	-2.5	-1.3	-1.6	+7.2	-0.3	+0.2	51.9
3. Shift (km)	347	440	110	156	220	550	110	156	110	156	116	
C. Shape												
1. Correlation-No Shift	0.46	0.52	0.77	0.52	0.69	0.57	0.74	0.51	0.65	0.66	0.80	
2. Correlation-With Shift ^{****}	0.70	0.73	0.79	0.68	0.76	0.74	0.76	0.71	0.67	0.78	0.83	
II Maxima^{*****}												
A. Location-Kriged (km)	0	0	0	0	0	0	0	0	0	0	0	
B. Magnitude-Kriged (%) ^{***}	0	0	0	+55	-35	-33	0	0	0	0	0	
Magnitude-Site (%) ^{***}	-7	0	-9	+98	-55	-53	-11	0	-17	0	-27	
III Temporal Pattern Replication												
A. Seasonal Contribution (%) (Percent Difference) ^{***}	23.2 -21	26.7 -9	31.2 +6	32.1 +10	30.4 +4	27.7 -5	24.7 -16	22.1 -25	23.7 -19	28.6 -2	22.7 -23	29.3

Underscored measures are primary performance measures.

* "+" and "-" denote the prevalence of overpredictions and underpredictions, respectively. Significant differences detected when the prediction falls outside the uncertainty range about each interpolated observation.

** The p-value is the probability that the differences occurred by chance.

*** Values listed for each model represent the value of the prediction minus the value of the observation. Percent differences are normalized by observed values.

**** Model pattern shifted to produce the highest possible correlation with observation.

***** Kriging was used to arrive at the maximum location and magnitude.

Table 3.3.12 Summary of model performance measures for Summer 1980

	AES	AST	MOE	REL	RIV	RTM	SER	SIM	STA	TVA	UMA	OBS
I. Spatial Patterns Replication												
A. Magnitude												
1. Area of Significant Differences (%)[*]												
a. Northeast	16.9-	1.1-	17.7-	7.5-	26.3-	22.9-	0.4-	29.3-	37.6-	22.3-	27.1-	
b. North Central	4.3-	6.4+	10.0-	5.9+	42.8-	48.0-	3.2+	38.7-	54.8-	16.3-	16.3-	
c. Southwest	14.5-	4.9+	17.1-	32.9+	46.5-	46.9-	4.4-	31.1-	29.8-	10.9-	31.1-	
d. Southeast	3.9+	48.7+	3.3-	90.1+	27.0-	26.3-	3.9+	3.3+	11.2-	2.0+	0.7	
e. All 4 regions	9.4-	10.6+	12.4-	23.7+	37.3-	38.6-	2.9	29.9-	39.2-	14.9-	20.0-	
2. Median (kg S/ha)	2.97	3.43	2.18	4.49	1.70	1.57	3.31	2.13	1.51	2.80	1.66	3.00
(p-value)^{**}	0.826	0.510	0.048	0.016	0.000	0.000	0.510	0.048	0.004	0.826	0.048	
3. Dispersion (kg S/ha)	1.63	4.33	1.28	12.07	0.25	0.20	1.11	1.12	0.98	1.83	1.50	2.71
(p-value)^{**}	0.055	0.069	0.009	0.000	0.010	0.000	0.003	0.003	0.001	0.105	0.031	
4. Bias-High (kg S/ha)	0.91	-0.84	1.24	-2.01	2.50	2.60	0.40	1.88	2.28	0.87	1.66	
(p-value)^{**}	0.01	0.04	0.00	0.03	0.00	0.00	0.13	0.00	0.00	0.02	0.00	
5. Bias-Low (kg S/ha)	0.10	-0.25	0.67	-1.07	0.91	0.92	-0.60	0.61	0.99	0.30	1.04	
(p-value)^{**}	0.33	0.17	0.00	0.02	0.00	0.00	0.00	0.01	0.00	0.11	0.00	
6. Mean Squared Error (kg S/ha)²	1.98	2.71	2.01	11.6	4.11	4.16	1.41	3.41	3.98	2.17	3.23	
B. Position												
1. Centroids (km)	100	63	51	147	33	54	10	127	92	94	42	
2. Major Axis (degrees)^{***}	+2.8	+8.5	+11.7	+10.3	+6.8	+6.2	+14.6	+13.4	+19.6	+12.5	-0.6	40.5
3. Shift (km)	190	220	156	348	220	141	190	453	110	245	156	
C. Shape												
1. Correlation-No Shift	0.56	0.68	0.77	0.38	0.81	0.80	0.75	0.30	0.64	0.54	0.74	
2. Correlation-With Shift^{****}	0.88	0.83	0.84	0.71	0.88	0.89	0.88	0.58	0.67	0.74	0.85	
II Maxima^{*****}												
A. Location-Kriged (km)	277	351	84	277	84	84	263	259	164	84	277	
B. Magnitude-Kriged (%)^{***}	-9	+1	-34	+85	-60	-59	-18	-32	-42	-14	-30	
Magnitude-Site (%)^{***}	-2	+1	-31	+89	-59	-56	-16	-27	-39	-7	-27	
III Temporal Pattern Replication												
A. Seasonal Contribution (%)^{***}	32.4	34.8	35.1	42.5	38.1	36.2	36.9	23.6	27.4	34.8	34.1	38.5
(Percent Difference)	-16	-10	-9	+10	-1	-6	-4	-39	-29	-10	-11	

Underscored measures are primary performance measures.

* "+" and "-" denote the prevalence of overpredictions and underpredictions, respectively. Significant differences detected when the prediction falls outside the uncertainty range about each interpolated observation.

** The p-value is the probability that the differences occurred by chance.

*** Values listed for each model represent the value of the prediction minus the value of the observation. Percent differences are normalized by observed values.

**** Model pattern shifted to produce the highest possible correlation with observation.

***** Kriging was used to arrive at the maximum location and magnitude.

3.3.4.e CURRENT OR FUTURE USE OF "LINEAR MODELS"

Although most developmental work on linear long-range transport models has been completed, they can still serve a function in emission reduction assessment. The input meteorological requirements of Lagrangian models are substantially less than those required for comprehensive models. The computer resource requirements for base case model runs and particularly for scenario runs are much lower than those required for comprehensive models. Correspondingly, Lagrangian models can be run for long time periods (1 to 5 years) to assess meteorological variability in deposition and concentration fields. This variability is best expressed as percentage changes from a base case run to reduce reliance on the absolute accuracy of the model results.

Depending on the final results of the comprehensive Eulerian models in determining the degree of nonlinearity of the system, Lagrangian models could also be used to assess emission reduction. If total deposition (dry plus wet) is nearly linear, then these models could be used directly to model detailed emission reduction scenarios. Even if the system is nonlinear to some degree there remains the possibility of using the comprehensive models to develop average relationships between total emission and deposition reductions. This might be a function of season and of large geographic areas. Lagrangian model results could then be scaled according to these relationships when detailed emission scenarios were run. The Lagrangian model would calculate the ranges of wet or dry deposition that could be expected from year to year for a particular emission cut. This information could be used when assessing monitoring results over a region. Comprehensive Eulerian model results could still be run for some episodes to indicate shorter term variability and to see whether or not the source-receptor relationships in the Lagrangian model results applied for the specific emission cuts examined.

3.3.5 NONLINEAR EULERIAN MODELS

Although attempts have been made to incorporate complex chemistry into Lagrangian models (Eliassen et al., 1982, Bottenheim et al., 1984), this approach is not well suited to multisource situations since chemistry is a function of the total concentrations in air rather than the concentrations due to individual sources or groups of sources. Lagrangian models with complex chemistry can be used to trace the evolution of plumes from major sources.

For multisource situations, an Eulerian framework is better suited to comprehensive acid deposition or oxidant modelling. The two comprehensive acid deposition models being used in North America are RADM (Regional Acid Deposition Model) and ADOM (Acid Deposition and Oxidants Model). Both the ADOM and RADM chemistry modules were condensed from detailed chemical schemes. Care was taken to ensure that the essence of the behaviour of the important species was captured in the condensed scheme. Inter-model comparison between the chemistry modules of ADOM and RADM was performed. Though the two modules were developed independently and two different schemes were

used to lump the organics, the comparisons of ozone, nitric acid, hydrogen peroxide and daily maximum sulphate for 100 different multi-day simulations show very little scatter. The R^2 correlation is always larger than 0.97. With the exception of H_2O_2 , where RADM systematically predicts about 28% less than ADOM, all the other species comparisons show a systematic bias of less than 10%. In this section of the report we will outline the evaluation of ADOM with four meteorological data sets.

Model runs have been performed for 1) a 20-day period in April 1981 (during OSCAR experiments); 2) a 44-day period during the ANATEX experiment in January and February 1987; 3) a 9-day long severe ozone episode in June 1983; and 4) a 10-day winter study in January and February 1985. Model outputs have then been examined for 3 of the 4 seasons during a range of meteorological conditions.

3.3.5.a BRIEF DESCRIPTION OF THE MODEL

A brief description of ADOM is provided in Venkatram et al. (1988) and Misra et al. (1989) with details of the modules presented in ERT (1984 & 1985). The model is run using 12 vertical levels extending to 10 km for a grid size of 127 km by 127 km over either a 33 by 33 grid domain as shown in Figure 3.3.6 or a 37 by 38 grid domain for the ANATEX simulations. Input meteorological data consist of horizontal and vertical wind fields, eddy diffusivity, temperature, humidity, surface precipitation and cloud information. These data are derived diagnostically using the Canadian Meteorological Centre's spectral weather prediction model as a dynamic interpolator to produce data on a 1-hour time step from observed dynamic fields.

The modules in ADOM are listed below. A cell centred flux formulation is used for advection and diffusion. The gas phase chemistry module includes 50 species involved in approximately 100 reactions to handle sulphur, nitrogen and oxidant chemistry. Emissions of SO_2 , SO_4^- , NO_x , NH_3 and 10 categories of RHC'S are provided as input data. Figure 3.3.6 gives the springtime SO_2 emission rate for each grid. ADOM uses both stratiform and cumulus cloud modules in wet scavenging and cloud mixing processes. Cloud and precipitation fields are derived using a combination of observed data and diagnostic output from the Canadian Meteorological Centre's spectral weather prediction model. Aqueous chemistry consists of 25 reactions among 13 air and aqueous species. Finally, dry deposition is modelled as a deposition velocity which is calculated as the inverse of the sum of the aerodynamic, deposition layer and surface canopy resistances.

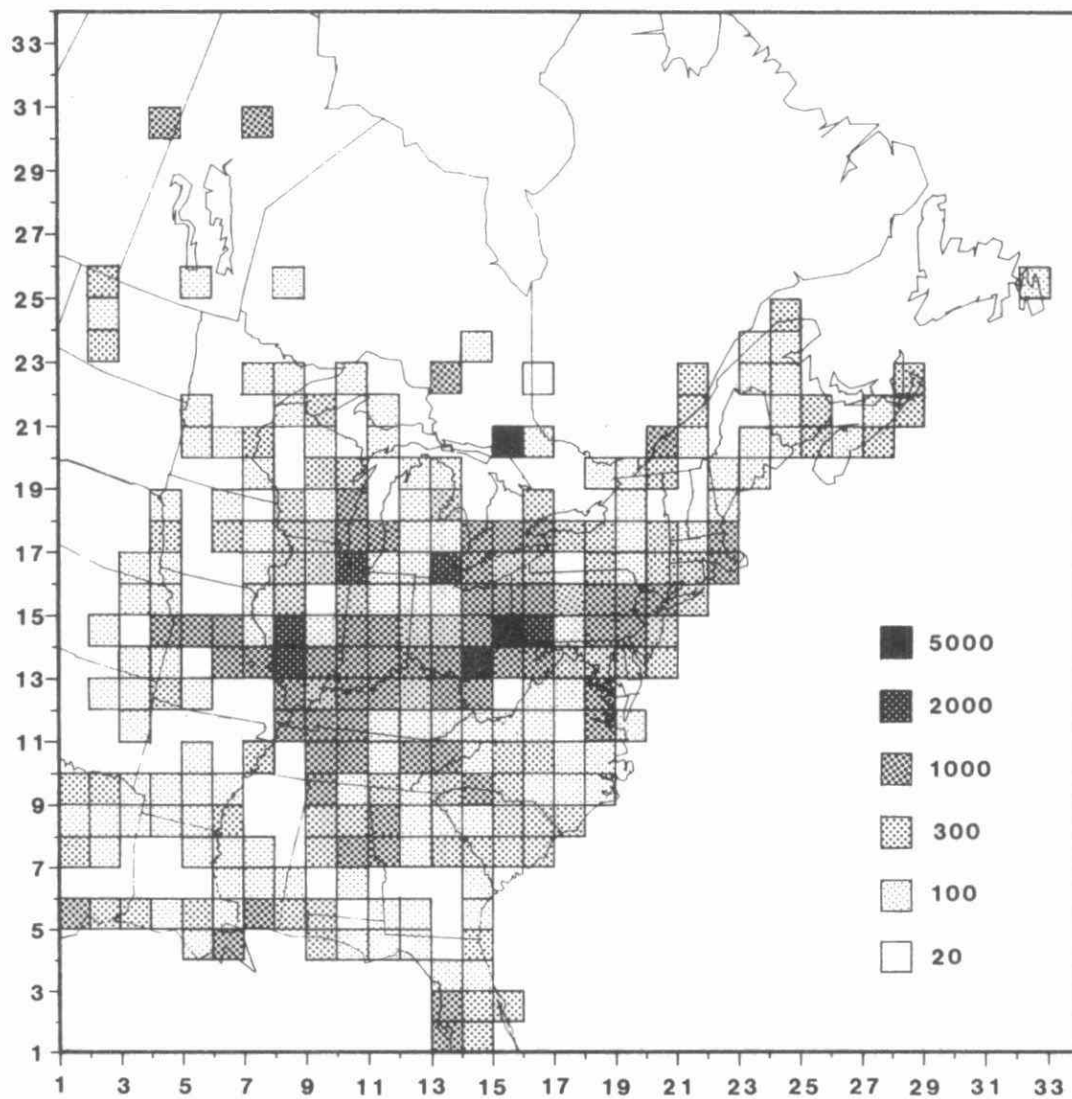


Fig. 3.3.6 Total SO₂ emission rate (metric tonnes per day) during springtime within each ADOM (127 x 127 km²) grid.

3.3.5.b OSCAR MODEL RUNS

The model was run for the period from April 10 to April 29, 1981 during the OSCAR field experiment. Figure 3.3.7 shows the total precipitation over the 20-day period. A series of frontal disturbances tracked through the northern United States and southern Canada over the 20-day period. Shower activities dominated in the western half of the domain with a mixture of drizzle, rain and showers in the east. Over the 20-day period, a maximum of more than 120 mm fell south of Lake Michigan.

Observed daily average $\text{SO}_4^{=}$ concentrations in precipitation were available at 34 sites in the northeastern U.S. and S. Ontario for 5 days during this period. A scatter graph of modelled versus observed $\text{SO}_4^{=}$ concentrations in precipitation averaged over the 5 days is given in Figure 3.3.8 for two different episodes. The average model result was 20% lower than the average observed value, but approximately 70% and 80% of the modelled results were within a factor of 2 of the observations for OSCAR II and IV, respectively. Given possible errors in the input NH_3 emission data as well as the fact that a modelled grid average is being compared to point data, these results are very encouraging. A similar scatter graph for nitrate in precipitation (Figure 3.3.9) shows a slight underprediction for the model results.

Figures 3.3.10 and 3.3.11 show the 16-day averaged $\text{SO}_4^{=}$ wet fluxes for runs with a Lagrangian model employing linear chemistry and with ADOM, respectively (Ellenton et al., 1988). The locations of the maxima were very similar for the two models. Overall the Lagrangian model produced larger sulphate deposition although that is due in part to a background deposition of $67 \mu\text{g m}^{-2} \text{h}^{-1}$ employed in the Lagrangian model. ADOM results indicate more deposition extending off the east coast. Since the Lagrangian model had no input precipitation over the oceans, this difference is not unexpected. Such limitations in the input data make percentage changes from baseline deposition a more reliable field than absolute changes in deposition.

The response of the two models to emission reductions is quite different. The Lagrangian model assumes that deposition decreases at the same rate as emissions (although background deposition remains unchanged). Figure 3.3.12 shows the percentage change in the 20-day average wet sulphate deposition resulting from a 50% cut in SO_2 emission across the domain of ADOM. In the main deposition area (which is removed from boundary value effects) reductions ranged from 30 to 45% with the lowest values near the strong source region. A Lagrangian model employing linear chemistry might perform well in simulating existing conditions, but it would not necessarily give the correct answer for an emission control scenario.

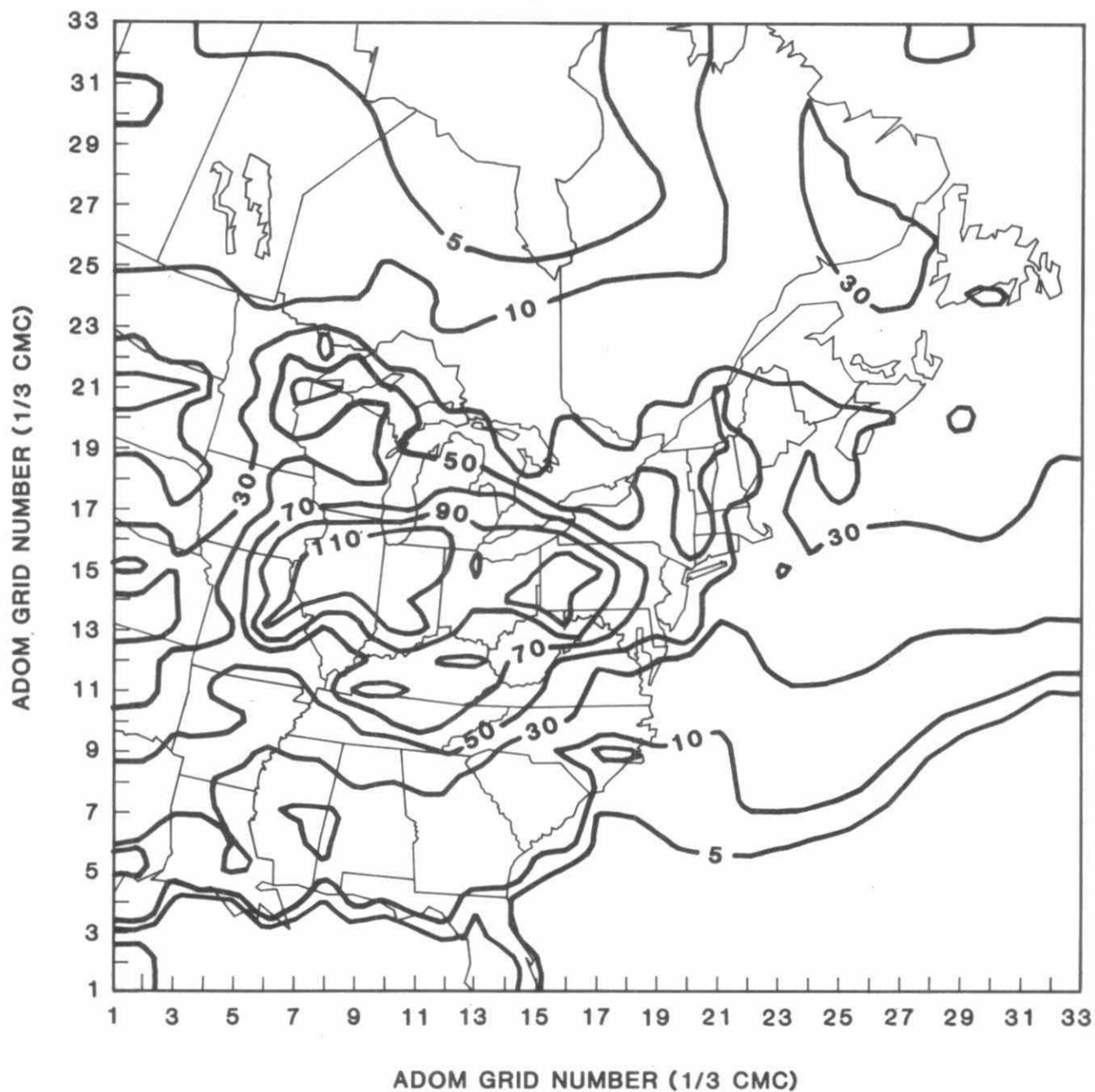
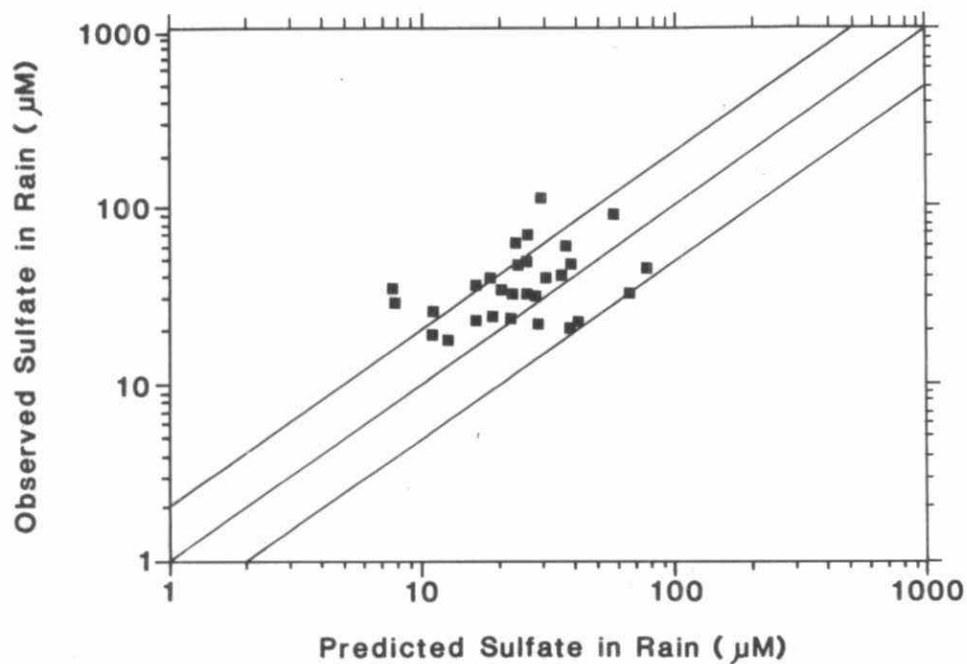


Fig. 3.3.7 The total precipitation amount (mm) during OSCAR II, III and IV (10-29 April 1981) plotted on the ADOM domain.

a)



b)

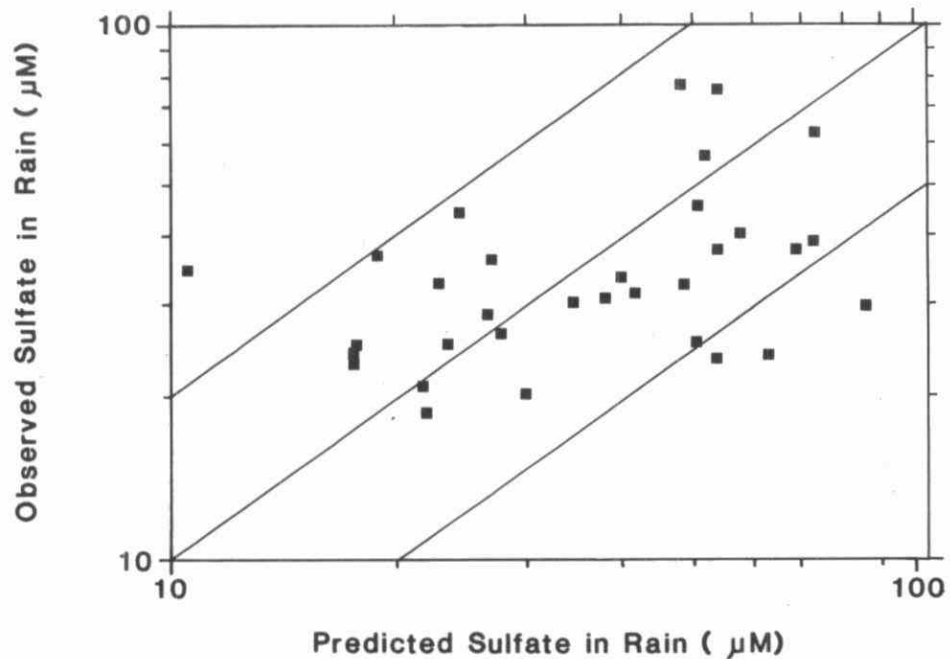
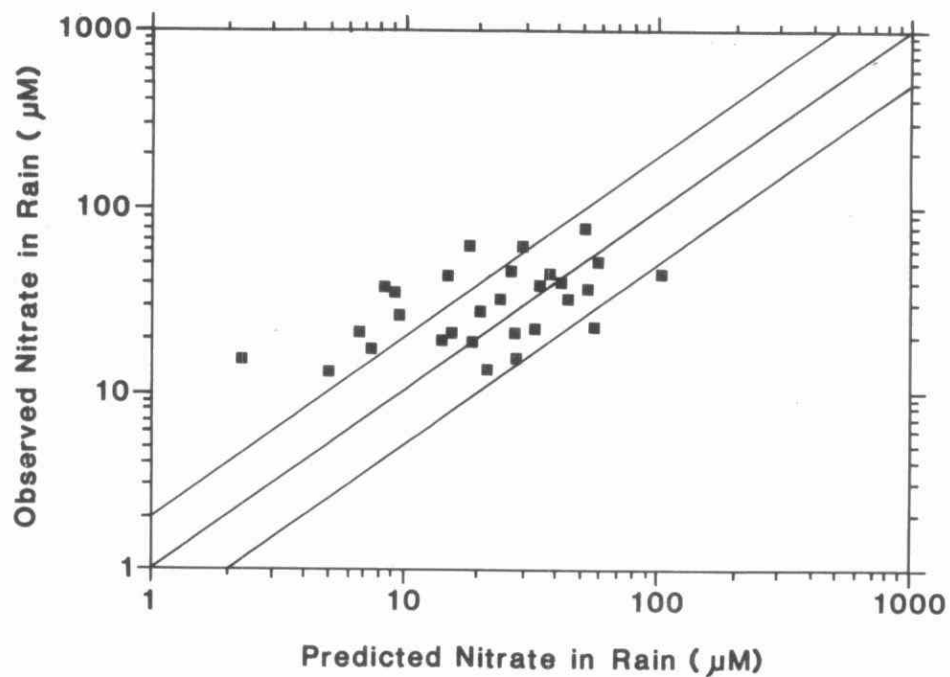


Fig. 3.3.8

(a) OSCAR II $\text{SO}_4^{=}$ concentrations in precipitation (new scavenging module).

(b) OSCAR IV $\text{SO}_4^{=}$ concentrations in precipitation (new scavenging module).

a)



b)

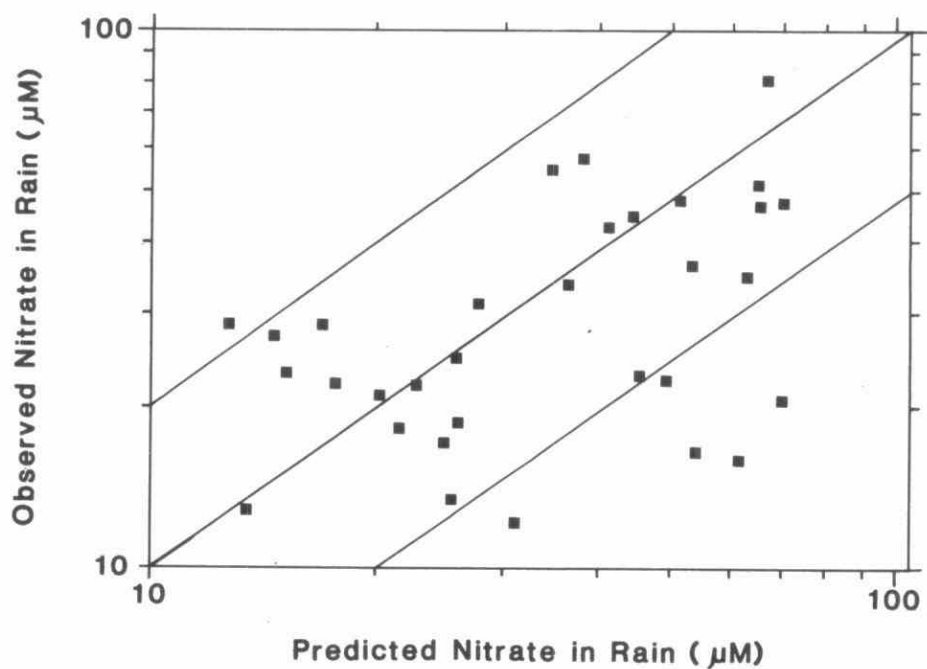


Fig. 3.3.9

(a) OSCAR II nitrate concentrations in precipitation (new scavenging module).

(b) OSCAR IV nitrate concentrations in precipitation (new scavenging module).

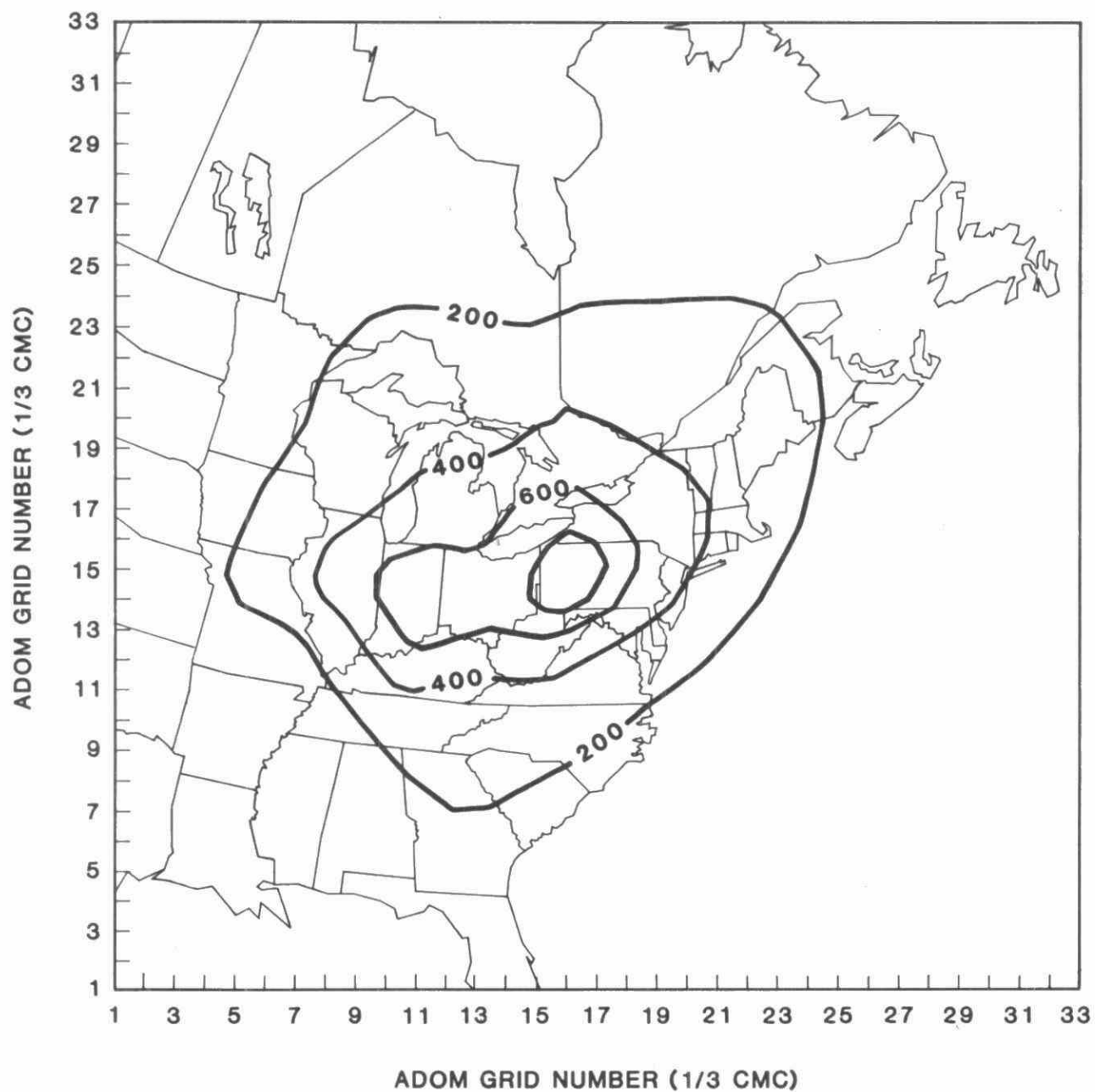


Fig. 3.3.10 16-day averaged (April 10-25, 1981) wet flux ($\mu\text{g m}^{-2}\text{h}^{-1}$) of SO_4^{2-} predicted by the Lagrangian model. This is given on the ADOM grid domain. A background deposition of $67 \mu\text{g m}^{-2}\text{h}^{-1}$ is added to the model output to account for non-anthropogenic and out-of-domain contributions.

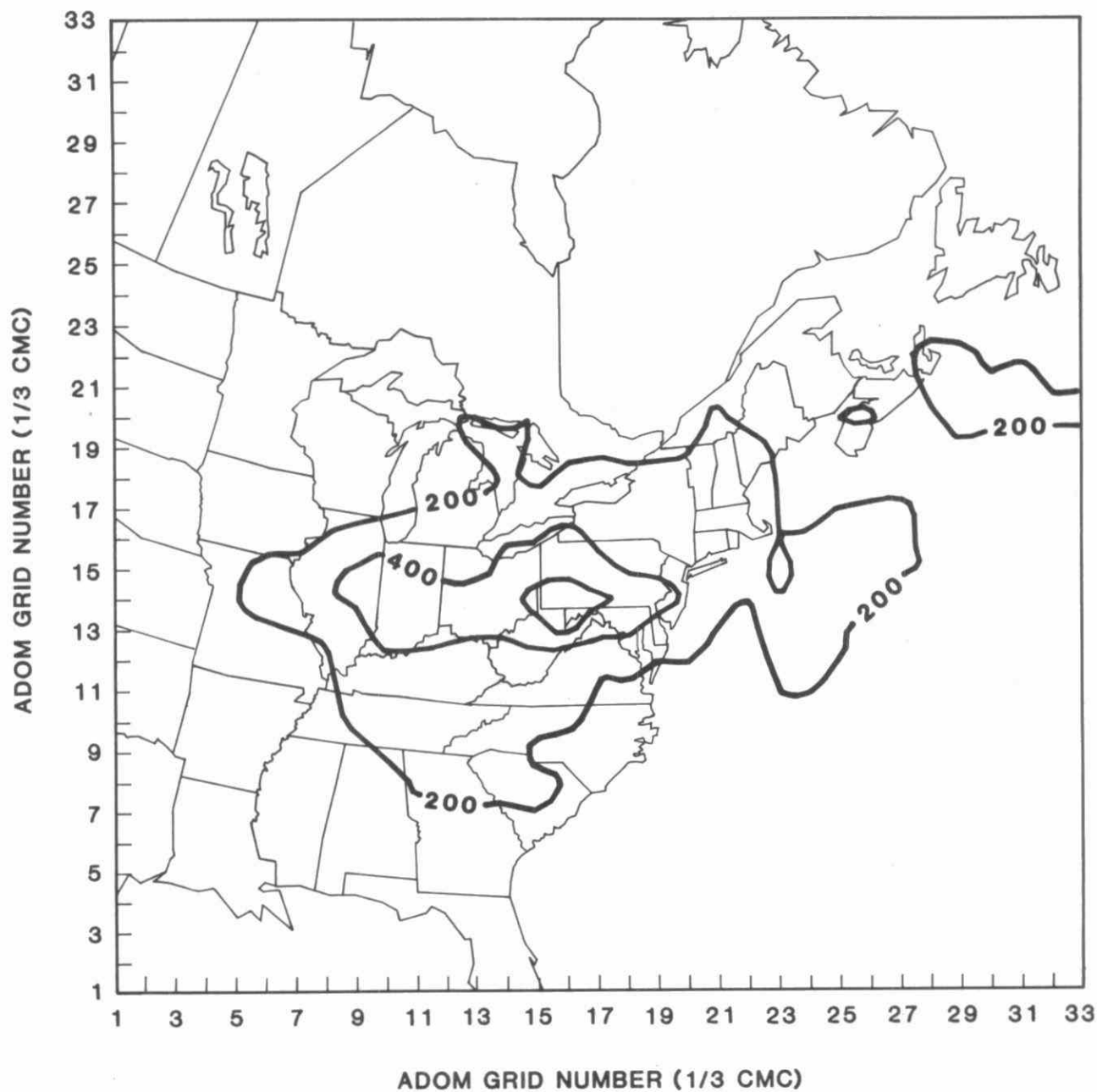


Fig. 3.3.11 16-day averaged (April 10-25, 1981) wet flux ($\mu\text{g m}^{-2}\text{h}^{-1}$) of $\text{SO}_4^{=}$ predicted by ADOM.

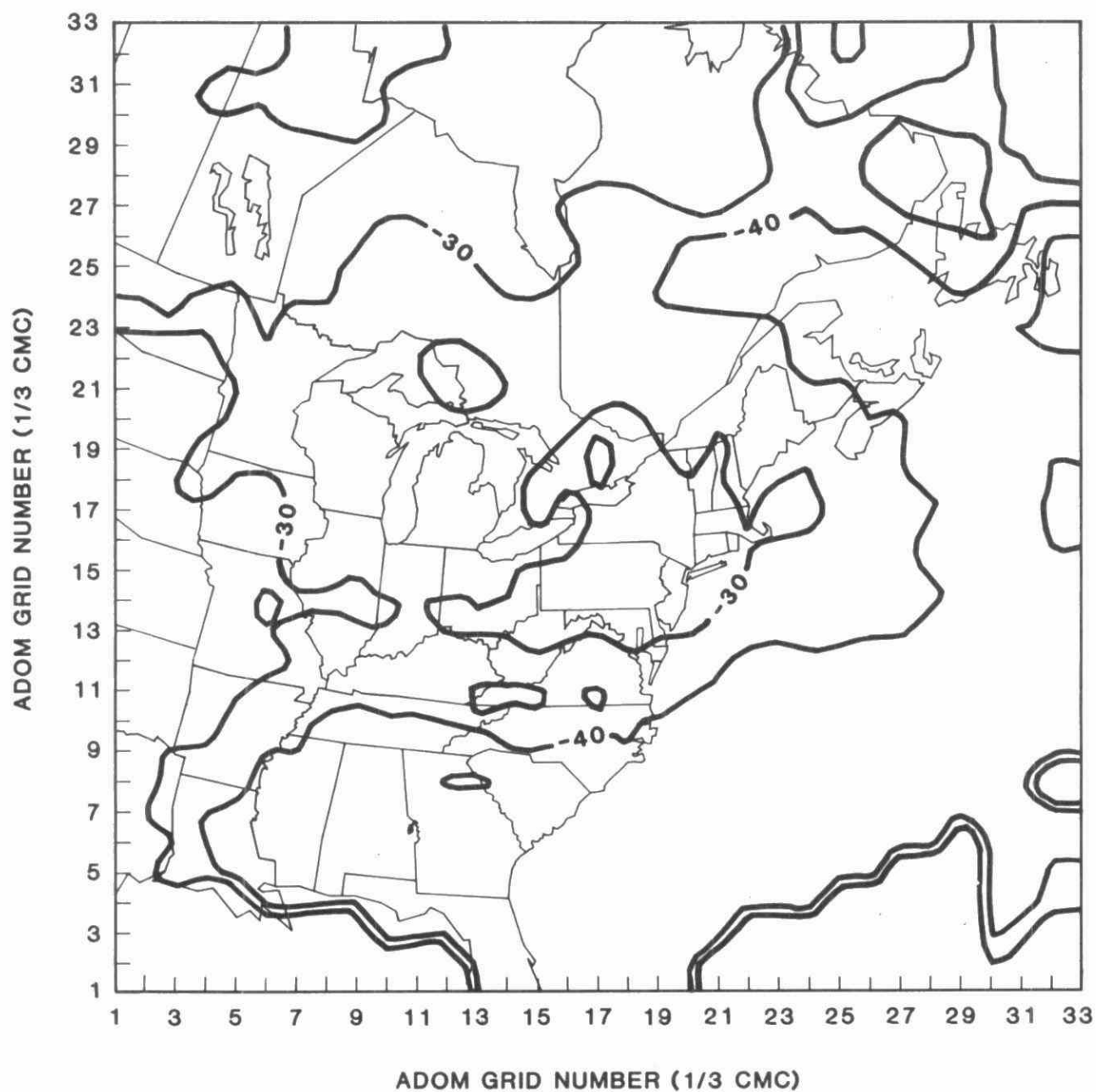


Fig. 3.3.12 20-day averaged (April 10-29, 1981) ADOM predicted percentage reduction in $\text{SO}_4^{=}$ precipitation concentration as a result of a 50% across-the-domain reduction of SO_2 and $\text{SO}_4^{=}$ emissions.

3.3.5.c ANATEX MODEL RUNS

During the Across North America Tracer Experiments in January-March 1987, three inert tracers were released from two sites (St. Cloud, Minnesota and Glasgow, Montana) at 2 1/2 day intervals and monitored at 77 fixed sites arranged at approximately equidistant arcs away from the release points (Figure 3.3.13).

A stripped-down version of ADOM (with the cloud scavenging, chemistry and dry-deposition modules removed because the tracers were not affected by any of these) was run over a domain which has been extended to the west to cover Glasgow (Olson et al., 1989b). In general, the model's performance for a point release on an episodic scale (1-3 days) is limited by the accuracy of the input meteorological data while the model reproduces a longer term average (44 days) fairly well (Figure 3.3.14). In this case, the modelled maximum coincides with the point of release (St. Cloud, Minnesota) while the observed maximum is about 1-2 grid cells to the northeast. This discrepancy is a consequence of the limited spatial resolution of the measuring network and the tendency of narrow plumes to frequently miss the nearest measuring stations.

The first release (about 1800 GMT January 5) from St. Cloud serves to illustrate the limitation the input data place on the results. The model wind field realistically simulates the flow around the major highs and lows but can smooth or miss the detailed flow pattern around fronts. Figure 3.3.15 shows that the modelled puff was advected too far to the west and out of the domain whereas the actual puff was advected south by January 6 (1300 GMT January 6 -1200 GMT January 7). In this case, the modelled wind field did not resolve the northerly flow behind a cold front which passed St. Cloud on January 6. Olson et al. (1989b) attributed discrepancies in short-term model prediction to small scale meteorology, initial pollutant spread over the 127 by 127 km grid, and numerical diffusion.

Consequently, without higher resolution meteorological data and an approach to restrict numerical diffusion and initial spread, the Eulerian model is better suited to multisource simulations on an episodic basis (a few days) or longer term simulations for a single source than to modelling a single source for 1-2 days.

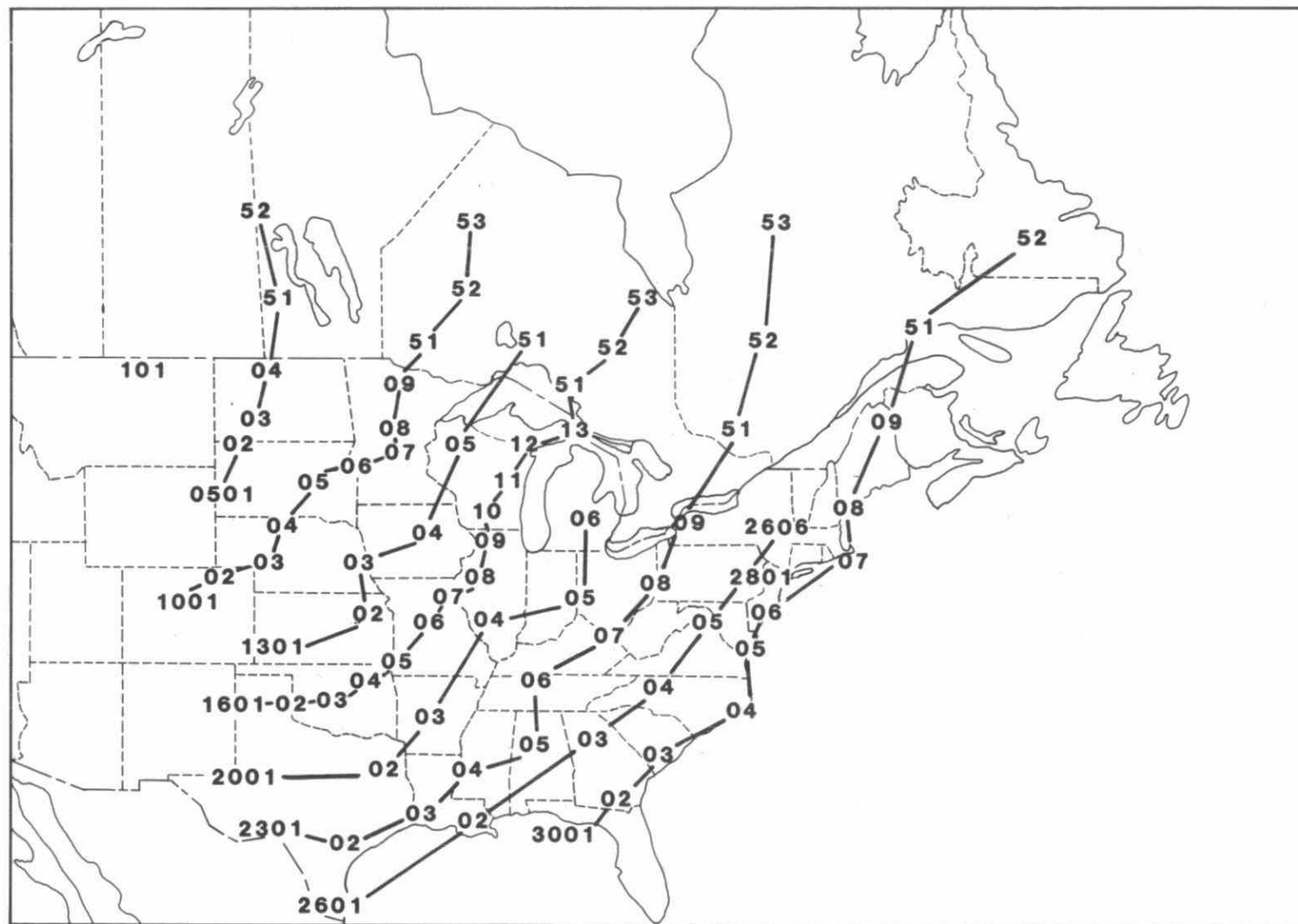


Fig. 3.3.13 Primary ground-level ANATEX sampling network. Exact station locations is at the centre of each site number.

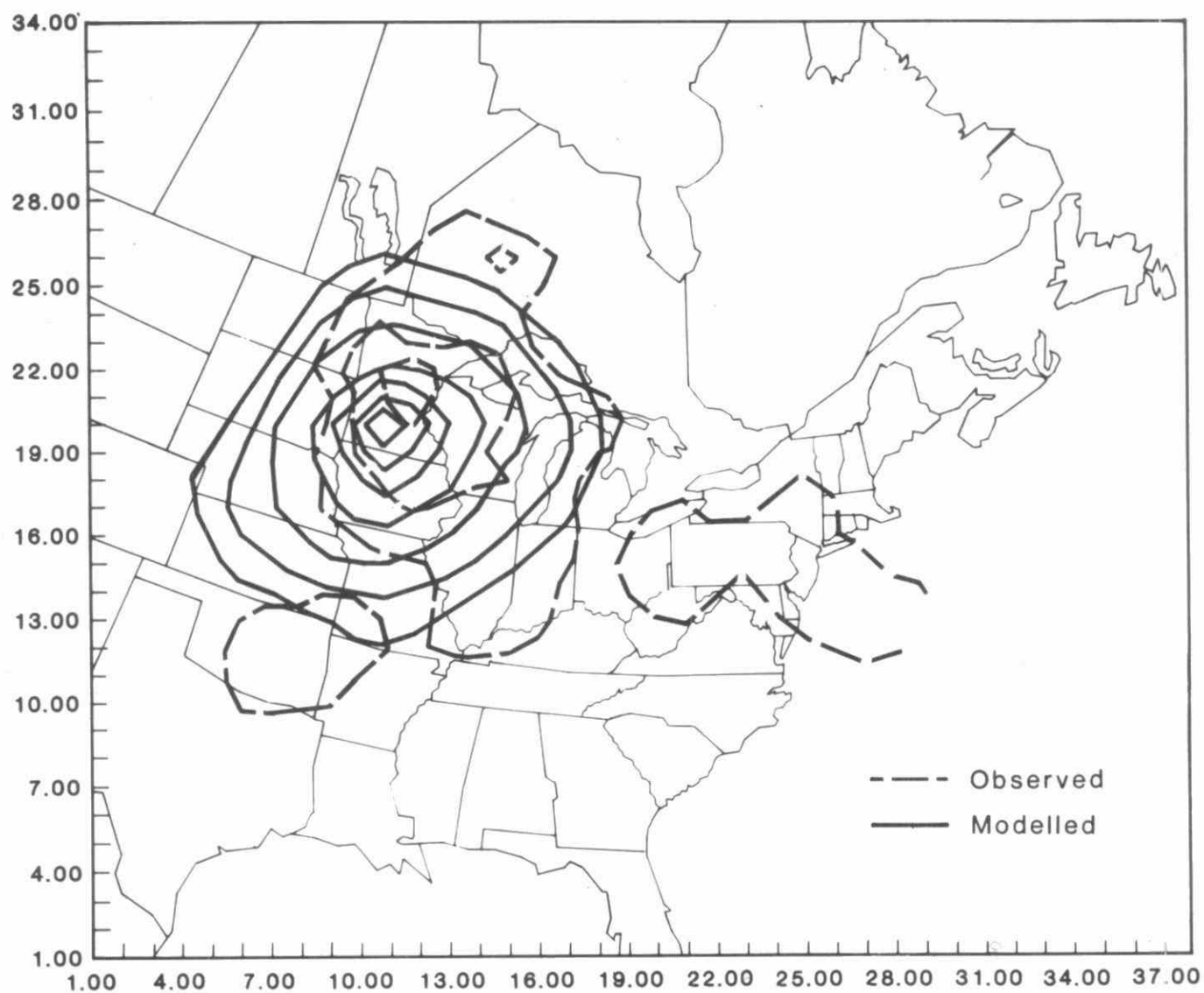


Fig. 3.3.14 The observed and predicted PDCH pattern for the first 44 days of the ANATEX run. The contours are 0.5, 1, 2, 5, 10, 20, 50, 100, fl/l with the outermost contour being 0.5.

fl/l: femtolitre per litre

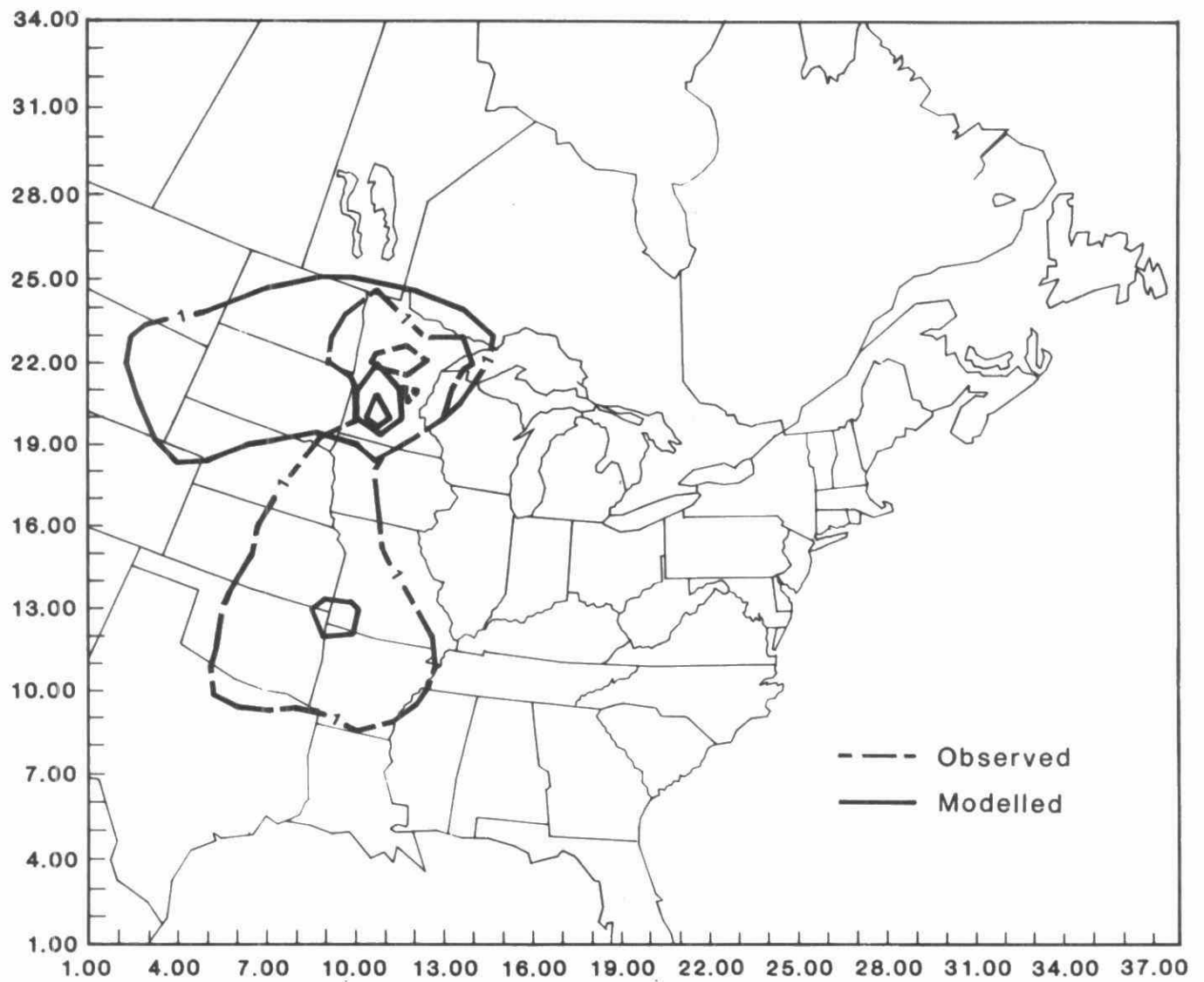


Fig. 3.3.15 The observed and predicted PDCH pattern for the first three days of the first release of the ANATEX run. The observed contours start at a fl/l on the outside and increase in steps of 4 fl/l. The predicted contours start at 1 fl/l on the outside and increase in steps of 10 fl/l.

fl/l: femtolitre per litre

3.3.5.d SUMMER OZONE EPISODE

Since oxidant concentrations, particularly H_2O_2 and O_3 , affect aqueous phase oxidation of SO_2 , it is important to evaluate the oxidant concentrations produced by the model. ADOM was run for a 9-day period in June 1983, during which ozone concentrations were above 80 ppb at many stations throughout the northeastern United States and southern Canada. For this set of model runs, a biogenic RHC inventory was included as part of the input data. The model was evaluated against observed ozone concentrations at 30 stations in Ontario and the northeastern United States

Figure 3.3.16 depicts the O_3 time series of model predictions and observations for a grid in southern Ontario and one in northern Ohio. The observed values are an average of 6 and 2 stations, respectively, within each grid square. The model reproduced the observed daily pattern and the daily maxima very well for most of the days examined. Statistical comparisons of observed and modelled daily maxima for 30 stations resulted in a geometric standard deviation of 1.4 which means that 95% of predictions were within a factor of 2 of observed values. The model bias was very small.

Scenario runs with reduced NO_x or RHC emissions indicated that very large changes in emissions are needed to produce significantly lower daytime O_3 maxima for the horizontal grid scale used in ADOM. The high RHC/ NO_x ratios through much of Ontario resulted in NO_x emission reductions having more influence on ozone concentrations than RHC emission reductions.

3.3.5.e WINTER STUDY

Since the behaviour of sulphur and nitrogen chemistry is very different in the winter than in the spring or summer, ADOM was run for a 10-day period in the winter of 1985. Figure 3.3.17 shows the scatter graph of precipitation event-averaged observed and modelled $\text{SO}_4^{=}$ concentrations in precipitation at sites throughout eastern North America. The circular points represent values which are made up of one day of measurements. The results showed more scatter than was found for the OSCAR episode. Comparisons of modelled precipitation with that observed at the chemistry sites showed a great deal of scatter which appears to adversely affect the correlation between model grid average and observed point aqueous concentrations. This is corroborated by the poorer performance of the points which only have one day in the average. Input data limitations could mean that the model would perform better for predicting percentage changes in deposition than absolute deposition on an episodic scale. Other comparisons with observations produced the following results:

- (a) Nitrate concentrations in precipitation showed considerable scatter when compared with observed data;
- (b) Modelled SO_2 air concentrations were well correlated with observed results but the model tended to overpredict the concentrations; and
- (c) The model systematically underpredicted air concentrations of sulphate and nitrate.

Table 3.3.13 gives an overall summary of the nitrate/sulphate ratios found in precipitation during OSCAR and for this winter study. For OSCAR the model predicted the average

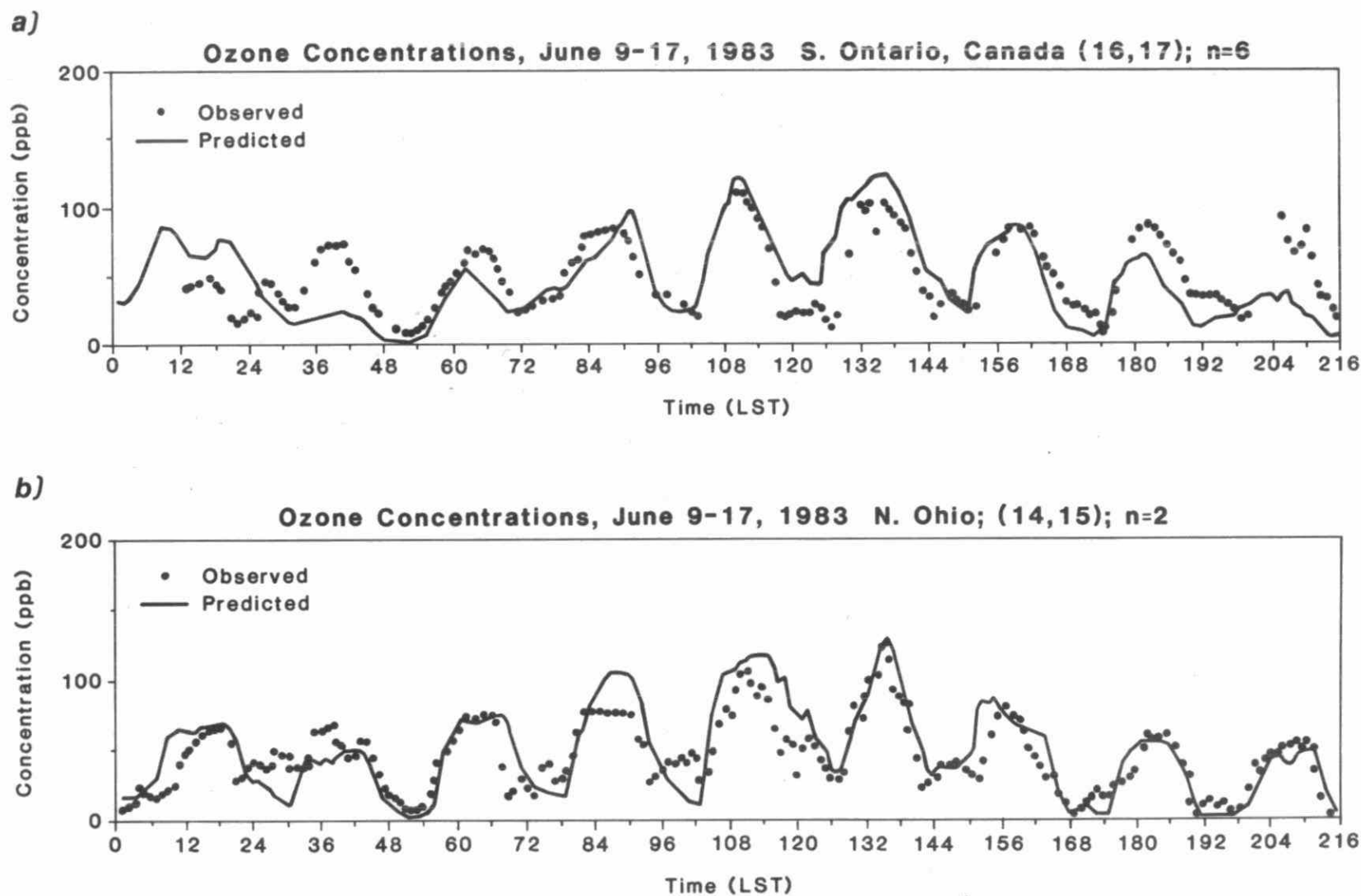


Fig. 3.3.16 Ozone concentrations, June 9-17, 1983, southern Ontario and northern Ohio.

ratio very well, although the modelled range of ratios was not as wide as observed at point locations during OSCAR II. For the winter study, the model predicted a larger nitrate/sulphate ratio but not as large as was observed. Some stations had observed ratios which were 3 times higher than the modelled ratios.

Figure 3.3.18 shows the percentage change in $\text{SO}_4^{=}$ concentrations in precipitation when SO_2 emissions were reduced uniformly by 50%. Through the central part of the grid the modelled reduction was from 20 to 35% with lowest values in the western part of the domain. This is more nonlinear than was found for the spring OSCAR study.

3.3.5.f EULERIAN MODEL EVALUATION FIELD STUDY

ADOM (Acidic Deposition and Oxidants Model) was evaluated using data from the Eulerian Model Evaluation Field Study (EMEFS). During this field study, an intensive effort was made to collect both surface and aircraft data.

A "Model-Evaluation Protocol" (Barchet, 1989) has been developed to provide guidance on the types of test to be carried out. This protocol has been reviewed by an external review panel consisting of 10 experts. It outlines tests to stress the ADOM and RADM models to determine their strengths and applicability. At this stage of the evaluation, only simple statistical techniques have been employed. Comparisons have so far been limited to ground level air and precipitation concentrations. The measured concentrations of most species are available as 24-hr averages while measured ozone concentrations are available hourly. The following sections describe the findings of the evaluation of ADOM with data from the July - September 1988 period.

The data from the measurement networks are stratified and averaged for comparison with model output. The EMEFS measurement sites are classified into nine regions (Figure 3.3.19) based on emissions and meteorological characteristics. Four sites, which were determined to be too close to urban areas were not classified into the nine regions. A site in Massachusetts did not fit into any region and was left as a site by itself. In the scatter plot to be presented, the points are designated by the region number.

Comparison of concentrations in precipitation is affected by occasional mismatch between the modelled grid-averaged precipitation and the observed precipitation point measurements. This may introduce an extreme value in the measured data, for example (if the precipitation amount is small at the monitoring station), and a large deviation between the measured (point) and modelled (grid-square) values. Although this qualitative agreement of the extreme values tends to support the modelling framework, it is not very useful in objective analyses of the comparison between model predictions and observations. By averaging over precipitation "events" of 4 to 7-day duration, the extreme values are somewhat filtered out making it easier to interpret the scatter plots. All the scatter plots of this section are for period-averaged data.

Two types of regression analysis were performed on ADOM's data presented below in scatter plot form: (1) regular linear regression yielding the slope and y-intercept of the best fit line and (2) best fit analysis that forces the line through the origin.

Event Averaged SO_4 Concentrations in Precipitation

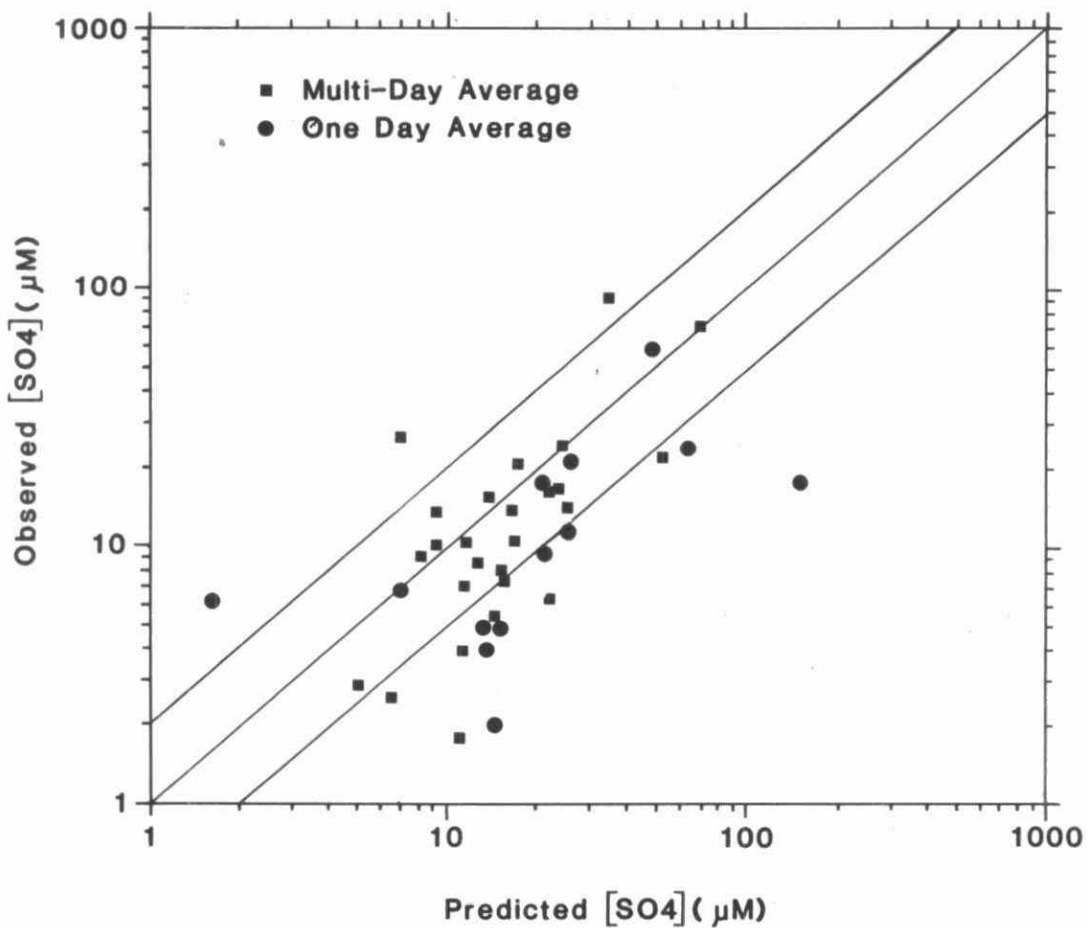


Fig. 3.3.17 Event averaged SO_4 concentrations in precipitation.

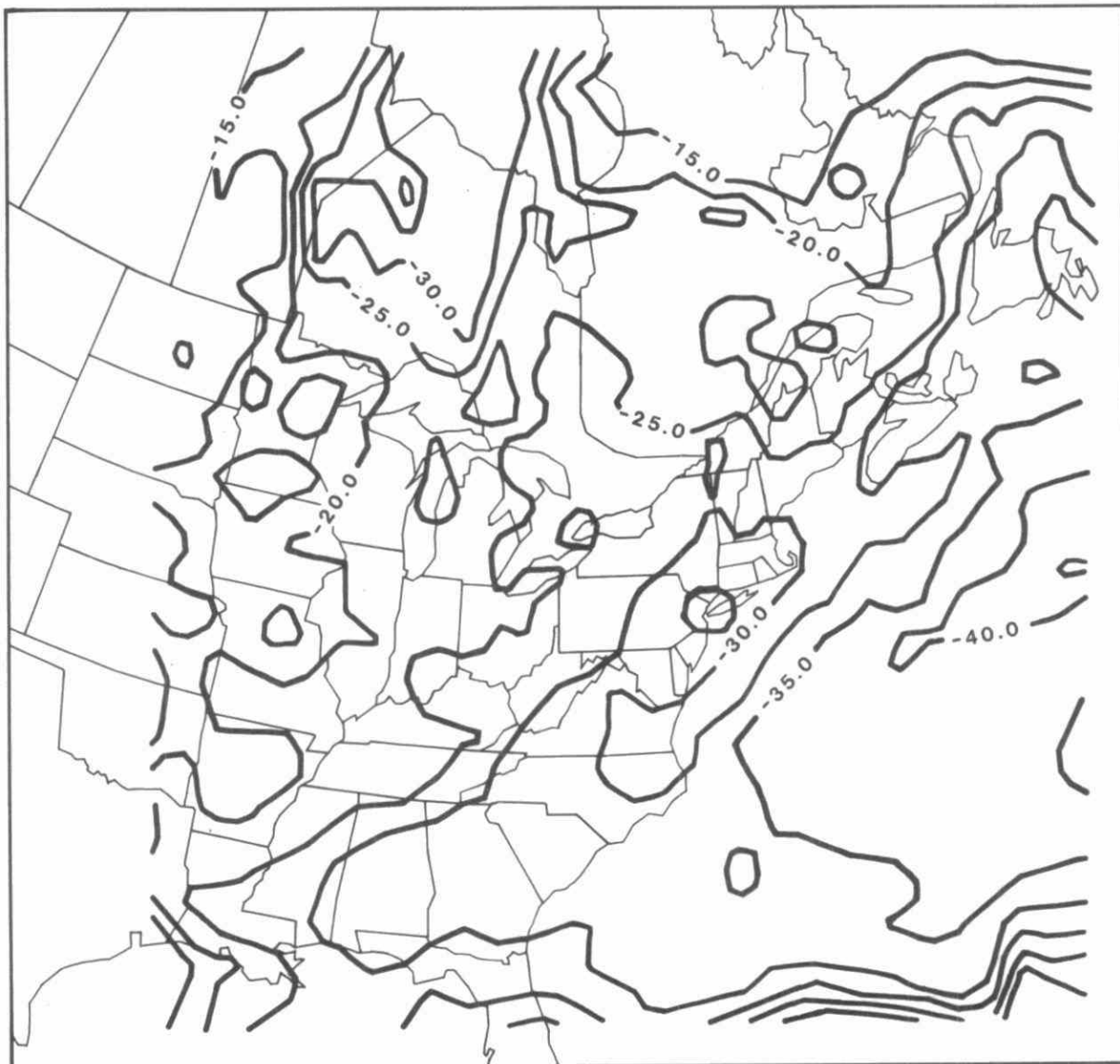


Fig. 3.3.18 Reduction (%) in wet sulphur deposition in response to 50% reduction in grid SO_x emissions.

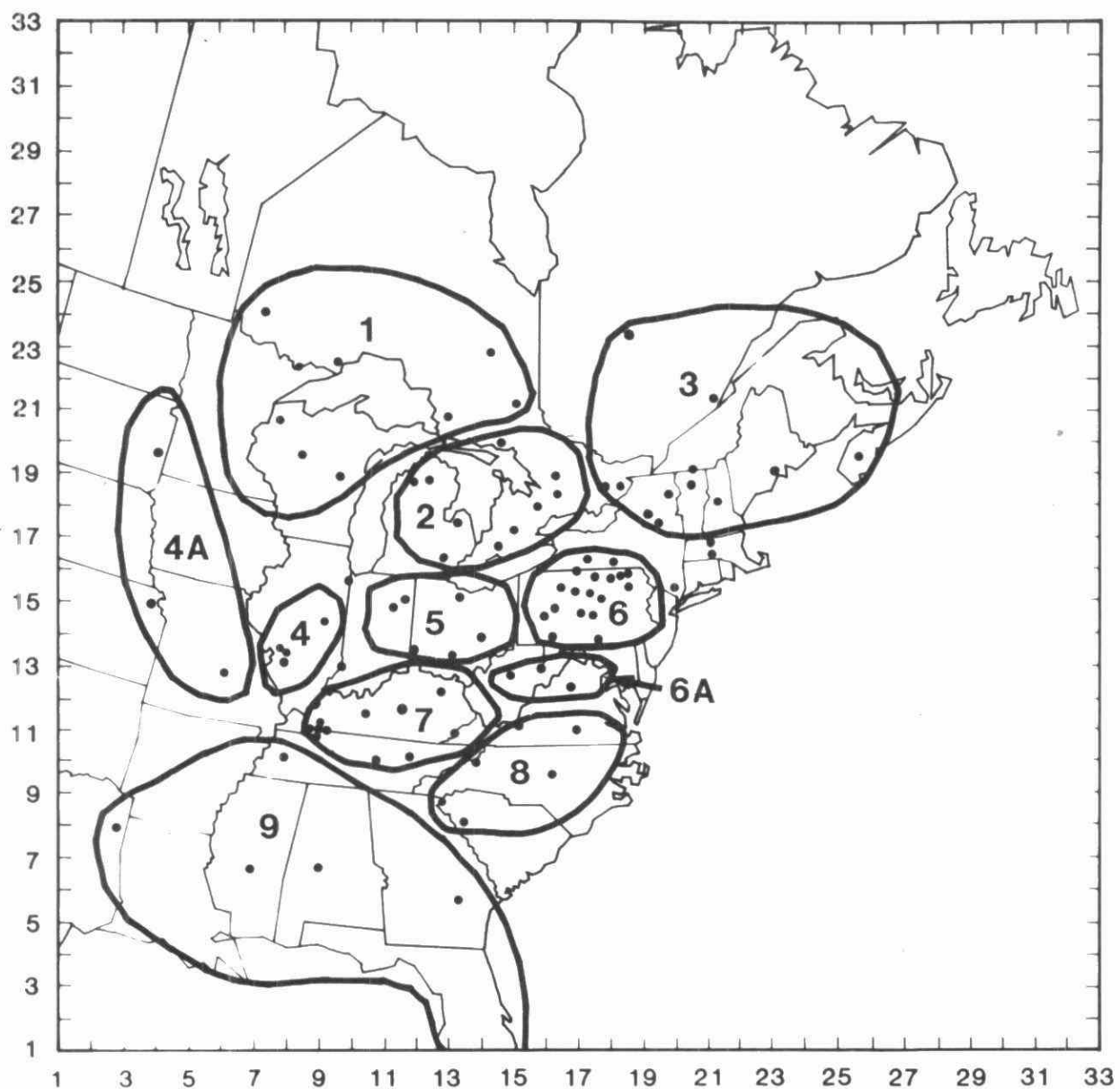


Fig. 3.3.19 Eulerian Model Evaluation Field Study (EMEFS) monitoring sites and regions.

Table 3.3.13

Ratios of $\text{NO}_3^-/\text{SO}_4^{2-}$ found in precipitation during OSCAR II and IV and a winter period

	Observed		Predicted	
Study	Range	Geometric Mean	Range	Geometric Mean
OSCAR II	0.21 - 2.53	0.89	0.55 - 1.19	0.82
OSCAR IV	0.53 - 1.49	0.91	0.52 - 1.47	0.83
WINTER	0.23 - 14.8	2.40	0.20 - 4.54	1.62

The following sections will present results of ADOM for two periods: July 28 - August 8, 1988 and August 25 - September 5, 1988. These will be referred to as Periods 1 and 2, respectively. The first period covers a high O_3 episode prevalent over southern Ontario. The second period covers the first twelve days of an evaluation period that was decided on for comparison. Since the sulphur and nitrogen species in the model do not interact directly, they are discussed separately below.

Figure 3.3.20 shows the modelled vs. observed ground level concentration for SO_2 for Periods 1 and 2. For Period 1, the mean of all the observed points is $6.33 \mu g/m^3$. This indicates an overall overprediction of about 10 per cent of the observed mean. On the other hand, the slope of the best fit line forced through the origin is 0.98. This slope is apparently driven by a few points showing underprediction at large observed values. Results of linear regression give a positive y-intercept of $1.86 \mu g/m^3$ and a slope of 0.8. For Period 2, the overprediction which is apparent from the scatter plot is confirmed by the mean of the observed ($5.39 \mu g/m^3$) and modelled ($6.98 \mu g/m^3$) values. This gives close to 30 per cent overprediction. The slope of the best fit line forced through the origin is 1.15, indicating overprediction. The results of linear regression are: slope of 0.9 and y-intercept of $2.15 \mu g/m^3$. This agrees with the results of Period 1. The R^2 correlation coefficients are 0.53 (Period 1) and 0.57 (Period 2). There is no spatial region that performs preferentially better or worse.

Figure 3.3.21 gives the time series plots for Periods 1 and 2 for Regions 3 and 5. The temporal trends can, to a first approximation, be attributed to the SO_2 response to precipitation. For Region 5 which covers the heavy emissions area of Ohio, an increasing SO_2 concentration can, to a first approximation be related to build up during a dry period, while a decreasing concentration can be attributed to scavenging and rapid in-cloud conversion. The behaviour of Region 3 can also be explained by the above factors, together with transport into and out of the region. During the first period, both Regions 3 and 5 show rather disorganized weather activity. The different parts of Region 3 experienced fog, drizzle, continuous rain and shower at various times. Region 5 during Period 1 experienced fog and haze. For Period 2, both regions experienced three well-defined precipitation events: 25-26 August; 28-29 August for Region 5 and 29-30 August for Region 3; and 4-5 September. Both Regions 3 and 5 for Period 1 do not show strong overpredictions while the regions for Period 2 show unmistakable overprediction. This is in agreement with the scatter plot analyses presented in Figure 3.3.20. The correlation between the observed and predicted concentrations for Period 2 is better than that for Period 1. This is probably because the weather pattern during Period 2 is better organized (e.g. clear break between wet and dry periods and having less subgrid scale precipitation) and consequently better represented as input data to the model. In fact, the plot for Region 5 of Period 1 does indicate rather complex fluctuations of the concentration, possibly due to complex meteorology. In this situation, the model can be highly stressed.

Figure 3.3.22 shows the modelled vs. observed ground level concentration of $SO_4^{=}$ for Periods 1 and 2, respectively. During Period 1, only 17 stations were measuring $SO_4^{=}$. These limited observations indicate consistent underprediction. The mean observed value is $8.23 \mu g/m^3$, more than twice the mean modelled value at the observed points of $3.89 \mu g/m^3$. Out of the 17 points, only two near the low end are overpredicted. The slope of the best fit line forced through the origin and that from standard linear regression are 0.41 and 0.45, respectively. The y-intercept from linear regression is $0.5 \mu g/m^3$. The

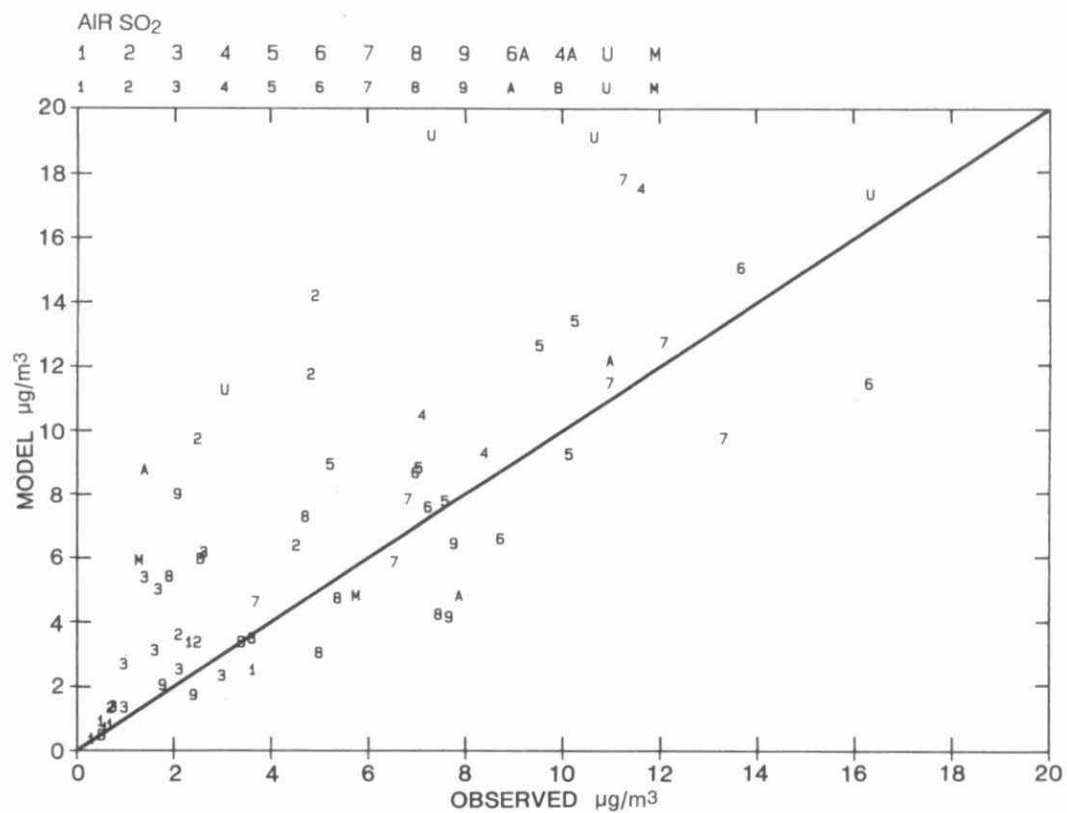
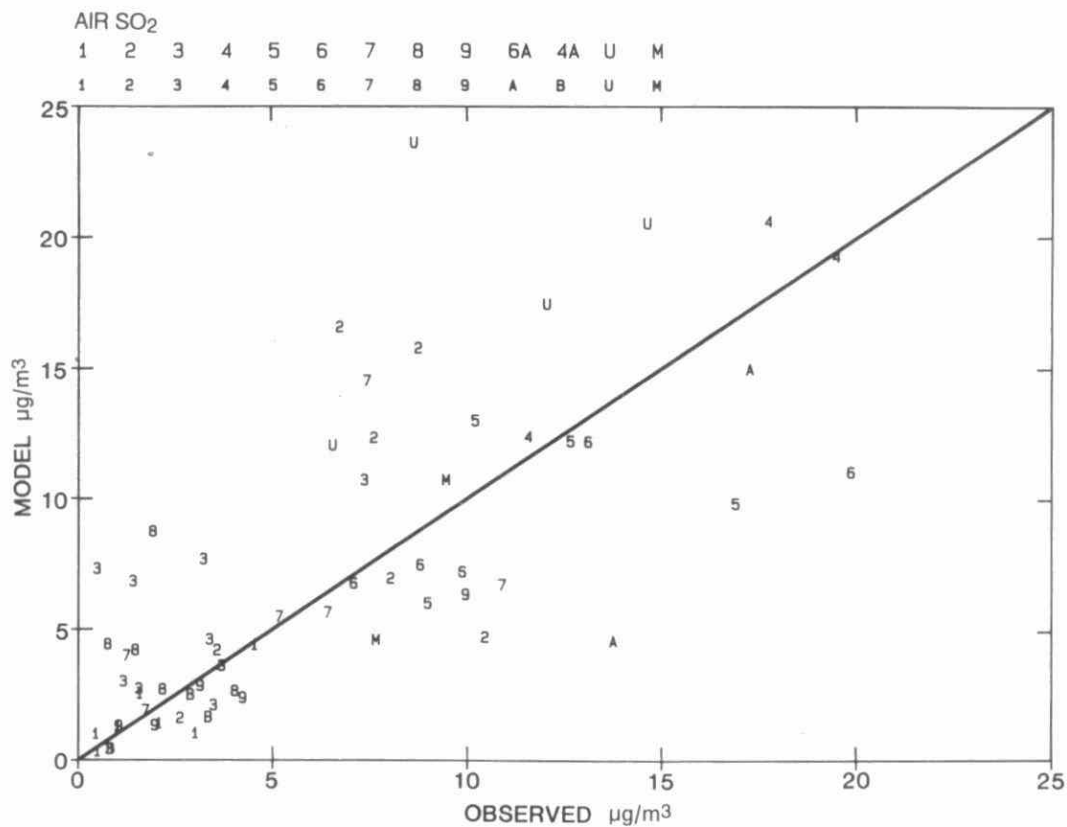


Fig. 3.3.20 Model predictions vs. observed ground level concentrations of SO_2 ($\mu\text{g}/\text{m}^3$) during July 28 - August 8 and August 25 - September 5, 1988.
Numbers refer to the regions shown in Fig. 3.3.19

REGIONAL SO₂ TREND

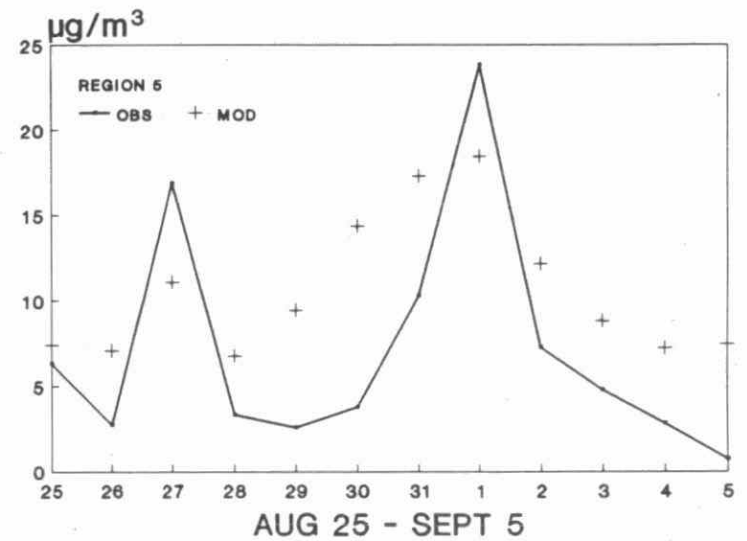
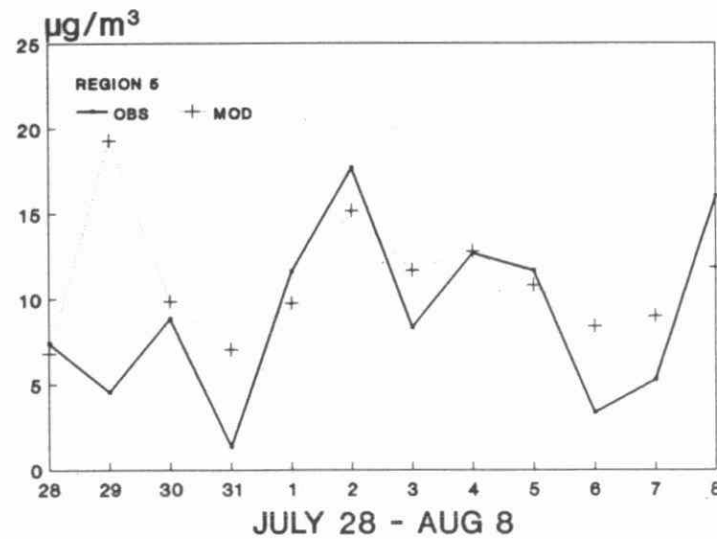
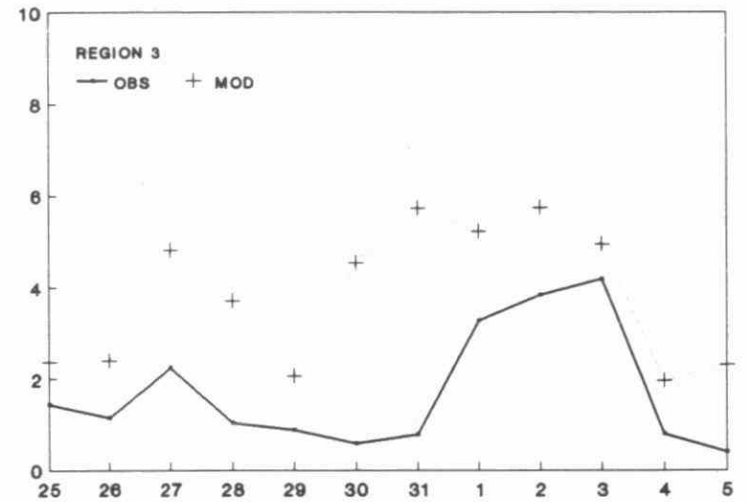
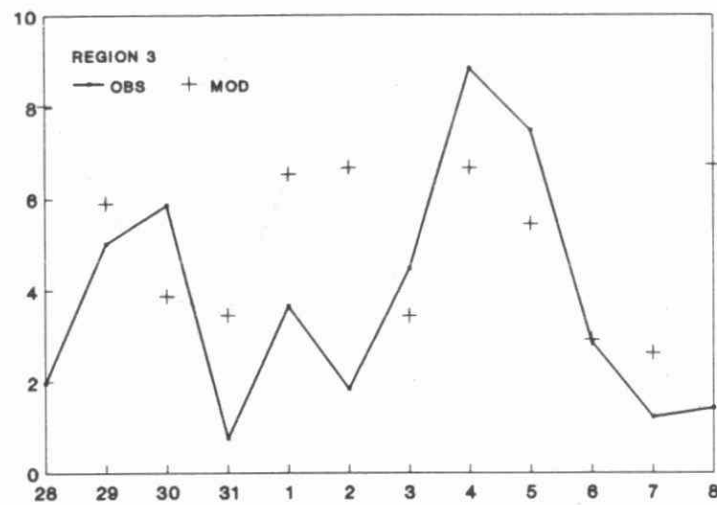


Fig. 3.3.21 Time series plot of averaged concentrations of observed and predicted SO₂ (μg/m³) for Regions 3 and 5 during Periods 1 and 2.

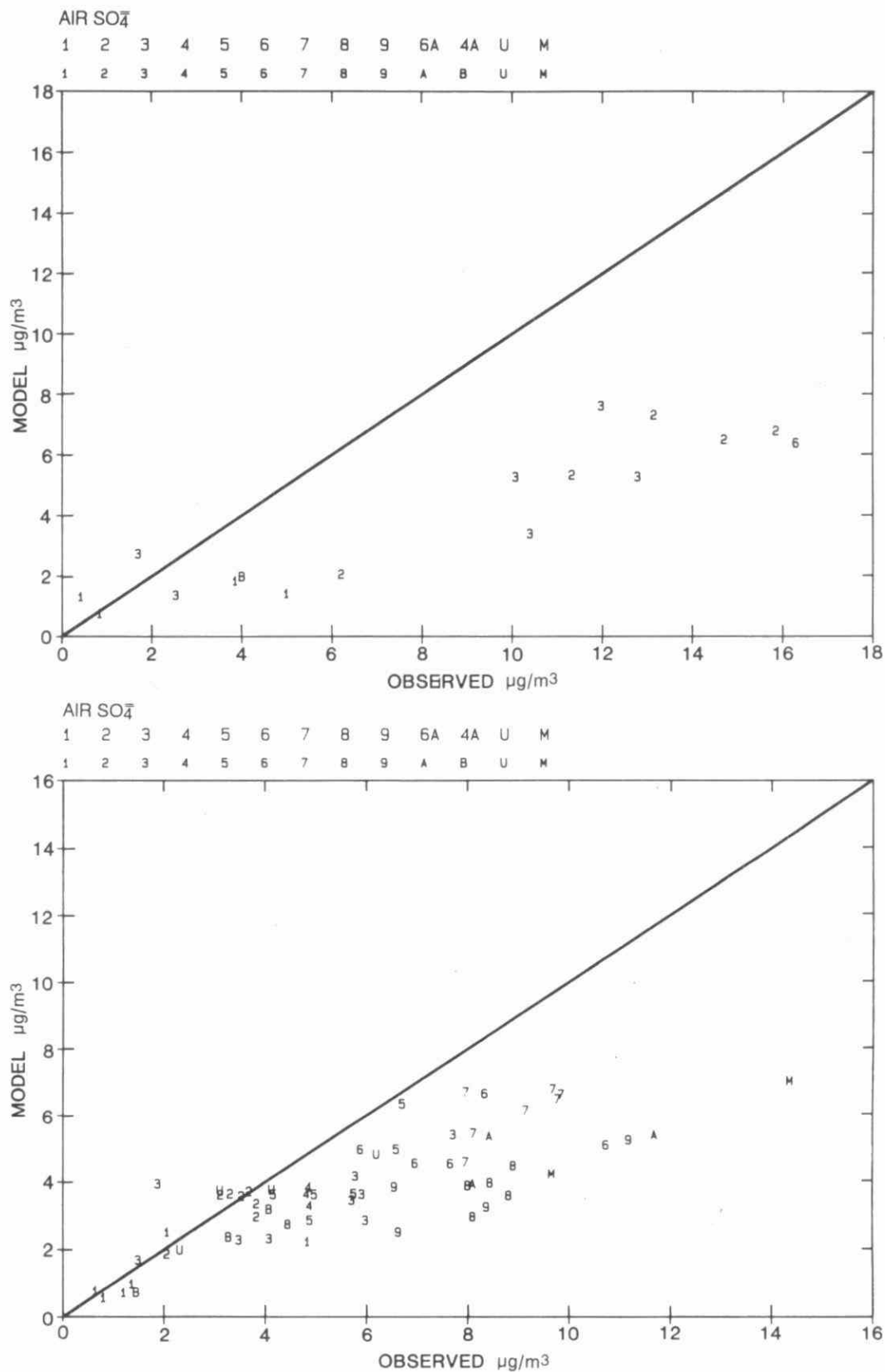


Fig. 3.3.22 Model predictions vs. observed ground level concentrations of SO₄⁼ ($\mu\text{g}/\text{m}^3$) during July 28 - August 8, and August 25 - September 5, 1988.
Numbers refer to the regions shown in Fig. 3.3.19

maximum value attained by the model at these points is less than $7.5 \mu\text{g}/\text{m}^3$ while the maximum of the observed (not the same points as the modelled) is over $16 \mu\text{g}/\text{m}^3$. For Period 2, $\text{SO}_4^{=}$ is still underpredicted. The mean observed value for the 65 points is $5.8 \mu\text{g}/\text{m}^3$. The mean modelled value at those points is $3.7 \mu\text{g}/\text{m}^3$. The few points that overpredicted are all found within the lower half of the range of observed values. The slope of the best fit line forced through the origin is 0.59. The linear regression results give a best fit slope of 0.42 and a y-intercept of $1.2 \mu\text{g}/\text{m}^3$. Like Period 1, the model maximum at these locations is less than $7.5 \mu\text{g}/\text{m}^3$ while the observed maximum is more than $14 \mu\text{g}/\text{m}^3$. The R^2 correlation coefficient for Period 1 is 0.84 and for Period 2 is 0.65. In general, the $\text{SO}_4^{=}$ ground level concentrations show less scatter than the SO_2 ground level concentrations and the ranges of values predicted for the two periods are similar.

The time series plots for Periods 1 and 2 for Regions 3 and 6 are given in Figure 3.3.23. There is no observed data for Region 5 during the first period. Two consistent trends can be seen: the periodicity of the observed data is accurately reproduced by the model and the observed peaks are underpredicted. For both regions, the fluctuation is caused by a combination of washout by precipitation and transport into and out of the region.

The comparison of the modelled vs. observed total sulphur (SO_2 and $\text{SO}_4^{=}$) concentration for Periods 1 and 2 are given in Figure 3.3.24. The analysis of Period 1 shows approximately 8 per cent underprediction. However, given the small number of points available (only 13 points covering 3 regions have observations of both SO_2 and $\text{SO}_4^{=}$ in air), the results of any analysis will have to be treated with caution. On the other hand, the small overprediction is certainly expected from the small overprediction for the air SO_2 and significant underprediction for the air $\text{SO}_4^{=}$ reported for this period. Again, all of the regions show points on both sides of the 1:1 line. For Period 2, 53 points make up the plot. Analysis shows overprediction of only 2 per cent. The slope of the best fit line forced through the origin is 1.00. Standard regression analysis gives a slope of 0.92, a y-intercept of $0.51 \mu\text{g}/\text{m}^3$ and an R^2 correlation coefficient of 0.67.

Figure 3.3.25 shows the modelled vs. observed $\text{SO}_4^{=}$ concentration in precipitation for Periods 1 and 2. For both periods, two characteristics are immediately apparent: there is little systematic bias and a large scatter. The first observation is supported by the mean of the observed and modelled values. For Period 1, the mean observed value is 3.49 mg/l and the mean modelled value is 3.71 mg/l. The two agree to within 10 per cent of each other. For Period 2, the mean observed and modelled values are 2.49 and 2.47 mg/l, respectively. For all practical purposes, this agreement to within 1 per cent indicates no bias. The large scatter is indicated by the low R^2 correlation coefficients for the two periods (0.07 for Period 1 and 0.16 for Period 2).

The large scatter can be attributed to two factors. First, the comparison shown in Figure 3.3.25 is between point (for observed) and area-averaged (for modelled) values. Subgrid scale variability in precipitation can cause considerable mismatch in the comparison if the observed precipitation amount deviates from the grid average. The highly sporadic nature of precipitation basically guarantees significant mismatch. Second, both of these periods are no longer than twelve days. Within each period, each site experienced no more than three to four precipitation events. This is too short to have averaged out the extreme values. This indicates that correlation coefficients are not meaningful in the interpretation of wet sulphate concentrations.

REGIONAL SO_4^{2-} TREND

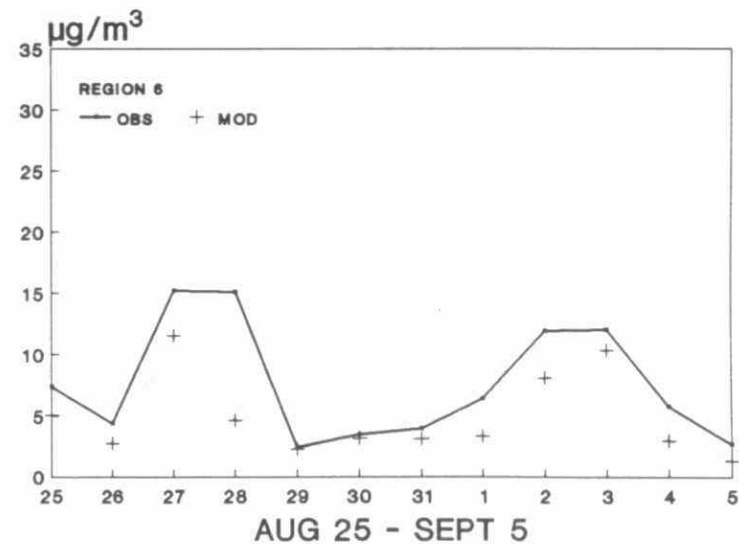
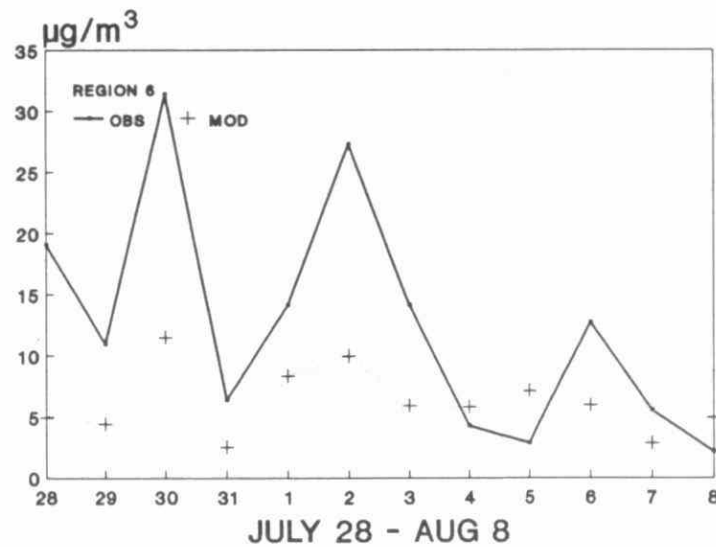
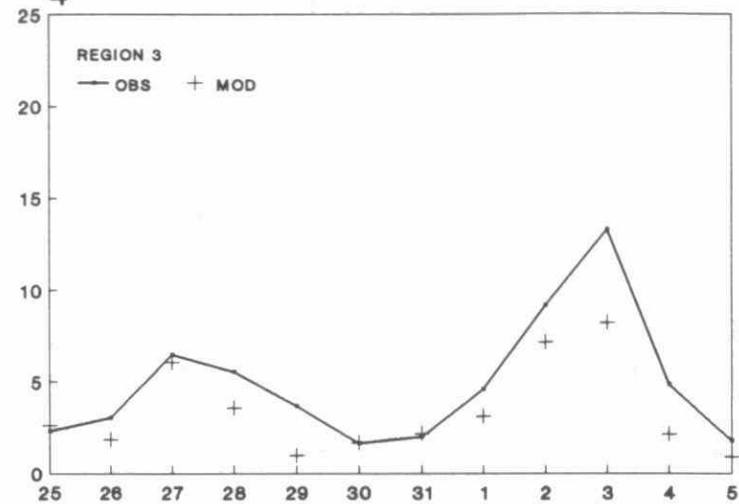
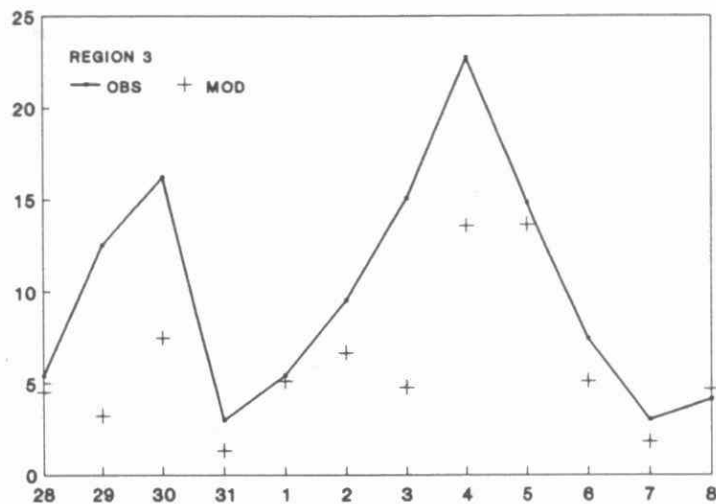


Fig. 3.3.23 Time series plots of averaged concentrations of observed and predicted SO_4 ($\mu\text{g}/\text{m}^3$) for Regions 3 and 6 during Periods 1 and 2.

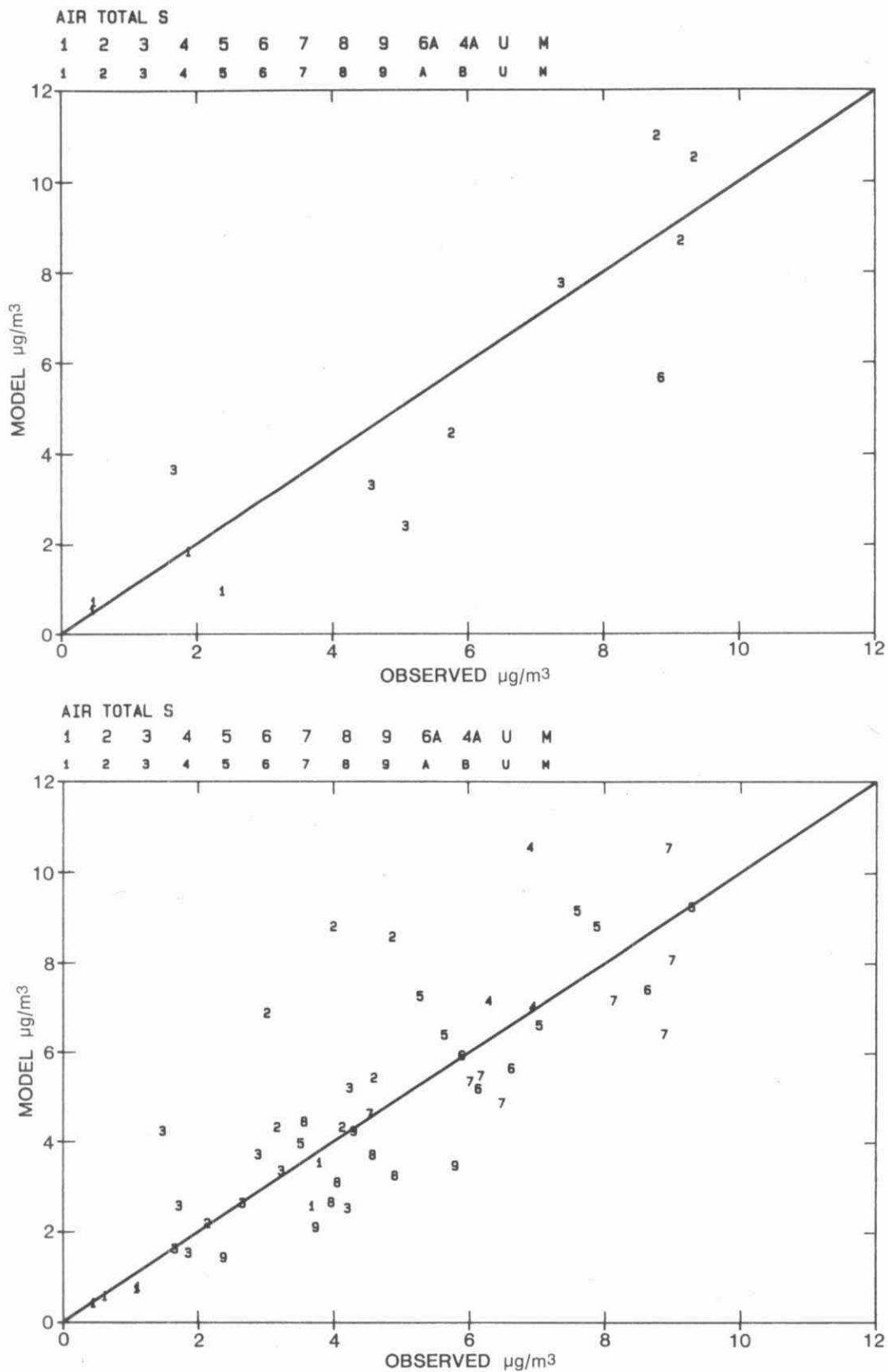


Fig. 3.3.24 Model predictions vs. observed ground level concentrations of total sulphur ($\mu\text{g}/\text{m}^3$) during July 28 - August 8 and August 25 - September 5, 1988. Numbers refer to the regions shown in Fig. 3.3.19

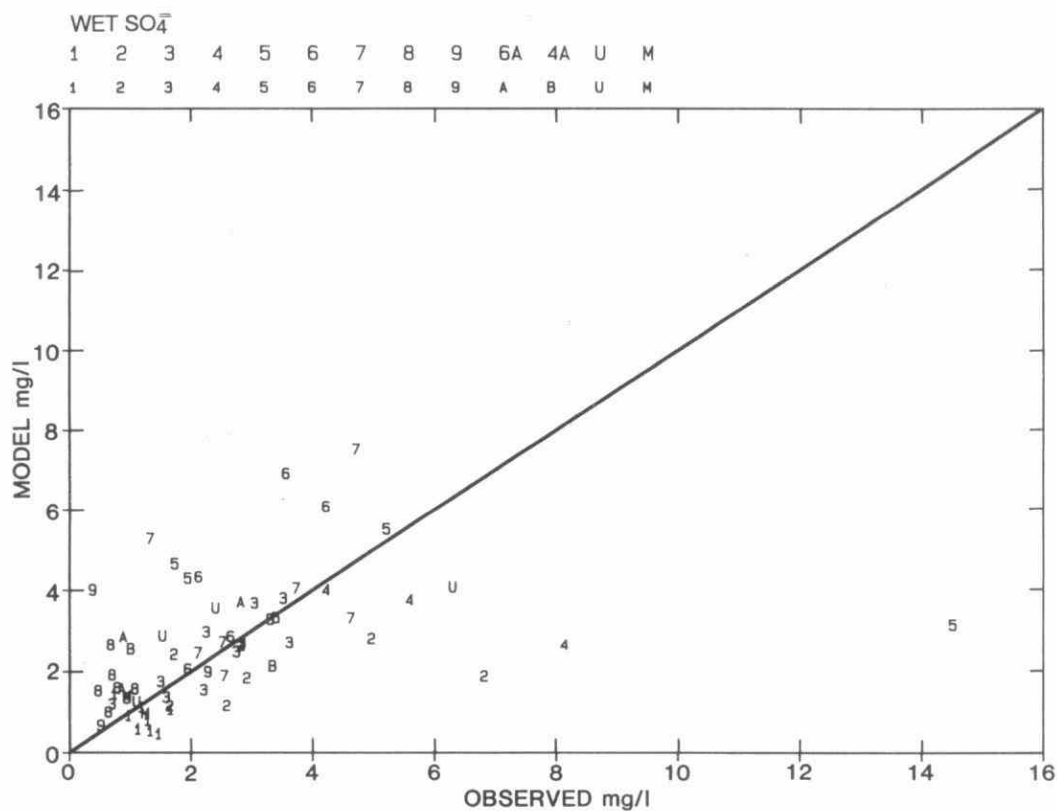
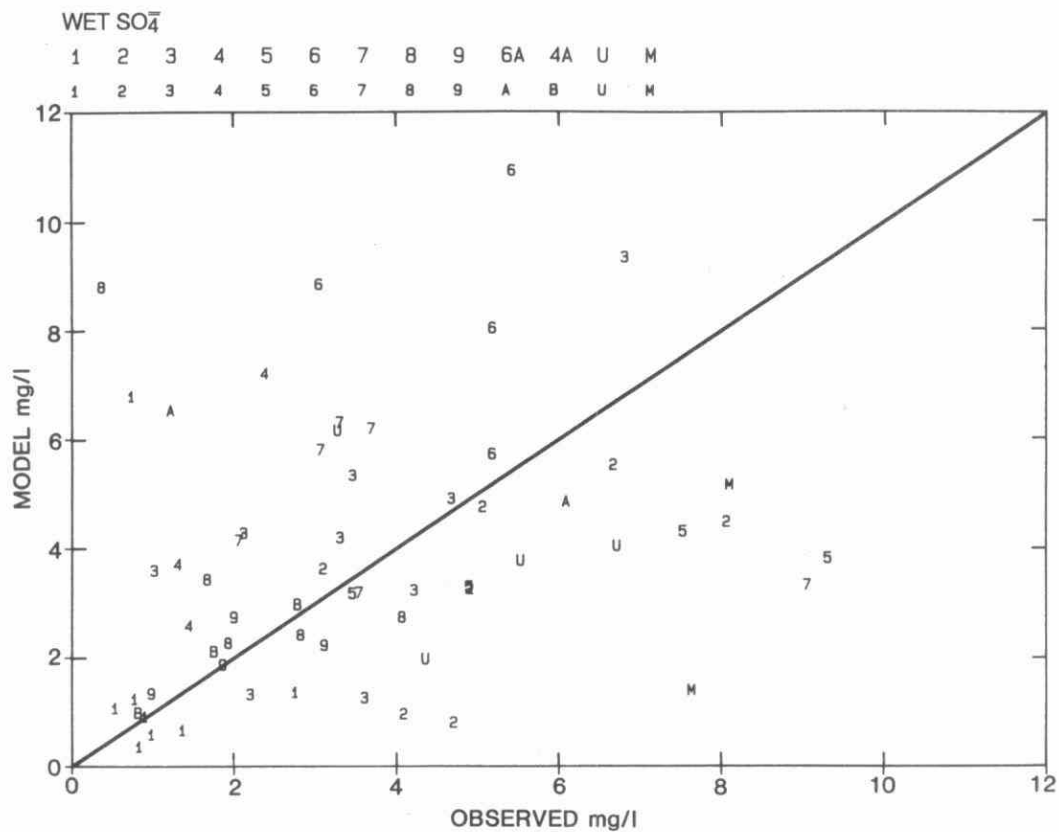


Fig. 3.3.25 Model predictions vs. observed concentrations in precipitation SO_4^- (mg/l) during July 28 - August 8 and August 25 - September 5, 1988. Numbers refer to the regions shown in Fig. 3.3.19

Figure 3.3.26 gives the modelled vs. observed NO_2 ground level concentration for Periods 1 and 2, respectively. For Period 1, the data show an underprediction of approximately 20 per cent ($6.8 \mu\text{g}/\text{m}^3$ for mean observed value vs. $5.5 \mu\text{g}/\text{m}^3$ for mean modelled value). The slope of the best fit line forced through the origin is 0.64. As a result of an outlying point (model prediction of more than $30 \mu\text{g}/\text{m}^3$), the R^2 correlation is very low (0.055). Consequently, the regression analysis which gives a slope of 0.28 and a positive y-intercept of $3.5 \mu\text{g}/\text{m}^3$ would not be very meaningful. This outlying point represents a one-day measurement (the station only measured for one day during the period) very close to New York City. The mean modelled value is also affected by this outlier. Without this point, the underprediction would be approximately 30 per cent. For Period 2, the model underpredicts by less than 5 per cent ($5.05 \mu\text{g}/\text{m}^3$ for mean observed vs. $4.86 \mu\text{g}/\text{m}^3$ for mean modelled). The R^2 correlation coefficient for this period is 0.47. Regression analysis for this period gives a slope of 0.87 and y-intercept of $0.46 \mu\text{g}/\text{m}^3$.

The region-averaged time series plots for Regions 3 and 6 for Periods 1 and 2 are given in Figure 3.3.27. Region 3 on July 31, 1988 shows a missing value because none of the stations in this region was operating. (Region 5 shows even more missing days and so the results for Region 6 were presented instead). The Region 3 data for Period 1 show opposite trends for the observed and modelled concentration after July 31. Region 6 shows significant underprediction almost throughout the entire Period 1. This is consistent with the underprediction indicated in the scatter plot. For Period 2, Region 3 shows consistent and significant overprediction. Overall overprediction is also noticed in the time series plots in some other regions (e.g. 2 and 5). Region 6 shows underprediction at the beginning and end of the period. Taken together, this seems to contradict the underprediction reported in the preceding paragraph. However, it was found that about 16 stations were reporting for Region 6 whereas between 1 and 3 stations were reporting during the same period for other regions. Thus, Region 6, which underpredicts, would be weighted more heavily.

Since NO_2 is mainly formed through gas-phase reactions and is not very soluble in water, the fluctuations in the time series are mainly a result of gas-phase chemical conversion and transport. The lack of correlation between the time trends in some regions may be attributed to the dominance of local sources (because of the rapid NO to NO_2 conversion) coupled with local air flow pattern.

The modelled vs. observed comparison of ground level total nitrate (nitric acid vapour plus particulate nitrate) concentrations for Periods 1 and 2 are given in Figure 3.3.28. The first period shows less than 10 per cent mean underprediction ($3.64 \mu\text{g}/\text{m}^3$ for mean observed value vs. $3.35 \mu\text{g}/\text{m}^3$ for mean modelled value), while the second period shows less than 4 per cent underprediction ($2.58 \mu\text{g}/\text{m}^3$ for mean observed value vs. $2.68 \mu\text{g}/\text{m}^3$ for mean modelled value). This is apparent from the scatter plots. The slopes of the best fit line forced through the origin are 0.92 and 0.99 for Periods 1 and 2, respectively. Regression analyses give slopes of 0.92 and 0.84 and positive y-intercepts of 0.02 and $0.51 \mu\text{g}/\text{m}^3$ for Periods 1 and 2, respectively. The R^2 correlation coefficients for the two periods are respectively 0.47 and 0.56.

The region-averaged nitrate concentration time series plots for Regions 3 and 5 during Periods 1 and 2 are given in Figure 3.3.29. For the first period, both regions do not capture the fluctuations very well. Inspection of the data shows that Regions 3 and 5 average 10 and 3 operating stations, respectively, during that period. Thus, the paucity of stations is not an explanation of the discrepancy. For Period 2, there are two well

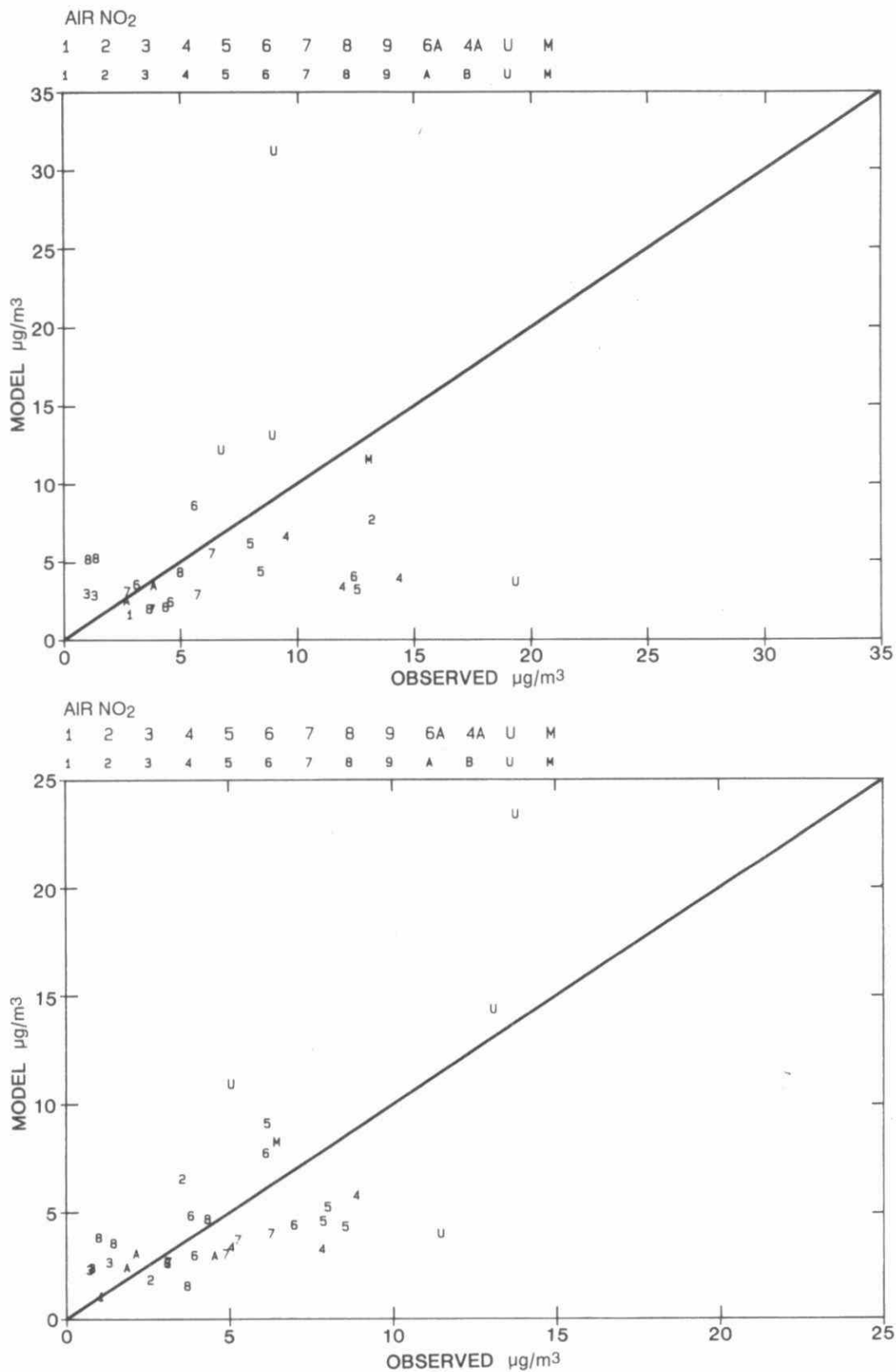


Fig. 3.3.26 Model predictions vs. observed concentrations NO₂ ($\mu\text{g}/\text{m}^3$) during July 28 - August 8 and August 25 - September 5, 1988. Numbers refer to the regions shown in Fig. 3.3.19

REGIONAL NO₂ TREND

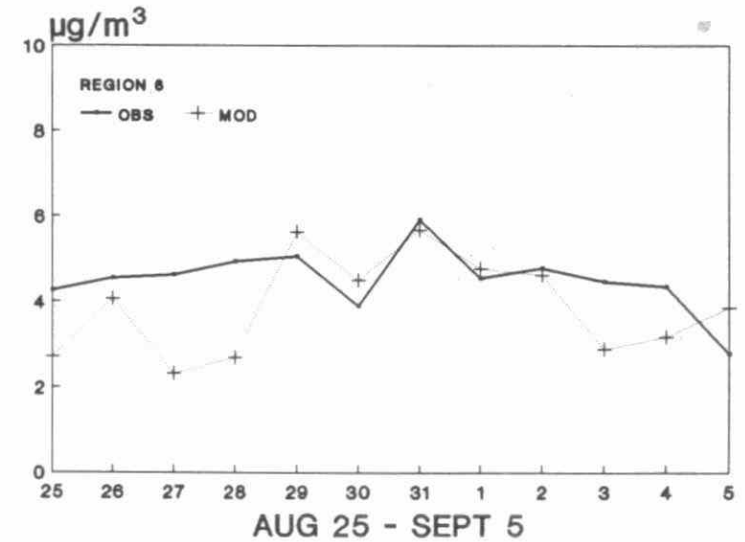
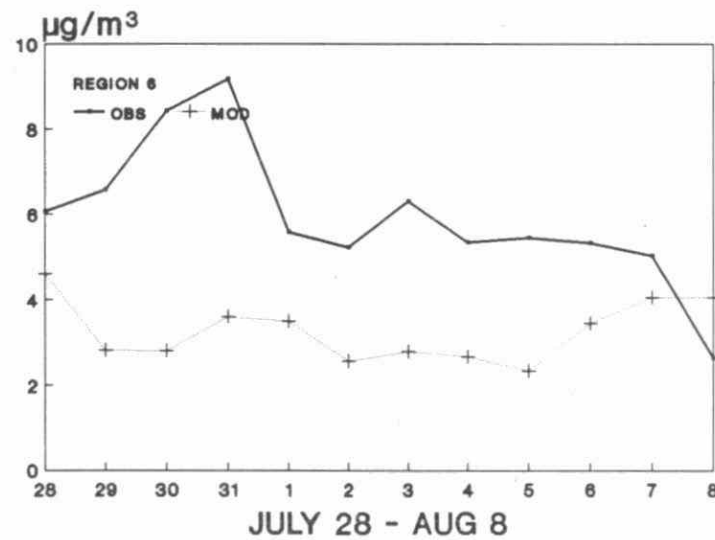
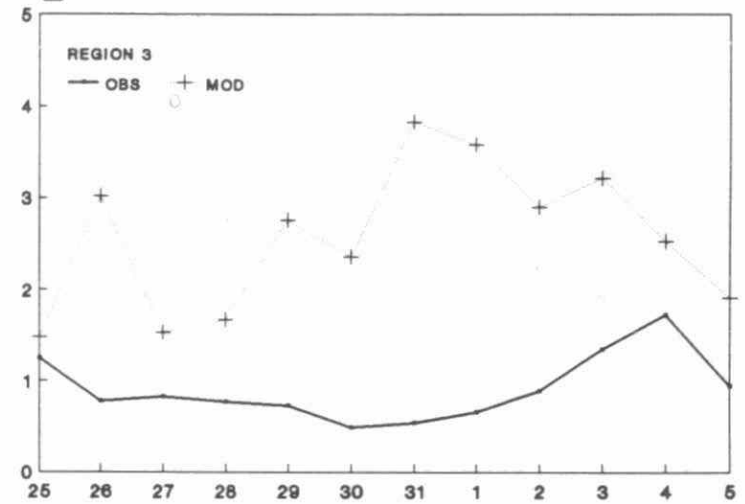
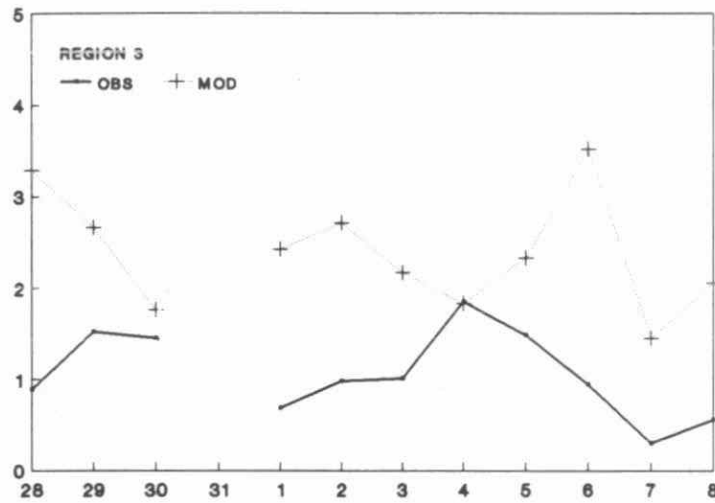


Fig. 3.3.27 Time series plots of averaged concentrations of observed and predicted NO₂ (µg/m³) for Regions 3 and 6 during Periods 1 and 2.

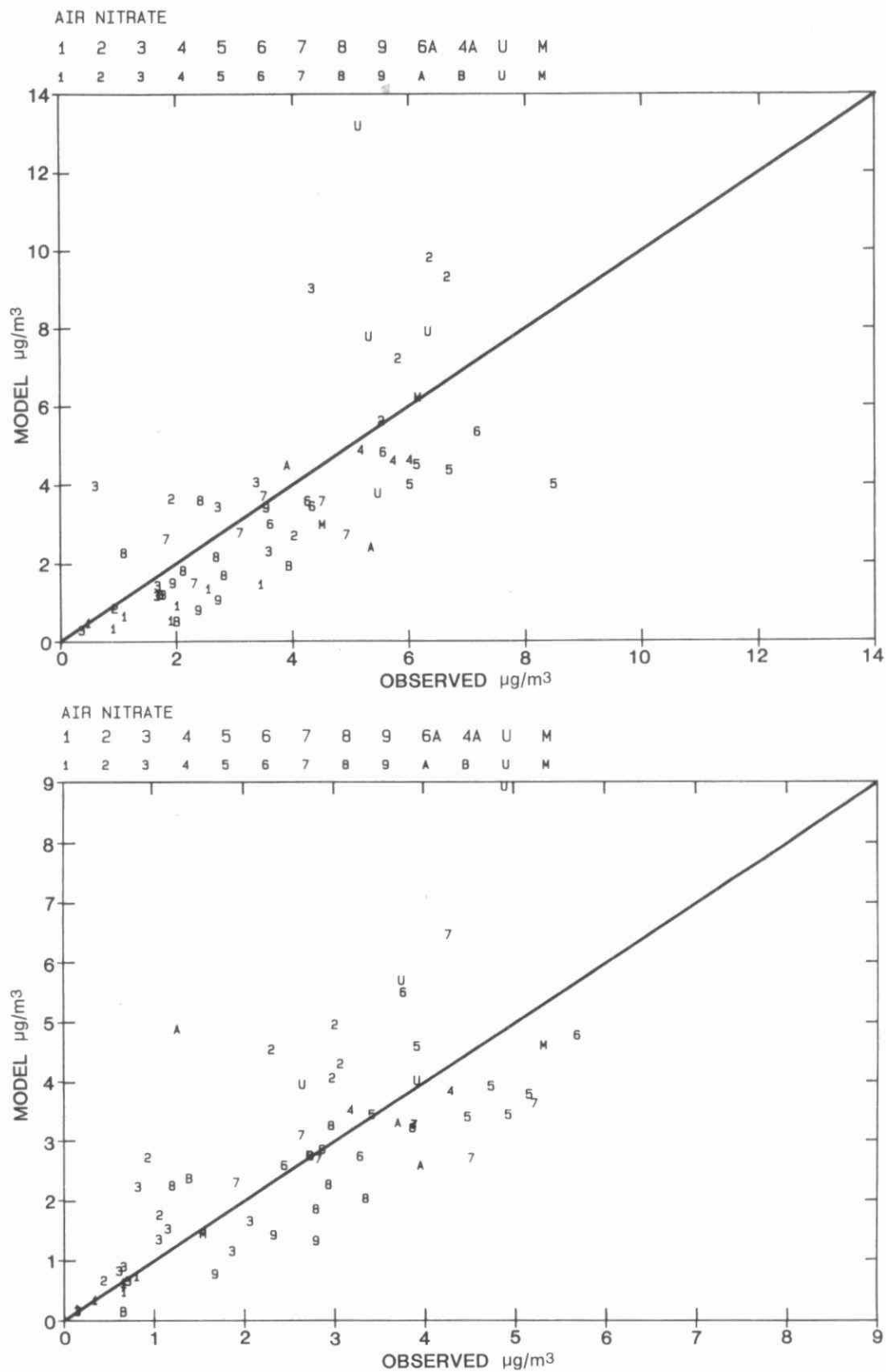


Fig. 3.3.28 Model predictions vs. observed ground level concentrations of total nitrate ($\mu\text{g}/\text{m}^3$) during July 28 - August 8 and August 25 - September 5, 1988. Numbers refer to the regions shown in Fig. 3.3.19

REGIONAL NITRATE TREND

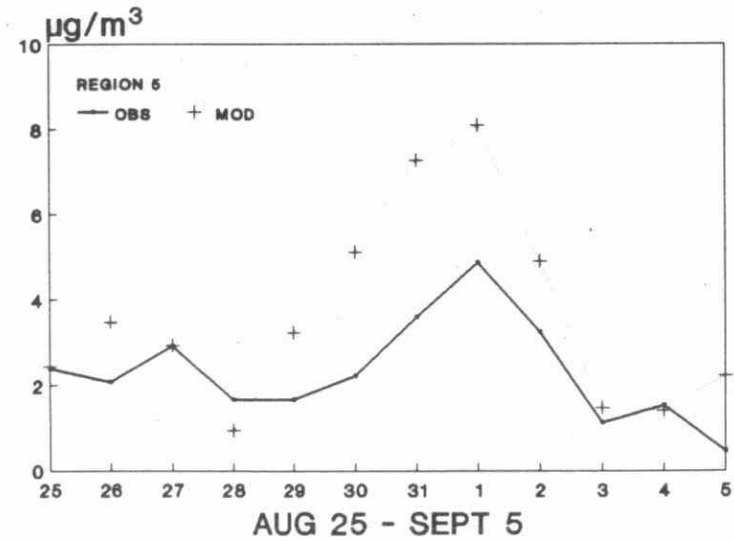
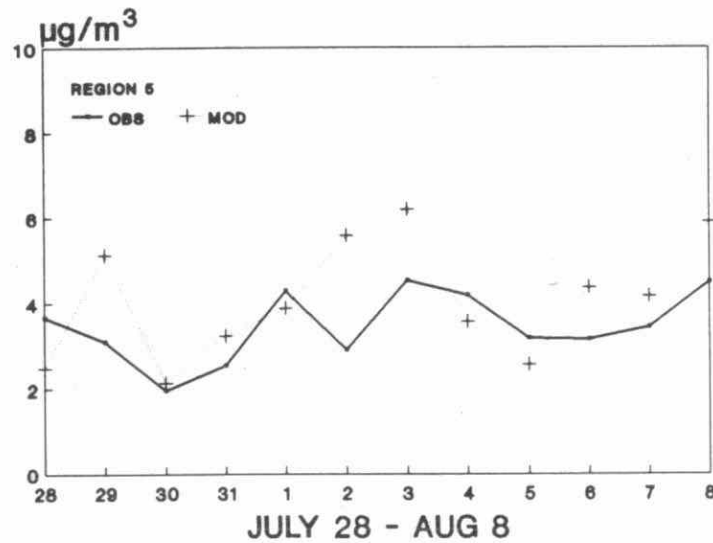
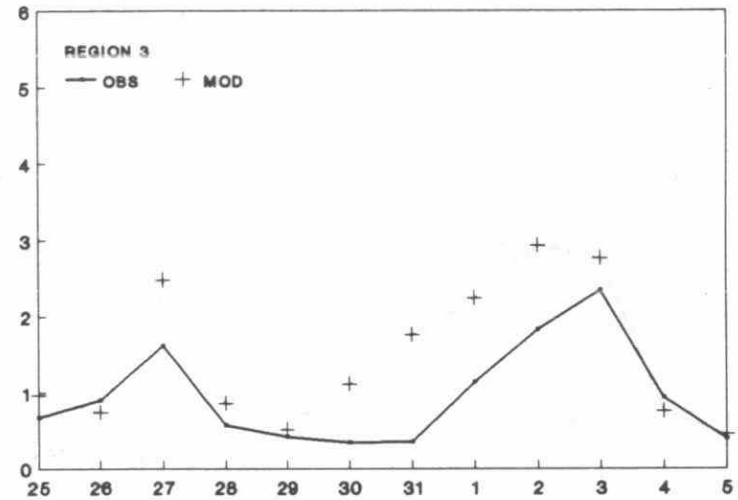
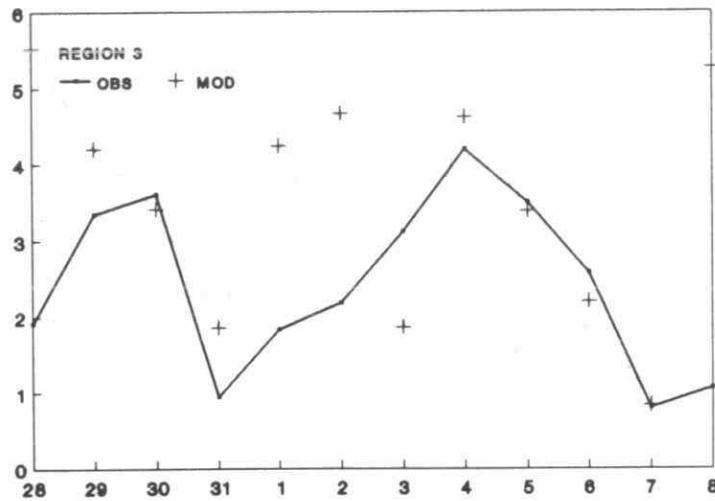


Fig. 3.3.29 Time series plots of averaged concentrations of observed and predicted nitrate concentration ($\mu\text{g}/\text{m}^3$) for Regions 3 and 5 during Periods 1 and 2.

defined peaks and the model captures both for the two regions though there is a phase lag of approximately two days in the second modelled peak. Since nitrate is readily scavenged by precipitation, the fluctuations can be interpreted as responses to precipitation, gas-phase conversion and transport. The trends of the first period indicate complex meteorology and subgrid scale precipitation which the model input data and grid resolution have been unable to capture.

The modelled vs. observed comparison plot for nitrate in precipitation is given in Figure 3.3.30 for Periods 1 and 2. For both periods, the nitrate in precipitation is underpredicted. The overall underprediction during both periods is similar: approximately 25 per cent for Period 1 and 20 per cent for Period 2. The average measured concentration for Period 1 is almost twice as high as that for Period 2 ($3.07 \mu\text{g/l}$ vs. $1.58 \mu\text{g/l}$). Like the $\text{SO}_4^{=}$ concentration in precipitation, there is considerable scatter during both periods resulting in R^2 correlation coefficient of 0.02 and 0.1 for Periods 1 and 2. With such a low R^2 correlation, regression and best fit line through origin analyses are of little significance.

The explanations of the scatter given for $\text{SO}_4^{=}$ concentration in precipitation also apply here.

Hourly observed and predicted ozone data have been plotted at three sites for Period 1: (16,18) in southern Ontario representing a heavy emissions of NO_x area; (13,16) in northern Michigan representing a semi-remote site; (23,19) in Maine representing a remote site. For Period 2, grids (16,18), (14,14) and (23,19) are given. Grid (14,14) is a site in Ohio which also represents a heavy emissions area. These plots are given in Figure 3.3.31. For grid (16,18), measurements at two sites from the Ontario Ministry of the Environment network are given. At North York West, which is part of Metro Toronto, the measured ozone level is, during most of the time, lower than model prediction. At night, this site frequently measured zero ozone concentration despite the fact that a major high ozone episode was experienced during the first few days of August. This is due to ozone scavenging by NO after photo-chemical reactions have been shut off after sunset. The other site, Stouffville, which is about thirty kilometres north of Metro Toronto, shows diurnal fluctuations in the measurements which are, during most of the period, higher than the model predictions. The discrepancy between the two sites is significant. This underlines the difficulty in model evaluation when subgrid scale variability is large. For this particular comparison, the measurements at Stouffville should be more representative of the region covered by the model grid cell. Consequently, the model captures the fluctuations but underpredicts.

For grid (13,16), during Period 1, the model agrees with the O_3 measurements both in magnitude and trend (fluctuations) for the first half of the period and overpredicts subsequently. The remote site (23,19) shows that the peaks of the concentrations are captured well except for August 4-6, 1988 when some 25-35 per cent underpredictions in the peak magnitudes are seen. The overall performance of this comparison is better than the preceding two.

For Period 2, the comparison at (16,18) is similar to what was found for Period 1: the model underpredicts the ozone peaks and captures the time trends. The Ohio site (14,14) which is also in a heavy emissions area also shows consistent underprediction while capturing the time trends. For (23,19), the remote site in Maine, the model overpredicts all but one peak during the period.

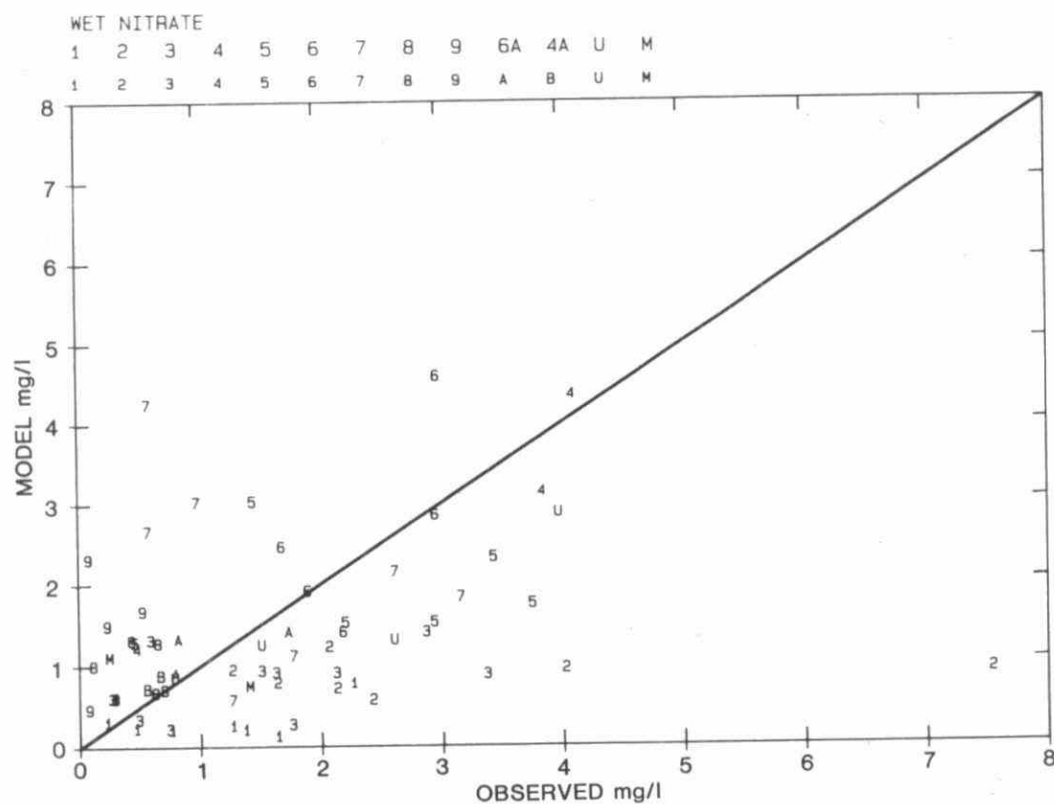
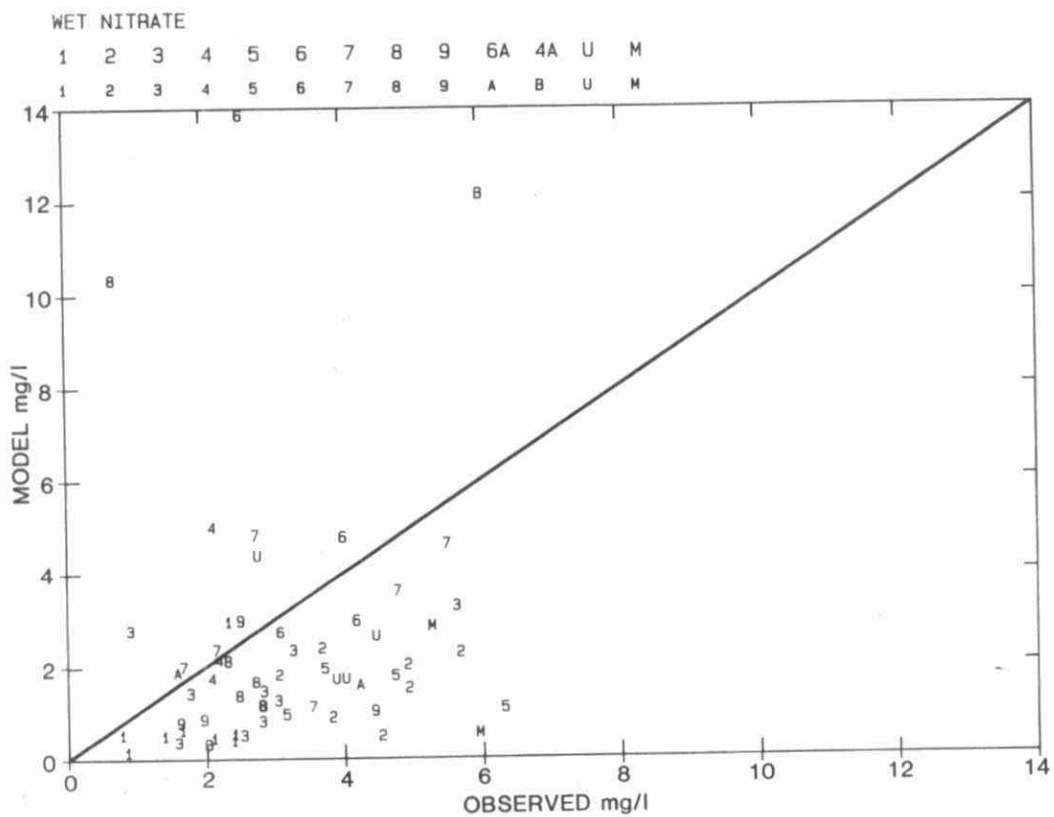


Fig. 3.3.30 Model predictions vs. observed concentrations in precipitation of total nitrate (mg/l) during July 28 - August 8 and August 25 - September 5, 1988.
Numbers refer to the regions shown in Fig. 3.3.19

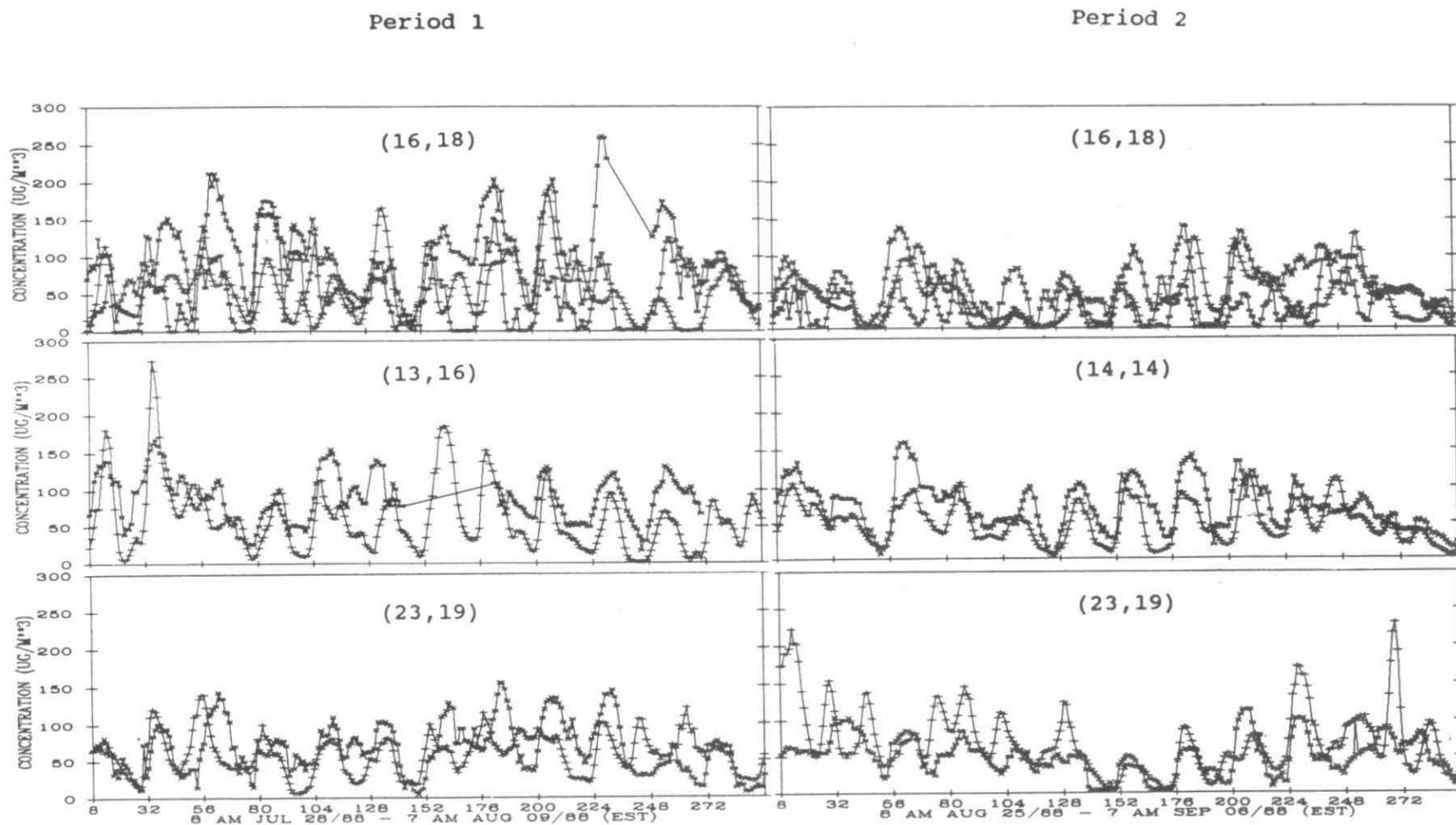


Fig. 3.3.31 Model predictions (dashes) vs. observed ozone concentrations (x's) at selected sites and model grid points in Ontario (16,18), Michigan (13,13) and Maine (23,19) for Period 1 (July 28 - August 8) and Period 2 (August 25 - September 6).

Interpretation of ADOM's Results

Eight species from the model have been evaluated. They are the ground level ambient concentrations of SO_2 , $\text{SO}_4^{=}$, total sulphur (SO_2 and particulate $\text{SO}_4^{=}$), NO_2 , NO_3^- and O_3 , and concentrations of $\text{SO}_4^{=}$ and NO_3^- in precipitation. The performance of these species is as follows:

Ground level SO_2 :	Mean overprediction by 10 to 30 per cent with higher overprediction at the low end. Model explains about 55 percent of the variance.
Ground level $\text{SO}_4^{=}$:	Mean underprediction of 40 to 60 per cent with higher underprediction at the low end. Model explains between 65 and 85 per cent of the variance.
Ground level Total Sulphur:	Mean modelled concentration is within 8 per cent of the observed mean.
$\text{SO}_4^{=}$ concentration in precipitation:	Mean precipitation weighted model concentration agrees to within 10 per cent of observed concentration. Model explains less than 16 per cent of the observed variance.
Ground Level NO_2 :	Mean underprediction by 5 to 20 per cent. Model explains between 5 to 47 per cent of the observed variance.
Ground level NO_3^- :	Mean underprediction by less than 10 per cent. The model explains about 50 per cent of the variance.
NO_3^- concentration in precipitation:	Mean underprediction by 20 to 25 per cent. Model explains less than 10 per cent of the observed variance.
Ground level O_3 :	Underpredicting the peaks in heavy emissions areas and reproducing the magnitude of peaks in remote areas.

The large scatter associated with concentrations in precipitation is largely a result of a basic mismatch of spatial representation. Unless a new approach in handling subgrid scale precipitation is developed or the period of averaging is increased or the measurement site density within each grid cell significantly increased thereby capturing the grid cell average, there is very little that can be done to improve the comparison results.

Given the large uncertainty in the measurements of the air concentrations of the nitrogen species, the present run shows that ADOM performs reasonably well for the nitrogen

species (especially for Period 2). A sensitivity run which was made necessary by an error (see #3 below) also shows that nitrate in air almost responds linearly to a change in NO emissions.

Various explanations have been put forward to explain the SO_2 and $\text{SO}_4^{=}$ in air discrepancy. To start, it is observed that the mean total sulphur concentration and mean sulphate concentration in precipitation have very little bias. This suggests, but does not prove, that the amount of sulphur in the domain is reasonable. Thus, the question revolves around the conversion of SO_2 to $\text{SO}_4^{=}$. The following possibilities have been put forward:

1. **Missing non-precipitation clouds which can be a major mechanism in $\text{SO}_4^{=}$ conversion.** However, sensitivity runs show that the effect in incorporating non-precipitating cloud is not unidirectional on ground level concentrations since non-precipitation clouds also include cloud vertical transport.
2. **Ground level $\text{SO}_4^{=}$ measurement data contaminated by fog.** The extent of widespread fog and monitor design have been investigated and found that fog contamination is not a potential cause of the discrepancy.
3. **The NO input to the model is incorrect.** Since both nitrogen and sulphur species compete for oxidants in gas-phase reactions, too much NO input would reduce the oxidant concentrations thus slowing SO_2 to $\text{SO}_4^{=}$ conversion. This possibility has actually been explored and led to the discovery of an error in the NO emissions. (NO about 30 per cent too high). However, with the problem corrected (the present run), the nitrogen species performance improved, but the $\text{SO}_4^{=}$ performance is not significantly affected.
4. **The oxidant level is too low.** It has already been pointed out that the ozone peak concentrations are underpredicted in heavy emissions areas that are not dominated by local NO_x emissions. This will lead to underproduction of OH radicals leading to slow conversion of SO_2 to $\text{SO}_4^{=}$.
5. **Inaccurate reaction rate constant between SO_2 and OH.** The previous possibility (#4) is predicated on a correct reaction rate. Since both ADOM and RADM behave similarly with regard to SO_2 and $\text{SO}_4^{=}$ (preliminary results conveyed by R. Dennis (U.S.EPA) and J. Chang (SUNY)), it seems that one mechanism common to both, thus producing similar results, would be the reaction rate constant. An increase in the reaction rate constant would convert SO_2 to $\text{SO}_4^{=}$ faster in both ADOM and RADM. On the other hand, this rate constant has been studied extensively and the value used in the current modes is a consensus reached among experts. Thus the value should be accurate.
6. **Missing a major gas-phase mechanism.** That model results have been used to diagnose parts of the source-receptor relationship is not new. The latest is actually in locating the problem with the NO emissions (see #3). It may be possible that a not-so-well-understood mechanism like $\text{SO}_2\text{-H}_2\text{O}_2$ is an important pathway for SO_2 to $\text{SO}_4^{=}$ conversion.

The last three and other possibilities will be pursued further.

3.3.5.g PRELIMINARY COMPARISON OF LINEAR AND COMPREHENSIVE MODELS

The question is now asked: Are comprehensive models better than simple linear models? To answer this, the Ontario Ministry of the Environment's (OME) linear Lagrangian model was run using the wind, precipitation and total emissions data that drove ADOM for the EMEFS period. The SO_2 ground level concentration, the $\text{SO}_4^{=}$ ground level concentration and the $\text{SO}_4^{=}$ concentration in precipitation predicted by the linear Lagrangian model are given in Figures 3.3.32 to 3.3.34. Concentrations of SO_2 in air are overpredicted by approximately 110 per cent (best fit line forced through the origin has a slope of 2.1) while the $\text{SO}_4^{=}$ concentrations in air are scattered about the 1:1 line. The best fit line forced through the origin for the $\text{SO}_4^{=}$ in precipitation has a slope of about 0.87, indicating a 10-15 per cent underprediction.

Linear Lagrangian models are usually simple enough that some parametric values can be adjusted to alter performance. For the OME Lagrangian model, the parameters that will affect model performance are: mixing height, conversion rate of SO_2 to $\text{SO}_4^{=}$, wet scavenging coefficients and dry deposition velocities.

Adjusting the mixing height in the OME Lagrangian model will affect all the species by changing the volume over which the species spread. For this run, a daily average mixing height of 800 m corresponding to fall conditions was used.

The conversion rate of SO_2 to $\text{SO}_4^{=}$ will change the ratio of SO_2 to $\text{SO}_4^{=}$ with distance away from the source. A higher conversion rate would see a greater decrease in the ratio of $\text{SO}_2/\text{SO}_4^{=}$ with distance away from the source and vice versa. The spatial pattern of both species will be affected.

The scavenging coefficient used in this model for $\text{SO}_4^{=}$ ($3 \times 10^{-4}/\text{s}$) is one order of magnitude higher than that for SO_2 . The coefficient for each species can be adjusted independently. If the SO_2 scavenging coefficient is adjusted, it will of course affect the amount of SO_2 available for conversion to $\text{SO}_4^{=}$ and the SO_2 spatial distribution. Though it appears from the relative magnitude of the scavenging coefficients of SO_2 and $\text{SO}_4^{=}$ that the same percentage change to the two coefficients would affect $\text{SO}_4^{=}$ more, the actual pattern is more complicated than that. During heavy precipitation, SO_2 and $\text{SO}_4^{=}$ can be scavenged out rapidly leaving insignificant amounts for subsequent scavenging. In this case, the amount scavenged is relatively insensitive to the values of the scavenging coefficients.

The dry deposition velocity used in this model is 5 mm/s for SO_2 and 0.5 mm/s for $\text{SO}_4^{=}$. Consequently, a change in the SO_2 dry deposition velocity would affect SO_2 directly. However, $\text{SO}_4^{=}$ would also feel the effect of such a change in SO_2 through SO_2 to $\text{SO}_4^{=}$ conversion. Thus, both SO_2 and $\text{SO}_4^{=}$ are affected.

The above discussion points up possibilities to improve the linear Lagrangian model performance though it would not be a straight-forward effort. Since a given parameter can affect SO_2 and $\text{SO}_4^{=}$ concentrations, several parameters must be changed at the same time to bring about a simultaneous improvement in air and precipitation concentrations.

Given the biases seen in the Lagrangian model concentrations, the following parameter adjustments could be considered:

- (1) Increase the mixed layer height and thus lower the SO_2 and $\text{SO}_4^{=}$ air concentrations.
- (2) Increase the conversion rate of SO_2 to $\text{SO}_4^{=}$ to reduce the positive bias of SO_2 in air and any negative bias of $\text{SO}_4^{=}$ in air produced by increasing the mixed layer height.
- (3) Adjust the dry deposition velocities and wet scavenging rates to tune the model to match the data further.

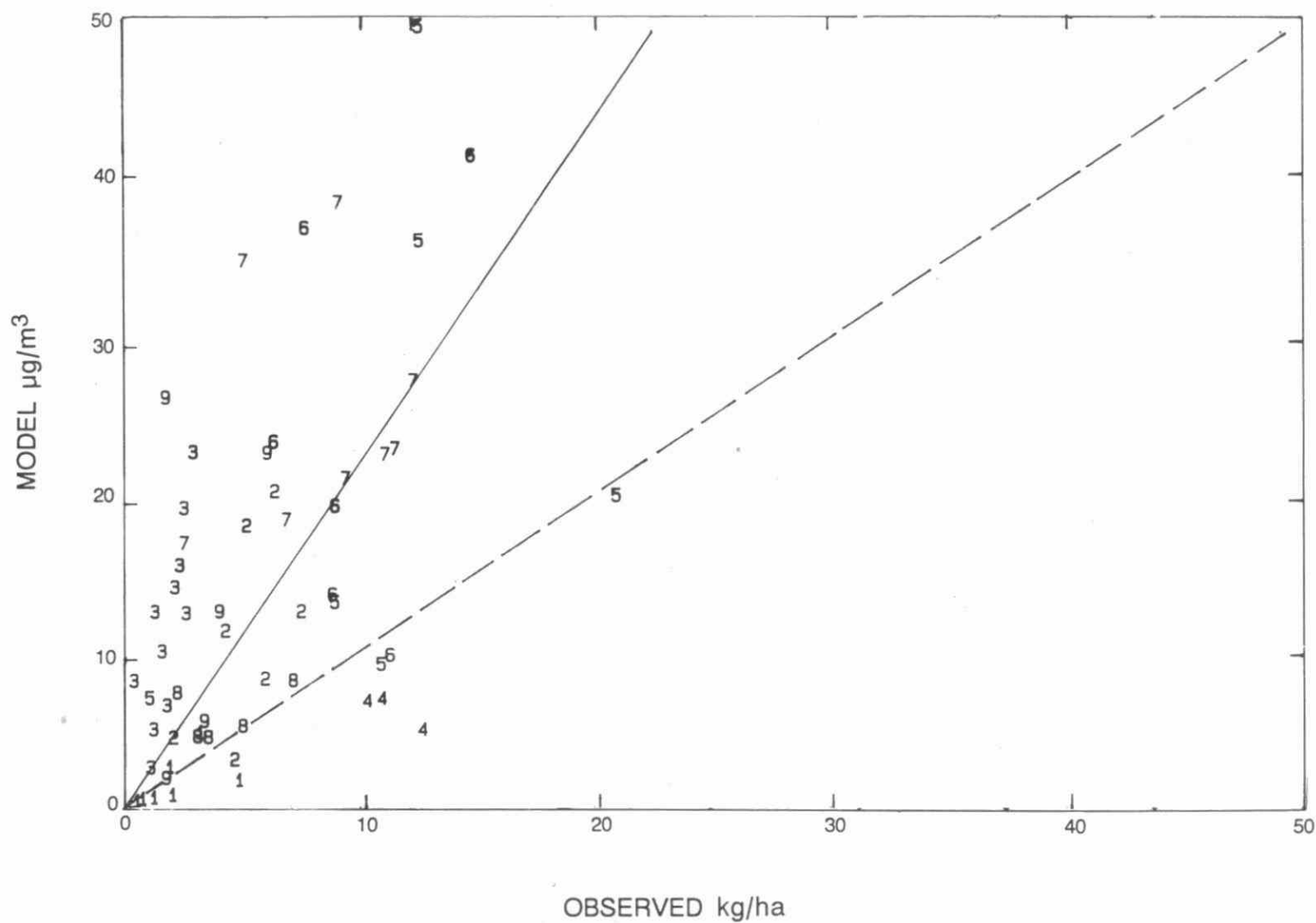
The question is whether or not a linear Lagrangian model designed to output SO_2 and $\text{SO}_4^{=}$ in air and $\text{SO}_4^{=}$ wet deposition with small biases (after tuning) is a better model than a comprehensive model? This question can have two parts: (1) Is the linear Lagrangian model, or for that matter, all linear Lagrangian models, better performing models? and (2) is the linear Lagrangian model a better scientific tool?

Since the Lagrangian model results can only be compared for 3 species (SO_2 and $\text{SO}_4^{=}$ in air and $\text{SO}_4^{=}$ in wet deposition), it is possible to produce good results at the expense of poor performance in dry deposition or in the vertical distribution of the species. For example, increasing the boundary layer height required to reduce SO_2 air concentrations will result in more SO_2 at higher levels. Also, any set of tuned parameters would be specific to the current distribution and magnitude of sources. Good model performance at ground level for the species examined could be limited to these specific conditions. Also, as can be seen by comparing the performance of the comprehensive and linear models (e.g. Figure 3.3.20 with Figure 3.3.32, Figure 3.3.21 with Figure 3.3.33), the comprehensive model shows less scatter than the linear model. It has been noted that the OME linear Lagrangian model produces a smoother field (Misra et al., 1989) than the comprehensive model. Thus, the comprehensive model has better resolution than linear models.

The second question on which type of tool is the better scientific model can be answered easily. In order to make the linear Lagrangian model perform better on the three species examined, the parametric values will be stressed to the extreme and more importantly, without any justification other than to make the results look good. This is difficult to defend scientifically. The other aspect of a good scientific model is its ability to address questions and to respond to different situations (i.e. different source mixes and locations). A model with limited physics and chemistry tuned to present conditions is not as useful for scientific purposes.

ADOM has been used successfully as a diagnostic tool in the case of the NO emissions. What allowed ADOM to be used in this way is the confidence that modellers have in the model, having incorporated what is currently known about the processes in the long-range transport of acidic precipitation. In the process of trying to explain the $\text{SO}_4^{=}$ in air underprediction in both ADOM and RADM, some processes which so far have been neglected or are still unknown may be found to be important, thus enhancing our understanding. In this way, comprehensive models can actually make contributions to the science of acidic precipitation.

In all, the performance and scientific utility of linear models are limited by their formulation and inherent assumptions. On the other hand, comprehensive models provide a framework for future improvements and can give the right answer for the correct reasons.

AIR SO₂, 8/28-9/28, OME LAGRANGIAN MODEL

AIR SO₄, OME LAGRANGIAN MODEL

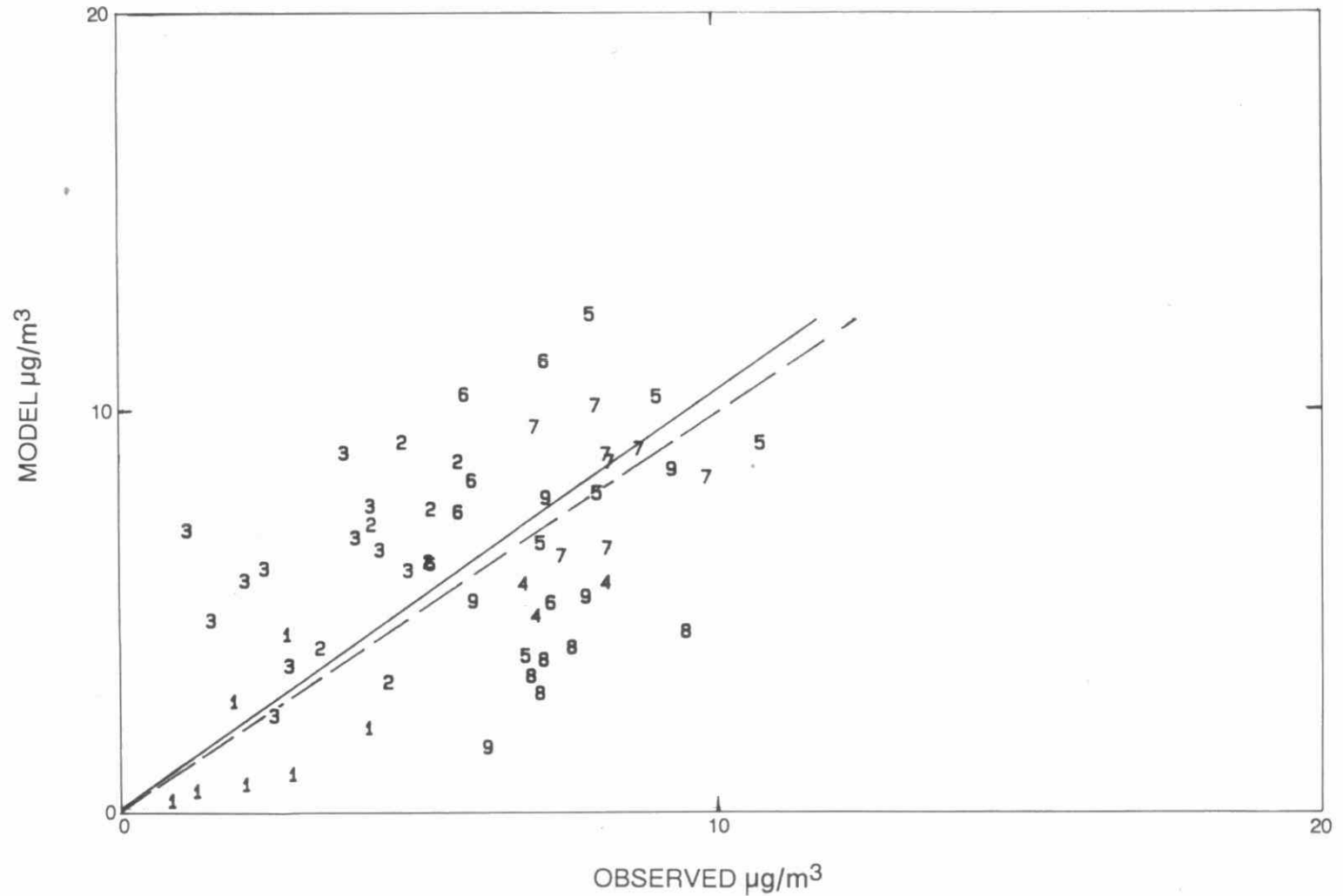


Fig. 3.3.33 Ontario Ministry of the Environment Lagrangian Model predictions for the EMEFS period - SO₄ ($\mu\text{g}/\text{m}^3$).
Numbers refer to the regions shown in Fig. 3.3.19

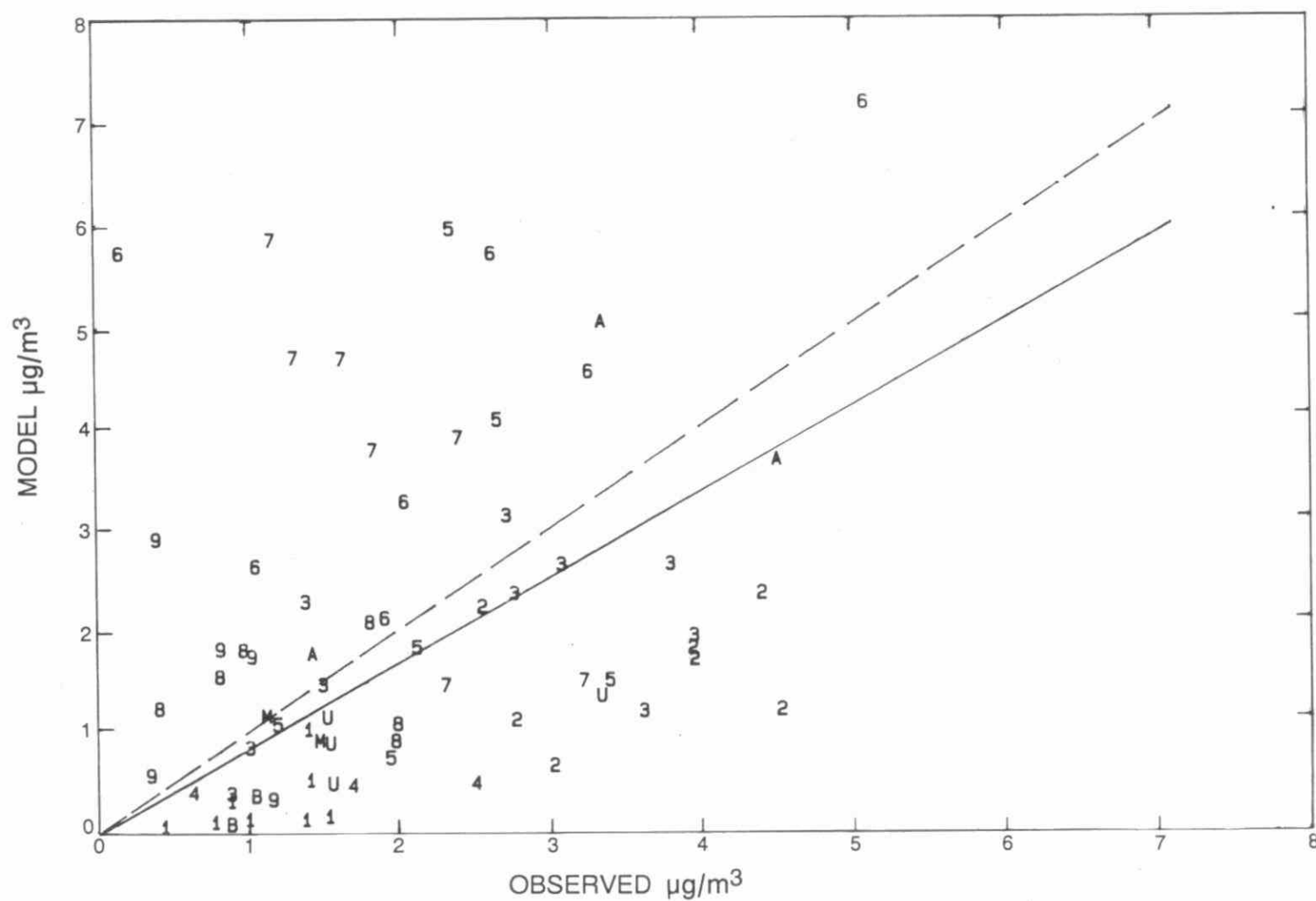
WET SO₄, OME LAGRANGIAN MODEL

Fig. 3.3.34 Ontario Ministry of the Environment Lagrangian Model predictions for the EMEFS period - SO₄²⁻ in precipitation (mg/l). Numbers refer to the regions shown in Fig. 3.3.19

3.3.6 DISCUSSION AND CONCLUSIONS

Mathematical models provide the most efficient means to establish source-receptor relationships. However, as shown in this chapter, the model results are not free of uncertainty. Thus interpretation of source-receptor relationships has to be done while keeping the model uncertainty in perspective. In this respect, it is the relative impacts of a change from a baseline case of the emission scenarios, which are more meaningful than the absolute model outputs.

The uncertainty of model results arises from many contributing factors (Demerjian, 1985, 1986). First, the model is formulated using various assumptions which give the possibility of introducing biases in model results. Second, the input parameters of a model may be incompletely known. Third, the number of variables used to formulate the model are usually much smaller than the number required to formulate the "perfect" model. Thus, the missing variables can assume infinitely many combinations for each set of prescribed variables introducing uncertainty in model results. Fourth, there is incompatibility in the spatial averaging of the model outputs and the observed data. For instance, if one makes the logical assumption that the appropriate spatial averaging of the current models' outputs is the same as the spatial averaging of input meteorological data, then on the average in North America, the model outputs are compatible with a spatial average over a grid size of approximately 100 x 100 km. Observations, on the other hand, are available mostly for one or two locations within this grid size. Finally, there is uncertainty in the inputs (meteorological, geophysical) and the observed data themselves.

An examination of the model uncertainty can be made by comparing the model outputs with observations. Most of the linear models can explain about 50 percent of the variance in observations of wet sulphur deposition (i.e. the R^2 value of the regression between observations and model outputs is approximately 0.5). Thus 50 percent of the unexplained variance can be attributed to model and data uncertainties. The paper by Fay et al. (1985) provides a clue to the origin of most of this uncertainty. When actual precipitation data were used with model generated air concentrations of sulphur, Fay et al. (1985) were able to explain as high as 80 percent of the variability in observed sulphur deposition. This indicates that the variability of precipitation amounts is responsible for most of the observed data variability and unless the models accurately include precipitation amounts in the input data sets, model results are bound to be uncertain by the corresponding amounts. Experiments with more comprehensive Eulerian models corroborate this conclusion. A significant portion of the lack of comparison between model outputs and observations can be attributed to errors in precipitation amounts. Ellenton et al. (1988) carried out model runs for 4 years using a linear Lagrangian model, where the emissions of SO_2 were fixed at their 1980 values and the meteorological data were varied between the years. They concluded that most of the variability of the observations could be attributed to meteorological variability. Streets et al. (1985) and Fernau and Samson (1986) reached similar conclusions using different models.

Bloxam et al. (1986) varied the scavenging coefficient in a Lagrangian model randomly and concluded that random space and time variations in this parameter contribute at most 20 percent to the uncertainty in model results. In the MOI exercise, several different models using very different parameterizations were tested with observations. They all showed similar skills in explaining observations. In a subsequent more detailed comparison (ISDME), the input data for these models were kept nearly the same. Once again, the relative skills of these models were comparable.

The above arguments point to the fact that errors in meteorological inputs and the missing variables in a model contribute the most to the model uncertainty. Although our discussion has relied heavily on the linear model performance, the conclusion can be extended to the more comprehensive Eulerian models as well.

In using a model to study the impact of future emission scenarios the meteorology is kept fixed for a "typical" year. Thus, even if the model were "perfect", the scenario results will be uncertain for reasons discussed above. Thus, the absolute predictions from a model for a given emission scenario are less useful to the decision making process than the relative impacts between the emission scenarios. In this respect, all linear models predict that a uniform percentage change in the current emission level will bring about a similar percentage change in the annual deposition of sulphur in North America (except for background deposition due to sources not included in the inventory). These linear models can differ in their predicted effects when emission reductions are targeted to specific source areas. However, the percentage contributions of source areas to receptors are predicted to be approximately the same for all models.

Thus, although model precision (uncertainty) is useful to understand model performance, it is not very useful in emission control scenario studies. However, the skill of the model in predicting the correct trend in the deposition of sulphur as a function of emission levels is fundamentally the most important factor in the decision making process. For instance, one can visualize three different relationships between emission levels of SO_2 and the wet deposition of sulphur. Depending on the degree of non-linearity that can be expected in the atmospheric processes, the wet deposition of sulphur can remain unchanged for a significant range of reduction of SO_2 emissions, it can reduce with emissions at a slower rate than the emissions reductions, or it can increase with emissions reduction. All available information suggest that the second of the above mentioned trends between SO_2 emissions and wet deposition of sulphur is most realistic. The first trend; i.e. no change in the wet deposition of sulphur for a change in SO_2 emissions, is possible but rarely observed. The third trend cannot be justified for sulphur species on the grounds of mass conservation.

Experimental data and experiments with the complex Eulerian models suggest that if meteorology is kept fixed, a decrease in the emission rate is always accompanied by a decrease in the wet deposition of sulphur everywhere in North America. The decrease, however, is less than the fractional decrease in emissions. For instance, an experiment with the Eulerian model, ADOM, for the month, April 1981, suggests that a 50 percent uniform reduction of SO_2 emissions in North America will produce a 30-40 percent change in the wet deposition of sulphur within the same domain. The non-linearity of wet SO_4 deposition in response to 50% SO_2 emissions cut over a year or more is not expected to exceed this magnitude. This is the consensus reached among scientists at the NAPAP International Conference held at the Hilton Head Island, South Carolina in February 1990 (Venkatram et al., 1989). The relationship between SO_2 emissions and wet deposition of sulphur is, therefore, non-linear. However, the degree of non-linearity, when model precision and uncertainty in observations are taken into account, is not so severe as to negate the conclusions of the linear models to-date especially when total (dry and wet) deposition is considered. Further comparison of the Eulerian models with the full data set from EMEFS is expected to shed more light on this issue.

In summary, the following statements can be supported from the modelling exercises to date:

1. A reduction of SO₂ emission by 50 percent from the current emission level will reduce the wet deposition of sulphur in springtime over southern Canada and northeastern U.S. by 30-40 percent. There is no evidence that wet deposition of sulphur will either remain unchanged or increase for a decrease in SO₂ emissions. When the total deposition of sulphur is considered, the non-linearity is mitigated by the almost linear response of dry deposition to emissions reduction.
2. Emission reductions targeted to a few key states in the U.S. are likely to be more beneficial than an across-the-board reduction of SO₂ emissions.
3. Uncertainty in the outputs of most models is within a factor of two, where the significant contributing factors to this uncertainty are input data uncertainty and missing variables in the model.
4. Most of the variability in observed data on wet deposition of sulphur can be attributed to meteorological variability. Thus one cannot expect to see a reduction in wet deposition of sulphur immediately following a reduction in SO₂ emission levels. However, in the long term, wet deposition of sulphur would obviously be expected to show a decreasing trend.

APPENDICES

APPENDIX 3A

**THE BEST ESTIMATE OF TOTAL DEPOSITION THAT IS
DRY DEPOSITION IN EASTERN CANADA**

LIST OF FIGURES

Figure#		Page#
3A-1	Best estimate of the fraction of total sulphur deposition that is dry deposition (%).	3-201
3A-2	Best estimate of the fraction of total NO_3^- deposition excluding NO_2 dry deposition that is dry (%).	3-202

APPENDIX 3A

THE BEST ESTIMATE OF TOTAL DEPOSITION THAT IS DRY DEPOSITION IN EASTERN CANADA

Deposition takes place via three processes: removal by rain and snow (wet deposition), direct uptake of particles and gases at the earth's surface (dry deposition) and fogwater deposition. In the following estimates, fogwater deposition is neglected even though in mountain top regions and along the east coast it may be a substantial fraction of the total (Barrie and Schemenauer, 1986).

Sulphur

In Figure 3A-1 are shown the estimates of the fraction of total deposition made up by dry deposition (FD) based on two data sets: the APIOS network data of Ontario Ministry of Environment for 1984 to 1986 and the APN network of Environment Canada for 1979 to 1982. Wet deposition is measured directly, while dry deposition is calculated from the product of an estimated dry deposition velocity for an area 100 km radius around the site and an observed monthly air concentration. The latter is comprised of a contribution for SO_2 gas and for $\text{SO}_4^{=}$ particulate matter. Dry deposition velocities are calculated using the scheme of Voldner et al. (1986) and are reported and discussed in Sirois and Barrie (1988).

The results indicate a range in FD from 8.5% to 37%. The results at Long Point are highest, because the area to which dry deposition was calculated (100 km radius around the site) was half covered by water, which is an effective sink for SO_2 gas. In general, FD is about 15%. Because of the uncertainty in estimation of dry deposition velocities, a significant spatial variation in the estimated FD in eastern Canada cannot be derived with any confidence at this time. This does not mean that there is no spatial variation, but just that the power of our observations and estimates is too weak to detect it. Nevertheless, it is fair to say that most of total deposition of sulphur in eastern Canada is wet deposition.

Nitrogen

There are three forms of nitrogen that are sufficiently soluble or surface reactive that they play a role in wet and dry deposition: particulate NO_3^- , gaseous HNO_3 and gaseous NO_2 . Since there are virtually no measurements of NO_2 , it is not included here in the estimate of dry deposition. Based on preliminary data, Sirois and Barrie (1988) estimate that the fraction of dry deposition made up of NO_2 is most probably in the range 35 to 88%. Thus, the estimates of FD that neglect NO_2 are a lower limit. They are shown for both networks in Figure 3A-2. Wet and dry deposition was calculated in a similar way as for that of sulphur.

There was a difference in the way that the dry deposition was estimated by the Ontario Ministry of the Environment (OME) and Environment Canada (AES). There are several explanations for this. OME assumed that all NO_3^- was in the form of HNO_3 , while AES calculated dry deposition for both HNO_3 and NO_3^- in particles. Since the deposition velocity for HNO_3 is much higher than that of NO_3^- particles, the OME estimates are higher, but this can account for only 20 to 30% difference because most dry deposition is in the form of HNO_3 . Another reason is that HNO_3 concentrations measured by OME are on average 30 to 40% higher than those determined by AES (personal communication

A. Wiebe, 1989). Furthermore, there are differences in the way deposition velocities are calculated. Thus, current information suggests two possibilities based (i) on OME estimates and (ii) on AES estimates. In the former, FD (excluding NO₂ contributions) is 40%; in the latter, it is 20%. With NO₂ contributing 50% more to dry deposition (as discussed above), this rises to 60% and 30%, respectively. This range likely is a realistic reflection of the uncertainty in the estimate of dry deposition of nitrates.

Summary

At the present time, the available data suggest that regional dry deposition of sulphur can be adequately estimated from the fairly detailed precipitation chemistry data in Canada by assuming that the fraction of total sulphur deposition made up by the dry component is 0.15. This number may not apply where there is a large local source of sulphur emissions, such as the smelters at Sudbury or Noranda. Better local estimates of dry deposition are possible if air concentrations are available. Since the fraction of the total deposition (in Canada) that is dry is relatively small, uncertainties in the dry contribution are not expected to markedly change the conclusions of aquatic and terrestrial effects work.

The uncertainty in the dry contribution due to nitrogen compounds is much greater, although it cannot be fully assessed at the present time due to lack of monitoring data, especially for NO₂. Unfortunately, for the nitrogen oxides, the dry contribution could be comparable to the wet contribution, based on the few available data.

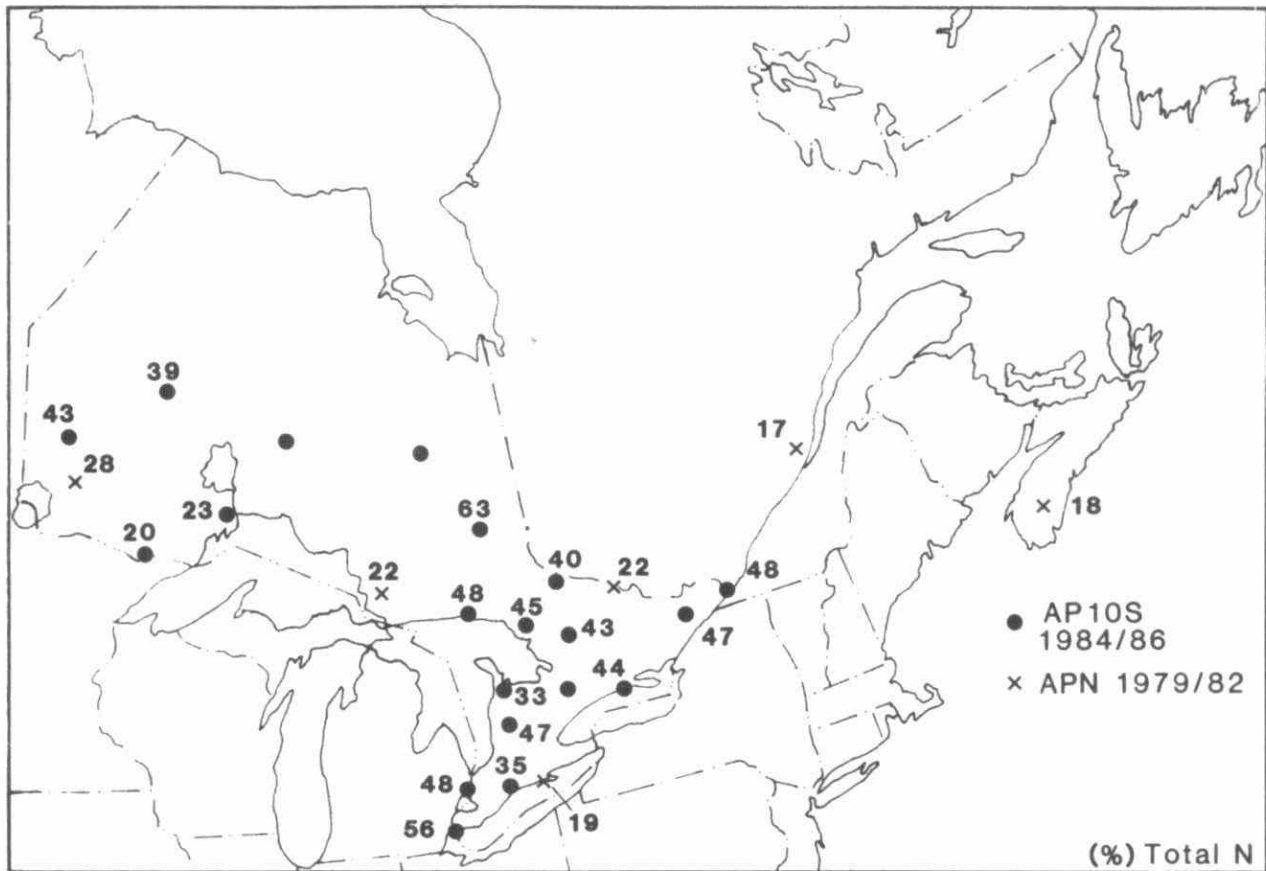


Fig. 3A-1 Best estimate of the fraction of total sulphur deposition that is dry deposition (%).

ERRATUM

Please note the Figures 3A-1 and 3A-2 have been reversed.

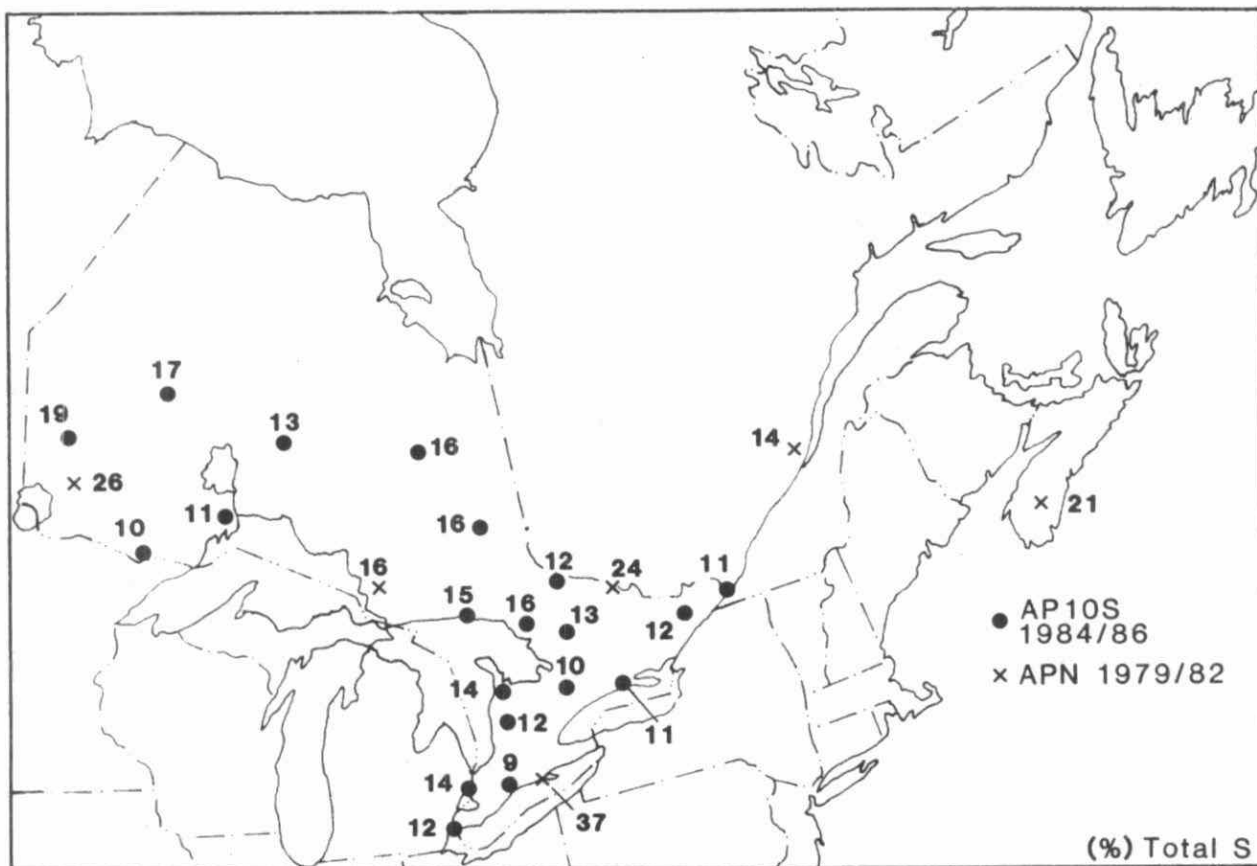


Fig. 3A-2 Best estimate of the fraction of total NO_3^- deposition excluding NO_2 dry deposition that is dry (%).

ERRATUM

Please note the Figures 3A-1 and 3A-2 have been reversed.

APPENDIX 3B

CONCENTRATION AND DEPOSITION PATTERNS

LIST OF FIGURES

Figure#		Page#
3B-1	Patterns of annual precipitation - weighted mean concentrations of $\text{SO}_4^{=}$ (mg/l): 1980-1983.	3-209
3B-2	Patterns of annual precipitation - weighted mean concentrations of $\text{SO}_4^{=}$ mg/l: 1984-1987.	3-210
3B-3	Patterns of annual wet deposition of $\text{SO}_4^{=}$ (kg/ha/yr): 1980-1983.	3-211
3B-4	Patterns of annual wet deposition of $\text{SO}_4^{=}$ (kg/ha/yr): 1984-1987.	3-212
3B-5	Patterns of annual precipitation - weighted mean concentrations of NO_3^{-} (mg/l): 1980-1983.	3-213
3B-6	Patterns of annual precipitation - weighted mean concentrations of NO_3^{-} (mg/l): 1984-1987.	3-214
3B-7	Patterns of annual wet deposition of NO_3^{-} (kg/ha/yr): 1980-1983.	3-215
3B-8	Patterns of annual wet deposition of NO_3^{-} (kg/ha/yr): 1984-1987.	3-216
3B-9	Patterns of annual mean pH distribution: 1980-1983.	3-217
3B-10	Patterns of annual mean pH distribution: 1984-1987.	3-218
3B-11	Patterns of annual precipitation - weighted mean H^{+} concentrations (mg/l): 1980-1983.	3-219
3B-12	Patterns of annual precipitation - weighted mean H^{+} concentrations (mg/l): 1984-1987.	3-220
3B-13	Patterns of annual wet deposition of H^{+} (kg/ha/yr): 1980-1983.	3-221
3B-14	Patterns of annual wet deposition of H^{+} (kg/ha/yr): 1984-1987.	3-222
3B-15	Patterns of annual precipitation-weighted mean concentrations of NH_4^{+} (mg/l): 1980-1983.	3-223
3B-16	Patterns of annual precipitation - weighted mean concentrations of NH_4^{+} (mg/l): 1984-1987.	3-224
3B-17	Patterns of annual wet deposition of NH_4^{+} (kg/ha/yr): 1980-1983.	3-225
3B-18	Patterns of annual wet deposition of NH_4^{+} (kg/ha/yr): 1984-1987.	3-226
3B-19	Patterns of annual precipitation-weighted mean concentrations of Ca^{+2} (mg/l): 1980-1983.	3-227
3B-20	Patterns of annual precipitation-weighted mean concentrations of Ca^{+2} (mg/l): 1984-1987.	3-228
3B-21	Patterns of annual wet deposition of Ca^{+2} (kg/ha/yr): 1980-1983.	3-229
3B-22	Patterns of annual wet deposition of Ca^{+2} (kg/ha/yr): 1984-1987.	3-230

LIST OF FIGURES (continued)

Figure#		Page#
3B-23	Patterns of annual precipitation-weighted mean concentrations of Mg^{+2} (mg/l): 1980-1983.	3-231
3B-24	Patterns of annual precipitation-weighted mean concentrations of Mg^{+2} (mg/l): 1984-1987.	3-232
3B-25	Patterns of annual wet deposition of Mg^{+2} (kg/ha/yr):1980-1983.	3-233
3B-26	Patterns of annual wet deposition of Mg^{+2} (kg/ha/yr):1984-1987.	3-234
3B-27	Patterns of annual precipitation-weighted mean concentrations of Cl^- (mg/l): 1980-1983.	3-235
3B-28	Patterns of annual precipitation-weighted mean concentrations of Cl^- (mg/l): 1984-1987.	3-236
3B-29	Patterns of annual wet deposition of Cl^- (kg/ha/yr)(1980-1983).	3-237
3B-30	Patterns of annual wet deposition of Cl^- (kg/ha/yr)(1984-1987).	3-238
3B-31	Patterns of annual precipitation-weighted mean concentrations of Na^+ (mg/l): 1980-1983.	3-239
3B-32	Patterns of annual precipitation-weighted mean concentrations of Na^+ (mg/l): 1984-1987.	3-240
3B-33	Patterns of annual wet deposition of Na^+ (kg/ha/yr):1980-1983.	3-241
3B-34	Patterns of annual wet deposition of Na^+ (kg/ha/yr):1984-1987.	3-242
3B-35	Patterns of annual precipitation-weighted mean concentrations of K^+ (mg/l): 1980-1983.	3-243
3B-36	Patterns of annual precipitation-weighted mean concentrations of K^+ (mg/l): 1984-1987.	3-244
3B-37	Patterns of annual wet deposition of K^+ (kg/ha/yr):1980-1983.	3-245
3B-38	Patterns of annual wet deposition of K^+ (kg/ha/yr):1984-1987.	3-246
3B-39	Patterns of total precipitation depth (cm):1980-1983.	3-247
3B-40	Patterns of total precipitation depth (cm):1984-1987.	3-248
3B-41	Six-year mean concentration and deposition patterns of $SO_4^{=}$ (1982-1987).	3-249
3B-42	Six-year mean pH distribution (1982-1987).	3-250
3B-43	Six-year mean concentration and deposition patterns of NH_4^+ (1982-1987).	3-251
3B-44	Six-year mean concentration and deposition patterns of Ca^{+2} (1982-1987).	3-252

LIST OF FIGURES (continued)

Figure#		Page#
3B-45	Six-year mean concentration and deposition patterns of Mg^{+2} (1982-1987).	3-253
3B-46	Six-year mean concentration and deposition patterns of Cl^- (1982-1987).	3-254
3B-47	Six-year mean concentration and deposition patterns of Na^+ (1982-1987).	3-255
3B-48	Six-year mean concentration and deposition patterns of K^+ (1982-1987).	3-256

APPENDIX 3B

CONCENTRATION AND DEPOSITION PATTERNS

(i) ANNUAL PATTERNS OF PRECIPITATION-WEIGHTED MEAN CONCENTRATION AND DEPOSITION (1980 - 1987)

This appendix contains maps showing the annual patterns of precipitation-weighted mean concentration and wet deposition for $\text{SO}_4^{=}$, NO_3^- , pH, H^+ , NH_4^+ , Ca^{++} , Mg^{++} , Cl^- , Na^+ , and K^+ . See chapter 3.2.2.b of the text for a description of the data, the interpolation program and the results.

The maps are shown in Figures 3B-1 to 3B-40.

(ii) SIX-YEAR AVERAGE PATTERNS OF PRECIPITATION-WEIGHTED MEAN CONCENTRATION AND DEPOSITION FOR THE YEARS 1982-87

Maps showing the six-year average (1982-87) patterns of precipitation-weighted mean concentration and wet deposition are presented for $\text{SO}_4^{=}$, pH (concentration only), NH_4^+ , Ca^{++} , Mg^{++} , Na^+ , Cl^- and K^+ . See text for a description of the data, the interpolation method, and the averaging process. The maps are shown in Figures 3B-41 to 3B-48.

A brief summary of the major characteristics of the concentration and deposition patterns is given below for each of the ions.

$\text{SO}_4^{=}$

The concentration and deposition patterns of $\text{SO}_4^{=}$ shown in Fig. 3B-41 are similar to those of excess $\text{SO}_4^{=}$ - except along the Atlantic seaboard. The differences reflect the fact that $\text{SO}_4^{=}$ was not corrected for the sea salt contribution of $\text{SO}_4^{=}$ (corrections ranged from 0 in the inland areas to as much as 21% at sites along the coastline). As a result, the patterns show higher concentration and deposition of $\text{SO}_4^{=}$ than excess $\text{SO}_4^{=}$ in the Atlantic provinces and states.

NH_4^+

High values of NH_4^+ concentration (>0.3 mg/l) and deposition (>4.0 kg/ha/yr) occurred in an area covering southern Manitoba, southern Ontario, southern Quebec, and portions of the US Great Plains and midwest (Fig. 3B-43). The primary land use in this area is agricultural, suggesting a strong influence of livestock and fertilizer on precipitation composition. This appears to be confirmed by the local concentration and deposition maxima (>0.5 mg/l and 4.0 kg/ha/yr, respectively) located in the intensive agricultural areas of southwestern Ontario and South Dakota, Nebraska and Iowa.

Ca^{++}

The Ca^{++} concentration and deposition patterns shown in Figure 3B-44 are strikingly similar to those of ammonium. Highest 6-year mean concentrations (> 0.2 mg/l) occurred in Manitoba, southern Ontario, the Great Plains and a number of midwest states. In fact, the 2 mg/l isopleth encompassed almost the same agricultural areas of eastern Canada and USA as the 0.3 mg/l NH_4^+ isopleth - a fact that undoubtedly reflects the

Canada and USA as the 0.3 mg/l NH_4^+ isopleth - a fact that undoubtedly reflects the strong influence of agriculturally-related soil material on precipitation chemistry. The deposition pattern of Ca^{++} displays two local maxima ($> 3 \text{ kg/ha/yr}$) - both in regions of intensive agricultural activity. One occurs in southwestern Ontario and the other in the Iowa, Kansas, Missouri area.

Mg^{++}

Maximum concentrations and deposition of Mg^{++} occurred along the Atlantic coast of both Canada and the USA and in the agricultural areas of southern Ontario and the American midwest (Figure 3B-45). The patterns reflect the strong influences of sea-salt magnesium (magnesium being the third largest elemental constituent of bulk seawater after Na^+ and Cl^- - Rahn, 1976) and agricultural activity (magnesium being a major constituent of soil dust).

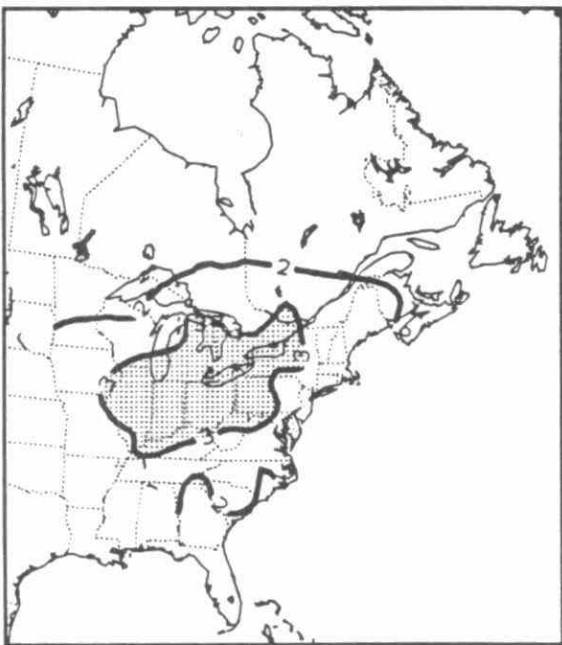
Na^+ and Cl^-

The spatial patterns of Cl^- and Na^+ (Figures 3B-46 and 3B-47) exhibit maximum concentrations and deposition along the Atlantic coast; this is followed by a steep decline to low values roughly 100 km inland. The patterns strongly reflect the influence of sea salt on coastal precipitation chemistry.

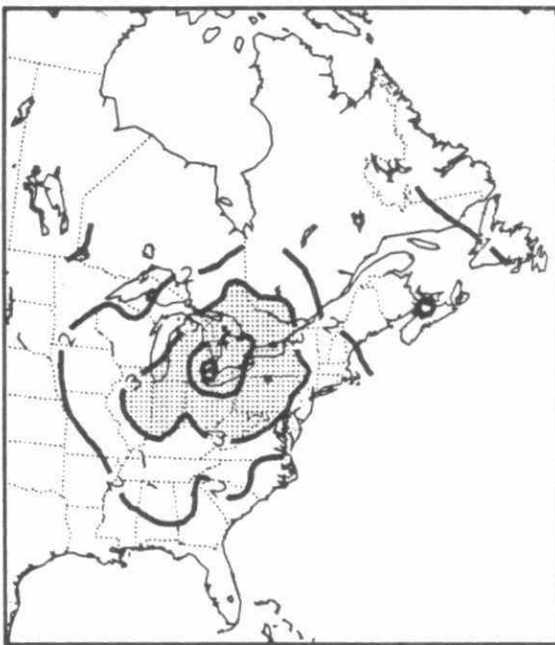
K^+

Concentration and deposition levels of K^+ are very low across most of eastern North America (Figure 3B-48). Highest values ($> 0.05 \text{ mg/l}$ and 0.6 kg/ha/yr) occur along the eastern seaboard, likely reflecting the influence of sea salt.

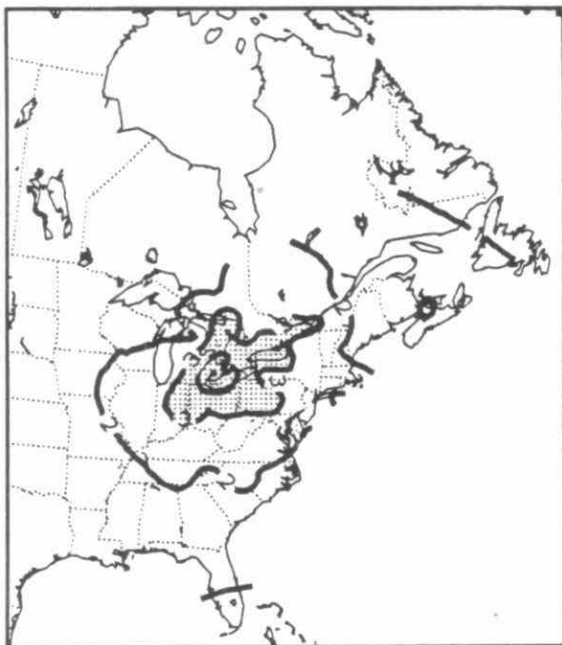
1980 ANNUAL MEAN SO₄ CONCENTRATION IN PRECIPITATION (MG/L)



1981 ANNUAL MEAN SO₄ CONCENTRATION IN PRECIPITATION (MG/L)



1982 ANNUAL MEAN SO₄ CONCENTRATION IN PRECIPITATION (MG/L)



1983 ANNUAL MEAN SO₄ CONCENTRATION IN PRECIPITATION (MG/L)

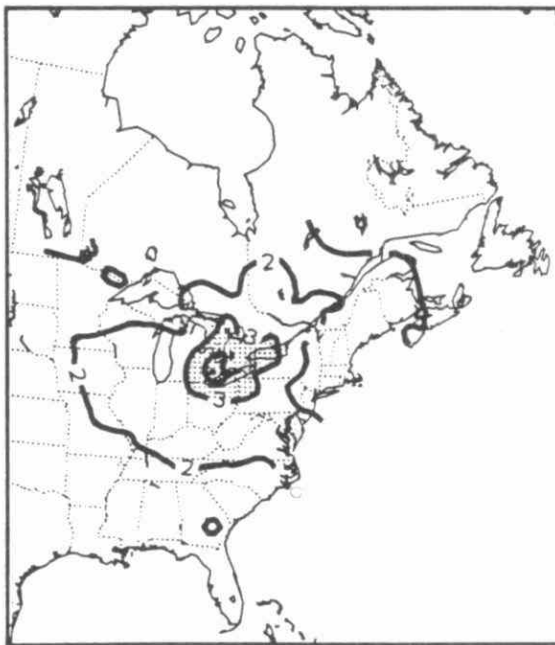
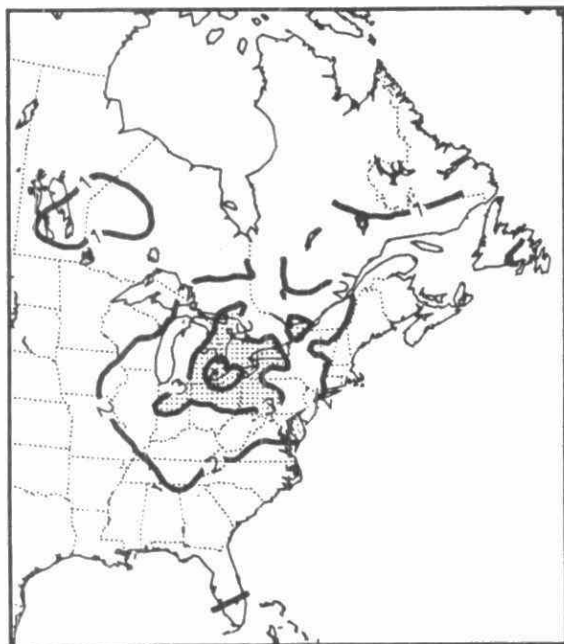
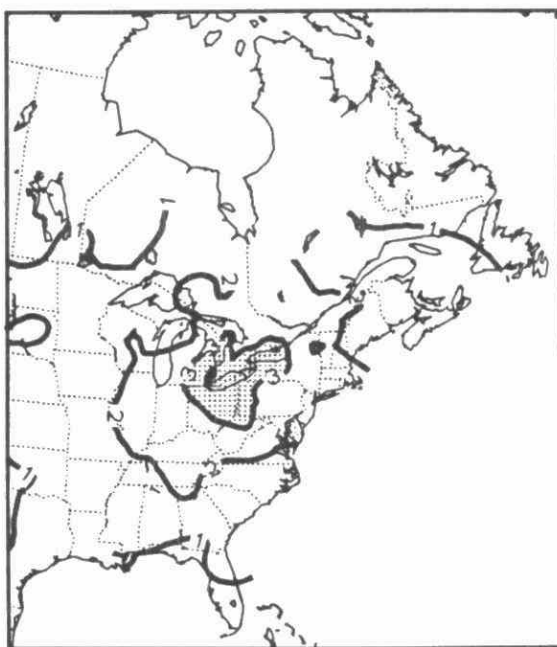


Fig. 3B-1 Patterns of annual precipitation - weighted mean concentrations of SO₄⁼ (mg/l): 1980-1983.

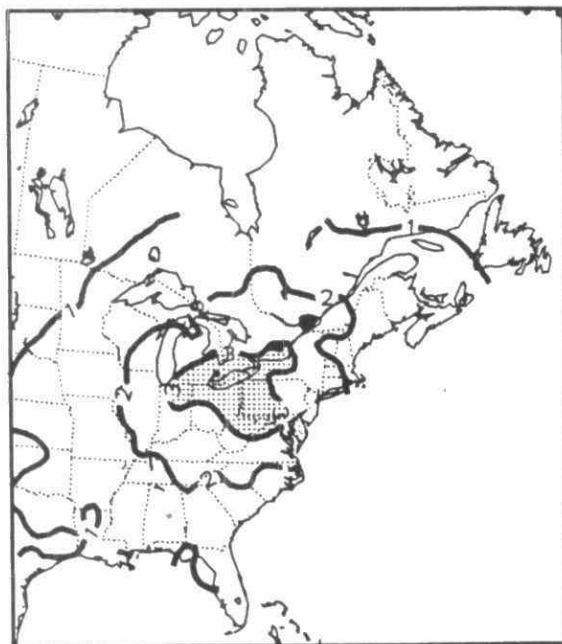
1984 ANNUAL MEAN SO₄ CONCENTRATION IN PRECIPITATION (MG/L)



1985 ANNUAL MEAN SO₄ CONCENTRATION IN PRECIPITATION (MG/L)



1986 ANNUAL MEAN SO₄ CONCENTRATION IN PRECIPITATION (MG/L)



1987 ANNUAL MEAN SO₄ CONCENTRATION IN PRECIPITATION (MG/L)

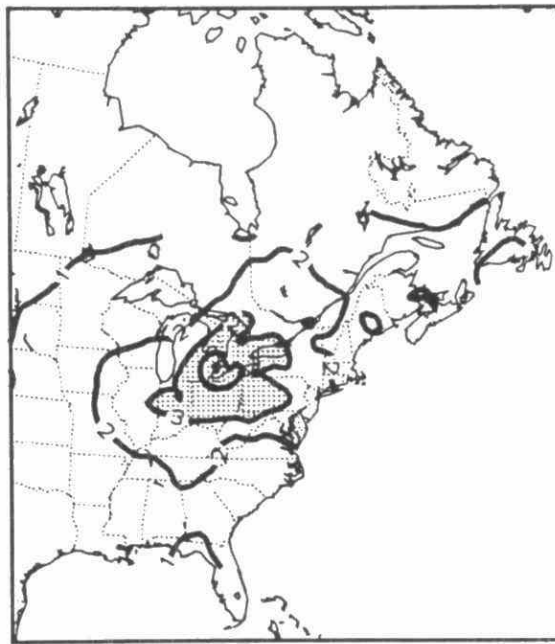
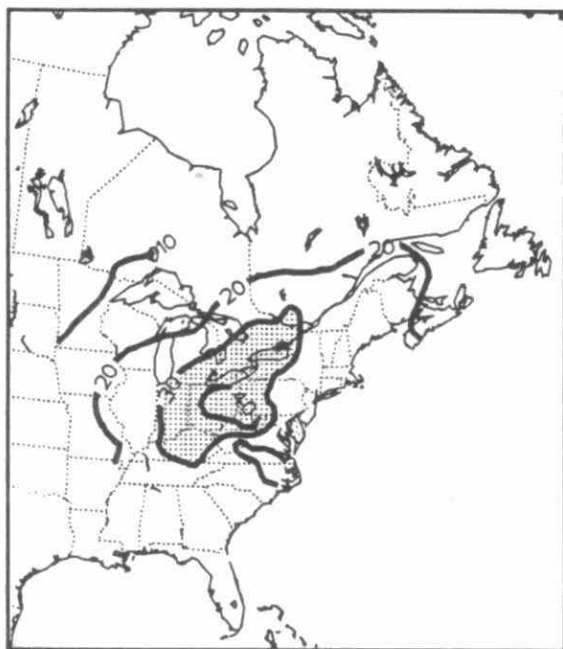
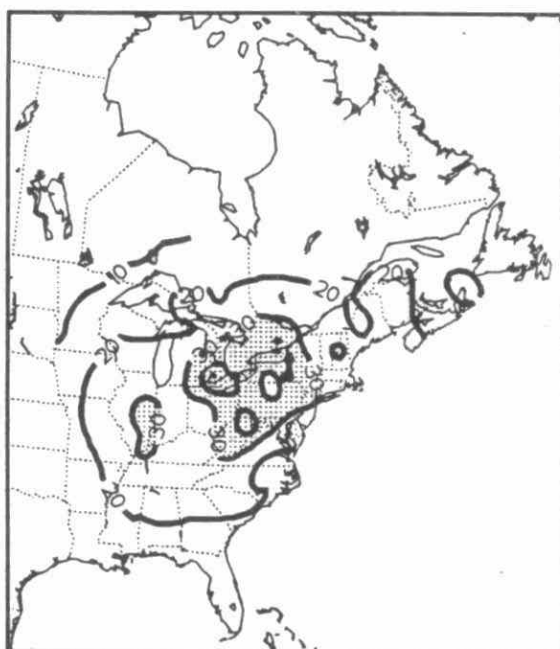


Fig. 3B-2 Patterns of annual precipitation - weighted mean concentrations of SO₄ = mg/l: 1984-1987.

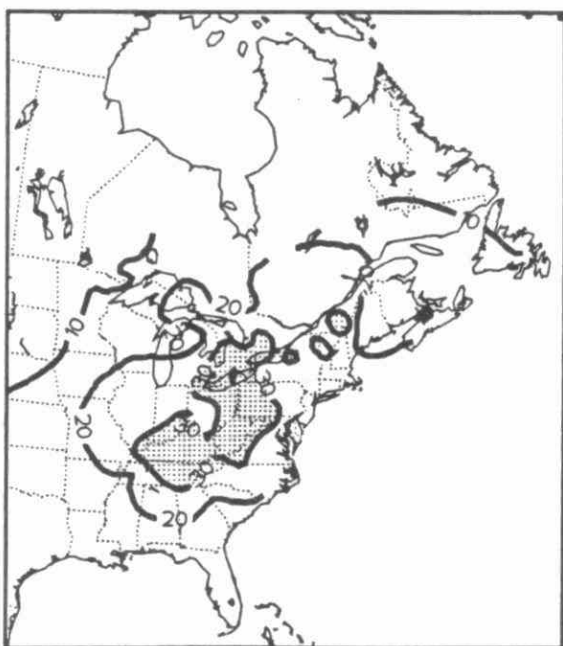
1980 WET SO₄ DEPOSITION (KG/HA/YR)



1981 WET SO₄ DEPOSITION (KG/HA/YR)



1982 WET SO₄ DEPOSITION (KG/HA/YR)



1983 WET SO₄ DEPOSITION (KG/HA/YR)

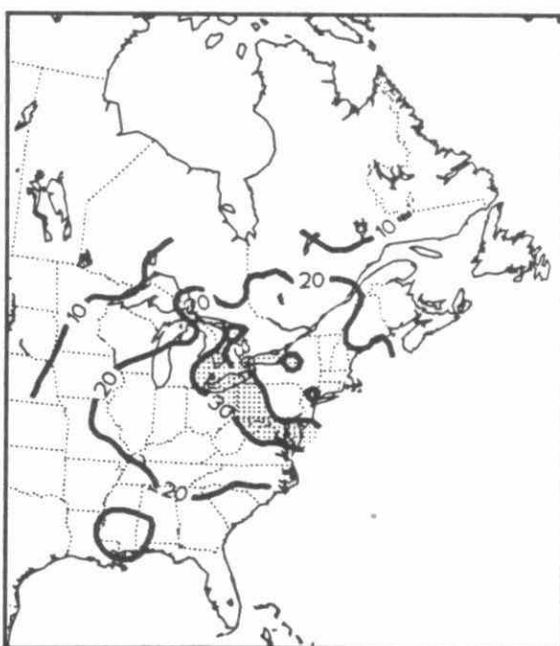
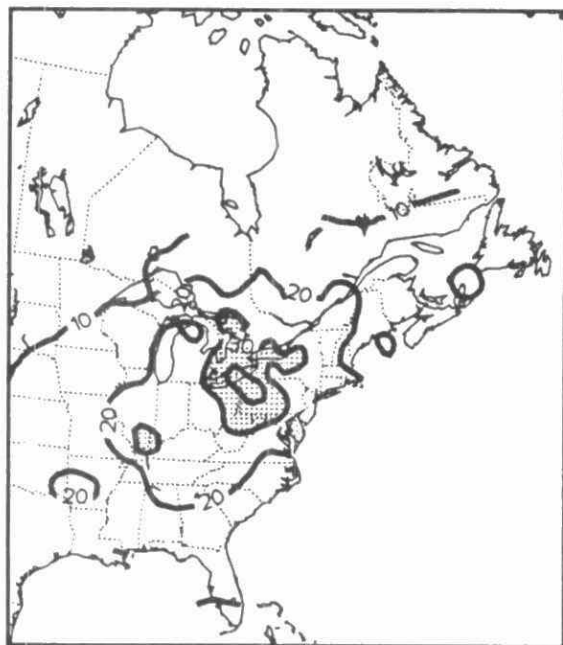
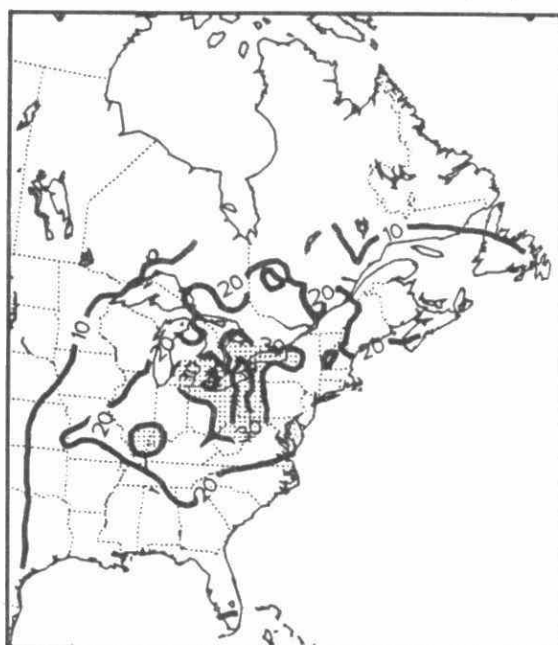


Fig. 3B-3 Patterns of annual wet deposition of SO₄⁼ (kg/ha/yr): 1980-1983.

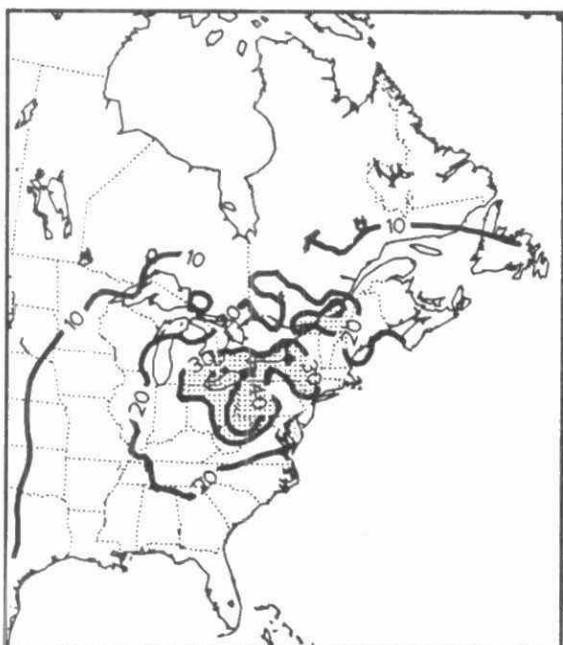
1984 WET SO₄ DEPOSITION (KG/HA/YR)



1985 WET SO₄ DEPOSITION (KG/HA/YR)



1986 WET SO₄ DEPOSITION (KG/HA/YR)



1987 WET SO₄ DEPOSITION (KG/HA/YR)

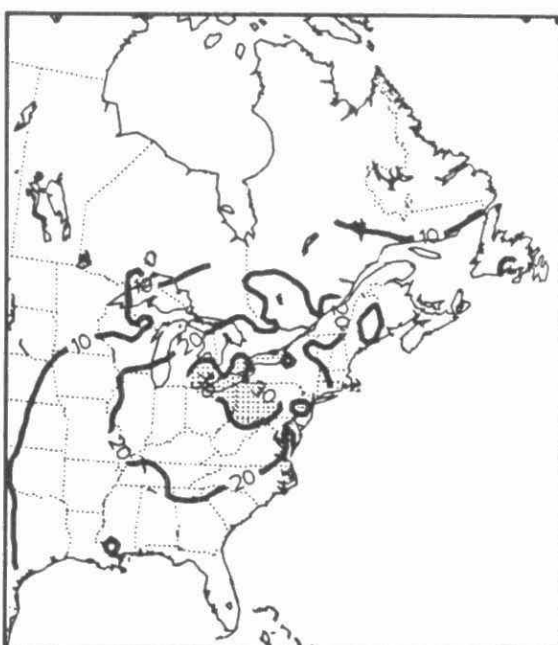
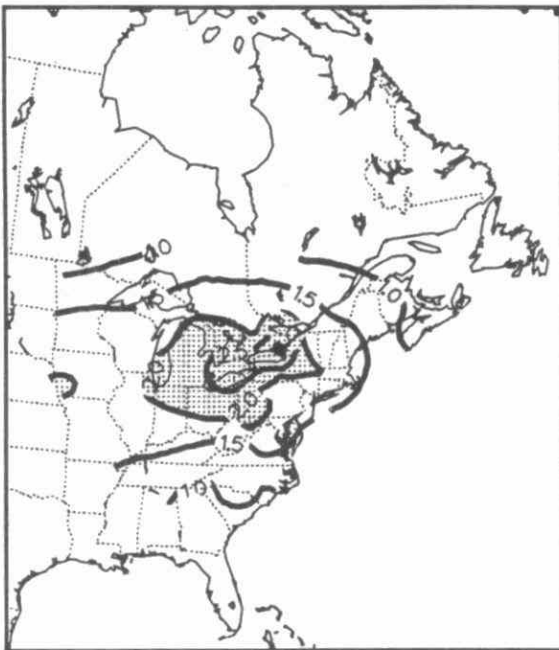
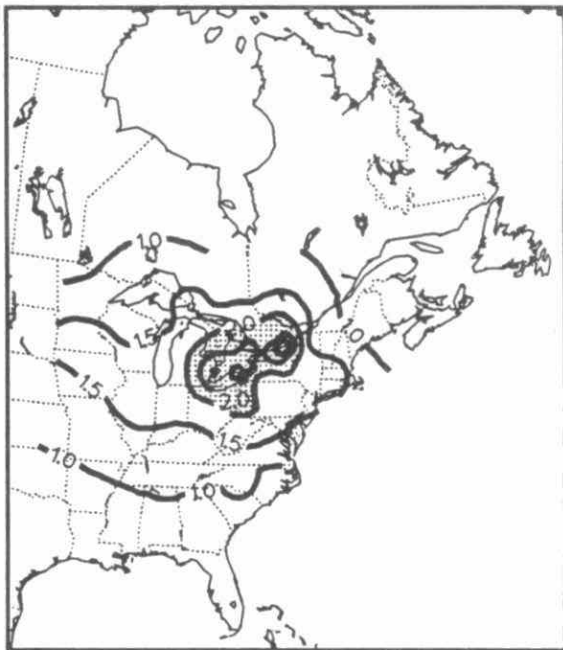


Fig. 3B-4 Patterns of annual wet deposition of SO₄²⁻ (kg/ha/yr):1984-1987.

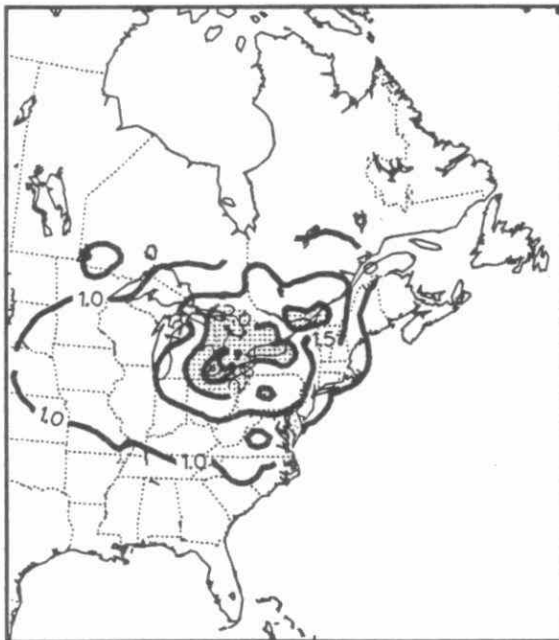
1980 ANNUAL MEAN NO₃ CONCENTRATION IN PRECIPITATION (MG/L)



1981 ANNUAL MEAN NO₃ CONCENTRATION IN PRECIPITATION (MG/L)



1982 ANNUAL MEAN NO₃ CONCENTRATION IN PRECIPITATION (MG/L)



1983 ANNUAL MEAN NO₃ CONCENTRATION IN PRECIPITATION (MG/L)

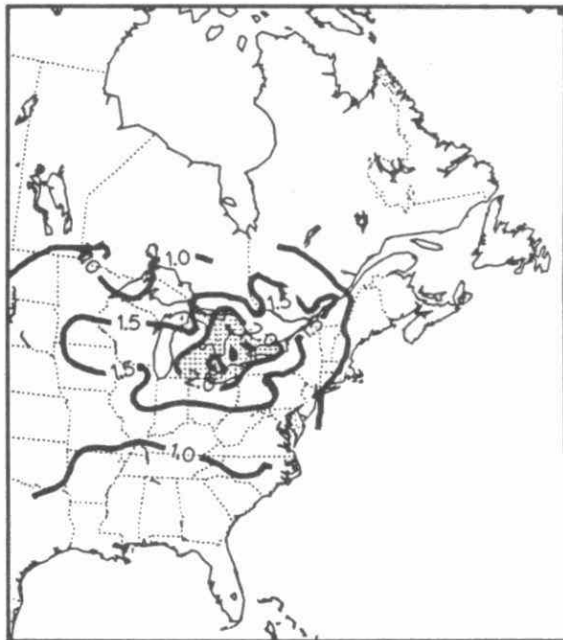
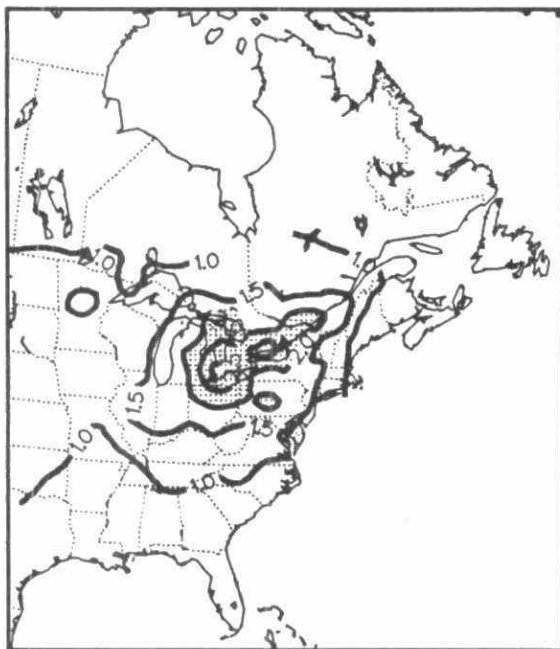
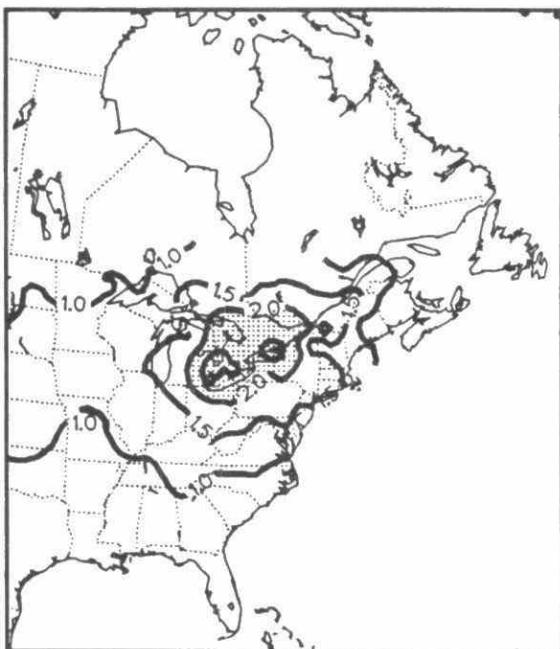


Fig. 3B-5 Patterns of annual precipitation - weighted mean concentrations of NO₃⁻ (mg/l): 1980-1983.

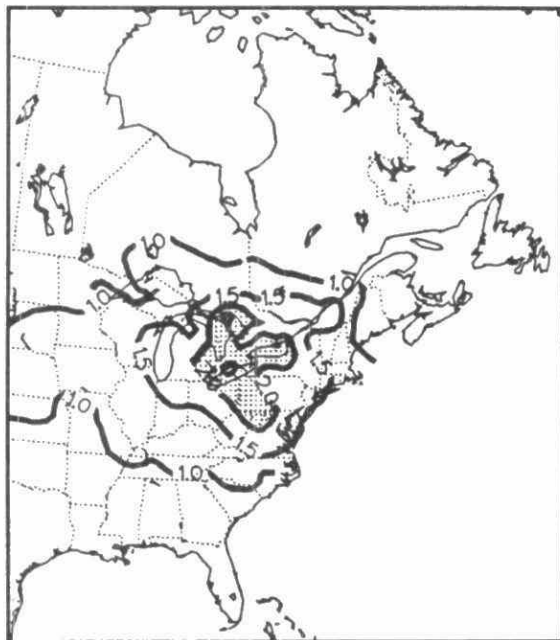
1984 ANNUAL MEAN NO₃ CONCENTRATION IN PRECIPITATION (MG/L)



1985 ANNUAL MEAN NO₃ CONCENTRATION IN PRECIPITATION (MG/L)



1986 ANNUAL MEAN NO₃ CONCENTRATION IN PRECIPITATION (MG/L)



1987 ANNUAL MEAN NO₃ CONCENTRATION IN PRECIPITATION (MG/L)

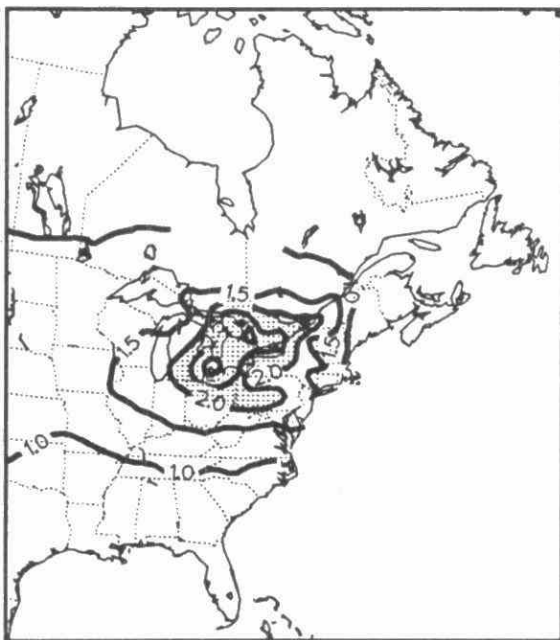
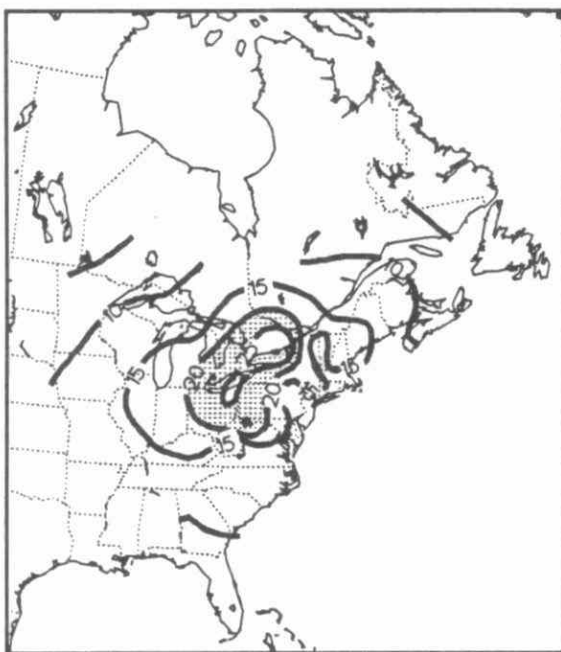
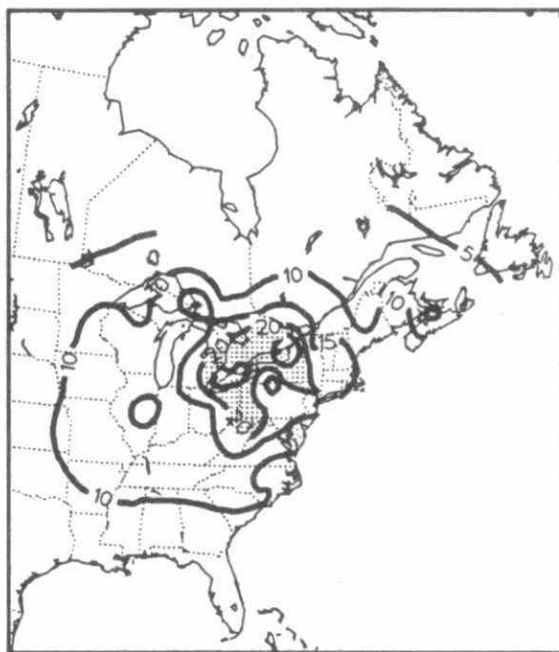


Fig. 3B-6 Patterns of annual precipitation - weighted mean concentrations of NO₃⁻ (mg/l): 1984-1987.

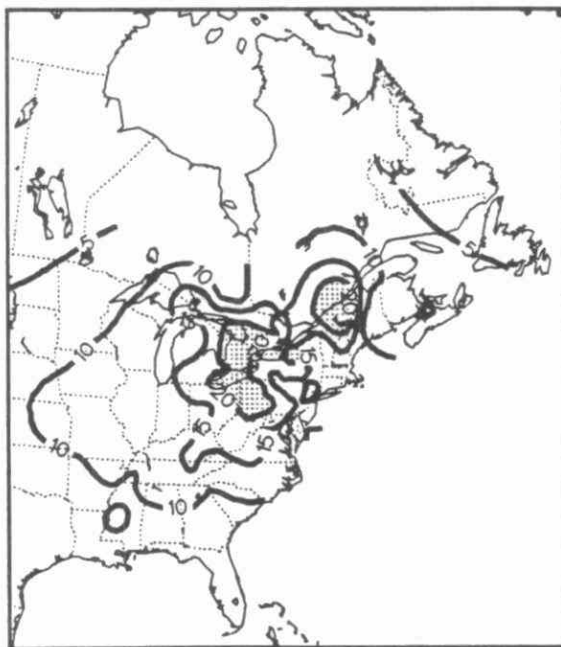
1980 WET NO₃ DEPOSITION (KG/HA/YR)



1981 WET NO₃ DEPOSITION (KG/HA/YR)



1982 WET NO₃ DEPOSITION (KG/HA/YR)



1983 WET NO₃ DEPOSITION (KG/HA/YR)

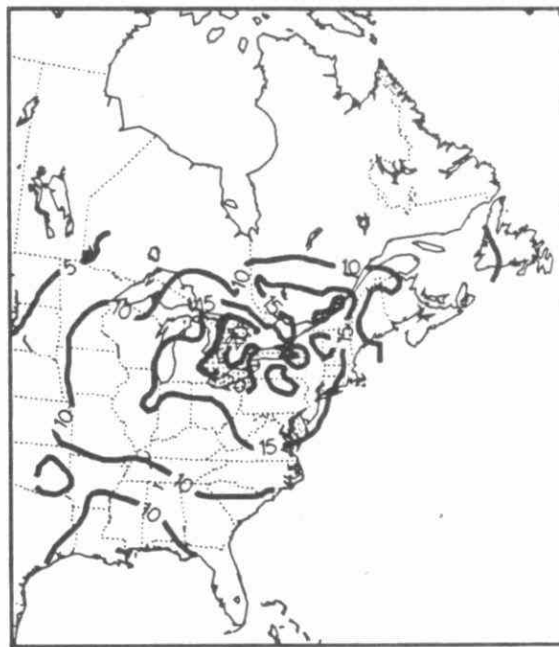
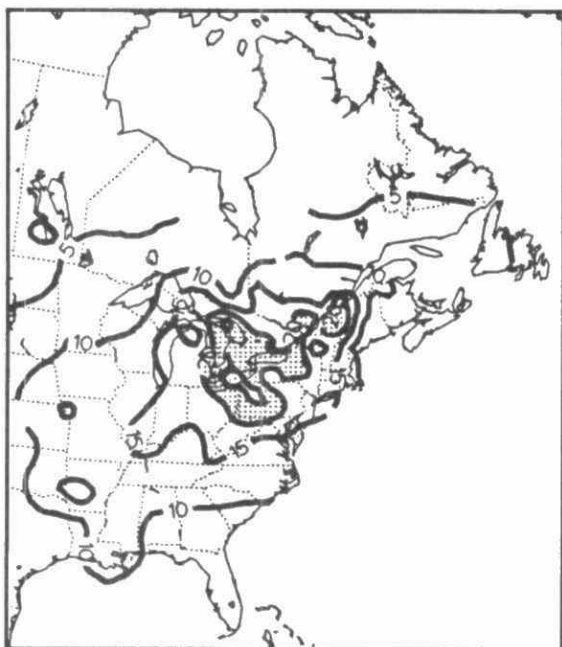
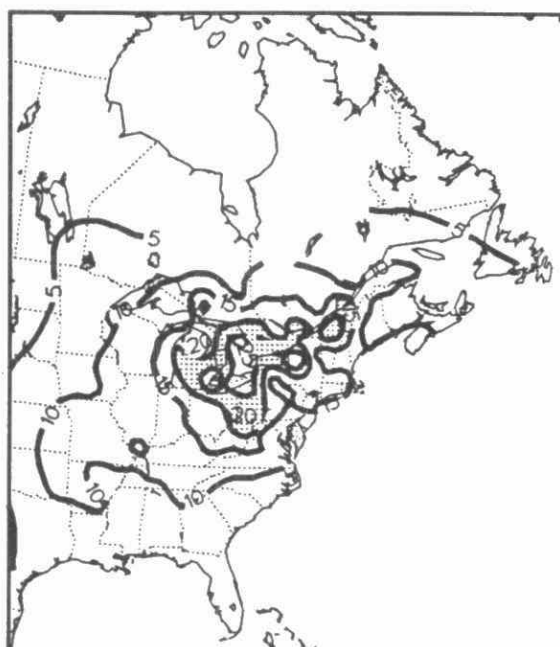


Fig. 3B-7 Patterns of annual wet deposition of NO₃⁻ (kg/ha/yr):1980-1983.

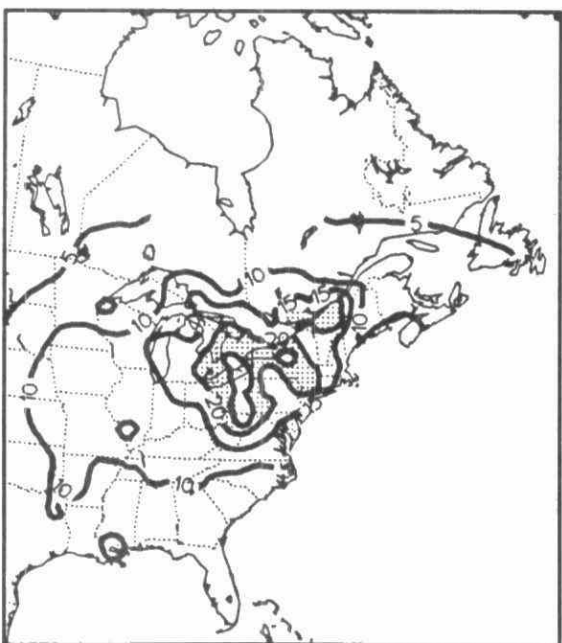
1984 WET NO₃ DEPOSITION (KG/HA/YR)



1985 WET NO₃ DEPOSITION (KG/HA/YR)



1986 WET NO₃ DEPOSITION (KG/HA/YR)



1987 WET NO₃ DEPOSITION (KG/HA/YR)

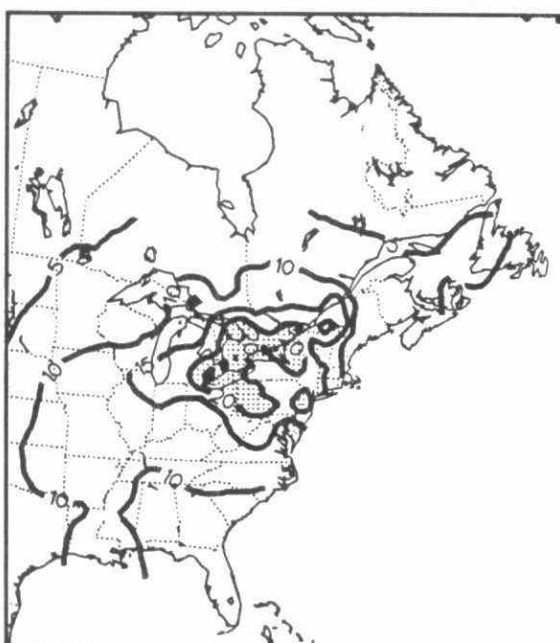
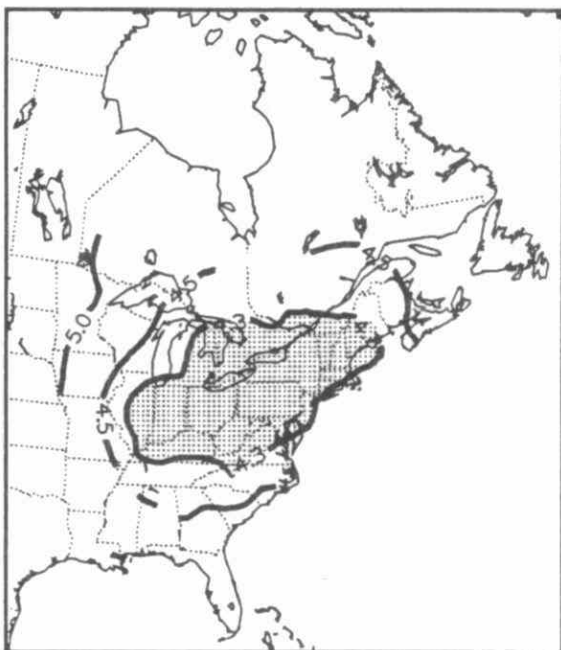
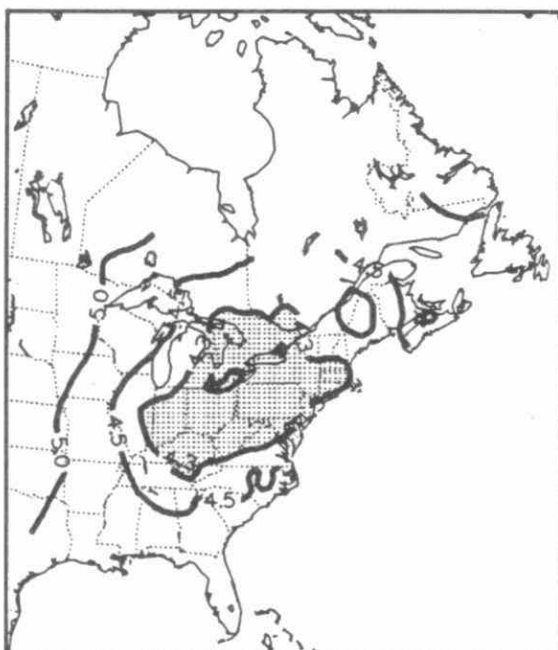


Fig. 3B-8 Patterns of annual wet deposition of NO₃⁻ (kg/ha/yr):1984-1987.

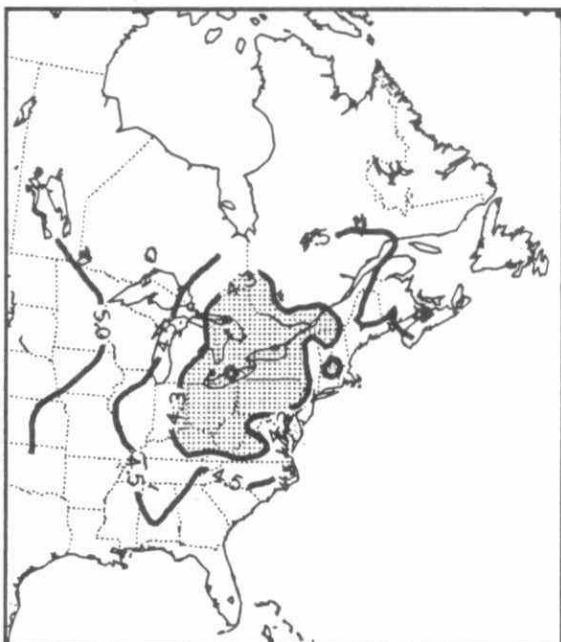
1980 ANNUAL MEAN PH DISTRIBUTION



1981 ANNUAL MEAN PH DISTRIBUTION



1982 ANNUAL MEAN PH DISTRIBUTION



1983 ANNUAL MEAN PH DISTRIBUTION

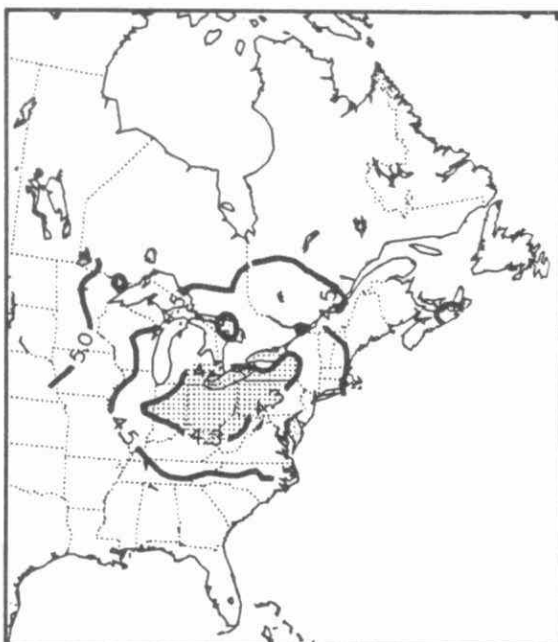
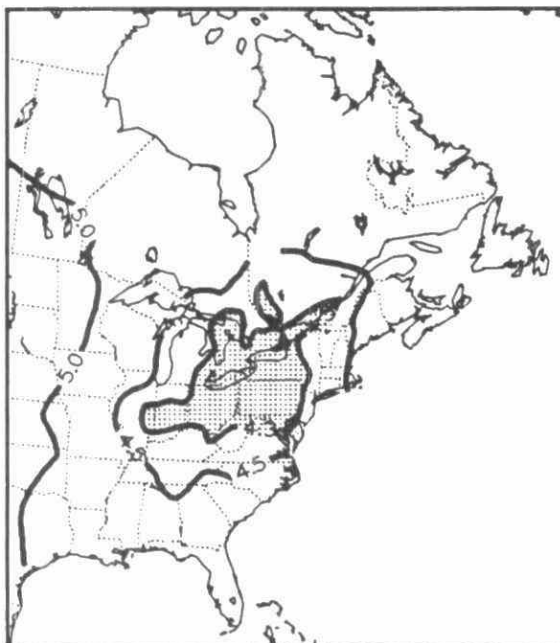
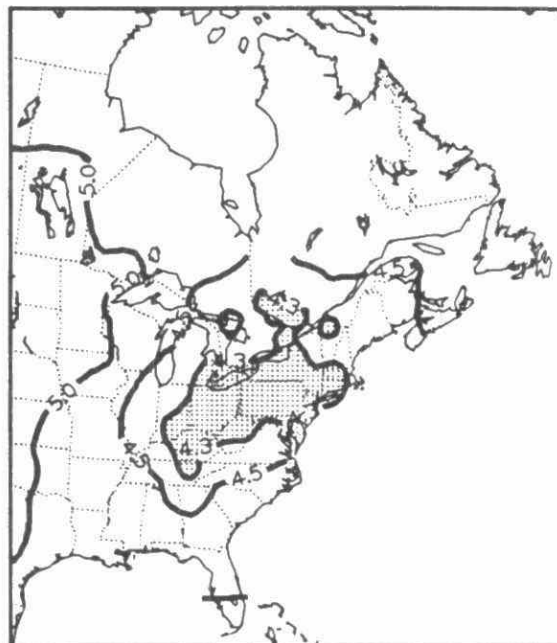


Fig. 3B-9 Patterns of annual mean pH distribution: 1980-1983.

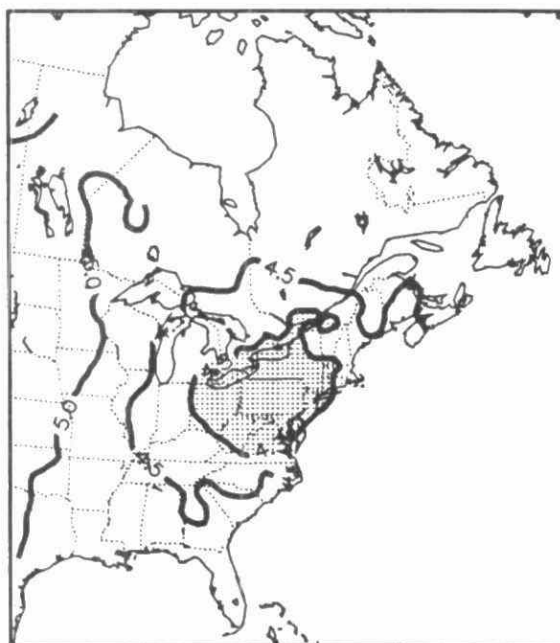
1984 ANNUAL MEAN PH DISTRIBUTION



1985 ANNUAL MEAN PH DISTRIBUTION



1986 ANNUAL MEAN PH DISTRIBUTION



1987 ANNUAL MEAN PH DISTRIBUTION

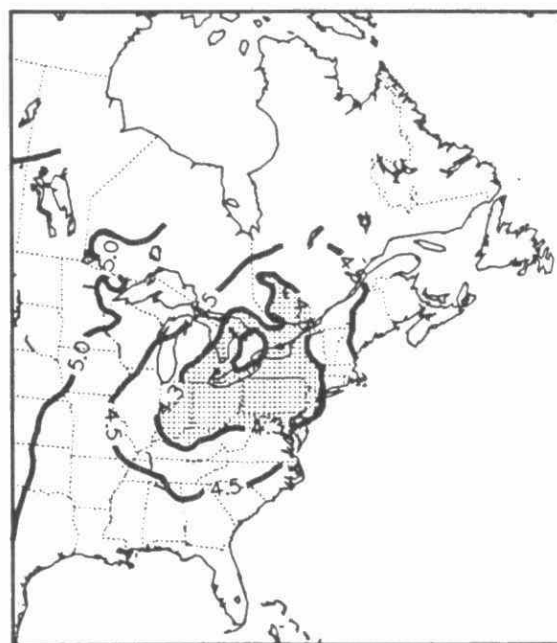
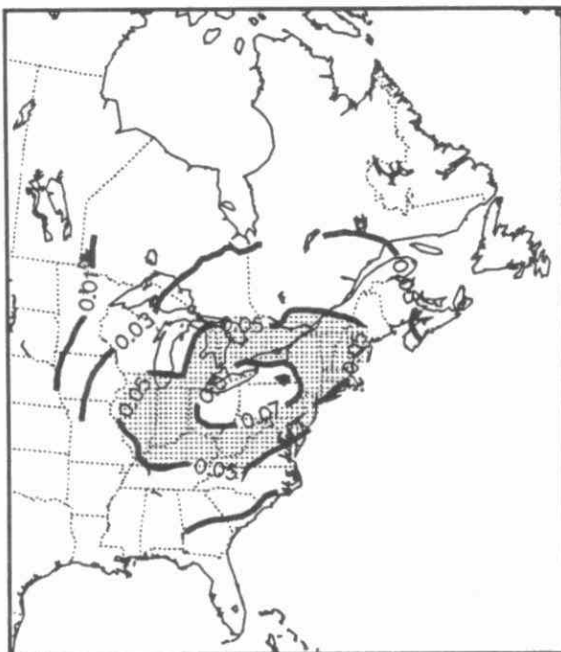
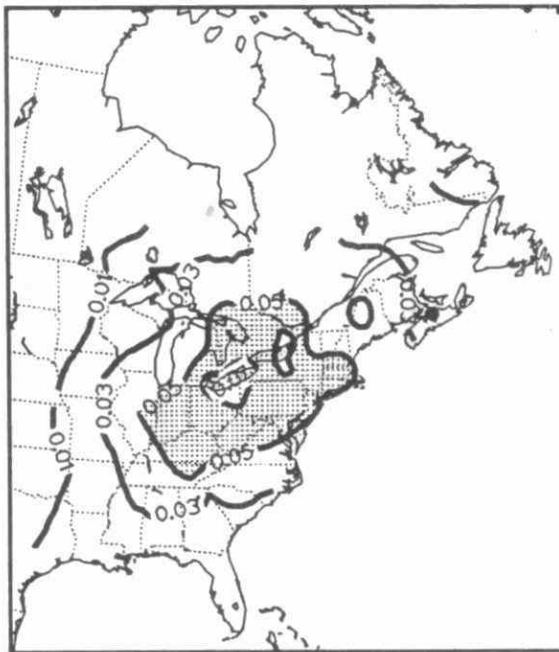


Fig. 3B-10 Patterns of annual mean pH distribution: 1984-1987.

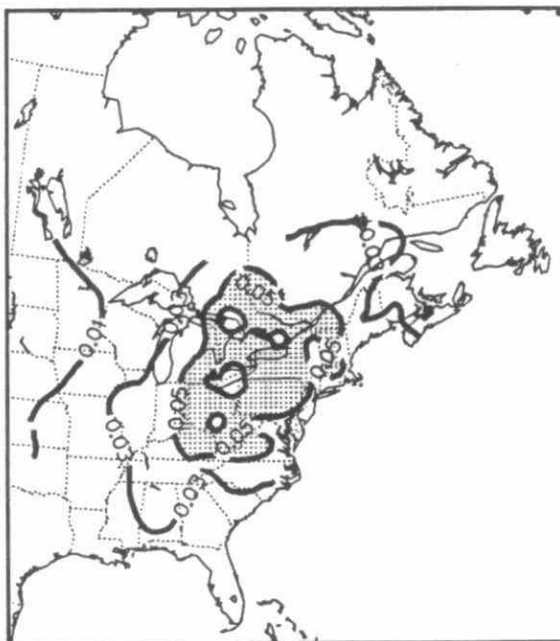
1980 ANNUAL MEAN H⁺ CONCENTRATION IN PRECIPITATION (MG/L)



1981 ANNUAL MEAN H⁺ CONCENTRATION IN PRECIPITATION (MG/L)



1982 ANNUAL MEAN H⁺ CONCENTRATION IN PRECIPITATION (MG/L)



1983 ANNUAL MEAN H⁺ CONCENTRATION IN PRECIPITATION (MG/L)

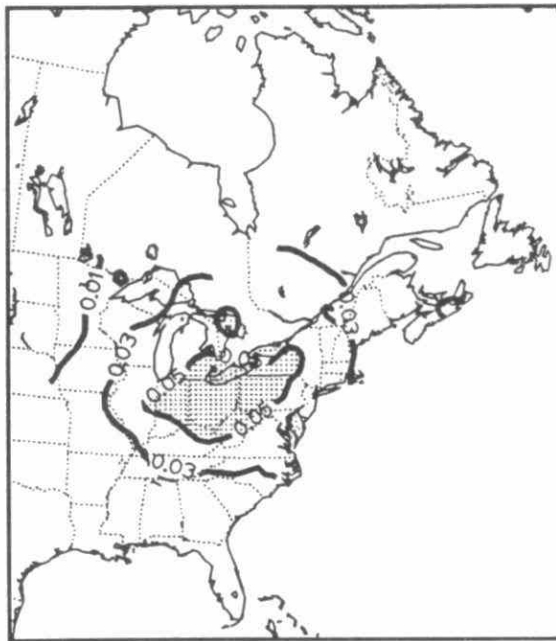
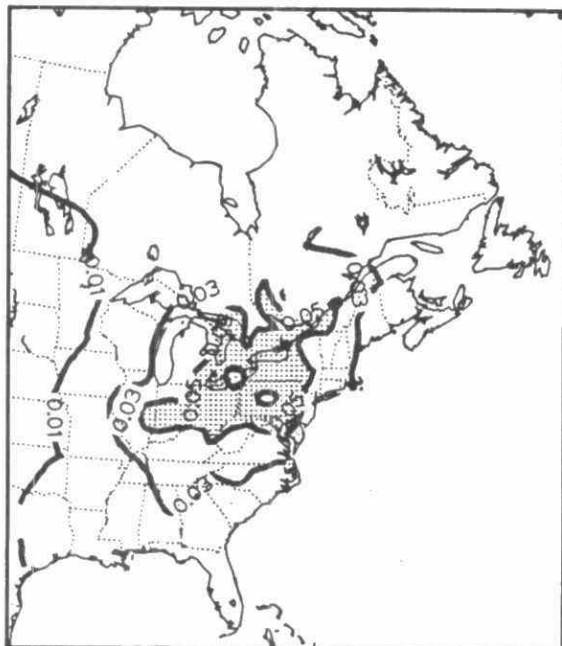
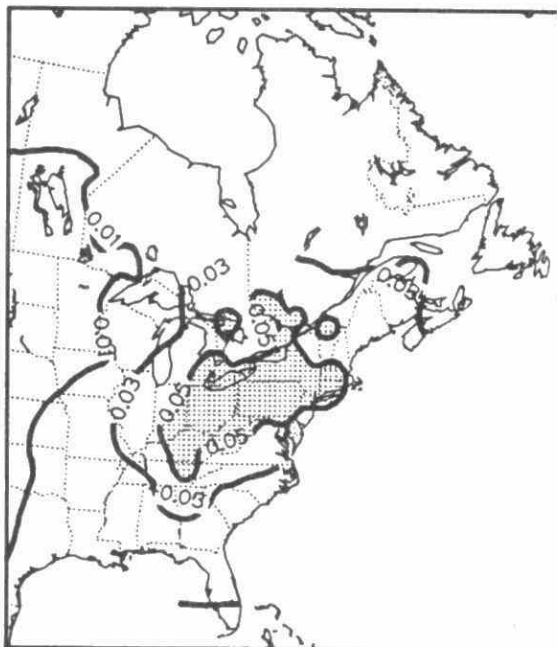


Fig. 3B-11 Patterns of annual precipitation - weighted mean H⁺ concentrations (mg/l): 1980-1983.

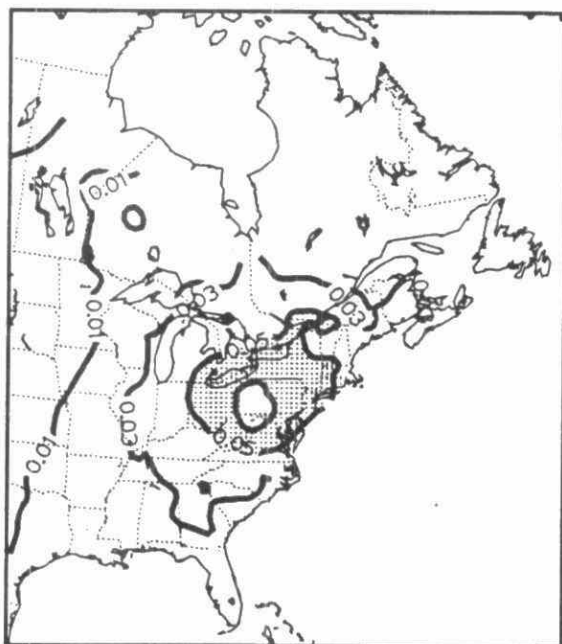
1984 ANNUAL MEAN H⁺ CONCENTRATION IN PRECIPITATION (MG/L)



1985 ANNUAL MEAN H⁺ CONCENTRATION IN PRECIPITATION (MG/L)



1986 ANNUAL MEAN H⁺ CONCENTRATION IN PRECIPITATION (MG/L)



1987 ANNUAL MEAN H⁺ CONCENTRATION IN PRECIPITATION (MG/L)

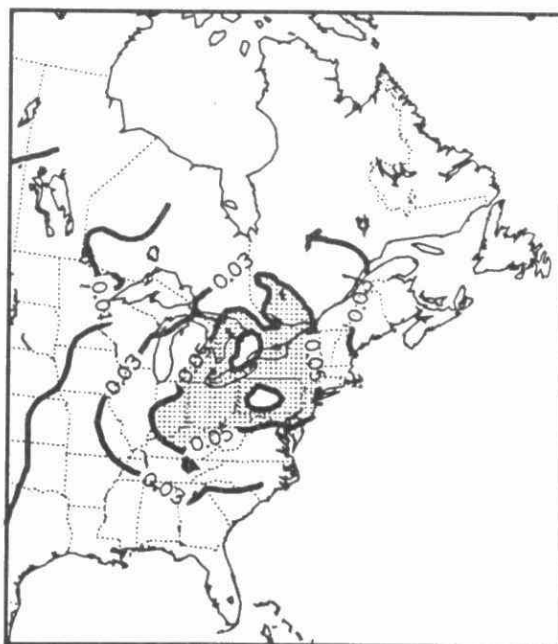
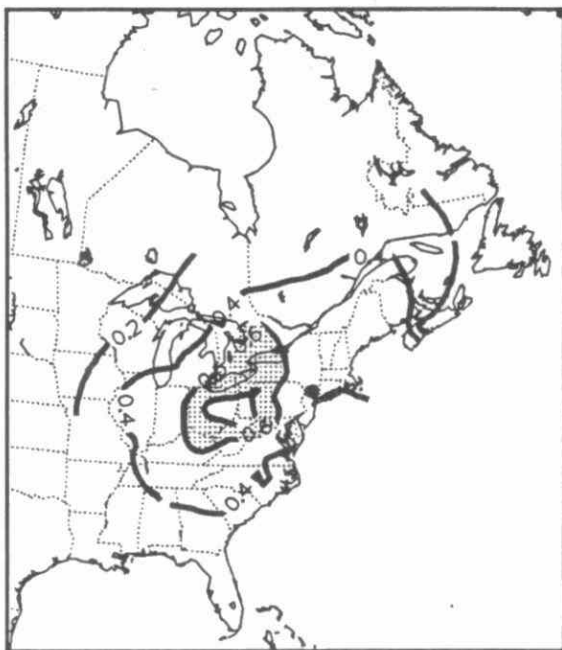
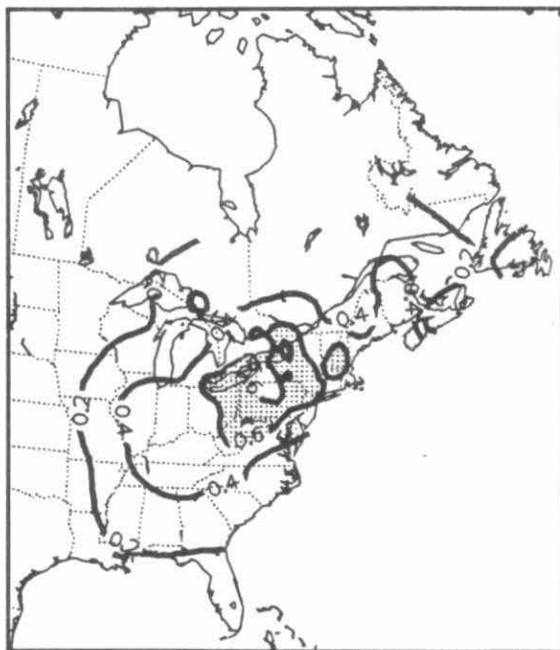


Fig. 3B-12 Patterns of annual precipitation - weighted mean H⁺ concentrations (mg/l): 1984-1987.

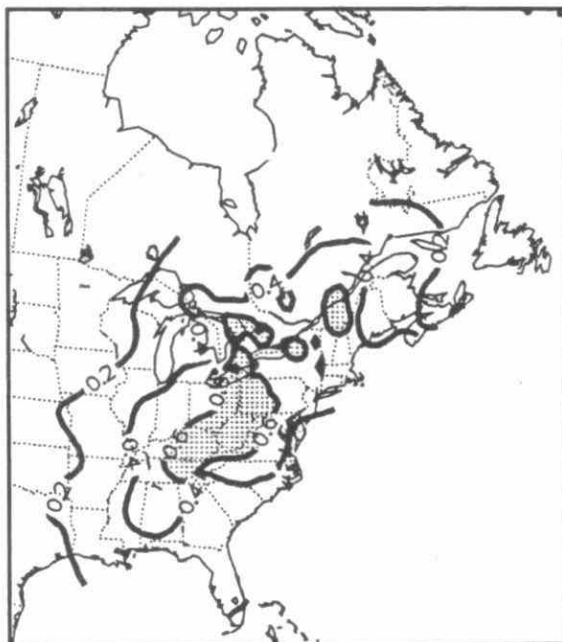
1980 WET H⁺ DEPOSITION (KG/HA/YR)



1981 WET H⁺ DEPOSITION (KG/HA/YR)



1982 WET H⁺ DEPOSITION (KG/HA/YR)



1983 WET H⁺ DEPOSITION (KG/HA/YR)

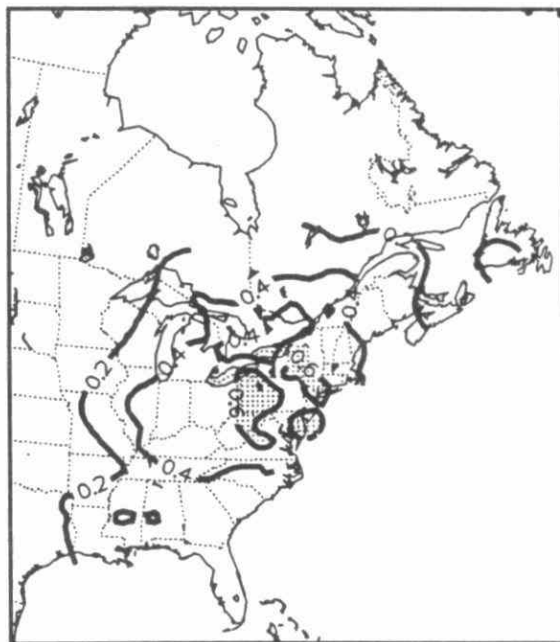
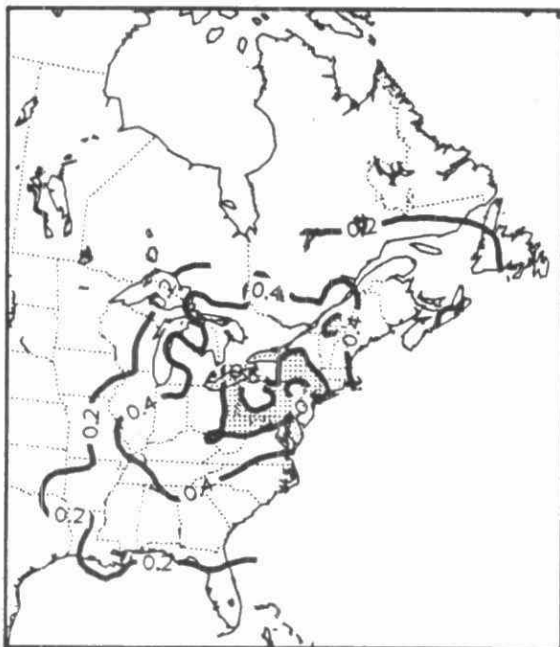
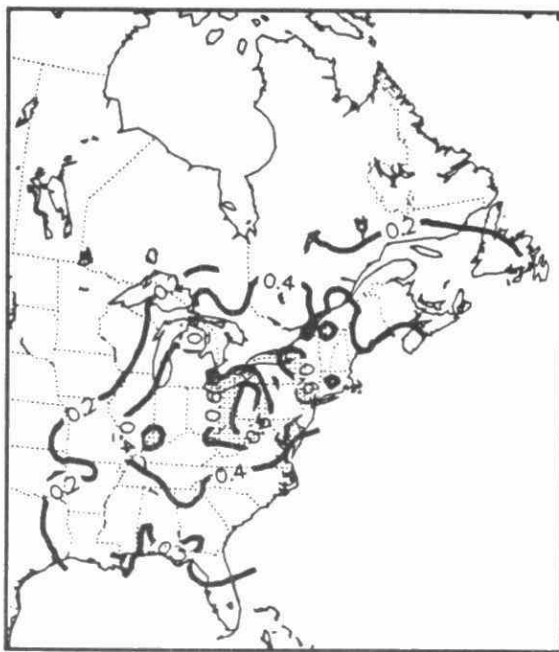


Fig. 3B-13 Patterns of annual wet deposition of H⁺ (kg/ha/yr): 1980-1983.

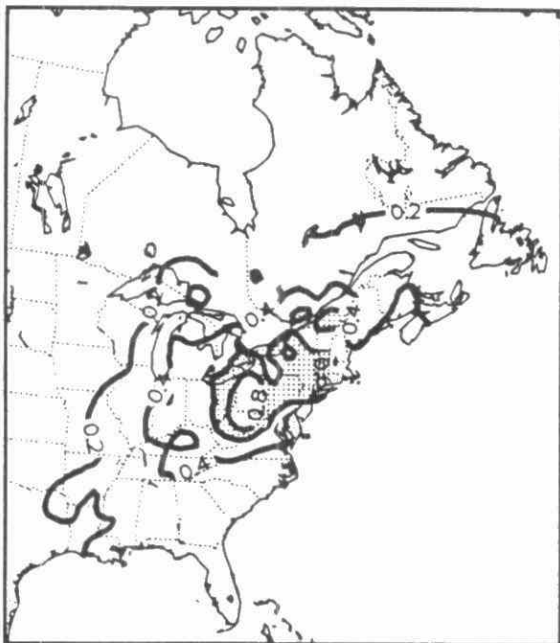
1984 WET H⁺ DEPOSITION (KG/HA/YR)



1985 WET H⁺ DEPOSITION (KG/HA/YR)



1986 WET H⁺ DEPOSITION (KG/HA/YR)



1987 WET H⁺ DEPOSITION (KG/HA/YR)

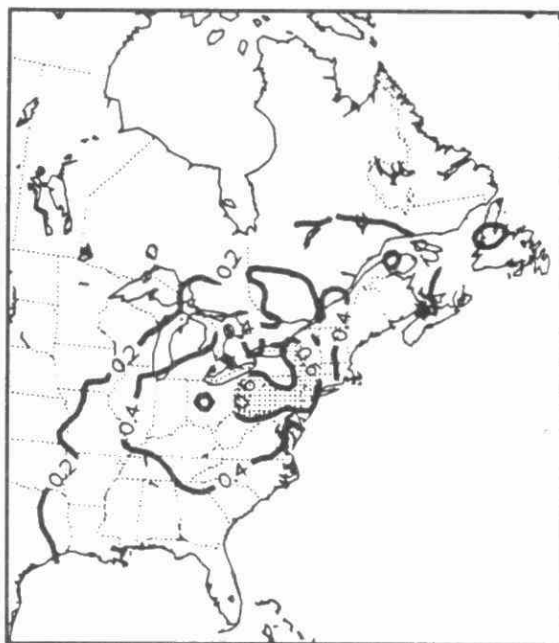
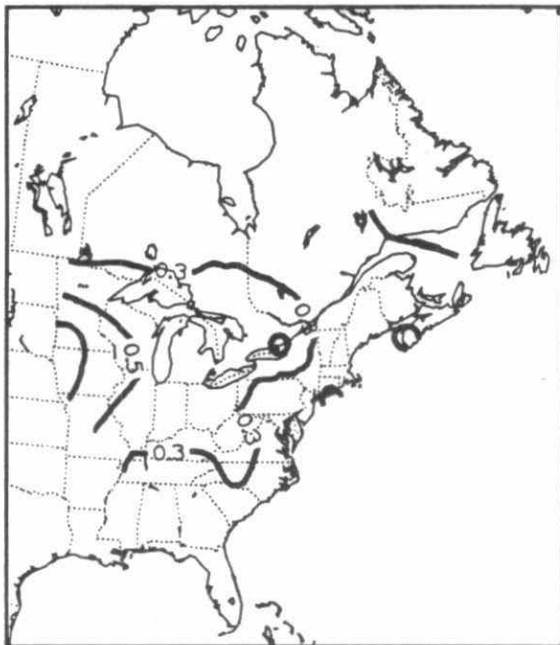
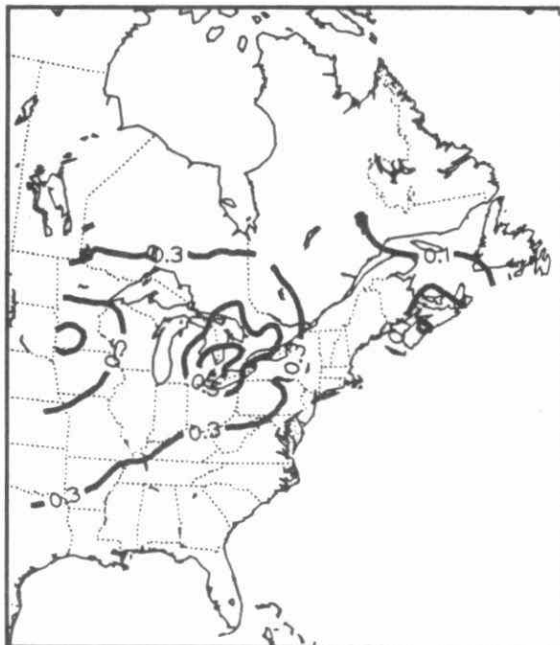


Fig. 3B-14 Patterns of annual wet deposition of H⁺ (kg/ha/yr): 1984-1987.

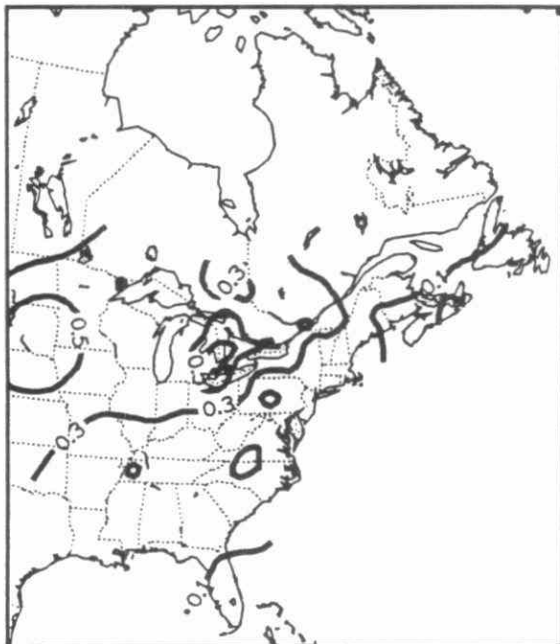
1980 ANNUAL MEAN NH_4 CONCENTRATION IN PRECIPITATION (MG/L)



1981 ANNUAL MEAN NH_4 CONCENTRATION IN PRECIPITATION (MG/L)



1982 ANNUAL MEAN NH_4 CONCENTRATION IN PRECIPITATION (MG/L)



1983 ANNUAL MEAN NH_4 CONCENTRATION IN PRECIPITATION (MG/L)

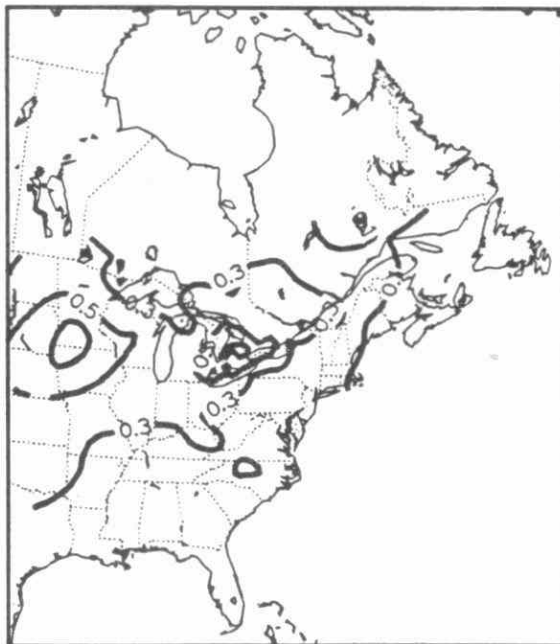
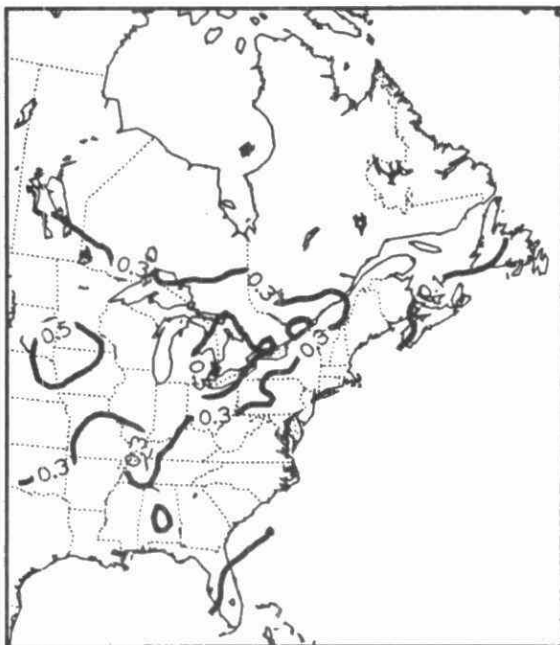
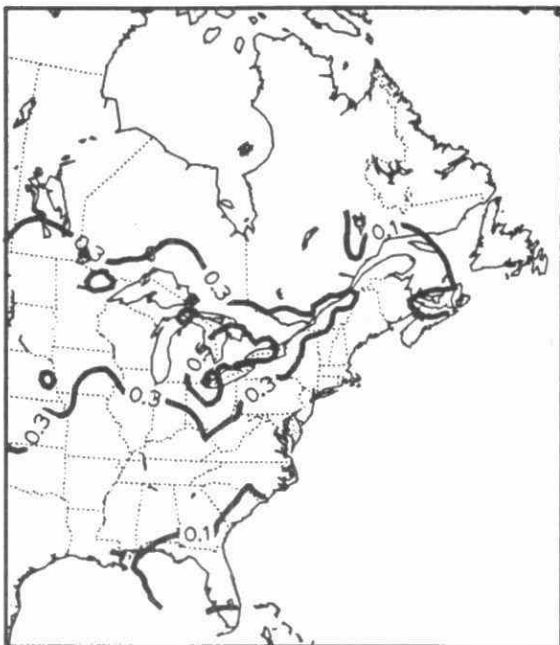


Fig. 3B-15 Patterns of annual precipitation-weighted mean concentrations of NH_4^+ (mg/l): 1980-1983.

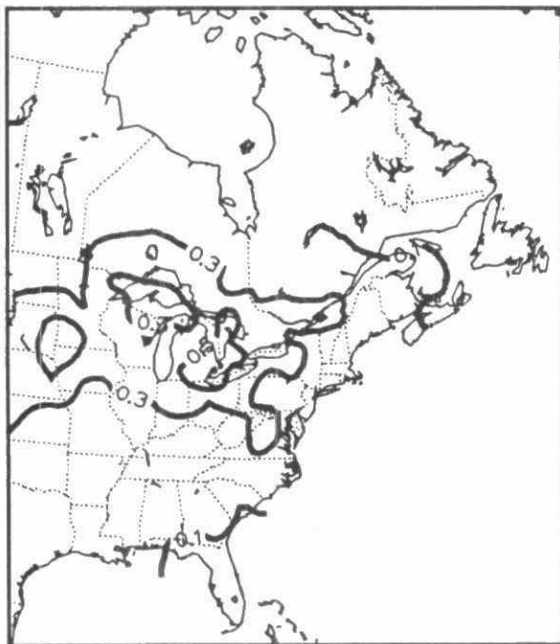
1984 ANNUAL MEAN NH_4 CONCENTRATION IN PRECIPITATION (MG/L)



1985 ANNUAL MEAN NH_4 CONCENTRATION IN PRECIPITATION (MG/L)



1986 ANNUAL MEAN NH_4 CONCENTRATION IN PRECIPITATION (MG/L)



1987 ANNUAL MEAN NH_4 CONCENTRATION IN PRECIPITATION (MG/L)

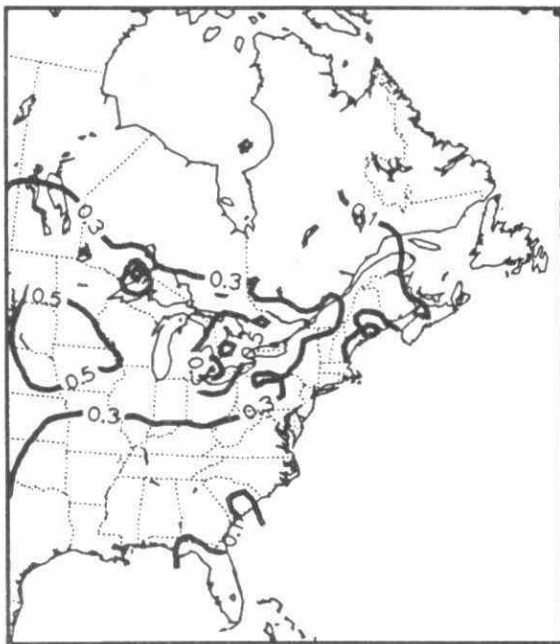
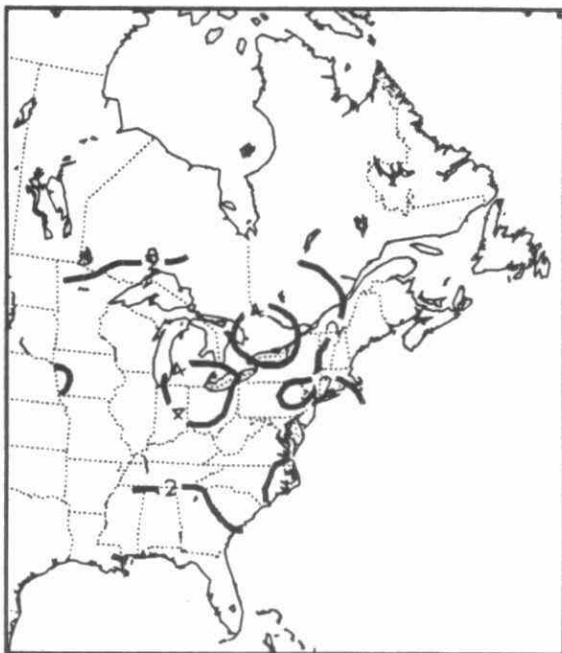
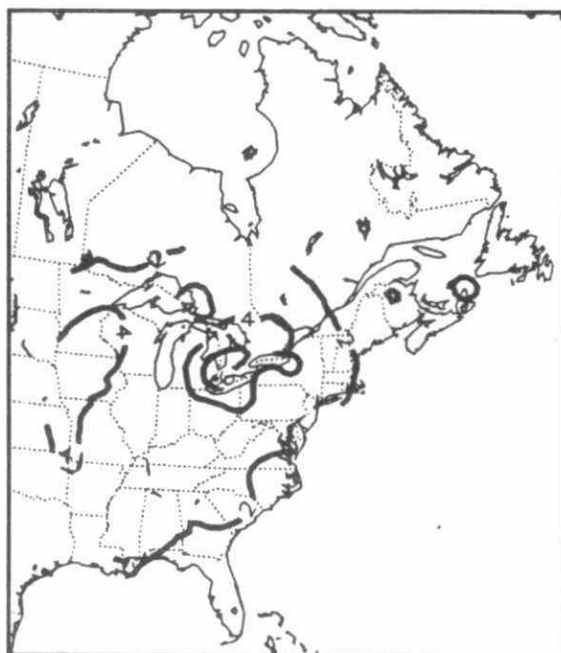


Fig. 3B-16 Patterns of annual precipitation - weighted mean concentrations of NH_4^+ (mg/l): 1984-1987.

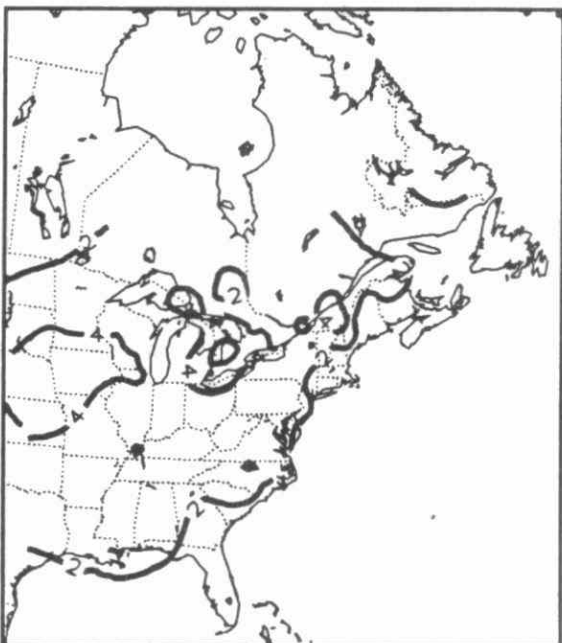
1980 WET NH₄ DEPOSITION (KG/HA/YR)



1981 WET NH₄ DEPOSITION (KG/HA/YR)



1982 WET NH₄ DEPOSITION (KG/HA/YR)



1983 WET NH₄ DEPOSITION (KG/HA/YR)

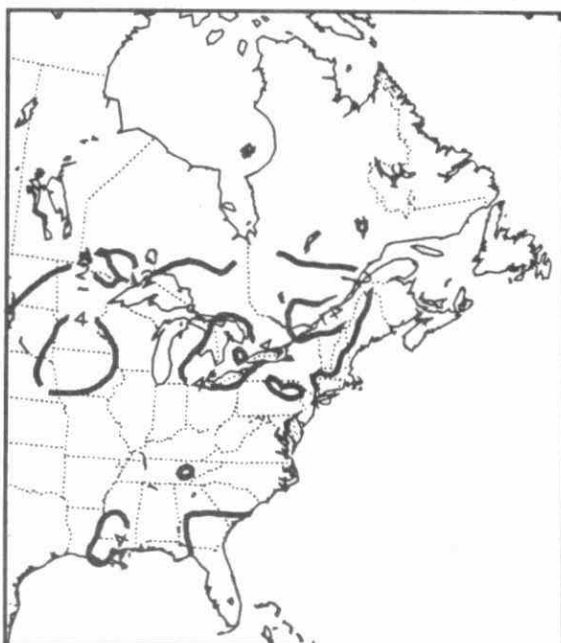
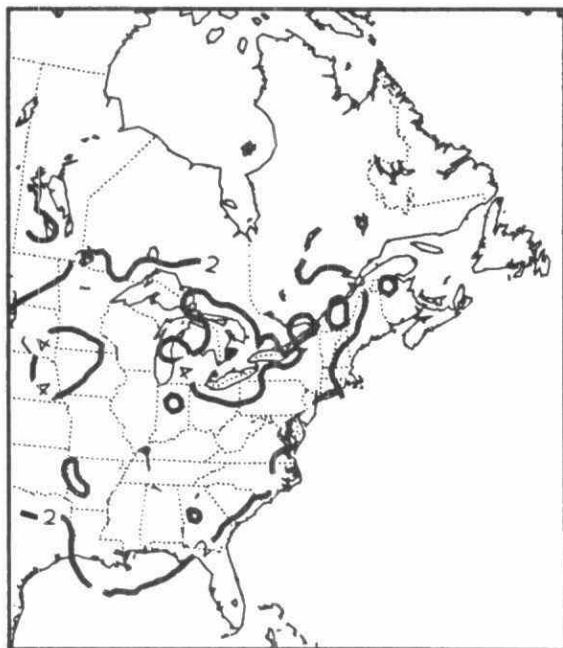
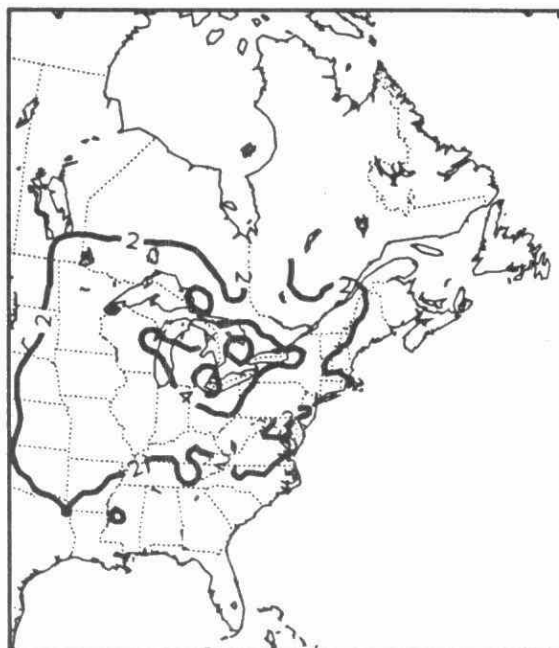


Fig. 3B-17 Patterns of annual wet deposition of NH₄⁺ (kg/ha/yr):1980-1983.

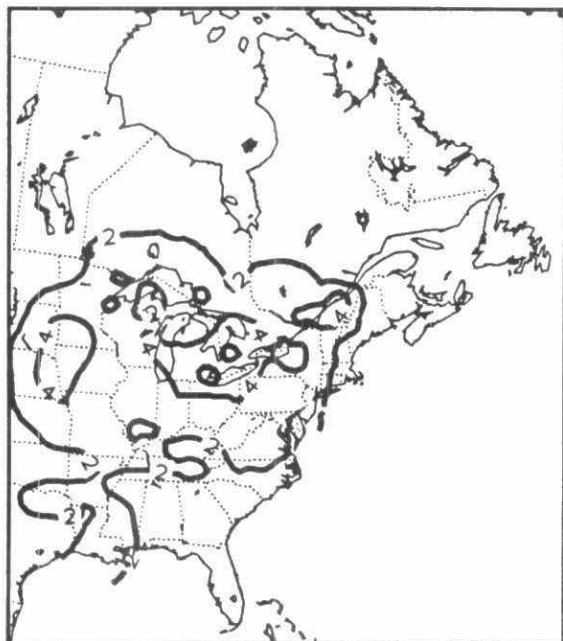
1984 WET NH₄ DEPOSITION (KG/HA/YR)



1985 WET NH₄ DEPOSITION (KG/HA/YR)



1986 WET NH₄ DEPOSITION (KG/HA/YR)



1987 WET NH₄ DEPOSITION (KG/HA/YR)

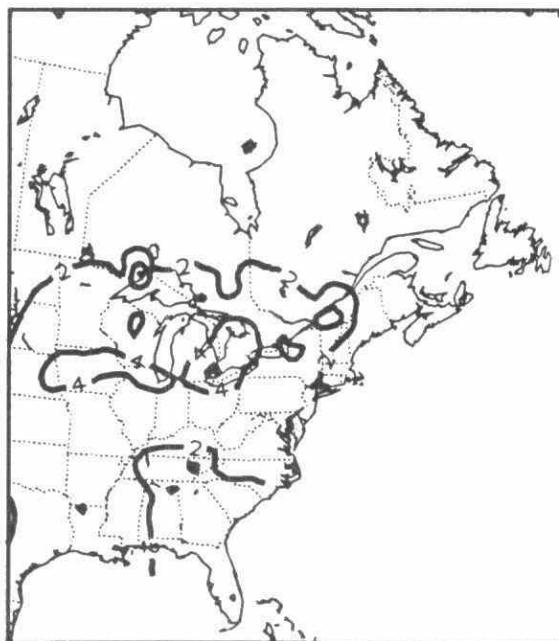
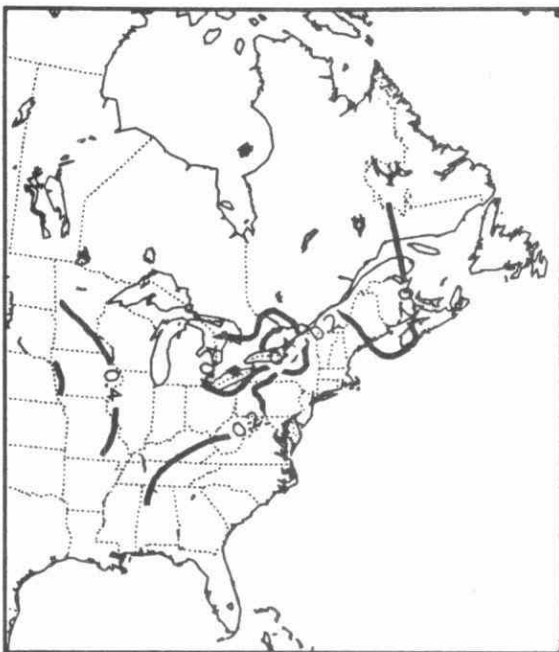
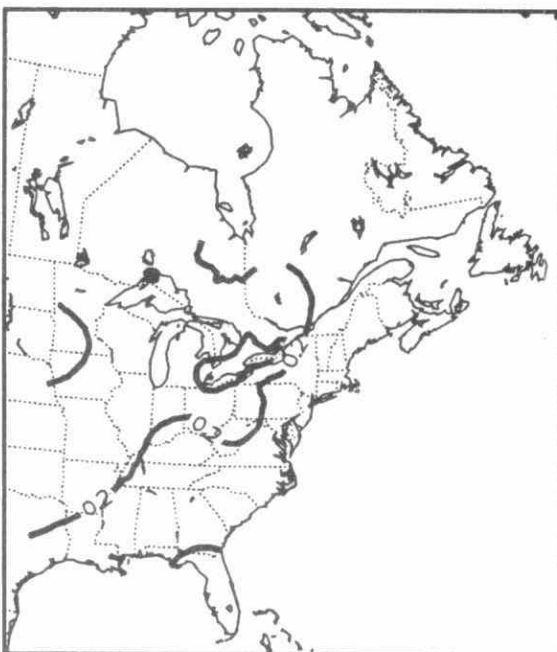


Fig. 3B-18 Patterns of annual wet deposition of NH₄⁺ (kg/ha/yr):1984-1987.

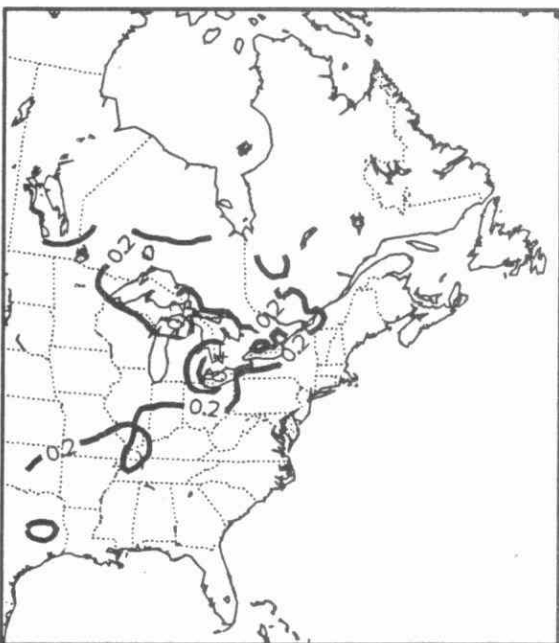
1980 ANNUAL MEAN CA CONCENTRATION IN PRECIPITATION (MG/L)



1981 ANNUAL MEAN CA CONCENTRATION IN PRECIPITATION (MG/L)



1982 ANNUAL MEAN CA CONCENTRATION IN PRECIPITATION (MG/L)



1983 ANNUAL MEAN CA CONCENTRATION IN PRECIPITATION (MG/L)

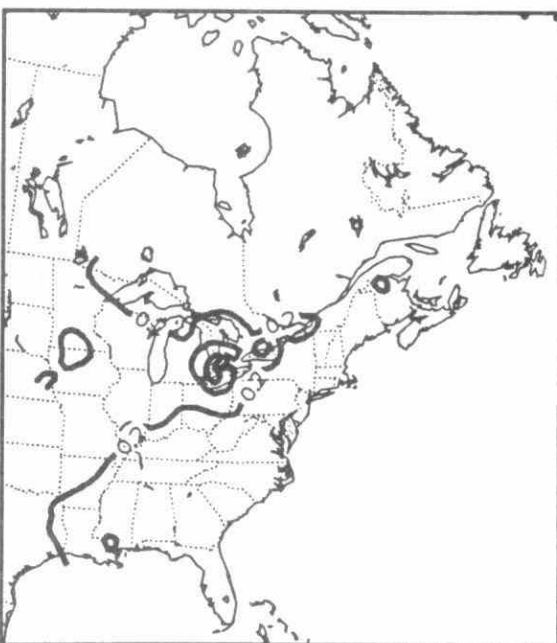
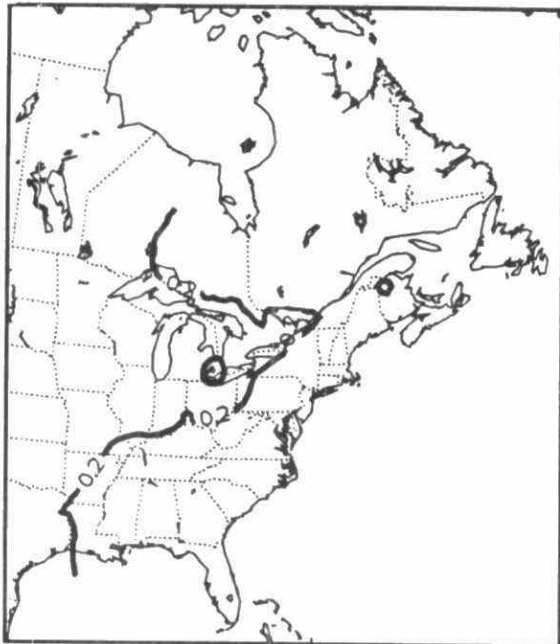
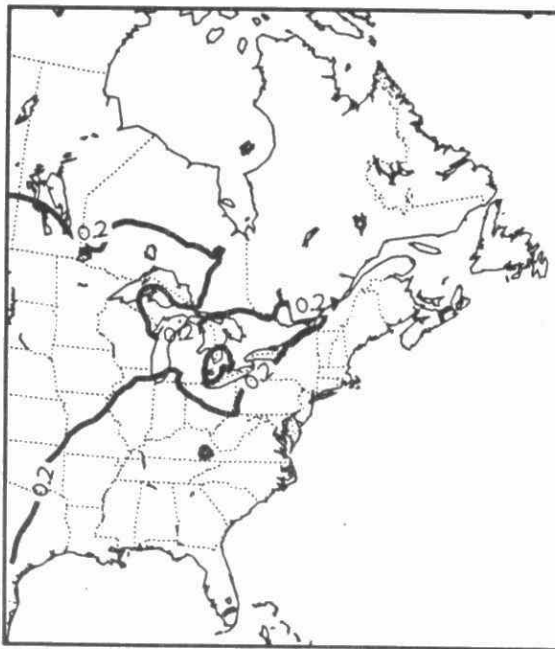


Fig. 3B-19 Patterns of annual precipitation-weighted mean concentrations of Ca^{+2} (mg/l): 1980-1983.

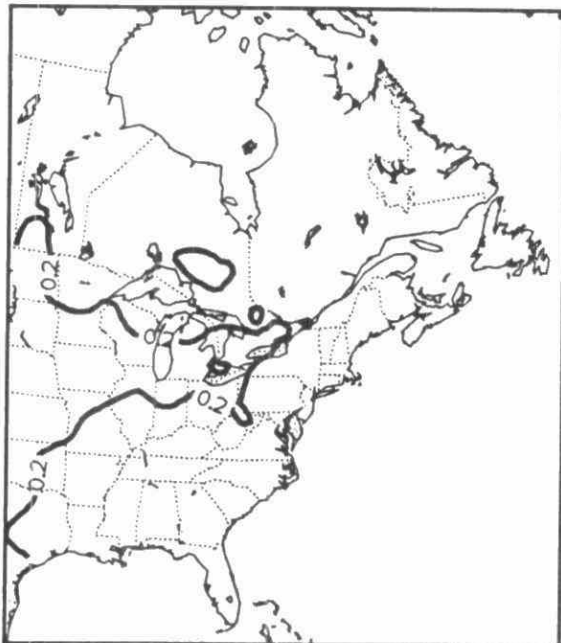
1984 ANNUAL MEAN CA CONCENTRATION IN PRECIPITATION (MG/L)



1985 ANNUAL MEAN CA CONCENTRATION IN PRECIPITATION (MG/L)



1986 ANNUAL MEAN CA CONCENTRATION IN PRECIPITATION (MG/L)



1987 ANNUAL MEAN CA CONCENTRATION IN PRECIPITATION (MG/L)

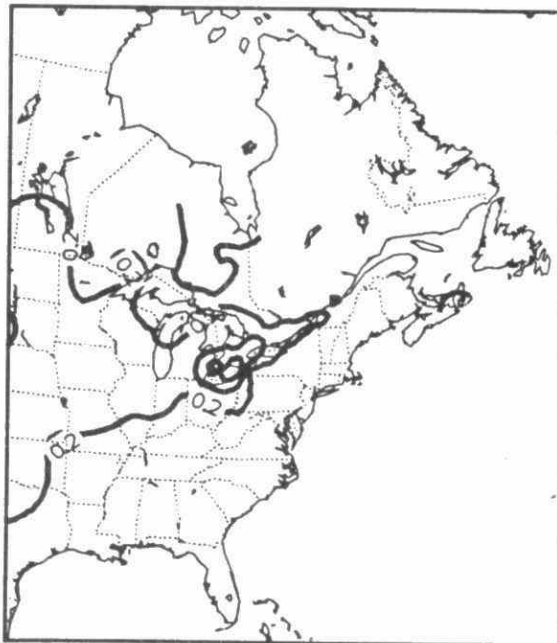
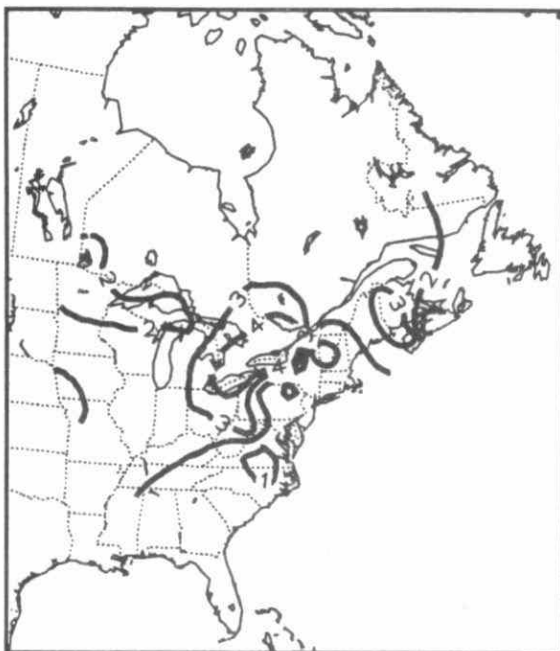
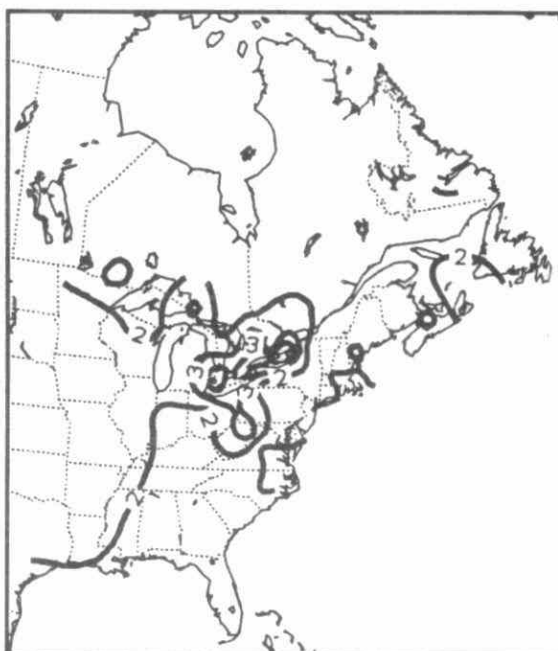


Fig. 3B-20 Patterns of annual precipitation-weighted mean concentrations of Ca^{+2} (mg/l): 1984-1987.

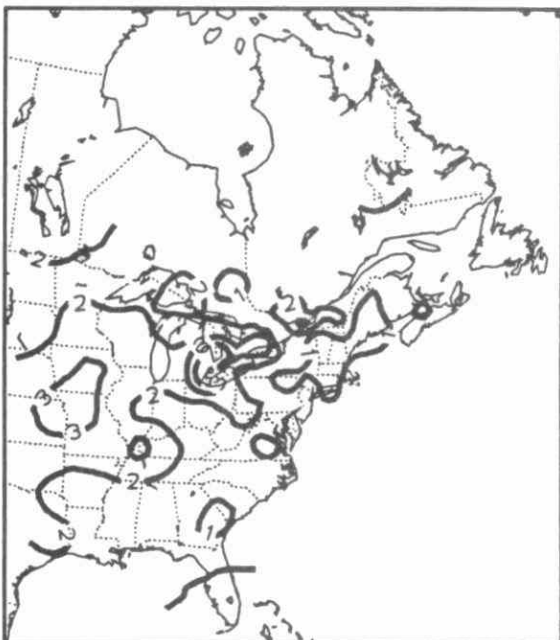
1980 WET CA DEPOSITION (KG/HA/YR)



1981 WET CA DEPOSITION (KG/HA/YR)



1982 WET CA DEPOSITION (KG/HA/YR)



1983 WET CA DEPOSITION (KG/HA/YR)

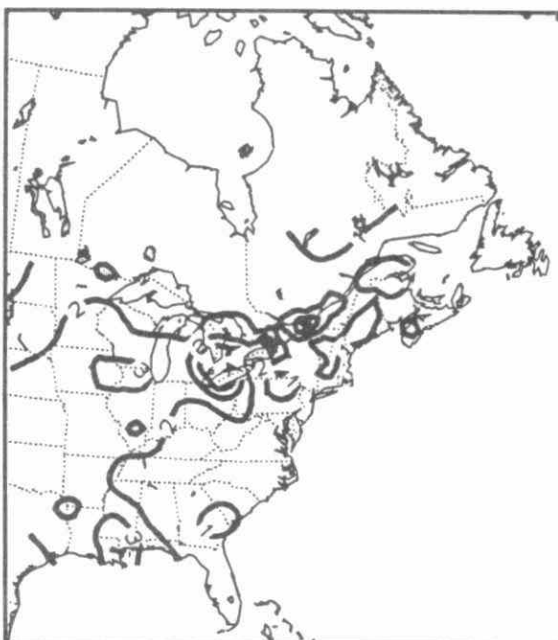
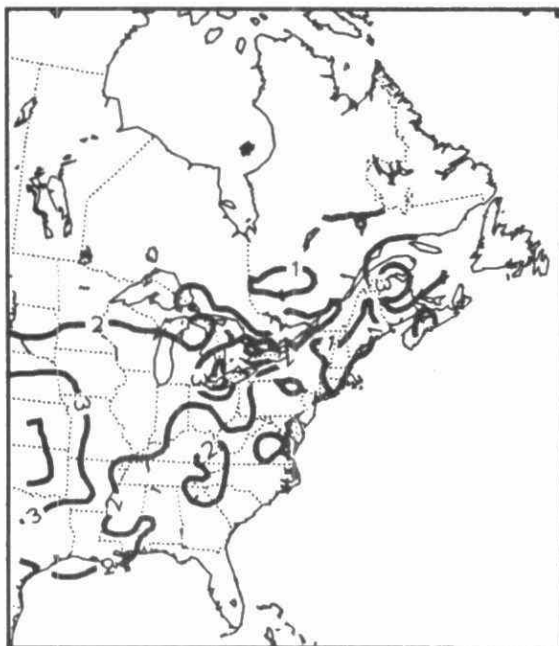
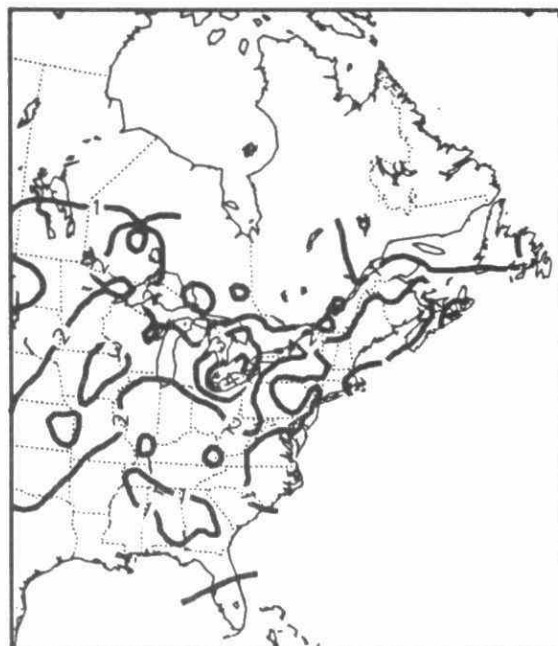


Fig. 3B-21 Patterns of annual wet deposition of Ca^{+2} (kg/ha/yr):1980-1983.

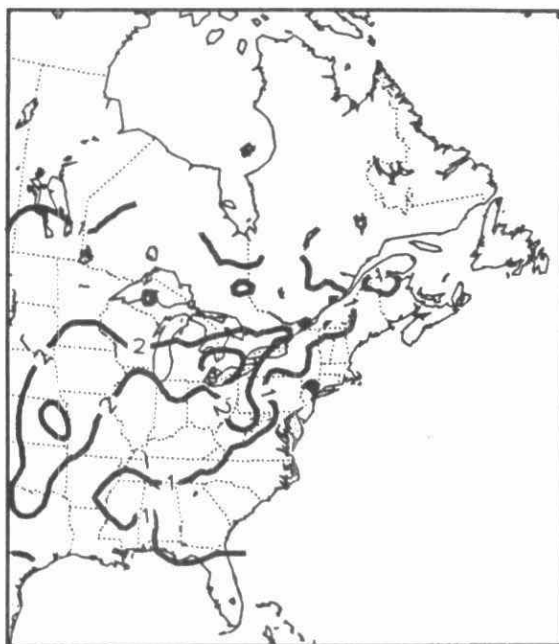
1984 WET CA DEPOSITION (KG/HA/YR)



1985 WET CA DEPOSITION (KG/HA/YR)



1986 WET CA DEPOSITION (KG/HA/YR)



1987 WET CA DEPOSITION (KG/HA/YR)

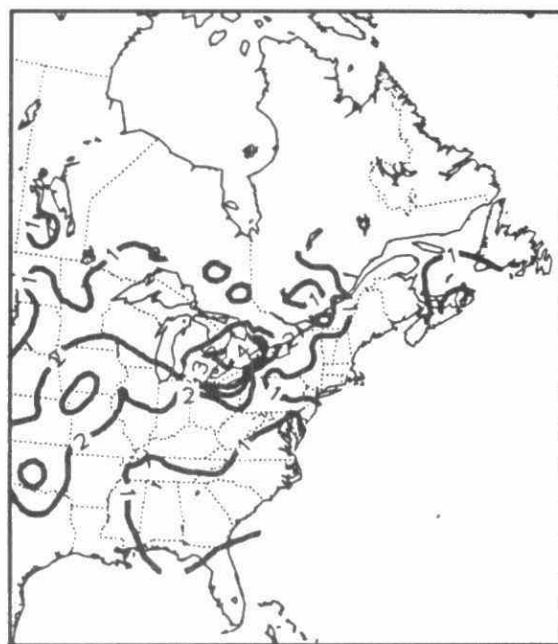
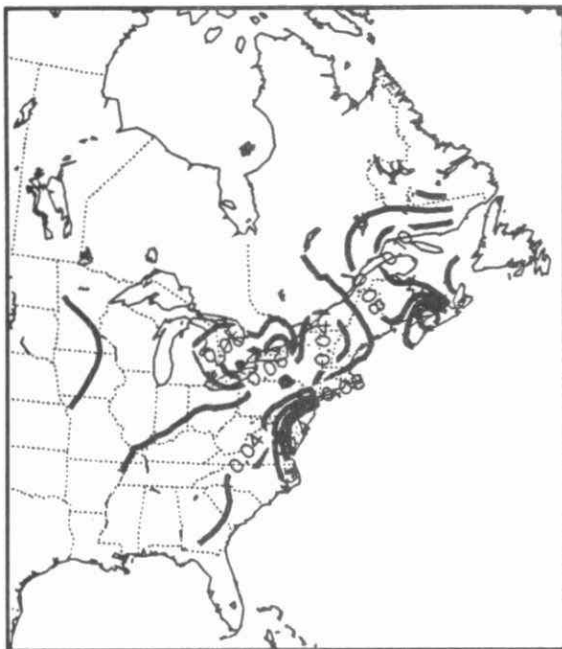
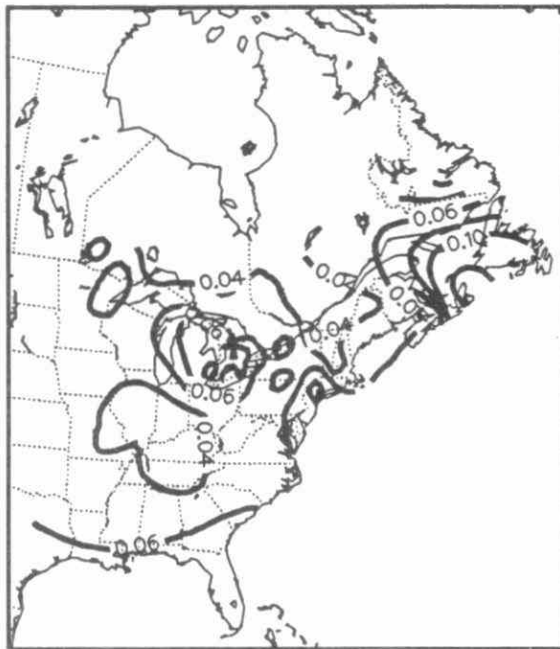


Fig. 3B-22 Patterns of annual wet deposition of Ca^{+2} (kg/ha/yr):1984-1987.

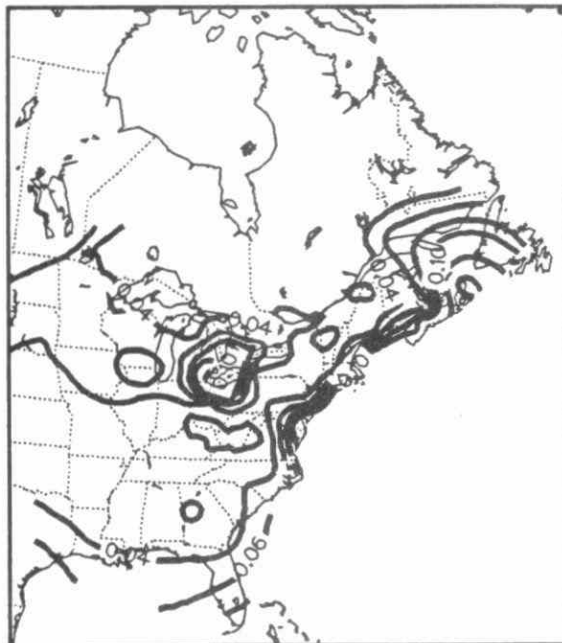
1980 ANNUAL MEAN MG CONCENTRATION IN PRECIPITATION (MG/L)



1981 ANNUAL MEAN MG CONCENTRATION IN PRECIPITATION (MG/L)



1982 ANNUAL MEAN MG CONCENTRATION IN PRECIPITATION (MG/L)



1983 ANNUAL MEAN MG CONCENTRATION IN PRECIPITATION (MG/L)

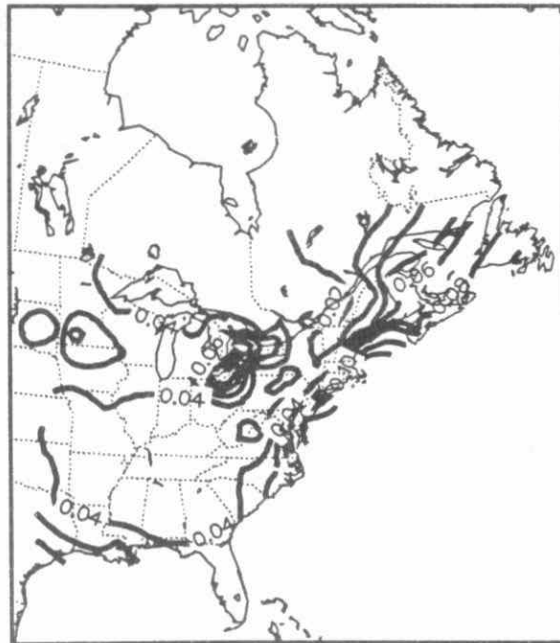
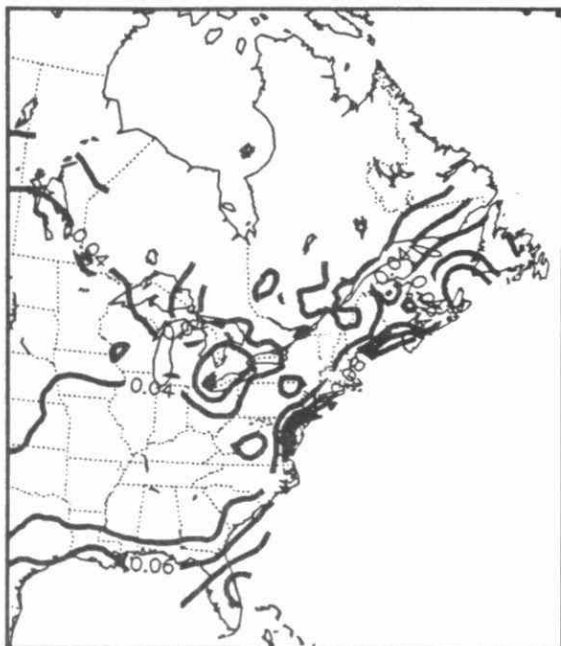


Fig. 3B-23 Patterns of annual precipitation-weighted mean concentrations of Mg^{+2} (mg/l): 1980-1983.

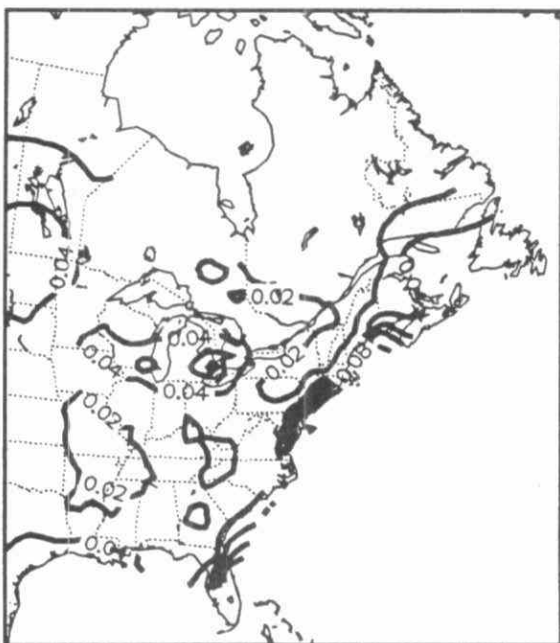
1984 ANNUAL MEAN MG CONCENTRATION IN PRECIPITATION (MG/L)



1985 ANNUAL MEAN MG CONCENTRATION IN PRECIPITATION (MG/L)



1986 ANNUAL MEAN MG CONCENTRATION IN PRECIPITATION (MG/L)



1987 ANNUAL MEAN MG CONCENTRATION IN PRECIPITATION (MG/L)

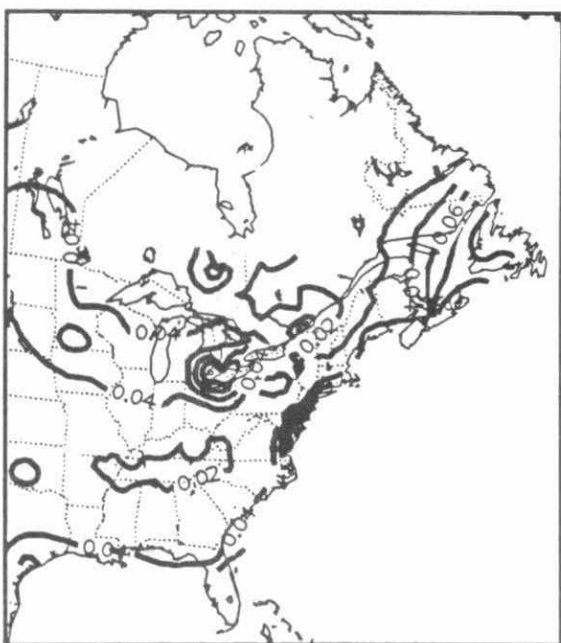
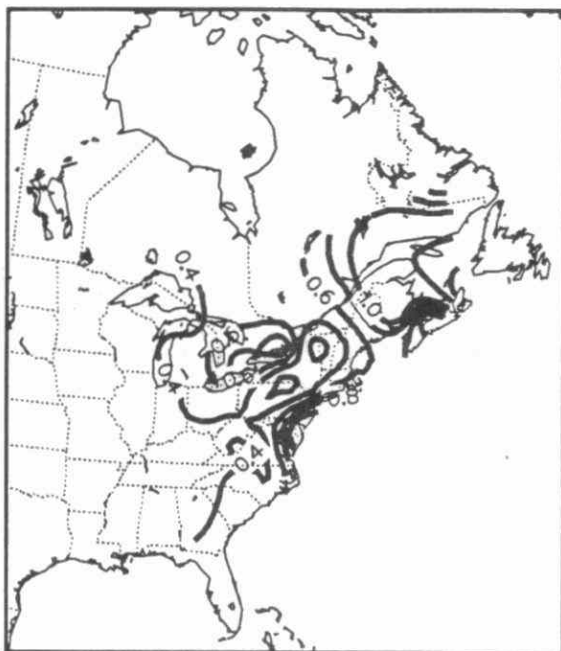
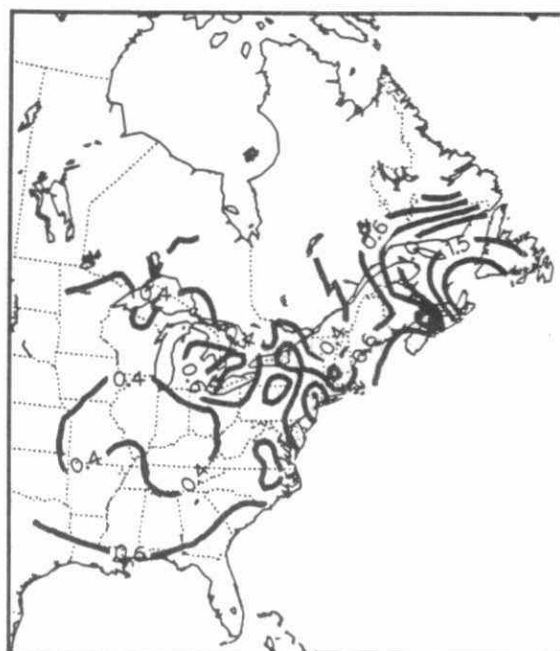


Fig. 3B-24 Patterns of annual precipitation-weighted mean concentrations of Mg^{+2} (mg/l): 1984-1987.

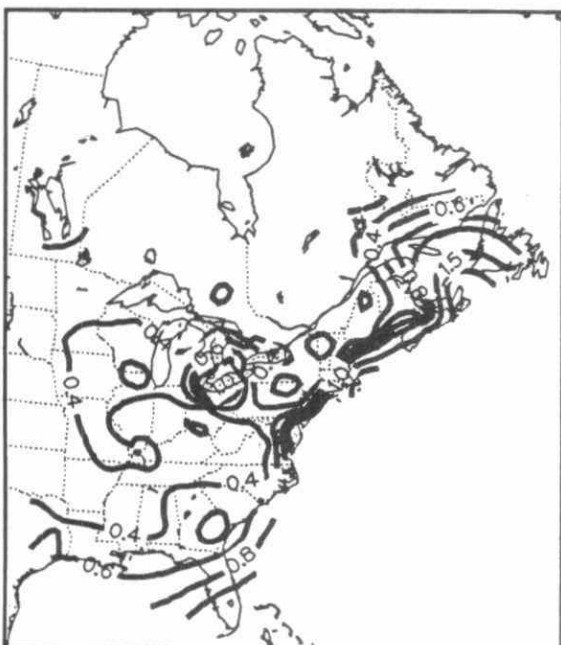
1980 WET MG DEPOSITION (KG/HA/YR)



1981 WET MG DEPOSITION (KG/HA/YR)



1982 WET MG DEPOSITION (KG/HA/YR)



1983 WET MG DEPOSITION (KG/HA/YR)

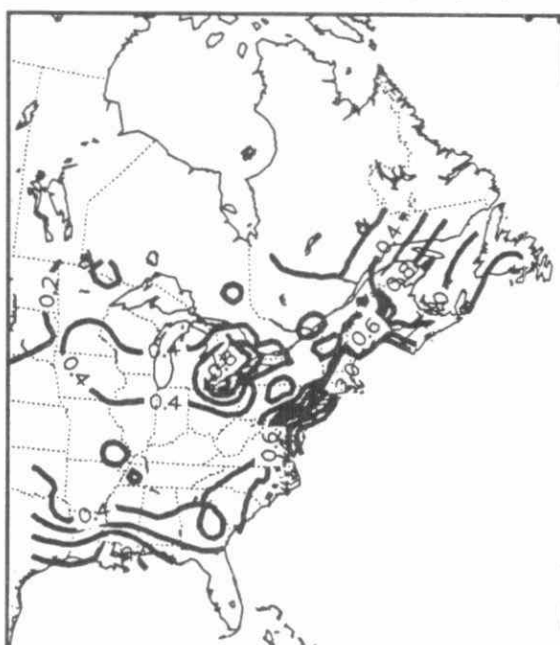
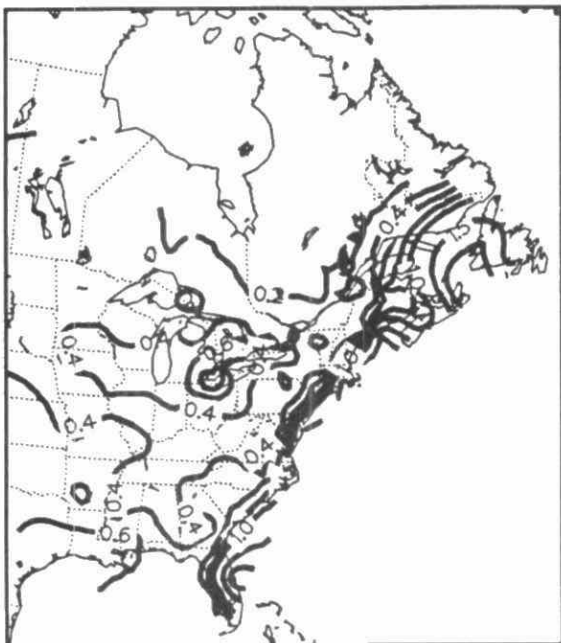
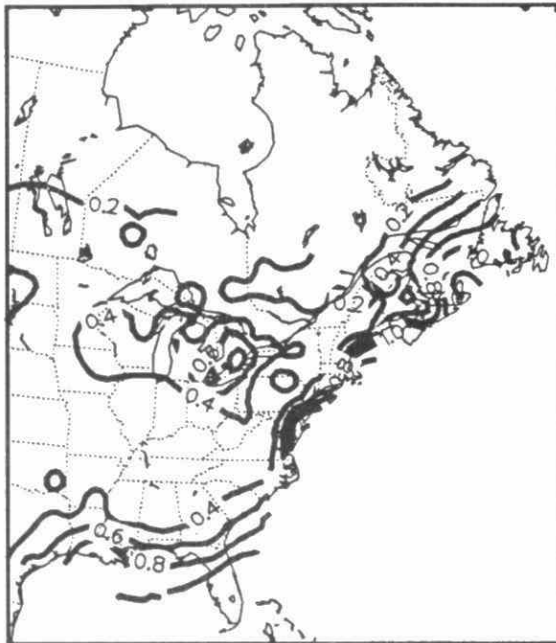


Fig. 3B-25 Patterns of annual wet deposition of Mg^{+2} (kg/ha/yr): 1980-1983.

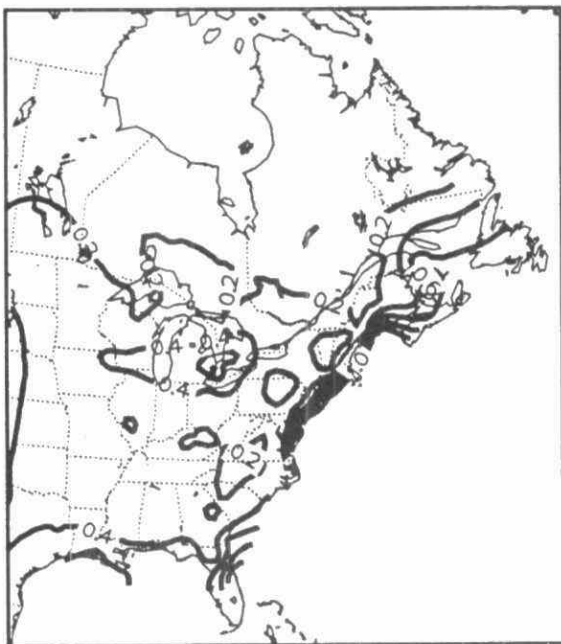
1984 WET MG DEPOSITION (KG/HA/YR)



1985 WET MG DEPOSITION (KG/HA/YR)



1986 WET MG DEPOSITION (KG/HA/YR)



1987 WET MG DEPOSITION (KG/HA/YR)

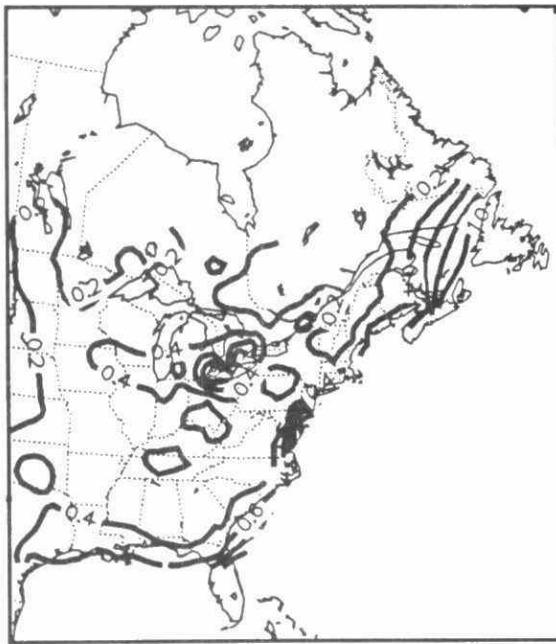
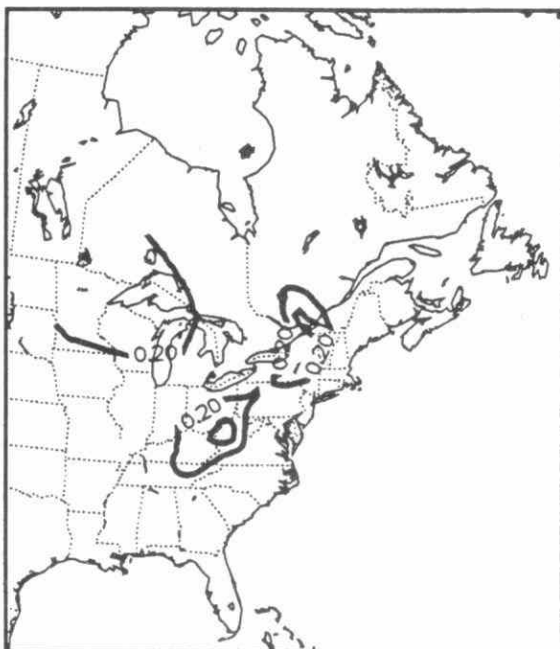
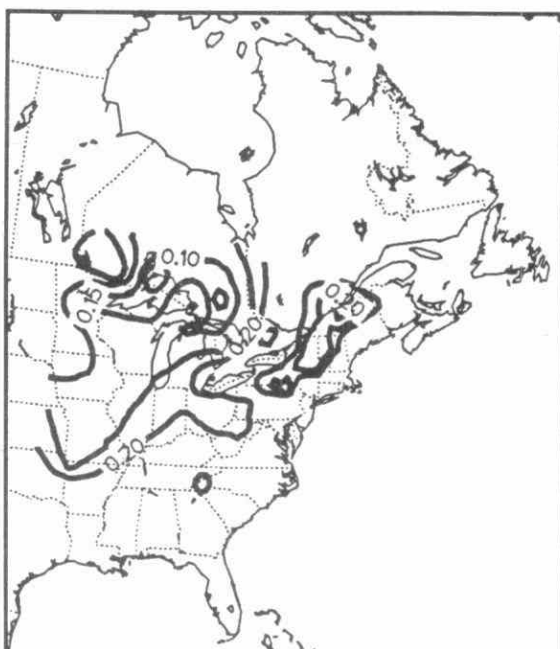


Fig. 3B-26 Patterns of annual wet deposition of Mg^{+2} (kg/ha/yr) 1984-1987.

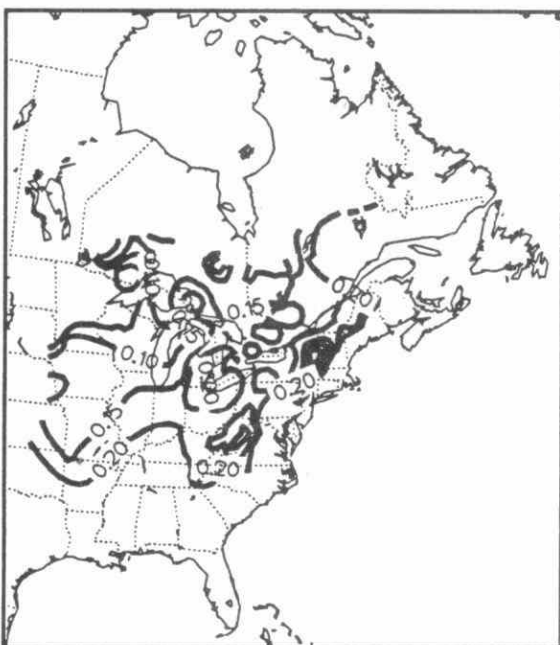
1980 ANNUAL MEAN CL CONCENTRATION IN PRECIPITATION (MG/L)



1981 ANNUAL MEAN CL CONCENTRATION IN PRECIPITATION (MG/L)



1982 ANNUAL MEAN CL CONCENTRATION IN PRECIPITATION (MG/L)



1983 ANNUAL MEAN CL CONCENTRATION IN PRECIPITATION (MG/L)

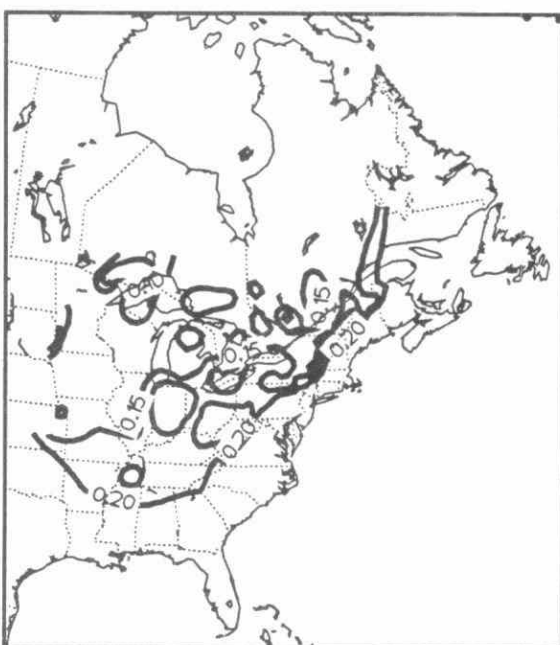
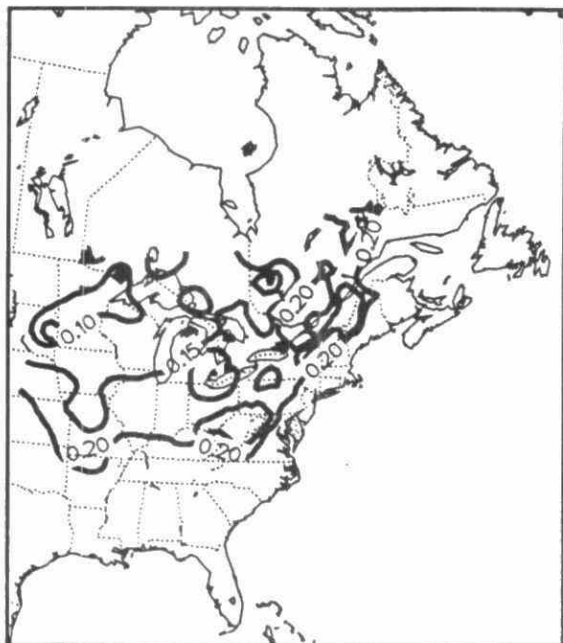
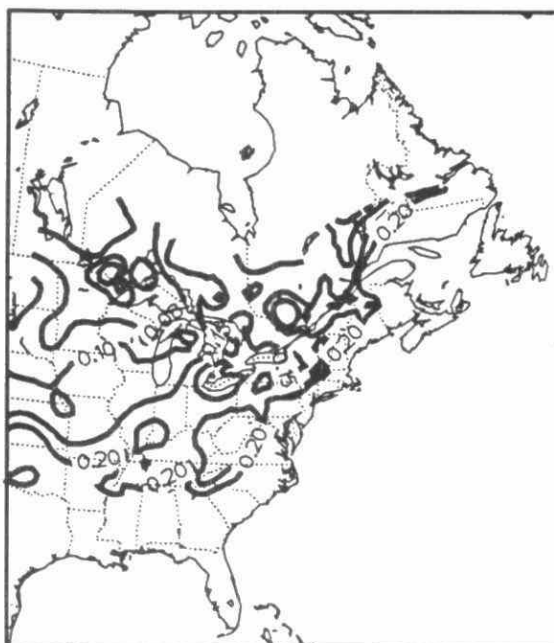


Fig. 3B-27 Patterns of annual precipitation-weighted mean concentrations of Cl^- (mg/l): 1980-1983.

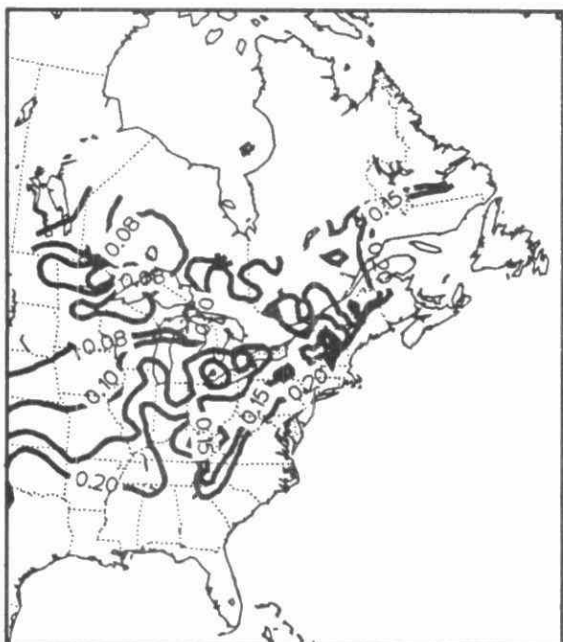
1984 ANNUAL MEAN CL CONCENTRATION IN PRECIPITATION (MG/L)



1985 ANNUAL MEAN CL CONCENTRATION IN PRECIPITATION (MG/L)



1986 ANNUAL MEAN CL CONCENTRATION IN PRECIPITATION (MG/L)



1987 ANNUAL MEAN CL CONCENTRATION IN PRECIPITATION (MG/L)

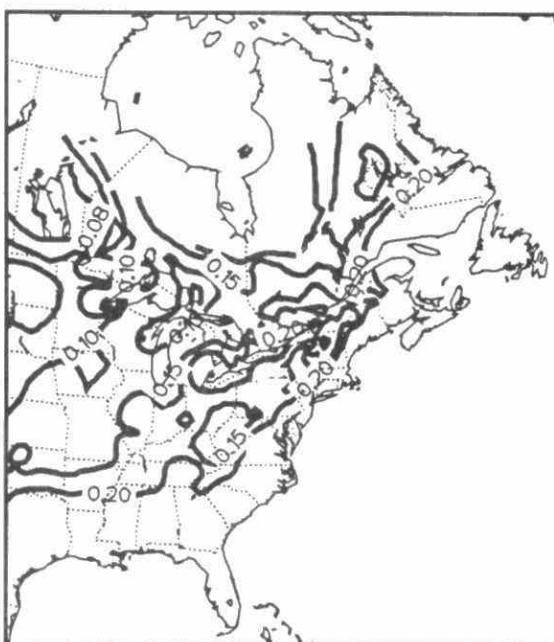
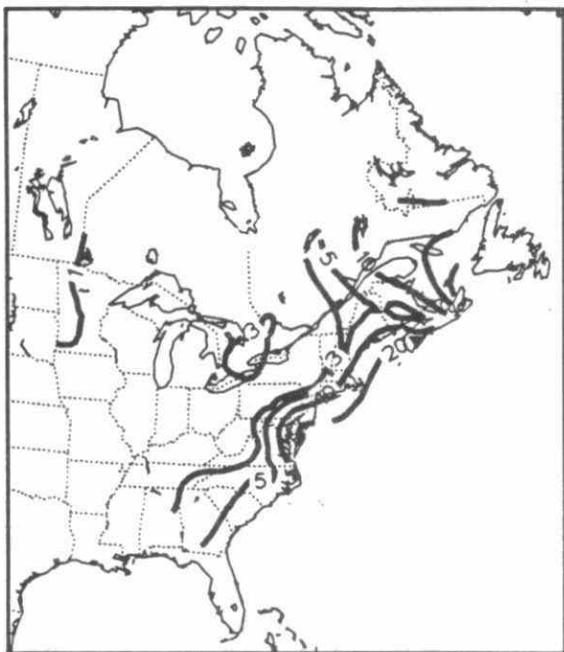
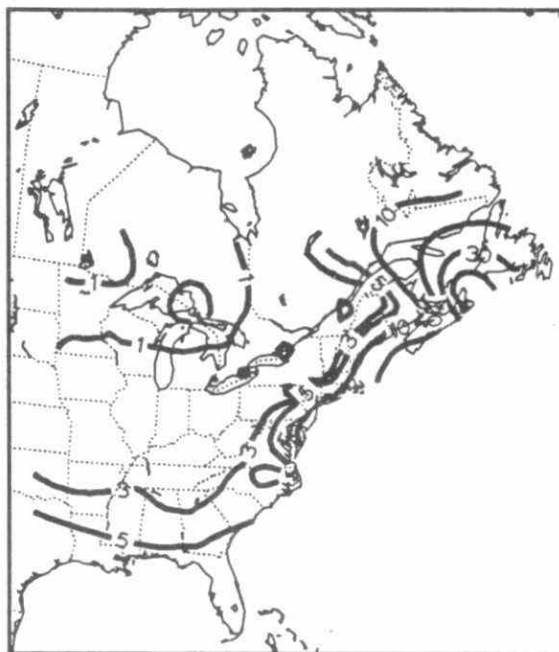


Fig. 3B-28 Patterns of annual precipitation-weighted mean concentrations of Cl^- (mg/l): 1984-1987.

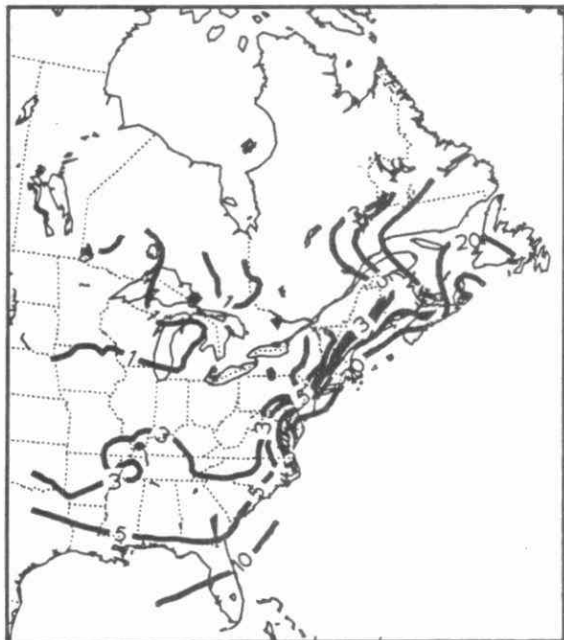
1980 WET CL DEPOSITION (KG/HA/YR)



1981 WET CL DEPOSITION (KG/HA/YR)



1982 WET CL DEPOSITION (KG/HA/YR)



1983 WET CL DEPOSITION (KG/HA/YR)

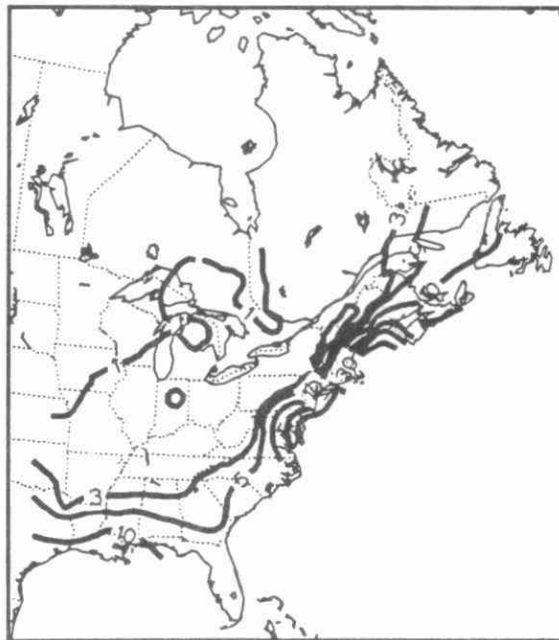
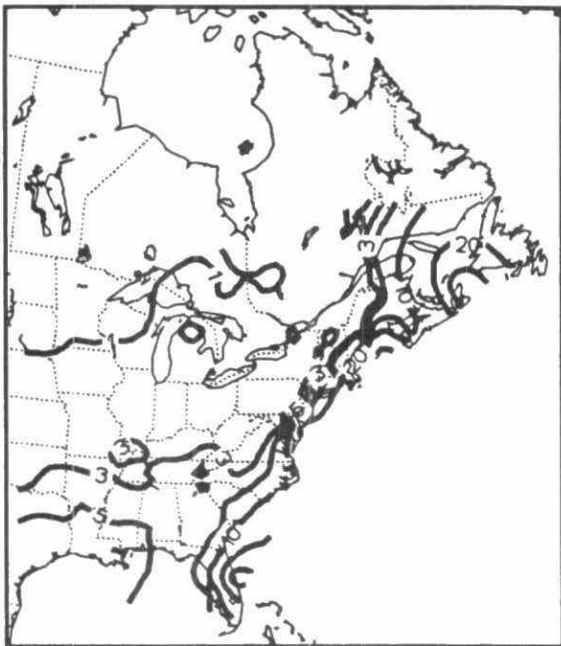
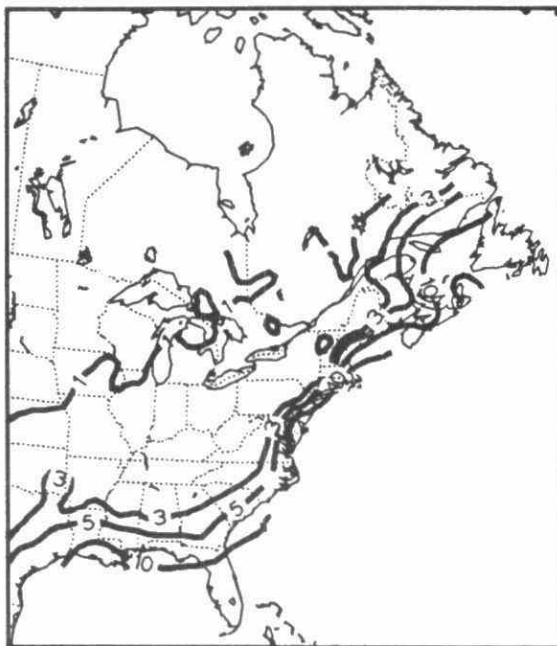


Fig. 3B-29 Patterns of annual wet deposition of Cl^- (kg/ha/yr)(1980-1983).

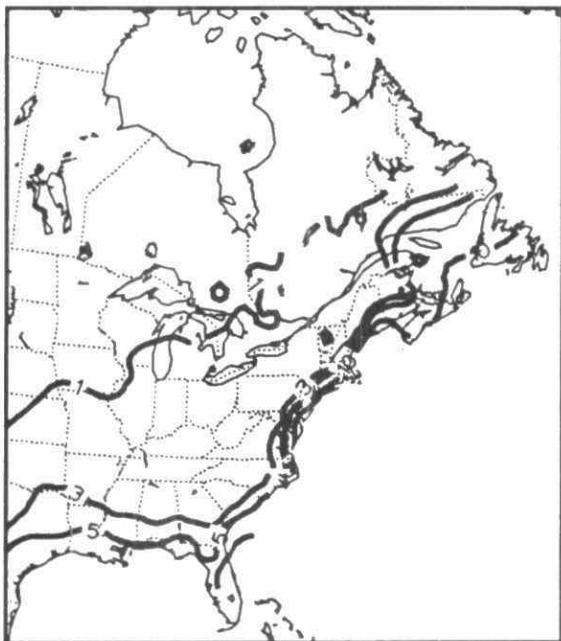
1984 WET CL DEPOSITION (KG/HA/YR)



1985 WET CL DEPOSITION (KG/HA/YR)



1986 WET CL DEPOSITION (KG/HA/YR)



1987 WET CL DEPOSITION (KG/HA/YR)

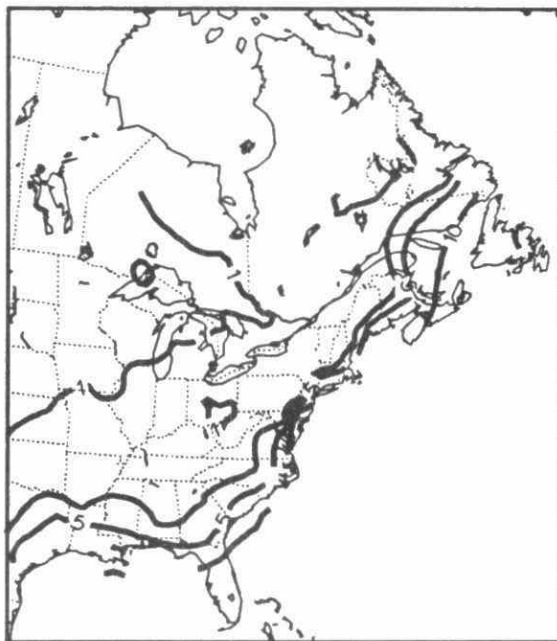
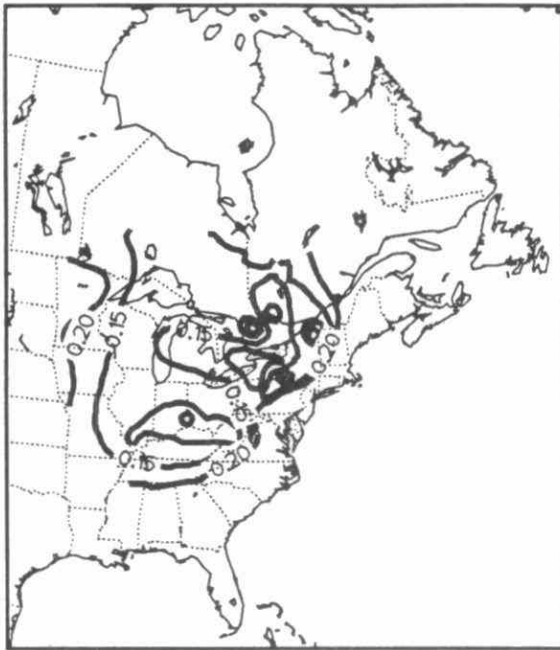
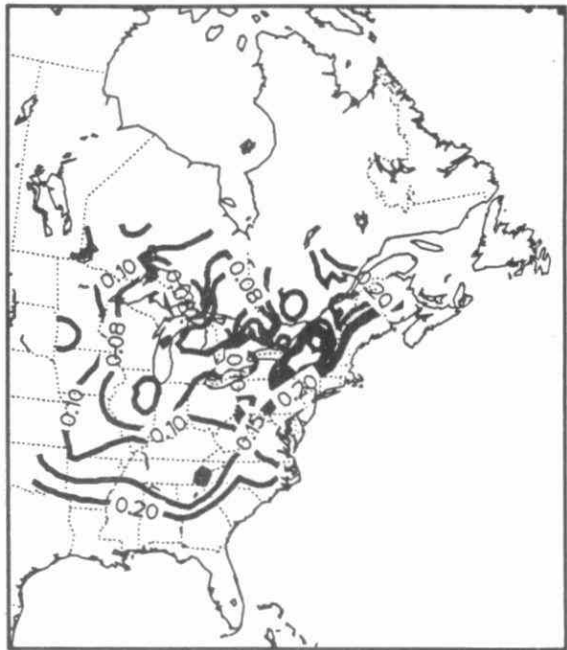


Fig. 3B-30 Patterns of annual wet deposition of Cl^- (kg/ha/yr)(1984-1987).

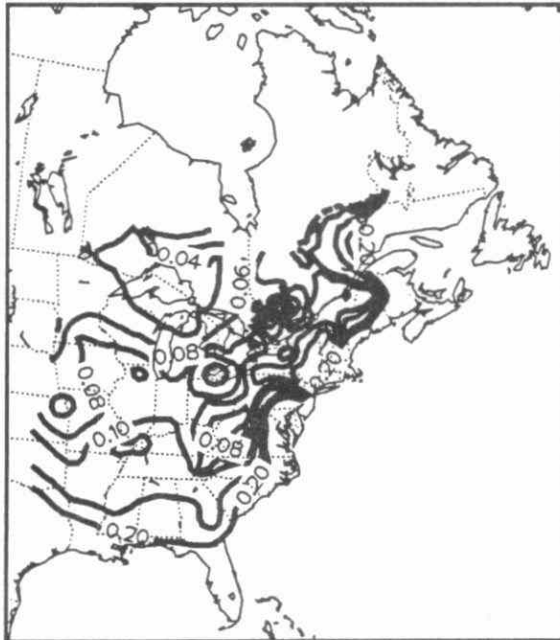
1980 ANNUAL MEAN NA CONCENTRATION IN PRECIPITATION (MG/L)



1981 ANNUAL MEAN NA CONCENTRATION IN PRECIPITATION (MG/L)



1982 ANNUAL MEAN NA CONCENTRATION IN PRECIPITATION (MG/L)



1983 ANNUAL MEAN NA CONCENTRATION IN PRECIPITATION (MG/L)

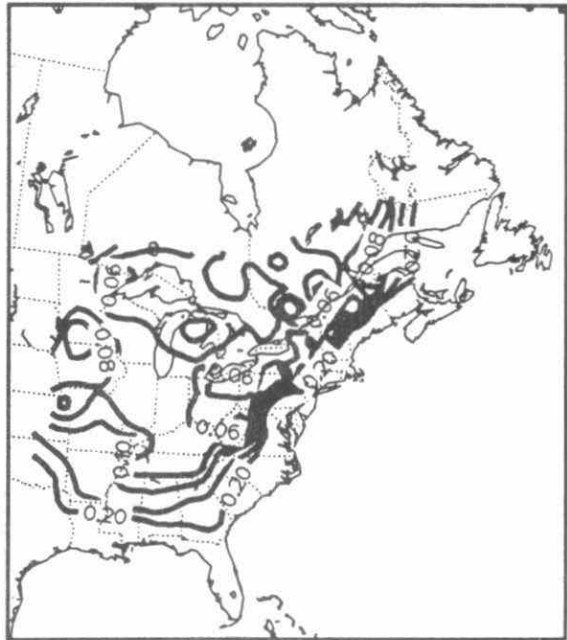
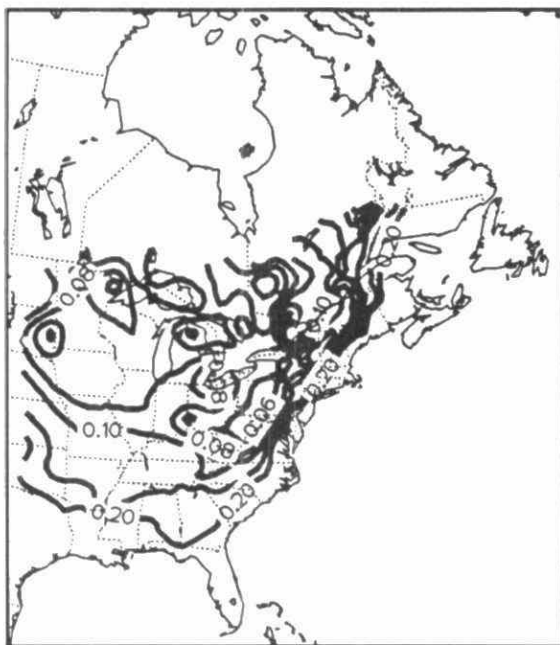
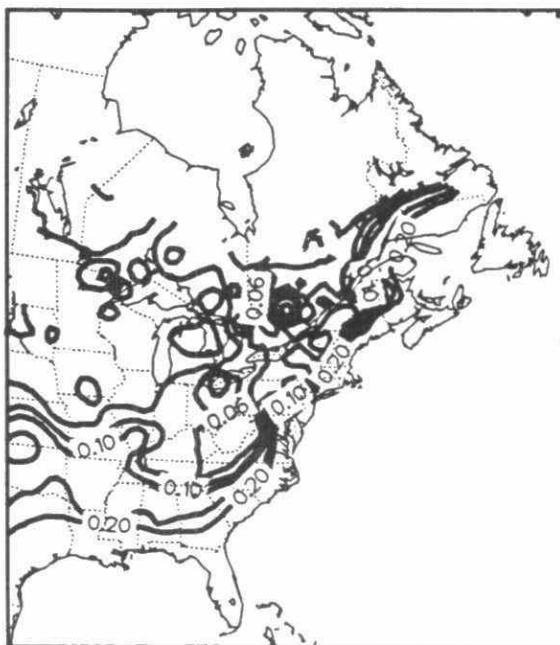


Fig. 3B-31 Patterns of annual precipitation-weighted mean concentrations of Na^+ (mg/l): 1980-1983.

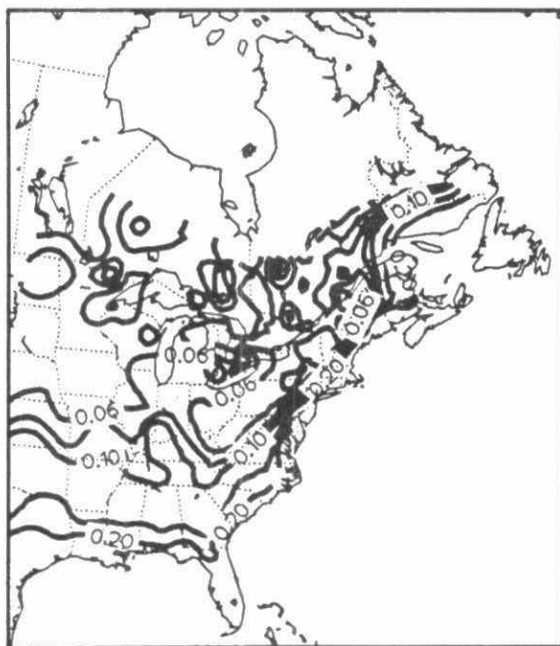
1984 ANNUAL MEAN NA CONCENTRATION IN PRECIPITATION (MG/L)



1985 ANNUAL MEAN NA CONCENTRATION IN PRECIPITATION (MG/L)



1986 ANNUAL MEAN NA CONCENTRATION IN PRECIPITATION (MG/L)



1987 ANNUAL MEAN NA CONCENTRATION IN PRECIPITATION (MG/L)

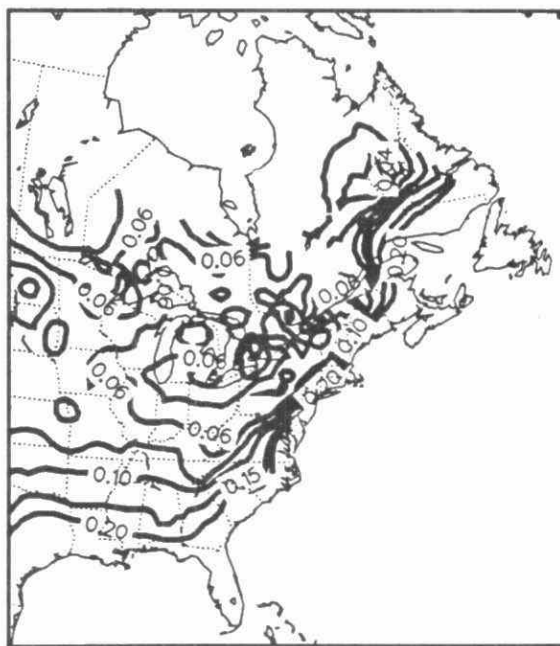
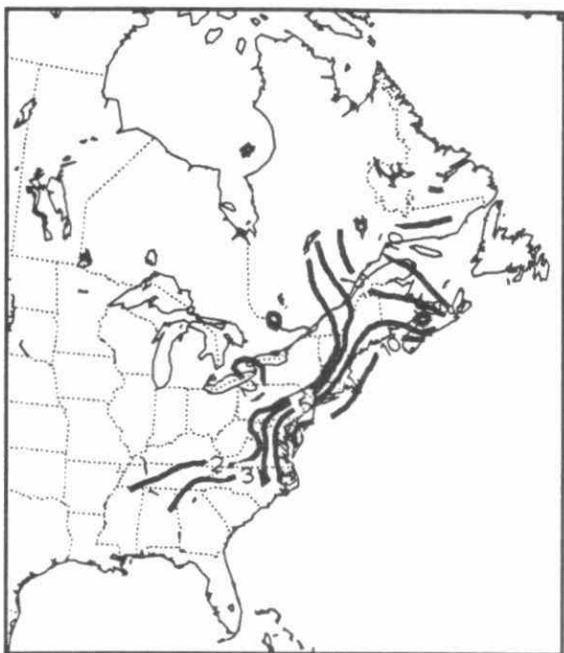
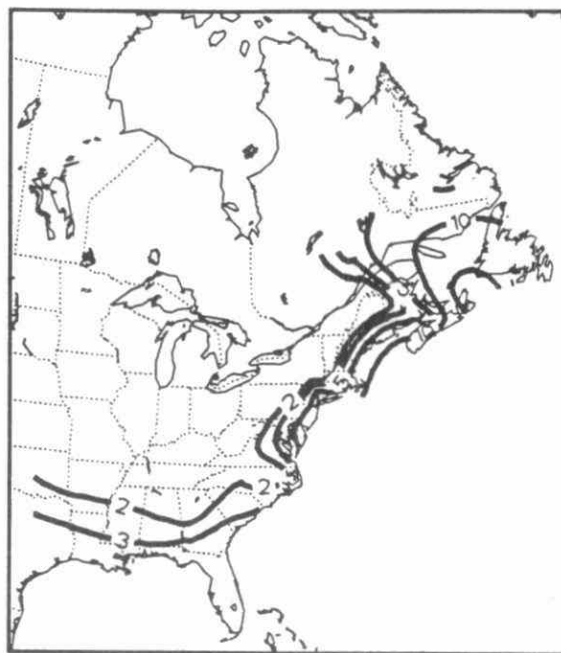


Fig. 3B-32 Patterns of annual precipitation-weighted mean concentrations of Na^+ (mg/l): 1984-1987.

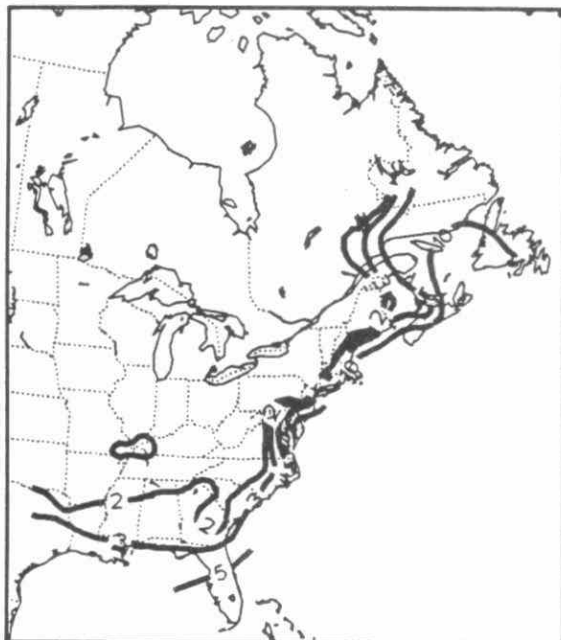
1980 WET NA DEPOSITION (KG/HA/YR)



1981 WET NA DEPOSITION (KG/HA/YR)



1982 WET NA DEPOSITION (KG/HA/YR)



1983 WET NA DEPOSITION (KG/HA/YR)

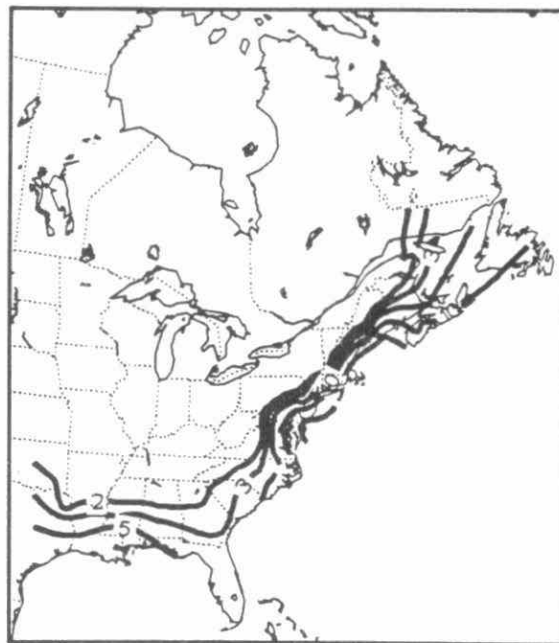
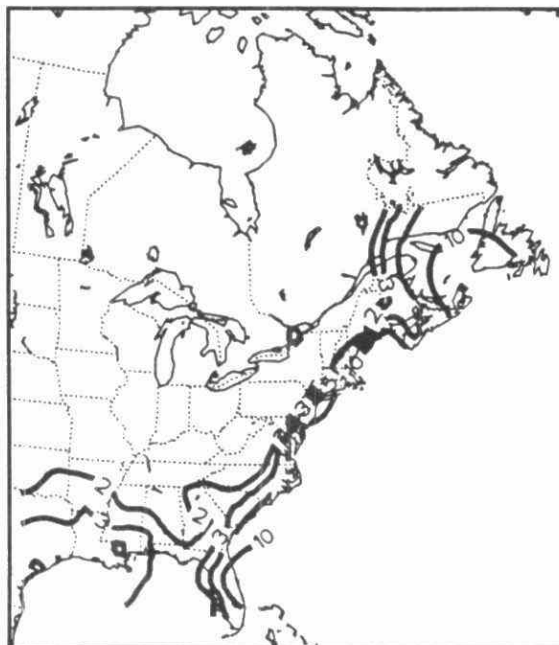
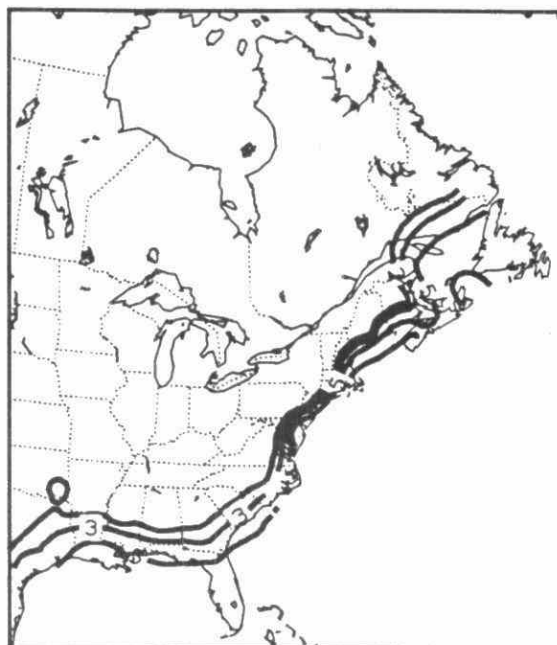


Fig. 3B-33 Patterns of annual wet deposition of Na^+ (kg/ha/yr):1980-1983.

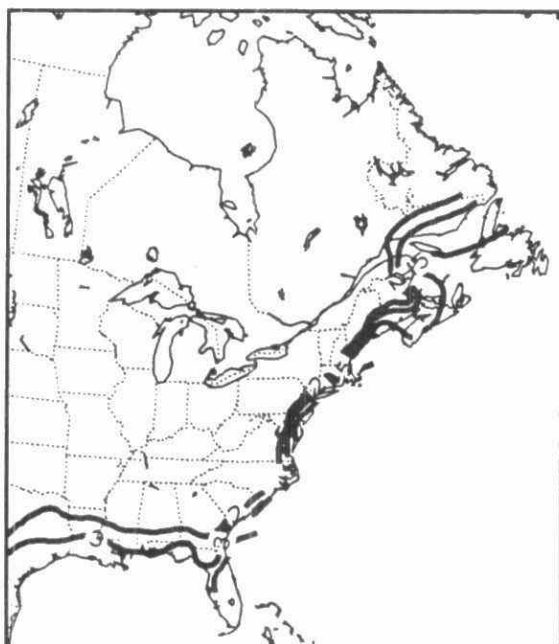
1984 WET NA DEPOSITION (KG/HA/YR)



1985 WET NA DEPOSITION (KG/HA/YR)



1986 WET NA DEPOSITION (KG/HA/YR)



1987 WET NA DEPOSITION (KG/HA/YR)

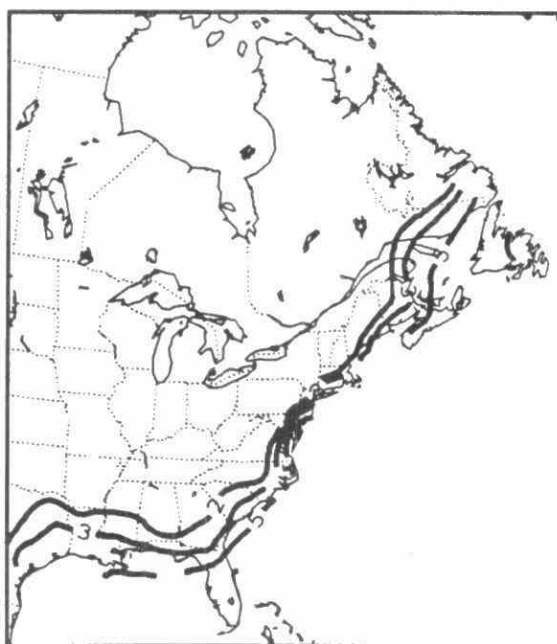
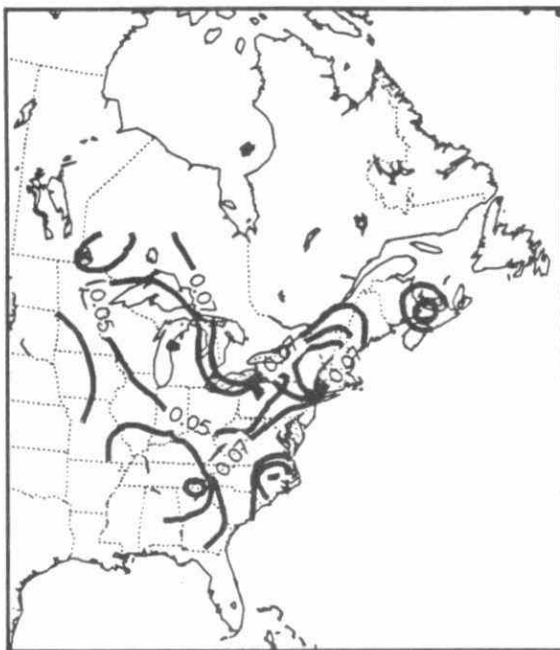
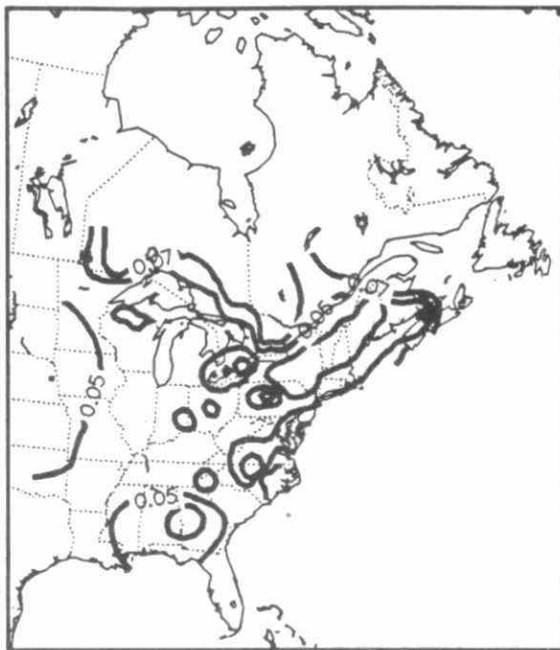


Fig. 3B-34 Patterns of annual wet deposition of Na^+ (kg/ha/yr):1984-1987.

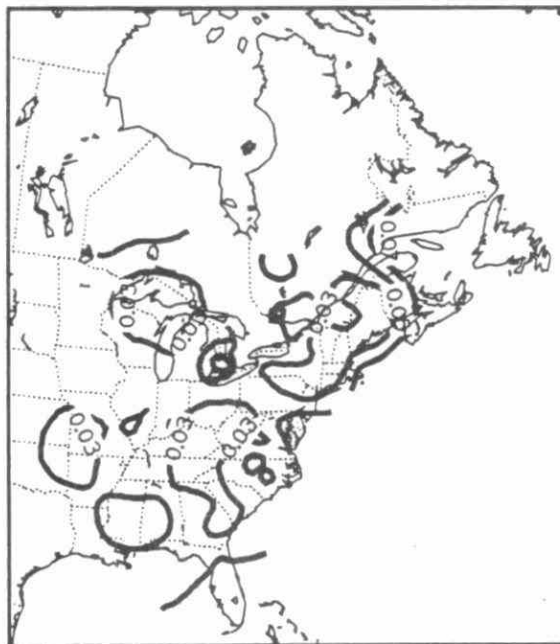
1980 ANNUAL MEAN K CONCENTRATION IN PRECIPITATION (MG/L)



1981 ANNUAL MEAN K CONCENTRATION IN PRECIPITATION (MG/L)



1982 ANNUAL MEAN K CONCENTRATION IN PRECIPITATION (MG/L)



1983 ANNUAL MEAN K CONCENTRATION IN PRECIPITATION (MG/L)

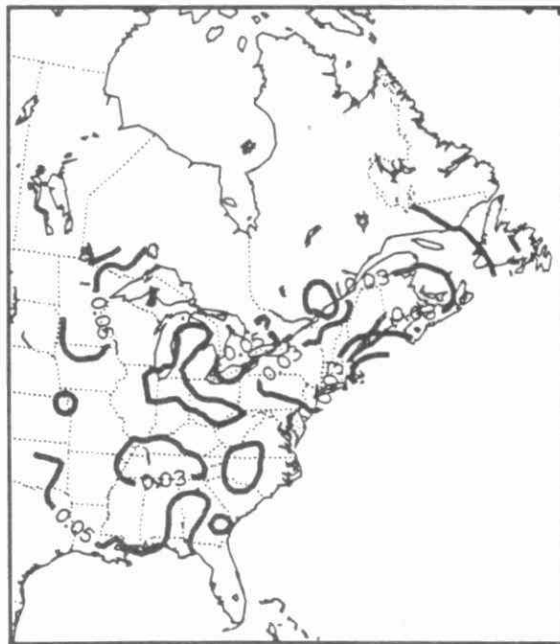
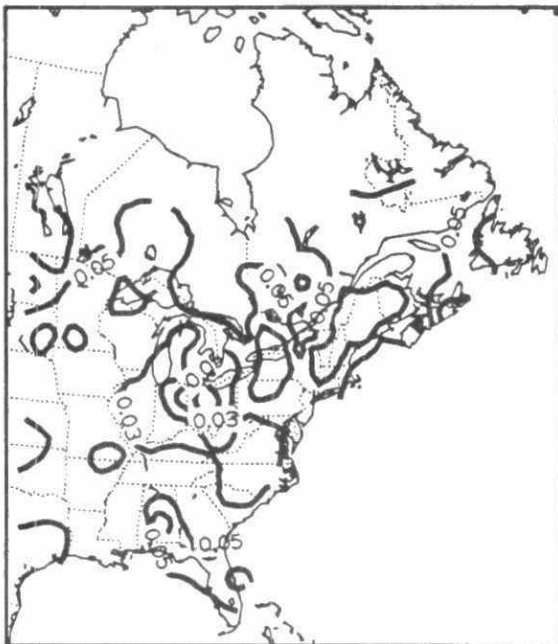
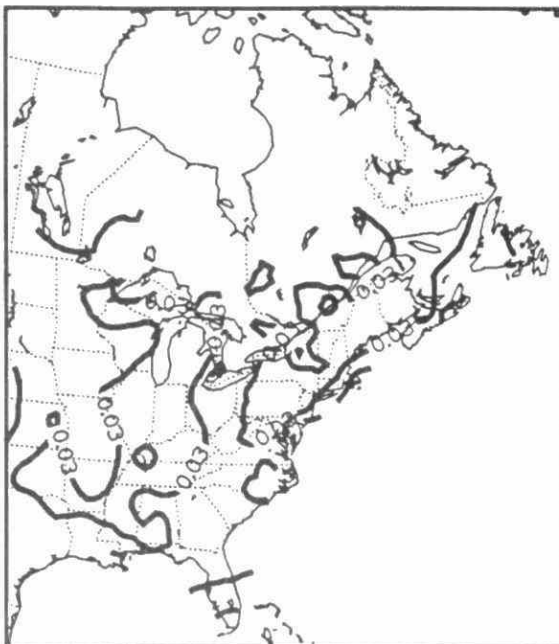


Fig. 3B-35 Patterns of annual precipitation-weighted mean concentrations of K^+ (mg/l): 1980-1983.

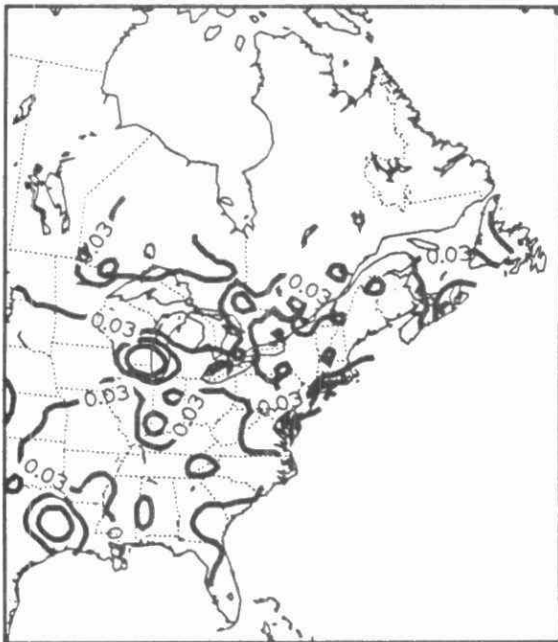
1984 ANNUAL MEAN K CONCENTRATION IN PRECIPITATION (MG/L)



1985 ANNUAL MEAN K CONCENTRATION IN PRECIPITATION (MG/L)



1986 ANNUAL MEAN K CONCENTRATION IN PRECIPITATION (MG/L)



1987 ANNUAL MEAN K CONCENTRATION IN PRECIPITATION (MG/L)

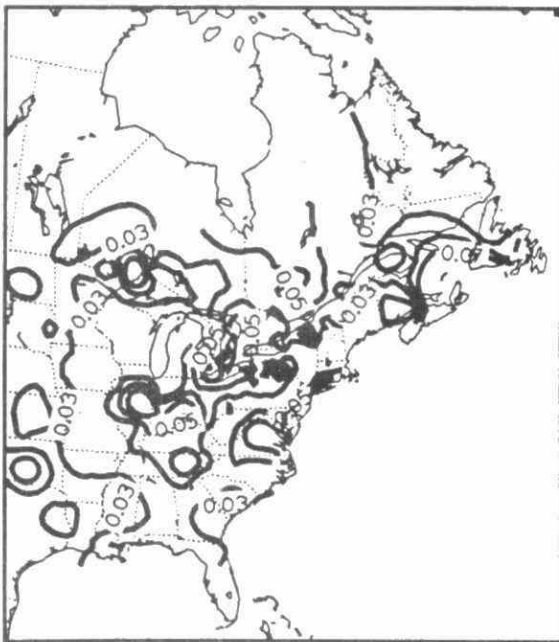
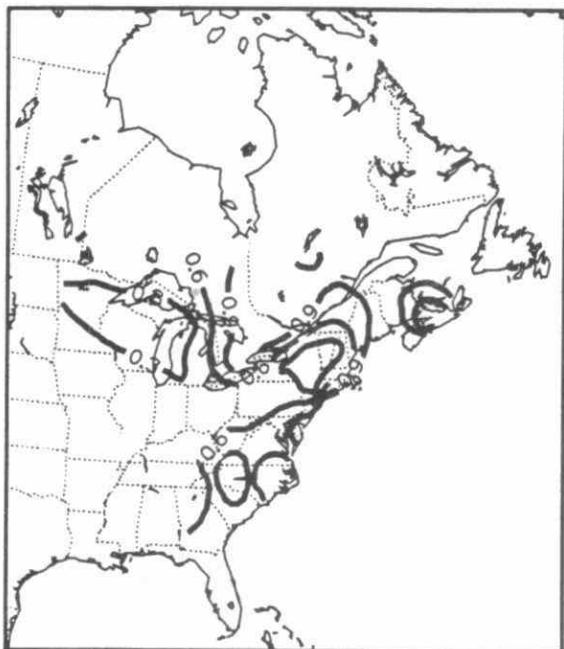
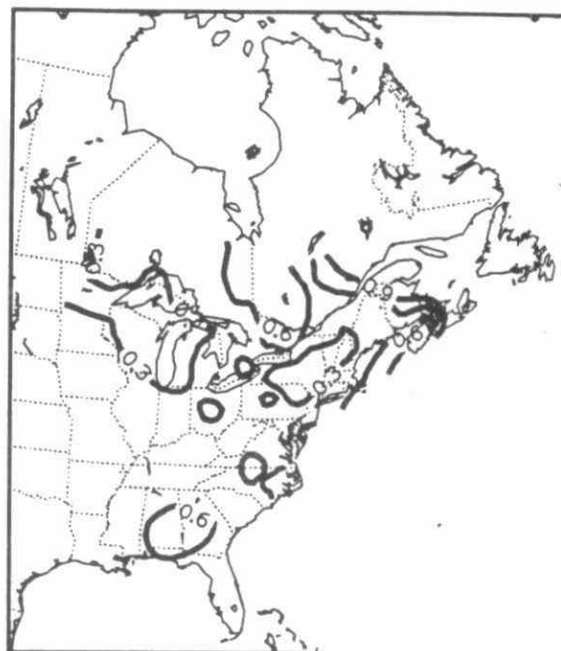


Fig. 3B-36 Patterns of annual precipitation-weighted mean concentrations of K^+ (mg/l): 1984-1987.

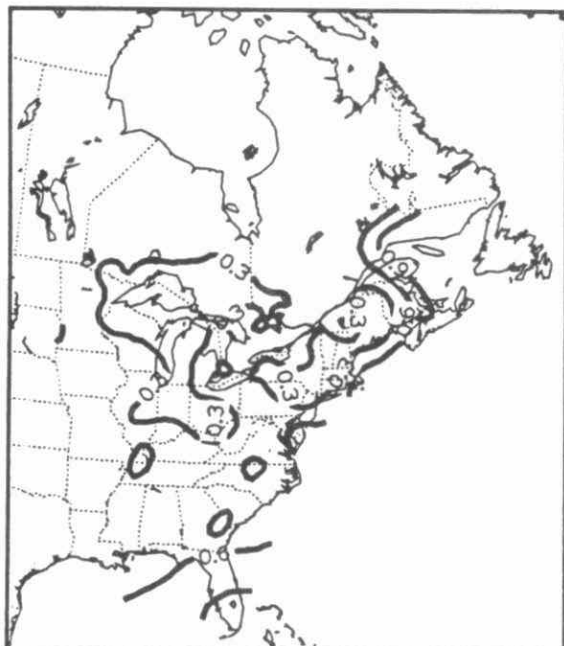
1980 WET K DEPOSITION (KG/HA/YR)



1981 WET K DEPOSITION (KG/HA/YR)



1982 WET K DEPOSITION (KG/HA/YR)



1983 WET K DEPOSITION (KG/HA/YR)

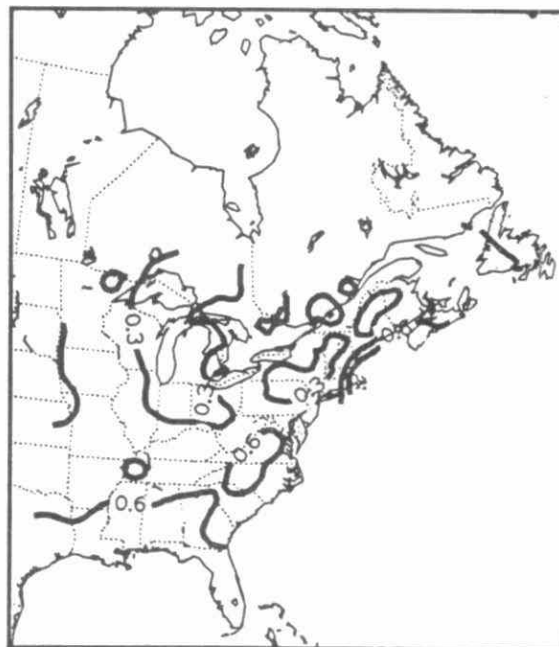
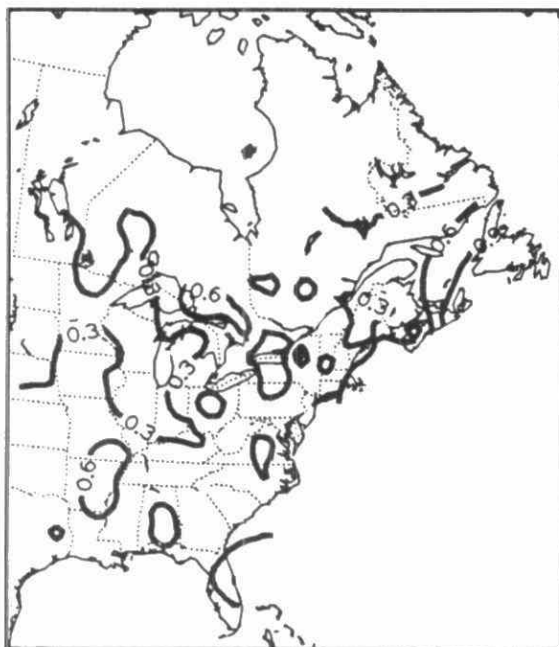
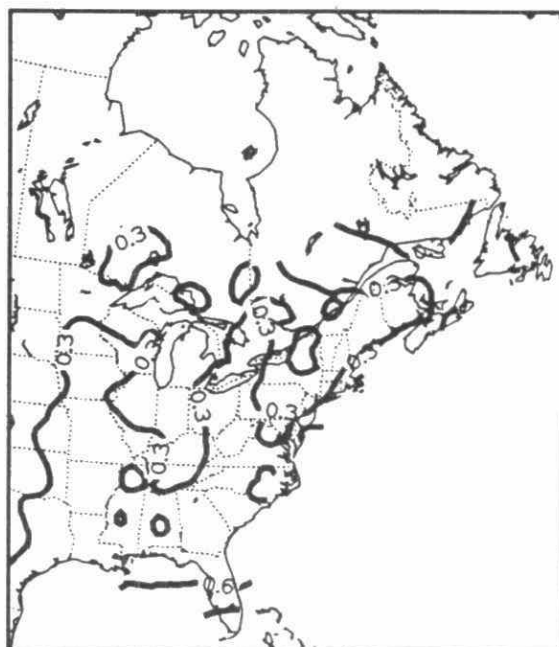


Fig. 3B-37 Patterns of annual wet deposition of K^+ (kg/ha/yr):1980-1983.

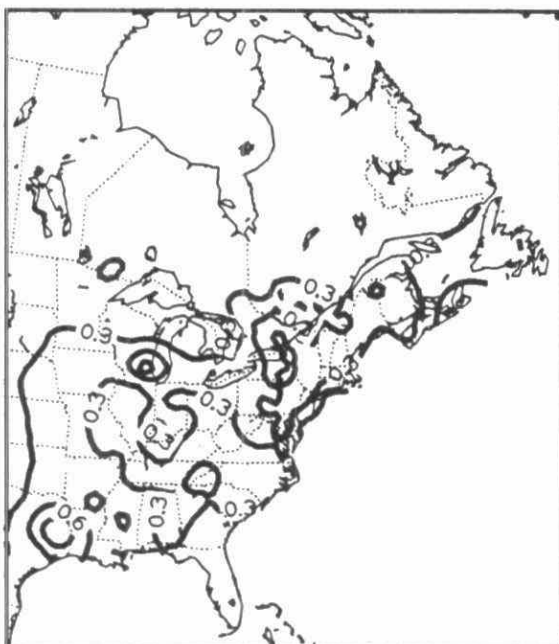
1984 WET K DEPOSITION (KG/HA/YR)



1985 WET K DEPOSITION (KG/HA/YR)



1986 WET K DEPOSITION (KG/HA/YR)



1987 WET K DEPOSITION (KG/HA/YR)

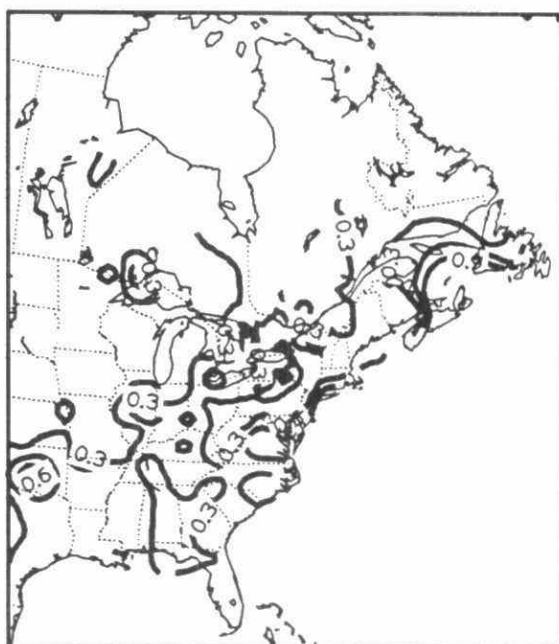
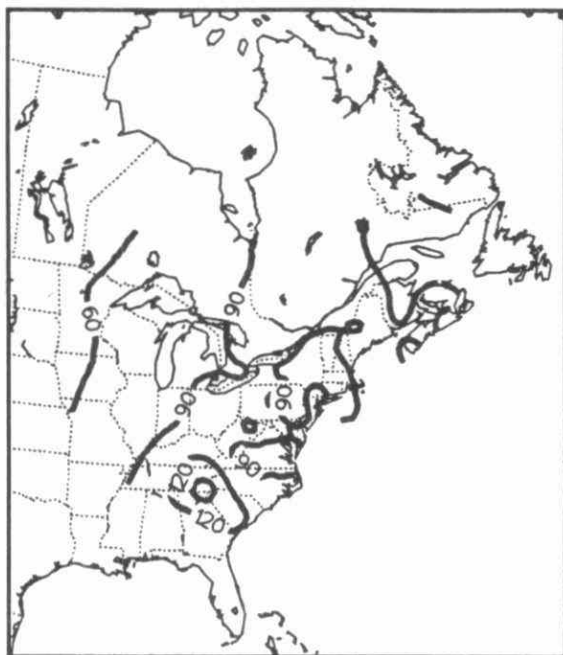
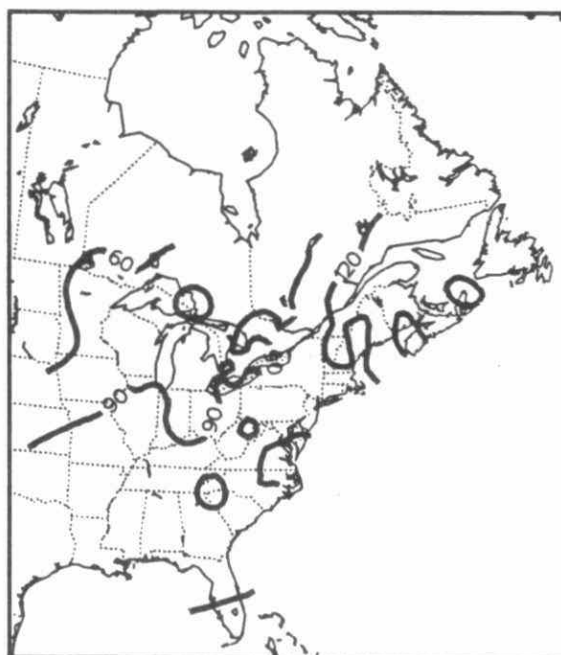


Fig. 3B-38 Patterns of annual wet deposition of K^+ (kg/ha/yr):1984-1987.

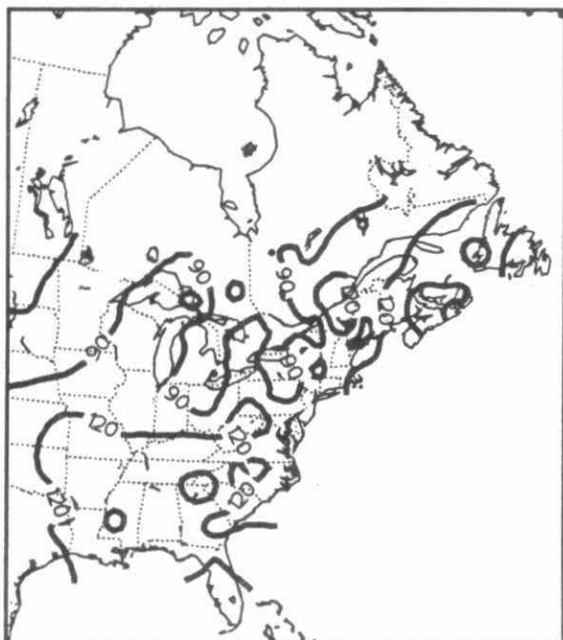
1980 TOTAL PRECIPITATION DEPTH (CM)



1981 TOTAL PRECIPITATION DEPTH (CM)



1982 TOTAL PRECIPITATION DEPTH (CM)



1983 TOTAL PRECIPITATION DEPTH (CM)

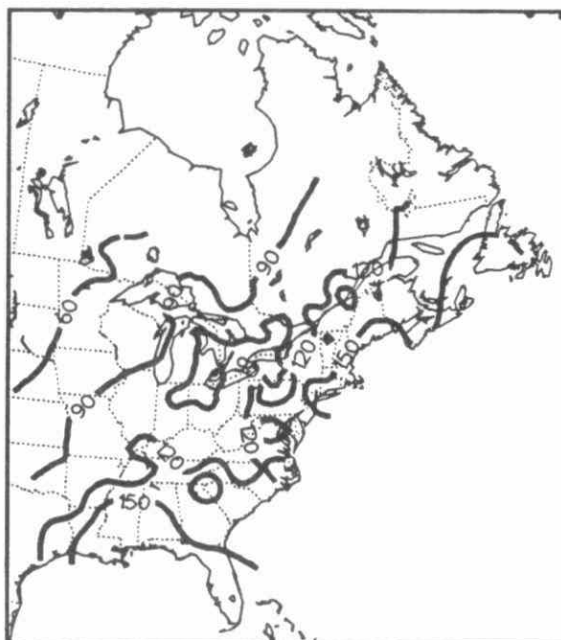
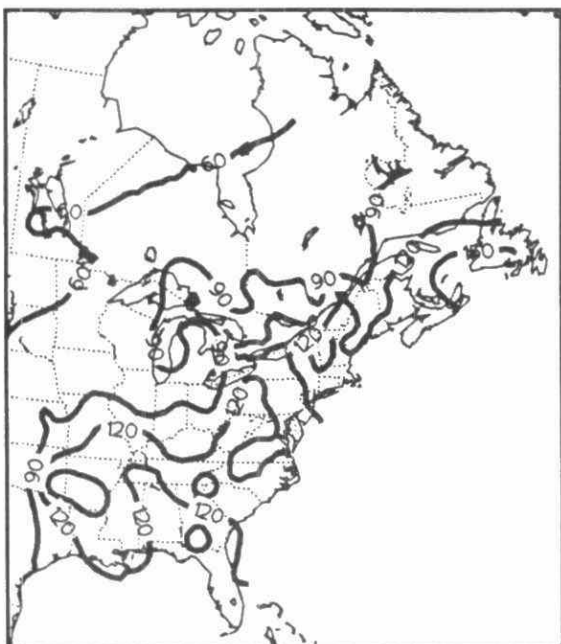
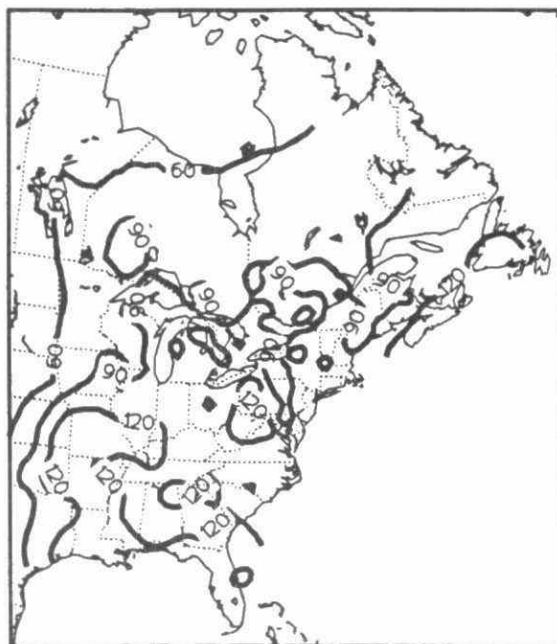


Fig. 3B-39 Patterns of total precipitation depth (cm):1980-1983.

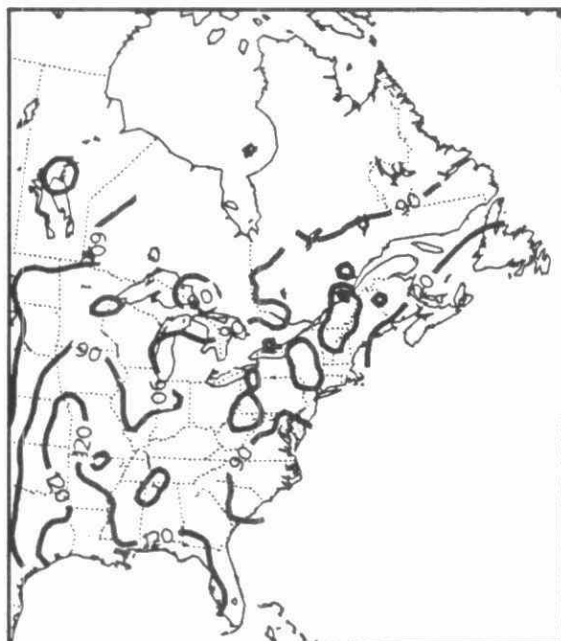
1984 TOTAL PRECIPITATION DEPTH (CM)



1985 TOTAL PRECIPITATION DEPTH (CM)



1986 TOTAL PRECIPITATION DEPTH (CM)



1987 TOTAL PRECIPITATION DEPTH (CM)

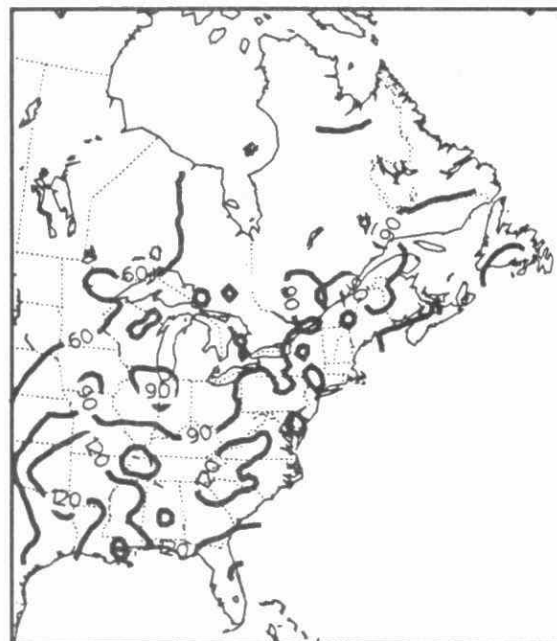
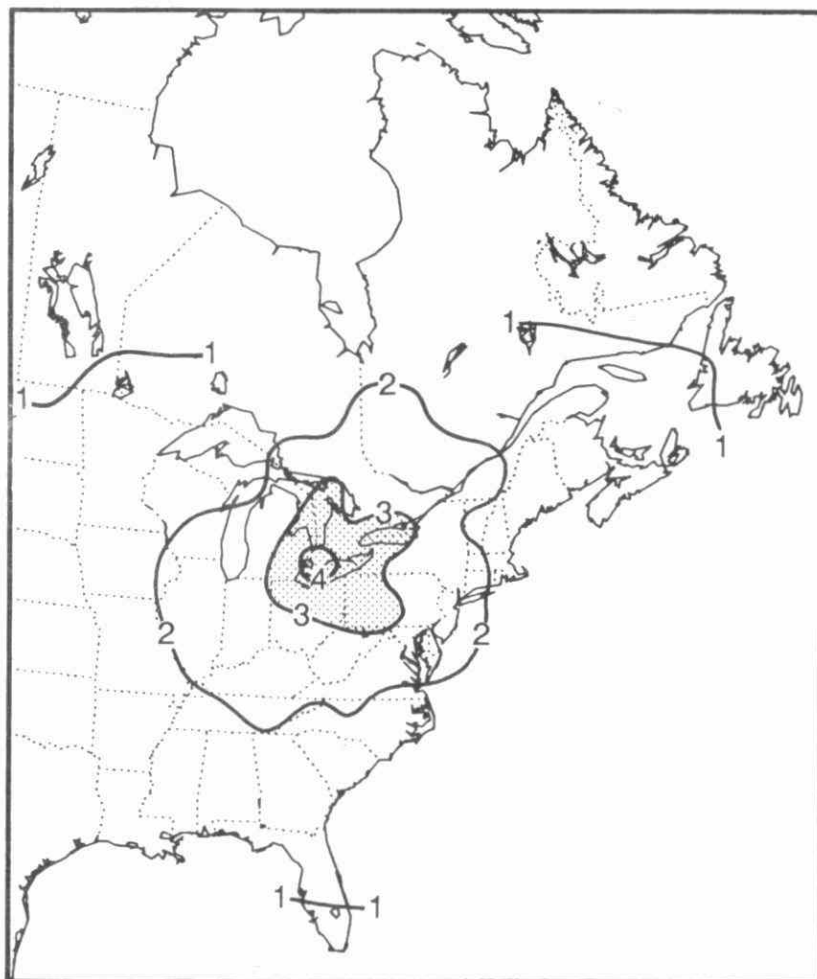


Fig. 3B-40 Patterns of total precipitation depth (cm):1984-1987.

6-YEAR (1982-87) MEAN SO_4^- CONCENTRATION
IN PRECIPITATION (mg/l)



6-YEAR (1982-87) MEAN SO_4^- DEPOSITION (kg/ha/yr)

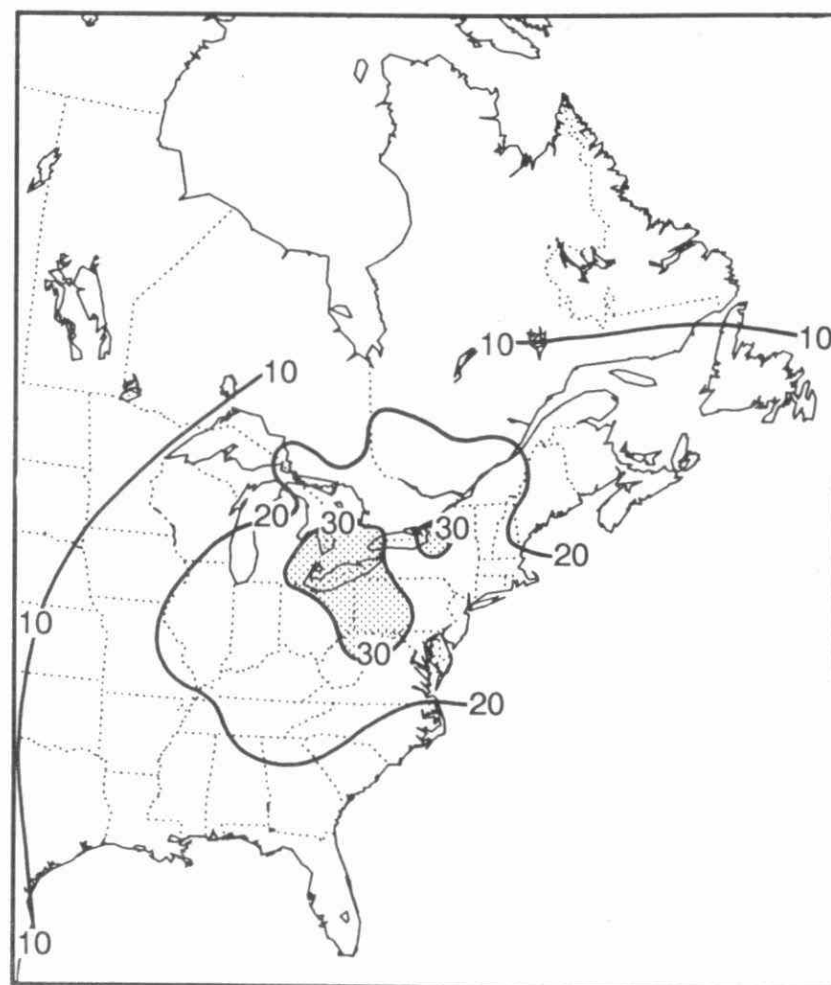


Fig. 3B-41 Six-year mean concentration and deposition patterns of SO_4^- (1982-1987).

6-YEAR (1982-87) MEAN PH DISTRIBUTION

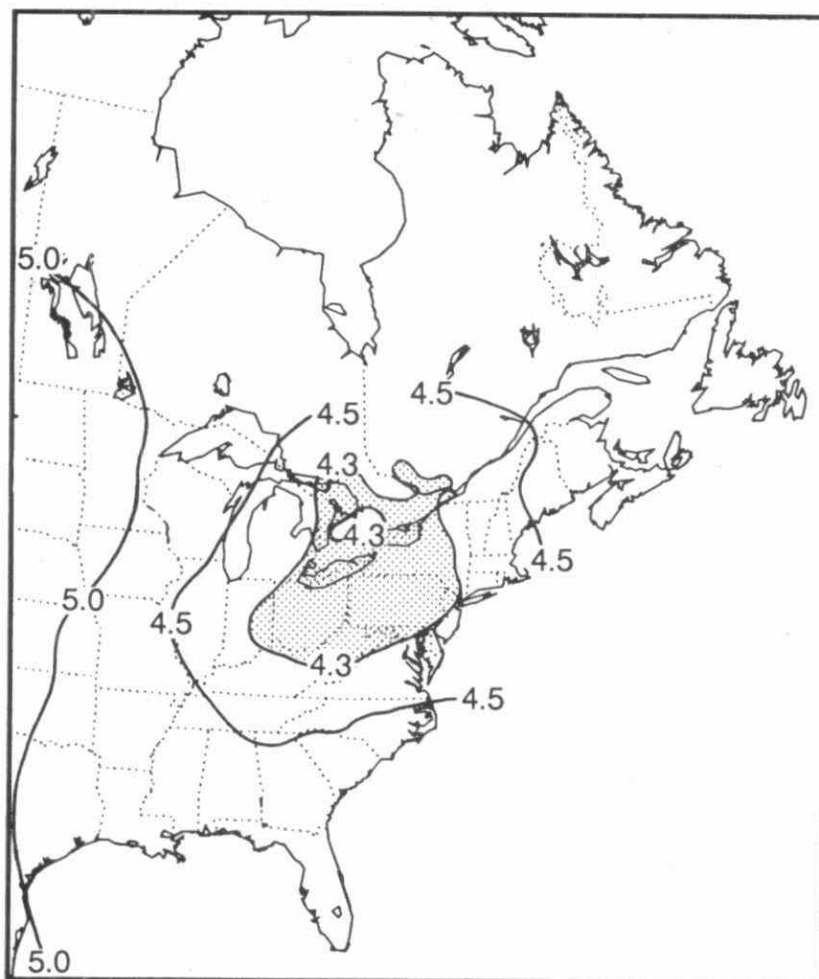
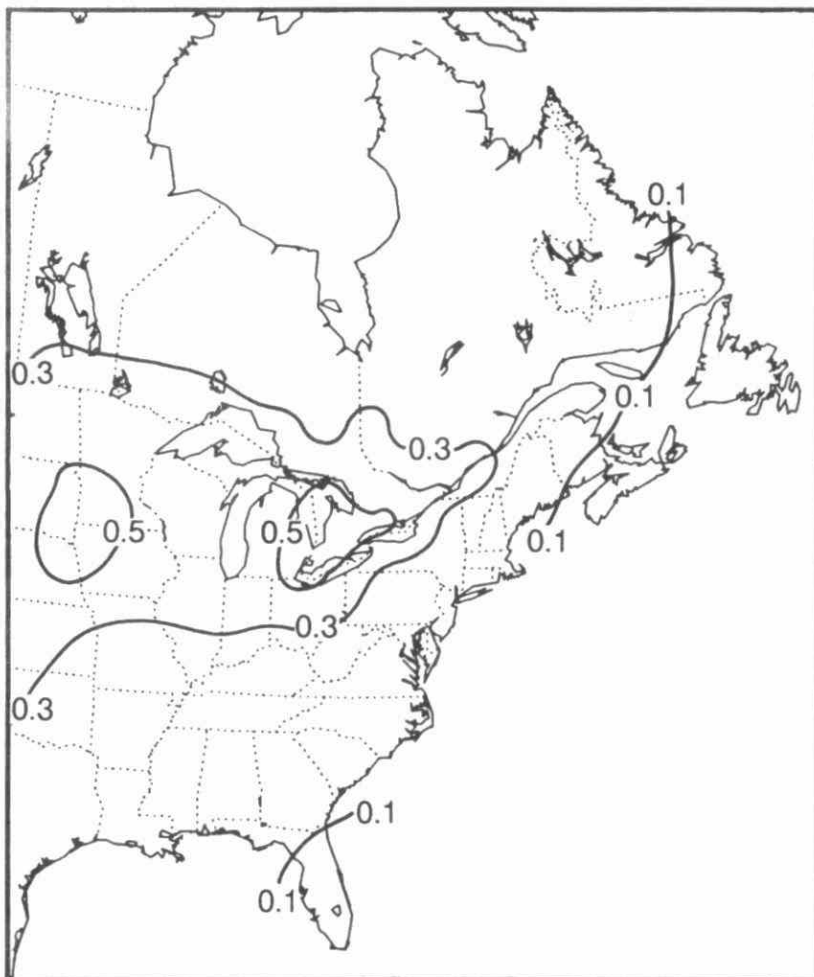


Fig. 3B-42 Six-year mean pH distribution (1982-1987).

6-YEAR (1982-87) MEAN NH_4^+ CONCENTRATION
IN PRECIPITATION (mg/l)



6-YEAR (1982-87) MEAN NH_4^+ DEPOSITION (kg/ha/yr)

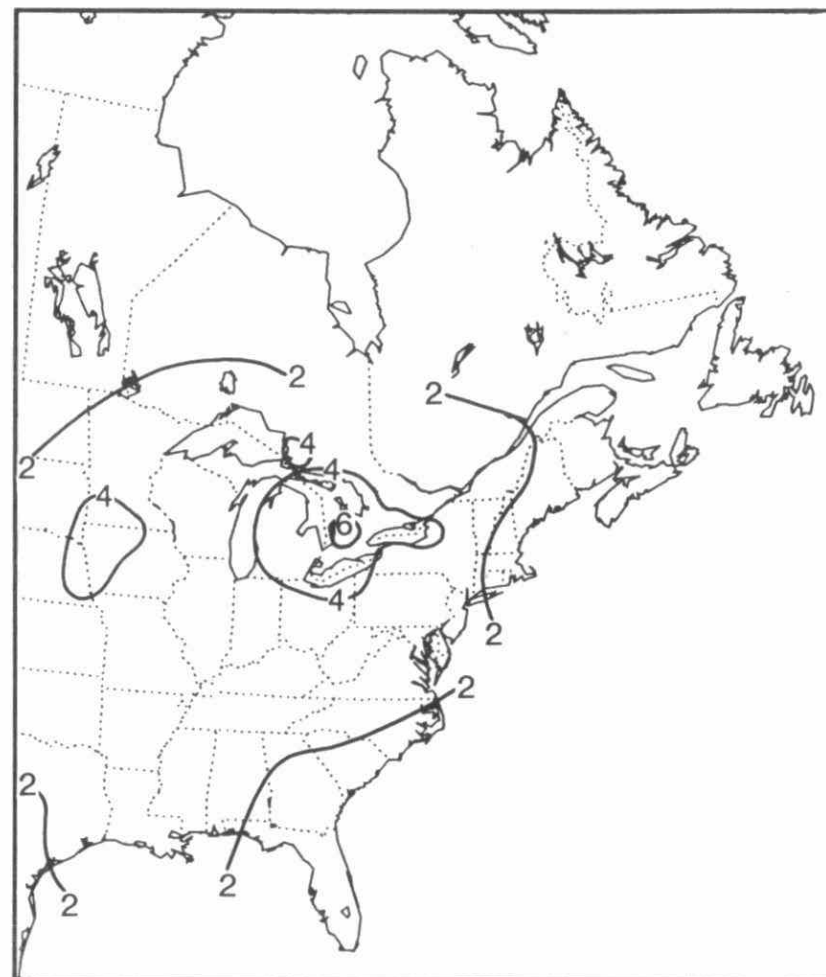
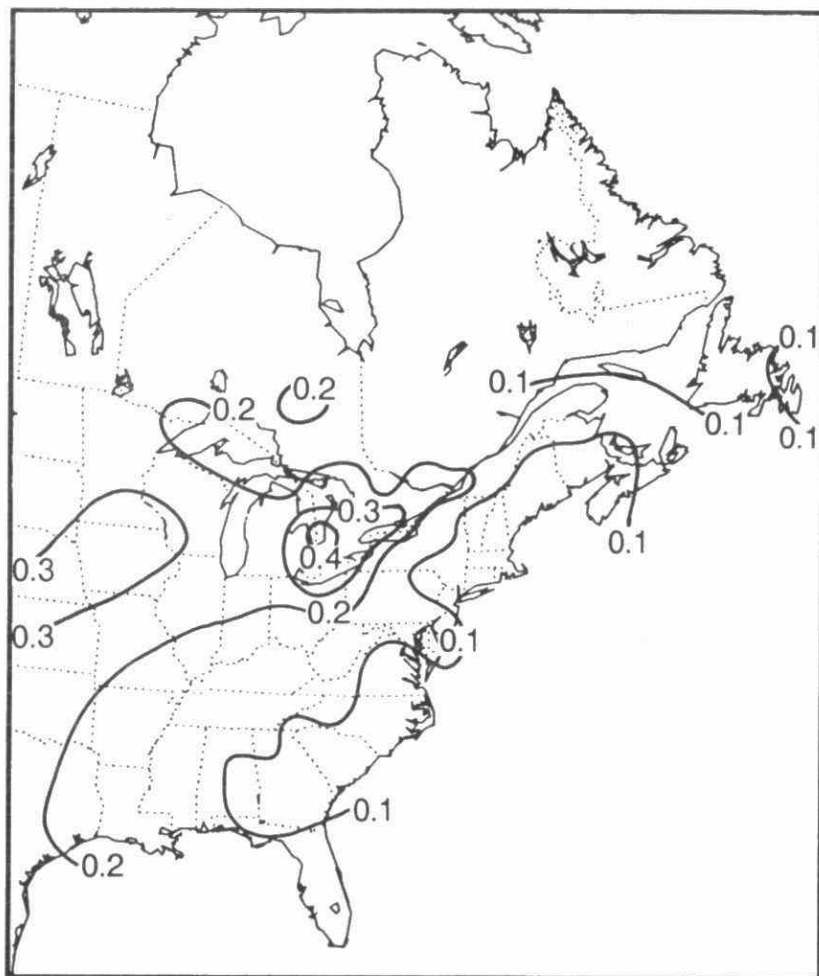


Fig. 3B-43 Six-year mean concentration and deposition patterns of NH_4^+ (1982-1987).

6-YEAR (1982-87) MEAN Ca^{++} CONCENTRATION
IN PRECIPITATION (mg/l)



6-YEAR (1982-87) MEAN Ca^{++} DEPOSITION (kg/ha/yr)

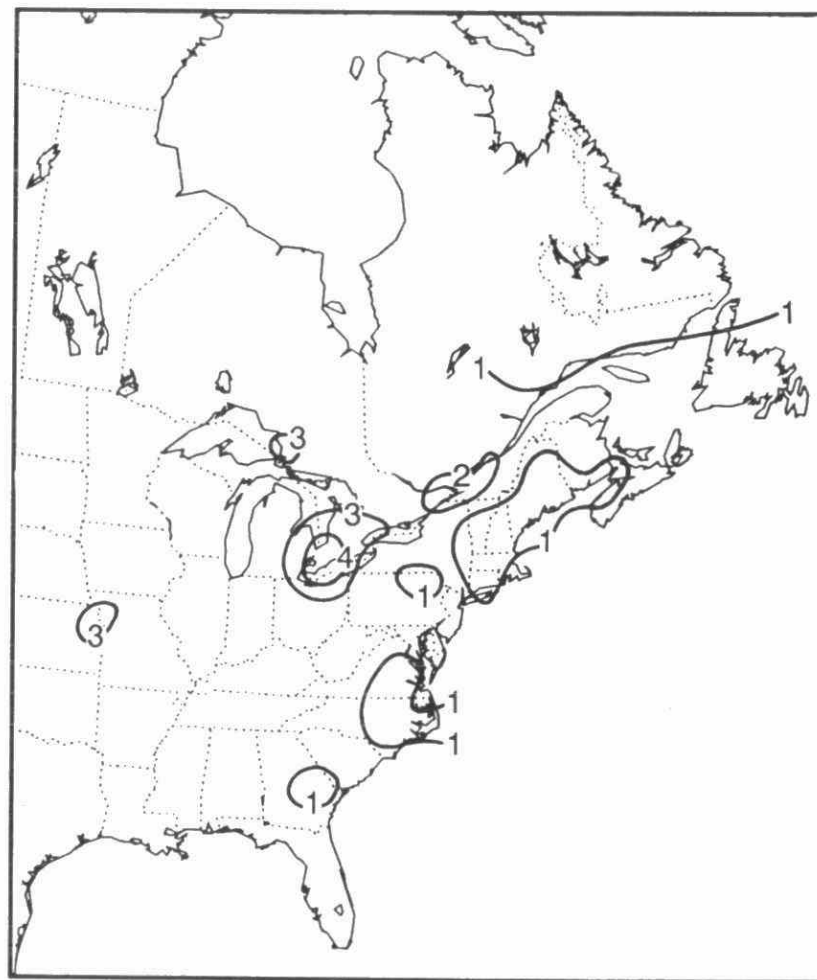
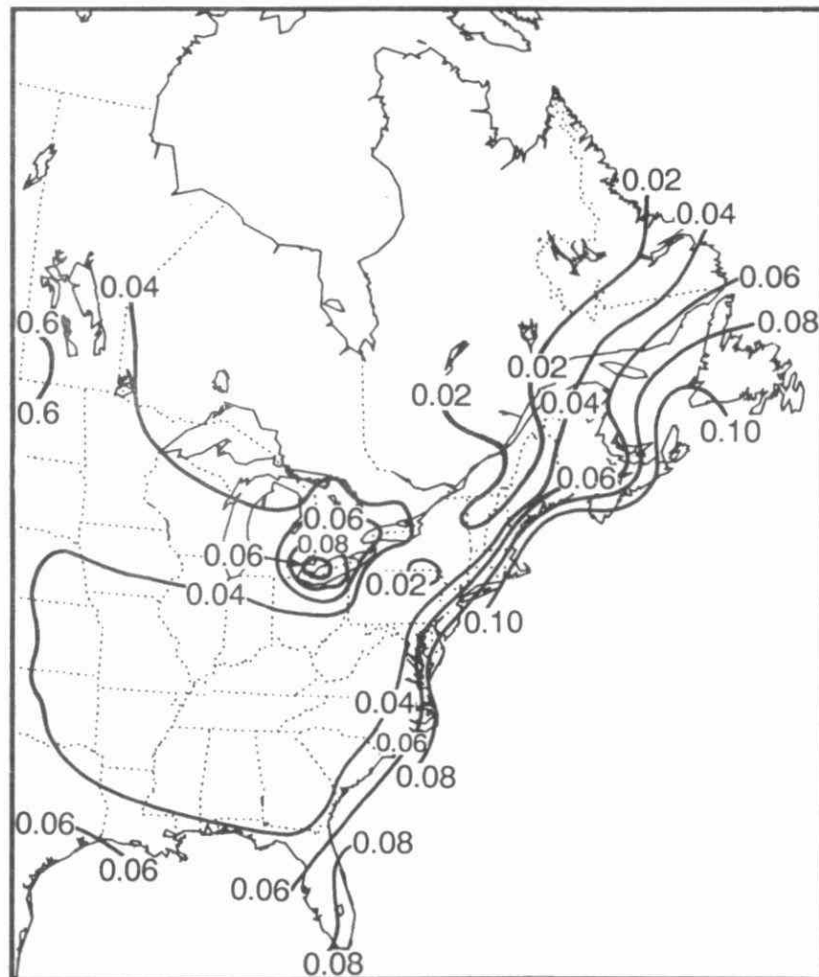


Fig. 3B-44 Six-year mean concentration and deposition patterns of Ca^{+2} (1982-1987).

6-YEAR (1982-87) MEAN Mg^{++} CONCENTRATION
IN PRECIPITATION (mg/l)



6-YEAR (1982-87) MEAN Mg^{++} DEPOSITION (kg/ha/yr)

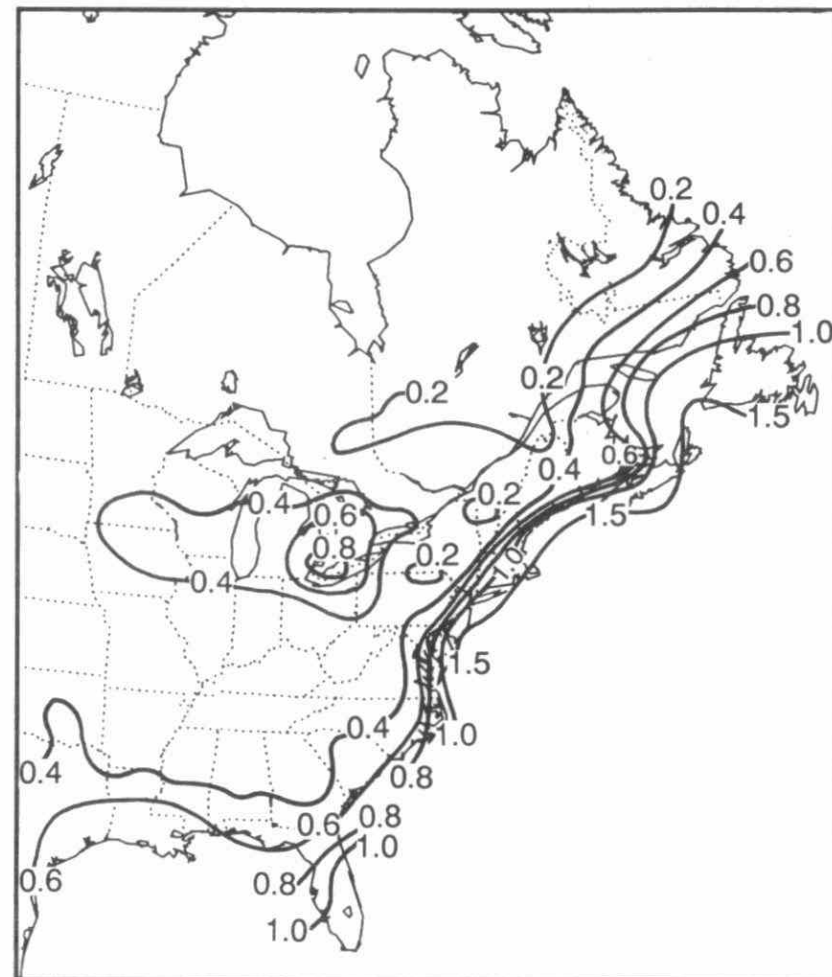
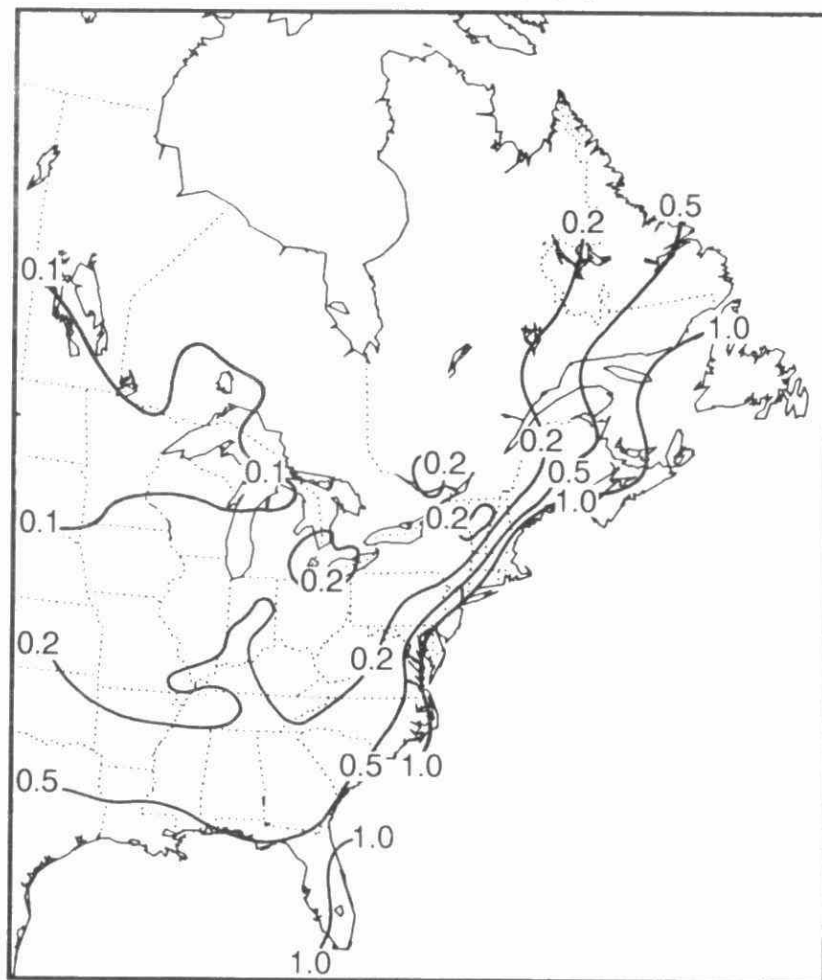


Fig. 3B-45 Six-year mean concentration and deposition patterns of Mg^{+2} (1982-1987).

6-YEAR (1982-87) MEAN Cl^- CONCENTRATION
IN PRECIPITATION (mg/l)



6-YEAR (1982-87) MEAN Cl^- DEPOSITION (kg/ha/yr)

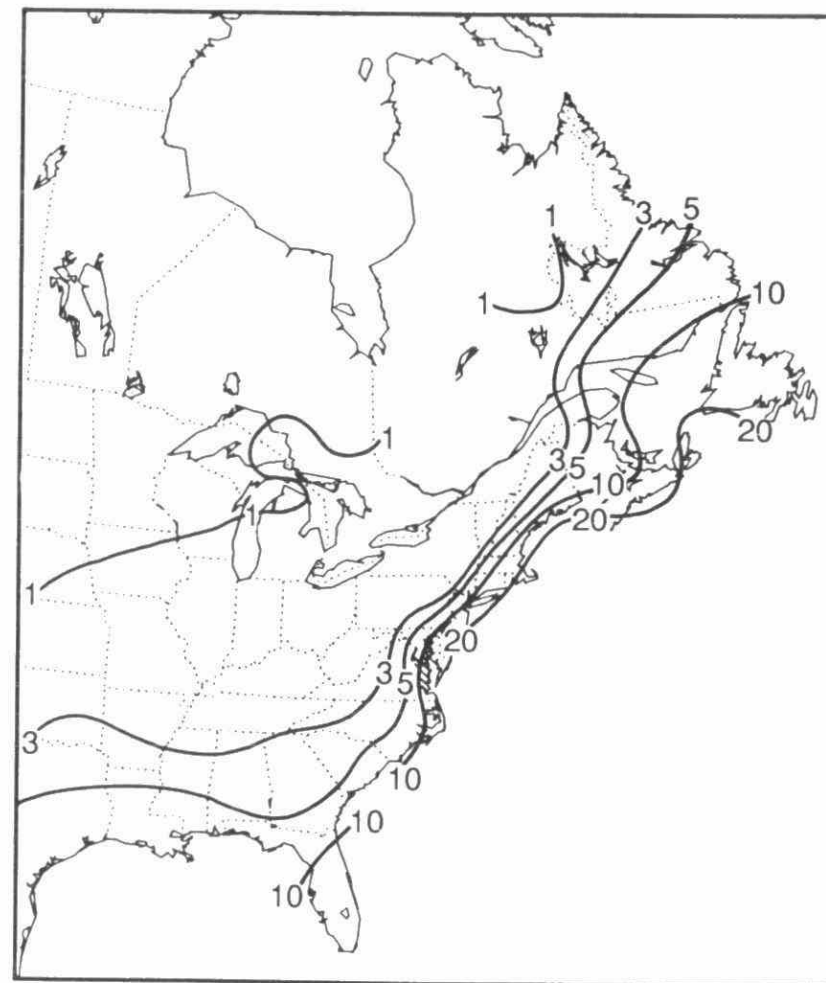
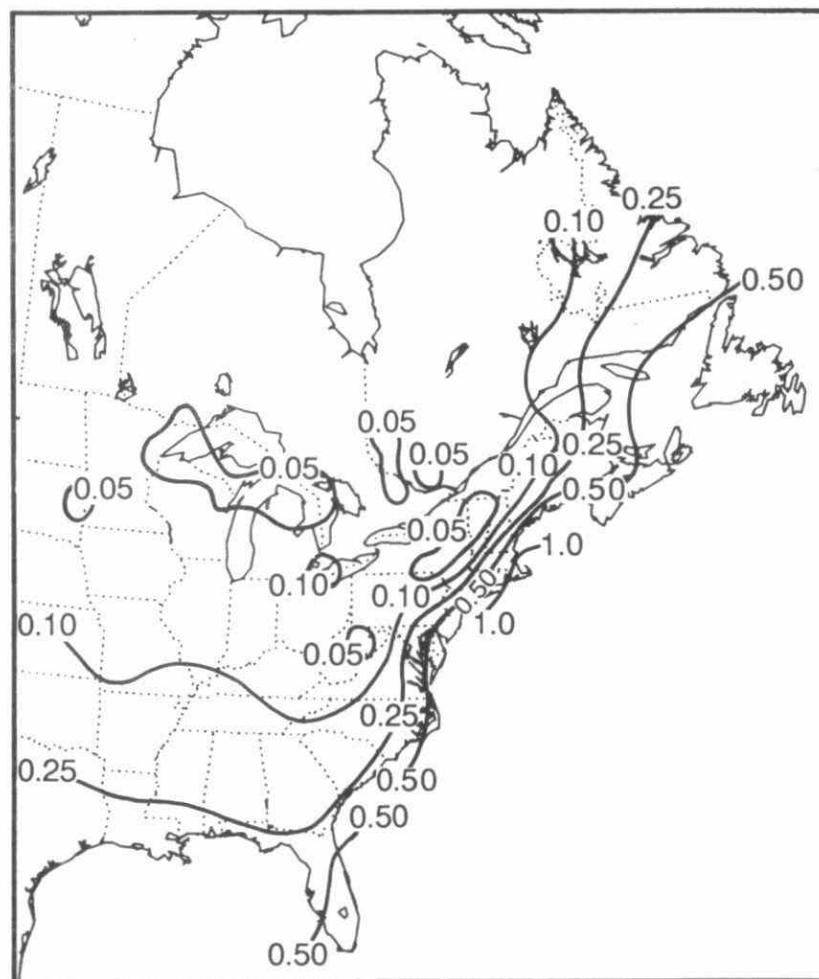


Fig. 3B-46 Six-year mean concentration and deposition patterns of Cl^- (1982-1987).

6-YEAR (1982-87) MEAN Na^+ CONCENTRATION
IN PRECIPITATION (mg/l)



6-YEAR (1982-87) MEAN Na^+ DEPOSITION (kg/ha/yr)

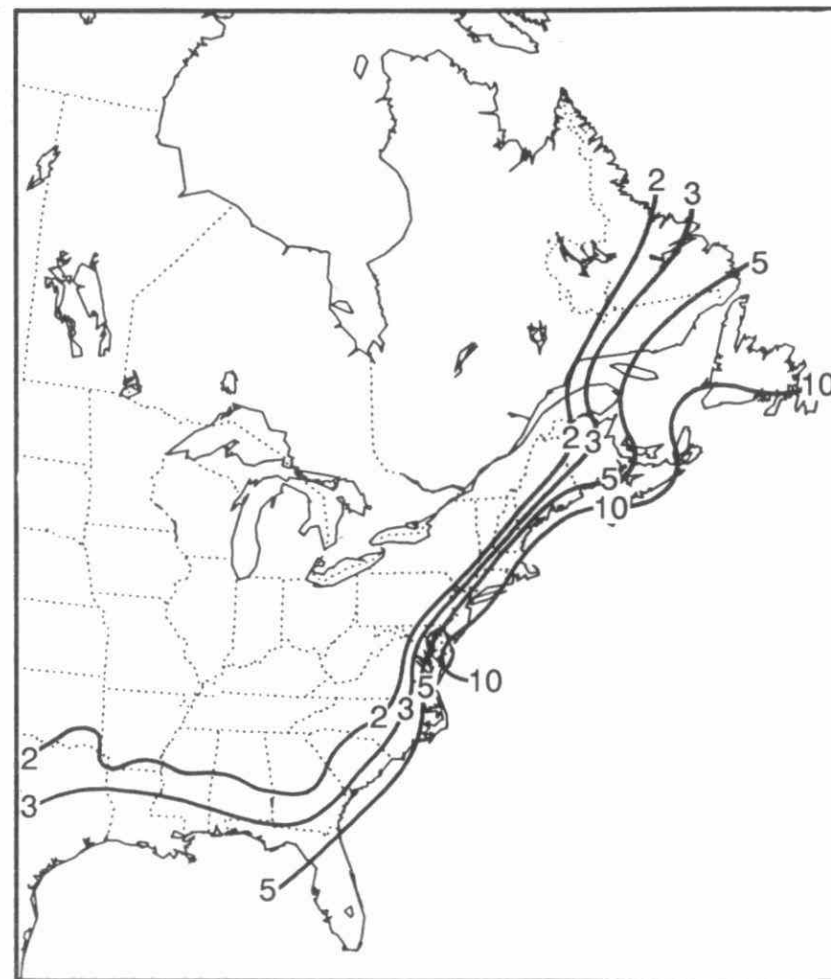
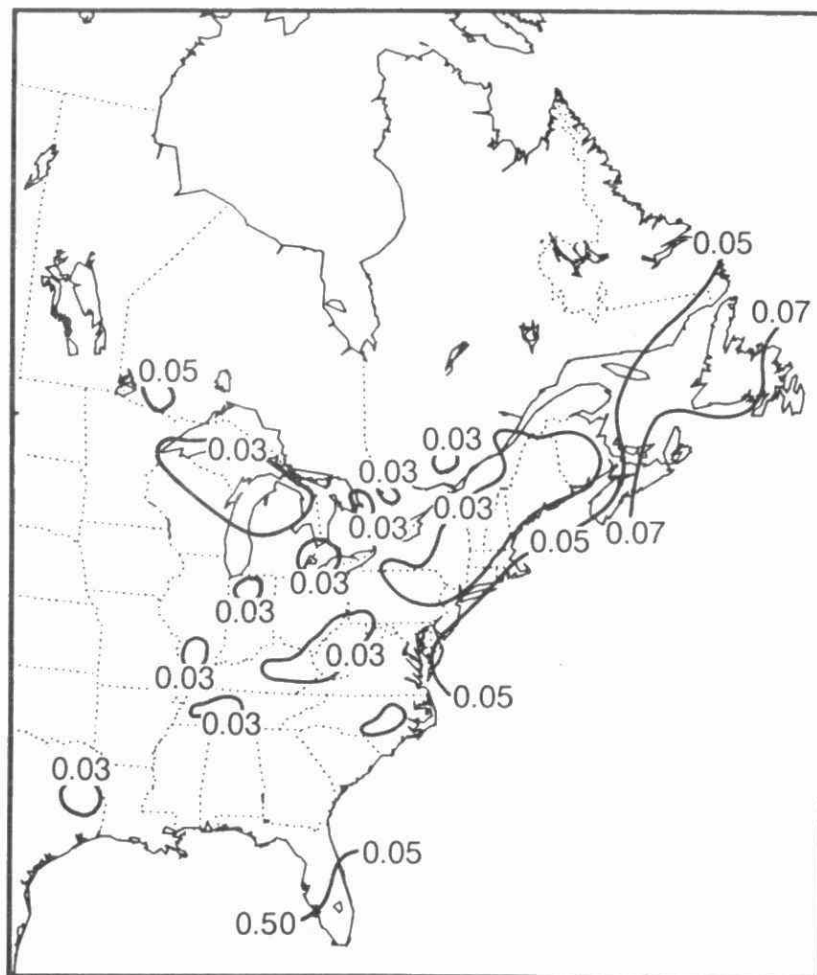
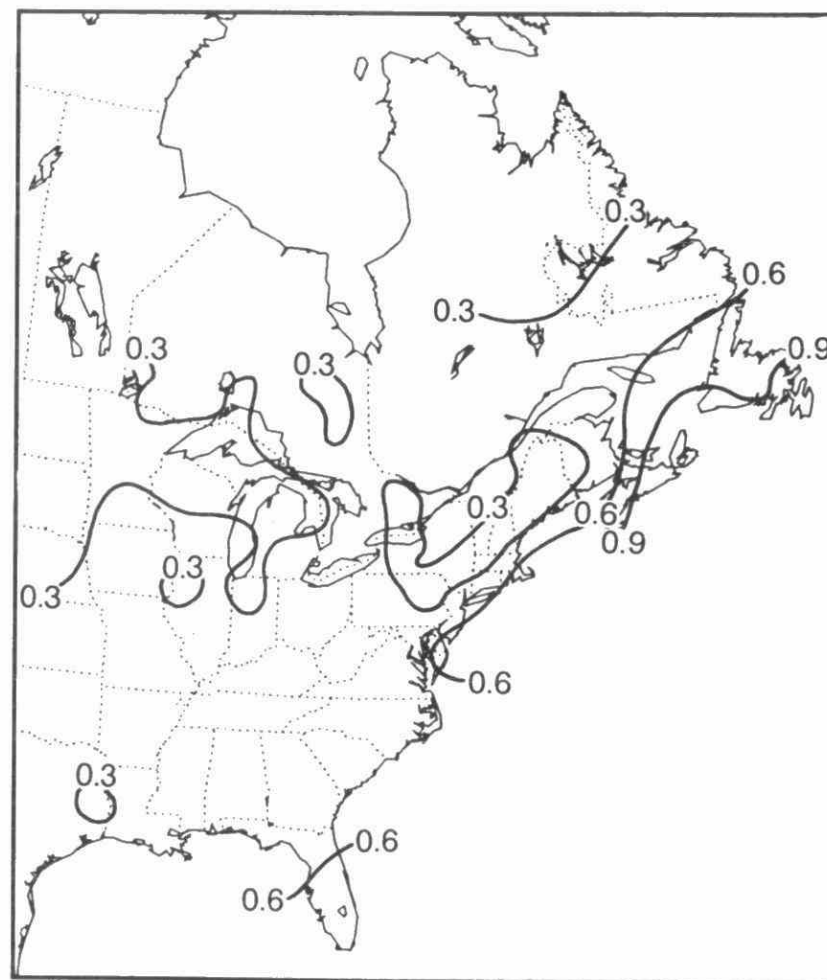


Fig. 3B-47 Six-year mean concentration and deposition patterns of Na^+ (1982-1987).

6-YEAR (1982-87) MEAN K^+ CONCENTRATION
IN PRECIPITATION (mg/l)6-YEAR (1982-87) MEAN K^+ DEPOSITION (kg/ha/yr)Fig. 3B-48 Six-year mean concentration and deposition patterns of K^+ (1982-1987).

APPENDIX 3C
THE SPATIAL AND TEMPORAL PATTERNS OF SULPHATE
AND NITRATE CONCENTRATIONS IN AIR IN ONTARIO

LIST OF FIGURES

<u>Figure#</u>		<u>Page#</u>
3C-1	Envelope of 1 and 4 $\mu\text{g}/\text{m}^3$ isopleths for SO_2 in Ontario:1982 - 1986.	3-261
3C-2	Envelope of 2 and 4 $\mu\text{g}/\text{m}^3$ isopleths for $\text{SO}_4^{=}$ in Ontario:1982 - 1986.	3-261
3C-3	Envelope of 0.2 and 0.6 $\mu\text{gN}/\text{m}^3$ isopleths for total NO_3^- in Ontario: 1982-1986.	3-261

APPENDIX 3C

THE SPATIAL AND TEMPORAL PATTERNS OF SULPHATE AND NITRATE CONCENTRATIONS IN AIR IN ONTARIO

Introduction

Concentrations of sulphate, sulphur dioxide and total nitrate in air (among other species) are measured in Ontario in the APIOS (Acidic Precipitation in Ontario Study) Cumulative Network (Chan et al., 1985). The annual average concentrations have been presented here as isopleth maps, to allow an assessment of the spatial patterns, and also so that the changes in patterns from year to year can be investigated.

Methodology

Air concentrations in the APIOS Cumulative Network are measured using a low volume filter pack technique. Particulate sulphate and nitrate are collected on a teflon filter. This is followed by a nylon filter which selectively absorbs nitric acid and a pair of cellulose filters impregnated with sodium carbonate in glycerol, which absorb SO_2 . The flow rate of air through the filter pack is 2 litres per minute, and the filters are exposed for 28 days. Because of the possible occurrence of artifacts in the partitioning of nitrate between particulate nitrate and nitric acid during the time that the filter packs are deployed in the field, no attempt is made to distinguish between the two in the Cumulative Network. Instead their sum is reported as total nitrate.

Isopleths of concentration were determined using a Kriging routine, and are presented as Figures 3.2.24a (SO_2), 3.2.24b (SO_4) and 3.2.24c (total nitrate). Data from 1982, the first complete year of network operation, to 1986 were available for this analysis.

Discussion

A strongly decreasing gradient from south to north in the province is evident for all of the species studied here. This is consistent with the known locations of the major source areas for SO_2 and NO_x which either lie in southern Ontario, or to the south, in the United States. The only exception to this is the smelters at Sudbury, and at Noranda in Quebec, which are large sources of SO_2 . However there is little evidence of the influence of these smelters in either the sulphate or sulphur dioxide concentration maps. These patterns are also consistent with the patterns of precipitation concentration discussed in Appendix 3B where the regions of highest concentration were also found to lie in southwestern Ontario.

The patterns of SO_2 concentration are very similar for 1982, 1983, 1984 and 1985, with the Muskoka-Haliburton region seeing about $3 \mu\text{g m}^{-3}$, and Thunder Bay about 1 to $2 \mu\text{g m}^{-3}$. There is evidence of a decrease in concentrations of sulphur dioxide in central and southern Ontario in 1986. The isopleth lines are all shifted southward in comparison with the preceding years, and correspondingly lower concentrations were determined in all areas of the province. These observations are summarised in Figure 3.2.25, which compares the averaged contours for 1982 and 1983 with those for 1985 and 1986.

A change in the appearance of the isopleths seems to have occurred since 1983, with higher concentrations of sulphur dioxide being observed on the north shore of Lake Huron than in preceding years. It is difficult to associate this change in the pattern with

emission changes in a specific region. However, it may be noted that SO₂ emissions in Ontario, Ohio and Indiana all increased between 1983 and 1984.

Sulphate concentration behaves in very much the same way as SO₂. That is, the patterns for the early years are very similar, but in this case it appears that there was a southerly shift of the isopleth lines in 1985, with 1985 and 1986 being similar. Sulphate concentrations were 3 to 4 µg m⁻³ in the Muskoka-Haliburton region. Figure 3.2.26 shows the contrast between the 1982/3 and 1985/6 average contours.

By way of contrast, changes in the concentration patterns for nitrate have been small, as is seen in the comparison of the 1982/3 and 1985/6 averages (Figure 3.2.27). Nitrate concentrations in air range between about 0.6 and 1.5 µg m⁻³ in southern Ontario and are less than 0.2 µg m⁻³ over most of northern Ontario.

Figure 3C-1 to 3C-3 shows the envelopes of selected isopleths for SO₂ (3C-1), sulphate (3C-2) and nitrate (3C-3). These envelopes cover the time period of the data, i.e., 1982 to 1986, and also indicate how little year to year change there has been for nitrate, as compared with the other two species.

The spatial patterns of the ambient concentrations of sulphur dioxide, sulphate and total nitrate are consistent with the location of the major source regions to the south and west of the sensitive regions in central Ontario. The changes in concentration patterns over the last several years are also consistent with the emission history of the major emitters. However, these data do not permit a more precise identification of source regions without a more detailed analysis.

Conclusions

The major conclusions of this study are:

- (i) concentrations of sulphur dioxide, sulphate and total nitrate in air decrease strongly from south to north in Ontario;
- (ii) isopleths for sulphur dioxide and sulphate have shown a small southward movement over the time period of this study, corresponding to a decrease in concentration at most locations;
- (iii) concentration patterns for nitrate have changed relatively little over the same time period.

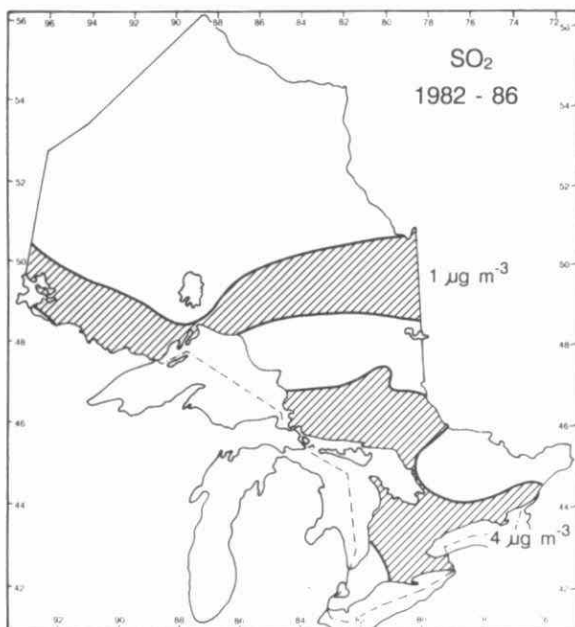


Fig. 3C-1 Envelope of 1 and 4 $\mu\text{g}/\text{m}^3$ isopleths for SO_2 in Ontario: 1982 - 1986.

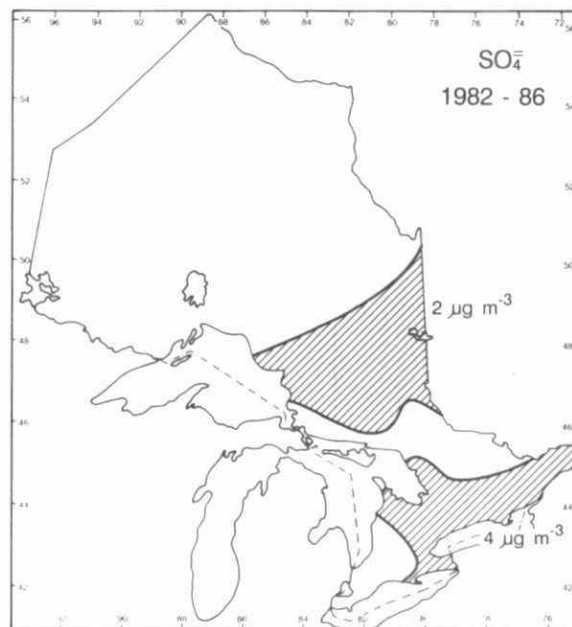


Fig. 3C-2 Envelope of 2 and 4 $\mu\text{g}/\text{m}^3$ isopleths for SO_4 in Ontario: 1982 - 1986.

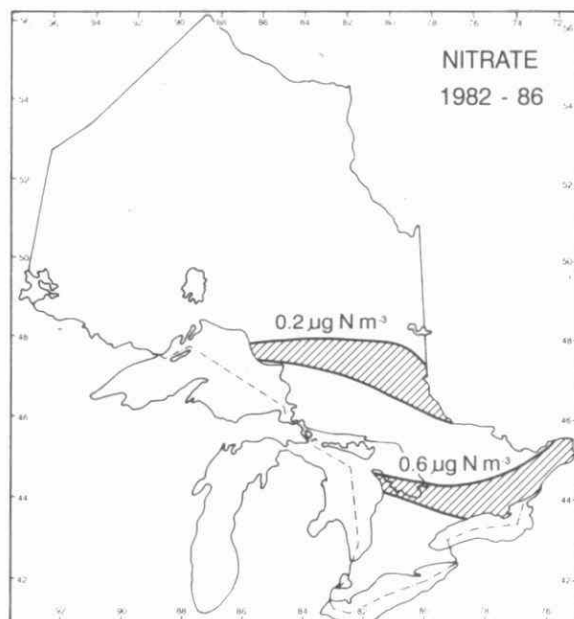


Fig. 3C-3 Envelope of 0.2 and 0.6 $\mu\text{gN}/\text{m}^3$ isopleths for total NO_3 in Ontario: 1982-1986.

APPENDIX 3D

**TEMPORAL VARIATION OF SULPHATE AND NITRATE
CONCENTRATION IN AIR AND PRECIPITATION
AT FIVE SITES IN EASTERN CANADA**

LIST OF FIGURES

Figure#		Page#
3D-1	Temporal variation of $\text{SO}_4^{=}$ monthly precipitation-weighted-mean concentration in precipitation at ELA (a) and Chalk River (b). The dots and the squares are for observed and modeled values, respectively.	3-278
3D-2	Intercept and long-term trend ($C_o + f^t(t)$) of $\text{SO}_4^{=}$ concentrations in precipitation normalized to 1980 (or first complete year of record). Dashed line-continuous trend; solid line-normalized annual values. Only sites with statistically significant long-term trends are shown.	3-279
3D-3	Same as Figure 3D-2 for NO_3^- in precipitation.	3-280
3D-4	Intercept, long-term trend and long-term cycle ($C_o + f^t(t) + f^c(t)$) of $\text{SO}_4^{=}$ concentration in precipitation normalized to 1980 (or first complete year of record). Dashed line-continuous trend; solid lines-annual normalized values. Only sites with statistically significant trends are shown.	3-281
3D-5	Same as Figure 3D-4 for NO_3^- in precipitation.	3-282
3D-6	Temporal variation of monthly median air concentrations at ELA for $\text{SO}_4^{=}$ (a), SO_2 (b) and Total NO_3^- (c). Dashed line - model; dots - observations.	3-283
3D-7	Same as Figure 3D-6 for Kejimkujik.	3-284
3D-8	Same as Figure 3D-2 except for monthly median $\text{SO}_4^{=}$ concentrations in air.	3-285
3D-9	Same as Figure 3D-8 for SO_2 in air.	3-286
3D-10	Same as Figure 3D-8 for Total NO_3^- in air.	3-287
3D-11	Same as Figure 3D-4 except for monthly median $\text{SO}_4^{=}$ concentrations in air.	3-288
3D-12	Same as Figure 3D-11 for SO_2 in air.	3-289
3D-13	Same as Figure 3D-11 for Total NO_3^- in air.	3-290
3D-14	Definition of sectors for sulphate and nitrate for ELA and Kejimkujik.	3-291

LIST OF FIGURES (continued)

Figure#		Page#
3D-15	Boxplots for the SO_3^- , SO_2 and Total NO_3^- concentrations in air for the sectors defined in Figure 3D-14 at E.L.A. and Kejimkujik. In each box, the central bar is the median and the lower and upper limits are the first and third quartiles, respectively. The lines extending vertically from the box indicate the spread of the distribution with the length being 1.5 times the difference between the first and third quartiles. Observations falling beyond the limits of those lines are considered to be outliers and are indicated by dots. The stars along the lines indicate the lowest and highest observations that were not outliers. The black squares are the monthly geometric means.	3-292
3D-16	Temporal variation of $\text{SO}_4^{=}$ monthly median concentration in air at ELA for the sectors defined in Figure 3D-14. Dashed line - model; dots - observations.	3-293
3D-17	Same as Figure 3D-16 for SO_2 .	3-294
3D-18	Same as Figure 3D-16 for Total NO_3^- .	3-295
3D-19	Temporal variation of $\text{SO}_4^{=}$ monthly median concentration in air at Kejimkujik for the sectors defined in Figure 3D-14. Dashed line model; dots - observations.	3-296
3D-20	Same as Figure 3D-19 for SO_2 .	3-297
3D-21	Same as Figure 3D-19 for Total NO_3^- .	3-298
3D-22	Intercept and long-term trend of monthly median SO_2 concentrations in air at ELA normalized to 1980 for the four sectors in Figure 3D-14. Dashed line - continuous trend; solid lines - normalized annual averages.	3-299
3D-23	Same as Figure 3D-22 except that it represents the intercept, long-term trend plus long-term cycle of $\text{SO}_4^{=}$ in air at ELA.	3-300
3D-24	Same as Figure 3D-23 for SO_2 in air.	3-301
3D-25	Same as Figure 3D-23 for Total NO_3^- in air.	3-302
3D-26	Intercept and long-term trend of monthly median SO_2 air concentrations at Kejimkujik normalized to 1980 for the four sectors in Figure 3D-14. Dashed line - continuous trend; solid lines - normalized annual averages.	3-303
3D-27	Same as Figure 3D-26 for SO_2 in air.	3-304
3D-28	Same as Figure 3D-26 for Total NO_3^- in air.	3-305

LIST OF TABLES

TABLE#		Page#
3D-1	Summary of results of time series analysis of $\text{SO}_4^{=}$ and NO_3^- concentration in air at 5 rural locations in eastern Canada.	3-275
3D-2	Summary of results of time series analysis of $\text{SO}_4^{=}$, SO_2 and Total NO_3^- concentration in air at 5 rural locations in eastern Canada.	3-275
3D-3	Summary of results of time series analysis of $\text{SO}_4^{=}$, SO_2 and Total NO_3^- concentration in air for the four different sectors of origin at E.L.A. and Kejimkujik.	3-276
3D-4	Frequency of occurrence of the four sectors defined in Figure 3D-14 for the daily $\text{SO}_4^{=}$, SO_2 and Total NO_3^- concentrations in air at E.L.A. and Kejimkujik.	3-277

APPENDIX 3D

TEMPORAL VARIATION OF SULPHATES AND NITRATES CONCENTRATION IN AIR AND PRECIPITATION AT FIVE SITES IN EASTERN CANADA

Introduction

The study of temporal variation requires many years of uninterrupted sampling with the minimum of changes in the sampling protocol used. In Canada, only sites that were part of the Air and Precipitation Monitoring Network (APN) and are presently in the Canadian Air and Precipitation Monitoring Network (CAPMoN) fulfill nearly this requirement. Only five sites have a long enough sampling history (i.e. seven years or more) to be considered. They are : Experimental Lakes Area (E.L.A.), Ontario; Chalk River, Ontario; Algoma, Ontario; Forêt Montmorency, Quebec; and Kejimikujik, Nova Scotia. Note that some important changes in the sampling protocol occurred during the existence of those sites. They will be described briefly in the next section.

A general and classical way of studying the time evolution of a variable is to decompose its variation as the sum of a deterministic and a stochastic part. The deterministic part is further broken down as the sum of annual cyclic components (i.e. cyclic variation with periods less than one year), long-term cyclic components (i.e. cyclic variation with periods longer than one year) and long-term trend components. The stochastic part is usually assumed to be generated randomly from a normal distribution with mean zero and constant standard deviation. It is also assumed that the stochastic component values are independent. In the present study, such an additive model was fitted using least-squares to the logarithmic transform of the concentration.

In the present study, only the temporal variation of $\text{SO}_4^{=}$ and NO_3^- concentration in precipitation and $\text{SO}_4^{=}$, SO_2 and total NO_3^- concentration in air will be discussed. In the case of Kejimikujik near the Atlantic ocean, the results for excess sulphate (i.e. $\text{SO}_4^{=}$ observations were corrected for sea salt contributions using Na^+ and a $\text{SO}_4^{=}/\text{Na}^+$ mass ratio of .25) will be presented. The model described in the preceding paragraph was fitted to the weekly mean/monthly median values and not the daily values. This was done because the stochastic component was, in the case of daily data, highly auto-correlated. The weekly precipitation-weighted-mean was used in the case of the concentration in precipitation and the monthly median in the case air concentration. Only weeks/months with sufficient data were used.

Network History

As mentioned earlier, important modifications were made to the sampling and chemical analysis protocols since the establishment of the monitoring sites which might influence the result obtained in the analysis. It is therefore important to bear these in mind when interpreting the results. Only the pertinent changes will be summarized here.

Precipitation Sampling

In the APN network, precipitation sampling was done on a daily basis using a Sangamo wet-only precipitation sampler (see Barrie et al., 1980). The precipitation samples were collected in a plastic container. The precipitation samples, if present, were collected at 08:00 LST. In addition to the precipitation chemistry collector, there are two standard

Canadian precipitation-amount gauges : a rain gauge and snow gauge with a Nipher shield. Every 2 weeks, the precipitation samples were sent to Environment Canada's National Water Quality Laboratory in Burlington (Ontario) for analysis. $\text{SO}_4^{=}$ and NO_3^- were analyzed using the automated methyl thymol blue and cadmium reduction techniques, respectively. Samples with low precipitation amounts were not analyzed.

In mid-1983, the APN sites, except for Algoma, were integrated into the CAPMoN network. Algoma was merged into the CAPMoN network in January 1985. In the CAPMoN network, the Type A-M Wet Deposition Collector is used (Vet et al., 1986). It differs from the Sangamo in many ways. The most important differences are : 1) a new precipitation sensor is used to control the bucket lid; 2) the bucket has a collecting area 2.7 times larger than the Sangamo collector and 3) the bucket is lined with a plastic collection bag. The plastic bags are changed each morning at 0800 LST. Note that the composition of the plastic bag was changed twice since the establishment of the CAPMoN network (Vet et al., 1986, 1988a, 1988b and 1989). Beginning in the summer of 1983, $\text{SO}_4^{=}$ and NO_3^- were analyzed using ion chromatography. Samples with low precipitation amount are diluted and then analyzed.

Air Sampling

A vacuum system consisting of several air filters mounted in series at the top of a 10-metre tower was used to measure air concentrations. Prior to December 1982, a two-stage system was employed enabling the determination of ambient air concentration of $\text{SO}_4^{=}$, SO_2 and total NO_3^- (see Barrie et al., 1980). The filters operated for 24-hour periods starting at about 0800 LST. $\text{SO}_4^{=}$ and total NO_3^- were analyzed using liquid ion chromatography. The automated Thorin method was used to determine the concentration of SO_2 . In December 1982, the two-filter system was replaced by a three-filter system which enables the measurement of particulate and gaseous nitrate individually (see Anlauf et al., 1985). The chemical analysis techniques remained the same except that the automated Thorin method for SO_2 was replaced by ion chromatography in January 1984.

Statistical Model

The general model described in the introduction can be written algebraically as:

$$\text{Log}(C(t)) = C_0 + f^t(t) + f^c(t) + f^s(t) + \epsilon(t)$$

where :

- $C(t)$ is the concentration at time t ;
- C_0 is a constant;
- $f^t(t)$ is the long-term trend component that can be approximated by a low order polynomial in t as $c_1^t t + c_2^t t^2 + \dots$. Polynomials up to the third degree were used in the present study;
- $f^c(t)$ is the cyclic components that can be approximated as a sum of sines and cosines with periods larger than one year but shorter than 6 years. Up to two different cycles were tested;

- $f^s(t)$ is the annual cyclic components that can be described as a sum of sines and cosines with periods less than or equal to one year. Annual cycles with periods of one year, six months, four months were used;
- $\epsilon(t)$ is the stochastic component.

In the case of the ionic concentration in precipitation, a sixth term was added to describe the relationship between concentration and precipitation amount. That term was $c^p \text{Log}(P)$, where P is the weekly total precipitation amount. Relation (1) was fitted to the weekly mean/monthly median concentrations using the least-squares technique.

To test the statistical significance of the different terms in relation (1), the Bonferroni's multiple testing technique at a 90% confidence level was used (see Miller, 1981). In this technique, it is assumed that the stochastic component is randomly generated from a normal distribution with mean zero and standard deviation constant with time. The monthly stochastic component values should also be independent. The normality of the stochastic components was tested using the Kolmogorov-Smirnov test (see Hollander and Wolfe, 1973) at a 95% confidence level. To test the independence of the stochastic components, the auto-correlation coefficients up to lag 14 were calculated and compared to the limit $1.96/\sqrt{n}$, where n is the number of data (see Chatfield, 1984).

Results

Precipitation Concentration

As mentioned in the preceding section, two hypotheses about the stochastic components were made: i.e. they are normally distributed and their values are independent from week to week. The 95% Kolmogorov-Smirnov tests used to test for normality indicated that the hypothesis of normality can be rejected for most of the models fitted. However, the non-normality of the stochastic components was small and would not influence noticeably the results presented in this section, because of the large number of observations available (more than 248 in all cases). However, the hypothesis of independence between the weekly stochastic component values could not be rejected.

The results of the model fitting for the sulphate and nitrate concentration in precipitation are summarized in Table 3D-1. Two examples of the fits between model and observations for sulphate are presented in Figure 3D-1. The dots are the observed weekly precipitation-weighted-mean concentrations and the boxes the values obtained using the fitted models. For all cases, except for NO_3^- at Forêt Montmorency, the fraction of the total variance explained by the model, is between 0.15 and 0.34.

For all sites, except at Algoma for NO_3^- , a significant relationship between weekly mean concentration and precipitation depth was found. For all significant cases, the logarithm of the weekly mean concentrations decreases with increasing values of the logarithm of the precipitation depth. For $\text{SO}_4^{=}$, the coefficient of the linear relationship between $\text{Log}(C)$ and $\text{Log}(P)$ was between -0.11 and -0.43. For NO_3^- , it was between -0.12 and -0.38. C was in mg l^{-1} and P in mm.

For $\text{SO}_4^{=}$, statistically significant long-term trends were found at all sites. The long-term trend components (i.e. $C_0 + f^t(t)$), relation (1) normalized by the mean value for 1980 or the first subsequent complete year of record are shown in Figure 3D-2. At all sites except

Forêt Montmorency, there was a decrease between 1980-1981 and 1987. The strongest decreases, about 40%, were at Chalk River and E.L.A. Decreases of about 25% were observed at Kejimikujik and Algoma. For NO_3^- , a statistically significant long-term trend was only found at Kejimikujik (Figure 3D-3). NO_3^- concentration increased by about 40% at this site between 1980 and 1987.

Long-term cyclic components ($f^c(t)$) were present at E.L.A. and Algoma for $\text{SO}_4^{=}$ and at all sites except Chalk River for NO_3^- . The periods of the long-term cycles vary between about 3 years at E.L.A. for sulphate to about 5.5 years for nitrate at E.L.A.. The combined long-term trend and cyclic components are shown in Figures 3D-4 and 3D-5 for $\text{SO}_4^{=}$ and NO_3^- respectively. There was no similar pattern between the temporal variation of the long-term cyclic components from site to site. For the same period, the long-term cyclic components can be minimum at some sites and maximum at others.

Statistically significant annual cycles in precipitation concentration were found for all cases (Table 3D-1). For $\text{SO}_4^{=}$, both a 12 month and a 6 month annual cycle were present, except at Kejimikujik where the 6 months cycles was not statistically significant. For NO_3^- , the periods of the annual cyclic components varied from a simple 12 month sine wave at Chalk River, with a maximum in February to a minimum in August, to more complicated combinations of sine and cosine waves with periods equal to 12, 6 and/or 4 months.

Air Concentration

The hypothesis that the stochastic components were from a normal distribution could not be rejected for any of the ions and sites studied, using 95% Kolmogorov-Smirnov tests. The hypothesis that the stochastic component values were independent from month to month could not be rejected in all cases except for SO_2 at Chalk River and E.L.A.. The auto-correlation coefficients of lag 1 were equal to .26 and .32, respectively. Therefore, the results presented for those two cases must be viewed with caution.

Table 3D-2 presents a summary of the model fitted for $\text{SO}_4^{=}$, SO_2 and Total NO_3^- concentration in air. The fits between observed monthly median concentrations and models are illustrated in Figures 3D-6 and 3D-7 for E.L.A. and Kejimikujik, respectively.

The greatest fraction of the total variance that can be explained by the model was for SO_2 (71 to 80%). This was due to the fact that more of the variance in the data was related to well defined annual cycles for SO_2 than for $\text{SO}_4^{=}$ and Total NO_3^- .

Long-term trends

For particulate $\text{SO}_4^{=}$, statistically significant long-term trends were found at Chalk River only (Figure 3D-8). In contrast for the SO_2 statistically significant long-term trend components were detected at all sites except Algoma, (Figure 3D-9). For E.L.A., the amplitude of the decrease in the long-term trend components compared with the other components can be seen in Figure 3D-6. The long-term trend components decreased by about 70% between 1980 and 1987. At Chalk River, most of the decrease in SO_2 concentration occurred between 1979 and 1983. The SO_2 concentration in 1987 was about half of its concentration in 1980. At Kejimikujik, it increased between 1979 and 1981; decreased until 1986 to a value equal to 40% of the 1980 concentration; and finally increased in the last year.

In the case of Total NO_3^- , statistically significant long-term trends were found at only the three most eastern sites; i.e. Chalk River, Forêt Montmorency and Kejimikujik (Figure 3D-10). However, only at Forêt Montmorency did it show a tendency to decrease with increasing time. The other two sites tended to peak in 1984 and 1985 then decrease in 1986 and 1987. At Forêt Montmorency, there was a decrease of about 40% between 1981 and 1987.

Long-term cycles

For particulate SO_4^{2-} , statistically significant long-term cycles were detected at all sites except Algoma (Figure 3D-11). The period of those cycles varied between about 3.0 and 4.5 years. The amplitudes of those cycles were small (see e.g. Figs 3D-6 and 3D-7). For gaseous SO_2 , long-term cyclic components, with periods of about 2.5 and 4.5 years, were present at all sites except Chalk River and Forêt Montmorency. (Figure 3D-12). Their amplitude was also small, as shown in Figures 3D-6 and 3D-7 for E.L.A. and Kejimikujik, respectively. In the case of Total NO_3^- in air, long-term cycles were present only at E.L.A. and Chalk River. They had periods equal to 3.0 and 3.5 years, respectively. The long-term trend and cyclic components are shown in Figure 3D-13.

Annual Cycles

Annual cycles were found in all cases except for particulate SO_4^{2-} at Chalk River. For most of the sites, complicated mixtures of sines and cosines with periods equal to 12 and 6 months were necessary to describe the annual cycle. Waves of a 4 month period were necessary at some sites for SO_2 and Total NO_3^- .

Trends in Air Concentrations Grouped by Sector of Origin

The non-random temporal variation of the concentration of a substance at a site is the end product of the interplay between two main factors, namely: variation in emissions and in meteorology. If emission changes were the only cause of temporal variation in air concentration, one would expect a net decrease in the concentration of sulphur between 1980 and 1985, as SO_2 emissions decreased over most of North America (Figure 3.2.42). However, between 1980 and 1985, statistically significant decreasing long-term trends could only be detected for SO_2 at Chalk River, E.L.A. and Forêt Montmorency. The inability to detect a trend is likely due to the strong noise caused by meteorology. One possible technique, that can be used to reduce the effects of meteorology, involves the use of air parcel back-trajectories to classify the observed concentrations according to origin and then testing for trends. This was done for SO_4^{2-} , SO_2 and Total NO_3^- air concentrations at two sites, namely; E.L.A. and Kejimikujik.

The four regions of origin chosen for sulphate and nitrate at E.L.A. and Kejimikujik are shown in Figure 3D-14. Back-trajectory information was used to assign each daily concentration to a particular region of origin or sector. For each month, the median value of the daily concentrations belonging to a sector was calculated. The model described by relation (1) was then fitted by least-squares to the monthly median values of each sector, giving four different models for each ion and site.

Before discussing the results obtained for the models, it will be useful to consider the distribution of the daily data when grouped by sector. Boxplots of the daily ionic concentrations grouped by sector are shown in Figure 3D-15. The frequencies of

occurrence of each sector are given in Table 3D-4. At E.L.A., the highest $\text{SO}_4^{=}$ concentrations are mainly from the eastern United States and southeastern Canada (sector IV) and the lowest from northeast and northwest sectors (I and III). The median value for sector IV was about twice the value for sector I. Similar results were obtained for SO_2 , except that the distribution for sectors II and III were not different. In the case of Total NO_3^- , most of the highest concentrations were found in the southwest sector (III). As with $\text{SO}_4^{=}$, the lowest values were still found in the north sector (I). The median value for the southwest sector (III) was about four times larger than that from the north sector (I). At Kejimikujik, the ionic concentrations increased when one goes from the north to east to west to southwest (sector I to sector IV) for both $\text{SO}_4^{=}$ and Total NO_3^- . The median value in the southwest sector (IV) was about 3.5 times higher than for the north sector (I) for both ions. For SO_2 , the lowest concentrations were from the east off the Atlantic ocean (sector II). The distributions for the west and southwest sectors (III and IV) were not different. In summary, those results indicate that a relationship between ionic concentrations and region of origin of the air existed. They also show that the highest ionic concentrations were mostly from regions of high emissions.

As in the preceding cases of model fitting the stochastic components (or residuals) were tested for normality and for independence. In all cases, the hypothesis of normality could not be rejected using the Kolmogorov-Smirnov test at a 95% confidence level. The hypothesis that the stochastic component values were independent from month to month could not be rejected in all cases using the test described earlier.

A summary of the model-fitting results is given in Table 3D-3. Figures 3D-16 to 3D-21 illustrate the fit between observation and models for the four sectors. At E.L.A. (Figures 3D-16 to 3D-18), no statistically significant long-term trend was detected in the case of particulate $\text{SO}_4^{=}$ and Total NO_3^- . On the other hand, long-term cycles were found for sectors I, II and III, and sectors I, II and IV for $\text{SO}_4^{=}$ and Total NO_3^- , respectively (Figures 3D-23 and 3D-25). Their periods varied between 2.0 and 5.0 years. Annual cycles were present for all sectors except the eastern United States and southeastern Canada sector (IV) for $\text{SO}_4^{=}$. For that last sector, no statistically significant non-random component was found in the case of particulate $\text{SO}_4^{=}$. A statistically significant long-term trend was detected for all sectors for SO_2 concentrations at E.L.A.. The terms $C_0 + f(t)$ of relation (1) normalized by the 1980 mean value, are shown in Figure 3D-22. For the southwest, northwest and southeast sectors (II, III and IV), the monthly median increased between January 1979 and the end of 1981 to the beginning of 1982, and then decreased. The long-term trend for the southeast and northwest sectors (II and III) are essentially identical. For the eastern United States and southeastern Canada sector (IV), and the north east sector (I) the long-term trend of the monthly median decreased by about 70% between 1980 and 1987. For the southwest and northwest sectors (III and II, respectively), the concentrations were about 60% lower in 1987 than in 1980. A long-term cycle, with period equal to 4.5 years, was only present for the northeast sector (I) (Figure 3D-24).

At Kejimikujik (Figures 3D-19 to 3D-21), long-term trends were found for some sectors for each ion. The statistically significant long-term trends are illustrated in Figures 3D-26 to 3D-28. For particulate $\text{SO}_4^{=}$, statistically significant long-term trends were detected for all sectors but the southwest (IV). It is interesting to notice that no long-term trend was encountered for the air coming from the southwest sector (IV) which is the region where the highest emissions are situated. For SO_2 , statistically significant long-term variation was found for the four sectors. The long-term trend with the highest amplitude was from

the sector off the Atlantic ocean (II). Note that this sector includes Halifax where, between 1980 and 1985, SO_2 emissions from two thermal generating stations decreased from 25713 to 5521 tonnes per annum. (J. Underwood, personal communication). For the west and southwest sectors (III and IV), the monthly median decreased slowly between January 1979 and December 1987 by about 60%. In the case of the north sector (I), the long-term trend also shows a decrease between 1979 and 1986 and then a small increase in 1987. The concentration was about 60% lower in 1986 than in 1980. For Total NO_3^- , (Figure 3D-28) statistically significant long-term trends were found only for the north and west sectors (I and III). In both cases, the long-term trend indicated that the monthly median increased and then decreased in the last few years.

In summary, the non-random components of the time series showed different patterns according to which sector one considers. At E.L.A., statistically significant long-term trends were found only for SO_2 . They showed a general decrease in the monthly median concentrations. The same general pattern was also present at Kejimikujik for SO_2 . At Kejimikujik, long-term trends were detected for SO_4^{2-} for sectors I, II and III. In the case of Total NO_3^- , only sectors I and III presented long-term trends.

Discussion

Because only between 7 and 9 years of observations were available, the results presented in the preceding section are only preliminary and must be interpreted with caution.

As mentioned earlier, the non-random temporal variation of sulphate and nitrogen ionic concentrations at a site are the end product of the interplay between two main factors, namely : 1) variation in the emission sources of SO_x and NO_x and 2) meteorological variability. A third factor that might influence the results obtained for the long-term trend components, is the changes that occurred in the sampling and analytical analysis protocols for both precipitation and ambient air.

The only perceptible effect of the changes in the sampling and analytical analysis protocols for precipitation was in the number of low sample volumes for which ionic concentrations were available. The effect of missing low volume samples before mid-1983 would be the introduction of a slight bias and greater uncertainty in the values obtained for the weekly precipitation-weighted-mean values (Sirois, 1990). The magnitude of both the bias and the uncertainties is a function of the number of samples missing and the total volume of precipitation missing. Since the percentage of event missing would be greater than the percentage of precipitation amount missing, the monthly precipitation-weighted-mean estimates should be negatively biased (Sirois, 1990). Therefore, the effect would tend to temper any decrease of the weekly mean concentration that might have occurred between the periods before and after the sampling protocol changes. That effect should however be small as the bias should in the majority of the cases be less than 5%.

If one considers the temporal variation of the daily ionic concentration in ambient air, one does not detect any major break in the time series associated with the change of sampling protocol in December 1982. Therefore, this change of sampling protocol should not have a significant effect on the results obtained in the preceding section.

In summary, one should expect that the deterministic part of the temporal variation in ion concentration in air and precipitation should be related mainly to variation in emissions

and meteorological variability. However, it is difficult to separate the relative importance of those two effects in generating the observed temporal variation in ionic concentration. The variation of the long-term trend components at a site would be driven by the long-term variations in the emission and by the long-term variation in the air circulation. Because temporal variation in emissions are region dependent, those two causes would not act independently. For example, a reduction in emission can be offset by a shift in general circulation causing an increase in the frequency of days when air is coming from regions of high emission.

As we have seen, statistically significant decreases in SO_4^{2-} , between 1980 and 1985, could be detected in precipitation at E.L.A., Algoma, Chalk River and Kejimikujik, and in air, for SO_2 concentration at Chalk River, E.L.A. and Forêt Montmorency. It is interesting to notice that the SO_2 air concentration which is sensitive to sources near the observation sites is the compound that reflects most, the general decrease in SO_x emissions. One should note that, for SO_4^{2-} concentration in precipitation, a similar decrease in the seasonal precipitation-weighted-mean concentration was detected at Dorset, Ontario (see Appendix 3F), a site close to Chalk River. For nitrate, because the pattern of NO_x emission changes is complicated (see Figure 3.2.43), it is difficult to relate these changes to the only statistically significant long-term trends observed for Total- NO_3^- in air at Chalk River, Forêt Montmorency and Kejimikujik. In summary, although long-term trends were observed for some cases, it is difficult to relate them to the variation in emissions because of the strong noise caused by meteorological variability.

Conclusion

A study of the temporal variation of the monthly mean concentrations of SO_4^{2-} and NO_3^- in precipitation and SO_4^{2-} , SO_2 and Total NO_3^- in air was presented for 5 rural sites in eastern Canada for the period 1979-1987. Weekly precipitation-weighted mean concentrations and monthly median concentrations were used for the ions in precipitation and air, respectively. Models that assume that the temporal variations is the sum of a long-term trend, long-term cycles, annual cycles and a random function were fitted to the logarithmic transform of the weekly mean or the monthly median ionic concentrations using least-squares. In the case of the ionic concentration in precipitation, a fifth term describing the relationship between concentration and precipitation amount was added.

The main findings of this study are :

- Statistically significant relationships between weekly mean ionic concentrations in precipitation and precipitation depth were found at all sites except Algoma for NO_3^- .
- For SO_4^{2-} in precipitation, the weekly mean concentrations decreased with time at E.L.A., Algoma, Chalk River and Kejimikujik by 25-40% between 1980 and 1987.
- In air, long-term trends (not necessarily monotonic) were detected in the monthly median ionic concentrations at Chalk River for SO_4^{2-} ; at Chalk River, Kejimikujik and Forêt Montmorency for Total NO_3^- ; and at all sites except Algoma for SO_2 . The logarithmic transform of the monthly median SO_2 concentrations decreased with time at E.L.A., Algoma and Chalk River.
- Statistically significant long-term cycles were present for most ions and sites;

- Statistically significant annual cycles were found for all ions and sites, except at Chalk River for $\text{SO}_4^{=}$ concentration in air.
- At E.L.A., when back-trajectories were used to classify daily samples by regions of origin or sectors, statistically significant long-term trends were encountered only for SO_2 . Also for all sectors at E.L.A., the long-term component of the monthly median SO_2 concentrations decreased by a factor of about 3 to 4 between January 1982 and December 1987.
- At Kejimikujik, long-term trends were found for all sectors and ions, except for the southwest sector (IV) in the case of particulate $\text{SO}_4^{=}$ and for the off Atlantic - Nova Scotia and southwest sectors (II and IV) in the case of Total- NO_3^- . For all sectors, the long-term component of the monthly median SO_2 concentration decreased by a factor 2 to 10 between January 1981 and December 1987. The highest decrease was for the relatively clean air coming off the Atlantic ocean - Nova Scotia sector (II) and the lowest for the air coming from the relatively polluted southwest sector (IV).

The present study makes clear two important facts. Firstly, more complicated models than a simple linear long-term trend and an annual cycle are necessary to describe the temporal variation of ionic concentration in air and precipitation. Secondly, although long-term variation can be detected, to link them with the temporal variation in emissions of the order of 18 to 30% is difficult. This is because of many factors including meteorological variability, length of observational record and continuity of observational method.

Table 3D-1

Summary of results of time series analysis of SO_4^{2-} and NO_3^- concentration in air at 5 rural locations in eastern Canada.

N is the number of data used and R^2 is the fraction of the total variance explained by the model.

"Y" means that model component is present and "N" that it is not present.

ION	SITE	N	R^2	PRECIP. DEPTH	LONG-TERM TREND	LONG-TERM CYCLE	ANNUAL CYCLE
SO_4^{2-}	E.L.A.	318	.34	Y	Y	Y	Y
	ALGOMA	302	.19	Y	Y	Y	Y
	CHALK RIVER	363	.34	Y	Y	N	Y
	MONTMORENCY	257	.27	Y	Y	N	Y
	KEJIMKUJIK	364	.31	Y	Y	N	Y
SO_2	E.L.A.	269	.19	Y	N	Y	Y
	ALGOMA	291	.15	N	N	Y	Y
	CHALK RIVER	325	.17	Y	N	N	Y
	MONTMORENCY	248	.06	Y	N	Y	Y
	KEJIMKUJIK	347	.20	Y	Y	N	Y

Table 3D-2

Summary of results of time series analysis of SO_4^{2-} , SO_2 and Total NO_3^- concentration in air at 5 rural locations in eastern Canada.

N is the number of data used and R^2 is the fraction of the total variance explained by the model.

"Y" means that model component is present and "N" that it is not present.

ION	SITE	N	R^2	LONG-TERM TREND	LONG-TERM CYCLE	ANNUAL CYCLE
SO_4^{2-}	E.L.A.	103	.52	N	Y	Y
	ALGOMA	84	.17	N	N	Y
	CHALK RIVER	105	.27	Y	Y	N
	MONTMORENCY	80	.35	N	Y	Y
	KEJIMKUJIK	98	.35	N	Y	Y
SO_2	E.L.A.	79	.71	Y	Y	Y
	ALGOMA	79	.71	N	Y	Y
	CHALK RIVER	104	.80	Y	N	Y
	MONTMORENCY	65	.77	Y	N	Y
	KEJIMKUJIK	83	.78	Y	Y	Y
T- NO_3^-	E.L.A.	102	.37	N	Y	Y
	ALGOMA	83	.12	N	N	Y
	CHALK RIVER	103	.40	Y	Y	Y
	MONTMORENCY	76	.19	Y	N	Y
	KEJIMKUJIK	98	.24	Y	N	Y

Table 3D-3

Summary of results of time series analysis of $\text{SO}_4^{=}$, SO_2 and Total NO_3^- concentration in air for the four different sectors of origin at E.L.A. and Kejimkujik.

N is the number of data used and R^2 is the fraction of the total variance explained by the model.

"Y" means that model component is present and "N" that it is not present.

ION	SECTOR	N	R^2	LONG-TERM TREND	LONG-TERM CYCLE	ANNUAL CYCLE
E.L.A.						
$\text{SO}_4^{=}$	I	96	.61	N	Y	Y
	II	103	.35	N	Y	Y
	III	98	.47	N	Y	Y
	IV	100	.00	N	N	N
SO_2	I	68	.66	Y	Y	Y
	II	82	.62	Y	N	Y
	III	72	.70	Y	N	Y
	IV	72	.31	Y	N	Y
T- NO_3^-	I	98	.56	N	Y	Y
	II	96	.56	N	Y	Y
	III	93	.39	N	N	Y
	IV	99	.21	N	Y	Y
KEJIMKUJIK						
$\text{SO}_4^{=}$	I	96	.37	Y	N	Y
	II	84	.11	Y	Y	N
	III	97	.20	Y	N	Y
	IV	98	.38	N	Y	Y
SO_2	I	82	.66	Y	Y	Y
	II	56	.81	Y	Y	Y
	III	84	.63	Y	Y	Y
	IV	82	.55	Y	Y	Y
T- NO_3^-	I	97	.24	Y	Y	Y
	II	82	.00	N	N	N
	III	97	.20	Y	N	Y
	IV	97	.15	N	Y	Y

Table 3D-4

Frequency of occurrence of the four sectors defined in Figure 3D-14 for the daily $\text{SO}_4^{=}$, SO_2 and Total NO_3^- concentrations in air at E.L.A. and Kejimkujik.

	E.L.A.			KEJIMKUJIK		
SECTOR	$\text{SO}_4^{=}$	SO_2	T- NO_3^-	$\text{SO}_4^{=}$	SO_2	T- NO_3^-
I	25.7	24.6	60.6	32.9	32.2	38.6
II	37.0	38.3	15.5	14.9	14.8	14.7
III	23.8	24.7	11.8	27.6	28.1	20.5
IV	13.5	12.4	12.1	24.6	24.8	26.2

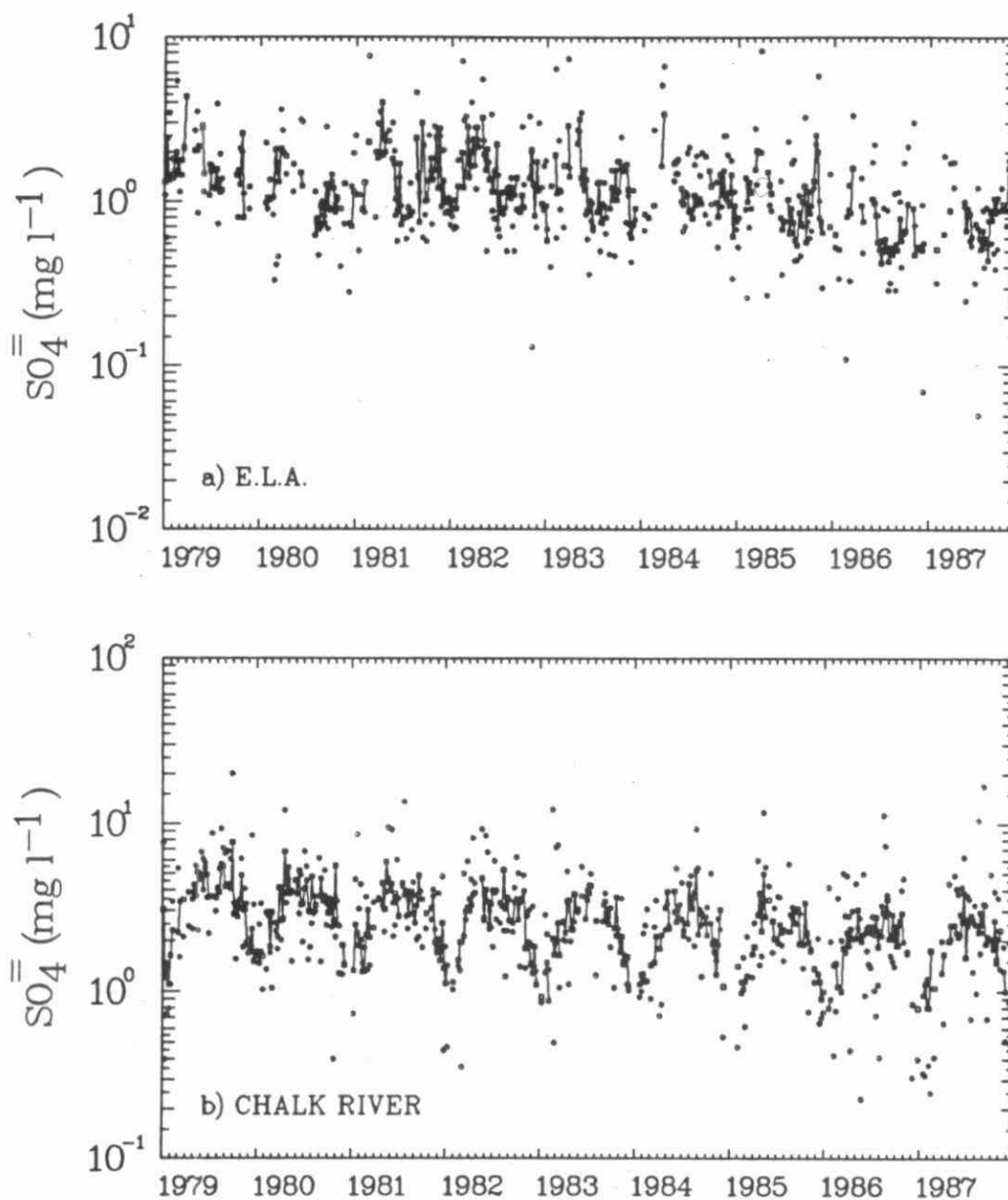


Fig. 3D-1 Temporal variation of $\text{SO}_4^=$ monthly precipitation-weighted-mean concentration in precipitation at ELA (a) and Chalk River (b). The dots and the squares are for observed and modeled values, respectively.

LONG-TERM TREND

$\text{SO}_4^{=}$

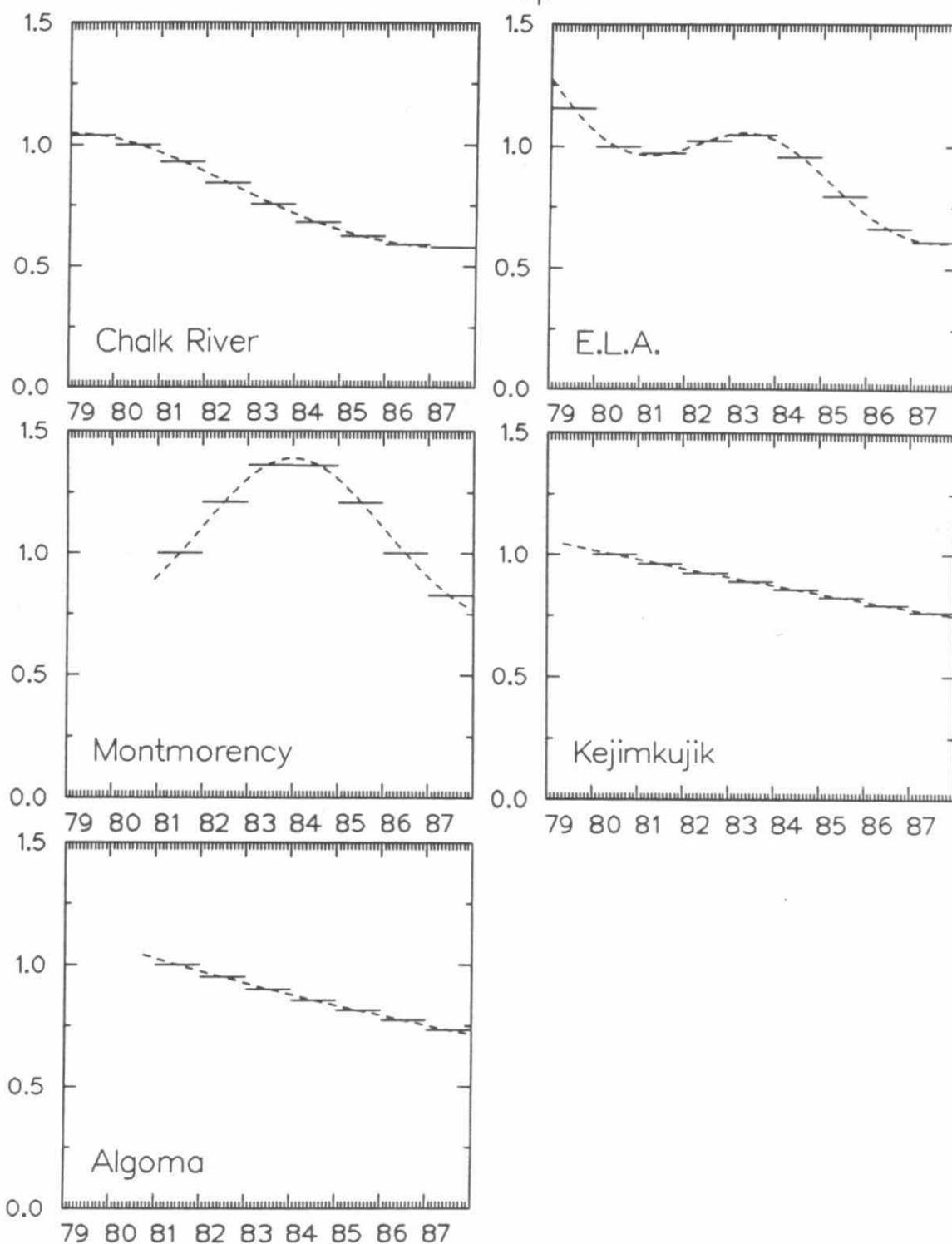


Fig. 3D-2 Intercept and long-term trend ($C_0 + f^t(t)$) of $\text{SO}_4^{=}$ concentrations in precipitation normalized to 1980 (or first complete year of record). Dashed line-continuous trend; solid line-normalized annual values. Only sites with statistically significant long-term trends are shown.

LONG-TERM TREND

NO_3^-

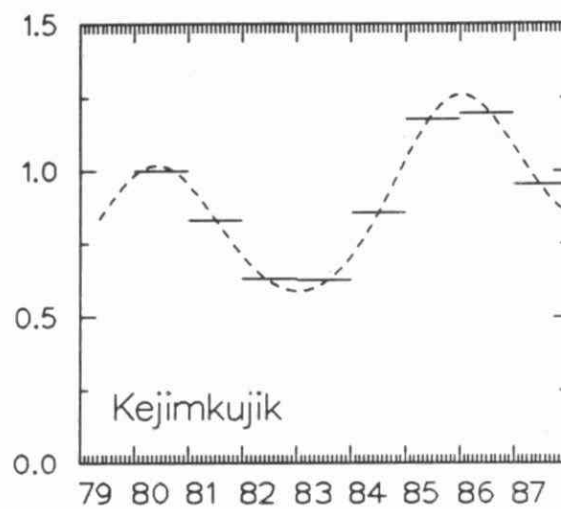


Fig. 3D-3 Same as Figure 3D-2 for NO_3^- in precipitation.

LONG-TERM TREND AND CYCLE

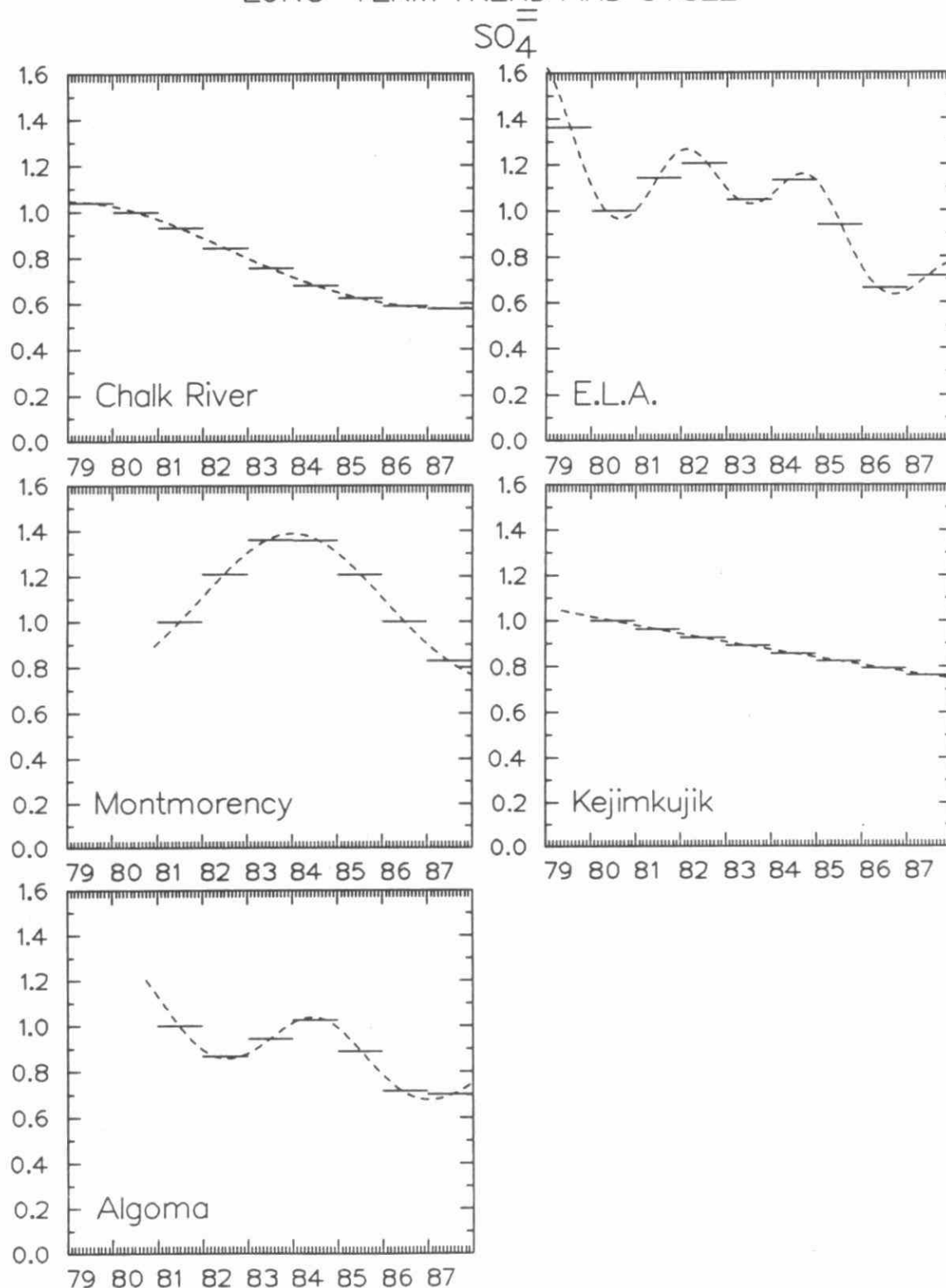


Fig. 3D-4 Intercept, long-term trend and long-term cycle ($C_0 + f^t(t) + f^c(t)$) of $\text{SO}_4^{=}$ concentration in precipitation normalized to 1980 (or first complete year of record). Dashed line-continuous trend; solid lines-annual normalized values. Only sites with statistically significant trends are shown.

LONG-TERM TREND AND CYCLE

NO_3^-

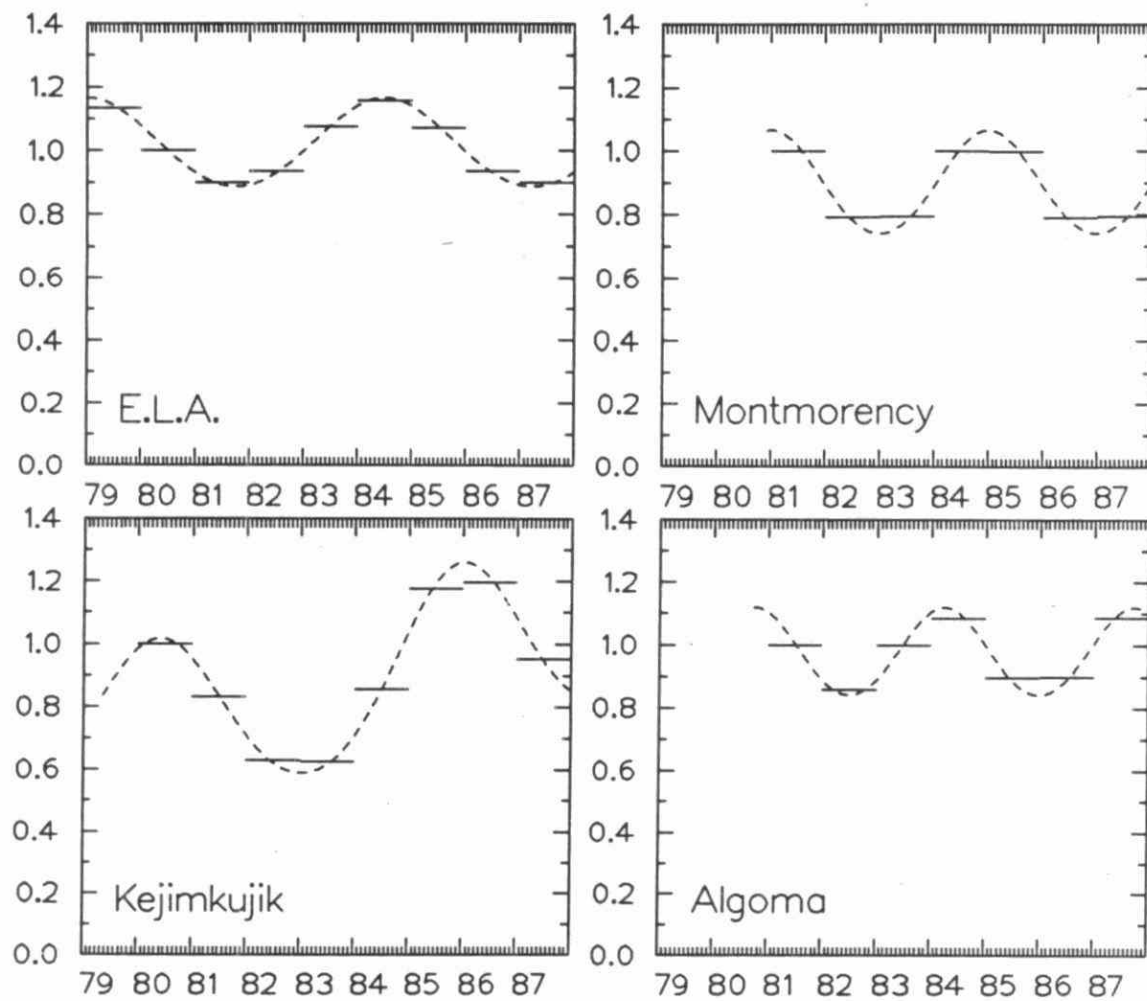


Fig. 3D-5 Same as Figure 3D-4 for NO_3^- in precipitation.

E.L.A.

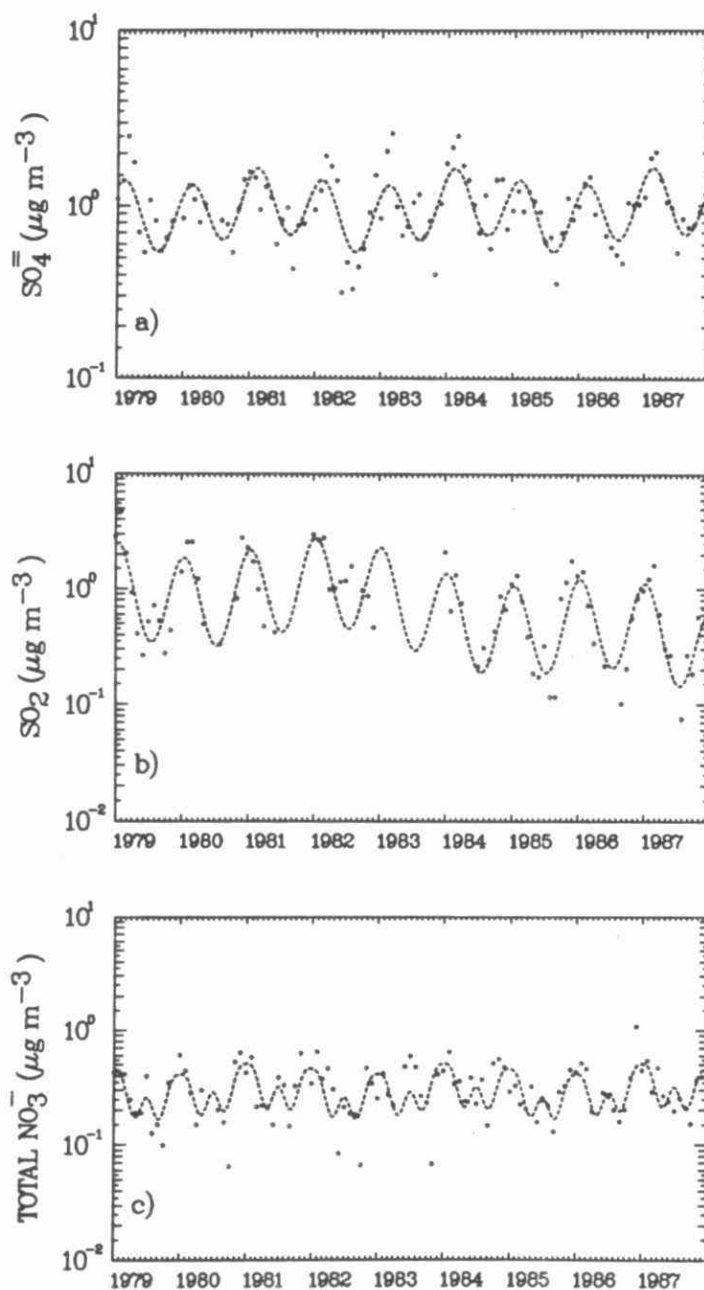


Fig. 3D-6 Temporal variation of monthly median air concentrations at ELA for SO_4^{2-} (a), SO_2 (b) and Total NO_3^- (c). Dashed line - model; dots - observations.

KEJIMKUJIK

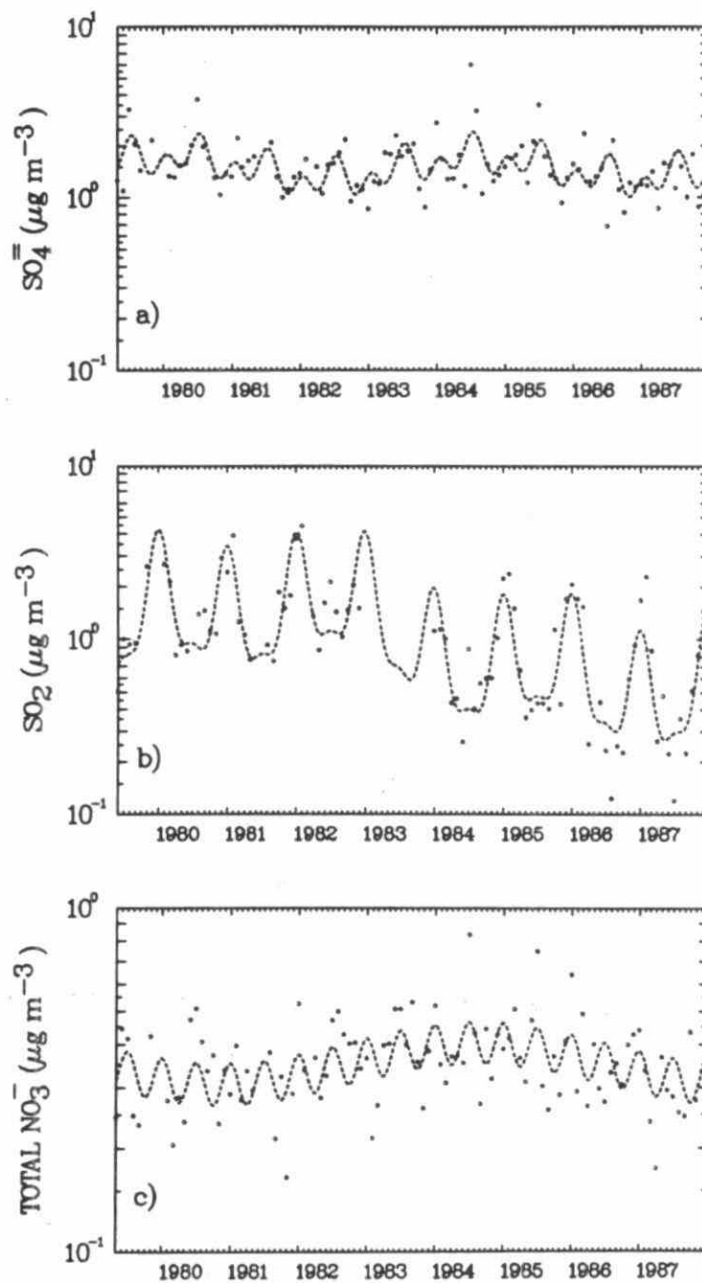


Fig. 3D-7 Same as Figure 3D-6 for Kejimkujik.

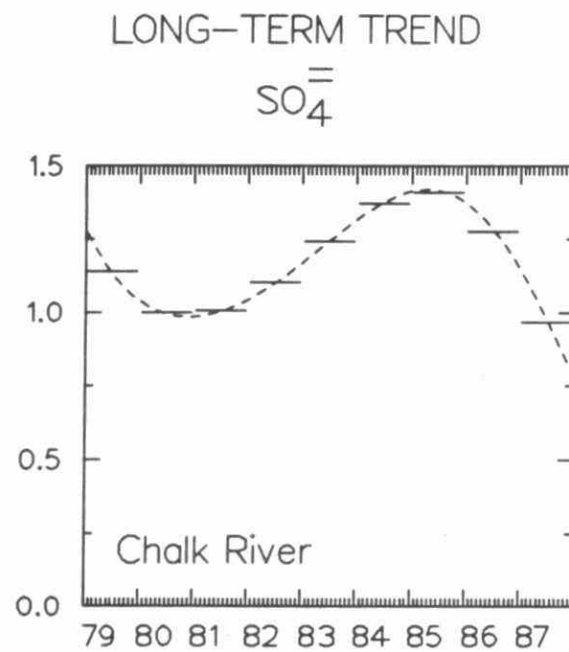


Fig. 3D-8 Same as Figure 3D-2 except for monthly median $\text{SO}_4^{=}$ concentrations in air.

LONG-TERM TREND

SO₂

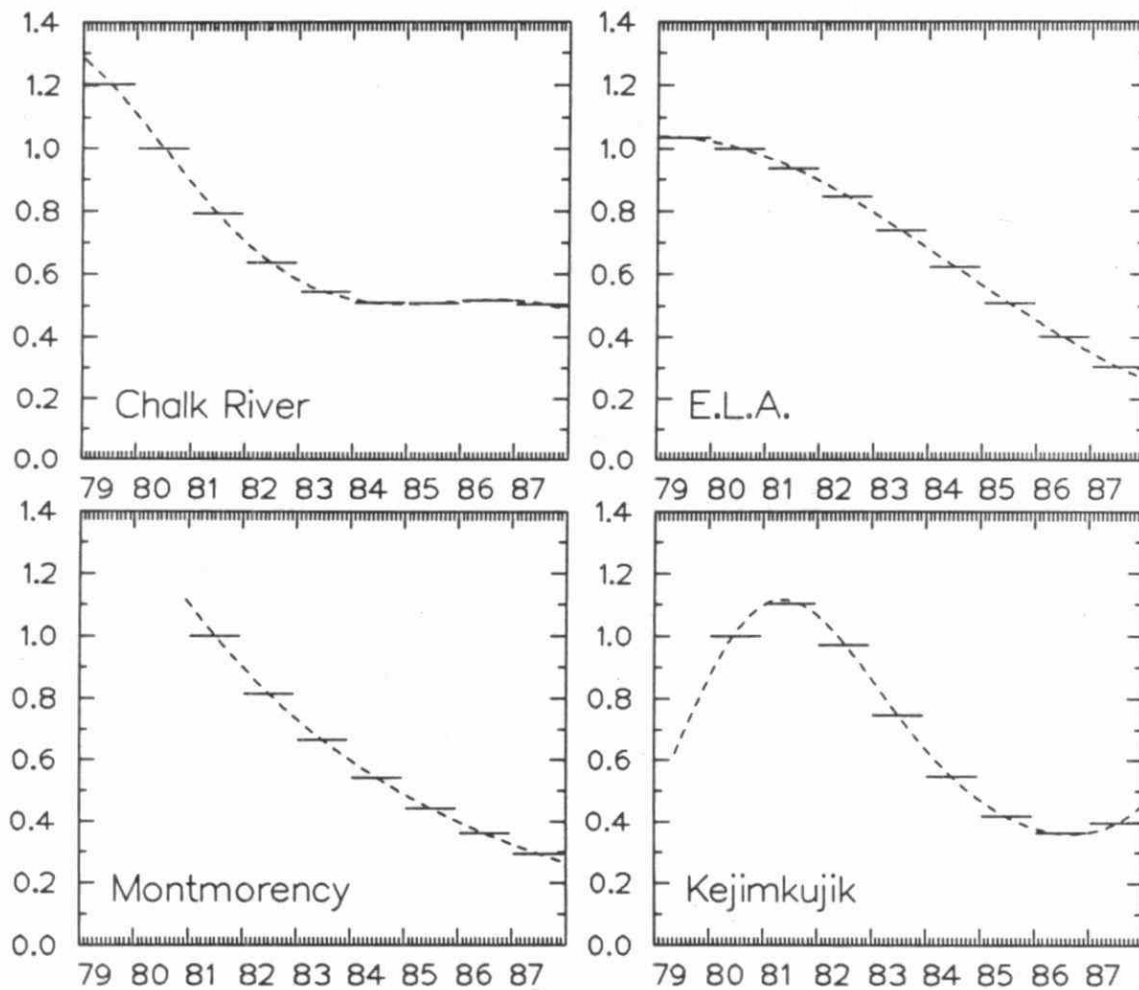


Fig. 3D-9 Same as Figure 3D-8 for SO₂ in air.

LONG-TERM TREND

Total NO_3^-

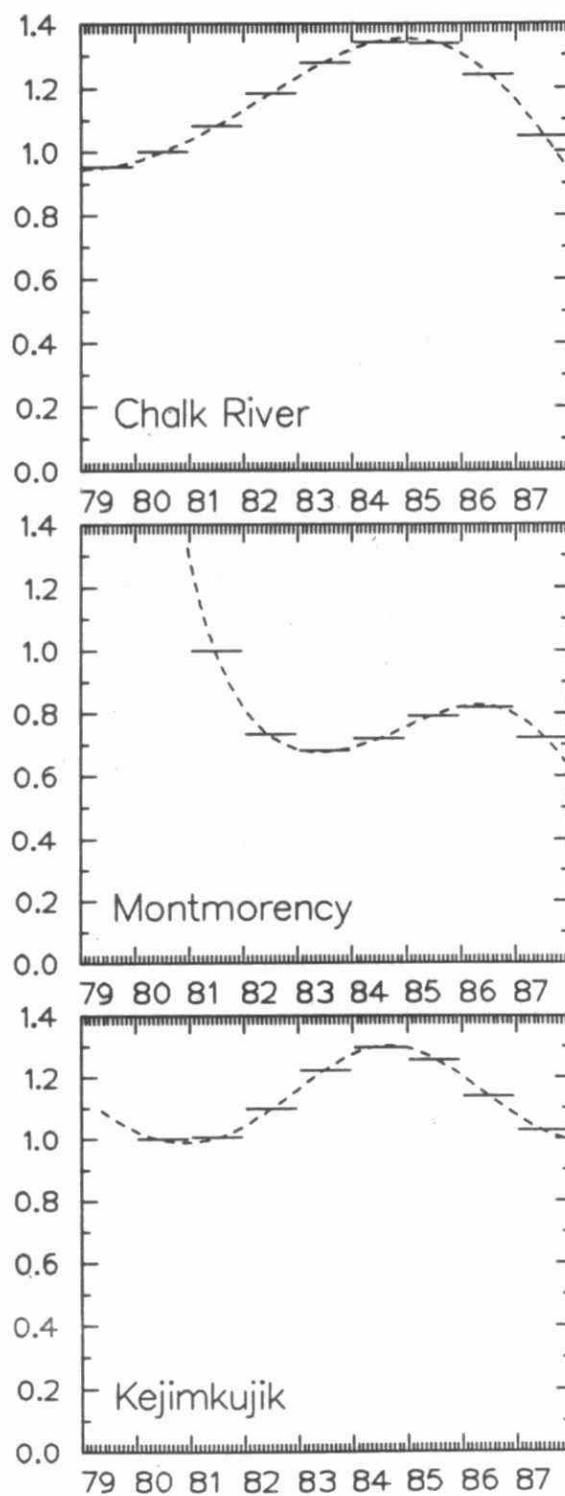


Fig. 3D-10 Same as Figure 3D-8 for Total NO_3^- in air.

LONG-TERM TREND AND CYCLE

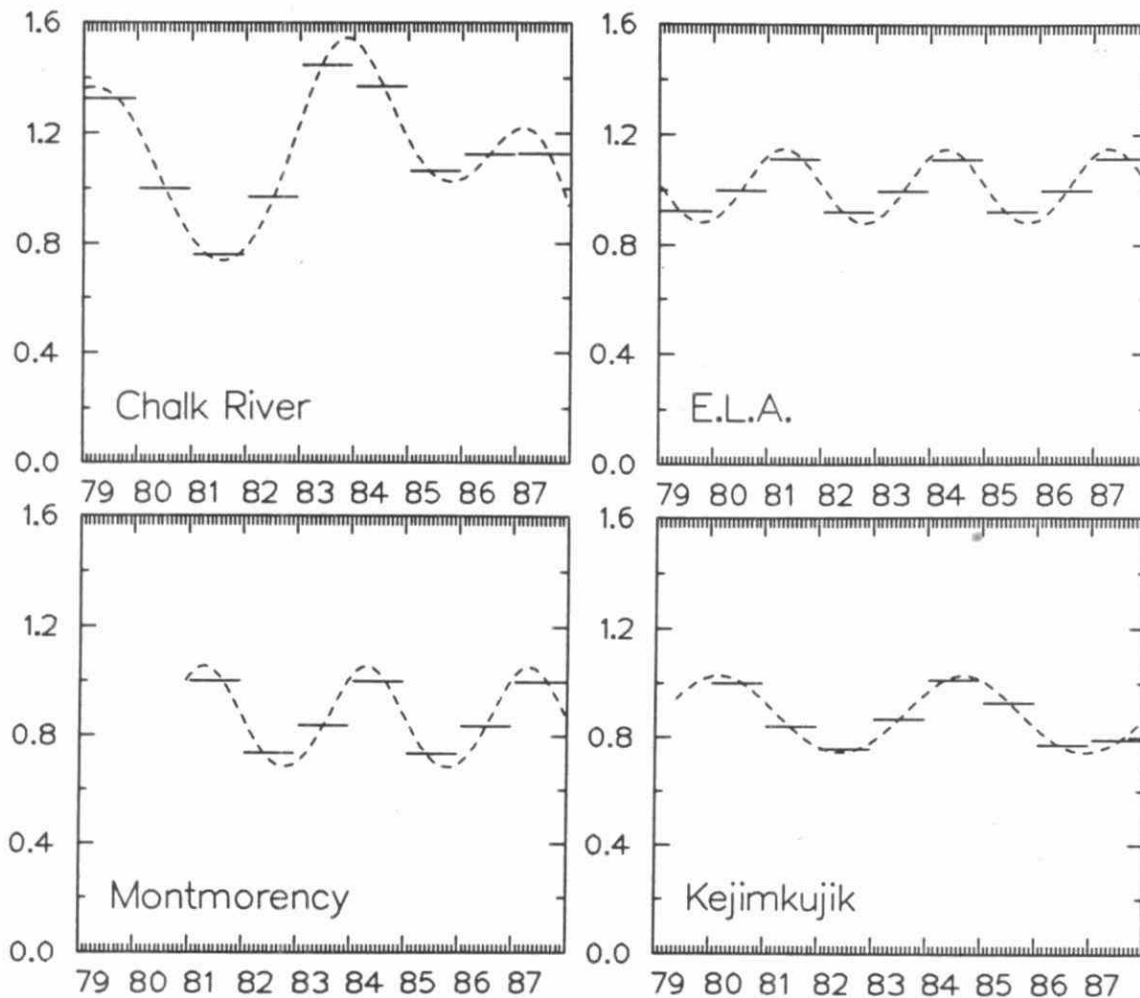


Fig. 3D-11 Same as Figure 3D-4 except for monthly median $\text{SO}_4^{=}$ concentrations in air.

LONG-TERM TREND AND CYCLE

SO₂

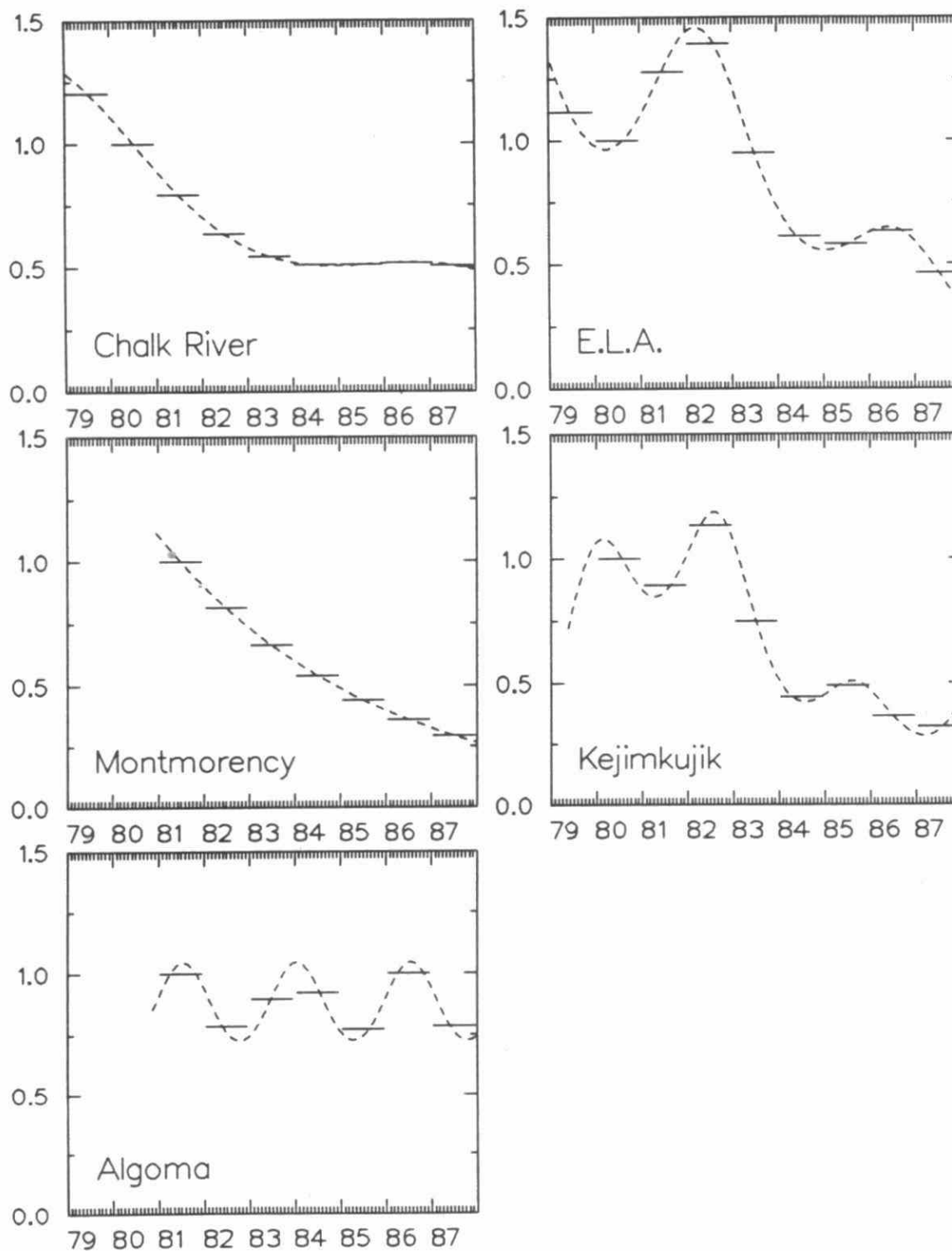


Fig. 3D-12 Same as Figure 3D-11 for SO₂ in air.

LONG-TERM TREND AND CYCLE

Total NO_3^-

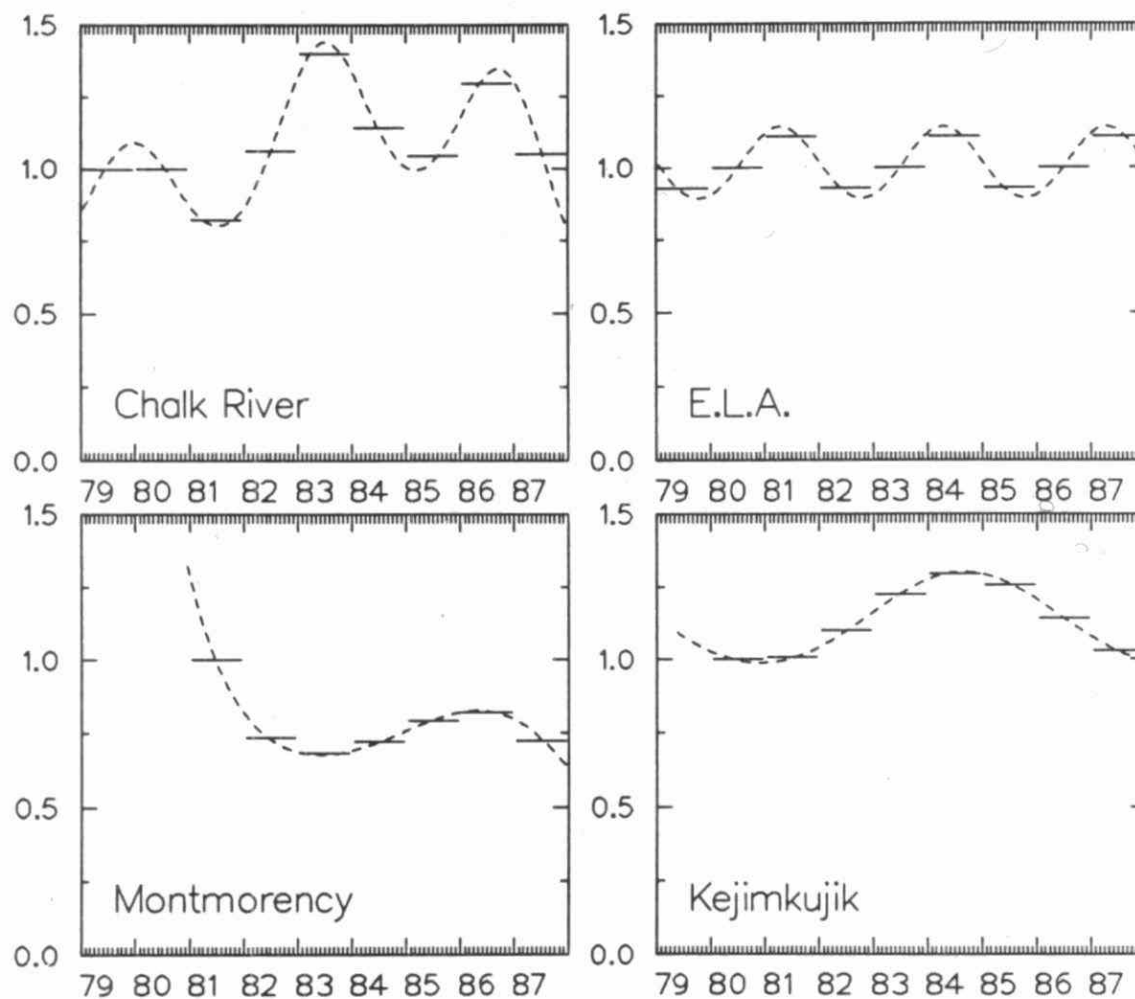


Fig. 3D-13 Same as Figure 3D-11 for Total NO_3^- in air.

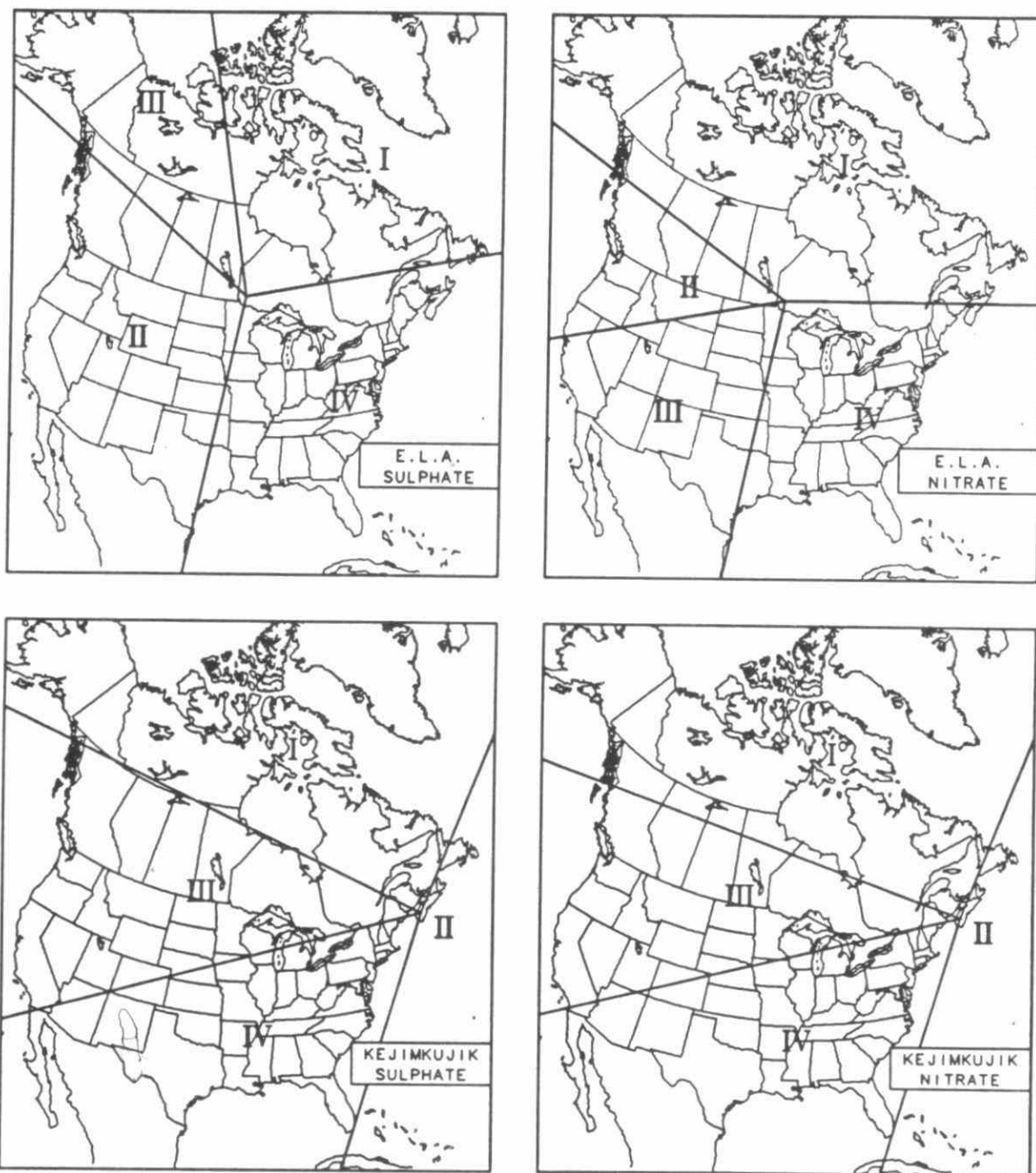


Fig. 3D-14 Definition of sectors for sulphate and nitrate for ELA and Kejimikujik.

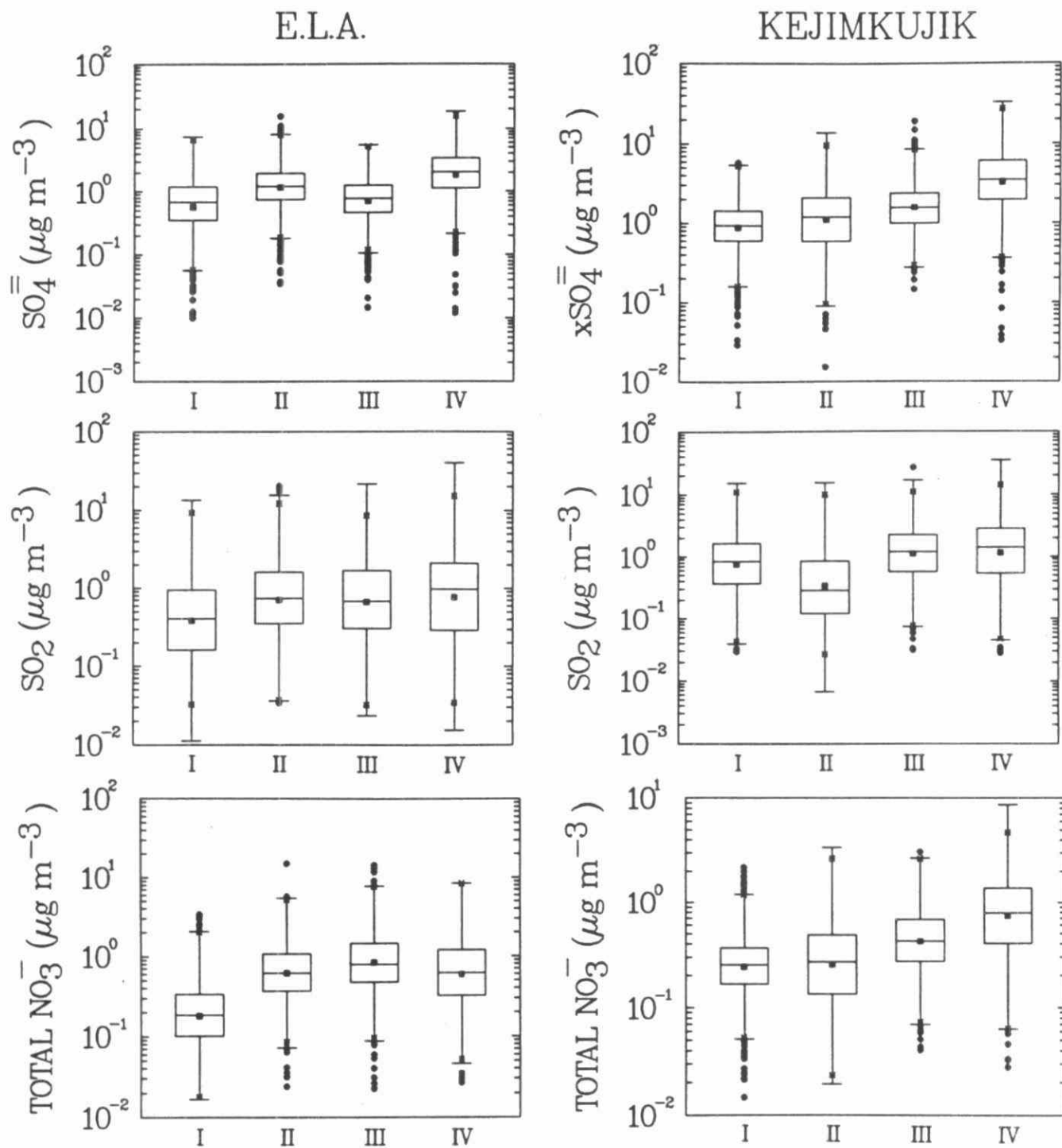


Fig. 3D-15 Boxplots for the SO_4^{2-} , SO_2 and Total NO_3^- concentrations in air for the sectors defined in Figure 3D-14 at E.L.A. and Kejimkujik. In each box, the central bar is the median and the lower and upper limits are the first and third quartiles, respectively. The lines extending vertically from the box indicate the spread of the distribution with the length being 1.5 times the difference between the first and third quartiles. Observations falling beyond the limits of those lines are considered to be outliers and are indicated by dots. The stars along the lines indicate the lowest and highest observations that were not outliers. The black squares are the monthly geometric means.

E.L.A.

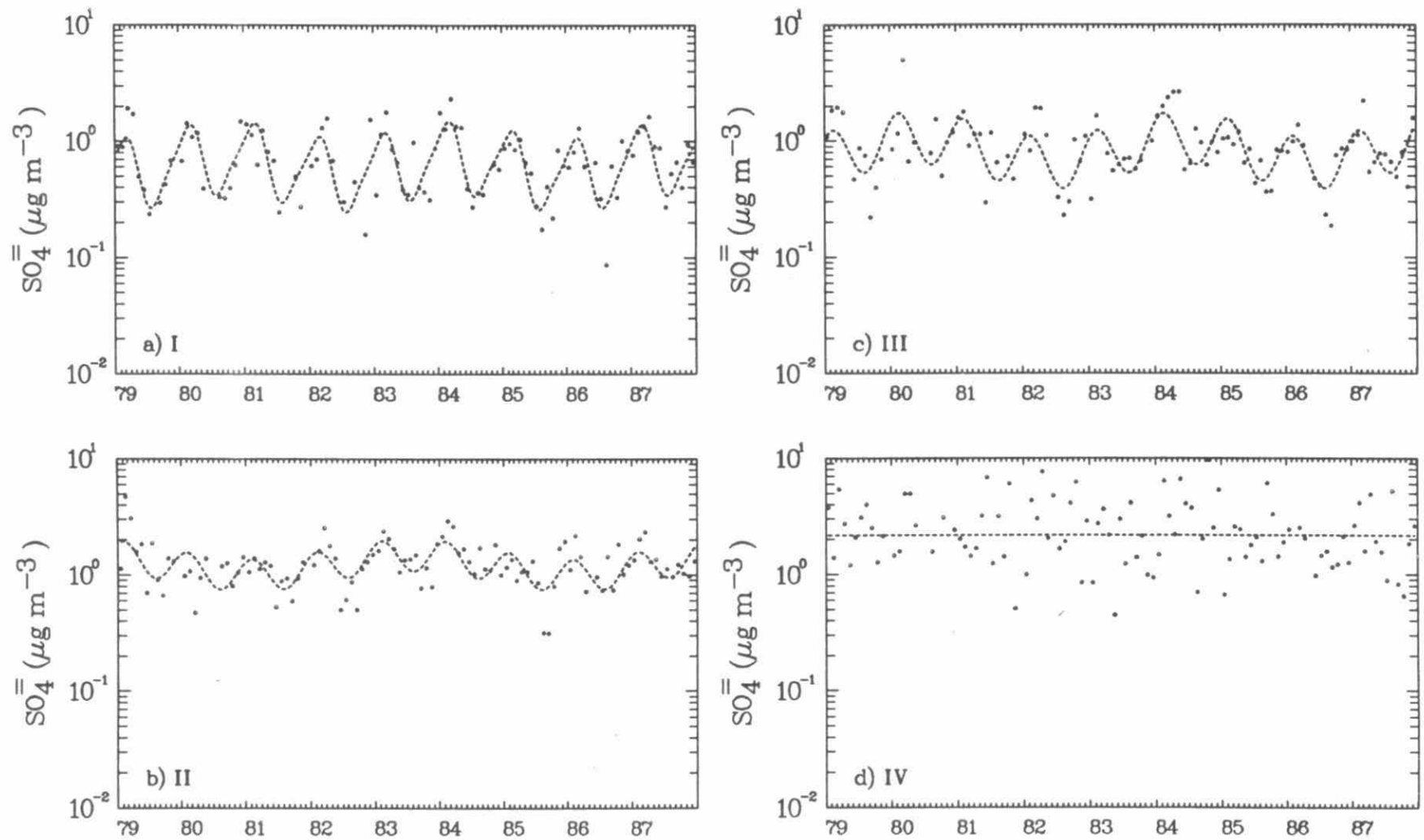
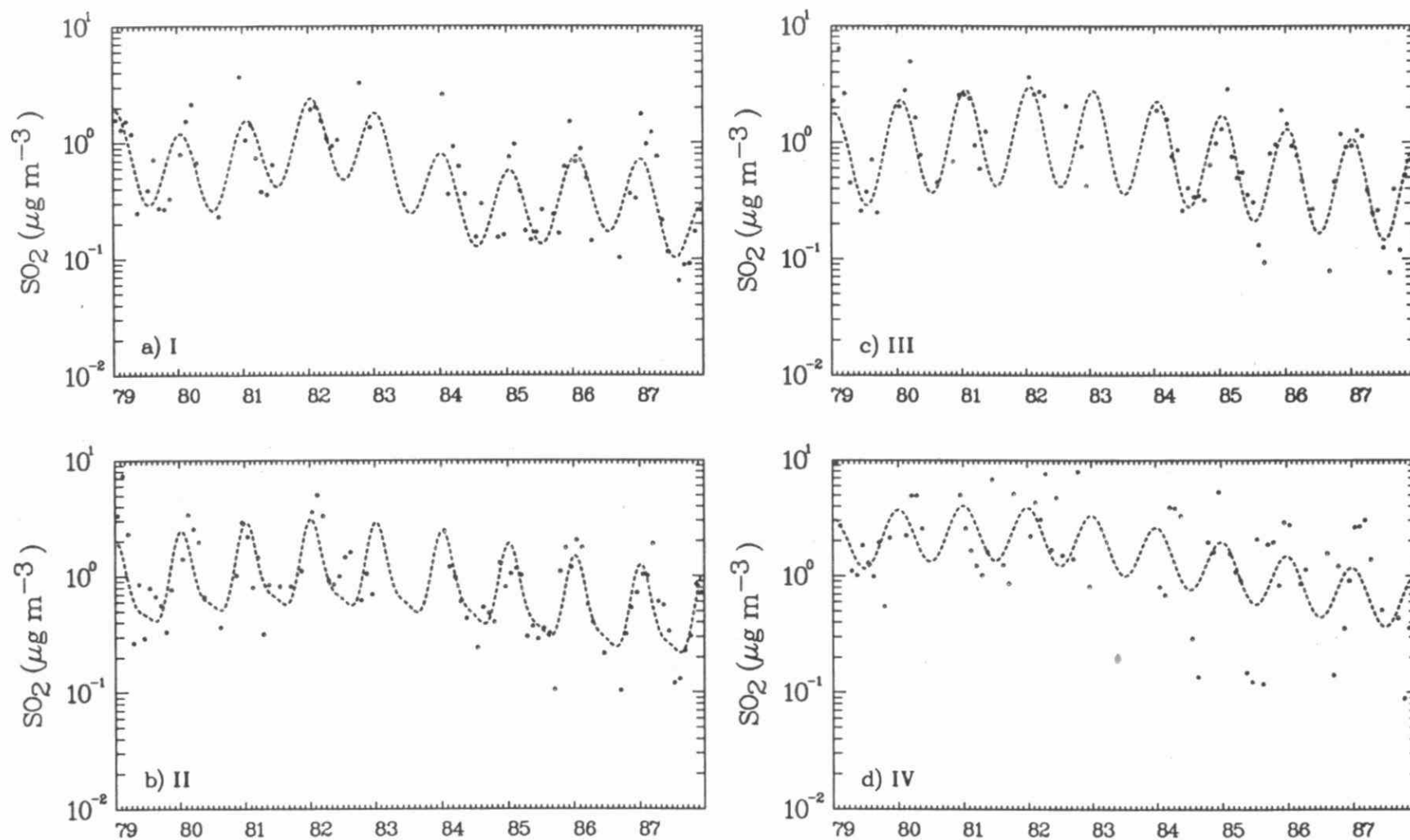


Fig. 3D-16 Temporal variation of $\text{SO}_4=$ monthly median concentration in air at ELA for the sectors defined in Figure 3D-14. Dashed line - model; dots - observations.

E.L.A.

Fig. 3D-17 Same as Figure 3D-16 for SO_2 .

E.L.A.

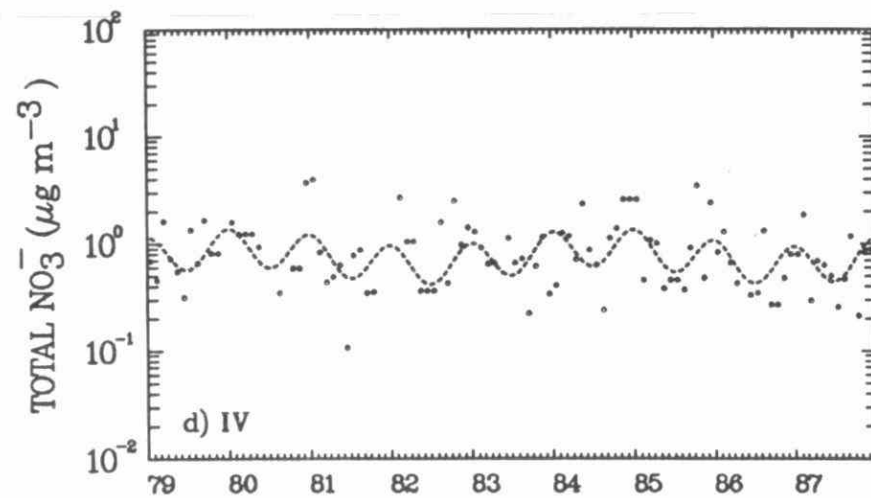
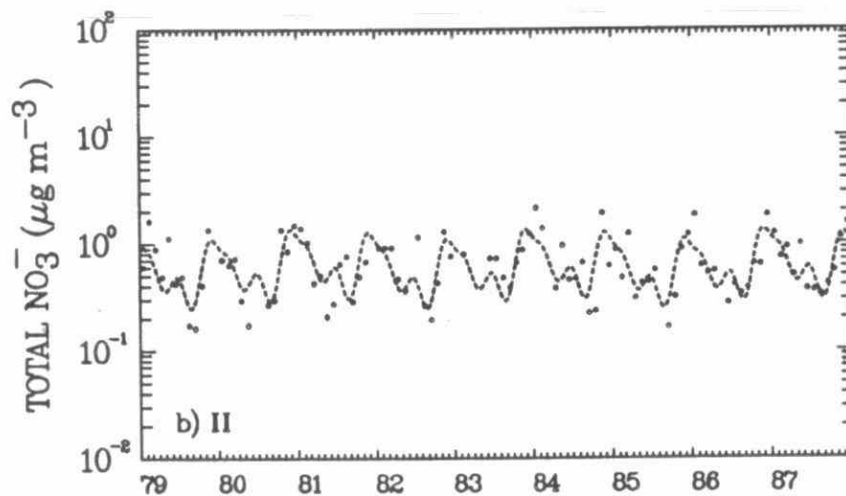
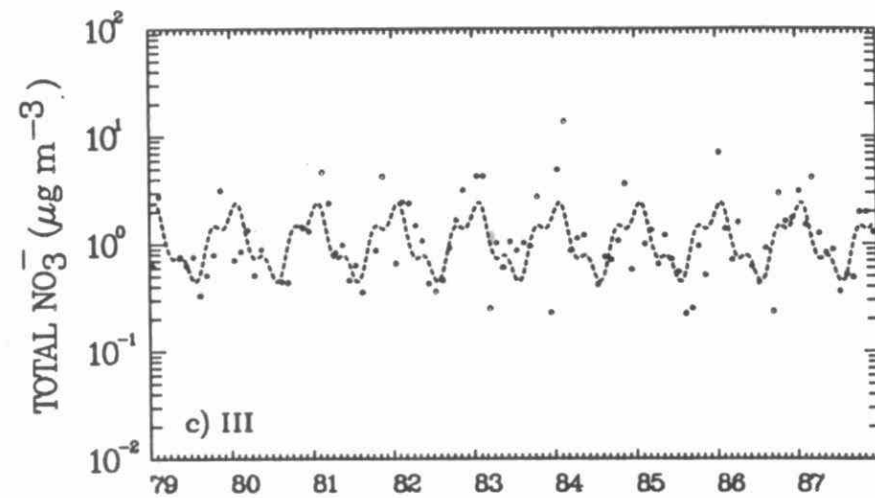
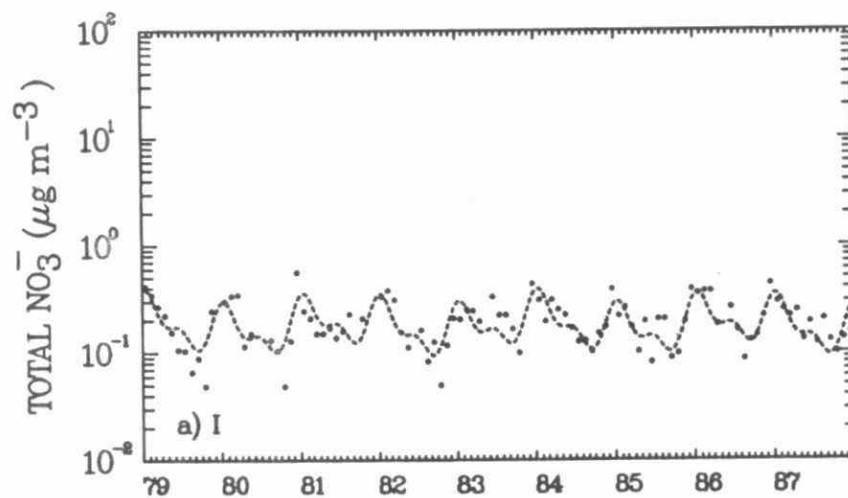


Fig. 3D-18 Same as Figure 3D-16 for Total NO_3^- .

KEJIMKUJIK

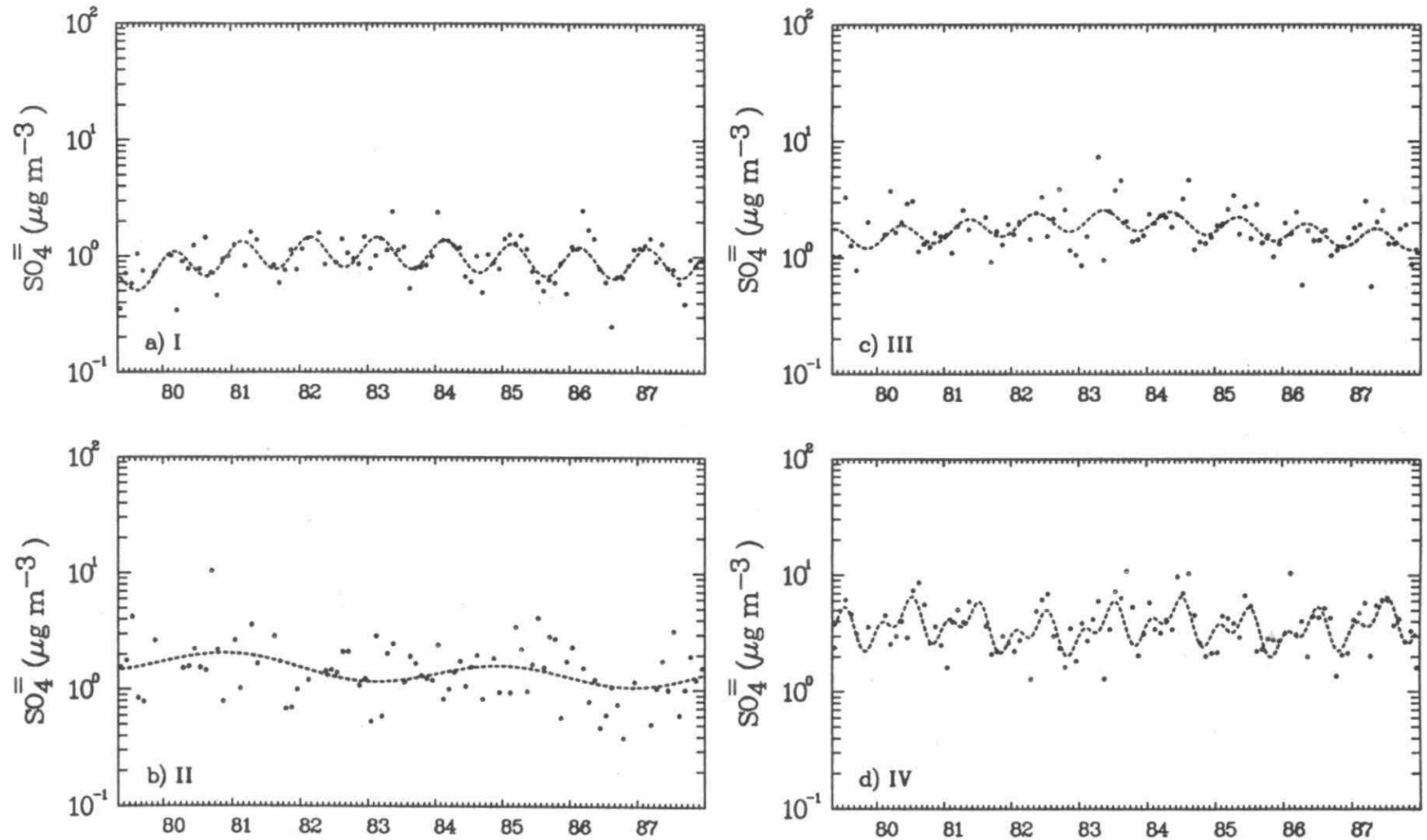


Fig. 3D-19 Temporal variation of $\text{SO}_4=$ monthly median concentration in air at Kejimikujik for the sectors defined in Figure 3D-14. Dashed line model; dots - observations.

KEJIMKUJIK

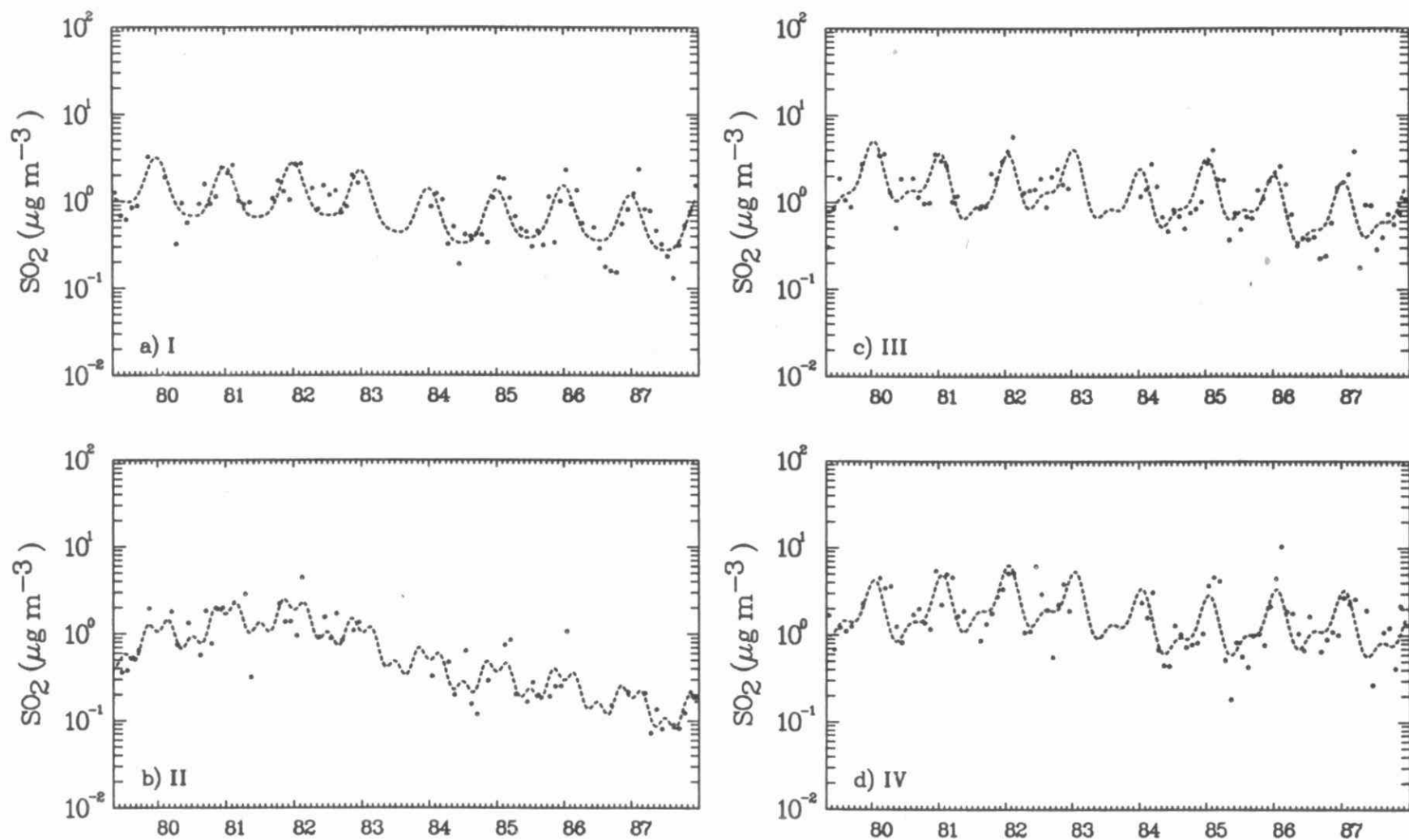


Fig. 3D-20 Same as Figure 3D-19 for SO_2 .

KEJIMKUJIK

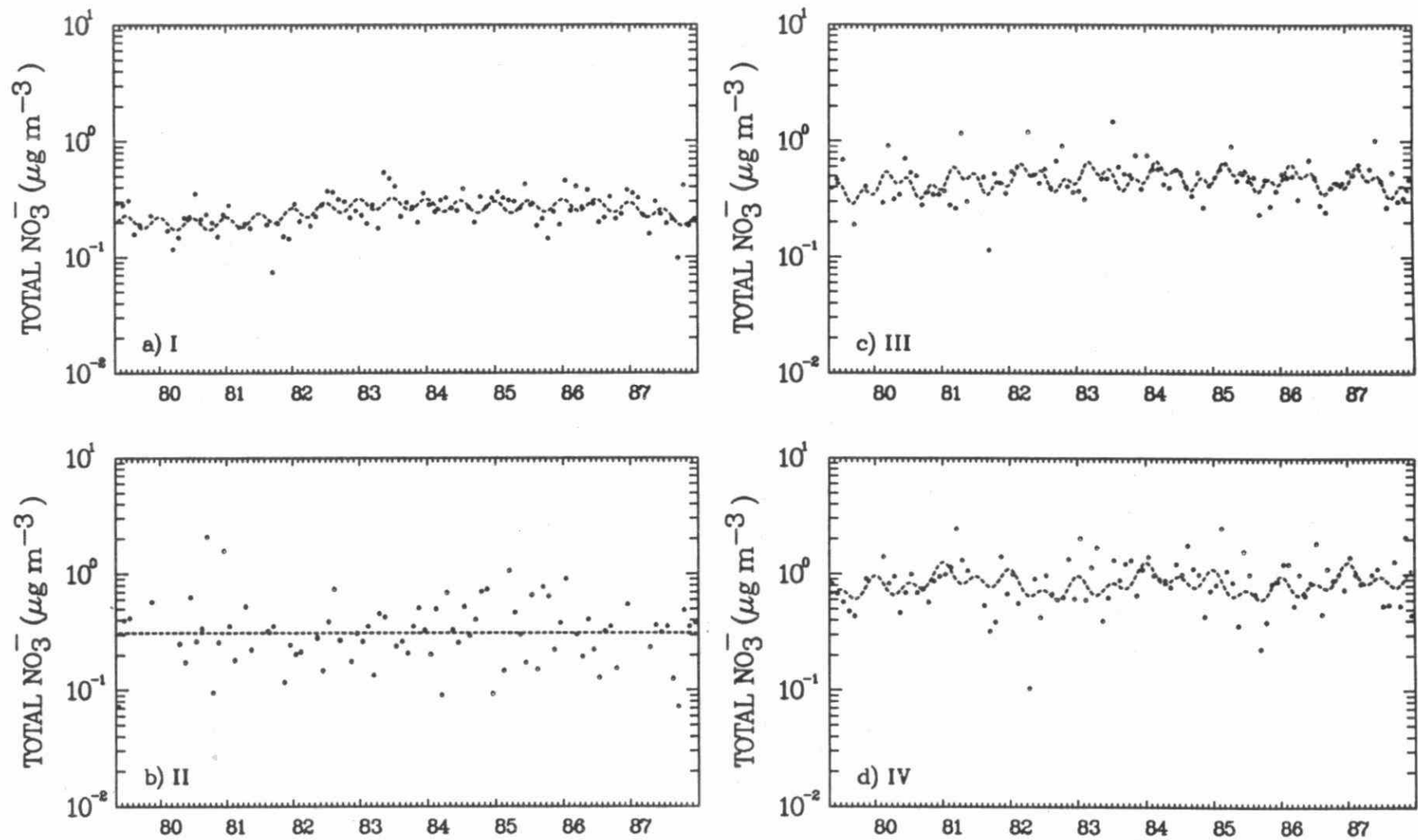


Fig. 3D-21 Same as Figure 3D-19 for Total NO_3^- .

LONG-TERM TREND

E.L.A.

SO₂

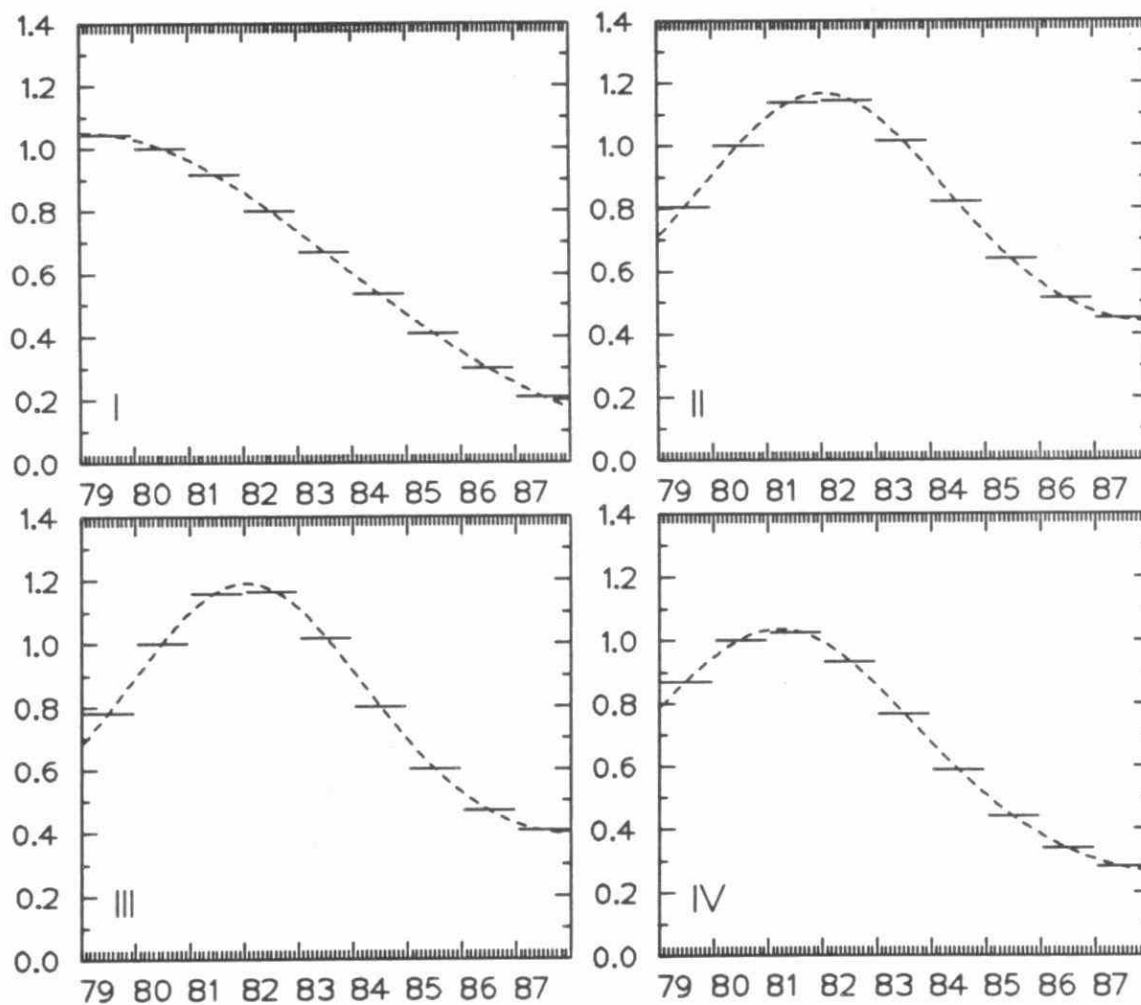


Fig. 3D-22 Intercept and long-term trend of monthly median SO₂ concentrations in air at ELA normalized to 1980 for the four sectors in Figure 3D-14. Dashed line - continuous trend; solid lines - normalized annual averages.

LONG-TERM TREND AND CYCLE

E.L.A.

$\text{SO}_4^=$

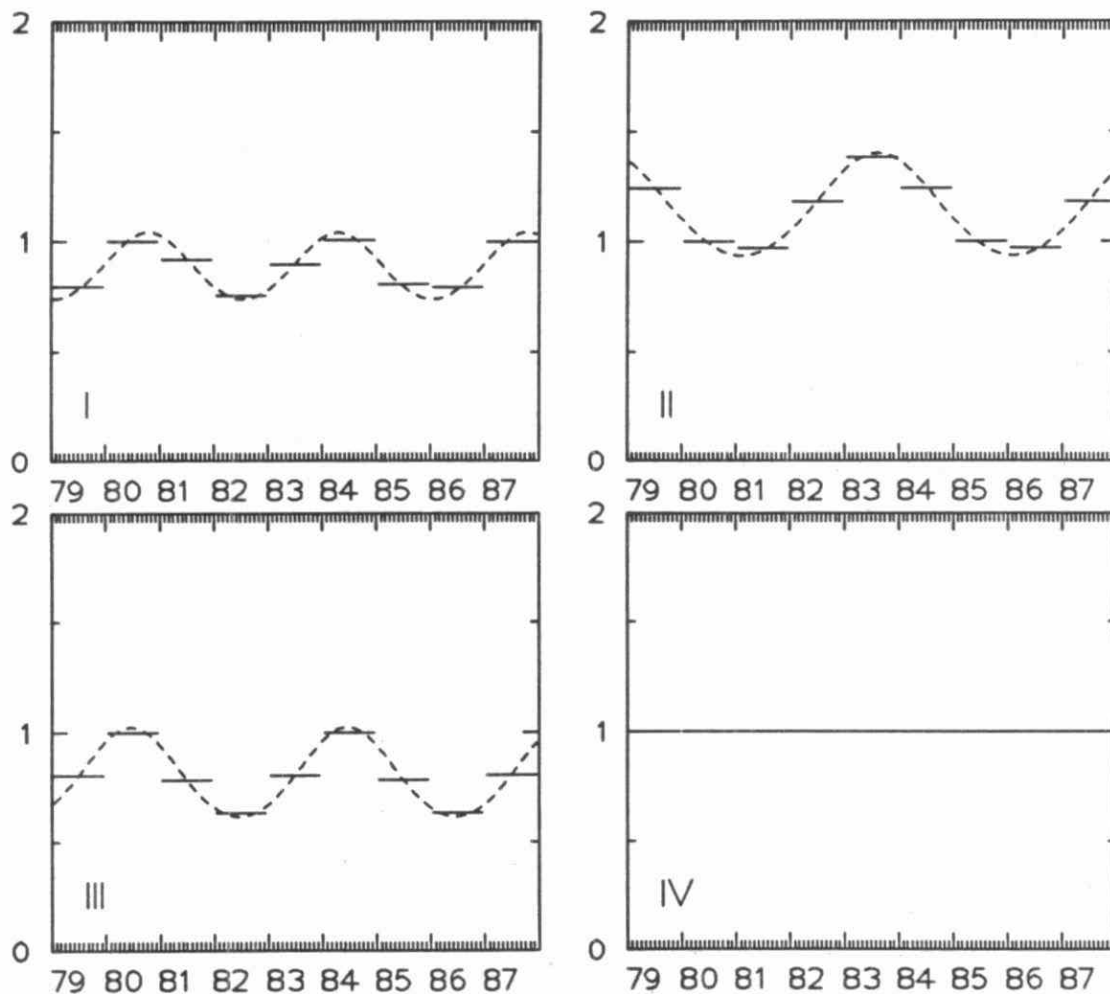


Fig. 3D-23 Same as Figure 3D-22 except that it represents the intercept, long-term trend plus long-term cycle of $\text{SO}_4^=$ in air at ELA.

LONG-TERM TREND AND CYCLE

E.L.A.

SO₂

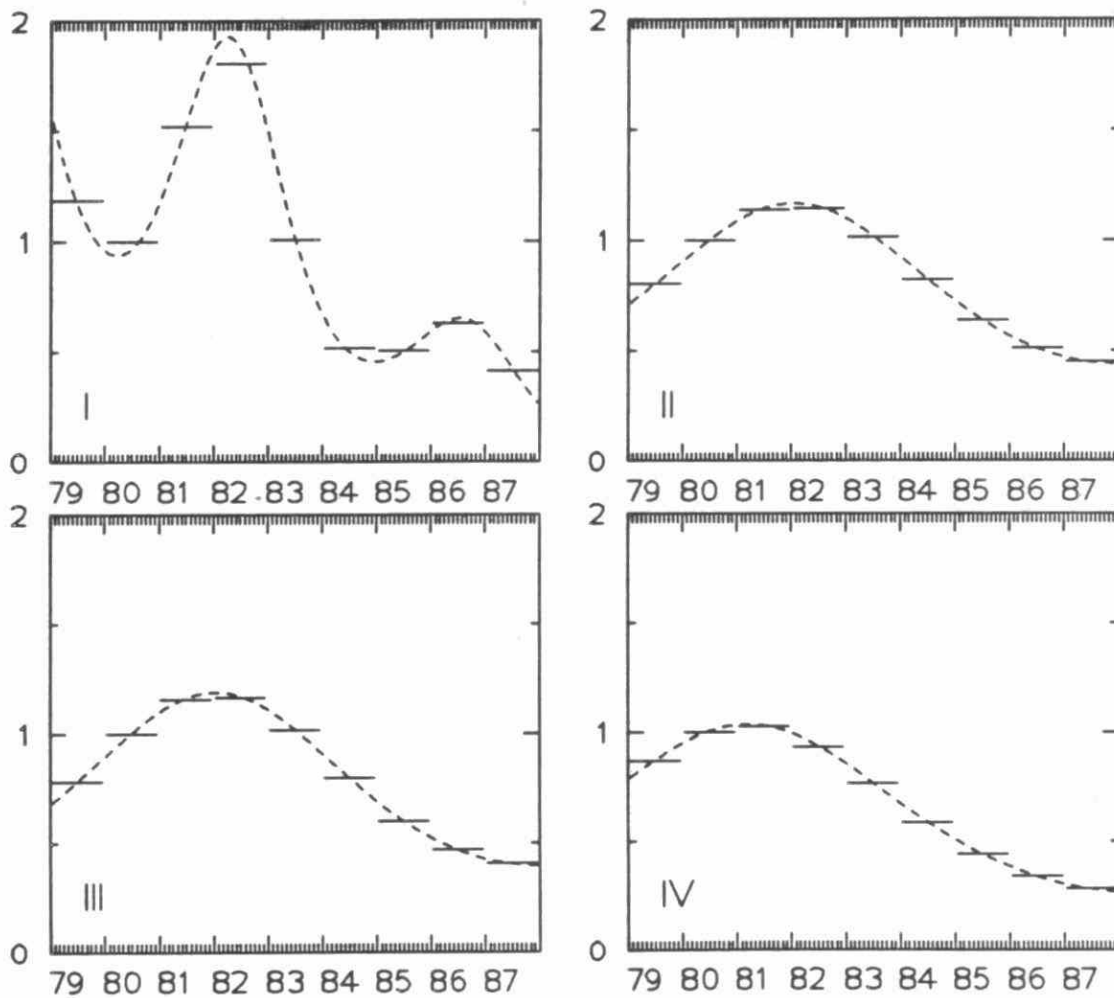


Fig. 3D-24 Same as Figure 3D-23 for SO₂ in air.

LONG-TERM TREND AND CYCLE

E.L.A.

Total NO_3^-

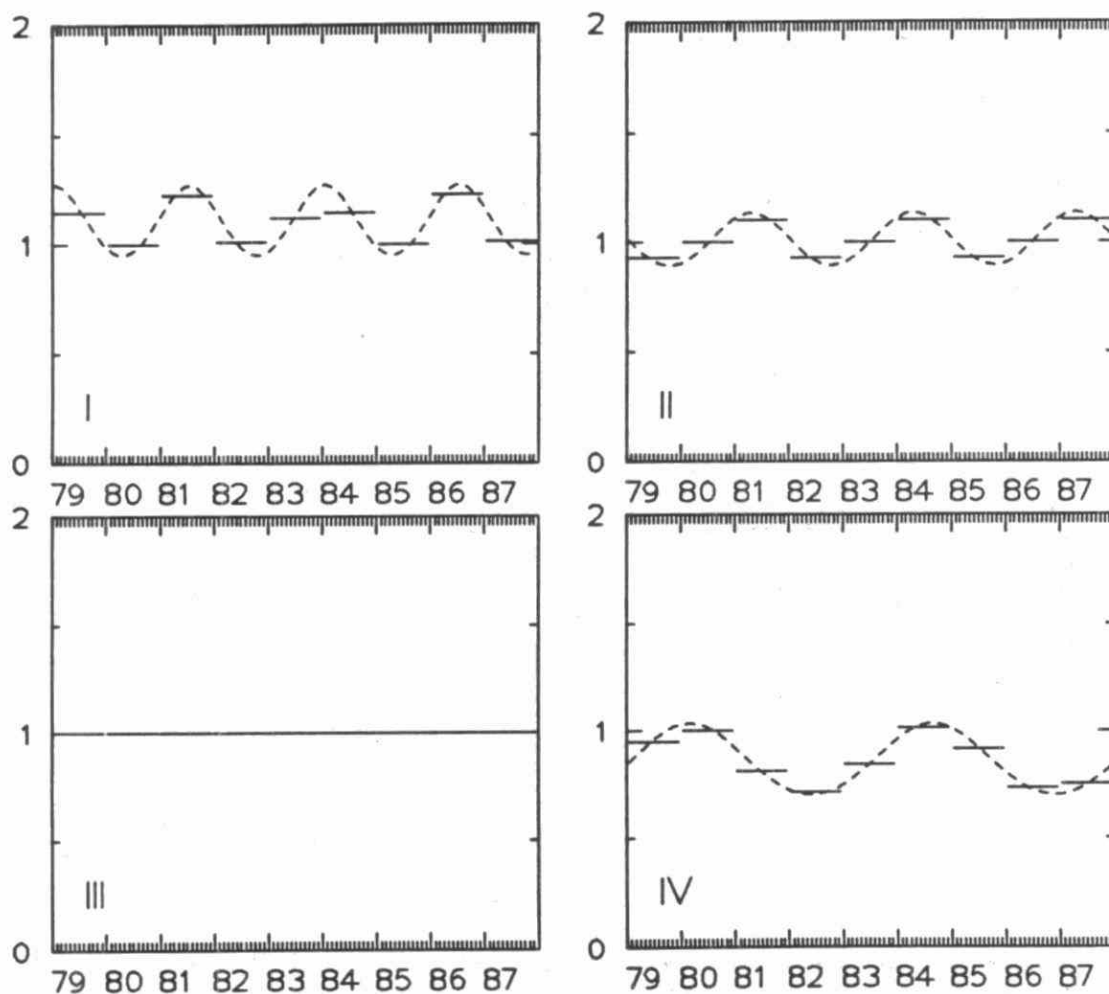


Fig. 3D-25 Same as Figure 3D-23 for Total NO_3^- in air.

LONG-TERM TREND

KEJIMKUJIK

SO_4

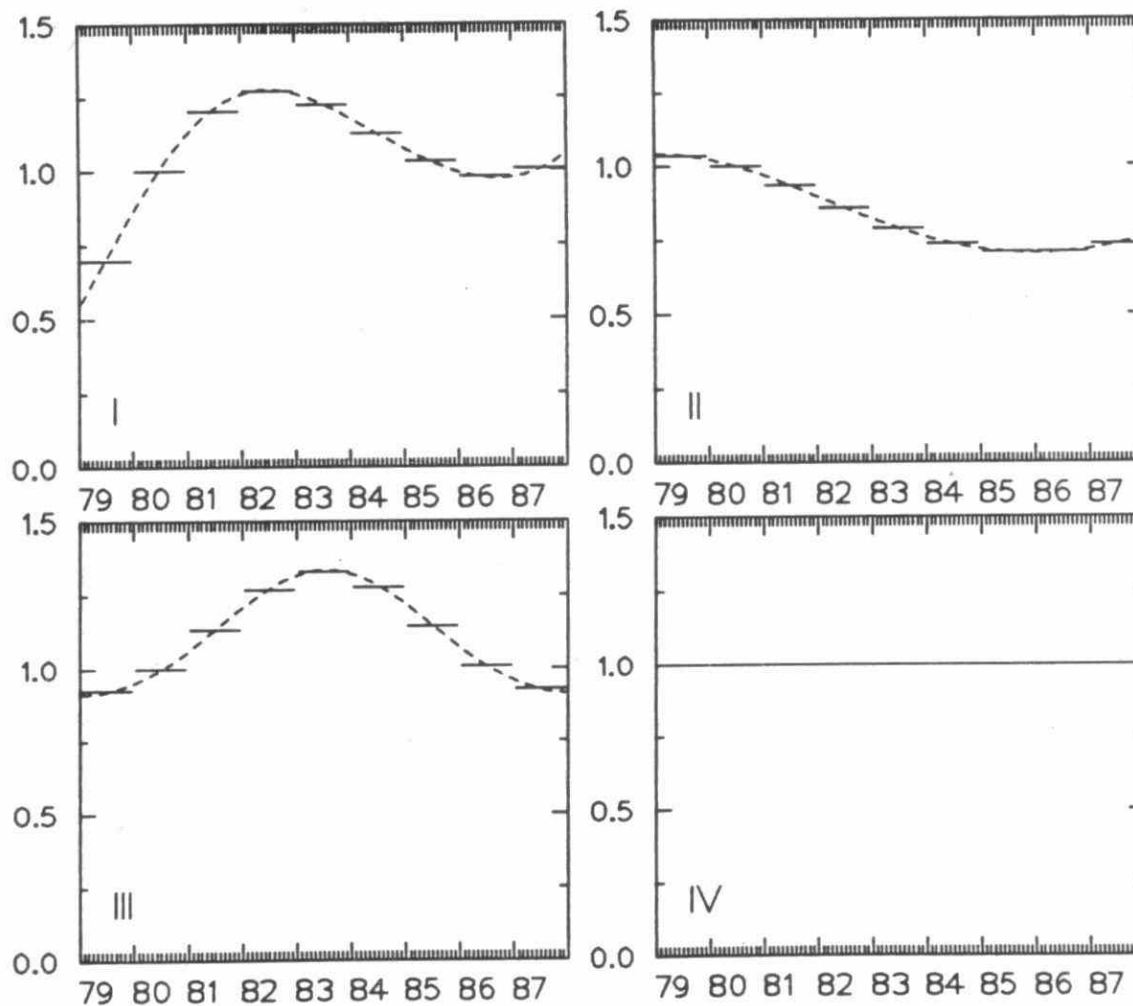


Fig. 3D-26 Intercept and long-term trend of monthly median SO_2 air concentrations at Kejimikujik normalized to 1980 for the four sectors in Figure 3D-14. Dashed line - continuous trend; solid lines - normalized annual averages.

LONG-TERM TREND

KEJIMKUJIK

SO₂

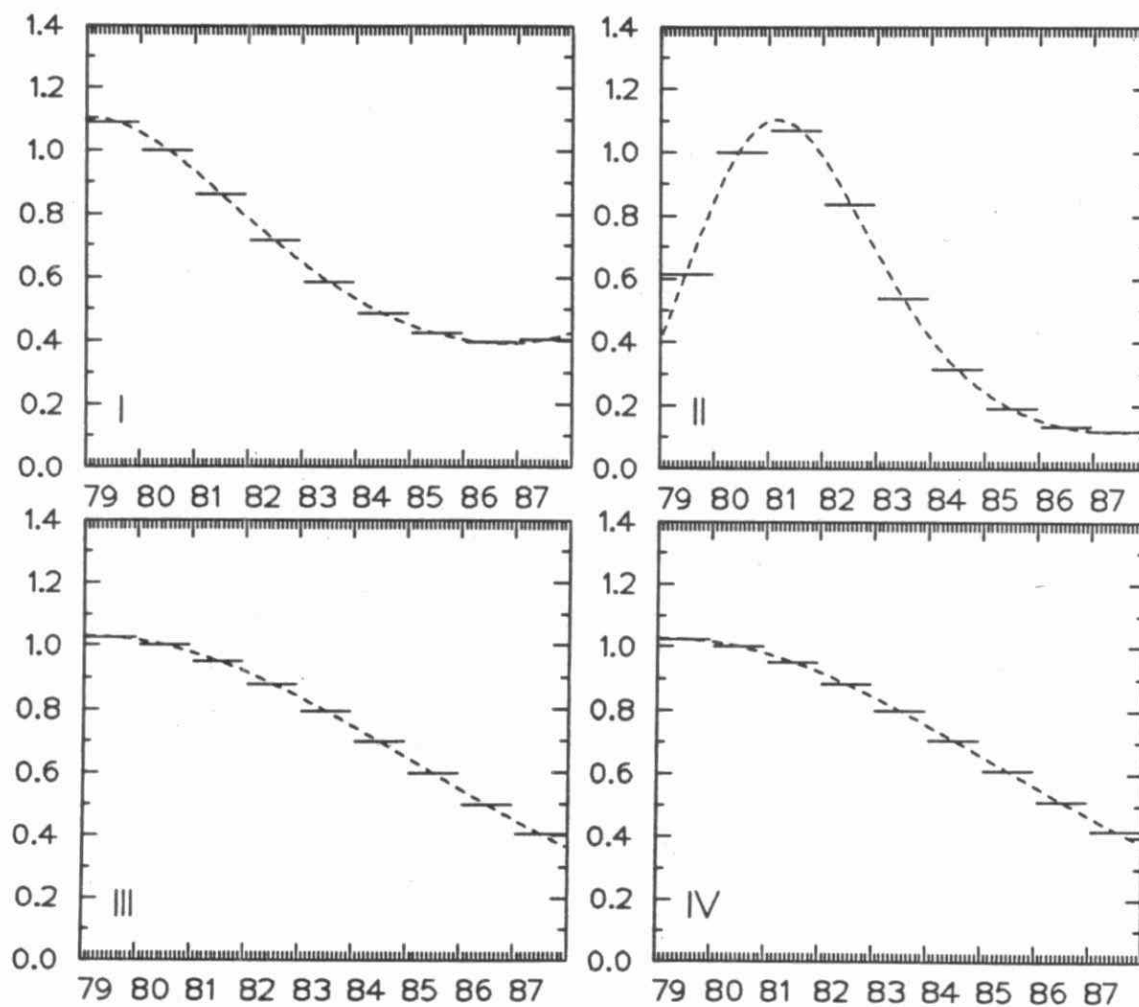


Fig. 3D-27 Same as Figure 3D-26 for SO₂ in air.

LONG-TERM TREND

KEJIMKUJIK

Total NO_3^-

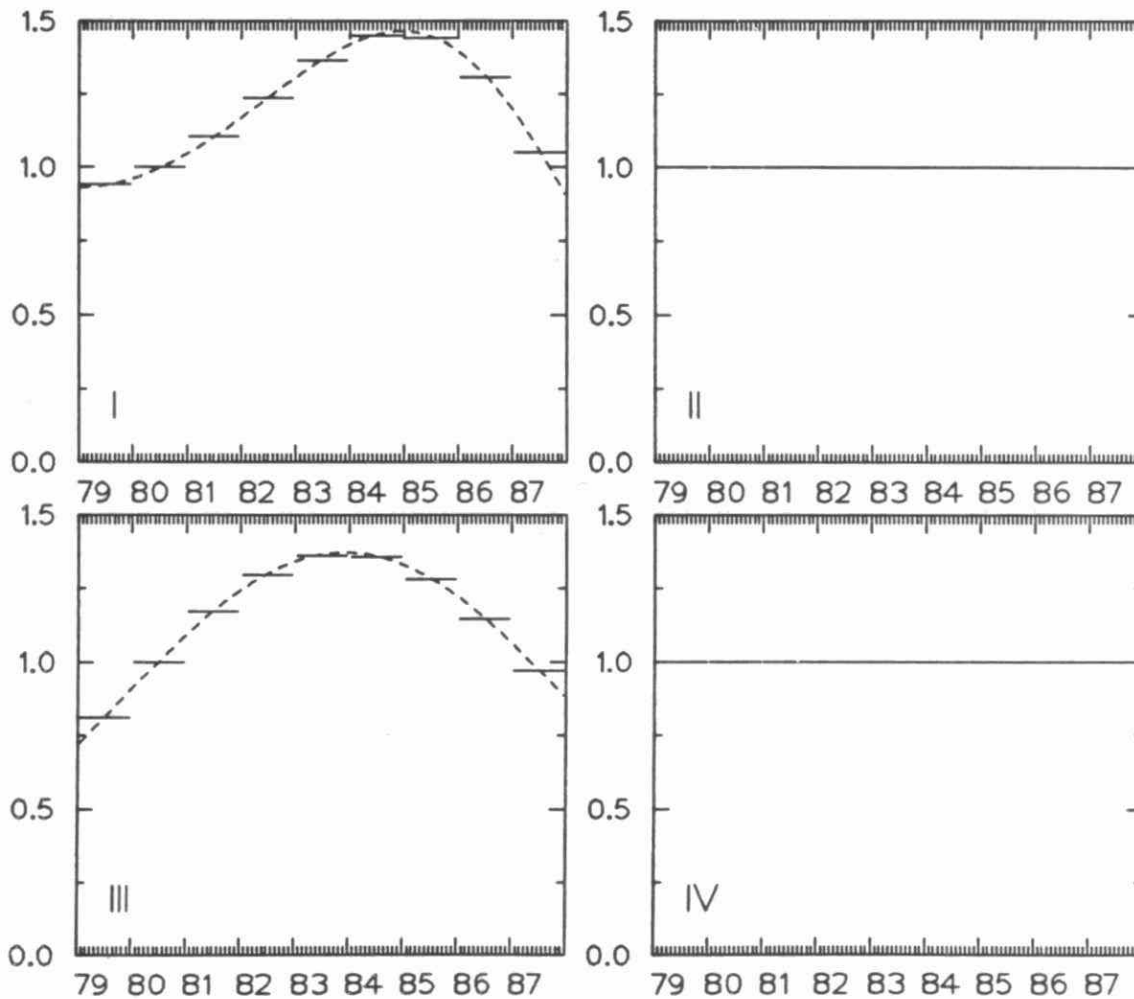


Fig. 3D-28 Same as Figure 3D-26 for Total NO_3^- in air.

APPENDIX 3E

**TRENDS IN PRECIPITATION CHEMISTRY IN NOVA SCOTIA:
1978-1987**

LIST OF FIGURES

Figure#	Page#
3E-1 Concentrations of excess $\text{SO}_4^{=}$, H^+ , NO_3^- , and NH_4^+ ($\mu\text{eq l}^{-1}$) in Nova Scotia, 1978-1987. Emissions of SO_2 and NO_2 from North America also shown (10^6 T).	3-309
3E-2 Deposition of excess $\text{SO}_4^{=}$, NO_3^- -N, and NH_4^+ -N in Nova Scotia, 1978-1987. Precipitation depth (cm) is also shown.	3-309
3E-3 Seasonal concentration of H^+ , excess $\text{SO}_4^{=}$, NO_3^- -N, and NH_4^+ -N ($\mu\text{eq l}^{-1}$). Seasonal deposition of excess $\text{SO}_4^{=}$ also shown (meq m^{-2}).	3-310
3E-4 Sulphate deposition in Nova Scotia (5 stations) and at Kejimikujik Park in south western Nova Scotia.	3-310

APPENDIX 3E

TRENDS IN PRECIPITATION CHEMISTRY IN NOVA SCOTIA: 1978-1987

More than 1400 precipitation samples were collected weekly from 5 sites in Nova Scotia between 1978 and 1987. High concentrations of H^+ , non-marine SO_4^{2-} , ($*SO_4^{2-}$) and NO_3^- were observed in 1978 and 1986. In 1983, concentrations of all three parameters were the lowest in the data record (Fig. 3E-1). Fluctuations in emissions for SO_2 and NO_2 are shown on Fig. 3E-1. They are insufficient to account for the variability observed in concentration and deposition values. Mean annual concentrations in 1983 were 13, 16, and 6 $\mu\text{eq/l}$ for H^+ , $*SO_4^{2-}$, and NO_3^- , respectively. In 1986 the values were 35, 28, and 13 $\mu\text{eq/l}$. Average pH of precipitation was 4.61 during the 10 year study. The two most acidic years were 1979 (4.47) and 1986 (4.46). In 1983, the average pH was 4.89.

Average provincial deposition of $*SO_4^{2-}$ (Fig. 3E-2) exceeded 20 kg/ha in 1978-80, while in 1983 it reached a low value of 11 kg/ha. The 1986 peak was 18 kg/ha. Neither $NO_3^- \cdot N$ nor $NH_4^+ \cdot N$ exceeded 3 kg/ha, and the sum of the two was less than 5 kg/ha during each of the 10 years. Calcium deposition did not show clear relationship to SO_4^{2-} deposition.

The ratio (equivalents) of NO_3^- to $*SO_4^{2-}$ was 0.4, so most acidity in the precipitation results from $H_2SO_4^{2-}$. However, multiple regression analysis revealed that H^+ is more sensitive to changes in NO_3^- concentrations than $*SO_4^{2-}$. The following equation explained 75% of the variance:

$$H^+ = 1.02 NO_3^- + 0.51 *SO_4^{2-} - 0.55 Ca^{+2} - 0.25 NH_4^+ 0.004 \quad (1).$$

Ratios of summer (JJA) vs winter (JFM) average concentrations were examined. During summer, $*SO_4^{2-}$ and H^+ were 1.8 times winter values. Ratios of JJA:JFM for NO_3^- and H^+ were 1.4 and 2.5, respectively (Fig. 3E-3).

A relatively steady decline in the annual ratios of $*SO_4^{2-}:NO_3^-$ ($\mu\text{eq/l}$) was also found. This ratio was about 2.5 during the first several years of the study, and approached 2.0 in 1987. This may indicate that SO_4^{2-} declined slightly during the study period (a deduction which is consistent with findings reported in Appendix 3D), although a decade of data is insufficient to demonstrate trends that may exist within the range of annual fluctuations.

Reliability of a data base compiled from samples collected weekly (Nova Scotia average) relative to samples collected daily (Kejimikujik Park) is demonstrated in Fig. 3E-4. Slight reductions in deposition in eastern portions of the province have previously been described (Underwood et al. 1987), and except for this phenomenon, it is clear that Kejimikujik data from CAPMoN (Summers, 1988 personal communication) are representative of rural Nova Scotia.

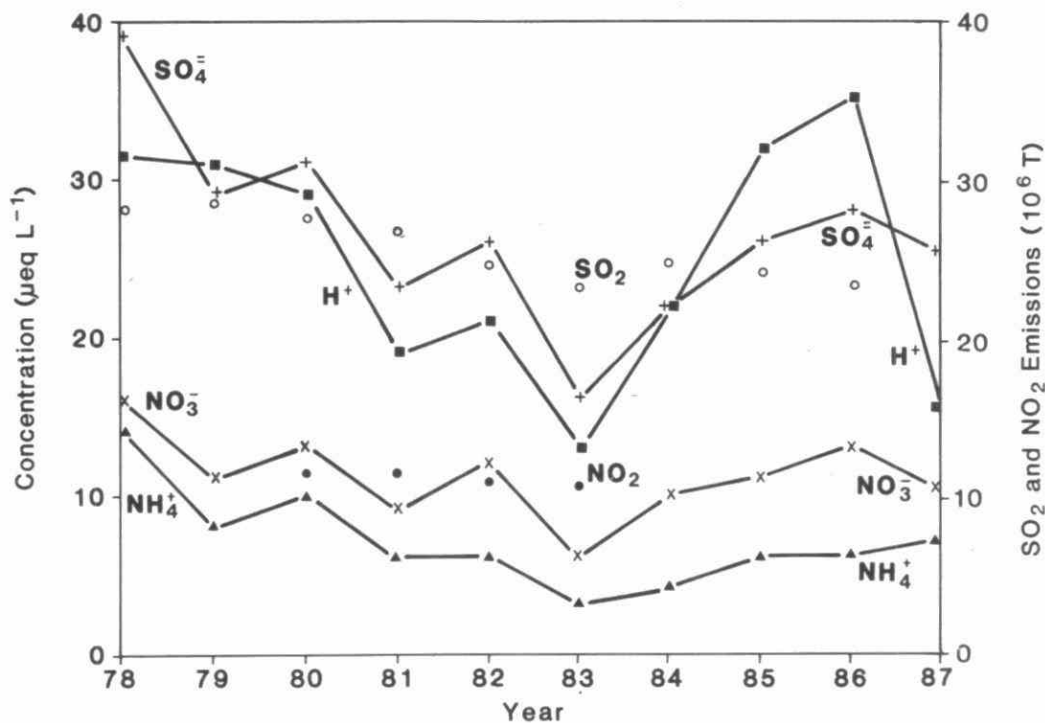


Fig. 3E-1 Concentrations of excess $\text{SO}_4^{=}$, H^+ , NO_3^- , and NH_4^+ ($\mu\text{eq L}^{-1}$) in Nova Scotia, 1978-1987. Emissions of SO_2 and NO_2 from North America also shown (10^6 T).

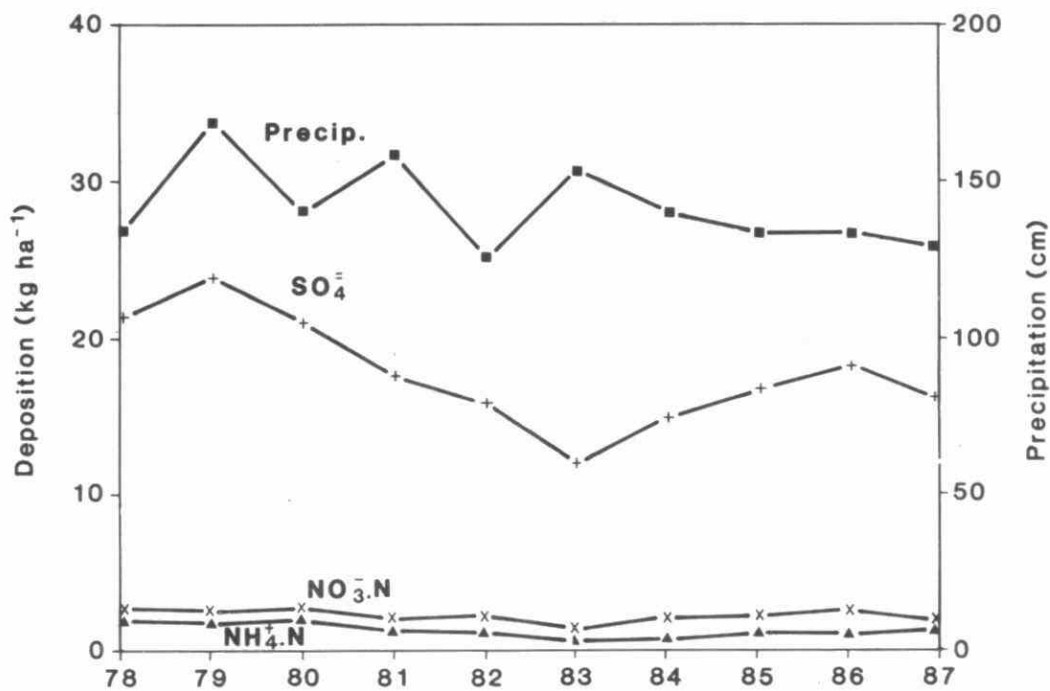


Fig. 3E-2 Deposition of excess $\text{SO}_4^{=}$, $\text{NO}_3\text{-N}$, and $\text{NH}_4\text{-N}$ in Nova Scotia, 1978-1987. Precipitation depth (cm) is also shown.

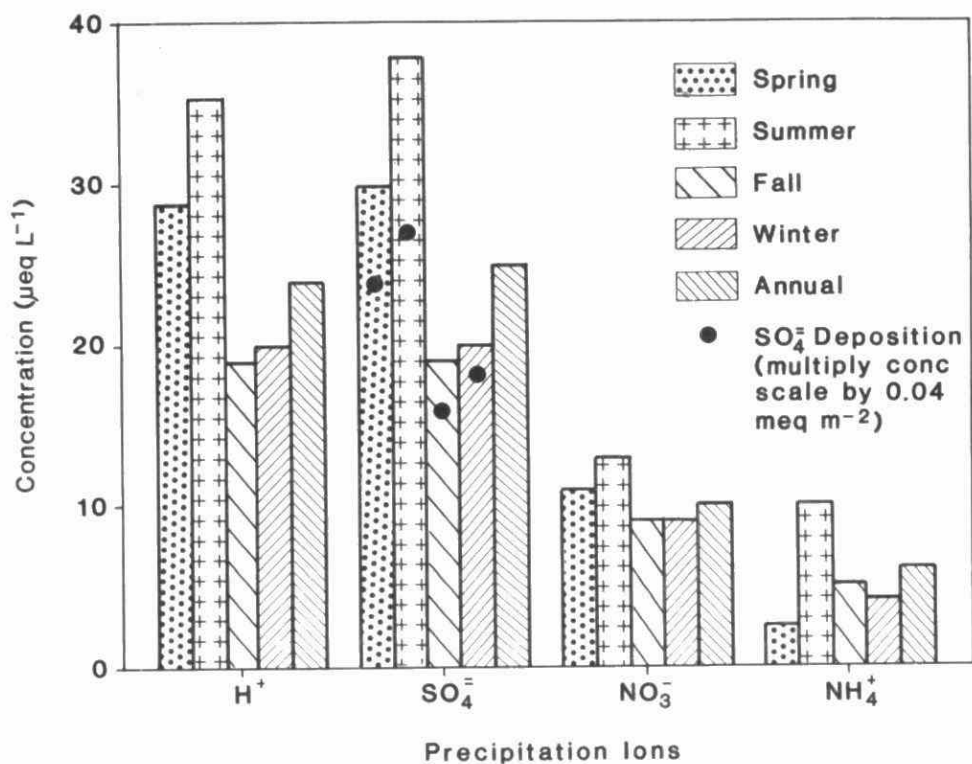


Fig. 3E-3 Seasonal concentration of H^+ , excess $\text{SO}_4^{=}$, NO_3^- -N, and NH_4^+ -N ($\mu\text{eq L}^{-1}$). Seasonal deposition of excess $\text{SO}_4^{=}$ also shown (meq m^{-2}).

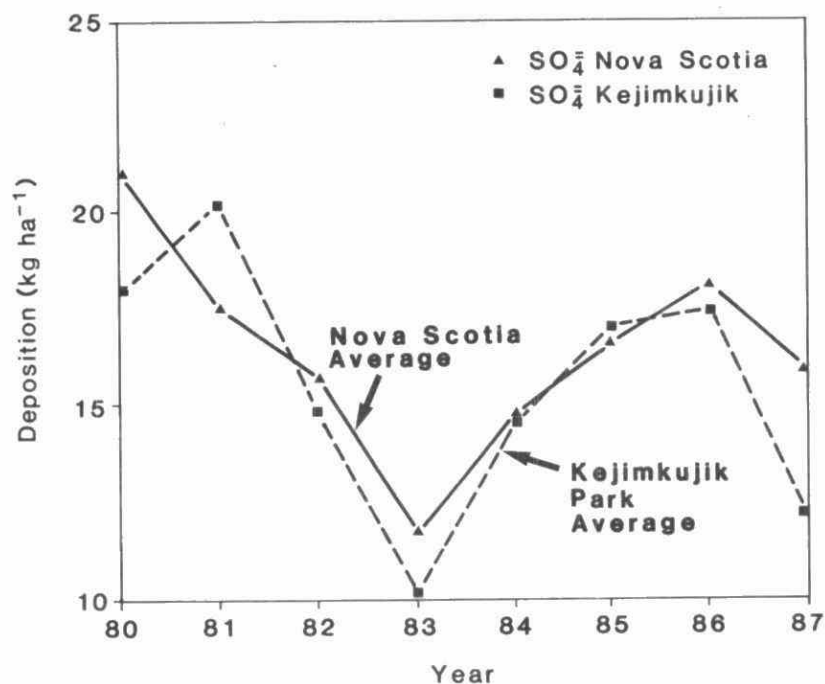


Fig. 3E-4 Sulphate deposition in Nova Scotia (5 stations) and at Kejimikujik Park in south western Nova Scotia.

APPENDIX 3F

**TEMPORAL VARIATION OF SULPHATE AND NITRATE
CONCENTRATIONS IN AIR AND PRECIPITATION AT DORSET,
ONTARIO**

LIST OF FIGURES

<u>Figure#</u>	<u>Page#</u>
3F-1 Seasonal sulphate concentrations in precipitation at Dorset, Ontario: 1980-1986.	3-324
3F-2 Seasonal sulphate concentrations in Winter precipitation at Dorset, Ontario: 1981-1986.	3-325
3F-3 Seasonal sulphate concentrations in Spring precipitation at Dorset, Ontario: 1981-1986.	3-325
3F-4 Seasonal sulphate concentrations in Summer precipitation at Dorset, Ontario: 1980-1986.	3-325
3F-5 Seasonal sulphate concentrations in Autumn precipitation at Dorset, Ontario: 1980-1986.	3-325
3F-6 Cyclical component of seasonal sulphate concentrations in precipitation at Dorset, Ontario: 1981-1986.	3-326
3F-7 Specific seasonal relativities of sulphate in precipitation by quarter at Dorset, Ontario: 1981-1986.	3-326
3F-8 Irregular component of seasonal sulphate concentrations vs. precipitation amount at Dorset, Ontario: 1981-1986.	3-326
3F-9 Precipitation amount corrected seasonal sulphate concentrations at Dorset, Ontario: 1981-1986.	3-326
3F-10 Precipitation amount corrected Winter sulphate concentrations at Dorset, Ontario: 1981-1986.	3-327
3F-11 Precipitation amount corrected Spring sulphate concentrations at Dorset, Ontario: 1981-1986.	3-327
3F-12 Precipitation amount corrected Summer sulphate concentrations at Dorset, Ontario: 1981-1986.	3-327
3F-13 Precipitation amount corrected Autumn sulphate concentrations at Dorset, Ontario: 1981-1985.	3-327
3F-14 Seasonal N-NO_3^- concentrations in precipitation samples at Dorset, Ontario: 1981-1986.	3-328
3F-15 Seasonal N-NO_3^- concentrations in Winter precipitation at Dorset, Ontario: 1981-1986.	3-329
3F-16 Seasonal N-NO_3^- concentrations in Spring precipitation at Dorset, Ontario: 1981-1986.	3-329
3F-17 Seasonal N-NO_3^- concentrations in Summer precipitation at Dorset, Ontario: 1981-1986.	3-329
3F-18 Seasonal N-NO_3^- concentrations in Autumn precipitation at Dorset, Ontario: 1981-1986.	3-329

LIST OF FIGURES (continued)

Figure#	Page#
3F-19 Cyclical component of seasonal N-NO_3^- concentrations at Dorset, Ontario: 1981-1986.	3-329
3F-20 Specific seasonal relativities of N-NO_3^- in precipitation by quarter at Dorset, Ontario: 1981-1986.	3-330
3F-21 Irregular component of seasonal N-NO_3^- concentrations vs. precipitation amount at Dorset, Ontario: 1981-1986.	3-331
3F-22 Precipitation amount corrected seasonal N-NO_3^- concentrations at Dorset, Ontario: 1981-1986.	3-331
3F-23 Precipitation amount corrected Winter N-NO_3^- concentrations at Dorset, Ontario: 1981-1986.	3-331
3F-24 Precipitation amount corrected Spring N-NO_3^- concentrations at Dorset, Ontario: 1981-1986.	3-331
3F-25 Precipitation amount corrected Summer N-NO_3^- concentrations at Dorset, Ontario: 1981-1985.	3-331
3F-26 Precipitation amount corrected Autumn N-NO_3^- concentrations at Dorset, Ontario: 1981-1985.	3-332
3F-27 Seasonal total sulphur concentrations in ambient air at Dorset, Ontario: 1981-1986.	3-332
3F-28 Winter total sulphur concentrations in ambient air at Dorset, Ontario: 1981-1986.	3-333
3F-29 Spring total sulphur concentrations in ambient air at Dorset, Ontario: 1982-1986.	3-333
3F-30 Summer total sulphur concentrations in ambient air at Dorset, Ontario: 1982-1986.	3-333
3F-31 Autumn total sulphur concentrations in ambient air at Dorset, Ontario: 1981-1986.	3-333
3F-32 Specific seasonal relativities of seasonal total sulphur in air at Dorset, Ontario: 1982-1986.	3-334
3F-33 Cyclical components of seasonal total sulphur in air at Dorset, Ontario: 1982-1986.	3-334
3F-34 Irregular components of seasonal total sulphur in air at Dorset, Ontario: 1982-1986.	3-334
3F-35 Climatological factor corrected seasonal total sulphur concentrations in air at Dorset, Ontario: 1982-1986.	3-334
3F-36 Climatological factor corrected Winter total sulphur concentrations in air at Dorset, Ontario: 1982-1986.	3-335

LIST OF FIGURES (continued)

Figure#	Page#
3F-37 Climatological factor corrected Spring total sulphur concentrations in air at Dorset, Ontario: 1982-1986.	3-335
3F-38 Climatological factor corrected summer total sulphur concentrations in air at Dorset, Ontario: 1982-1986.	3-335
3F-39 Climatological factor corrected Autumn total sulphur concentrations in air at Dorset, Ontario: 1982-1985.	3-335
3F-40 Seasonal total nitrate concentrations in ambient air at Dorset, Ontario: 1982-1986.	3-336
3F-41 Winter total nitrate concentrations in ambient air at Dorset, Ontario: 1982-1986.	3-337
3F-42 Spring total nitrate concentrations in ambient air at Dorset, Ontario: 1982-1986.	3-337
3F-43 Summer total nitrate concentrations in ambient air at Dorset, Ontario: 1982-1986.	3-337
3F-44 Autumn total nitrate concentrations in ambient air at Dorset, Ontario: 1982-1986.	3-337
3F-45 Specific seasonal relativities of seasonal total nitrate in air at Dorset, Ontario: 1982-1986.	3-338
3F-46 Cyclical components of seasonal total nitrate in air at Dorset, Ontario: 1982-1986.	3-338
3F-47 Irregular components of seasonal total nitrate in air at Dorset, Ontario: 1982-1986.	3-338
3F-48 Climatological factor corrected total nitrate concentrations in air at Dorset, Ontario: 1982-1986.	3-338
3F-49 Climatological factor corrected total nitrate concentration in air: Winter.	3-339
3F-50 Climatological factor corrected total nitrate concentration in air: Spring.	3-339
3F-51 Climatological factor corrected total nitrate concentration in air: Summer.	3-339
3F-52 Climatological factor corrected total nitrate concentration in air: Autumn.	3-339

LIST OF TABLES

Table#		Page#
3F-1	Seasonal Time Series Analysis: Dorset Sulphate Data	3-340
3F-2	Seasonal Time Series Analysis: Dorset Total Nitrate in Precipitation	3-341
3F-3	Seasonal Time Series Analysis: Dorset Sulphur Air Data	3-342
3F-4	Seasonal Time Series Analysis: Dorset Total Nitrate Air Data	3-343

Appendix 3F

Temporal Variation of Sulphate and Nitrate Concentrations in Air and Precipitation at Dorset, Ontario

Introduction

It is generally agreed that a time period of at least ten years is required before trends in precipitation concentration or deposition can be assessed. However, the existing APIOS (Acidic Precipitation in Ontario Study) data base, which now extends over six years for validated data (1981 to 1986), has a long enough period of record for at least some of the features of the temporal patterns to be elucidated. Data from the Dorset site were used in this study. Dorset is a rural site, located in Central Ontario, in the sensitive Muskoka region. The data were from the APIOS Cumulative Network (Chan et al., 1985), which was specifically set up to monitor long term trends in deposition.

Procedure

The procedure followed in this study was a Classical Time Series Analysis, which is thoroughly explained in standard texts (e.g., Reinmuth, 1977). Briefly, the procedure is as follows.

In general, the Classical Time Series Analysis model comprises four components. These are the Trend (T), Cyclical (C), Seasonal (S) and Irregular (I) components, which are considered to be multiplicative. The analysis was applied to seasonal average concentrations, with the seasons defined so that January, February, and March constitute winter, etc. Each component has a particular meaning, and describes specific features of the temporal behaviour of the data.

- the trend component describes the net effect of long term factors, and is usually modelled as a straight line or a smooth curve
- the cyclical component describes periodic factors with periods longer than one year, including climate change cycles; it may contain two or more cycles of different period and amplitude
- the seasonal component, as the name implies, describes seasonal effects, and consists of a repetitive cycle of period one year (or less)
- the irregular component consists of the residuals which remain after the other components have been extracted.

The decomposition procedure, by which these components are extracted, is as follows:

1. Calculate the trend component (T) by fitting a line or smooth curve to the data by simple regression.
2. Calculate the cyclical-seasonal-irregular component (CSI) by dividing each data point by the corresponding trend value.

3. Calculate the trend-cyclical (TC) component, using a centred, four-quarter moving average of the original time series. This averaging smooths out the seasonal and irregular components.
4. Calculate the seasonal-irregular (SI) component by dividing each data point by the corresponding TC value.
5. Calculate the cyclical component (C). This is the smoothed result of dividing TC (step 3) by the trend values.
6. Extract the seasonal (S) component from SI. If SI is stable this is done by averaging the SI values for each quarter. The irregular effects will tend to cancel out, so that the result reflects the seasonal effects. In this study medians were used to avoid the possibility that an outlier will distort the average.
7. Determine the cyclical-irregular component (CI), as the quotient of CSI (step 2) and S (step 6).
8. Obtain the irregular component by dividing CI (step 7) by C.

The analysis presented here differs from the one described in Appendix 3D in that the components are extracted successively from the time series of the data, rather than fitting the complete model to the data in one step. This allows greater flexibility in the fitting of repetitive cycles, but is possibly more restrictive in the extraction of the trend component. In this work a linear trend is postulated, since this model is fitted to the entire data set. Because of the short term noise in the data almost any trend model (within reason) would give an equivalent goodness of fit. The possible restrictions inherent in assuming a linear trend are, however, offset by the fact that departures from linearity will be determined in the cyclical or irregular components, or both.

Results and Discussion

Sulphate in Precipitation

The results of the decomposition of the time series of sulphate concentrations in precipitation are listed in Table 3F-1.

Figure 3F-1 shows a time plot of the original data. The strong seasonal cycle is clearly visible in this plot. A linear trend was fitted to this series, as described in above. The trend is given by:

$$\text{SO}_4^- = 3.4244 - 0.0515 \times t$$

where t denotes time in seasons. This corresponds to a decrease in sulphate concentration of 1.5% per season, or 6% per year. The time plots for individual seasons are shown in Figures 3F-2 to 3F-5.

The cyclical component is plotted in Figure 3F-6. It contains a one year cycle of small amplitude (0.01), and a two-year cycle of larger amplitude (0.2). The superposition of these two cycles results in a complex waveform, in which the global maxima and minima

recur every five years. This is approximately equal to the time coverage of the data. It therefore follows that the cyclical component is subject to significant uncertainty, and is liable to change when the data record is lengthened.

The seasonal component is plotted in Figure 3F-7. Averaged over the period 1981 to 1986 these components are 0.50 for winter, 1.13 for spring, 1.38 for summer and 0.87 for autumn. These results are in agreement with those of many other studies in which sulphate concentrations in precipitation were found to be highest in summer and lowest in winter.

Figure 3F-8 contains a plot of the irregular component. Also included in Figure 3F-8 is an indication of precipitation depth for each season. There are clear indications in this figure of an inverse correlation between the irregular component and precipitation depth. It is possible to use these data to correct for the effect of precipitation depth, by regressing the irregular component against precipitation depth (a linear fit was found). A correction factor was then calculated for each season. Figure 3F-9 contains a plot of sulphate concentration after correction for precipitation amount. Corresponding plots for individual seasons are shown in Figures 3F-10 to 3F-13.

The slow decreasing trend in sulphate concentration is more clearly evident in these corrected plots, particularly in the case of the spring and autumn seasons. In both cases, however, it appears that the decrease occurred prior to 1984, and that sulphate concentrations have been relatively constant since then. This feature was also found in a similar analysis of bulk sampler data, also collected at Dorset. An analysis of these data has previously been reported by Dillon et al. (1988).

An interesting feature of the sulphate data after normalisation for precipitation depth is that the winter time concentrations have not changed significantly from year to year, whereas the other seasons all show a decrease. This decrease is consistent, in that it occurred mainly in the first two or three years of the series. As was noted above, conversion of SO_2 to sulphate is relatively limited in winter, which suggests that the normalised winter-time sulphate concentrations shown in Figures 3F-9 and 3F-11 correspond essentially to scavenged primary sulphate. This component has not changed with time, and comprises a background level for the Dorset site. It could be attributed to one or more of the following sources:

- anthropogenic emissions of primary sulphate
- continental background sulphate
- sea salt emissions of sulphate

It is difficult to explain why anthropogenic primary sulphate emissions would remain unchanged with time while SO_2 emissions have changed, and the sea salt component is expected to be small at Dorset because of its distance from the nearest ocean. We therefore conclude that the winter-time precipitation sulphate concentrations at Dorset result from the scavenging of continental background sulphate aerosol.

Nitrate in Precipitation

The corresponding analysis for seasonally averaged nitrate concentrations in precipitation is summarised in Table 3F-2. In this case the linear trend is given by

$$\text{NO}_3^- = 0.5197 - 0.00266 \times t$$

The decrease in total nitrate concentration therefore averages to 0.5% per season, or 2% per year. However, this slope is not statistically different from zero, as judged by the fact that the standard error of estimate of the slope of the trend line exceeds the coefficient.

The complete time series of the data is plotted in Figure 3F-14. The seasonal cycle is not as well developed for nitrate as it is for sulphate; however, concentrations were generally highest in summer or spring. The plots for the individual seasons (Figures 3F-15 to 3F-18) show a substantial year-to-year variability, which results in the lack of a clear seasonal cycle. These figures include also an indication of seasonal precipitation depth, and the inverse correlation between concentration and precipitation amount is clearly marked.

The cyclical component is plotted in Figure 3F-19. It consists of the superposition of a two year and a four year cycle, and presents a clear contrast with the cyclical component for sulphate shown in Figure 3F-6. This difference suggests that the cyclical component is not associated with meteorological factors (or there would be greater similarities between different species in precipitation). However, it should again be noted that the overall period of the cycle is close to the period covered by the available data, and is therefore subject to considerable uncertainty.

The seasonal components are plotted in Figure 3F-20. Averaged over the period 1981 to 1986 the components are 0.85 for winter, 1.13 for spring, 1.13 for summer and 0.93 for autumn. This is in accordance with the many earlier studies which have found a much smaller season to season variation for nitrate concentration than is found for sulphate. These components also confirm the qualitative appearance of Figure 3F-14, namely that concentrations tend to be highest in the spring and summer, and lowest in the winter.

Figure 3F-21 contains the plot of the irregular component, which, as in the case of sulphate, shows a strong inverse correlation with precipitation depth. A correction factor for precipitation amount was calculated for nitrate, as was described for sulphate, and seasonal nitrate concentrations, corrected for precipitation amount, are plotted in Figure 3F-22. Corresponding plots for the individual seasons are shown in Figures 3F-23 to 3F-26. A linear fit to the corrected concentrations gives the same slope as for the uncorrected data, i.e., a decrease of 2% per year. However, a considerable amount of variation remains after adjustment, and this slope is not significantly different from zero.

Total Sulphur in Air

Dry deposition of acidifying compounds in Ontario is inferred from measured concentrations in air and a calculated deposition velocity. In this section we report the temporal patterns of air concentrations of total sulphur (sulphur dioxide plus sulphate). The patterns for dry deposition will be similar, provided that no changes in deposition velocity have occurred during the study period. This requirement will usually be met if no major changes in land use have taken place in the vicinity of the monitoring site. The Dorset site meets this requirement. Total sulphur was used in this analysis, rather than

analysing sulphur dioxide and sulphate separately, since this is consistent with the methods used in analysing the time series of precipitation concentrations; the quantity reported as sulphate in precipitation by the APIOS network actually includes a contribution from dissolved sulphur dioxide, since no measures are taken to determine this species separately. The results of the decomposition are listed in Table 3F-3.

Figure 3F-27 shows a time plot of the original data. The strongest distinguishing feature in this plot is the very high value for the winter of 1984. This high value arises from very high sulphur dioxide concentrations; sulphate concentrations were similar to those determined during other winter seasons. Although the high concentration is anomalous in terms of the time series, it is not incorrect. High sulphur dioxide concentrations were also determined at nearby sites in the cumulative network, and also at the daily network sampler located at Dorset.

However, this high value was replaced by the median of all wintertime sulphur concentrations in the fitting of the trend, to avoid an undue influence by a single value. The trend line is shown in Figure 3F-27, and corresponds to

$$S = 3.36 - 0.0712 \times t$$

where t denotes time in seasons. This corresponds to a decrease in sulphur concentration of 2.1% per season or 8.4% per year. The time plots for individual seasons are shown in Figures 3F-28 to 3F-31.

The cyclical component contains a two-year cycle of variable amplitude, and is plotted in Figure 3F-32. This is assumed to reflect the influence of climatological factors, noting that the analysis of precipitation data also revealed a two-year cycle.

The seasonal component is plotted in Figure 3F-33. The median values over the period 1981 to 1986 for these components are 1.37 for winter, 0.99 for spring, 0.76 for summer and 0.83 for autumn. These results, which are in contrast with the case of precipitation, where the highest component is found in the summer, reflect the higher concentrations of sulphur dioxide found in the winter, when deposition, ventilation and chemical conversion to sulphate are at a minimum.

Figure 3F-34 contains a plot of the irregular component. The values for this component range from 0.76 to 1.35, which is smaller than the range found for precipitation (0.74 to 1.78).

On the assumption that the cyclical component indeed represents climatological effects, a correction may be made by dividing the original data series by the cyclical component. Figure 3F-35 contains a plot of sulphur concentration after this correction. Corresponding plots for individual seasons are shown in Figures 3F-36 to 3F-39.

The slow decreasing trend in sulphur concentration is more clearly evident in these corrected plots. As was found in the analysis of precipitation data, it appears that the decrease occurred prior to 1984, and that sulphur concentrations have been relatively constant since then.

The very high concentrations found for total sulphur in air in the winter of 1984 are not reflected in the concentrations observed in precipitation; see Figure 3F-2 or Figure 3F-11.

This is consistent with the expectation that atmospheric SO_2 is not scavenged to any significant extent in the winter.

Total Nitrate in Air

The decomposition of the time series for total nitrate in air is summarised in Table 3F-4, and the original time series is plotted in Figure 3F-40. As was the case for total sulphur in air, the concentration for the winter of 1984 was found to be very high. Again, this high concentration was confirmed by comparing Dorset data with results obtained from neighbouring sites.

Because the winter 1984 concentration was more comparable with other high seasonal concentrations (e.g., the winters of 1982, 1983 and 1986), it was retained in the fitting of the linear trend. This trend was found to amount to a decrease of 0.9% per season or 3.6% per year. However, as in the case of nitrate in precipitation, it was found that this slope was not statistically distinguishable from zero.

The apparent lack of a trend in the concentrations of nitrate in air is borne out in the plots of the seasonal concentrations in Figures 3F-41 to 3F-44. For spring and autumn the concentrations were highest in 1982. This was followed by a substantial decrease to 1983, with an apparent increase for every subsequent year. For winter and summer there is no systematic increase or decrease. The seasonal components are plotted in Figure 3F-45.

The cyclical components are plotted in Figure F-45, with the seasonal and irregular components being shown in Figures F-46 and F-47 respectively. A climatological correction was derived, as was done for sulphur, and the corrected total nitrate concentrations are given in Figure F-48 (all data), and Figures F-49 to F-52 (individual seasons). The corrected data confirm the original conclusion about the temporal behaviour of total nitrate, namely that there is substantial year to year variability, but no systematic long term trend.

In comparing the concentrations of total nitrate in air (Figure 3F-40) and precipitation (Figure 3F-22), much greater correspondence is seen than was the case for sulphate. For example, high concentrations are seen in both time series for the winters of 1982 and 1984, and the winter and spring of 1985. The agreement is not quantitative, but this is not unexpected because the incorporation of nitrate in air into precipitation depends on other factors in addition to its concentration.

The cyclical and irregular components are plotted in Figures 3F-46 and 3F-47, respectively, and the climatological factor-corrected concentrations are plotted in Figure 3F-48.1

Discussion

The variation with time of the concentrations of pollutants in air and precipitation can result from a number of factors, including

- changes in sampling methodology
- changes in emissions

- changes in meteorological factors, affecting the delivery of pollutants to the sampling location, or the scavenging of pollutants on route, or at the sampler.

Great care has been taken in the APIOS Cumulative Network to ensure continuity of the data record, by keeping changes in methodology to a minimum, and by ensuring that those new methods that have been introduced were completely comparable with the existing procedures. The time trends observed in these analyses of the data must therefore be associated with changes in emissions, and with meteorological variability. As has been discussed above, we believe that a significant portion of the meteorological variability is found in the cyclical or irregular components. The trend component is believed to reflect, at least in some measure, the changes in precursor emissions during the corresponding time period.

Annual emissions of SO_2 and NO_x for eastern North America are given in Table 3.2.5 for the time period corresponding to this analysis.

For sulphur dioxide it is clear that there was a systematic reduction in emissions over the study period, amounting to approximately 3% per year. This is to be compared with the linear downward trends for sulphur compound concentrations found in this work of 6% per year (sulphate in precipitation) and 8% per year (total sulphur in air). Quantitatively there is some difference, but this is to be expected because of the many compounding factors contributing to the temporal variability of ambient pollutant concentrations. However, the qualitative agreement is good, even to the observation of the relatively sharp initial decrease in emissions, followed by a more gradual change, which is mirrored in the observations presented earlier.

In the case of nitrogen oxides, emissions have remained approximately constant during the study period. This, too, is consistent with the analysis of concentration data, where no significant trend could be detected.

The trends found in this work are consistent with the findings of others. For example, Dillon et al. (1988) using a different set of data, but also obtained at Dorset, found that sulphate in precipitation decreased by 6% per year, while nitrate decreased by about 1.6% per year, but with much greater scatter.

In Appendix 3D it was found that concentrations of sulphate in precipitation have decreased with time at Chalk River, which is approximately 150 kilometres from Dorset. A linear trend was not fitted to the data, but the overall rate of change was approximately 5% per year. Also no significant changes were found in nitrate concentration in air or precipitation over the study period.

Appendix 3D analysed data for sulphate and sulphur dioxide in air separately. No significant long term change was found in sulphate at Chalk River, but the sulphur dioxide concentrations decreased by about 7% per year on average. Since the sulphur dioxide concentrations were at all times significantly higher than sulphate at Chalk River, the corresponding rate of decrease for total sulphur in air will also be approximately 7% per year, in good agreement with the present finding of 8% per year.

Fay et al. (1989) studied the time trends of sulphate and nitrate in eastern North America, using data from 17 sites which have a long term record. They found decreasing linear trends of 6.4% per year for sulphate and 0.6% per year for nitrate at Chalk River.

Conclusions

The major conclusions of this study are:

- Concentrations of sulphate in precipitation measured at Dorset in Ontario show a decreasing trend of about 6% per year over the period 1981 to 1986. The trend is most clearly discernible in data for spring and autumn, after a correction has been made for the dependence of concentration on precipitation amount.
- Sulphur concentrations in air decreased by approximately 8% per year over the same time period.
- Nitrate concentrations in air and precipitation did not show a significant change over this time period.
- These changes in pollutant concentration are consistent with the changes in precursor emissions over the study period.
- An adjustment for the effect of precipitation amount on pollutant concentration could be derived from the analysis presented here. Adjustment for this factor allowed the temporal trend for sulphate to be more clearly delineated.

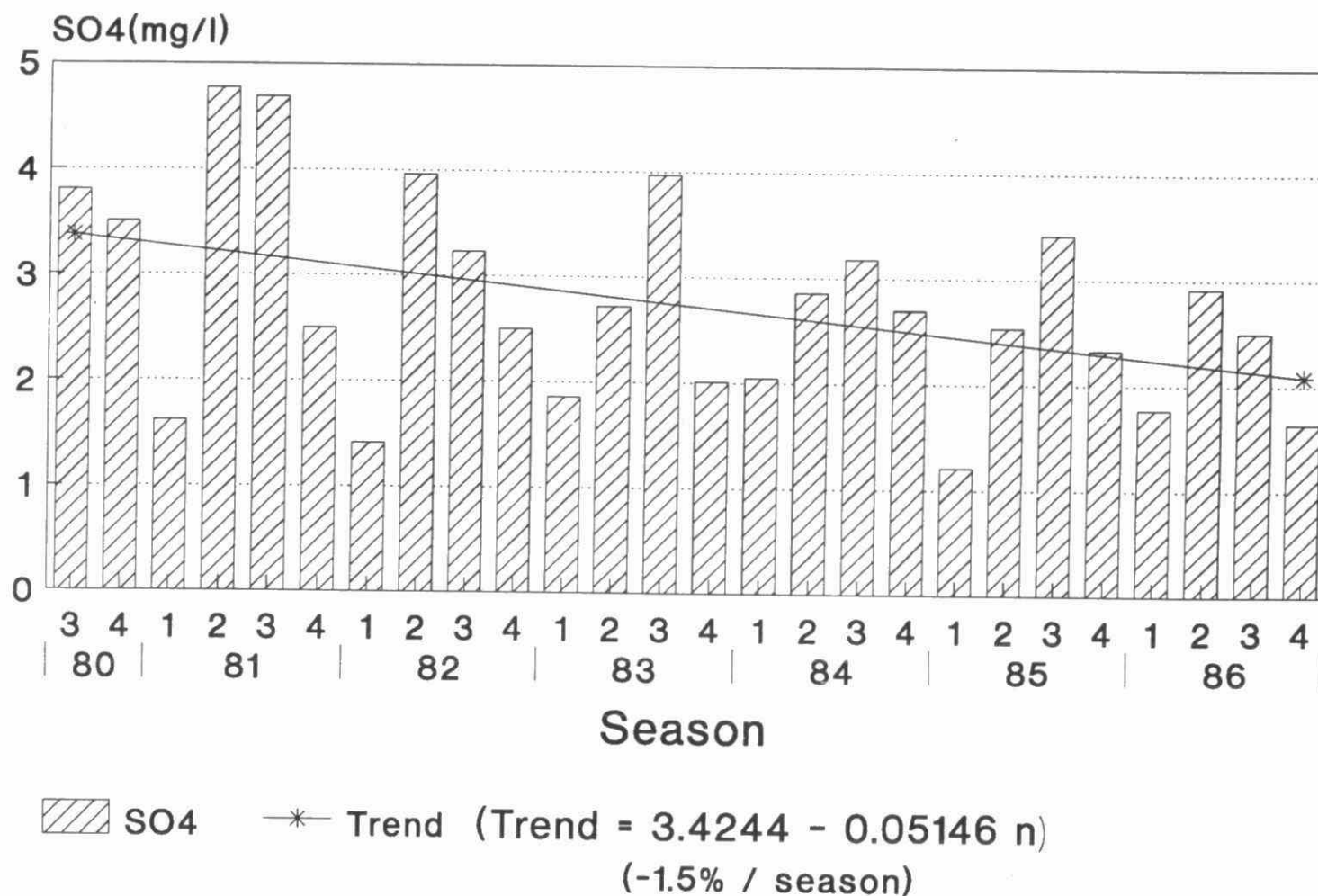


Fig. 3F-1 Seasonal sulphate concentrations in precipitation at Dorset, Ontario: 1980-1986.

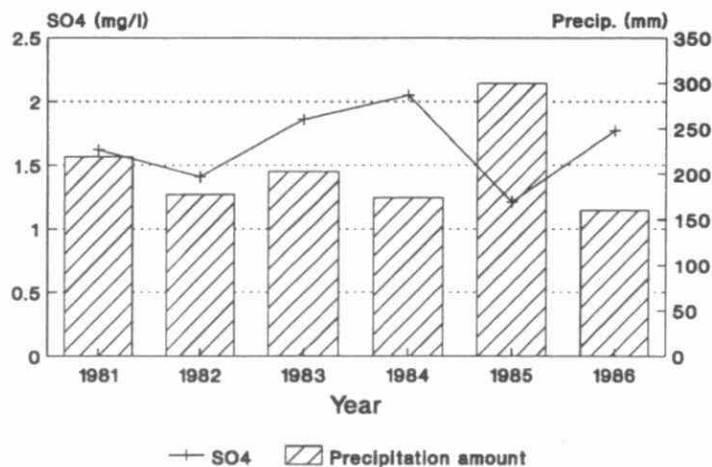


Fig. 3F-2 Seasonal sulphate concentrations in Winter precipitation at Dorset, Ontario: 1981-1986.

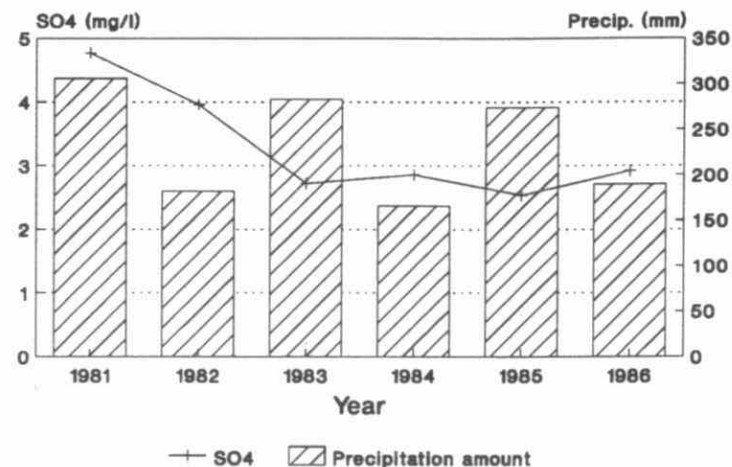


Fig. 3F-3 Seasonal sulphate concentrations in Spring precipitation at Dorset, Ontario: 1981-1986.

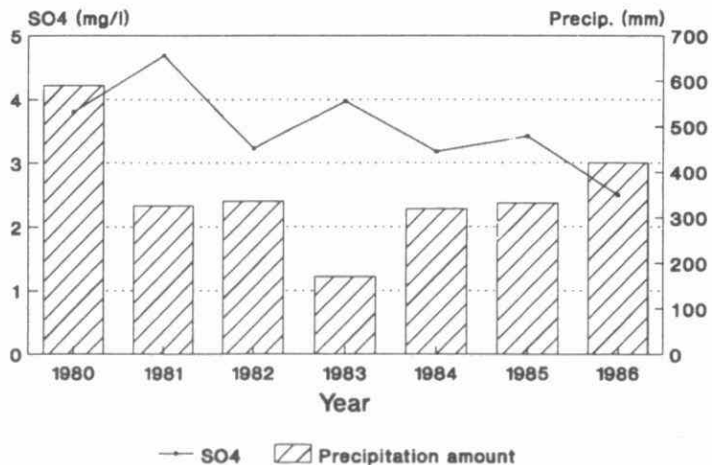


Fig. 3F-4 Seasonal sulphate concentrations in Summer precipitation at Dorset, Ontario: 1980-1986.

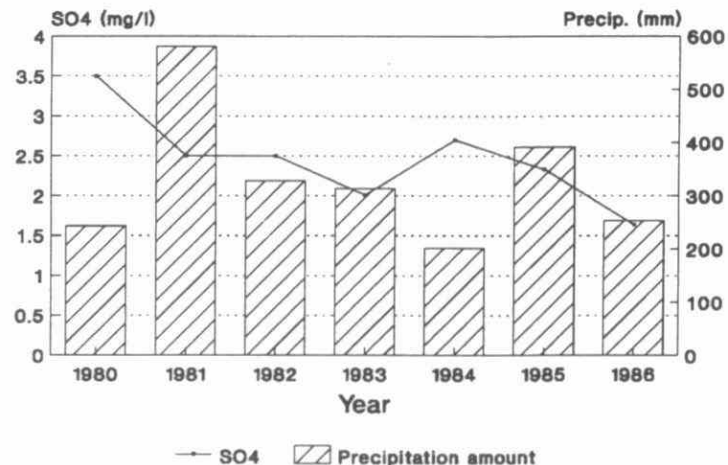


Fig. 3F-5 Seasonal sulphate concentrations in Autumn precipitation at Dorset, Ontario: 1980-1986.

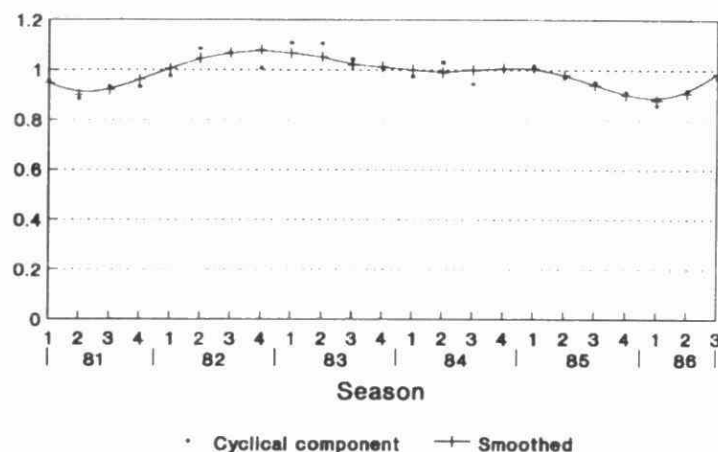


Fig. 3F-6 Cyclical component of seasonal sulphate concentrations in precipitation at Dorset, Ontario: 1981-1986.

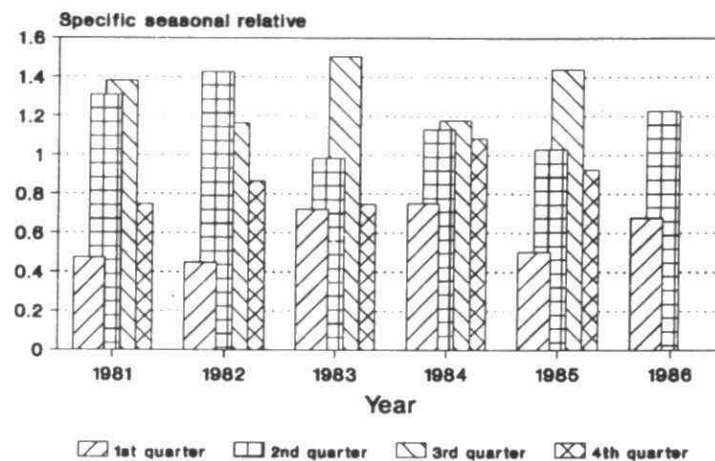


Fig. 3F-7 Specific seasonal relativities of sulphate in precipitation by quarter at Dorset, Ontario: 1981-1986.

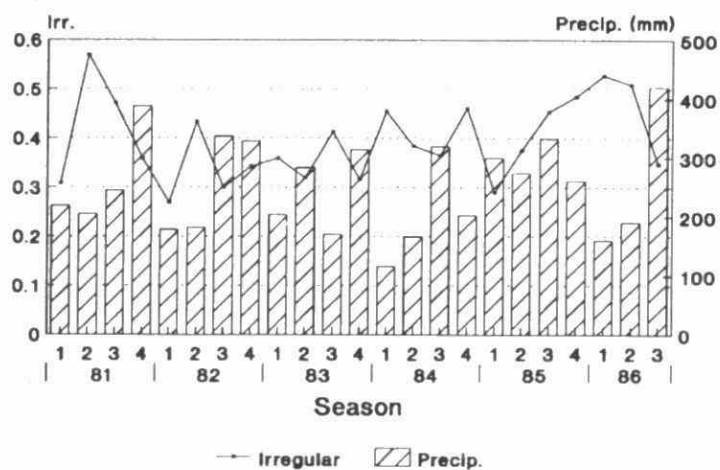


Fig. 3F-8 Irregular component of seasonal sulphate concentrations vs. precipitation amount at Dorset, Ontario: 1981-1986.

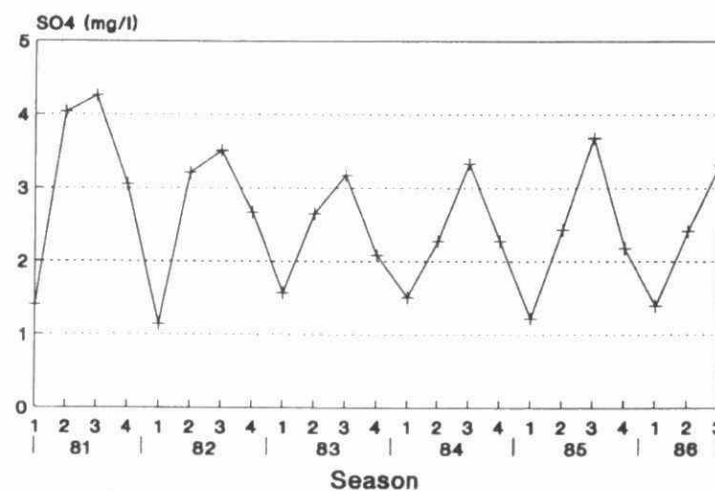


Fig. 3F-9 Precipitation amount corrected seasonal sulphate concentrations at Dorset, Ontario: 1981-1986.

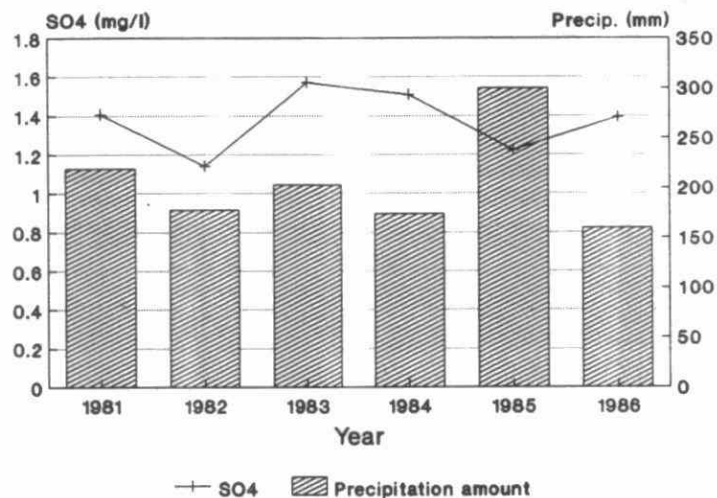


Fig. 3F-10 Precipitation amount corrected Winter sulphate concentrations at Dorset, Ontario: 1981-1986.

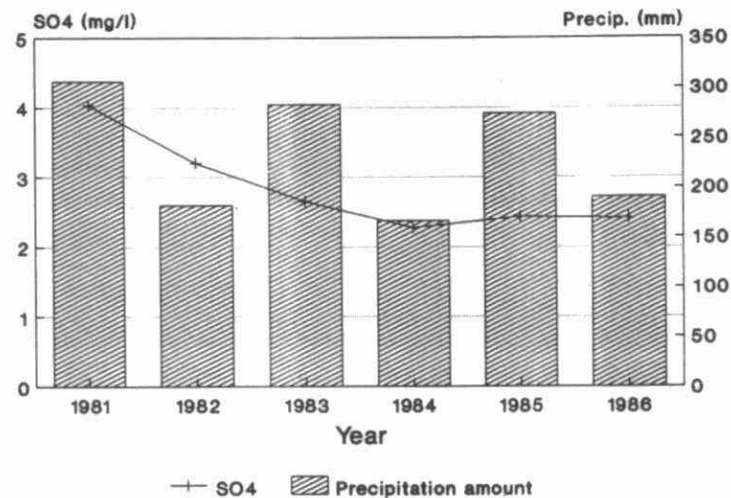


Fig. 3F-11 Precipitation amount corrected Spring sulphate concentrations at Dorset, Ontario: 1981-1986.

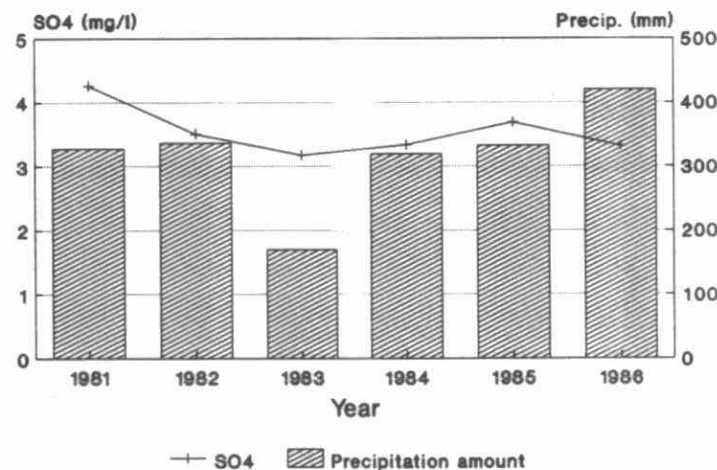


Fig. 3F-12 Precipitation amount corrected Summer sulphate concentrations at Dorset, Ontario: 1981-1986.

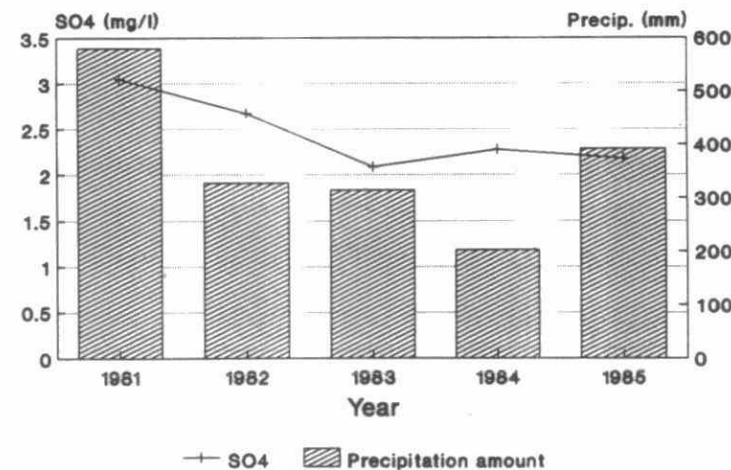


Fig. 3F-13 Precipitation amount corrected Autumn sulphate concentrations at Dorset, Ontario: 1981-1985.

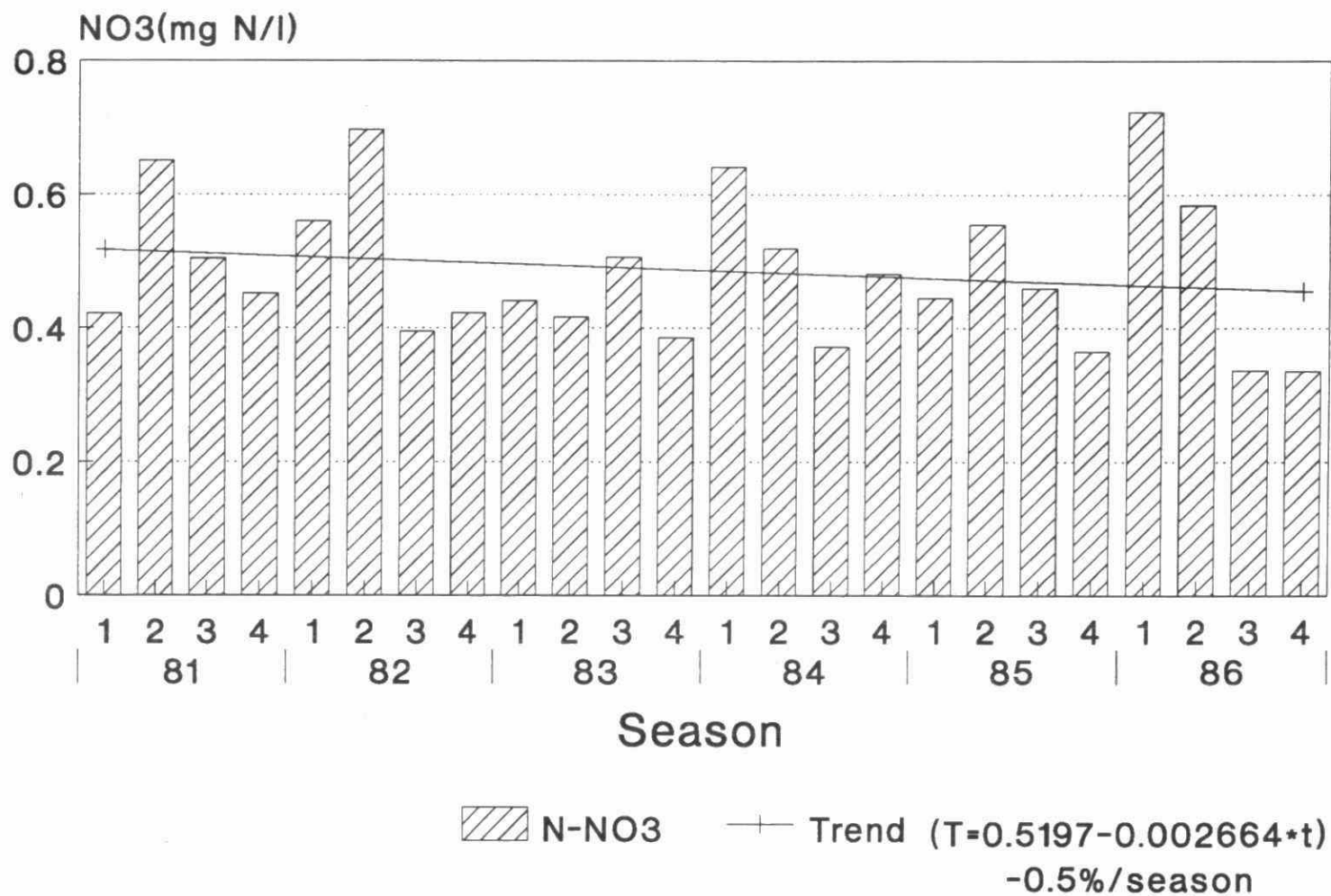


Fig. 3F-14 Seasonal N-NO₃⁻ concentrations in precipitation samples at Dorset, Ontario: 1981-1986.

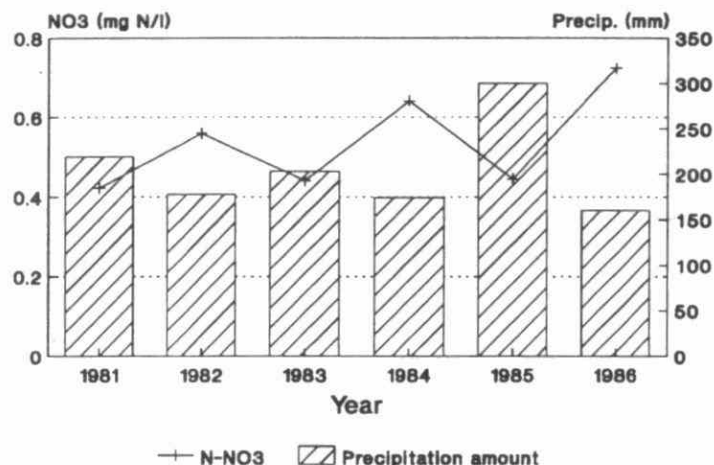


Fig. 3F-15 Seasonal N-NO₃⁻ concentrations in Winter precipitation at Dorset, Ontario: 1981-1986.

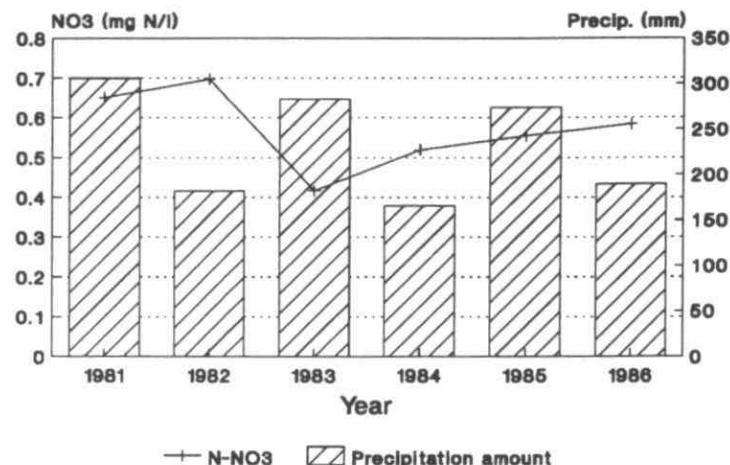


Fig. 3F-16 Seasonal N-NO₃⁻ concentrations in Spring precipitation at Dorset, Ontario: 1981-1986.

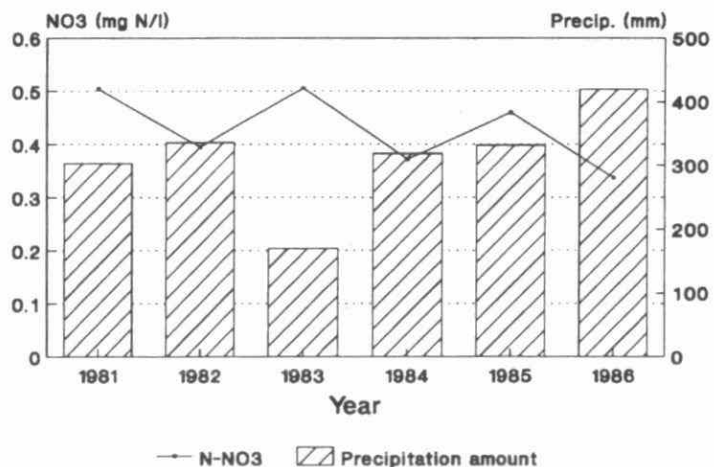


Fig. 3F-17 Seasonal N-NO₃⁻ concentrations in Summer precipitation at Dorset, Ontario: 1981-1986.

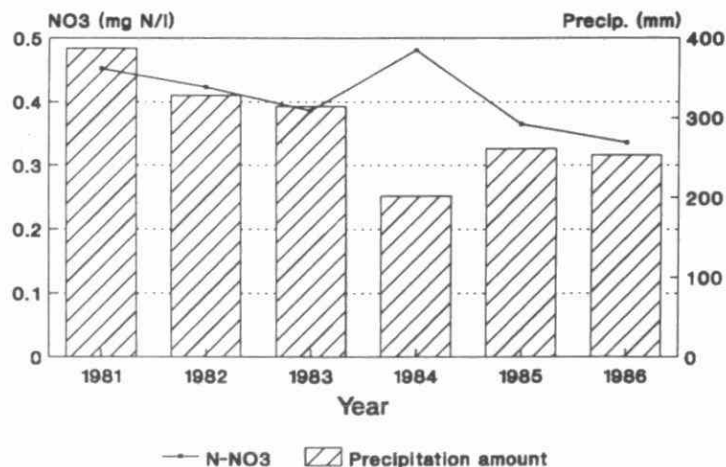


Fig. 3F-18 Seasonal N-NO₃⁻ concentrations in Autumn precipitation at Dorset, Ontario: 1981-1986.

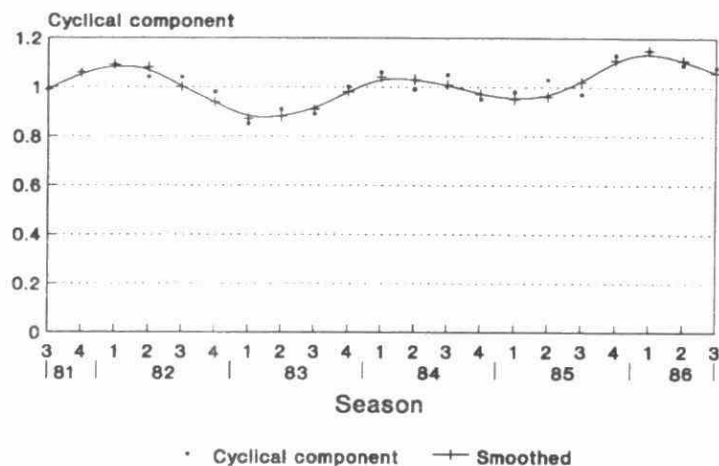


Fig. 3F-19 Cyclical component of seasonal N-NO_3^- concentrations at Dorset, Ontario: 1981-1986.

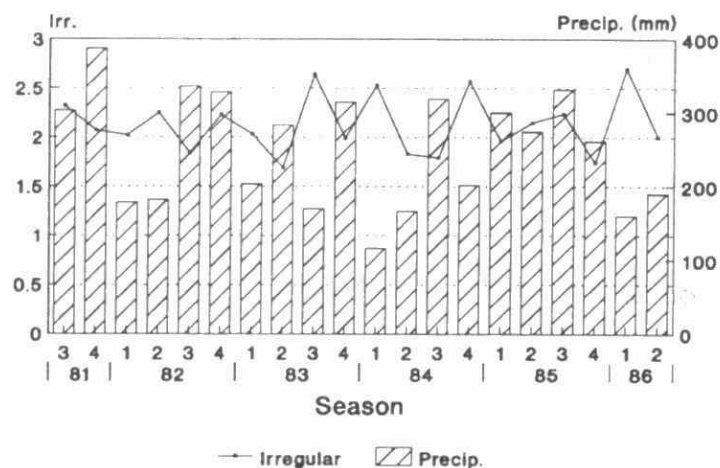


Fig. 3F-21 Irregular component of seasonal N-NO_3^- concentrations vs. precipitation amount at Dorset, Ontario: 1981-1986.

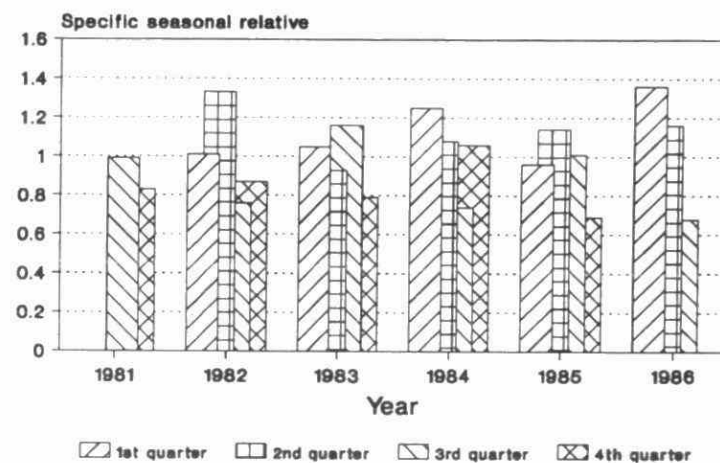


Fig. 3F-20 Specific seasonal relative of N-NO_3^- in precipitation by quarter at Dorset, Ontario: 1981-1986.

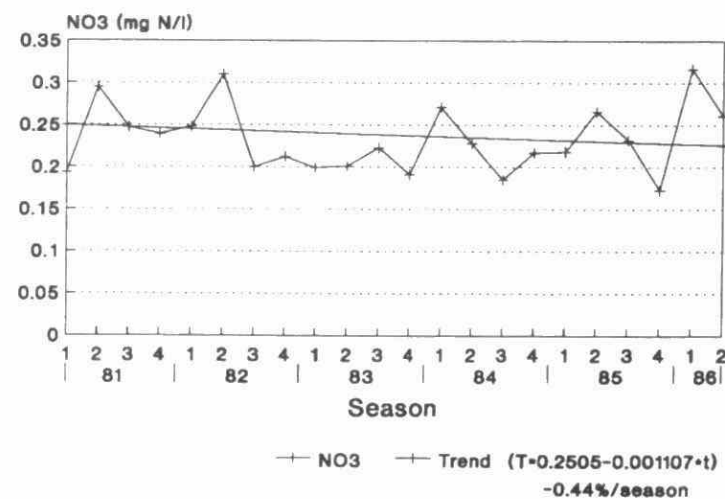


Fig. 3F-22 Precipitation amount corrected seasonal N-NO_3^- concentrations at Dorset, Ontario: 1981-1986.

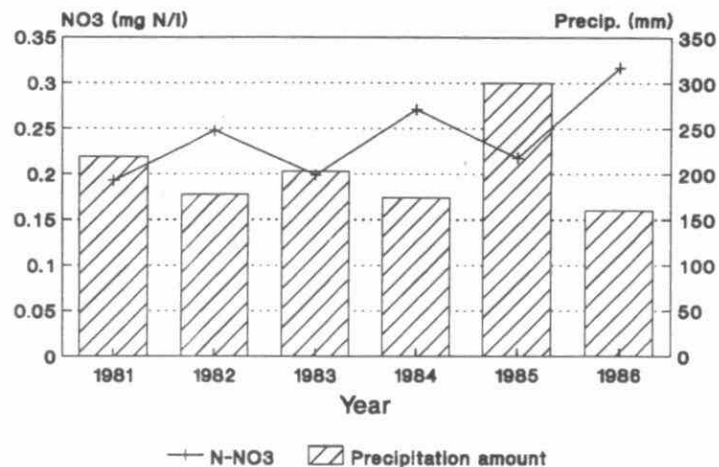


Fig. 3F-23 Precipitation amount corrected Winter N-NO₃⁻ concentrations at Dorset, Ontario: 1981-1986.

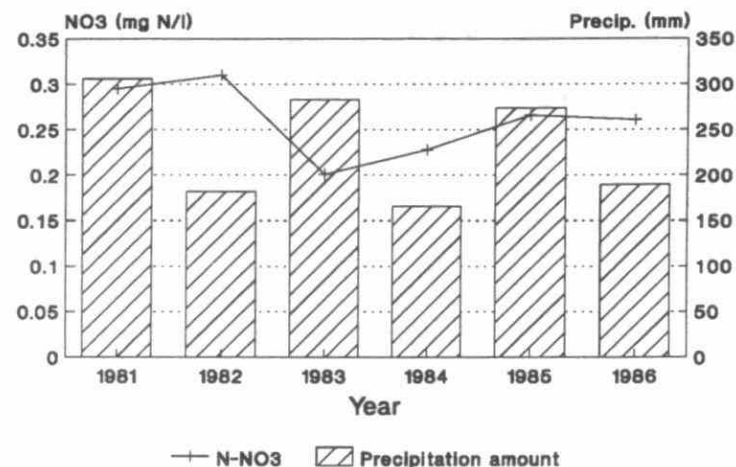


Fig. 3F-24 Precipitation amount corrected Spring N-NO₃⁻ concentrations at Dorset, Ontario: 1981-1986.

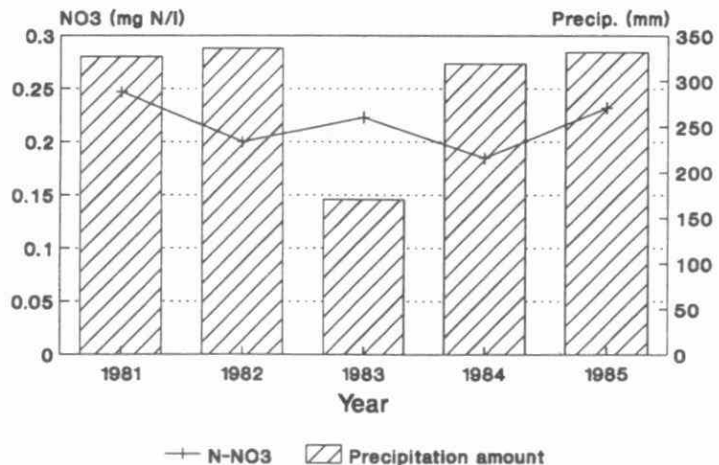


Fig. 3F-25 Precipitation amount corrected Summer N-NO₃⁻ concentrations at Dorset, Ontario: 1981-1985.

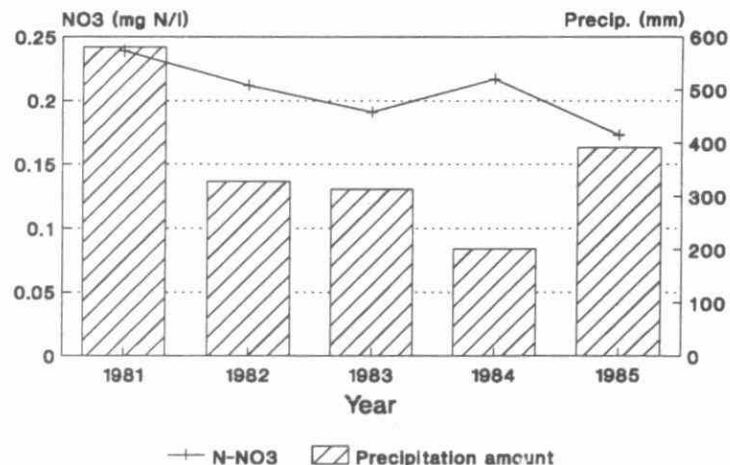


Fig. 3F-26 Precipitation amount corrected Autumn N-NO₃⁻ concentrations at Dorset, Ontario: 1981-1985.

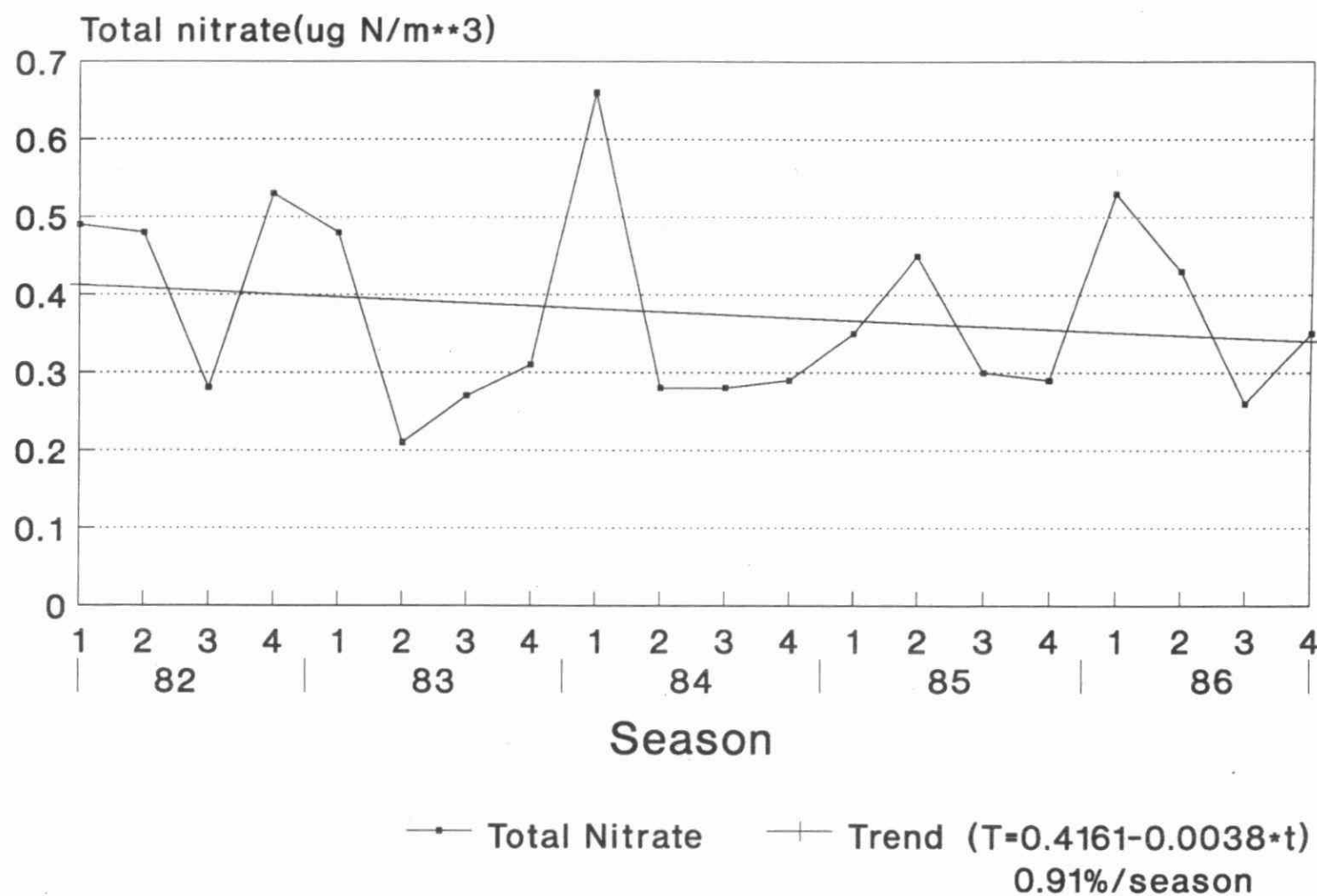


Fig. 3F-27 Seasonal total sulphur concentrations in ambient air at Dorset, Ontario:
1981-1986.

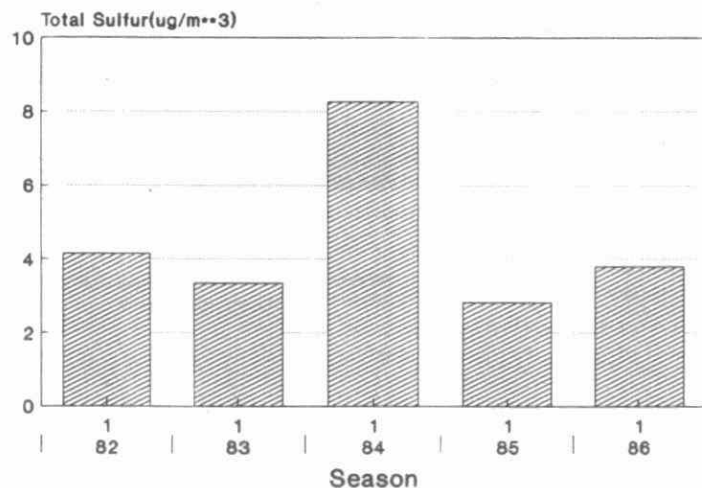


Fig. 3F-28 Winter total sulphur concentrations in ambient air at Dorset, Ontario: 1981-1986.

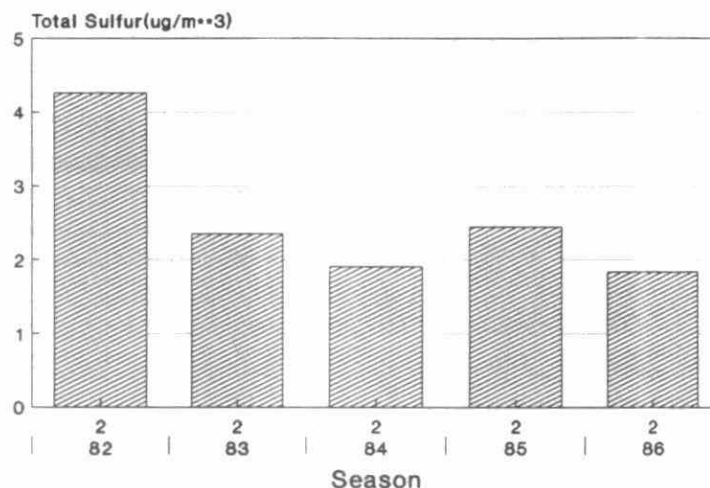


Fig. 3F-29 Spring total sulphur concentrations in ambient air at Dorset, Ontario: 1982-1986.

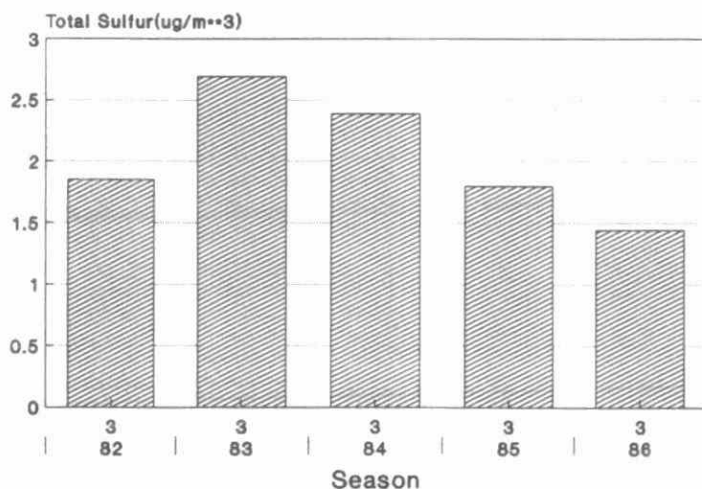


Fig. 3F-30 Summer total sulphur concentrations in ambient air at Dorset, Ontario: 1982-1986.

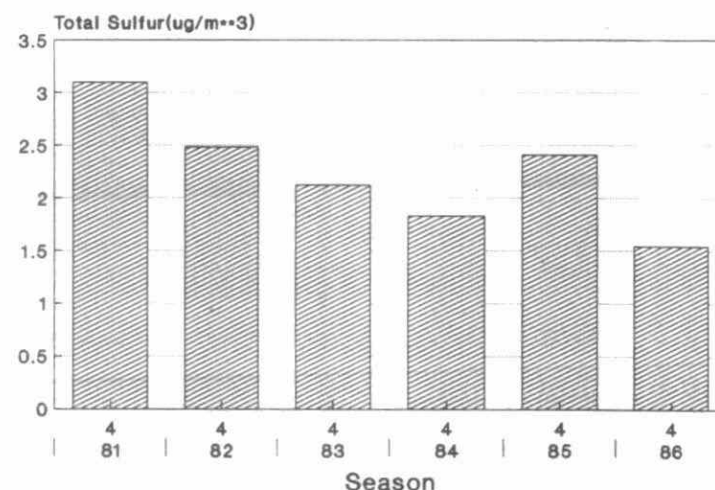


Fig. 3F-31 Autumn total sulphur concentrations in ambient air at Dorset, Ontario: 1981-1986.

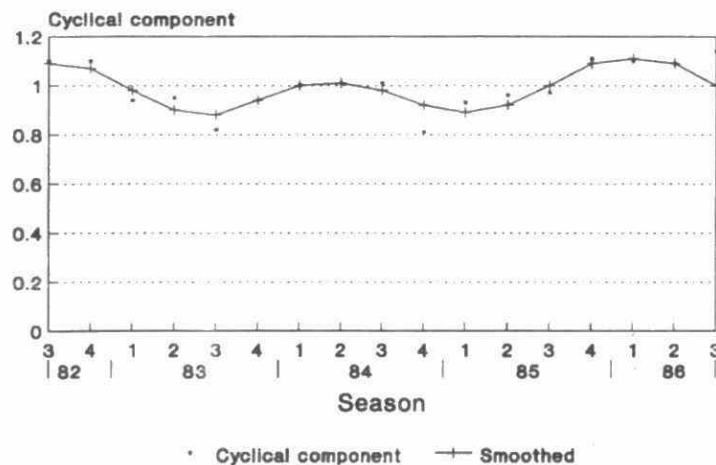


Fig. 3F-32 Specific seasonal relativities of seasonal total sulphur in air at Dorset, Ontario: 1982-1986.

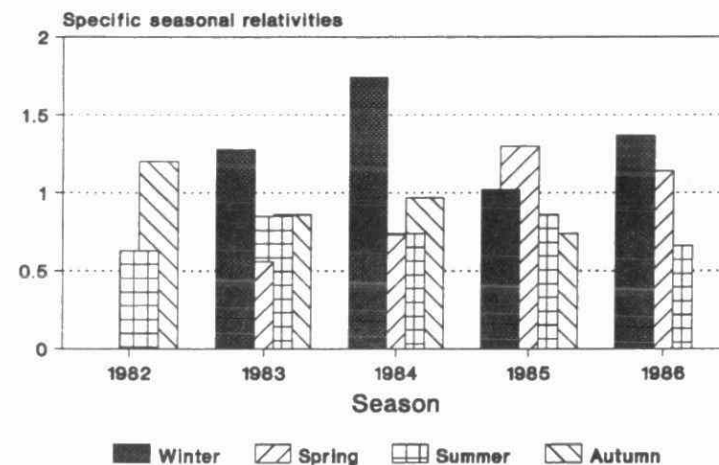


Fig. 3F-33 Cyclical components of seasonal total sulphur in air at Dorset, Ontario: 1982-1986.

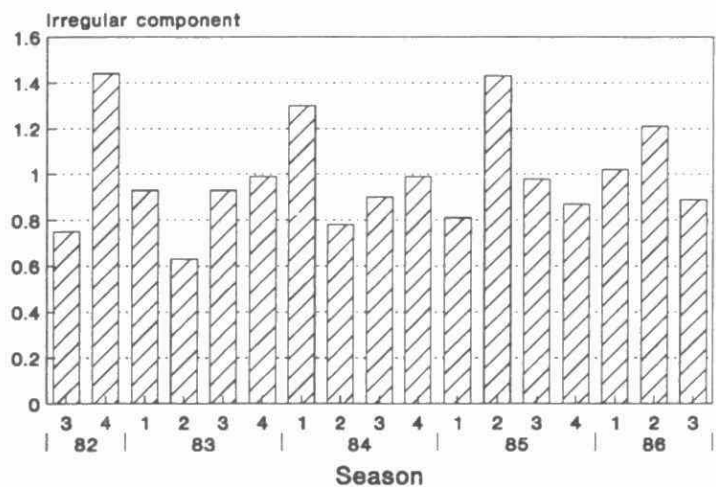


Fig. 3F-34 Irregular components of seasonal total sulphur in air at Dorset, Ontario: 1982-1986.

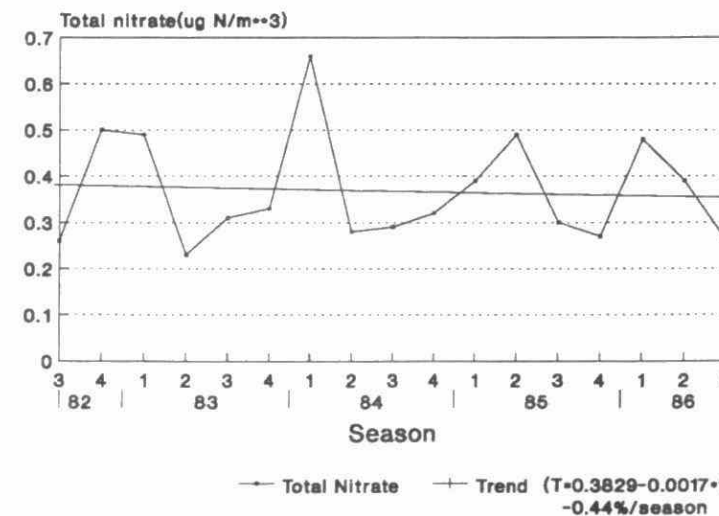


Fig. 3F-35 Climatological factor corrected seasonal total sulphur concentrations in air at Dorset, Ontario: 1982-1986.

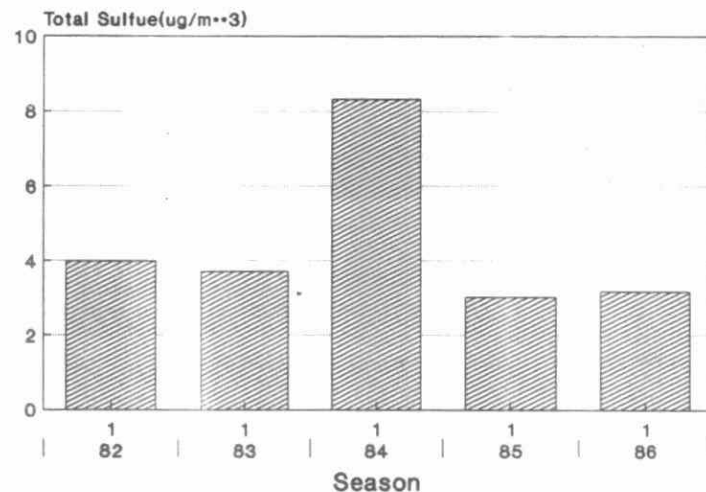


Fig. 3F-36 Climatological factor corrected Winter total sulphur concentrations in air at Dorset, Ontario: 1982-1986.

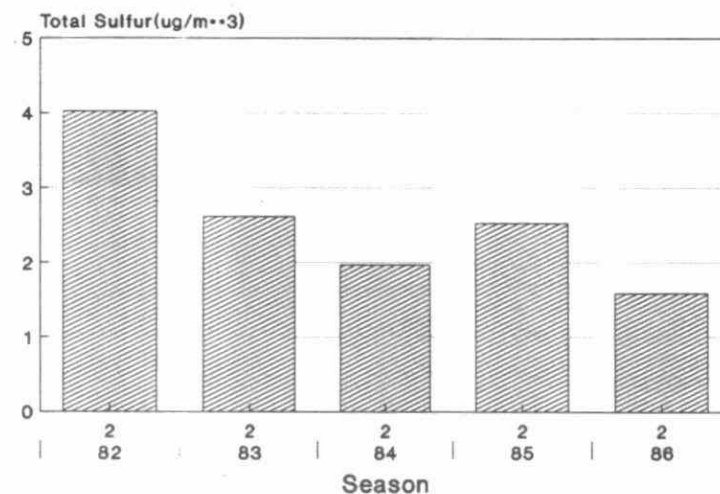


Fig. 3F-37 Climatological factor corrected Spring total sulphur concentrations in air at Dorset, Ontario: 1982-1986.

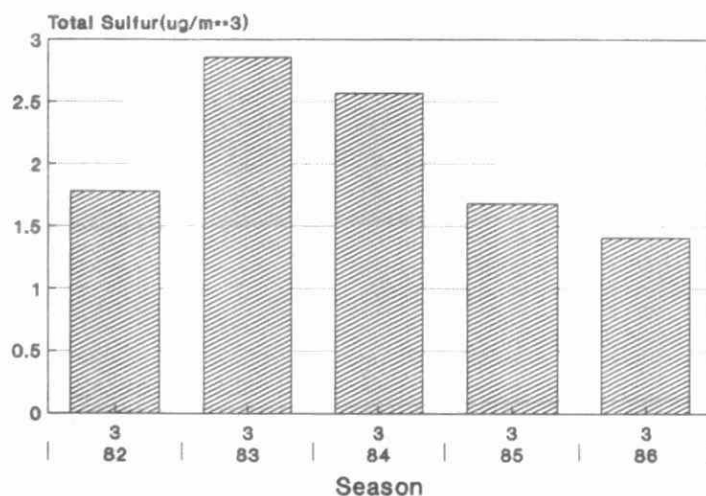


Fig. 3F-38 Climatological factor corrected summer total sulphur concentrations in air at Dorset, Ontario: 1982-1986.

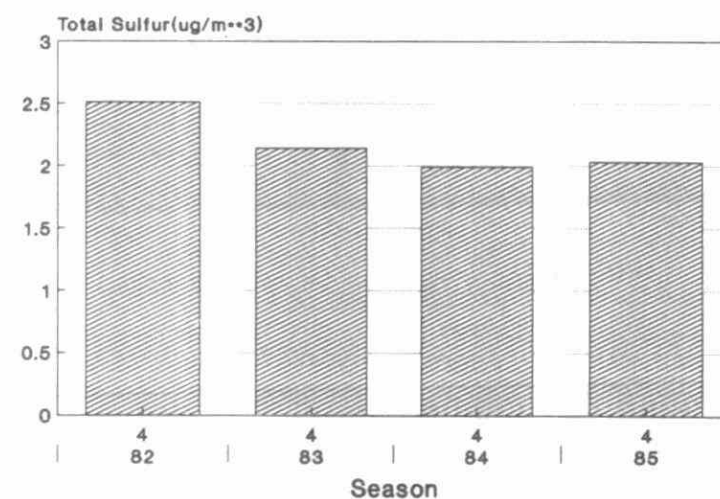


Fig. 3F-39 Climatological factor corrected Autumn total sulphur concentrations in air at Dorset, Ontario: 1982-1985.

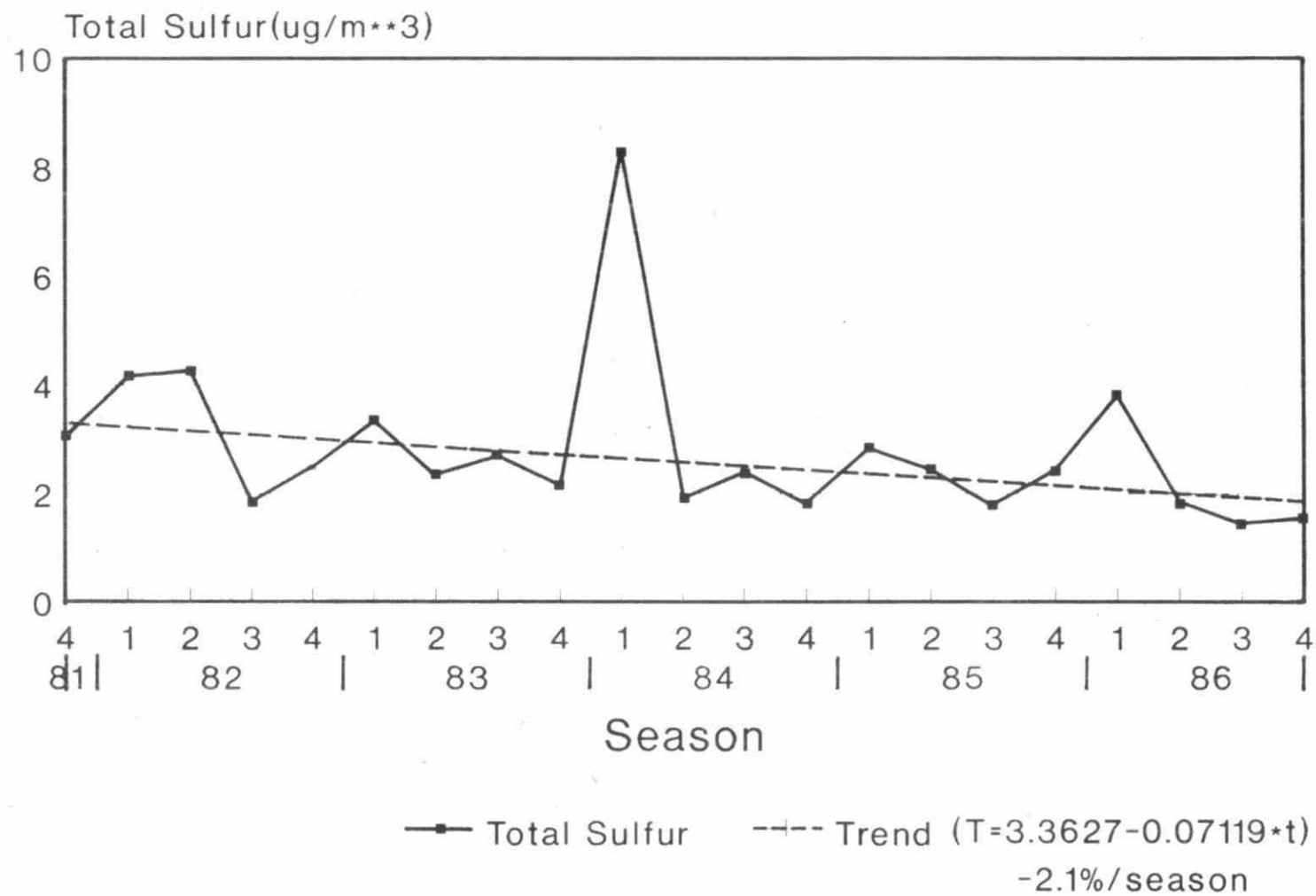


Fig. 3F-40 Seasonal total nitrate concentrations in ambient air at Dorset, Ontario: 1982-1986.

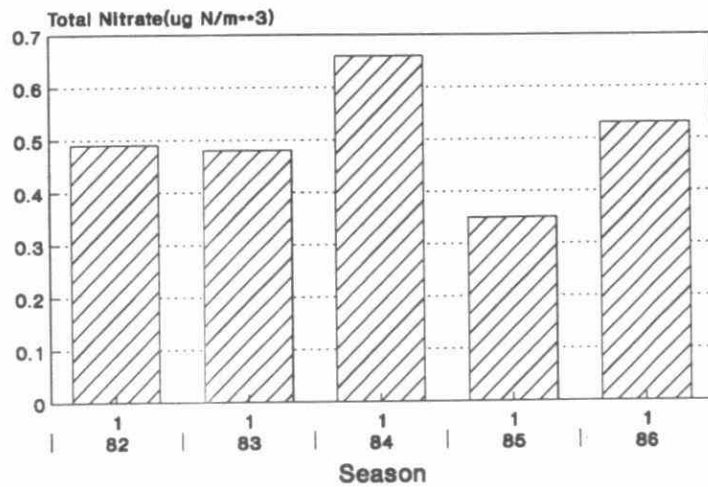


Fig. 3F-41 Winter total nitrate concentrations in ambient air at Dorset, Ontario: 1982-1986.

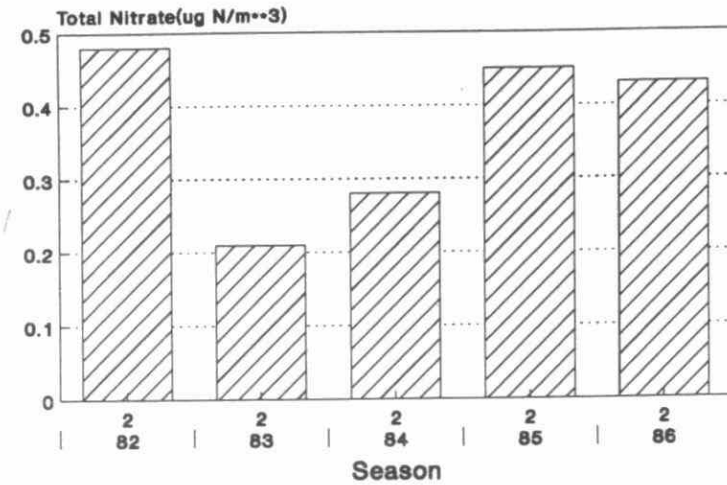


Fig. 3F-42 Spring total nitrate concentrations in ambient air at Dorset, Ontario: 1982-1986.

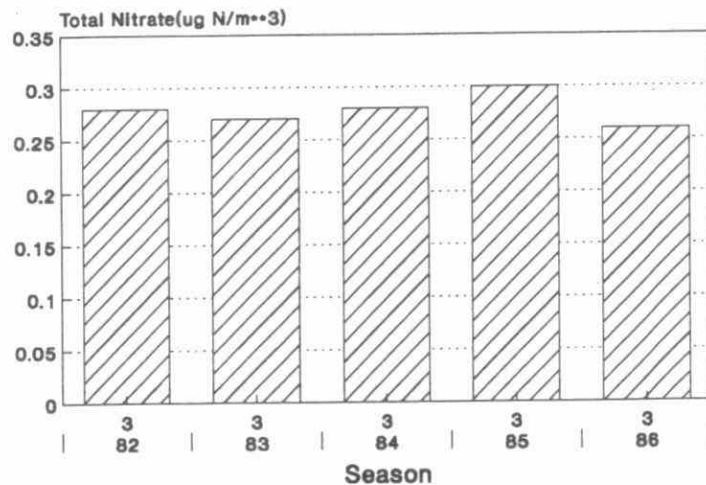


Fig. 3F-43 Summer total nitrate concentrations in ambient air at Dorset, Ontario: 1982-1986.

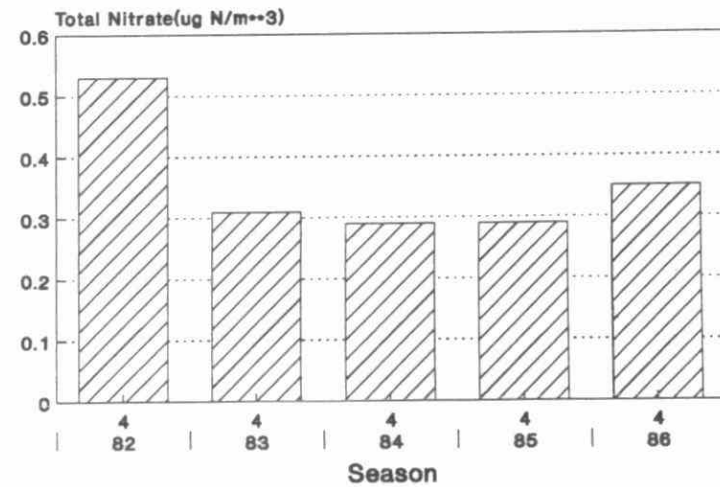


Fig. 3F-44 Autumn total nitrate concentrations in ambient air at Dorset, Ontario: 1982-1986.

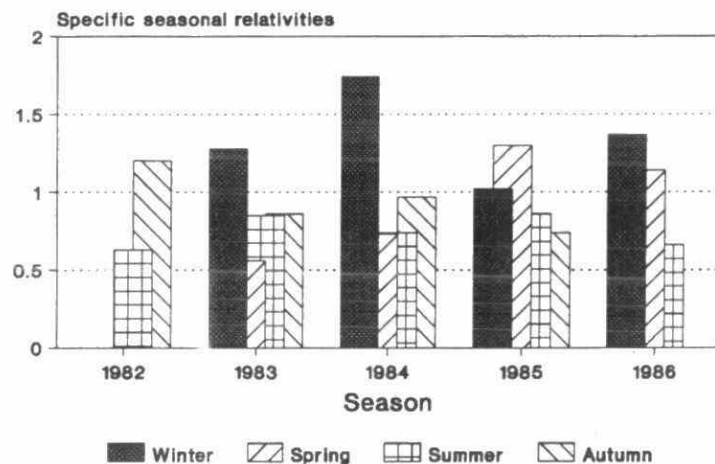


Fig. 3F-45 Specific seasonal relativities of seasonal total nitrate in air at Dorset, Ontario: 1982-1986.

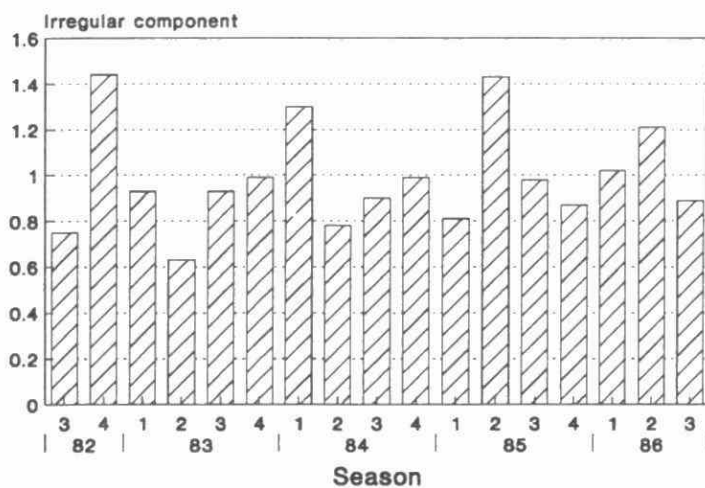


Fig. 3F-47 Irregular components of seasonal total nitrate in air at Dorset, Ontario: 1982-1986.

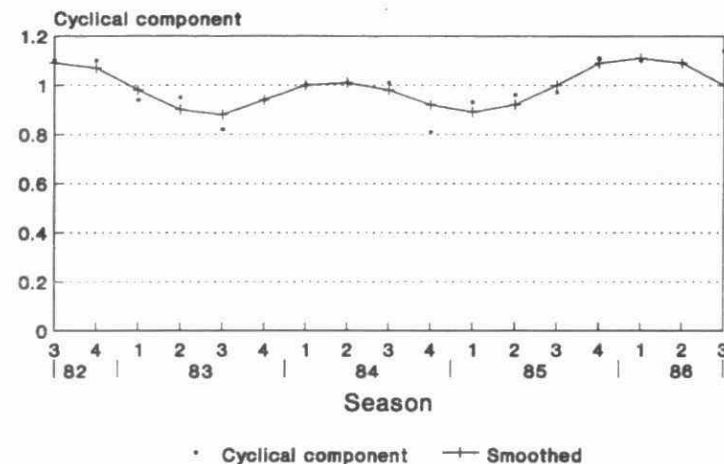


Fig. 3F-46 Cyclical components of seasonal total nitrate in air at Dorset, Ontario: 1982-1986.

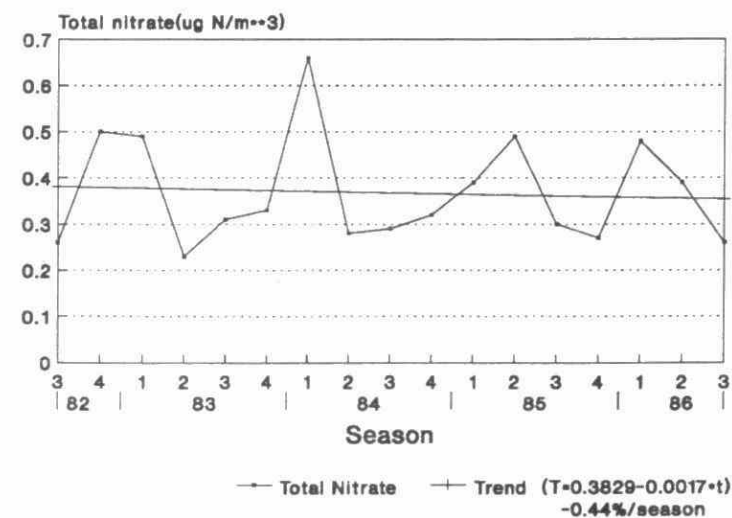


Fig. 3F-48 Climatological factor corrected total nitrate concentrations in air at Dorset, Ontario: 1982-1986.

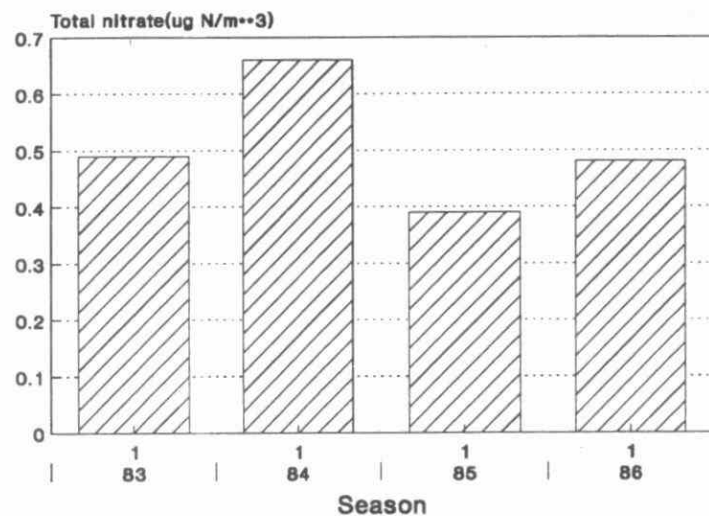


Fig. 3F-49 Climatological factor corrected total nitrate concentration in air: Winter.

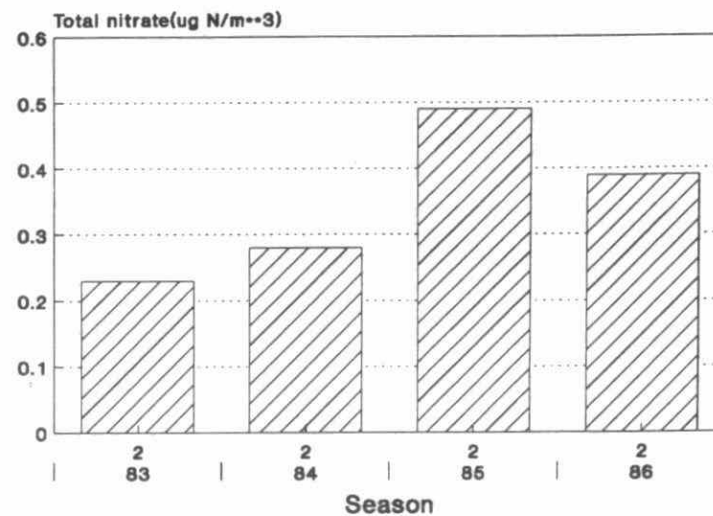


Fig. 3F-50 Climatological factor corrected total nitrate concentration in air: Spring.

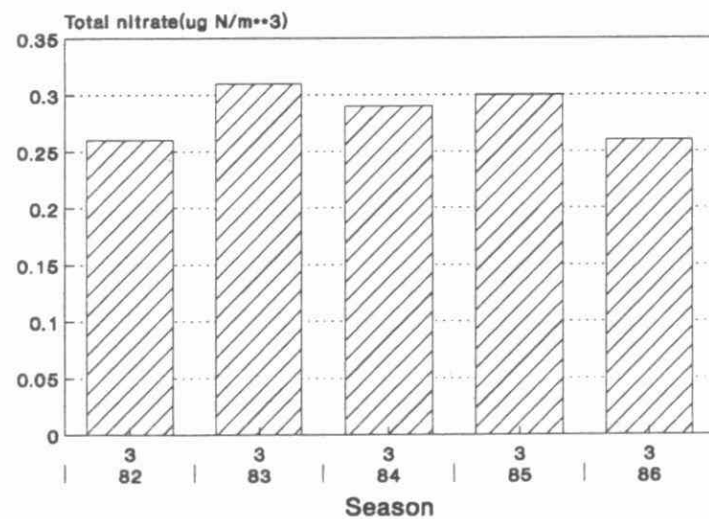


Fig. 3F-51 Climatological factor corrected total nitrate concentration in air: Summer.

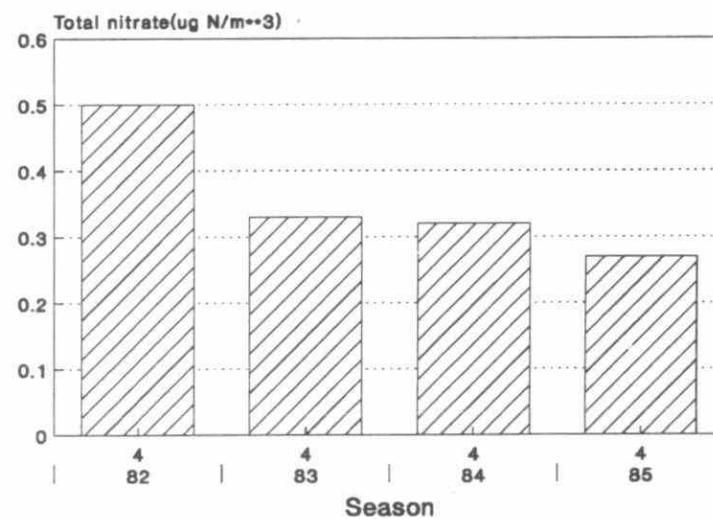


Fig. 3F-52 Climatological factor corrected total nitrate concentration in air: Autumn.

Table 3F-1

Seasonal Time Series Analysis: Dorset Sulphate Data

Season	Sulphate(mg/L)	Trend (T)	Cyclical (C)	Seasonal (S)	Irregular (I)
W81	1.62	3.27	0.96	0.50	1.04
S81	4.77	3.22	0.88	1.13	1.45
S81	4.69	3.17	0.93	1.38	1.17
A81	2.50	3.12	0.93	0.87	0.97
W82	1.41	3.06	0.98	0.50	0.91
S82	3.96	3.01	1.09	1.13	1.08
S82	3.23	2.96	1.07	1.38	0.74
A82	2.50	2.91	1.01	0.87	0.92
W83	1.86	2.86	1.11	0.50	1.21
S83	2.72	2.81	1.02	1.13	0.81
S83	3.97	2.76	1.04	1.38	1.02
A83	2.01	2.70	1.01	0.87	1.02
W84	2.05	2.65	0.97	0.50	1.54
S84	2.86	2.60	1.03	1.13	1.98
S84	3.18	2.55	0.95	1.13	0.90
A84	2.70	2.50	1.00	0.87	1.24
W85	1.21	2.45	1.02	0.50	0.88
S85	2.54	2.40	0.97	1.13	0.96
S85	3.42	2.34	0.95	1.38	1.13
A85	2.33	2.29	0.91	0.87	1.30
W86	1.77	2.24	0.86	0.50	1.78
S86	2.92	2.19	0.92	1.13	1.30
S86	2.50	2.14	0.97	1.38	0.86
A86	1.64	2.09			

Table 3F-2

Seasonal Time Series Analysis: Dorset Total Nitrate in Precipitation

Season	Nitrate (mg/L)	Trend (T)	Cylcal (C)	Seasonal (S)	Irregular (I)
S81	0.504	0.512	0.99	0.43	2.32
A81	0.452	0.509	1.06	0.41	2.07
W82	0.560	0.506	1.09	0.50	2.02
S82	0.697	0.504	1.04	0.57	2.25
S82	0.395	0.501	1.04	0.43	1.84
A82	0.423	0.498	0.98	0.41	2.23
W83	0.441	0.496	0.85	0.50	2.03
S83	0.417	0.493	0.91	0.57	1.69
S83	0.506	0.490	0.89	0.43	2.64
A83	0.386	0.488	1.00	0.41	1.99
W84	0.641	0.484	1.06	0.50	2.53
S84	0.519	0.482	0.99	0.57	1.83
S84	0.372	0.480	1.05	1.43	1.79
A84	0.481	0.477	0.95	0.41	2.57
W85	0.445	0.474	0.98	0.50	1.96
S85	0.555	0.472	1.03	0.57	2.15
S85	0.460	0.469	0.97	0.43	2.24
A85	0.365	0.466	1.13	0.41	1.74
W86	0.724	0.464	1.15	0.50	2.70
S86	0.584	0.461	1.09	0.57	2.00
S86	0.337	0.458	1.08	0.43	2.00

Table 3F-3

Seasonal Time Series Analysis: Dorset Total Sulphur Air Data

Season	Sulphate($\mu\text{g}/\text{m}^3$)	Trend (T)	Cyclical (C)	Seasonal (S)	Irregular (I)
A81	3.10	3.29			
W82	4.15	3.22			
S82	4.26	3.15	1.06	0.99	1.29
S82	1.85	3.08	1.04	0.76	0.76
A82	2.48	3.01	0.99	0.83	1.00
W83	3.34	2.93	0.85	1.37	0.92
S83	2.35	2.86	0.95	0.99	0.92
S83	2.69	2.79	0.94	0.76	1.35
A83	2.12	2.72	1.42	0.83	0.95
W84	8.25	2.65	1.41	1.37	2.29
S84	1.91	2.58	1.42	0.99	0.77
S84	2.39	2.51	1.43	0.76	1.35
A84	1.83	2.44	0.92	0.83	0.98
W85	2.82	2.36	1.00	1.37	0.94
S85	2.45	2.29	0.97	0.99	1.11
S85	1.80	2.22	1.07	0.76	1.00
A85	2.41	2.15	1.22	0.83	1.13
W86	3.80	2.08	1.18	1.37	1.11
S86	1.84	2.01	1.18	0.99	0.80
S86	1.44	1.94	1.11	0.76	0.96
A86	1.54	1.87			

Table 3F-4.

Seasonal Time Series Analysis: Dorset Total Nitrate Air Data

Season	Nitrate ($\mu\text{g}/\text{m}^3$)	Trend (T)	Cyclical (C)	Seasonal (S)	Irregular (I)
W82	0.49	0.412			
S82	0.48	0.409	1.10	0.85	0.75
S82	0.28	0.405	1.10	0.86	1.44
A82	0.53	0.401	0.94	1.33	0.93
W83	0.48	0.397	0.95	0.94	0.63
S83	0.21	0.393	0.82	0.85	0.93
S83	0.27	0.390	0.94	0.86	0.99
A83	0.31	0.386	1.00	1.33	1.30
W84	0.66	0.382	1.01	0.94	0.78
S84	0.28	0.378	1.01	0.85	0.90
S84	0.28	0.374	0.81	0.86	0.99
A84	0.29	0.371	0.93	1.33	0.81
W85	0.35	0.367	0.96	0.94	1.43
S85	0.45	0.363	0.97	0.85	0.98
S85	0.30	0.359	1.11	0.86	0.87
A85	0.29	0.355	1.10	1.33	1.02
W86	0.53	0.352	1.09	0.94	1.21
S86	0.43	0.348	1.14	0.85	0.89
S86	0.26	0.344			
A86	0.35	0.340			

APPENDIX G
LAGRANGIAN MODEL SCENARIO RUNS

LIST OF FIGURES

<u>Figure#</u>	<u>Page#</u>
3G-1 Wet SO ₄ Deposition Data 1982 - 1986 (kg/ha/yr). Current conditions- The observed 5 year (1982 - 1986) mean deposition values.	3-347
3G-2 Predicted Wet SO ₄ Deposition (kg/ha/yr). Model projections of deposition under conditions of full implementation of the SO ₂ control program in eastern Canada and the U.S. SO ₂ emissions equal to 1980 levels.	3-347
3G-3 Model projections of deposition under conditions of full implementation of the SO ₂ control program in eastern Canada and a 5 million ton (4.3 million metric tonne) reduction in 1980 emissions in the U.S. (i.e. first phase of control program to be implemented by 1995, announced by President Bush in the summer of 1989.)	3-348
3G-4 Model predictions of deposition under conditions of full implementation of the SO ₂ control program in eastern Canada and a 10 million ton (9 million metric tonne) reduction in 1980 emissions in the U.S. (i.e. full implementation of control program by 2000-2003 announced by President Bush in the summer of 1989.)	3-348

LIST OF TABLES

<u>Table#</u>	<u>Page#</u>
3G-1 Emission estimates used to evaluate effect of U.S. control program of sulphate deposition and transboundary flows.	3-349

FUTURE DEPOSITION SCENARIO RUNS

The analysis of the effectiveness of the Canadian and U.S. control programs offered in the assessment reports is based on the actual details of the SO₂ Control Program in Eastern Canada and the RMCC's best judgement on the distribution of the 10 million ton reduction in SO₂ announced by President Bush in the summer of 1989. The specific U.S. emission levels used to predict future deposition are listed in Table 3G-1.

In order to predict future deposition levels the Ontario Ministry of the Environment (OME)'s linear Lagrangian trajectory model was run for four emission conditions: a) the base case 1980 emissions; b) 1994 Canadian SO₂ emission levels under full implementation of the Canadian Acid Rain Control Program and 1980 base case emissions for the U.S.; c) 1994 Canadian SO₂ emission levels and U.S. emissions with a 4.5 million metric tonne (5 million ton) cut in 1980 levels (ie. the first phase of the control program to be implemented by 1995, announced by President Bush in the summer of 1989) and; d) 1994 Canadian SO₂ emission levels and U.S. emissions with a 9 million metric tonne (10 million ton) cut in 1980 levels (ie, the second phase of the control program to be implemented by 2000-2003, announced by President Bush in the summer of 1989). These model runs provided predictions of annual average wet sulphate deposition.

In the Lagrangian trajectory puff model, continuous emissions from a point source are idealized as discrete puffs which travel along time-varying trajectories following surface geostrophic winds. Trajectories are initiated at three-hour intervals from each of the 182 representative source points in North America east of the Rockies. The model runs for the three scenarios were performed using annual average SO₂ emissions and meteorology for 1980. The processes included in the model are (1) expansion of the puff as it travels downwind, (2) linear chemical conversion of SO₂ to SO₄⁻, (3) dry deposition of SO₂ and SO₄⁻. The model is described in Ellenton et al. (1985, 1988). Evaluations of the model against measured monthly average SO₂ wet deposition have been performed for a number of monitoring sites in Canada and U.S. Model results showed reasonable agreement with the monthly variability of measured data.

Since the model uses only anthropogenic SO₂ emissions for North America east of the Rockies, a background wet deposition was added to the model results. The background SO₄⁻ deposition was derived using a fixed precipitation concentration of 0.4 mg SO₄⁻/l. This concentration was multiplied by the annual precipitation amount at each grid cell to produce a variable background deposition. This deposition is due to emissions outside the grid domain and natural emissions within the grid domain.

The model is better at predicting relative changes in deposition under different emission conditions than quantifying the actual deposition levels. For this reason the percentage changes between the 1980 wet deposition and the future deposition conditions, as predicted by the OME model, were applied to the observed mean excess sulphate deposition for the period 1982-1986, in order to prepare maps showing future deposition scenarios (see Figures 3G1-3G4). These results indicate some reductions in wet sulphate deposition with the 1994 Canadian emission cuts: the region receiving wet sulphate deposition greater than 20 kg/ha/yr is reduced. When the control programs in both the U.S. and Canada are fully implemented the region of Eastern Canada receiving sulphate deposition greater than 20 kg/ha/yr is essentially eliminated.

SCENARIO 1

Wet SO₄ Deposition Data
1982 - 86 (kg/ha/yr)

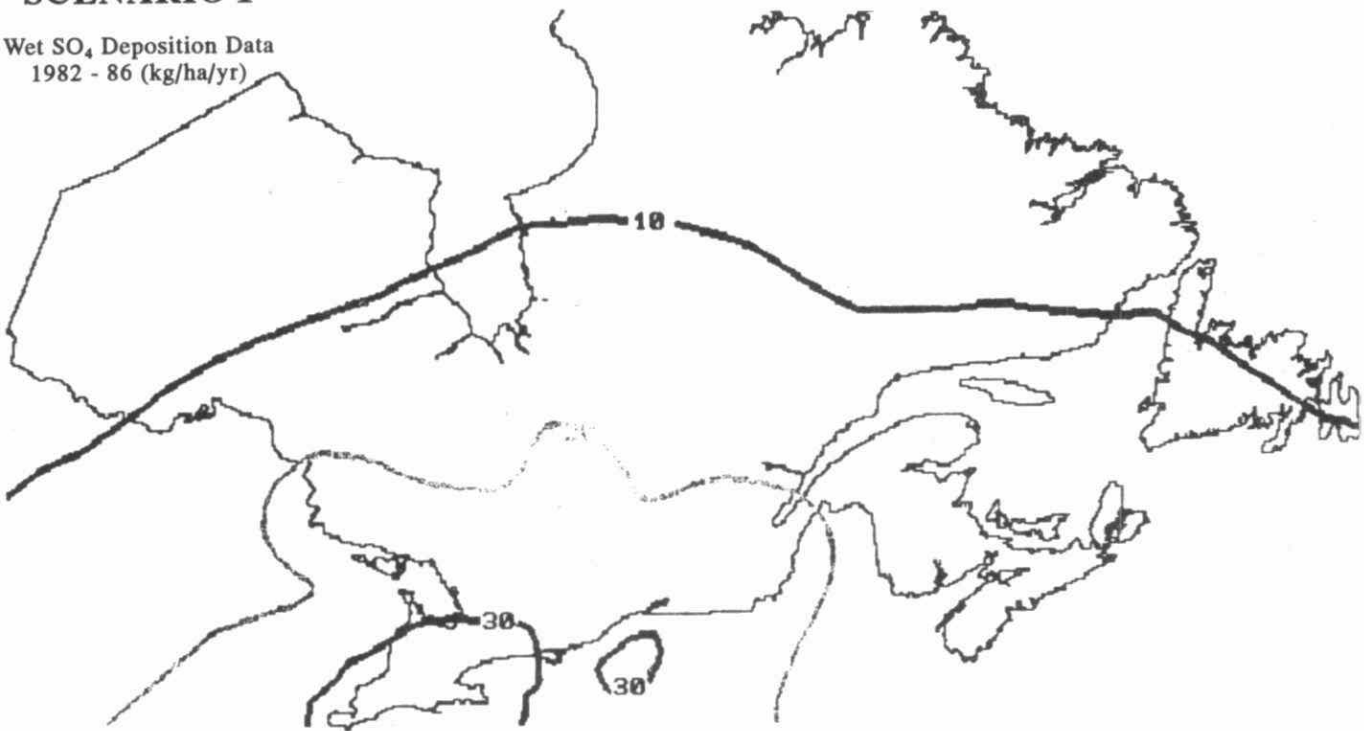


Fig. 3G-1 Wet SO₄ Deposition Data 1982 - 1986 (kg/ha/yr). Current conditions--The observed 5 year (1982 - 1986) mean deposition values.

SCENARIO 2

Predicted Wet SO₄ Deposition
(kg/ha/yr)

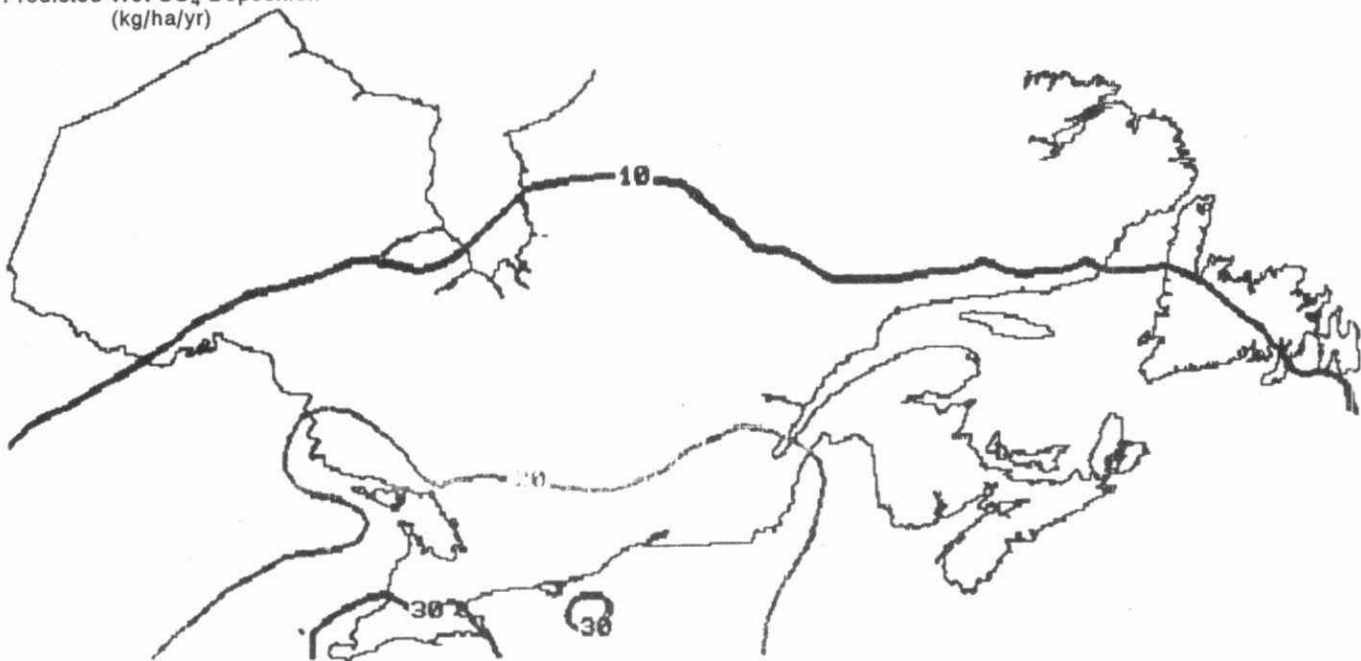


Fig. 3G-2 Predicted Wet SO₄ Deposition (kg/ha/yr). Model projections of deposition under conditions of full implementation of the SO₂ control program in eastern Canada and the U.S. SO₂ emissions equal to 1980 levels.

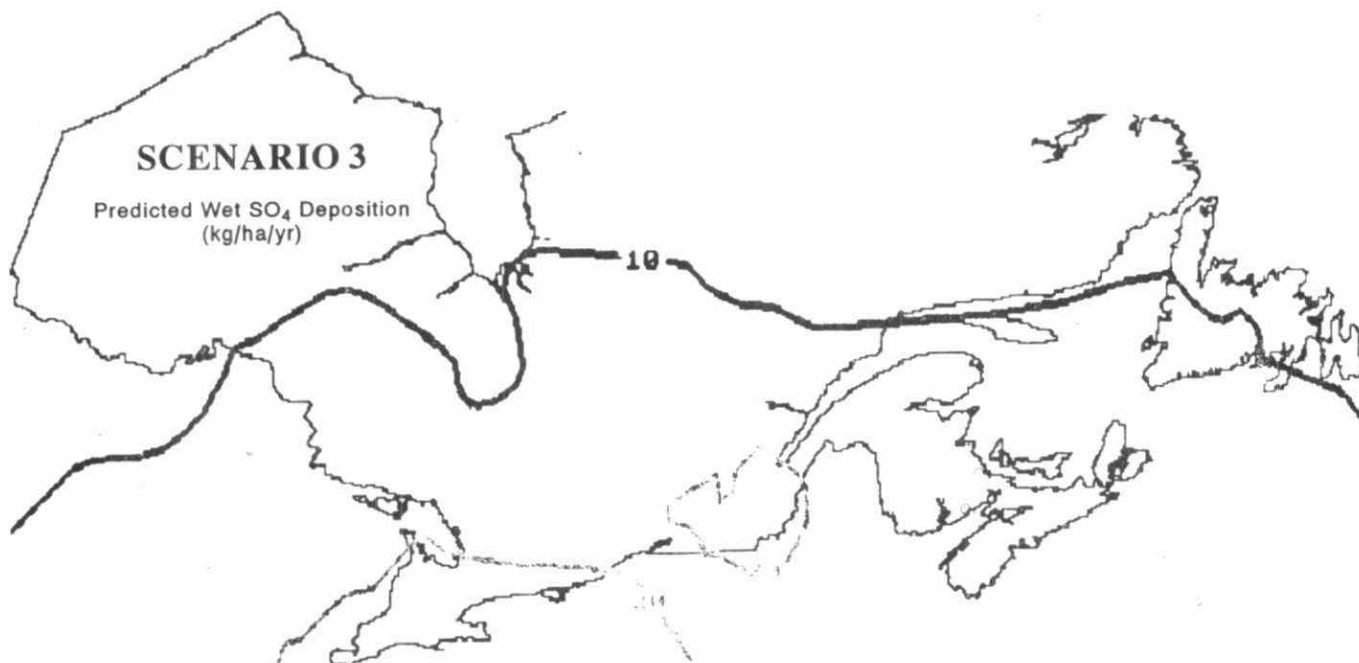


Fig. 3G-3 Model projections of deposition under conditions of full implementation of the SO₂ control program in eastern Canada and a 5 million ton (4.3 million metric tonne) reduction in 1980 emissions in the U.S. (i.e. first phase of control program to be implemented by 1995, announced by President Bush in the summer of 1989.)



Fig. 3G-4 Model predictions of deposition under conditions of full implementation of the SO₂ control program in eastern Canada and a 10 million ton (9 million metric tonne) reduction in 1980 emissions in the U.S. (i.e. full implementation of control program by 2000-2003 announced by President Bush in the summer of 1989.)

Table 3G-1

Emission Estimates used to Evaluate Effect of US Control Program of Sulphate Deposition and Transboundary Flows

Region	1980 SO ₂ Emissions		1st Phase of US Control Program (5 million tons)		Full US Control Program (10 million tons)	
	Kilotons	Kilotonnes (metric)	Kilotons	Kilotonnes (metric)	Kilotons	Kilotonnes (metric)
Ohio	2884	2616	2009	1822	1133	1028
Illinois	1537	1394	1070	971	604	548
Pensylvania	1908	1730	1329	1205	749	680
Indiana	1922	1743	1338	1214	755	685
Michigan	896	813	688	624	479	435
West Virginia	1150	1043	802	727	452	410
New York	869	788	667	605	465	422
Wisconsin/Iowa	1186	1076	911	826	635	576
Minnesota	273	248	210	190	146	133
Maine	158	143	121	110	85	77
Vermont/N.Hampshire	120	109	93	84	64	58
Kentucky	1175	1066	1004	911	834	757
Tennessee	1158	1050	1072	972	986	894
Missouri	1295	1175	1200	1088	1103	1001
Alabama	841	763	778	706	717	650
Virginia/North Carolina	1062	963	983	892	904	820
Florida	1226	1112	1136	1030	1044	947
Giorgia/South Carolina	1249	1133	1156	1049	1064	965
Maryland/Delaware/New Jersey/D.C.	778	706	721	654	663	601
Arkansas/Louisiana/Mississippi	905	821	838	760	771	699
Mass./Conn./Rhode Island	435	394	402	365	374	336
Western States	4763	4320	4262	3866	3763	3413
U.S. Total	27790	25206	22790	20671	17790	16135

REFERENCES

REFERENCES

- Anlauf, K., Fellin, P., Wiebe, H.A., Schiff, H.L., Mackay, G.I., Braman, R.S. and Gilbert, R. 1985. A comparison of three methods for measurement of atmospheric nitric acid and aerosol nitrate and ammonium, Atmos. Environ. **19**, 325-333.
- Anlauf, K., Olson, M., Wiebe, H.A. and Lusi, M. 1980. Atmospheric transport of particulate sulphate and ozone into the Toronto region and its correlation with visibility. Studies in Environmental Science **8**, 153-138.
- Ashbaugh, L.L. 1983. A statistical trajectory technique for determining air pollution source regions. J. Air Poll. Control Assoc., **33**, 1096-1098.
- Banic, C.M., Isaac, G.A., Cho, H.R. and Iribane, J.V. 1986. The Redistribution of Pollutants near a Frontal Surface: A Comparison Between Field Experiment and Modelling. Water, Air and Soil Pollution, **30**, 171-177.
- Barchet, R.W. 1989. NAPAP Model Evaluation, Volumes 1 and 2. Prepared for USEPA, Atmospheric Research and Exposure Assessment Laboratory, Research Triangle Park NC, 27711.
- Barchet, R.W. 1987. Acidic deposition and its gaseous precursors. Volume III, Chapter 5. The National Acid Precipitation Assessment Program Interim Assessment - The Causes and Effects of Acid Deposition. Office of the National Acid Precipitation Assessment Program, Washington, D.C.
- Barrie, L.A. 1988. Aspects of atmospheric pollutant origin and deposition revealed by multielemental observations at a rural location in eastern Canada. J. Geophys. Res. **93**, 3773-3788.
- Barrie, L.A. and Hales, J.M. 1984. The Spatial Distributions of Precipitation Acidity and Major Ion Wet Deposition in North America During 1980. Tellus **36B**, 333-355.
- Barrie, L.A. and Schemenauer, R.S. 1989. Wet deposition of heavy metals. NATO Advanced Research Workshop on the Control and Fate of Atmospheric Heavy Metals, 12-16 September, Oslo, Norway, in press.
- Barrie, L.A. and Schemenauer, R.S. 1986. Pollutant wet deposition mechanisms in precipitation and fog water. Water, Air, Soil Pollut. **30**, 91-104.
- Barrie, L.A., Wiebe, H.A., Fellin, P. and Anlauf, K. 1980. The Canadian Air and Precipitation Monitoring Network (APN): A description and results for November 1978 to June 1979. AQRB Internal Report # ARQB-80-002-T, Atmospheric Environment Service, 4905 Dufferin Street, Downsview, Ontario, Canada, M3H 5T4.
- Beattie, B.L., and Whelpdale, D.M. 1989. Meteorological Characteristics of Large Acidic Deposition Events at Kejimikujik, Nova Scotia. Water, Air, Soil Pollut. **46**, 45-59.
- Benkley, C.W. and Bass, A. 1979. User's Guide to MESOPUFF (Mesoscale PUFF Model). EPA 600/7-79, 141 pp.
- Bhumralkar, C.M., Mancuso, R.L., Wolf, D.E. and Johnson, W.B. 1981. Regional Air Pollution Model for Calculating Short-Term (daily) Patterns and Transfrontier Exchanges of Airborne Sulfur in Europe. Tellus **33**, 142-161.

REFERENCES (continued)

- Bottenheim, J.W., Brice, K.A. and Anlauf, K.G. 1984. Discussion of a Lagrangian Trajectory Model Describing Long-Range Transport of Oxides of Nitrogen, the Incorporation of PAN in the Chemical Mechanism and Supporting Measurements of PAN and Nitrate Species at Rural Sites in Ontario. Atmos. Envir. **18**, 2609-2619.
- Bloxam, R.M., Misra, P.K. and Ley, B.E. 1986. Variable Washout Ratios in Lagrangian Models. 2nd International Specialty Conference on Meteorology of Acidic Deposition. J.Laznow and G. Steusland, Eds. APCA Publication.
- Buch, H., Pedersen, H.B and Sztokhamer, I.S. 1976. The variations of the concentrations of airborne particulate matter with wind direction and wind speed in Denmark. Atmos. Environ. **10**, 159-162.
- Calvert, J.G. and Stockwell, W.R. 1984. Mechanism and Rates of the Gas Phase Oxidation of Sulphur Dioxide and the Nitrogen Oxides in the Atmosphere in SO₂, NO and NO₂ Oxidation Mechanisms: Atmospheric Considerations, Acid Precipitation Series, Volume 3, J.I. Teasley; Series Ed., Butterworth Boston.
- Carmichael, G.R. and Peters, L.K. 1984. An Eulerian Transport/Transformation Removal Model for SO₂ and Sulfate. Atmos. Environ. **18**, 937-967.
- Chan, W.H., Orr, D.B., Bardswick, W.S. and Vet, R.J. 1985. An Overview: The Cumulative Wet/Dry Deposition Network. Ontario Ministry of the Environment Report ARB-141-85-AQM.
- Chang, J.S., Brost, R.A., Isaksen, I.S.A., Madronich, S., Middleton, P., Stockwell, W.R. and Walcek, C.J. 1987. A Three-Dimensional Eulerian Acid Deposition Model: Physical Concepts and Formulation. Geophys. Res. **92**, **14**, 681,700.
- Chatfield, C. 1984. The Analysis of Time Series : An Introduction, Third Edition. Chapman and Hall, London, 286pp.
- Ching, J.K.S. and Alkezweeny, A.J. 1986. Tracer Study of Vertical Exchange by Cumulus Clouds. J.Clim. & Appl. Meteorol. **25**, 1702-1711.
- Chung, Y.S. 1977. Ground-level Ozone and Regional Transport of Air Pollutants, J. Appl. Meteorol., **16**, 1127-1136.
- Clark, T.L., Denise, R.L., Seilkop, S.K., Voldner, E.C., Olson, M.P. and Alvo, M. 1987. International sulfur deposition model evaluation. Atmospheric Environment Service Publication No. ARD-87-1, 4905 Dufferin Street, Downsview, Ontario.
- Cox, R.M., Spanold-Tims, J. and Hughes, R.N. 1989. Acid fog and ozone: their possible role in birch deterioration around the Bay of Fundy, Canada. Water Air and Soil Pollution, **481**, 263-276.
- Crocker, T.D. and Regens, J.L. 1985. Acid Deposition Control. Environ. Sci.& Technol., **19**, 112-116.
- Dann, T. 1988. Trends in Ambient Ozone Concentrations in Canada. Preprint, 81st Ann. Air Poll. Control Assoc. Meeting, Dallas, June 19-24.

REFERENCES (continued)

- Davis, C.S., Moran, M.D., Portelli, R.V., Reid, N.W., Bates, D.V. and Scheer, D.B. 1984. Initial Assessment Report on Photo-chemical Oxidant Air Pollutants in Canada. Report Prepared by Concord Scientific Corporation for Environment Canada, Environmental Protection Service, April 1984.
- Davis, C.S., Reid, N.W., Heidorn, K.C. and Ormrod, D.P. 1986. Oxidant Assessment Ontario Database-Phase I. Report Prepared by Concord Scientific Corporation for Environment Canada, 1986.
- Demerjian, K.L. 1986. Workshop Report on Sources and Evaluation of Uncertainty in Long-Range Transport Models. Joint Report EPA/AES/OME. American Meteorological Society, 45 Beacon St. Boston, Mass. 01208.
- Demerjian, K.L. 1985. Quantifying Uncertainty in Long-Range Transport Models. Bull. Amer. Met. Soc., Vol. 66 12, 1533-1540.
- Dickerson, R.R., Huffman, G.J., Luke, W.T., Nunnermacker, L.J., Pickering, K.E., Leslie, A.C.D., Lindsey, C.G., Slinn, W.G.N., Kelly, T.J., Daum, P.H., Delany, A.C., Greenberg, J.P., Zimmerman, P.R., Boatman, J.F., Ray, J.D. and Stedman, D.H. 1987. Thunderstorms: An Important Mechanism in the Transport of Air Pollutants. Science 235, 460-465.
- Dillon, P.J., Lusi, M.A., Reid, R. and Yap, D. 1988. Ten-year trends in sulphate, nitrate and hydrogen deposition in central Ontario. Atmos. Environ. 22, 901-905.
- Draxler, R.R. and Hefter, J.L., 1989, Eds. Across North America Tracer Experiment (ANATEX) Volume I: Description, ground - level sampling at primary sites, and meteorology. NOAA Tech. Memorandum ERL ARL-167. Air Resources Lab., Silver Spring, MD, USA. 83pp.
- Dutkiewicz, V.A., Parekh, P.P. and Husain, L. 1987. An evaluation of regional elemental signatures relevant to the Northeastern United States, Atmos. Environ. 21, 1033-1044.
- Eder, B.K., Coventry, D.H., Clark, T.L. and Bollinger, C.E. 1986. RELMAP: A Regional Lagrangian Model of Air Pollution, User's Guide. EPA Report EPA/600/8-86/013.
- Eliassen, A. 1980. The OECD Study on Long Range Transport of Air Pollutants: Long Range Transport Modelling, Atmos. Environ. 12, 479-487.
- Eliassen, A., Hov, O., Isaksen, I.S.A., Saltbones, J. and Stordal, F. 1982. A Lagrangian Long-Range Transport Model with Atmospheric Boundary Layer Chemistry. J. Appl. Met. 21, 1645-1661.
- Eliassen, A. and Saltbones, J. 1983. Modelling of Long-Range Transport of Sulphur over Europe: A Two-Year Model Run and Some Model Experiments. Atmos. Environ., 17, 1457-1473.
- Eliassen, A. and Saltbones, J. 1975. Decay and Transformation Rates of SO₂ as Estimated from Emissions Data, Trajectories and Measured Air Concentrations. Atmos. Environ., 9, 425-429.
- Ellenton, G., Misra, P.K. and Ley, B. 1988. The Relative Roles of Emission Changes and Meteorological Variability in Variations of Wet Sulphur Deposition: A Trajectory Model Study. Atmos. Environ. 22, 547-556.
- Ellenton, G., Ley, B. and Misra, P.K. 1985. A Trajectory Puff Model of Sulphur Transport for Eastern North America. Atmos. Environ., 19, 727-737.

REFERENCES (continued)

- Endlich, R.M., Nitz, K.C., Brodziwsky, R. and Bhurmalkar, C.M. 1983. The ENAMAP-2 Air Pollution Model for Long Range Transport of Sulphur and Nitrogen Compounds, EPA Report 600/7-83-059, 217 pp.
- EPA. 1988. National Air Quality and Emissions Trends Report, 1986. USEPA Report No. EPA-450/4-88-001.
- EPRI. 1984. Regional Air Quality Model Assessment and Evaluation, Report EPRI EA-3671.
- ERT. 1985. Development of a Model for the Transport and Deposition of Acidifying Pollutants, ERT No. P-B866-450. Environmental Research and Technology Inc., Newsbury Park, Ca. 91320.
- ERT. 1984. ADOM/TADAP Model Development Programs, Vols. 1-7. ERT No. P-B980-535, July 1984. Environmental Research and Technology Inc., Newsbury Park, CA. 91320.
- Faulkner, D.A. 1987. The Effect of a Major Emitter on the Rain Chemistry of Southwestern British Columbia. Report No. PAES 68-1. Atmospheric Environment Service, Vancouver, Canada.
- Fay, J.A., Golomb, D., and Kumar, S. 1986. Annual and semi-annual anthropogenic sulphur budget for eastern North America, Atmos. Environ. **20**, 1497-1500.
- Fay, J.A., Golomb, D. and Kumar, S. 1985. Source Apportionment of Wet Sulphate Deposition in Eastern North America. Atmos. Environ. **19**, 1773-1782.
- Fay, J.A., Golomb, D. and Zemba, S.G. 1989. Observed and modeled trend of sulphate and nitrate in precipitation in eastern North America. Atmos. Environ. **23**, 1863-1866.
- Fay, J.A. and Rosenzweig, J.J. 1980. An Analytical Diffusion Model for Long Distance Transport of Air Pollutants, Atmos. Environ. **14**, 355-365.
- Ferber, G.J. (Editor). 1985. Cross-Appalachian Tracer Experiment (CAPTEX) Operations Review, NOAA Technical Memorandum ERL ARL-138, Air Resources Laboratory, Silver Spring, MD, USA.
- Ferber, G.J., Hefftes, J.L., Draxler, R.R., Lagomarsino, R.J., Thomas, F.L., Dietz, R.N., and Benkovitz, C.M. 1986. Cross-Appalachian Traces Experiment (CAPTEX '83) Final Report. NOAA Tech. Mem. ERL ARL-142, January, 1986, 60 pp.
- Fernau, M. and Samson, P.J. 1986. The Effect of Meteorological Variability on Targeted Emission Control Strategies. Paper presented at the Second International Specialty Conference on Meteorology of Acidic Deposition, Albany, New York. March. 418 pp.
- Finlayson-Pitts, B.J., and Pitts, J.N. 1986. Atmospheric Chemistry. John Wiley and Son.
- Fisher, B.E.A. 1978. The Calculation of Long Term Sulphur Deposition in Europe, Atmos. Environ. **12**, 489-501.
- Fisher, B.E.A. 1975. The Long Range Transport of Sulphur Dioxide. Atmos. Environ. **9**, 1063-1070.
- Forland, E.J. 1973. A study of the acidity in the precipitation in southwestern Norway. Tellus **25**, 291-299.

REFERENCES (continued)

- Fung, C., Misra, P.K., Bloxam, R. and Wong, S. 1989. Non-linear Response of SO_4^{2-} in Precipitation to Emission Reduction: A Model Study. Reprints of the Sixth Joint Conference on Applications of Air Pollution Meteorology. Jan 30-Feb.3, 1989. Anaheim, CA, p. 11-14.
- Galloway, J.N., Likens, G.E., and Hawley, M.E. 1984. Acid Precipitation: Natural versus anthropogenic components, Science **226**, 829-831.
- Galloway, J.N., and Whelpdale, D.M. 1987. WATOX-86 Overview and Western North Atlantic ocean S and atmospheric budgets. Global Biogeochemical Cycles **1**, 261-281.
- Galloway, J.N., and Whelpdale, D.M. 1980. An atmospheric sulfur budget for eastern North America. Atmos. Environ. **14**, 409-417.
- Haagenson, P.L., Kuo, Y.H. and Skumanich, M. 1987. Tracer Verification of Trajectory Models. J. of Clim. and Appl. Meteor. **26**, 410-426.
- Heidorn, K. and Yap, D. 1986. A Synoptic Climatology for Surface Ozone Concentrations in Southern Ontario, 1976-1981. Atmos. Environ. **20**, 695-703.
- Heisler, S.L., Sellars, F.M. and Mosbley, J.D. 1986. Comparison of the 1980 NAPAP and 1982 EPRI Emission Inventories - Preliminary Results. Air Pollution Control Association Annual Meeting, Minneapolis, Minnesota.
- Hidy, G.M. 1984. Source-Receptor Relationships for Acid Deposition: Pure and Simple? A Critical Review, J. Air Poll. Control Assoc. **34**, 518-531.
- Hollander, M. and Wolfe, D.A. 1973. Nonparametric Statistical Methods. John Wiley and Sons, New York, 503 pp.
- Hopper, J.F. and Barrie, L.A. 1988. Regional and background aerosol trace elemental composition observed in eastern Canada. Tellus **40B**, 446-462.
- Isaac, G.A., Joe, P.I. and Summers, P.W. 1983. The Vertical Transport and Redistribution of Pollutants by Clouds. Proceedings of the APCA Specialty Conference on Meteorology of Acid Deposition, Hartford, Conn. 496-512.
- Kahl, J.D., Harris, J.M., Herbert, G.A. and Olson, M.P. 1989. Intercomparison of Three Long-Range Trajectory Models Applied to Arctic Haze. Tellus, in press.
- Kelly, N.A., Ferman, M.A. and Wolff, G.T. 1986. The Chemical and Meteorological Conditions Associated with High and Low Ozone Concentrations in Southeastern Michigan and Nearby Areas of Ontario. J. Air Pollut. Control Ass. **36**, 150-158.
- Kroll, G. and Winkler, P. 1989. Trace substances input to coniferous forests via cloud interception. Mechanisms and Effects of Pollutant-Transfer into Forests, H.W., Georgii (ed.), Kluwer Academic Publishers, 205-211.
- Kurtz, J., Tang, A.J.S., Kirk, R.W. and Chan, W.H. 1984. Analysis of an acid rain deposition episode at Dorset, Ontario. Atmos. Environ. **18**, 387-394.

REFERENCES (continued)

- Kurtz, J., Yap, D., Bloxam, R., Shenfeld, L. and Kiely, P. 1989. The impact of Longe Range Transport on Oxidant Levels -The Southern Ontario Situation, Seminar on the Contemporary Oxidant Problem, Vancouver, February 27-28.
- Lamb, R.G. 1985. A Regional Scale (1000 km) Model of Photochemical Air Pollution 3. Tests of Numerical Algorithms. Report, Off. of Res. and Dev., Environ. Sci. Res. Lab., USEPA, Research Triangle Park, N.C.
- Lamb, R.G. 1983. A Regional Scale (1000 km) Model of Photochemical Air Pollution 2. Input Processor Network Design. Report, Off. of Res. and Dev. Environ. Sci. Res. Lab., USEPA, Research Triangle Park, N.C.
- Lamb, R.G. 1982. A Regional Scale (1000 km) Model of Photochemical Air Pollution 1. Theoretical Formulation. Report, Off. of Res. and Dev., Environ. Sci. Res. Lab., USEPA, Research Triangle Park, N.C.
- Liu, M.D., Stewart, D.A. and Henderson, D. 1981. A Mathematical Model for the Analysis of Acid Deposition, System Application Inc. San Rafael, Ca.
- Lovett, G.M. 1984. Rates and mechanisms of cloud water deposition to a subalpine balsam fir forests. Atmos. Environ. **18**, 361-371
- Lowenthal, D.H. and Rahn, K.A. 1988. Discussion of an evaluation of regional elemental signatures relevant to the Northwestern United States. Atmos. Environ. **22**, 609-616.
- Lusis, M.A., Anlauf K.G., Chung Y.S. and Wiebe H.A. 1976. Aircraft O₃, measurements in the vicinity of Toronto, Canada. Preprint, 69th Ann. Air Poll. Control Assoc. Meeting, Portland, 76-7-1.
- Lusis, M.A., Sahota, H. and Yap, D. 1985. The Sarnia Oxidants Study (27 June - 18th July 1984): Analysis of the air quality and meteorological data. MOE Report ARB-124-85-AQM.
- Mathews, T. 1987. Manual of the National Atmospheric Chemistry Contouring System (NAtCon). Atmospheric Environment Service, 4905 Dufferin St., Downsview, Ontario.
- McCormick, W.J., Fung, C.S., and Alp, E. 1989. Evaluation of ADOM Using ANATEX Observations. Concord Scientific Corporation Report J1464.2, Downsview, Ontario.
- Miller, R.G. Jr. 1981. Simultaneous Statistical Inference. Second Edition, Springer-Verlag, New York, 300pp.
- Misra, P.K., Bloxam, R., Fung, C., and Wong, S. 1989. Non-linear response of Wet Deposition to Emissions reduction: A Model Study. Atmos. Environ. **23**, 671-687.
- Mohnen, V.A. 1988. Mountain Cloud Chemistry Project. Report to U.S. Environmental Protection Agency, AREAL, Research Triangle Park, N.C. 27711. Contact Number CR 813934-01-2, pp. 32.
- MOI. 1982a. Emissions, Costs and Engineering Assessment. Work Group 3B. U.S.-Canada Memorandum of Intent on Transboundary Air Pollution, Final Report, June 1982.

REFERENCES (continued)

- MOI. 1982b. Atmospheric Sciences and Analysis, Work Group 2. Modelling Subgroup Final Report 2F-M. US-Canada Memorandum of Intent November 1, 1982.
- MOI. 1982c. United States-Canada Memorandum of Intent on Transboundary Air Pollution Report No. 2F-1.
- Mukammal, E.I., Neumann, H.H. and Gillespie, T.J. 1982. Meteorological Conditions Associated with Ozone in South-western Ontario, Canada. Atmos. Environ. **16**, 2095-2106.
- Mukammal, E.I., Neumann, H.H. and Nichols, T.R. 1985. Some Features of the Ozone Climatology of Ontario, Canada and Possible Contributions of Stratospheric Ozone to Surface Concentrations. Arch. Met. Geoph. Biocl. Ser. A **34**, 179-211.
- Munn, R.E. 1973. Secular Increases in Summer Haze in the Atlantic Provinces. Atmosphere **11**, 156-161.
- National Academy of Sciences. 1983. Jack Calvert et al Editors. Acid Deposition, Atmospheric Process in Eastern North America. A Review of Current Scientific understanding. National Academy Press, Washington, D.C.
- NAPAP. 1985. Annual Report, 1985. National Acid Precipitation Assessment Program, Washington, D.C.
- NAPAP. 1989. Deposition Monitoring: Methods and Results. State of Science/Technology Report 6. National Acid Precipitation Assessment Program, Washington, D.C.
- Olson, M.P. 1989. Authors' Reply to Discussion on Interannual Variability of Transboundary Sulphur Flux. Atmos. Environ. **23**, 2864-2867.
- Olson, M.P. and Oikawa, K.K. 1989. International Variability of Transboundary Sulphur Flux. Atmos. Environ. **23**, 333-340.
- Olson, M.P., Bottenheim, J.W. and Oikawa, K.K. 1989a. Nitrogen Budget for Eastern Canada. Atmos. Environ., in press.
- Olson, M.P., Puckett, K.J., Davies, D. and Oikawa, K.K. 1989b. A comparison between the ADOM Model and the ANATEX Tracer Data. Presented at Association of Chemical Engineers Conference, San Francisco, Nov. 1, 1989.
- Olson, M.P., Voldner E.C., and Oikawa K.K. 1983. Transfer Matrices from the AES-LRT Model. Atmosphere-Ocean **21 Vol. 3**, 344-361.
- Olson, M.P., Oikawa, K.K. and MacAfee, A.W. 1978. A Trajectory Model Applied to the Long-Range Transport of Air Pollutants, LRTAP 78-4, Atmospheric Environment Service, Downsview, Ontario.
- Pacyna, J.M. 1986. Source-receptor relationships for trace elements in northern Europe. Water, Soil and Air Poll. **30**, 825-835.
- Pinard, P. 1989. Deux indicateurs de performance environnementales concernant l'acidite des precipitations. Rapport M-89-3, Direction de la meteorologie, ministere de l'Environnement du Quebec.

REFERENCES (continued)

- Poirot, R.L. and Wishinski, P.R. 1986. Visibility, sulfate and air mass history associated with the summertime aerosol in northern Vermont. Atmosph. Environ. **20**, 1457-1469.
- Pudykiewicz J. 1988. Numerical Formulation of the Transport of Radioactive Cloud from the Chernobyl Nuclear Accident. Tellus **40B**, 241-259.
- Raatz, W.E., and Shaw, G.E. 1984. Long-range transport of pollution aerosols into the Alaskan Arctic. J. Clim. Appl. Met. **23**, 1052-1064.
- Rahn, K.A. and Lowenthal, D.H. 1985. Pollution aerosols in the Northeast: northeastern and midwestern contributions. Science **228**, 275-284.
- Rahn, K.A., and Lowenthal, D.H. 1984. Elemental Tracers of Distant Regional Pollution Aerosols. Science **223**, 132-139.
- Rahn, K.A. 1982. On the causes, characteristics and potential environmental effects of aerosol in the Arctic atmosphere. Proc. Conf. on the Arctic Hydrographic Environment and the Fate of Pollutants, pp. 163-195.
- Rahn, K.A., and Heidam, N.Z. 1981. Progress in Arctic air chemistry, 1977-1980: a comparison of the first and second symposia. Atmosph. Environ. **15**, 1345-1348.
- Rahn K.A. 1976. The chemical composition of the atmospheric aerosol. Technical Report, Graduate School of Oceanography, University of Rhode Island, Kingston, RI.
- Reinmuth, M. 1977. Time Series, in Modern Elementary Statistics. Freund, J.E. (Ed). Prentice Hall Press, New York, pp 605-655.
- RMCC 1986. Assessment of the State of Knowledge on the Long-Range Transport of Air Pollutants and Acid Deposition: Part 2 Atmospheric Sciences, Federal/Provincial Research and Monitoring Coordinating Committee, August, 1986, 108 pp.
- Rodhe, H. and Grandel, H. 1972. On the Removal Time of Aerosol Particles from the Atmosphere by Precipitation Scavenging. Tellus **24**, pp.442-454.
- Rodhe, H. and Herrera, R. 1988. Acidification in tropical countries. Scope **36**. John Wiley & Sons.
- Rodhe, H., Persson, C. and Akesson, O. 1972. An investigation into regional transport of soot and sulphate aerosols. Atmos. Environ. **6**, 675-693.
- Samson, P. 1978. Ensemble trajectory analysis of summertime sulfate concentrations in New York State. Atmosph. Environ. **12**, 1889-1893.
- Samson, P.J. 1989. Aggregation of Pollutant Deposition Episodes into Seasonal and Annual Estimates. The University of Michigan Department of Atmospheric, Oceanic and Space Studies Report.
- Samson, P.J. and Keeler, G.J. 1987. Empirical evidence of source-receptor relationships for atmospheric pollutants. Proc. EMEP-Workshop on Data Analysis and Presentation. Cologne, FRG. 15-17 June 1987, 221-236.

REFERENCES (continued)

- Schemenauer, R.S. 1986. Acidic deposition to forests: The 1985 Chemistry of High Elevation Fog Project. Atmosphere-Ocean **24**, 303-328.
- Schemenauer, R.S., Schuepp, P., Kermasha, S. and Cereceda, P. 1988. Measurements of the properties of high elevation fog in Quebec, Canada. NATO Advanced Research Workshop: Acid Deposition Processes at High Elevation Sites, D. Reidel Publ., 359-374.
- Schemenauer, R.S. and Winston, C. 1988. The 1986 Chemistry of High Elevation Fog Project, Air Pollution Control Association, 81st Annual General Meeting, 20-14 June, 88-129.6, 1-16.
- Schwartz, S.E. 1982. Gas Aqueous Reactions of Sulphur and Nitrogen Oxides in Liquid-Water Clouds, in SO_2 , NO and NO_2 Oxidation Mechanisms: Atmospheric Conditions, ed. J.G. Calvert, Ann Arbor Science, Woburn, M.A.
- Schwartz, S.E. and Daum, P.H. 1988. Sulphur Dioxide - Hydrogen Peroxide Relationships in Clean Air, Clouds and Precipitation, Presented at the American Chemical Society Meeting in Toronto, Canada. June 5-11. p.4.
- Scire, J.S., Lurmann, F., Bass, A. and Hanna, S. 1984. User's Guide to the MESOPUFF II Model and Related Processor Programs. U.S. EPA 600/58-84-013.
- Scire, J.S., Lurmann, F., Bass, A. and Hanns, S. 1983. Development of the MESOPUFF II Dispersion Model. U.S. EPA.
- Seinfeld, J.H. 1980. Lectures in Atmospheric Chemistry, American Institute of Chemical Engineers, Monograph Series 12, Volume 76, 1980, 98 pp.
- Shannon, J.D. 1981. A Model of Regional Long-Term Average Sulphur Atmospheric Pollution, Surface Removal and Net Horizontal Flux. Atmos. Environ. **15**, 689-701.
- Shannon, J.D. and Lesht, B.M. 1986. Modeled Trends and Climatological Variability of the Net Transboundary Flux of Airborne Sulphur Between the United States and Canada. Internat. Specialty Conference, Albany N.Y., March 1986.
- Shenfeld, L., Yap, D. and Kurtz, J. 1978. Long-range Transport of Ozone into and Across Southern Ontario, Canada. Conference on the Long-Range Transport of Photochemical Oxidants, Oslo, September 1978.
- Sirois, A. 1990. The effects of missing data on the calculation of precipitation-weighted-mean concentration in wet deposition. Atmos. Environ., in press.
- Sirois, A. and Barrie, L.A. 1988. An estimate of the importance of dry deposition as a pathway of acidic substances from the atmosphere to the biosphere in eastern Canada. Tellus **40B**, 59-80.
- Smith, F.B. 1981. The Significance fo Wet and Dry Synoptic Regions on long-Range Transport of pollution and Its Deposition. Atmos. Environ. **15**, 863-873.
- Smith, F.B. and Hunt, R.D. 1978. Meteorological aspects of the transport of pollution over long distances. Atmos. Environ. **12**, 461-477.

REFERENCES (continued)

- Spicer, C.W. 1983. Smog Chamber Studies of NO_x Transformation Rates in Nitrate Precursor Relationship. Environ. Sci. & Technol. **17**, p.112.
- Spicer, C.W. and Holdren, M. 1983. Laboratory Studies of the Rates and Mechanism of NO_x Reaction in Known Urban Air. Paper presented at the CACGP symposium on Tropospheric Chemistry. Oxford, U.K. Aug. 28-Sept. 3.
- Stockwell, W.R., and Calvert, J.G. 1983. The Mechanism of the HO-SO_2 reaction. Atmos. Environ. **17**, 2231-2236.
- Strauss, B., Martin, D. and Cuillier, C. 1986. Une methode nouvelle en climatologie de trajectoires de masses d'air. Proc. Seventh World Clean air Congress, Sydney Australia, 25-29 Aug. 1986, Vol. I, 326-333.
- Streets, D.G., Lesht, B.M., Shannon, J.D. and Veselka, T.D. 1985. Climatological Variability - Effects on Strategies to Reduce Acid Deposition. Environ. Sci. & Technol. **19**, 887-893.
- Sturges, W.I. and Barrie, L.A., 1989. The use of stable lead 206/207 isotope ratios and elemental composition to discriminate the origins of lead in aerosols at a rural site in eastern Canada. Atmos. Environ. **23**, 1645-1657.
- Summers, P.W. 1987. Empirical source-receptor relationships in Eastern Canada determined from monitoring data and air-mass trajectory climatologies. Proc. EMEP-Workshop on Data Analysis and Presentation. Cologne, FRG, 15-17 June 1987, 165-192.
- Summers, P.W. 1984. Discussion of G. Hidy's Critical Review of Source-Receptor Relationships, J. Air Poll. Control Assoc. **34**, 906-911.
- Summers, P.W., 1982. From emission to deposition: Processes and Budgets. Proc. Specialty Conf. on Atmospheric Deposition. Air Pollution Control Association Report Sp-49.
- Summers, P.W. and Fricke, W. 1989. Atmospheric decay distances and times for sulphur and nitrogen oxides estimated from air and precipitation monitoring in eastern Canada. Tellus **41B**, 286-295.
- Summers, P.W. and Olson, M.P. 1985. A Comparison between AES-LRTAP Model Trajectories and Observed Tracer Concentrations during CAPTEX-83. Presented at the Muskoka 85 Acid Rain Conference, September 1985. Atmospheric Environment Service, Downsview, Ontario.
- Tang, A.J.S., Ahmed, A. and Lusi, M.A. 1986. Summary: Some results from the APIOS Atmospheric Deposition Monitoring Program (1981-1984). Report No. ARB-110-86, AP105. 011-86, Ont. Ministry of Environment.
- Underwood, J.K., Ogden, III, J.G., Kerekes, J.J., and Vaughan, H.H. 1987. Acidification of Nova Scotia Lakes.III: Atmospheric Deposition of SO_4 and NO_3 and Effects on Urban and Rural Lakes. Water, Air, and Soil Pollut. **32**, 77.
- Unified Deposition Data Base Committee (UDDBC). 1985b. A unified wet deposition data base for Eastern North America: Data Screening, Calculation Procedures, and results for sulphates and nitrates (1980) and Addendum with results for sulphates and nitrates (1980-1983). Edited by M. Lusi, Ontario Ministry of the Environment, 880 Bay Street, Toronto, Ont.

REFERENCES (continued)

- Vachon, M. 1988. Analyses statistiques de l'évolution temporelle des précipitations acides au Québec. Mémoire de maîtrise, Faculté des Études supérieures, Université de Montréal.
- Venkatram, A., Karamchandi, P.K., and Misra, P.K. 1988. Testing a Comprehensive Acid Deposition Model. Atmos. Environ. **22**, 737-747.
- Venkatram, A., Ley, B.E., and Wong, S.Y. 1982. A Statistical Model to Estimate Long-Term Concentrations of Pollutants Associated with Long-Range Transport. Atmos. Environ. **16**, pp. 249-257.
- Venkatram, A., McNaughton, D., Karamchandi, P., Shannon, J., Sisterson, D., and Fernau, M. 1989. State of the Science Document - 8. Relationships between Atmospheric Emissions and Deposition/Air Concentrations. National Acid Precipitation Assessment Program. Draft Report.
- Vet, R.J., Sukloff, W.B., Still, M.E. and Gilbert, R., 1986. Canadian Air and Precipitation Monitoring Network (CAPMoN): Precipitation Chemistry Data Summary, 1983-1984. Air Quality Monitoring and Assessment Division, Air Quality and Inter-Environmental Research Branch, Atmospheric Environment Service, 4905 Dufferin Street, Downsview, Ontario, M3H 5T4.
- Vet, R.J., Sukloff, W.B., Still, M.E., Martin, J.B., Kobelka, W.F. and Gaudenzi, A. 1988a. Canadian Air and Precipitation Monitoring Network (CAPMoN): Precipitation Chemistry Data Summary, 1985. Air Quality Monitoring and Assessment Division, Air Quality and Inter-Environmental Research Branch, Atmospheric Environment Service, 4905 Dufferin Street, Downsview, Ontario, M3H 5T4.
- Vet, R.J., Sukloff, W.B., Still, M.E., Martin, J.B., Kobelka, W.F. and Gaudenzi, A. 1988b. Canadian Air and Precipitation Monitoring Network (CAPMoN): Precipitation Chemistry Data Summary, 1986. Air Quality Monitoring and Assessment Division, Air Quality and Inter-Environmental Research Branch, Atmospheric Environment Service, 4905 Dufferin Street, Downsview, Ontario, M3H 5T4.
- Vet, R.J., Sukloff, W.B., Still, M.E., McNair, C.S., Martin, J.B., Kobelka, W.F. and Gaudenzi, A. 1989. Canadian Air and Precipitation Monitoring Network (CAPMoN): Precipitation Chemistry Data Summary, 1987. Air Quality Monitoring and Assessment Division, Air Quality and Inter-Environmental Research Branch, Atmospheric Environment Service, 4905 Dufferin Street, Downsview, Ontario, M3H 5T4.
- Vogelmann, H.W. 1982. Catastrophe on Camels Hump. Natural History **91**, 8-14.
- Voldner, E.C., Barrie, L.A. and Sirois, A. 1986. A Literature Review of Dry Deposition of Oxides of Sulphur and Nitrogen with Emphasis on Long-Range Transport Modelling in North America. Atmos. Environ. **20**, 2101-2123.
- Voldner, E.C. and Olson, M.P. 1982. Analysis of Transfer Matrices. Report AQRB-82-004-T. Atmospheric Environment Service, Downsview, Ontario. M3H 5T4.
- Voldner, E.C., Olson, M.P., Oikawa, K.K. and Loiselle, M. 1981. Comparison Between Measured and Computed Concentrations of Sulphur Compounds in Eastern North America. J. Geophys. Res. **86**, 5334-5346.
- Vong, R.J., Moseholm, L., Covert, D.S., Sampson, P.D., O'Loughlin, J.F., Stevenson, M.N., Charlson, R.J., Zoller, W.H., and Larson, T.V. 1988. Changes in rainwater acidity associated with closure of a copper smelter. J. Geophys. Res., **93**, 7169-7179.

REFERENCES (continued)

- Walmsley, J.L. and Mailhot, J. 1983. On the Numerical Accuracy of Trajectory Models for Long-Range Transport of Atmospheric Pollutants. Atmos.-Ocean **21**, 14-39.
- Yap, D. and Chung, Y.S. 1977. Relationship of Ozone to Meteorological Conditions in Southern Ontario. Preprint, 70th Ann. Air Poll. Control Assoc. Meeting, June 20-24, Toronto.
- Yap, D., Ning, D.T. and Dong, W. 1988. An Assessment of Source Contributions to the Ozone Concentrations in Southern Ontario, Atmos. Environ. **22**, 1161-1168.
- Young, J.W.S. 1988. Source-Receptor Relationships: The Canadian Experience. In: Acid Rain: The Relationship Between Sources and Receptors. J.C. White (Ed.), pp. 151-163.
- Young, J.W.S. and Shaw, R.W. 1986. A Proposed Strategy for Reducing Sulphate Deposition in North America - I. Methodology for Minimizing Sulphur Removal, Atmos. Environ. **20**, 189-199.
- Zeng, Y., and Hopke, P.K. 1989. A study of the sources of Acidic precipitation in Ontario, Canada. Atmos. Environ. **23**, 1499-1509.
- Zimmerman, D., Tak, W., Smith, M., Demmy, J. and Battye, R. 1988. Anthropogenic Emissions Data for the 1985 NAPAP Inventory. U.S. EPA, Report # EPA-600/7-88-022.

TD
195.54
.C36
1990
part 3

The 1990 Canadian long-range
transport of air pollutants and
acid deposition assessment
report.
77963

